

Nachhaltige katalytische Transformationen von Carbonsäuren

Decarboxylierende Kreuzkupplungen und Carboxylat-dirigierte Arylierungen



vom Fachbereich Chemie der Technischen Universität Kaiserslautern

zur Verleihung des akademischen Grades

„Doktor der Naturwissenschaften“

genehmigte Dissertation

D 386

vorgelegt von

Dipl.-Chem. Dagmar Hackenberger

angefertigt im Arbeitskreis von

Prof. Dr. L. J. Gooßen

Datum der wissenschaftlichen Aussprache: 17.08.2017

Kaiserslautern, 2017

Meinen Eltern

Promotionskommission

Vorsitzender: Prof. Dr.-Ing. Stefan Ernst

Berichterstatter: Prof. Dr. Lukas J. Gooßen

Berichterstatter: Prof. Dr. Werner R. Thiel

Die vorliegende Arbeit wurde im Zeitraum von Januar 2014 bis Juni 2017 im Arbeitskreis von Prof. Dr. Lukas J. Gooßen am Fachbereich Chemie der Technischen Universität Kaiserslautern und an der Fakultät für Chemie und Biochemie der Ruhr-Universität Bochum angefertigt.

Eidesstattliche Erklärung

Hiermit versichere ich, dass ich die vorliegende Arbeit eigenständig verfasst und keine anderen als die angegebenen Quellen und Hilfsmittel verwendet sowie Literaturzitate kenntlich gemacht habe. Kooperationsprojekte sind ausdrücklich als solche gekennzeichnet und die Mitarbeiter genannt. Die Arbeit liegt weder in gleicher noch in ähnlicher Form in einem anderen Prüfungsverfahren vor.

Kaiserslautern, den _____

Dagmar Hackenberger

Danksagung

Mein besonderer Dank gebührt Herrn Prof. Dr. Lukas J. Gooßen für seine stetige Unterstützung, das mir entgegengebrachte Vertrauen sowie für die herausfordernden Aufgabenstellungen, an denen ich gewachsen bin. Frau Dr. Käthe Gooßen danke ich für die Unterstützung beim Durchsehen der Manuskripte.

Herrn Prof. Dr. Werner R. Thiel danke ich für seine Tätigkeit als Zweitgutachter dieser Arbeit und Herrn Prof. Dr.-Ing. Stefan Ernst danke ich für die Übernahme des Prüfungsvorsitzes.

Allen aktuellen und ehemaligen Mitarbeitern des Arbeitskreises danke ich für die tolle Atmosphäre im Labor, die stete Hilfsbereitschaft und die Freundschaften, die in den letzten Jahren entstanden sind. Besonderer Dank gilt meinen Projektpartnern für die erfolgreiche Zusammenarbeit. Außerdem danke ich im Speziellen Agostino, Bilguun, Christian, Thilo und Timo für den Rückhalt und die schöne Zeit über den Laboralltag hinaus.

Christian, Thilo, Timo und Silke danke ich vielmals für Korrekturen dieser Arbeit.

Den Serviceabteilungen des Fachbereichs Chemie der Technischen Universität Kaiserslautern, insbesondere Frau Ruth Maria Bergsträßer und Herrn Dr. Uwe Bergsträßer, danke ich für die zuverlässigen Dienste. Weiterhin bin ich unserer Sekretärin Susanne zu großem Dank verpflichtet.

Für die finanzielle Unterstützung danke ich der Stipendienstiftung Rheinland-Pfalz.

Meiner Familie danke ich von ganzem Herzen für die uneingeschränkte Unterstützung, ihre Rücksichtnahme und den Rückhalt während meiner Doktorarbeit.

Veröffentlichungen

Die meisten Ergebnisse dieser Arbeit wurden bereits in wissenschaftlichen Fachzeitschriften veröffentlicht:

1. A. Fromm, C. van Wüllen, D. Hackenberger, L. J. Gooßen, *J. Am. Chem. Soc.* **2014**, *136*, 10007–10023: *Mechanism of Cu/Pd-Catalyzed Decarboxylative Cross-Couplings: A DFT Investigation.*
2. L. Huang, D. Hackenberger, L. J. Gooßen, *Angew. Chem.* **2015**, *127*, 12798–12802: *Iridium-katalysierte ortho-Arylierung von Benzoessäuren mit Aryldiazoniumsalzen; Angew. Chem. Int. Ed.* **2015**, *54*, 12607–12611: *Iridium-Catalyzed ortho-Arylation of Benzoic Acids with Arenediazonium Salts.*
3. D. Hackenberger, B. Song, M. F. Grünberg, S. Farsadpour, F. Menges, H. Kelm, C. Groß, T. Wolff, G. Niedner-Schatteburg, W. R. Thiel, L. J. Gooßen, *ChemCatChem* **2015**, *7*, 3579–3588: *Bimetallic Cu/Pd Catalysts with Bridging Aminopyrimidinyl Phosphines for Decarboxylative Cross-Coupling Reactions at Moderate Temperature.*
4. D. Katayev, D. Hackenberger, L. J. Gooßen, *The Catalyst Review* **2015**, *28*, 6–11: *Decarboxylative and Decarbonylative Reactions: An Industrial Perspective.*
5. J. Tang, D. Hackenberger, L. J. Gooßen, *Angew. Chem.* **2016**, *128*, 11466–11470: *Verzweigte Arylalkene aus Zimtsäuren: Selektivitätsumkehr in Heck-Reaktionen durch Carboxylate als abfallende dirigierende Gruppen; Angew. Chem. Int. Ed.* **2016**, *55*, 11296–11299: *Branched Arylalkenes from Cinnamates: Selectivity Inversion in Heck Reactions by Carboxylates as Deciduous Directing Groups.*
6. A. Biafora, T. Krause, D. Hackenberger, F. Belitz, L. J. Gooßen, *Angew. Chem.* **2016**, *128*, 14972–14975; *Angew. Chem. Int. Ed.* **2016**, *55*, 14752–14755: *ortho-C–H Arylation of Benzoic Acids with Aryl Bromides and Chlorides Catalyzed by Ruthenium.*
7. D. Hackenberger, P. Weber, D. C. Blakemore, L. J. Goossen, *J. Org. Chem.* **2017**, *82*, 3917–3925: *Synthesis of 3-Substituted 2-Arylpyridines via Cu/Pd-Catalyzed Decarboxylative Cross-Coupling of Picolinic Acids with (Hetero)Aryl Halides.*

Posterpräsentationen

Teile dieser Arbeit wurden bereits auf internationalen Konferenzen vorgestellt:

1. *14th Belgian Organic Synthesis Symposium* in Louvain-la-Neuve, **2014**: *Low-Temperature Cu/Pd-Catalyzed Decarboxylative Cross-Coupling with Bidentate Ligands.*
2. *48. Jahrestreffen deutscher Katalytiker* in Weimar, **2015**: *Cu/Pd-Catalysts with Bridging Aminopyrimidinyl Phosphines for Low-Temperature Decarboxylative Cross-Couplings.*
3. *GDCh-Wissenschaftsforum* in Dresden, **2015**: *Iridium-Catalyzed ortho-Arylation of Benzoic Acids with Arenediazonium Salts.*
4. *9th CaRLa Winter School* in Heidelberg, **2016**: *Bimetallic Cu/Pd Catalysts with Bridging Aminopyrimidinyl Phosphines for Decarboxylative Cross-Couplings at Moderate Temperature.*
5. *15th Belgian Organic Synthesis Symposium* in Antwerpen, **2016**: *Iridium-Catalyzed ortho-Arylation of Benzoic Acids with Arenediazonium Salts und Branched Arylalkenes from Cinnamates: Selectivity Inversion in Heck Reactions by Carboxylates as Deciduous Directing Groups.*

Abkürzungen

Ac	Acetyl	EI	Elektronenstoßionisation
acac	Acetylaceton	ESI	Elektrosprayionisation
Ad	Adamantyl	Et	Ethyl
Ala	Alanin	et al.	und andere
aq.	aqueous	EWG	Electron withdrawing group
Äquiv.	Äquivalent	Fa.	Firma
Ar	Aryl	F ₆ -acac	1,1,1,5,5,5-Hexafluoracetylaceton
ATR	Attenuated total reflection	FT	Fourier-Transform
BINAP	2,2'-Bis(diphenylphosphino)-1,1'-binaphthyl	GC	Gaschromatographie
bisSO	1,2-Bis(phenylsulfinyl)ethan	Gua	Guanidinium
Boc	<i>tert</i> -Butyloxycarbonyl	Het	Hetero
bpy	2,2'-Bipyridin	HFIP	1,1,1,3,3,3-Hexafluor-2-propanol
calcd.	calculated	HRMS	High Resolution Mass Spectrometry
CAS	Chemical Abstracts Service	Ile	Isoleucin
Cbz	Benzyloxycarbonyl	<i>i</i> -Pr	<i>iso</i> -Propyl
CMPhos	2-[2-(Dicyclohexylphosphino)-phenyl]-1-methyl-1 <i>H</i> -indol	IR	Infrarotspektroskopie
COD	1,5-Cyclooctadien	<i>J</i>	Kopplungskonstante
Cp*	1,2,3,4,5-Pentamethylcyclopentadienyl	JohnPhos	(2-Biphenyl)di- <i>tert</i> -butylphosphine
Cy	Cyclohexyl	KHMDS	Kaliumhexamethyldisilazid
CyJohnPhos	2-(Dicyclohexylphosphino)biphenyl	L	Ligand
Cym	Cymol	LM	Lösungsmittel
δ	Chemische Verschiebung	M	Metall
DavePhos	2-Dicyclohexylphosphino-2'-(<i>N,N</i> -dimethylamino)biphenyl	Me	Methyl
dba	Dibenzylidenacetone	Me ₄ -Phen	3,4,7,8-Tetramethyl-1,10-phenanthrolin
DCE	Dichlorethan	Mes	Mesitylen oder Mesityl
DCM	Dichlormethan	MIDA	<i>N</i> -Methyliminodiessigsäure
DFT	Dichtefunktionaltheorie	m.p.	Melting point
DG	Dirigierende Gruppe	MS	Molekularsieb oder Massenspektrometrie
Diglyme	Diglycoldimethylether	<i>n</i>	normal, unverzweigt
DMAc	<i>N,N</i> -Dimethylacetamid	Naph	Naphthyl
DMAP	4- <i>N,N</i> -Dimethylaminopyridin	<i>n</i> -Bu	<i>n</i> -Butyl
DME	Ethylenglycoldimethylether	n.d.	nicht detektiert
DMF	<i>N,N</i> -Dimethylformamid	NHPI	<i>N</i> -Hydroxyphthalimid
DMSO	Dimethylsulfoxid	NMP	<i>N</i> -Methyl-2-pyrrolidon
DMPU	Dimethylpropylenharnstoff	NMR	Nuclear Magnetic Resonance
DPEPhos	Bis[(2-diphenylphosphino)-phenyl]ether	NO ₂ -Phen	5-Nitro-1,10-phenanthrolin
dppe	1,2-Bis(diphenylphosphino)ethan	[O]	Oxidationsmittel
DPPF	1,1'-Bis(diphenylphosphino)ferrocen	Oct	Octyl
		OMs	Methansulfonyl
		OTf	Trifluormethansulfonyl
		OTs	<i>para</i> -Toluolsulfonyl

<i>o</i>	<i>ortho</i>	<i>t</i> -BuXPhos	2-Di- <i>tert</i> -butylphosphino-2',4',6'-
<i>p</i>	<i>para</i>		triisopropylbiphenyl
PEPPSI-IPr	[1,3-Bis(2,6-diisopropylphenyl)- imidazol-2-yliden](3-chloropyridyl)- palladium(II)-dichlorid	TEMPO	2,2,6,6-Tetramethylpiperidinyloxy
Ph	Phenyl	TFA	Trifluoracetat
Phe	Phenylalanin	TFE	Trifluorethanol
Ph ₂ -Phen	4,7-Diphenyl-1,10-phenanthrolin	THF	Tetrahydrofuran
1,10-Phen	1,10-Phenanthrolin	TMEDA	Tetramethylethylendiamin
Pro	Prolin	TOF	Time of flight
Py	Pyridin	Tol	Tolyl
R	organischer Rest	μW	Mikrowelle
RT	Raumtemperatur	Val	Valin
SET	Single electron transfer	White-Katalysator	1,2-Bis(phenylsulfinyl)ethan- palladium(II)acetat
SPhos	2-Dicyclohexylphosphino-2',6'- dimethoxybiphenyl	X	Halogen
<i>t</i> -Bu	<i>tert</i> -Butyl	XPhos	2-Dicyclohexylphosphino-2',4',6'- triisopropylbiphenyl
		Xyl	Xylol

Nummerierung der Verbindungen

Die vorliegende Doktorarbeit besteht zu einem großen Teil aus originalen Veröffentlichungstexten, in denen die Verbindungen unabhängig voneinander nummeriert wurden. Zum besseren Verständnis wurde die Nummerierung der Publikationen beibehalten und die Verbindungen in den jeweiligen Unterkapiteln getrennt voneinander nummeriert. Verbindungen, die nicht in einer Publikation enthalten sind, werden im entsprechenden Kapitel entweder neu nummeriert oder die Nummerierung knüpft an die einer vorhandenen Publikation an. Die Bezeichnung setzt sich jeweils aus der Nummer der dritten Überschriftsebene und einer durchlaufenden Nummer (mit Buchstabe) zusammen, sodass Doppelbenennungen vermieden werden. Trägt beispielsweise die 3. Verbindung aus der Publikation in Kapitel 5.1.2 die Nummer **3a**, dann trägt diese Verbindung in den zusätzlich verfassten Textpassagen und im experimentellen Teil die Nummer **5.1.2-3a**. Auf eine Nummerierung der Strukturen in der Einleitung sowie von stark verallgemeinerten Strukturen in generellen Schemata oder Abbildungen wurde verzichtet.

Inhaltsverzeichnis

1	Kurzzusammenfassung	1
2	Struktur der Arbeit	2
3	Einleitung	3
3.1	Darstellung und Reaktivität von Carbonsäuren	3
3.1.1	Darstellung von Carbonsäuren	3
3.1.2	Die Reaktivität der Carboxygruppe	6
3.2	Carbonsäuren als Substrate für Übergangsmetall-katalysierte Kupplungen.....	6
3.2.1	Übergangsmetall-vermittelte Aktivierungsmodi von Carbonsäuren	6
3.2.2	Redox-neutrale decarboxylierende Kreuzkupplungen	8
3.2.3	Carboxylat-dirigierte <i>ortho</i> -C–H-Funktionalisierungen	15
4	Aufgabenstellung	22
5	Ergebnisse und Diskussion	24
5.1	Kupfer/Palladium-katalysierte decarboxylierende Kreuzkupplungen bei moderaten Reaktionstemperaturen.....	24
5.1.1	Eingehende Untersuchungen zum Mechanismus der Reaktion	24
5.1.2	Decarboxylierende Kreuzkupplungen bei 100–120 °C mit bidentaten Liganden.....	46
5.2	Decarboxylierende Kreuzkupplungen heteroaromatischer Carbonsäuren.....	65
5.2.1	Hintergrund	65
5.2.2	Protodecarboxylierung von Pyridin-2-carbonsäure	66
5.2.3	Decarboxylierende Kreuzkupplung von Pyridin-2-carbonsäure	71
5.2.4	Decarboxylierende Kreuzkupplung 3-substituierter Pyridin-2-carbonsäuren.....	79
5.2.5	Decarboxylierende Kreuzkupplung von Pyrimidin-2-carbonsäure	92
5.3	Iridium-katalysierte <i>ortho</i> -Arylierung mit Aryldiazoniumsalzen.....	95
5.3.1	Hintergrund	95
5.3.2	Amid-dirigierte <i>ortho</i> -Arylierung.....	96
5.3.3	Alternative Iridium-katalysierte C–H-Arylierung von Benzamiden mit Aryldiazoniumsalzen.....	102
5.3.4	Carboxylat-dirigierte <i>ortho</i> -Arylierung.....	103
5.4	Ruthenium-katalysierte <i>ortho</i> -Arylierung von Benzoessäuren	115
5.4.1	Hintergrund	115
5.4.2	Ruthenium-katalysierte <i>ortho</i> -C–H-Arylierung mit Arylchloriden und -bromiden ...	116
5.4.3	Alternative Protokolle	127
5.5	Decarboxylierende Mizoroki-Heck-Reaktion von Arylhalogeniden mit Zimtsäuren zur Synthese von 1,1-Diarylalkenen	128
5.5.1	Hintergrund	128

5.5.2	Selektivitätsumkehr in Heck-Reaktionen durch Carboxylate als abfallende dirigierende Gruppen	129
5.5.3	1,1-Diarylalkene aus Zimtsäuren und Arenen.....	138
6	Zusammenfassung und Ausblick	139
7	Experimenteller Teil	143
7.1	Anmerkung.....	143
7.2	Allgemeine Arbeitstechniken.....	143
7.2.1	Chemikalien und Lösungsmittel.....	143
7.2.2	Durchführung von Parallelreaktionen	143
7.2.3	Analytische Methoden.....	145
7.3	Bimetallic Cu/Pd Catalysts with Bridging Aminopyrimidinyl Phosphines for Decarboxylative Cross-Coupling Reactions at Moderate Temperature.....	147
7.3.1	General remarks.....	147
7.3.2	General procedure for the protodecarboxylation experiments	147
7.3.3	Preparation of starting materials.....	147
7.3.4	Optimization of the Cu/Pd-catalyzed decarboxylative cross-coupling at 100 °C	148
7.3.5	General procedure for the biaryl synthesis	150
7.3.6	Synthesis and characterization of the corresponding products	151
7.3.7	Ligand synthesis	159
7.3.8	Synthesis and characterization of the palladium complex.....	166
7.3.9	Details and simulations of isotopic distributions of the ESI-MS studies	167
7.4	Synthesis of 2-Arylpyridines <i>via</i> Cu/Pd-Catalyzed Decarboxylative Cross-Coupling of Picolinic Acids with (Hetero)Aryl Halides	170
7.4.1	General remarks.....	170
7.4.2	General method for the catalyst screening in section 5.2.3 and 5.2.5 and the protodecarboxylation studies	170
7.4.3	Preparation of starting materials.....	170
7.4.4	Optimization of the decarboxylative cross-coupling of potassium 3-fluoropicolinate	171
7.4.5	General procedure for the biaryl synthesis	173
7.4.6	Synthesis and characterization of the corresponding products	173
7.4.7	Nucleophilic aromatic fluorine substitutions	190
7.5	Iridium-Catalyzed <i>ortho</i> -Arylation of Benzoic Acids and Benzamides with Arenediazonium Salts	191
7.5.1	Preparation of starting materials.....	191
7.5.2	General method for the catalyst screening.....	191
7.5.3	General procedure for the Ir-catalyzed <i>ortho</i> -arylation.....	192
7.5.4	Synthesis and characterization of the corresponding products	193
7.5.5	Procedure for the one-pot <i>ortho</i> -C–H arylation and protodecarboxylation.....	220
7.5.6	Procedure for the one-pot <i>ortho</i> -C–H arylation and cyclization	221

7.5.7	Control experiments	222
7.6	<i>ortho</i> -C–H Arylation of Benzoic Acids with Aryl Bromides and Chlorides	
	Catalyzed by Ruthenium	222
7.6.1	General remarks.....	222
7.6.2	Optimization of the Ru-catalyzed <i>ortho</i> -arylation.....	222
7.6.3	General procedure for the Ru-catalyzed <i>ortho</i> -arylation.....	224
7.6.4	Synthesis and characterization of the corresponding products	225
7.6.5	Procedure for the one-pot <i>ortho</i> -C–H arylation and protodecarboxylation.....	238
7.6.6	Procedure for the one-pot <i>ortho</i> -C–H arylation and decarboxylative cross coupling	240
7.6.7	Synthesis of [Ru(2-Me-benzoato ²⁻ -C ⁶ ,O ¹)(<i>p</i> -cymene)(pyridine)]	241
7.6.8	Mechanistic studies	241
7.7	Branched Arylalkenes from Cinnamates: Selectivity Inversion in Heck Reactions	
	by Carboxylates as Deciduous Directing Groups	242
7.7.1	General remarks.....	242
7.7.2	General procedure for the protodecarboxylation experiments	242
7.7.3	Preparation of starting materials.....	242
7.7.4	Optimization of the decarboxylative Mizoroki-Heck coupling.....	243
7.7.5	General procedure for the decarboxylative Mizoroki-Heck coupling.....	245
7.7.6	Synthesis and characterization of the corresponding products	245
7.7.7	Procedure for the one-pot three-step process	261
7.7.8	Control experiments	262
8	Literaturverzeichnis	263
9	Curriculum Vitae	275

1 Kurzzusammenfassung

Im Rahmen dieser Arbeit wurden neue nachhaltige Methoden zur selektiven C–C-Bindungsknüpfung ausgehend von Carbonsäuren entwickelt. Dabei wurden die Reaktionskonzepte der decarboxylierenden Biarylsynthese sowie der Carboxylat-dirigierten Arylierung verfolgt.

Geleitet von eingehenden DFT-Studien wurde ein Katalysatorsystem entwickelt, mit dem die Reaktionstemperatur der Kupfer/Palladium-katalysierten decarboxylierenden Kreuzkupplung von ursprünglich über 150 °C auf 100–120 °C abgesenkt werden konnte. Dazu wurden bidentate *P,N*-Liganden eingesetzt, die die Katalysatormetalle verbrückend koordinieren können und so die geschwindigkeitsbestimmende Transmetallierung erleichtern.

Daneben gelang es, ein bimetallisches Kupfer/Palladium-Katalysatorsystem zu entwickeln, welches die Synthese 3-substituierter 2-(Hetero-)Arylpyridine bei nur 130 °C ermöglicht. Dies basierte auf der Entdeckung, dass ein Substituent *ortho* zur Carboxygruppe der Pyridin-2-carbonsäure ebenso wie im Fall von Benzoesäuren eine Decarboxylierung begünstigt.

Neben den decarboxylierenden *ipso*-Arylierungen wurden auch neue Protokolle für Carboxylat-dirigierte *ortho*-Arylierungen von Benzoesäuren entwickelt. So wurde diese erstmals mit Aryldiazoniumsalzen als Kupplungspartner realisiert. Das neue Protokoll unter Verwendung eines Iridium-basierten Katalysatorsystems gewährleistet eine Reaktionsführung unter vergleichsweise milden Bedingungen. Zudem wird eine Orthogonalität zu Kupplungen mit Arylhalogeniden geschaffen.

Daneben wurde ein Protokoll für die *ortho*-Arylierung von Benzoesäuren mit Arylhalogeniden entwickelt, welches erstmals auf kostengünstigen Ruthenium-Katalysatoren basiert.

Die Überlegenheit der Carboxylatgruppe im Vergleich zu anderen dirigierenden Gruppen konnte demonstriert werden, indem sie im Anschluss an die jeweilige *ortho*-Arylierung entfernt sowie als Ankerpunkt in weiteren Funktionalisierungen genutzt wurde.

Weiterhin gelang es, eine Kupfer/Palladium-katalysierte decarboxylierende Mizoroki-Heck-Reaktion von Zimtsäuren mit Arylhalogeniden zu entwickeln, welche selektiv 1,1-Diarylalkene zugänglich macht. Dabei agiert die Carboxylatgruppe als abfallende dirigierende Gruppe.

Das synthetische Potential der neu entwickelten Methoden wurde jeweils anhand eines diversen Substratspektrums demonstriert. Darüber hinaus lieferten mechanistische Studien zu den Carboxylat-dirigierten Transformationen Einblicke zum Ablauf der Reaktionen.

2 Struktur der Arbeit

Die vorliegende Doktorarbeit wurde kumulativ verfasst. Sie besteht aus fünf Teilprojekten, die sich thematisch mit decarboxylierenden Kreuzkupplungen und Carboxylat-dirigierten Arylierungen befassen. Aufgrund der kumulativen Promotionsform enthält diese Ausarbeitung sechs englischsprachige Originaltexte. Zudem wurden deutschsprachige Passagen hinzugefügt. Diese leiten die Teilprojekte thematisch ein oder enthalten ergänzende und unveröffentlichte Ergebnisse.

In der Einleitung wird zunächst die Substanzklasse der Carbonsäuren vorgestellt und deren Bedeutung als Substrate in Übergangsmetall-katalysierten Kupplungsreaktionen dargelegt. Schwerpunktmäßig wird dabei auf redox-neutrale decarboxylierende Kreuzkupplungen und Carboxylat-dirigierte *ortho*-Arylierungen von Benzoesäuren eingegangen. Nach der Aufgabenstellung folgt der Ergebnis- und Diskussionsteil. Darin werden die einzelnen Teilprojekte jeweils kurz eingeleitet und die entsprechenden Originalveröffentlichungen abgebildet. Zusätzlich werden ergänzende und unveröffentlichte Ergebnisse zu den jeweiligen Teilprojekten diskutiert. In den ersten beiden Unterkapiteln dieses Abschnitts werden die im Rahmen der vorliegenden Arbeit erzielten Fortschritte auf dem Gebiet der decarboxylierenden Kreuzkupplung vorgestellt. Die nachfolgenden drei Unterkapitel beinhalten die Resultate zu den Carboxylat-dirigierten Arylierungen. Im anschließenden Abschnitt werden die erzielten Ergebnisse zusammengefasst und es erfolgt ein Ausblick. Der experimentelle Teil enthält die Spezifikationen der eingesetzten Messinstrumente sowie alle verwendeten Versuchsvorschriften und die Charakterisierungen der hergestellten Verbindungen. Dieses Kapitel wurde hauptsächlich auf Englisch verfasst, da es zum größten Teil aus dem Material der englischsprachigen „Supporting Information“ der Veröffentlichungen besteht. Im Anschluss daran folgen das Literaturverzeichnis und ein kurzer Lebenslauf.

Die Beiträge der einzelnen Autoren und Projektpartner werden vor den abgebildeten Publikationen beziehungsweise unmittelbar vor der Diskussion der Ergebnisse in den entsprechenden Unterkapiteln des Ergebnis- und Diskussionsteils beschrieben. Herr Prof. Dr. Lukas J. Gooßen unterstützte alle Arbeiten beratend.

3 Einleitung

Die Entwicklung nachhaltiger Methoden zur selektiven Darstellung komplexer Moleküle stellt eine Hauptdisziplin der modernen organischen Synthesechemie dar.^[1,2] In diesem Zusammenhang haben sich Übergangsmetall-katalysierte C–C- und C–Heteroatom-Bindungsknüpfungen als effizientes und vielseitig einsetzbares Synthesewerkzeug etabliert.^[3] Im Zuge der Implementierung von Nachhaltigkeitsaspekten, die sich an den Prinzipien der "Grünen Chemie" ausrichten, liegt dabei gegenwärtig ein Schwerpunkt auf der Erschließung abfallminimierter Verfahren ausgehend von ungiftigen und aus natürlichen Quellen verfügbaren Edukten.^[4–9] Vor diesem Hintergrund haben Carbonsäuren als Ausgangsstoffe für Übergangsmetall-katalysierte Kupplungsreaktion in den letzten Jahren an enormer Bedeutung gewonnen.^[10–12] Carbonsäuren sind gut lagerfähig und einfach handhabbar.^[10,12,13] Zudem sind sie in großer struktureller Vielfalt sowohl aus natürlichen Quellen als auch über zahlreiche etablierte Synthesemethoden zugänglich.^[13,14]

Auf die Darstellung von Carbonsäuren und deren Reaktivität in Übergangsmetall-katalysierten Kupplungsreaktion sowie auf die Vorteile, die sich aus deren Nutzung ergeben, wird nachfolgend näher eingegangen.

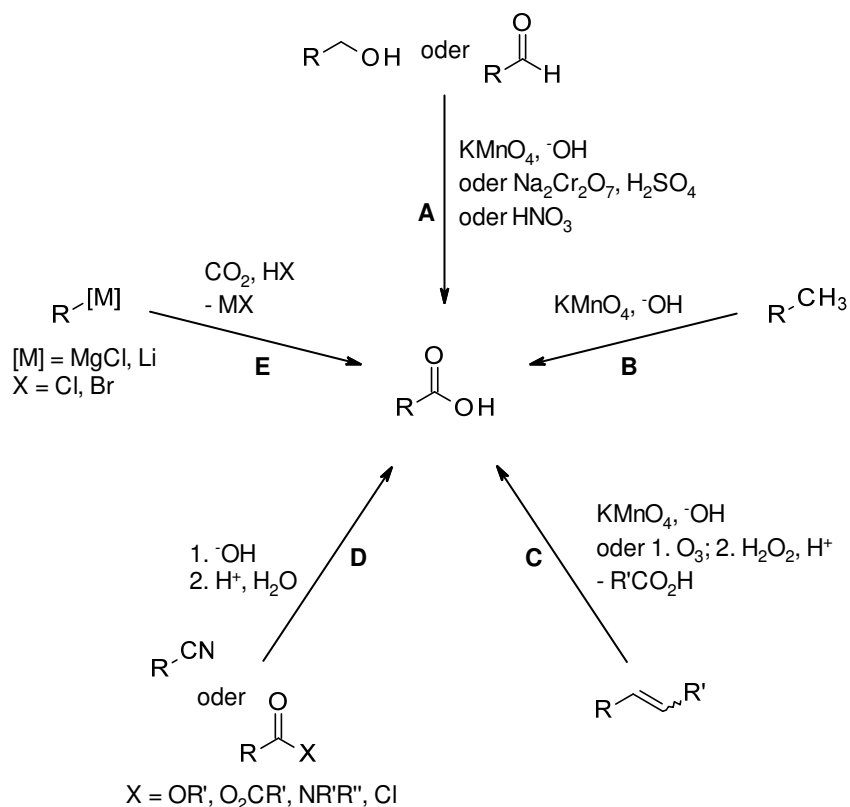
3.1 Darstellung und Reaktivität von Carbonsäuren

3.1.1 *Darstellung von Carbonsäuren*

Carbonsäuren können über eine Reihe bewährter Oxidationsreaktionen ausgehend von verschiedenen Verbindungsklassen dargestellt werden.^[13–15] So lassen sich primäre Alkohole oder Aldehyde in Gegenwart von beispielsweise Kaliumpermanganat im Basischen, Natriumdichromat im Sauren oder Salpetersäure in die entsprechenden Carbonsäuren überführen (Schema 1, Weg A).^[13,15] Sekundäre Alkohole und Ketone werden von Salpetersäure in Gegenwart von Vanadumpentoxid unter C–C-Bindungsspaltung oxidiert. Auf diese Weise lässt sich z. B. Adipinsäure aus Cyclohexanol darstellen.^[13,15] Auch aliphatische Seitenketten von Aromaten können mithilfe von Kaliumpermanganat oxidiert werden (Weg B)^[13] und Alkene reagieren unter oxidativer Spaltung zu Carbonsäuren (Weg C).^[13,15]

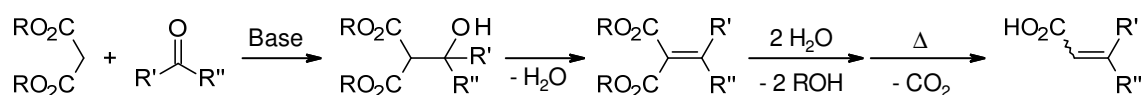
Weiterhin sind Carbonsäuren durch die Hydrolyse von Carbonsäurederivaten, wie z. B. Estern, Anhydriden oder Amidin, sowie von Nitrilen, welche über ein Säureamid als Zwischenstufe abläuft, zugänglich (Weg D).^[13,15]

Die Carboxylierung von metallorganischen Verbindungen, wie beispielsweise Grignard- oder Organolithiumverbindungen, mit CO_2 und anschließender Hydrolyse ermöglicht ebenfalls den Zugang zu Carbonsäuren (Weg E).^[13,15] Weiterhin lässt sich Natriumphenolat in einer elektrophilen Substitution zu Salicylsäure carboxylieren.^[15,16] Diese Reaktion ist unter dem Namen Kolbe-Schmitt-Synthese bekannt.



Schema 1: Ausgewählte traditionelle Methoden zur Darstellung von Carbonsäuren.

Ein Syntheseweg, der α, β -ungesättigte Carbonsäuren zugänglich macht, ist die Reaktion von Dialkylmalonaten mit Aldehyden oder Ketonen, die sogenannte Knoevenagel-Kondensation (Schema 2).^[13,15,17] In Gegenwart starker Basen greift das Malonat nukleophil am Carbonylkohlenstoff des Reaktionspartners an. Der resultierende β -Hydroxymalonsäurediester dehydratisiert zu einem Alkylidenmalonsäurediester, dessen Hydrolyse mit nachfolgender Decarboxylierung schließlich die α, β -ungesättigte Carbonsäure ergibt.^[15] Nach einem analogen Mechanismus reagiert Essigsäureanhydrid mit Arenaldehyden zu α, β -ungesättigten Carbonsäuren.^[15] Diese Variante ist unter dem Namen Perkin-Reaktion bekannt.^[18] Über beide Methoden lässt sich beispielsweise Zimtsäure aus Benzaldehyd und Malonsäurediethylester beziehungsweise Essigsäureanhydrid darstellen.^[15]



Schema 2: Synthese α,β -ungesättigter Carbonsäuren.

Auch für die großtechnische Darstellung von Carbonsäuren existiert eine Vielzahl an Verfahren. So sind über Oxidationsreaktionen mit Luftsauerstoff oder Carbonylierungsreaktionen wichtige Basischemikalien zugänglich:^[19,20]

Die bereits zuvor erwähnte Darstellung von Adipinsäure, welche überwiegend für die Produktion von Nylon verwendet wird, erfolgt im industriellen Maßstab ausgehend von Cyclohexan. Dieses wird in einer Flüssigphasenoxidation mit Luftsauerstoff bei 150–160 °C und 8–20 bar in Gegenwart eines Cobalt-Katalysators zu einem Gemisch aus Cyclohexanol und Cyclohexanon umgesetzt. Im Folgeschritt wird dieses Gemisch dann bei 75–80 °C und 1–4 bar durch Salpetersäure unter Verwendung von Vanadium(V)- oder Kupfer(II)-Katalysatoren zur Adipinsäure oxidiert.^[19]

Terephthalsäure lässt sich durch Oxidation von *para*-Xylol mit Luftsauerstoff darstellen. Dies erfolgt bei 175–225 °C und 12–30 bar in Essigsäure unter Verwendung eines Cobalt-Katalysators in Kombination mit Mangan- und Bromidionen.^[19,21] In ähnlichen Prozessen sind ebenso Benzoessäure und Isophthalsäure aus Toluol beziehungsweise *meta*-Xylol zugänglich.^[19]

Acrylsäure wird in einem zweistufigen Prozess durch Oxidation von Propen dargestellt. Letzteres wird zunächst in Gegenwart eines Bismuthmolybdat-Katalysators zu Acrolein und dann mit Hilfe eines Bismuthvanadat-basierten Katalysators weiter zu Acrylsäure umgesetzt.^[19]

Die oxidative Fermentation von Zuckern über Ethanol zu Essigsäure ist ein wichtiges Herstellungsverfahren in der Nahrungsmittelindustrie.^[19,22] In früheren Zeiten waren zudem die Luftoxidation von Butan oder Naphtha sowie von Acetaldehyd, welches durch die Kupfer/Palladium-katalysierte Oxidation von Ethen mit Luftsauerstoff im Wacker-Prozess leicht zugänglich ist, gängige Methoden zur Darstellung von Essigsäure.^[19] Gegenwärtig stellt die Carbonylierung von Methanol die bedeutendste Herstellungsmethode von Essigsäure dar. Dies erfolgt beispielsweise im Monsanto-Prozess in Gegenwart eines Rhodium-Katalysators bei 150–200 °C und 30–60 bar in Essigsäure mit einem Iodid-Cokatalysator.^[19] Im verwandten Cativa-Prozess werden anstelle des Rhodium-Katalysators ein Iridium-Katalysator und ein Ruthenium-Promotor eingesetzt.^[19,23] Dieses Verfahren kann bei einer deutlich geringeren Wasserkonzentration durchgeführt werden, was die anschließende Produktaufreinigung

erleichtert. Zudem zeigt der Katalysator eine höhere Stabilität sowie eine verbesserte Selektivität.^[19]

Weiterhin werden Carbonsäuren großtechnisch über die Hydroxycarbonylierung von Alkenen dargestellt.^[19] Auf diese Weise ist z. B. Propionsäure ausgehend von Ethen, Kohlenstoffmonoxid und Wasser unter Verwendung eines Nickel-Katalysators bei 250–320 °C und 100–300 bar zugänglich.

Von industrieller Bedeutung sind neben petrochemischen Verfahren weiterhin solche, bei denen Carbonsäuren aus nachwachsenden Rohstoffen gewonnen werden.^[24] So sind durch Hydrolyse der Triglyceride pflanzlicher oder tierischer Öle und Fette gesättigte und ungesättigte Fettsäuren unterschiedlicher Kettenlänge zugänglich.^[25,26]

3.1.2 Die Reaktivität der Carboxygruppe

Kennzeichnend für die Verbindungsklasse der Carbonsäuren ist die Carboxygruppe.^[13,15] Ihre Reaktivität wird durch die Carbonylgruppe und den daran gebundenen sauren Hydroxysubstituenten bestimmt.^[13] Unter basischen Bedingungen wird die Carboxygruppe deprotoniert und es bildet sich ein resonanzstabilisiertes Carboxylat. Die Protonierung des Carbonylsauerstoffatoms erfolgt unter sauren Bedingungen. Daran anschließend kann ein nukleophiler Angriff am Carbonylkohlenstoff mit Substitution der Hydroxygruppe erfolgen. Diese Reaktivität wird beispielsweise bei der Veresterung genutzt. Ebenso können aktivierte Derivate der Carbonsäure, z. B. Anhydride, Säurehalogenide oder Ester, über einen Addition-Eliminierungs-Mechanismus in einer nukleophilen Substitution umgesetzt werden, dies sowohl unter sauren als auch unter basischen Bedingungen.^[13]

3.2 Carbonsäuren als Substrate für Übergangsmetall-katalysierte Kupplungen

3.2.1 Übergangsmetall-vermittelte Aktivierungsmodi von Carbonsäuren

Der Nutzung von Carbonsäuren als Substrate in Übergangsmetall-katalysierten Transformationen liegen verschiedene Aktivierungsmodi zugrunde. Diese werden im Folgenden näher erläutert (Schema 3).

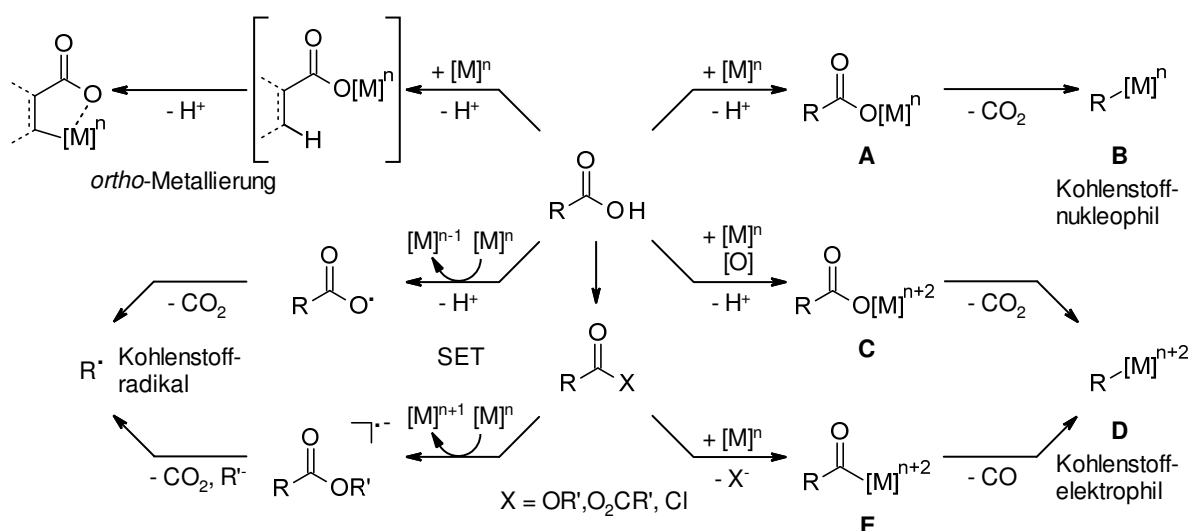
Wird ausgehend von der Säure eine Metallcarboxylatspezies gebildet, so kann diese selbst mit anderen Reaktionspartnern Kupplungsreaktionen eingehen.^[10] Schließt sich an die redox-neutrale Bildung der Spezies **A** eine Decarboxylierung an, so entsteht ein Metallorganyl **B**, welches analog zu präformierten Organometallverbindungen als Kohlenstoffnukleophil genutzt werden kann.^[10,11,27]

Erfolgt die zuvor beschriebene Aktivierung unter oxidativen Bedingungen, so sind Metallorganyle **D** höherer Oxidationsstufe zugänglich, die formal oxidativen Additionsprodukten von Kohlenstoffelektrophilen, wie z. B. Arylhalogeniden, entsprechen und analog in Kupplungsreaktionen genutzt werden können.^[11,27]

Alternativ ist Spezies **D** unter redox-neutralen Bedingungen ausgehend von Carbonsäurederivaten durch Insertion in die C(Acyl)–X-Bindung mit anschließender Decarbonylierung der Acyl-Metall-Spezies **E** zugänglich.^[10,27] Letztere kann außerdem in Acylierungsreaktionen genutzt werden.^[10]

Ein weiterer Aktivierungsmodus ist die Carboxylat-dirigierte *ortho*-Metallierung, an welche sich eine Funktionalisierung der einstigen C–H-Bindung anschließen kann. Die Carboxygruppe steht anschließend für weitere Funktionalisierungen zur Verfügung oder kann über eine Protodecarboxylierung entfernt werden.^[28–33]

Insbesondere aliphatische Carbonsäuren beziehungsweise deren Aktivester (X = OR', z. B. basierend auf NHPI-Derivaten) können außerdem als Quelle für Radikale dienen, die sich dann in Übergangsmetall-katalysierten Kupplungen weiter mit nukleophilen oder elektrophilen Reaktionspartnern umsetzen lassen.^[11,34–36] Dabei erfolgt die Aktivierung im Gegensatz zu den anderen Modi indirekt über einen Einelektronentransfer-Schritt zwischen Substrat und einem geeigneten Katalysatormetall. Eine nachfolgende radikalische Decarboxylierung liefert schließlich das Kohlenstoffradikal.



Schema 3: Übergangsmetall-vermittelte Aktivierung von Carbonsäuren.

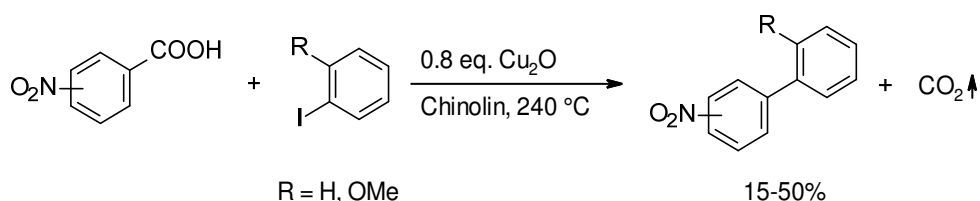
Basierend auf den beschriebenen Aktivierungswegen wurden zahlreiche katalytische Transformationen entwickelt. Dazu zählen unter anderem Protodecarboxylierungen,

decarboxylierende beziehungsweise decarbonylierende Biarylsynthesen und Varianten der Heck-Reaktion sowie decarboxylierende C–Heteroatom-Bindungsknüpfungen und Allylierungen.^[10–12,27,37,38] Zudem sind über die nicht-decarboxylierenden oder decarbonylierenden Routen beispielsweise Ester oder Arylketone^[10] zugänglich und auch auf dem Gebiet der Carboxylat-dirigierten *ortho*-C–H-Funktionalisierung wurden verschiedenste Methoden zur C–C- und C–Heteroatom-Bindungsknüpfung erschlossen.^[33,39–41] Aktuell erfahren die auf der radikalischen Decarboxylierung basierenden Kupplungen große Aufmerksamkeit; im besonderen Maße solche, die sich das Konzept der Photo-Redox-Katalyse zu Nutze machen.^[42] Auch in diesem Zusammenhang wurde eine Vielzahl an Protokollen zur C–C- und C–Heteroatom-Bindungsknüpfung entwickelt.^[34,35,43–49]

Da sich die vorliegende Arbeit mit redox-neutralen decarboxylierenden Kreuzkupplungen und Carboxylat-dirigierten *ortho*-C–H-Funktionalisierungen von Benzoesäuren beschäftigt, werden diese Reaktionskonzepte nachfolgend näher diskutiert. Schwerpunktmäßig erfolgt dies für Arylierungen zur Darstellung von Biarylen, einem Strukturmotiv, welches in Arzneistoffen, Agrochemikalien oder Funktionsmaterialien weit verbreitet ist.^[50–58]

3.2.2 Redox-neutrale decarboxylierende Kreuzkupplungen

Bereits im Jahre 1966 beschrieb Nilsson die erste Kupfer-vermittelte Synthese unsymmetrischer Biaryle ausgehend von aktivierten aromatischen Carbonsäuren und Aryliodiden (Schema 4).^[59,60]

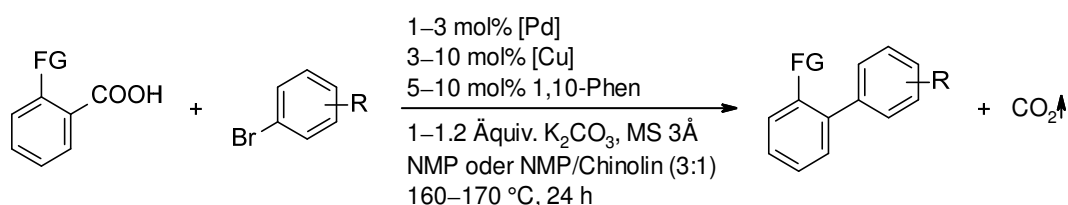


Schema 4: Kupfer-vermittelte decarboxylierende Kreuzkupplung.

Diese Entdeckung beruhte auf der Annahme, dass die Kupfer-vermittelte Ullmann-Reaktion^[61] sowie die Kupfer-vermittelte Protodecarboxylierung aromatischer Carbonsäuren^[62] über die gleichen Intermediate ablaufen.^[59] Zwar wurde mit diesen Pionierarbeiten die generelle Durchführbarkeit einer decarboxylierenden Kreuzkupplung bereits demonstriert, doch konnten nur geringe Ausbeuten erreicht werden und es waren zudem hohe Kupfermengen und harsche Reaktionsbedingung notwendig. Daher erlangte dieses Verfahren synthetisch keine Bedeutung.^[10,11]

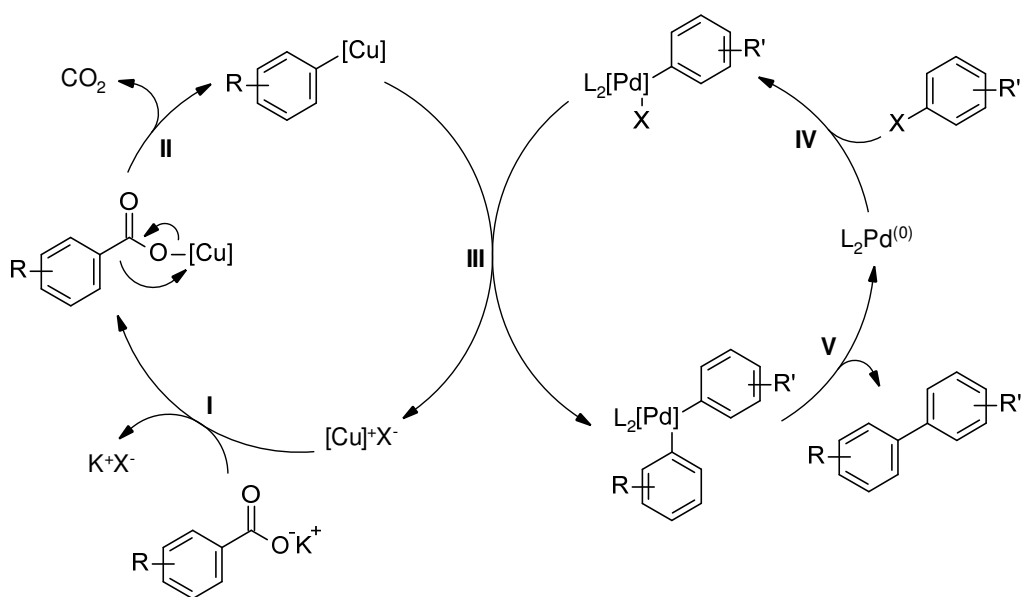
3.2.2.1 Kupfer/Palladium-katalysierte decarboxylierende Kreuzkupplungen

Erst 40 Jahre später gelang es Gooßen und Mitarbeitern, ein präparativ nützliches Protokoll für die decarboxylierende Kreuzkupplung aromatischer Carbonsäuren zu entwickeln, dies durch die Kombination eines Kupfer-basierten Decarboxylierungskatalysators mit einem Palladium-basierten Kreuzkupplungskatalysator. In Gegenwart von 1.5 Äquiv. CuCO_3 , 2 mol% $\text{Pd}(\text{acac})_2$, 6 mol% $\text{P}(i\text{-Pr})\text{Ph}_2$, 1.5 Äquiv. KF und Molekularsieb konnten vorwiegend *ortho*-substituierte Carbonsäuren mit diversen Arylbromiden in NMP bei 120 °C zu den entsprechenden Biarylen umgesetzt werden.^[63] Ein System, welches sowohl katalytisch in Kupfer (CuI oder CuBr) als auch in Palladium ($\text{Pd}(\text{acac})_2$ oder PdBr_2) ist, konnte durch Zusatz von 1,10-Phenanthrolin als Ligand realisiert werden und ermöglichte die Kupplung eines noch breiteren Substratspektrums (Schema 5).^[63,64]



Schema 5: Cu/Pd-Katalysierte decarboxylierende Kreuzkupplung.

Der angenommene Mechanismus dieser Reaktion ist in Schema 6 dargestellt.^[63,64] Im ersten Schritt erfolgt die Salzmetathese (**I**) zwischen dem Kaliumbenzoat und dem Kupfer-Katalysator. Eine anschließende Decarboxylierung (**II**) des Kupfercarboxylats führt zur Bildung einer Arylkupferspezies. In einer Transmetallierung (**III**) überträgt diese schließlich ihren organischen Rest auf den Palladiumkomplex, der aus der oxidativen Addition (**IV**) des Arylhalogenids an den Palladium-Katalysator hervorgeht und es kommt zur Regenerierung des Kupfer-Katalysators. Im letzten Schritt erfolgt die reduktive Eliminierung (**V**) des Biaryls, wodurch auch der zweite Zyklus geschlossen wird.

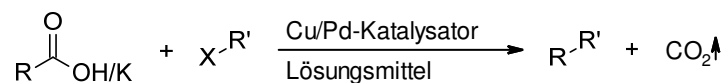


Schema 6: Mechanismus der Cu/Pd-katalysierten decarboxylierenden Kreuzkupplung.

Zusammenfassend eröffnet dieses Reaktionsprotokoll eine attraktive Alternative zu klassischen Kreuzkupplungen präformierter Organometallverbindungen.^[3] Letztere sind kostspielig, teilweise toxisch und müssen in vorangestellten Syntheseschritten aufwendig dargestellt werden.^[3,64–66] Zudem fallen bei deren Verwendung stöchiometrische Mengen an Metallsalzen an, die im Anschluss entsorgt werden müssen.^[5] Im Gegensatz dazu entsteht bei der decarboxylierenden Kreuzkupplung, der die *in situ*-Generierung der Metallorganyle zugrunde liegt, lediglich CO₂ als Nebenprodukt.^[63,64]

Basierend auf den beschriebenen Arbeiten wurde dieses Reaktionskonzept in den darauffolgenden Jahren stetig weiterentwickelt (Schema 7). So gelang es, kostengünstigere aber auch unreaktivere Arylchloride als Kupplungspartner durch eine Katalysatorkombination aus CuI, PdI₂, 1,10-Phenanthrolin und dem elektronenreichen, sterisch anspruchsvollen Phosphanliganden JohnPhos zugänglich zu machen.^[67] Die Erweiterung des Substratspektrums auf nicht-*ortho*-substituierte Benzoessäuren konnte mit einem Katalysatorsystem aus Cu₂O, PdI₂, 1,10-Phenanthrolin und Tol-BINAP oder P(*p*-Tol)₃ und Aryltriflaten als elektrophiler Kupplungspartner realisiert werden.^[2,68] Es wurde angenommen, dass die im Verlauf der Reaktion freigesetzten schwach koordinierenden Triflationen verglichen mit Halogeniden deutlich weniger mit den Benzoaten um die Koordination an den Kupfer-Katalysator konkurrieren, wodurch die Salzmetathese zur Bildung des Kupferbenzoats für nicht-*ortho*-substituierte Substrate erleichtert wird.^[2] Auch die kostengünstigeren Aryltosylate konnten durch weitere Optimierung des Palladium-Katalysators unter Verwendung des elektronenreichen, sterisch anspruchsvollen Phosphanliganden XPhos für die

decarboxylierende Kreuzkupplung zugänglich gemacht werden.^[69] Daneben konnten auch Kupplungen von unreaktiven Arylmesylaten durch den Einsatz maßgeschneiderter Imidazolylphosphane realisiert werden.^[70]



R = (Het)Ar, Alkenyl, Acyl; R' = (Het)Ar, Alkenyl; X = I, Br, Cl, OTf, OTs, OMs

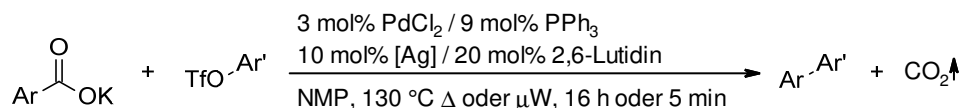
Schema 7: Anwendungsbreite Cu/Pd-katalysierter decarboxylierender Kreuzkupplungen.

Die Praktikabilität Cu/Pd-katalysierter decarboxylierender Kreuzkupplungen konnte durch die Synthese von Intermediaten für die Darstellung der Blutdrucksenker Valsartan^[71] und Telmisartan^[72] sowie Biarylsynthesen im Multigramm-Maßstab demonstriert werden.^[73] Daneben wurde das Konzept auch für die Darstellung von Arylketonen und Iminen ausgehend von α -Oxosäuren^[74,75] sowie Arylalkenen ausgehend von Alkenylhalogeniden oder -mesylaten genutzt.^[70,76] Weiterhin konnten auch intramolekulare Varianten dieser Reaktion realisiert werden.^[77] Neben einer konventionellen Reaktionsführung existieren zudem Verfahren im Durchflussreaktor oder in der Labormikrowelle, die deutlich verringerte Reaktionszeiten ermöglichen.^[78,79]

3.2.2.2 Silber/Palladium-katalysierte decarboxylierende Kreuzkupplungen

Bereits im ursprünglichen Protokoll zur decarboxylierenden Kreuzkupplung konnte demonstriert werden, dass sich anstelle von CuCO₃ auch stöchiometrische Mengen an Ag₂CO₃ mit einem Palladium-Katalysator kombinieren lassen.^[64] Nachfolgend wurde von Becht *et al.* ein Katalysatorsystem bestehend aus PdCl₂ und AsPh₃ oder DPEPhos in Gegenwart von 3 Äquiv. Ag₂CO₃ zur Kupplung von Aryliodiden beziehungsweise Aryliodoniumsalzen mit *ortho*-substituierten Benzoesäuren entwickelt.^[80,81] Ein ähnliches Protokoll zur Kupplung von Aryliodiden mit Benzoesäuren oder Zimtsäuren wurde später von Wu und Mitarbeitern beschrieben.^[82,83] Nachteilig bei diesen Verfahren sind zum einen die hohen Palladium-Katalysatorbeladungen (10–30 mol%) sowie die Notwendigkeit stöchiometrischer Silbermengen. Letzteres ist der Bildung stabiler Silberhalogenide im Verlauf der Reaktion zuzuschreiben, welche aufgrund ihrer Stabilität nicht wieder in den Katalysezyklus eintreten können.^[12]

Goßen und Mitarbeitern gelang es, eine Ag/Pd-katalysierte Kreuzkupplung von Aryltriflaten mit *ortho*-Nitrobenzoaten und heteroaromatischen Carboxylaten zu entwickeln (Schema 8).^[84]

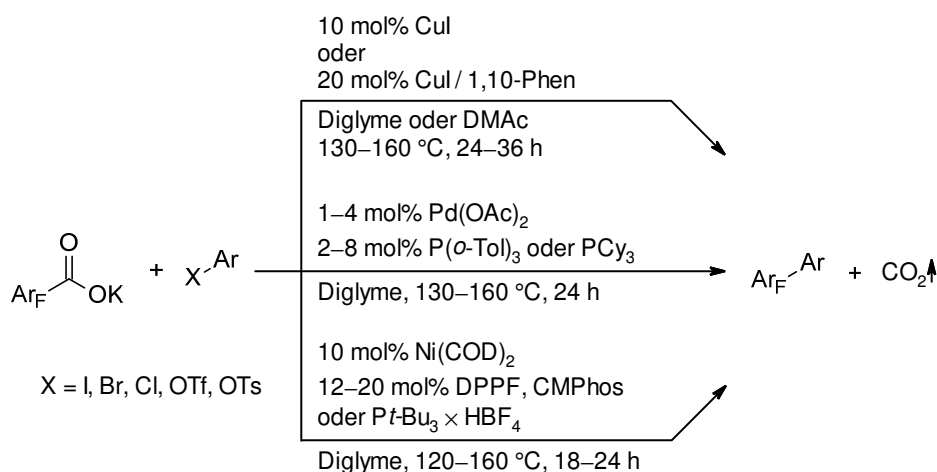


Schema 8: Ag/Pd-Katalysierte decarboxylierende Kreuzkupplung.

Diesen Arbeiten gingen ausführliche DFT-Rechnungen und experimentelle Studien zur Silber-katalysierten Protodecarboxylierung voraus.^[85,86] Entscheidend ist, dass mit diesem Katalysatorsystem eine Reaktionsführung bei nur 130 °C möglich wurde, während für Cu/Pd-basierte Katalysatorsysteme Reaktionstemperaturen von meist 170–190 °C notwendig sind.^[84]

3.2.2.3 Monometallische Katalysatorsysteme

Decarboxylierende Biarylsynthesen, die mit monometallischen Katalysatorsystemen durchführbar sind, existieren ausschließlich für polyfluorierte Benzoate. In Gegenwart von Kupfer-,^[87] Palladium-^[88] oder Nickel-Katalysatoren^[89] lassen sich letztere mit Arylhalogeniden oder -sulfonaten zu den entsprechenden Biarylen umsetzen (Schema 9).

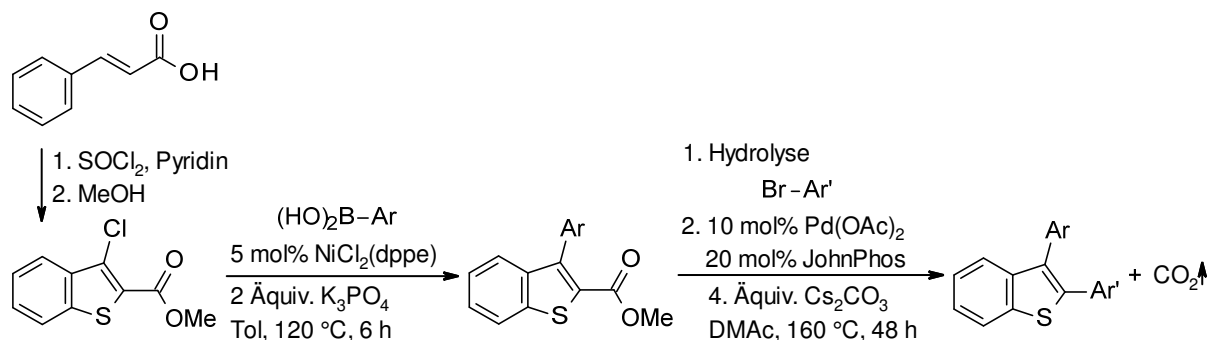


Schema 9: Decarboxylierende Kreuzkupplung mit monometallischen Katalysatorsystemen.

Ferner wurden monometallisch-katalysierte decarboxylierende Kupplungen von beispielsweise Zimtsäuren, Alkyloxalaten oder Alkynylcarbonsäuren beschrieben.^[90–93]

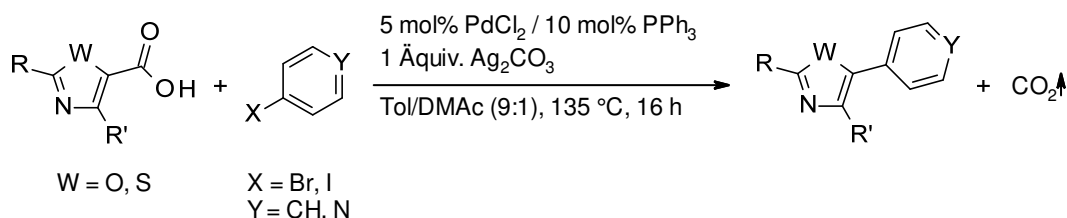
3.2.2.4 Decarboxylierende Kreuzkupplungen mit heteroaromatischen Carbonsäuren

Die Palladium-katalysierte decarboxylierende Kreuzkupplung fünfgliedriger heteroaromatischer Carbonsäuren mit Arylhalogeniden wurde von Forgione und Bilodeau *et al.* beschrieben (Schema 10).^[94,95] Zwar ist der Mechanismus dieser Reaktion noch nicht vollends geklärt, doch wird angenommen, dass dieser über eine Carbopalladierung mit anschließender Decarboxylierung und C–C-Bindungsknüpfung verläuft. Im Gegensatz dazu wurde für eine



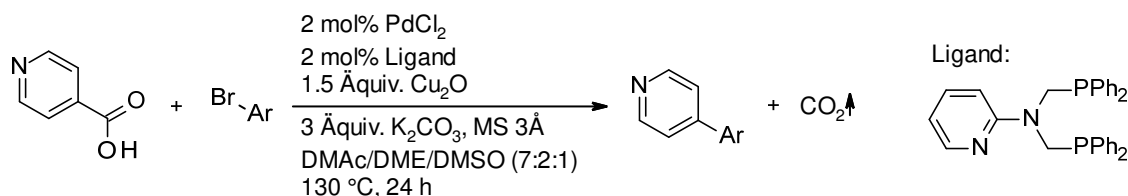
Schema 12: Sequenzielle Arylierung von 3-Chloro-2-methoxycarbonylbenzo[b]thiophen.

Weiterhin beschrieben Zhang und Greaney ein Palladium-basiertes Katalysatorsystem, welches in Gegenwart stöchiometrischer Mengen Ag_2CO_3 die Kupplung von Thiazol- und Oxazol-5-carbonsäuren mit Aryl- und Heteroaryl bromiden sowie -iodiden ermöglicht (Schema 13).^[100]



Schema 13: Decarboxylierende Kreuzkupplung von Thiazol- und Oxazol-5-carbonsäuren.

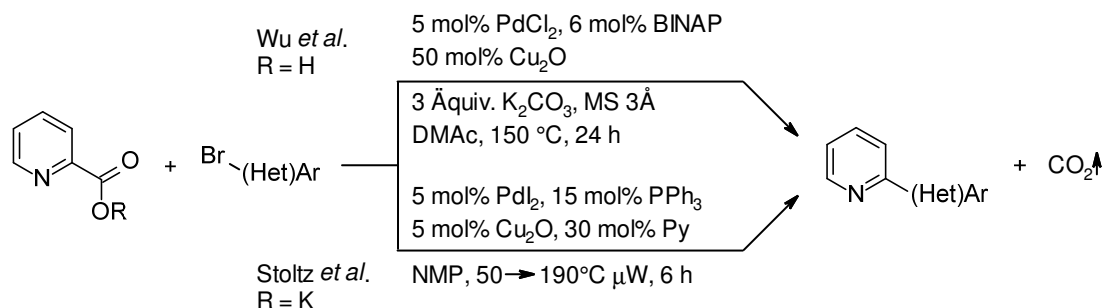
Neben decarboxylierenden Kreuzkupplungen von fünfgliedrigen Heteroarylcarbonsäuren wurden auch solche von sechsgliedrigen Derivaten, insbesondere von Pyridincarbonsäuren, entwickelt. Kupplungen von Pyridin-4-carbonsäuren mit Arylbromiden wurden von He *et al.* beschrieben (Schema 14).^[101] Das Katalysatorsystem basiert auf einer Kombination aus PdCl_2 und einem mehrzähligen *P,N*-Liganden. Nachteilig an diesem Verfahren ist der Einsatz überstöchiometrischer Kupfermengen. Dahingegen können Pyridin-3-carbonsäuren mit klassischen Cu/Pd-Katalysatorsystemen in moderaten Ausbeuten umgesetzt werden.^[68,69]



Schema 14: Decarboxylierende Kreuzkupplung von Pyridin-4-carbonsäuren.

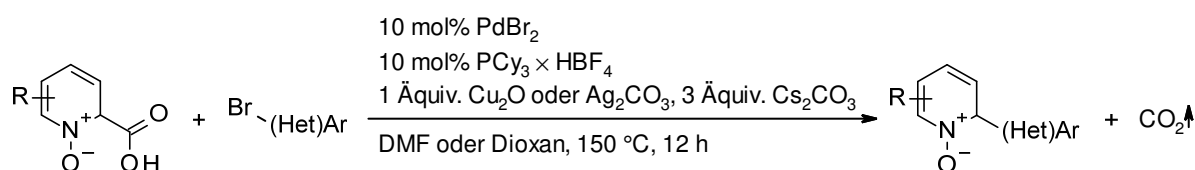
Decarboxylierende Kreuzkupplungen von Pyridin-2-carbonsäuren mit Aryl- und Heteroaryl bromiden wurden unabhängig voneinander von den Gruppen um Wu und Stoltz beschrieben (Schema 15).^[102,103] Diese Kupplungen sind besonders herausfordernd, da die intermediär gebildeten Heteroaryl-Metall-Spezies allgemein sehr instabil sind und zu

Protodemetallierung neigen.^[104] Die korrespondierenden Biaryle konnten in moderaten Ausbeuten erhalten werden. Während im Protokoll von Wu und Mitarbeitern relativ hohe Katalysatorbeladungen verwendet werden,^[102] sind im Verfahren nach Stoltz und Mitarbeitern vergleichsweise hohe Reaktionstemperaturen notwendig.^[103]



Schema 15: Decarboxylierende Kreuzkupplung von Pyridin-2-carbonsäuren.

Die Erschließung einer Palladium-katalysierten decarboxylierenden Kreuzkupplung der Chinolin- und der Pyridin-2-carbonsäure-*N*-oxide erfolgte durch Hoarau und Mitarbeiter (Schema 16).^[105]



Schema 16: Decarboxylierende Kreuzkupplung von Pyridin-2-carbonsäure-*N*-oxiden.

Die Reaktion erfolgt in Gegenwart substöchiometrischer bis stöchiometrischer Mengen Ag₂CO₃ oder Cu₂O. Insbesondere im Fall des Cu/Pd-basierten Systems ist ein Mechanismus anzunehmen, der über eine Protodecarboxylierung mit nachfolgender C–H-Arylierung erfolgt.^[105]

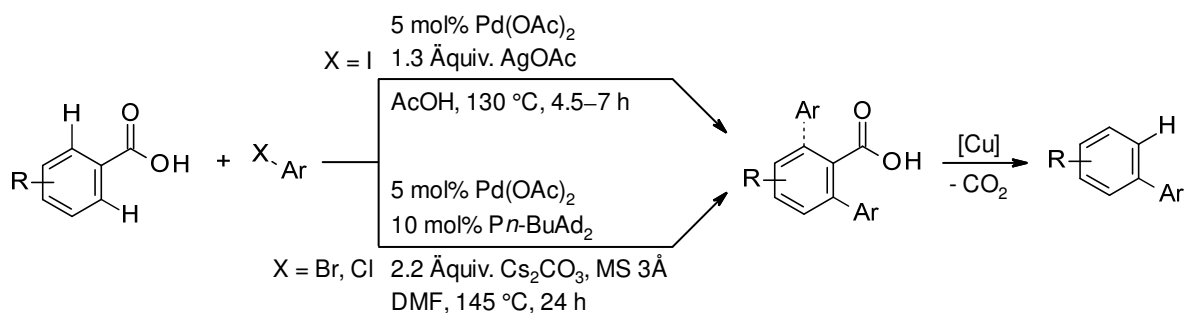
3.2.3 Carboxylat-dirigierte *ortho*-C–H-Funktionalisierungen

Übergangsmetall-katalysierte dirigierte C–H-Funktionalisierungen haben sich in den vergangenen Jahren zu einer wertvollen Methode zur selektiven C–C- und C–Heteroatom-Bindungsknüpfung etabliert.^[106–112] Insbesondere die Funktionalisierung aromatischer C–H-Bindungen kann durch eine Vielzahl dirigierender Gruppen, beispielsweise Pyridine, Amide, Anilide, Oxazoline, Imine oder Ketone, spezifisch in *ortho*-,^[106–112] aber auch in *meta*- und *para*-Position gelenkt werden.^[113–116] Ein Nachteil dieser Strategie ist, dass die dirigierende Gruppe meist vor der eigentlichen Reaktion in das entsprechende Substrat eingeführt werden muss, was mit einem zusätzlichen Synthesaufwand einhergeht.^[33] Weiterhin lassen sich viele

dirigierende Gruppen nur schwer nach der C–H-Funktionalisierung wieder entfernen.^[117–119] Die Verwendung von Carbonsäuren als dirigierende Gruppen bietet hingegen entscheidende Vorteile, die sich zum einen auf der breiten Verfügbarkeit dieser Substrate und zum anderen auf der Vielzahl an etablierten Funktionalisierungsmöglichkeiten der Carboxygruppe gründen.^[33] So könnte letztere bei Bedarf beispielsweise im Anschluss an die C–H-Funktionalisierung über eine Protodecarboxylierung entfernt oder in weiteren Kupplungsreaktionen umgesetzt werden.^[11,12] Zwar ist die Verwendung dieser dirigierenden Gruppe aufgrund ihrer geringen Koordinationsfähigkeit mit enormen Herausforderungen verbunden, doch konnte der große synthetische Nutzen dieses Reaktionskonzepts bereits anhand einer Vielzahl an *ortho*-C–H-Funktionalisierungen, insbesondere aromatischer C–H-Bindungen, demonstriert werden.^[32,33,39,120,121]

3.2.3.1 Redox-neutrale *ortho*-Arylierungen von Benzoesäuren

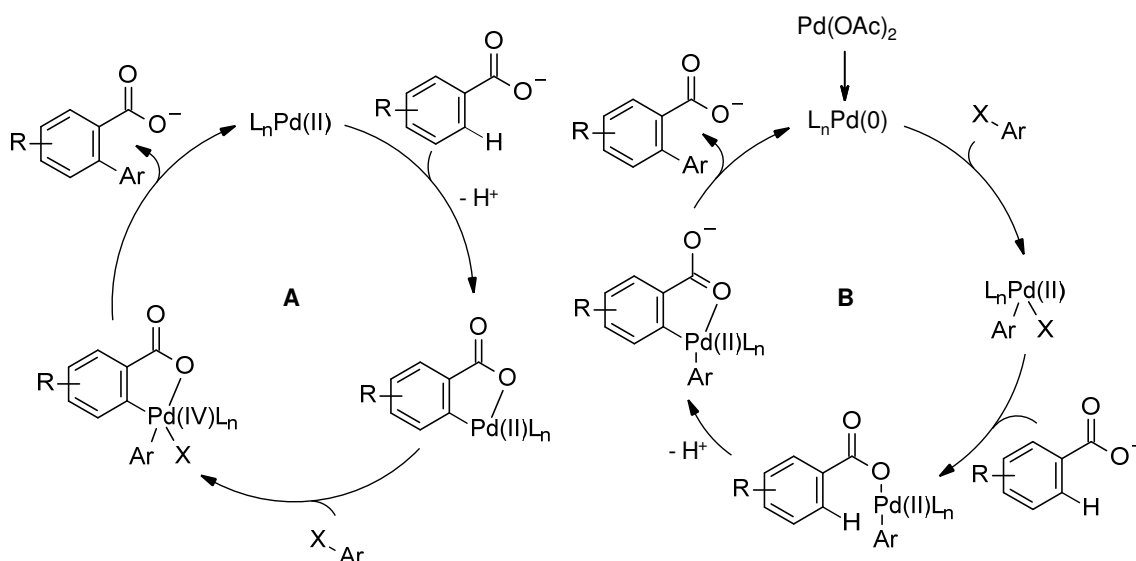
Die erste Carboxylat-dirigierte *ortho*-Arylierung wurde im Jahre 2007 von Daugulis und Mitarbeitern beschrieben.^[28] In Gegenwart eines Palladium-Katalysators und stöchiometrischer Mengen AgOAc als Base und Halogenidionenfänger lassen sich diverse Benzoesäuren mit Aryliodiden in die korrespondierenden Biarylcarbonsäuren überführen. Eine zweite Variante unter Einsatz eines Palladium/Phosphan-Katalysatorsystems ermöglichte weiterhin die Verwendung von Arylbromiden und -chloriden in dieser Transformation (Schema 17).



Schema 17: Palladium-katalysierte *ortho*-Arylierung von Benzoesäuren.

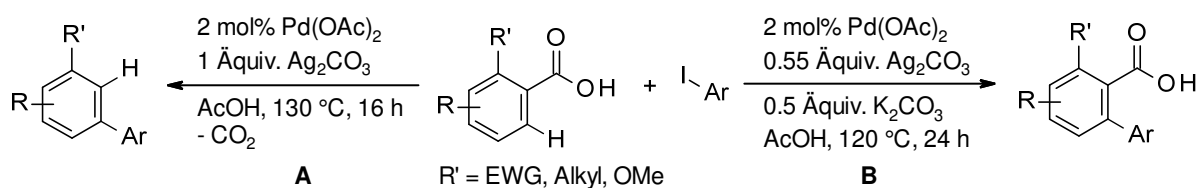
Während im Fall von *meta*-substituierten oder *meta,para*-disubstituierten Benzoesäuren meist ausschließlich die monoarylierten Produkte gebildet werden, erhält man im Fall von *para*- oder unsubstituierten Benzoesäuren die diarylierten Produkte. Dass sich die dirigierende Carboxylatgruppe bei Bedarf rückstandslos entfernen lässt, demonstrierten die Autoren exemplarisch anhand der Kupfer-katalysierten Protodecarboxylierung einer Biarylcarbonsäure.^[28]

Für die Reaktionsvariante unter Verwendung von Aryliodiden wird ein Pd(II)/Pd(IV)-Mechanismus angenommen (Schema 18, **A**). Im Fall der Arylchloride hingegen schlagen die Autoren einen Pd(0)/Pd(II)-Mechanismus vor (Schema 18, **B**).^[28]



Schema 18: Vorgeschlagene Mechanismen für die Carboxylat-dirigierte *ortho*-Arylierung.

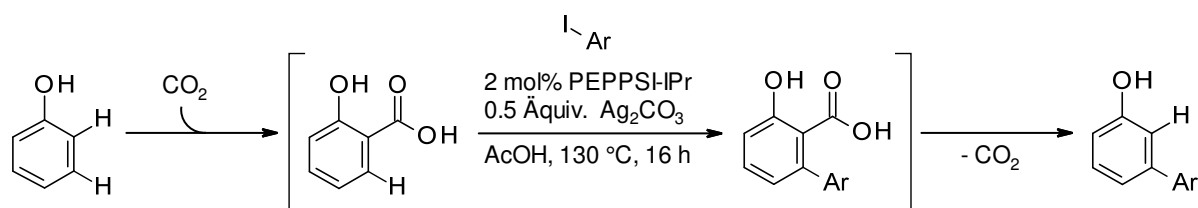
Eine Palladium-katalysierte *ortho*-Arylierung von Benzoesäuren mit einer im Reaktionsverlauf stattfindenden Protodecarboxylierung wurde von Larrosa und Mitarbeitern beschrieben (Schema 19, **A**).^[122] Auf diese Weise lassen sich selektiv *meta*-arylierte Aromaten darstellen. Mechanistische Studien weisen darauf hin, dass der Palladium-Katalysator nicht nur für die eigentliche *ortho*-Funktionalisierung verantwortlich ist, sondern auch die nachfolgende Decarboxylierung, die durch sterische Faktoren begünstigt wird, vermittelt.



Schema 19: *ortho*-Arylierung mit nachfolgender Protodecarboxylierung **A** und Variante ohne Protodecarboxylierung **B**.

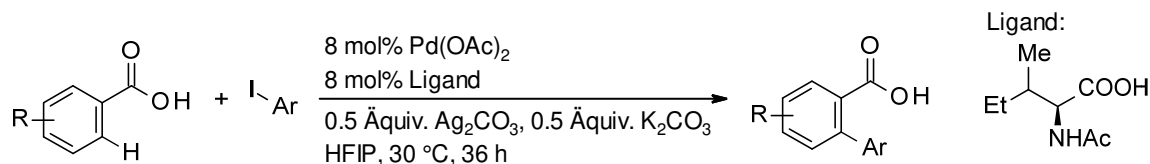
Die selbe Gruppe beschrieb außerdem ein Verfahren, bei dem die Protodecarboxylierung der *ortho,ortho*-disubstituierten Benzoesäuren unterdrückt werden kann (Schema 19, **B**).^[123] Verglichen mit dem zuvor beschriebenen System, werden in diesem Fall nur substöchiometrische Mengen des Halogenidionenfängers Ag_2CO_3 verwendet. Entscheidend ist hingegen der Zusatz von K_2CO_3 , welches einen Ligandenaustausch mit dem intermediären Palladiumbenzoat ermöglicht und so die Decarboxylierung verhindert.

Eine Strategie zur Darstellung *meta*-substituierter Phenole ausgehend von Salicylsäure oder Salicylaldehyd, welcher durch Oxidation zunächst *in situ* in die Säure überführt wird, wurde ebenfalls von der Gruppe um Larrosa beschrieben.^[124,125] Interessanterweise lassen sich die Produkte auch ausgehend von Phenol darstellen, wobei dies über eine Sequenz aus Carboxylierung mit nachfolgender *ortho*-Arylierung und Protodecarboxylierung in einem Eintopf-Verfahren erfolgt (Schema 20).^[126] Bei dieser Reaktionsvariante fungiert die Carboxylatgruppe als eine transiente dirigierende Gruppe, die *in situ* eingeführt und im Anschluss an die Arylierung wieder entfernt wird.



Schema 20: *meta*-Selektive Arylierung von Phenolen.

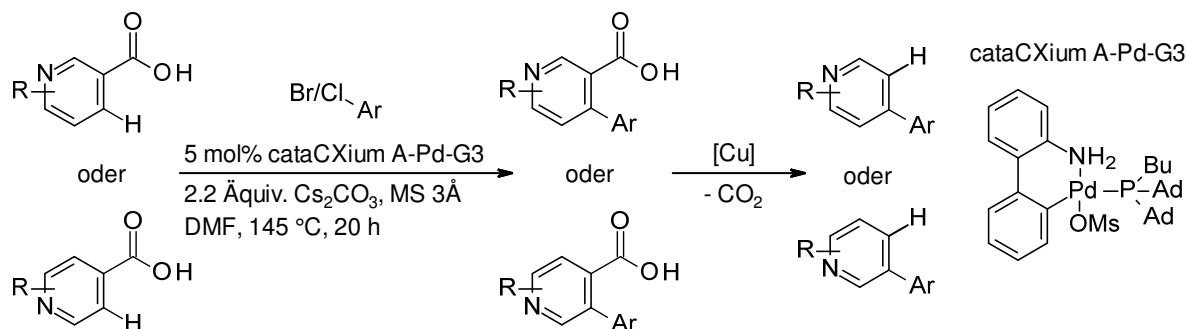
Eine monoselektive *ortho*-Arylierung elektronenarmer Benzoessäuren mit Aryliodiden wurde weiterhin von Su und Mitarbeitern beschrieben (Schema 21).^[127] Dabei ermöglicht insbesondere die Verwendung von Hexafluorisopropanol als Lösungsmittel sowie eines *N*-geschützten Aminosäureliganden eine Reaktionsführung unter besonders milden Bedingungen.



Schema 21: *ortho*-Arylierung in Gegenwart eines Aminosäureliganden bei 30 °C.

Weiterhin gelang es, ein Katalysatorsystem für die Kupplung mit Aryliodiden zu entwickeln, bei dem auf den Einsatz von Silbersalzen als Halogenidionenfänger verzichtet werden kann.^[128] In diesen Studien konnte Tetramethylammoniumchlorid als kostengünstige und umweltfreundlichere Alternative identifiziert werden, die in Kombination mit Pd(OAc)₂ und KOAc in Essigsäure die *ortho*-Arylierung von Benzoessäuren ermöglicht. Eine weitere silbersalzfreie Methode zur *ortho*-Arylierung von Benzoessäuren wurde von Zhou und Mitarbeitern beschrieben.^[129] Dabei dienen Diaryliodoniumsalze als Kupplungspartner in der Palladium-katalysierten Reaktion unter Verwendung von Wasser als Reaktionsmedium.

Erst kürzlich beschrieben Larrosa und Mitarbeiter die *ortho*-Arylierung von Picolin-3- und -4-carbonsäuren (Schema 22).^[130]

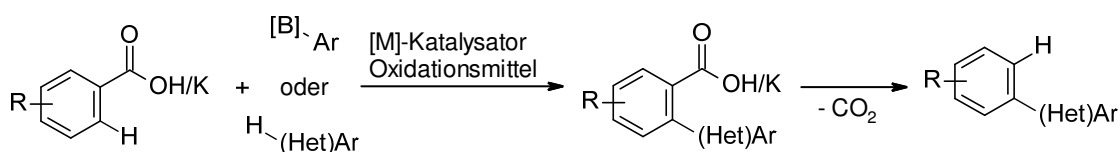


Schema 22: *ortho*-Arylierung von Picolin-3- und -4-carbonsäuren.

In Gegenwart eines Buchwald-Katalysators der dritten Generation lassen sich diese aufgrund des deaktivierenden Effekts des sp^2 -Stickstoffs anspruchsvollen Substrate mit Arylbromiden und -chloriden zu den entsprechenden Biarylcarbonsäuren umsetzen. Weiterhin lässt sich dieses Protokoll mit einer anschließenden Kupfer-vermittelten Protodecarboxylierung zu einem sequenziellen Eintopf-Verfahren kombinieren.^[130]

3.2.3.2 Oxidative *ortho*-Arylierungen von Benzoessäuren

Neben den bereits diskutierten redox-neutralen *ortho*-Arylierungen von Benzoessäuren mit Arylhalogeniden existieren auch oxidative Varianten unter Verwendung von Arylboronsäureestern oder Aryltrifluorboraten in Gegenwart von Palladium-Katalysatoren (Schema 23).^[30,131]



Schema 23: Oxidative *ortho*-Arylierungen von Benzoessäuren.

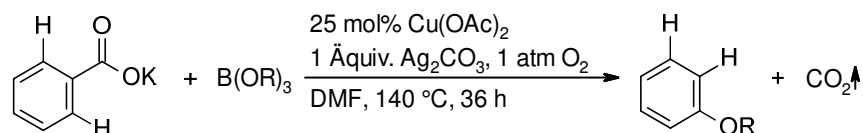
Außerdem wurden Carboxylat-dirigierte dehydrierende *ortho*-Arylierungen entwickelt, bei denen die Rhodium-katalysierte Aktivierung zweier C–H-Bindungen (Hetero-)Biaryle zugänglich macht (Schema 23).^[132–135] Dieses Reaktionskonzept wurde beispielsweise anhand der Homodimerisierung von Benzoessäuren sowie der *ortho*-Arylierung mit ausgewählten Heteroaromaten, die eine selektive Aktivierung gewährleisten, demonstriert. Im letzteren Fall sind zudem Varianten unter rückstandsloser Entfernung der Carboxylatgruppe mittels Protodecarboxylierung bekannt.^[132,133]

Da sich die vorliegende Arbeit mit redox-neutralen *ortho*-Arylierungen von Benzoessäuren beschäftigt, werden die oxidativen Varianten in diesem Rahmen nicht näher erläutert.

3.2.3.3 Carboxylate als abfallende dirigierende Gruppen

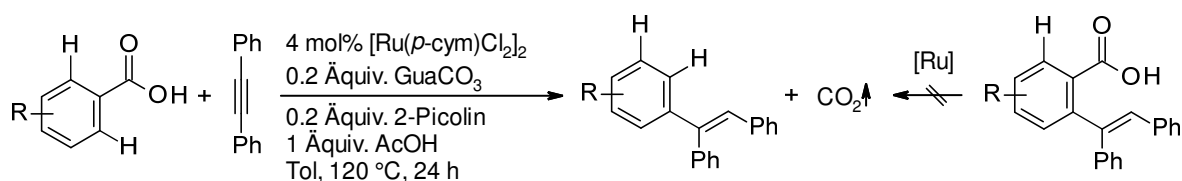
Neben den zuvor diskutierten Varianten der Carboxylatgruppe als rückstandslos entfernbare oder transiente dirigierende Gruppe in *ortho*-C–H-Funktionalisierungen existiert ein weiterer Reaktionsmodus: Carboxylate als abfallende dirigierende Gruppen.^[136] Dabei bleibt die Carboxylatgruppe gerade so lange im Substratmolekül wie es zur gewünschten *ortho*-Funktionalisierung notwendig ist und wird anschließend aufgrund einer aus der Bindungsknüpfung resultierenden Destabilisierung der C–COOH-Bindung abgespalten. Dies führt schließlich dazu, dass eine unerwünschte Difunktionalisierung, die häufig bei nicht-*ortho*-substituierten Benzoessäuren zu beobachten ist, unterbunden wird.^[136]

Ein frühes Beispiel, dem das Konzept der abfallenden dirigierenden Gruppe zugrunde liegt, ist die Carboxylat-dirigierte *ortho*-Alkoxylierung von Benzoessäuren zur Darstellung von Arylethern (Schema 24).^[137] Dabei führt die C–O-Bindungsknüpfung dazu, dass eine nachfolgende Protodecarboxylierung begünstigt wird, wodurch letztlich eine zweite Alkoxylierung ausbleibt und ausschließlich monoalkoxylierte Arene entstehen.



Schema 24: *ortho*-Alkoxylierung von Benzoessäuren.

Weiterhin beschrieben Gooßen und Mitarbeiter eine Ruthenium-katalysierte C–H-Hydroarylierung interner Alkine mit Benzoessäuren. Dabei wurde eine decarboxylierende Reaktionsvariante beschrieben, die selektiv das monofunktionalisierte Produkt liefert (Schema 25).^[138] Interessanterweise lässt sich das decarboxylierte Produkt nicht ausgehend von der entsprechenden isolierten 2-Alkenylbenzoessäure erhalten, was darauf hindeutet, dass die Reaktion nicht über eine Sequenz aus Hydroarylierung und Protodecarboxylierung abläuft, sondern dass die Decarboxylierung direkt im Zuge der Hydroarylierung erfolgt.



Schema 25: Ruthenium-katalysierte C–H-Hydroarylierung interner Alkine mit Benzoessäuren.

Ähnliche Protokolle wurden außerdem von Ackermann und Mitarbeitern sowie der Gruppe um Hartwig und Zhao beschrieben.^[139–141] Weiterhin konnte das Konzept auf eine zweifach regioselektive C–H-Hydroarylierung unsymmetrischer interner Alkine erweitert werden.^[142]

4 Aufgabenstellung

Das Ziel dieser Arbeit bestand in der rationalen Entwicklung neuer katalytischer Transformationen ausgehend von Carbonsäuren. Insbesondere sollten nachhaltige Methoden zur selektiven C–C-Bindungsknüpfung erschlossen werden, denen das Reaktionskonzept der decarboxylierenden Kreuzkupplung oder das der Carboxylat-dirigierten Funktionalisierung zugrunde liegt.

Zunächst sollten die auf neuen Erkenntnissen aus eingehenden DFT-Rechnungen basierenden Studien zur Cu/Pd-katalysierten decarboxylierenden Kreuzkupplung bei vergleichsweise milden Reaktionstemperaturen aus meiner Diplomarbeit fortgeführt werden. Im Rahmen dieses Projektes sollten bidentate *P,N*-Liganden verwendet werden, die in der Lage sind, die Katalysatormetalle verbrückend zu koordinieren, um schließlich die geschwindigkeitsbestimmende Transmetallierung zu erleichtern. Weiterführende Katalyseexperimente sollten ein tieferes Verständnis für diese Reaktion sowie für den Einfluss der *P,N*-Liganden schaffen. Daneben sollte die Anwendungsbreite der Reaktion ergänzend untersucht werden.

In einem weiteren Projekt sollten decarboxylierende Kreuzkupplungen von Pyridin-2-carbonsäure als Alternative zu Kupplungen präformierter 2-Pyridylorganometallverbindungen untersucht werden. Dabei sollte insbesondere der Einfluss eines aktivierenden *ortho*-Substituenten auf die Reaktivität dieses Substrats überprüft und ein Protokoll, welches eine Reaktionsführung unter vergleichsweise milden Bedingungen gewährleistet, entwickelt werden. In diesem Rahmen sollte zudem die Reaktivität anderer Heteroarylcarbonsäuren in der decarboxylierenden Kreuzkupplung evaluiert werden.

Eine weitere Aufgabe bestand darin, ein Reaktionsprotokoll für die *ortho*-Arylierung von Benzoessäuren mit Aryldiazoniumsalzen zu entwickeln. Zunächst sollte ein effizientes Katalysatorsystem für diese Transformation identifiziert und anschließend die Anwendungsbreite des neuen Verfahrens untersucht werden. Daneben sollte die Überlegenheit der Carboxylatgruppe im Vergleich zu anderen dirigierenden Gruppen demonstriert werden, indem sie im Anschluss an die Reaktion entfernt oder in weiteren Funktionalisierungen genutzt wird.

Weiterhin sollte ein Protokoll für die *ortho*-Arylierung von Benzoessäuren mit Arylhalogeniden entwickelt werden, welches auf kostengünstigen Ruthenium-Katalysatoren basiert. Dies würde eine ideale Alternative zu den bislang verwendeten Palladium- und Rhodium-katalysierten

Verfahren darstellen. Auch in diesem Fall sollte die Anwendungsbreite untersucht sowie demonstriert werden, dass die Carboxylatgruppe im Anschluss an die Reaktion entfernt oder als Ankerpunkt für eine weitere Funktionalisierung genutzt werden kann.

Daneben bestand die Aufgabe, eine decarboxylierende Mizoroki-Heck-Reaktion von Zimtsäuren mit Arylhalogeniden zu entwickeln. Dem Konzept der abfallenden dirigierenden Gruppe folgend, sollte dabei die Carboxylatgruppe zunächst eine Palladium-katalysierte Arylierung in die β -Position der Säure dirigieren und anschließend rückstandslos über eine Protodecarboxylierung durch einen geeigneten Metall-Katalysator entfernt werden. Im Erfolgsfall sollte die Praktikabilität dieser neuen Methode anhand der Synthese einer Vielzahl divers funktionalisierter 1,1-Diarylalkene aufgezeigt werden.

Insbesondere die Carboxylat-dirigierten Reaktionen sollten von eingehenden mechanistischen Studien begleitet werden, um nähere Einblicke zum Ablauf der Reaktionen zu erhalten.

5 Ergebnisse und Diskussion

5.1 Kupfer/Palladium-katalysierte decarboxylierende Kreuzkupplungen bei moderaten Reaktionstemperaturen

5.1.1 Eingehende Untersuchungen zum Mechanismus der Reaktion

5.1.1.1 Hintergrund

Wie bereits in Abschnitt 3.2.2.1 diskutiert, haben sich Cu/Pd-katalysierte decarboxylierende Kreuzkupplungen zu einem effizienten Werkzeug für die Biarylsynthese entwickelt. Dabei brachten stetige Optimierungsarbeiten immer effizientere Katalysatorsysteme hervor, die diesem Reaktionskonzept letztendlich zu einer synthetischen Reife verholfen haben. Dennoch existieren zwei zentrale Limitierungen, welche dessen praktische Anwendbarkeit einschränken.

Ein Nachteil besteht in den vergleichsweise hohen Reaktionstemperaturen, die meist über 150 °C liegen.^[63,64,67–70] In früheren Arbeiten wurde die Decarboxylierung als geschwindigkeitsbestimmend angenommen.^[86] Aufgründessen zielten bisherige Untersuchungen in Form von DFT-Rechnungen, die von eingehenden experimentellen Studien begleitet wurden, auf die Optimierung dieses Teilschritts ab.^[86,143] Dabei diente die Protodecarboxylierung als vereinfachte Testreaktion. Zwar führten diese Studien zu einem vertieften Verständnis über den Einfluss von Substituenten auf die Reaktion und brachten potente Katalysatorsysteme hervor,^[86,143] doch konnten darauf basierend bislang keinerlei Fortschritte hinsichtlich einer Cu/Pd-katalysierten decarboxylierenden Kreuzkupplung bei milderer Reaktionstemperaturen erzielt werden. Dies, obwohl weiterhin beobachtet wurde, dass mit einem optimierten Katalysatorsystem eine nahezu quantitative Protodecarboxylierung von *ortho*-Nitrobenzoesäure bereits bei 120 °C erfolgt.^[144] Dahingegen zeigte sich, dass Silberbasierte Katalysatoren die Protodecarboxylierung *ortho*-substituierter und heteroaromatischer Säuren bei nur 120 °C ermöglichen.^[85,86] Daraufhin gelang es, eine Ag/Pd-katalysierte Kreuzkupplung von *ortho*-Nitrobenzoaten und heteroaromatischen Carboxylaten mit Aryltriflaten zu entwickeln, welche bereits effizient bei 130 °C abläuft (Abschnitt 3.2.2.2).^[84]

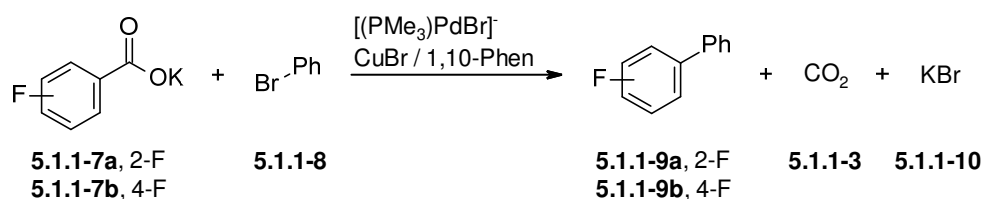
Ein weiterer Nachteil ist die Beschränkung auf *ortho*-substituierte Benzoate in der Kupplung mit Arylhalogeniden. Bereits in frühen Studien wurde festgestellt, dass die Anwesenheit von Halogenidsalzen, die in der Kupplung mit Arylhalogeniden im Verlauf der Reaktion freigesetzt werden, die Decarboxylierung nicht-*ortho*-substituierter Benzoate unterdrückt.^[64] Folglich wurde bislang angenommen, dass die Salzmetathese für Substrate mit koordinierenden

Gruppen in *ortho*-Position erleichtert ist und es gelang lediglich durch Verwendung von vergleichsweise teuren Aryltriflaten als elektrophilem Kupplungspartner nicht-*ortho*-substituierte Benzoate umzusetzen.^[2,68] Im Verlauf dieser Reaktion werden lediglich schwach koordinierende Triflationen freigesetzt, die deutlich weniger mit den Benzoaten um die Koordination an den Kupfer-Katalysator konkurrieren. Dadurch wird die Salzmetathese zur Bildung des Kupferbenzoats für nicht-*ortho*-substituierte Substrate erleichtert.^[2]

Um diese Limitierungen zu überwinden, ist ein vertieftes Verständnis über den Mechanismus der Cu/Pd-katalysierten decarboxylierenden Kreuzkupplung unabdingbar. Gerade die Diskrepanz zwischen der Temperatur für die Protodecarboxylierung der *ortho*-Nitrobenzoesäure^[144] und die im Vergleich dazu deutlich höheren Temperaturen, die für die Kreuzkupplung notwendig sind,^[63,64,67,69,70] lässt darauf schließen, dass der Decarboxylierungsschritt nicht notwendigerweise geschwindigkeitsbestimmend ist. Daher ist die Betrachtung aller Teilschritte des Mechanismus von zentraler Bedeutung.

5.1.1.2 DFT-Studien

Nachfolgend wurde der Mechanismus der Cu/Pd-katalysierten decarboxylierenden Kreuzkupplung mit Hilfe von DFT-Rechnungen eingehend untersucht. Dabei diente die Kupplung von Kalium-2- bzw. Kalium-4-fluorbenzoat (**5.1.1-7**) mit Brombenzol (**5.1.1-8**) als Modellsystem. Als Katalysatorsystem wurde Kupfer(I)-bromid mit 1,10-Phenanthrolin als Ligand und der anionische Komplex $[(\text{PMe}_3)\text{PdBr}]^-$ gewählt (Schema 26).



Schema 26: Modellreaktion für die DFT-Studien.

Die Ergebnisse dieser mechanistischen Untersuchungen werden in der nachfolgend abgebildeten Publikation diskutiert. Sie bildeten die Grundlage für die Entwicklung eines Katalysatorsystems, welches erstmals die Cu/Pd-katalysierte decarboxylierende Kreuzkupplung bei einer Reaktionstemperatur von nur 100 °C ermöglichte. Eine ergänzende Erläuterung der neuen Befunde sowie eine Diskussion der Voraussagen, die die Rechnungen zuließen, folgen im Anschluss an das Manuskript.

Beiträge der Autoren: Die nachfolgende Veröffentlichung entstand im Rahmen eines Kooperationsprojekts. Die DFT-Studien wurden von Herrn Andreas Fromm in enger Zusammenarbeit mit Herrn Prof. Dr. Christoph van Wüllen durchgeführt. Herr Dr. Bingrui Song begann mit der Entwicklung des Katalysatorsystems und den Optimierungsarbeiten zur decarboxylierenden Kreuzkupplung. Diese Arbeiten wurden zunächst von Herr Dr. Matthias Grünberg und dann eigenständig von mir fortgeführt sowie von mir fertiggestellt. Die Protodecarboxylierungsstudien wurden von mir mit Unterstützung von Herr Grünberg bearbeitet. Das Manuskript und die „Supporting Information“ wurden von Herrn Fromm verfasst, wobei ich den Abschnitt „Experimental Studies“ und die entsprechenden Hintergrundinformationen anfertigte. Herr Prof. Dr. L. J. Gooßen überarbeitete das Manuskript in Kooperation mit Herrn Prof. Dr. C. van Wüllen.


Die DFT-Studien sowie die daraus resultierende Entwicklung des Cu/Pd-basierten Katalysatorsystems unter Verwendung des *P,N*-Liganden für die decarboxylierende Kreuzkupplung bei 100 °C sind in der nachfolgenden Publikation aufgeführt. Diese wurde im *Journal of the American Chemical Society* veröffentlicht, für die vorliegende Arbeit angepasst und mit Erlaubnis des Verlags beigelegt:

"Reprinted (adapted) with permission from A. Fromm, C. van Wüllen, D. Hackenberger, L. J. Gooßen, *J. Am. Chem. Soc.* **2014**, *136*, 10007–10023: *Mechanism of Cu/Pd-Catalyzed Decarboxylative Cross-Couplings: A DFT Investigation*. Copyright 2014 American Chemical Society."

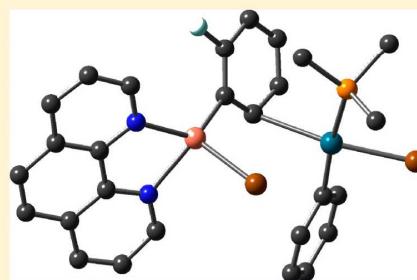
Mechanism of Cu/Pd-Catalyzed Decarboxylative Cross-Couplings: A DFT Investigation

Andreas Fromm, Christoph van Wüllen, Dagmar Hackenberger, and Lukas J. Gooßen*

Fachbereich Chemie und Forschungszentrum OPTIMAS, TU Kaiserslautern, Erwin-Schrödinger-Straße, 67663 Kaiserslautern, Germany

 Supporting Information

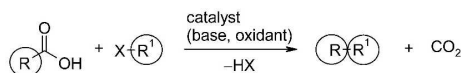
ABSTRACT: The reaction mechanism of decarboxylative cross-couplings of benzoates with aryl halides to give biaryls, which is cooperatively catalyzed by copper/palladium systems, was investigated with DFT methods. The geometries and energies of all starting materials, products, intermediates, and transition states of the catalytic cycle were calculated for the two model reactions of potassium 2- and 4-fluorobenzoate with bromobenzene in the presence of a catalyst system consisting of copper(I)/1,10-phenanthroline and the anionic monophosphine palladium complex $[\text{Pd}(\text{PMe}_3)\text{Br}]^-$. Several neutral and anionic pathways were compared, and a reasonable catalytic cycle was identified. The key finding is that the transmetalation has a comparably high barrier as the decarboxylation, which was previously believed to be solely rate-determining. The electronic activation energy of the transmetalation is rather reasonable, but the free energy loss in the initial Cu/Pd adduct formation is high. These results suggested that research aimed at further improving the catalyst should target potentially bridging bidentate ligands likely to assist in the formation of bimetallic intermediates. Experimental studies confirm this somewhat counterintuitive prediction. With a bidentate, potentially bridging ligand, designed to support the formation of bimetallic adducts, the reaction temperature for decarboxylative couplings was reduced by 70 °C to only 100 °C.



INTRODUCTION

Decarboxylative couplings have become a powerful tool for the selective formation of carbon–carbon and carbon–heteroatom bonds. In these transformations, CO_2 is extruded from a carboxylic acid precursor, and the carbon atom that has carried the carboxylic group then forms a bond with an electrophilic carbon or heteroatom. Following pioneering contributions by Nilsson, Tsuji, and Myers,¹ a redox-neutral decarboxylative biaryl synthesis was discovered in 2006 in which aromatic carboxylic acids are coupled with various aryl bromides in the presence of a copper/palladium bimetallic catalyst system (Scheme 1).²

Scheme 1. Decarboxylative Coupling Reactions



Since then, bimetallic systems have been used for decarboxylative couplings of benzoates and α -imino-³ and α -oxocarboxylates⁴ with aryl iodides, bromides,⁵ chlorides,⁶ triflates,⁷ tosylates,⁸ and mesylates.⁹ Decarboxylative couplings with monometallic catalysts include Cu-mediated arylations of perfluorinated arenecarboxylic acids,¹⁰ Rh-catalyzed decarboxylative 1,2-additions,¹¹ Pd-catalyzed decarboxylative allylations¹² and arylations of five-ring heteroarene carboxylates,¹³ and of alkynylcarboxylates,¹⁴ and of oxalic acid monoesters,¹⁵ and

Mannich-type reactions.¹⁶ Oxidative decarboxylative cross-couplings have been used for Heck-type vinylations,^{1f–h,17} C–H arylations,¹⁸ couplings of amino acids,¹⁹ and various C–heteroatom bond formations.²⁰

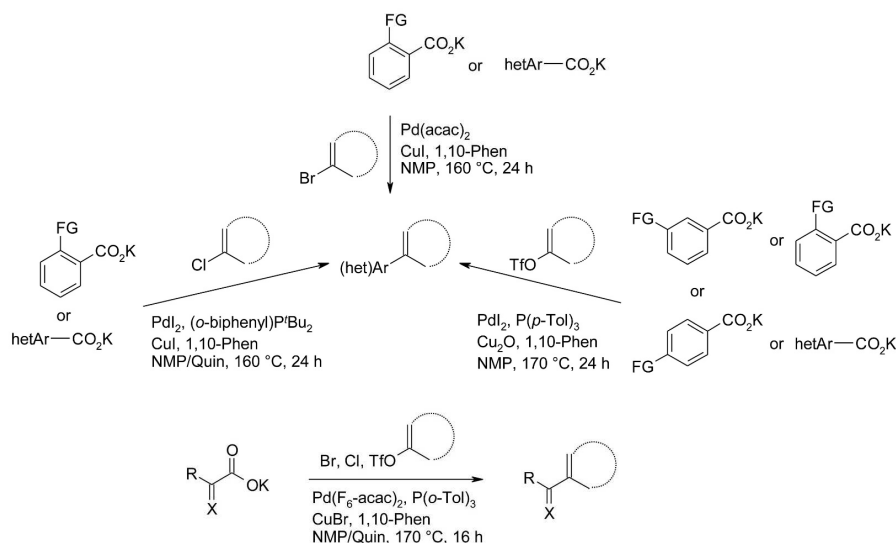
The concept of decarboxylative couplings has distinct advantages over traditional cross-coupling reactions in the regiospecific formation of C–C bonds, because it relies on inexpensive and broadly available carboxylate salts instead of expensive and sensitive preformed organometallic reagents as the source of carbon nucleophiles.

Typical catalyst systems and the reaction scope are shown in Scheme 2.

Especially in redox-neutral couplings of aromatic carboxylate salts, bimetallic copper/palladium systems have proven to be the most generally applicable catalysts. For these systems, a mechanistic outline consisting of two interlinked catalytic cycles has been proposed (Scheme 3).^{2,5} The ligand environment at the copper center is designed to promote the extrusion of CO_2 with the highest possible efficiency, while the palladium catalyst is independently optimized for the cross-coupling step. The proposed catalytic cycle starts with an anion exchange at the copper center, in the course of which the aromatic carboxylate is transferred to the copper complex a to give the metal carboxylate b. In the decarboxylation step, an organocopper

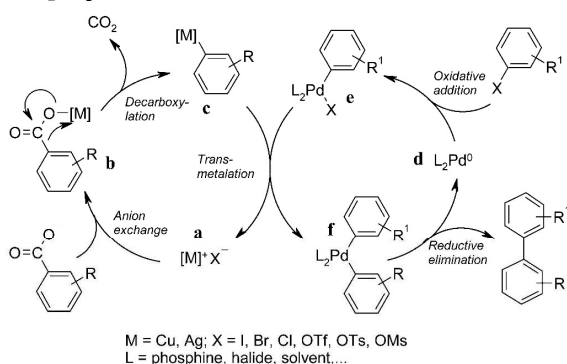
Received: April 2, 2014

Published: June 26, 2014

Scheme 2. Representative Decarboxylative Cross-Couplings with Bimetallic Cu/Pd Catalyst Systems^a


^aAr = aryl, FG = functional group, hetAr = heteroaryl, Phen = phenanthroline, Quin = quinoline, X = O, NR.

Scheme 3. Mechanism Proposed for Decarboxylative Cross-Couplings



species **c** is generated by extrusion of CO₂. A subsequent transmetalation links the two catalytic cycles. In this step, an aryl residue is transferred from the copper species **c** onto a palladium species **e** that has been generated by oxidative addition of the aryl electrophile to a low-valent palladium(0) cocatalyst **d**, and the original copper species **a** is regenerated. The resulting diaryl palladium species **f** undergoes reductive elimination, in which the new carbon–carbon bond is formed, the biaryl product is released, and the palladium(0) species **d** is regenerated.

At present, most decarboxylative couplings still require temperatures in excess of 160 °C, which, in practice, represents the main limitation of this elegant reaction type. The rational development of catalysts that promote decarboxylative couplings at lower temperatures is, thus, in the focus of current research activities. In this context, mechanistic investigations and theoretical studies are of vital importance.²¹

However, DFT modeling of the mechanistically complex decarboxylative couplings catalyzed by bimetallic systems poses a considerable challenge, which has so far precluded the

calculation even of simplified models. Computational studies of this reaction have to date been limited to the decarboxylation step (**b** → **c** in Scheme 3).²² That this step was rate-determining in the early reaction protocols became evident from the observation that Cu-catalyzed protodecarboxylations required temperatures that were at least as high as those of decarboxylative cross-couplings (170 °C). In contrast, Pd-mediated cross-couplings of aryl–copper species are known to proceed at much lower temperatures.

These DFT calculations confirmed²² that the extrusion of CO₂ from phenanthroline copper benzoates is endothermic by 9.9–28.8 kcal mol^{−1} and endergonic (0.8–17.5 kcal mol^{−1}) and has a considerable activation barrier of 27.2–36.1 kcal mol^{−1}.^{21c} Another correct prediction derived from these calculations was that for a narrow range of substitution patterns, e.g. *o*-methoxybenzoates, the energy barrier for the decarboxylation is substantially lower when copper is replaced by silver, whereas the majority of carboxylates lose CO₂ more easily when coordinated to copper rather than silver complexes.^{7c}

Pd-catalyzed cross-couplings of organometallic reagents have been intensively studied by DFT calculations.²³ For Suzuki-type couplings of carboxylic anhydrides with arylboronic acids, various catalytic cycles were computed starting from neutral (PMe₃)₂Pd(0) (**4**), anionic tricoordinate Amatore–Jutand-type [(PMe₃)₂Pd(0)OAc][−] (**5**), and anionic dicoordinate [(PMe₃)PdOAc][−] (**6**) (Figure 1).²⁴ With the anionic dicoordinate palladium complex **6**, the energy profile obtained was most favorable overall so that this species appears to be the optimal candidate for calculations of related Pd-catalyzed couplings.

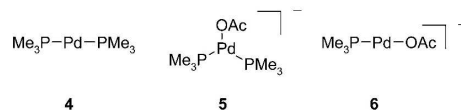
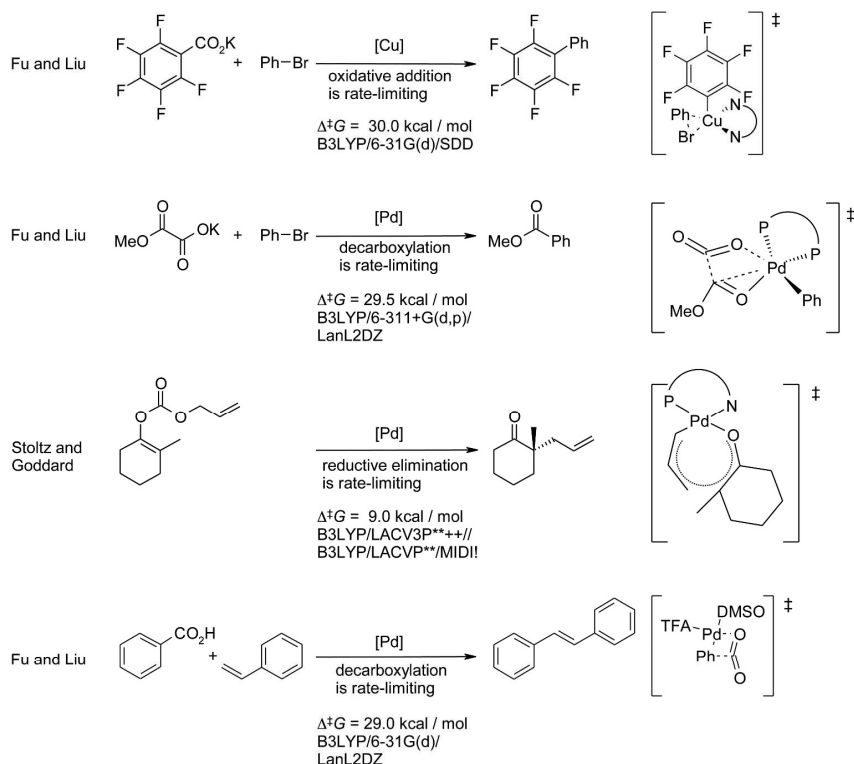
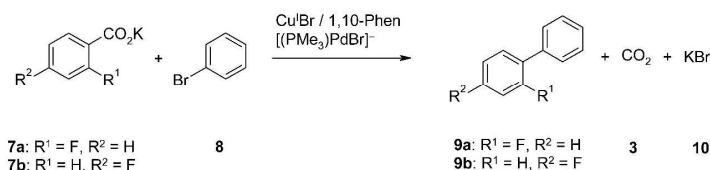


Figure 1. Pd-species investigated in Suzuki-type cross-couplings.

Scheme 4. DFT Investigations of Decarboxylative Cross-Couplings with Monometallic Catalysts



Scheme 5. Model Reactions of Potassium 2- and 4-Fluorobenzoate with Bromobenzene



As mentioned above, some particularly activated substrates can be decarboxylatively coupled with aryl electrophiles by using monometallic catalysts. The reduced complexity of such monometallic systems has permitted in-depth mechanistic investigations (see Scheme 4). DFT studies were reported for Pd-catalyzed decarboxylative cross-couplings of oxalic acid monoesters,¹⁵ decarboxylative allylations of enol carbonates,^{12,25} decarboxylative cross-couplings of polyfluorobenzoates with aryl electrophiles,²⁶ Myers' Pd-catalyzed decarboxylative Heck vinylation,^{17a} and certain intramolecular decarboxylative couplings.²⁷

For the mechanistically more complex decarboxylative couplings mediated by bimetallic catalyst systems, a similarly detailed computational study would be of substantial value. With state-of-the-art catalysts, the protodecarboxylation of *o*-nitrobenzoic acids with a copper/phenanthroline system can meanwhile be performed at 100 °C,²⁸ while decarboxylative cross-couplings with aryl triflates, in which copper/phenanthroline systems are employed as the decarboxylation cocatalysts, still do not proceed below 150 °C.^{7a,b} Thus, the decarboxylation is not necessarily rate-determining, and it is no longer sufficient to single out the decarboxylation step in computa-

tional studies to obtain a lead for further catalyst optimization. Instead, computational modeling should cover the entire catalytic cycle. A particular challenge lies in modeling the transmetalation step, in which an organic residue is transferred from a fully ligated copper complex to a phosphine-stabilized arylpalladium species.²⁹

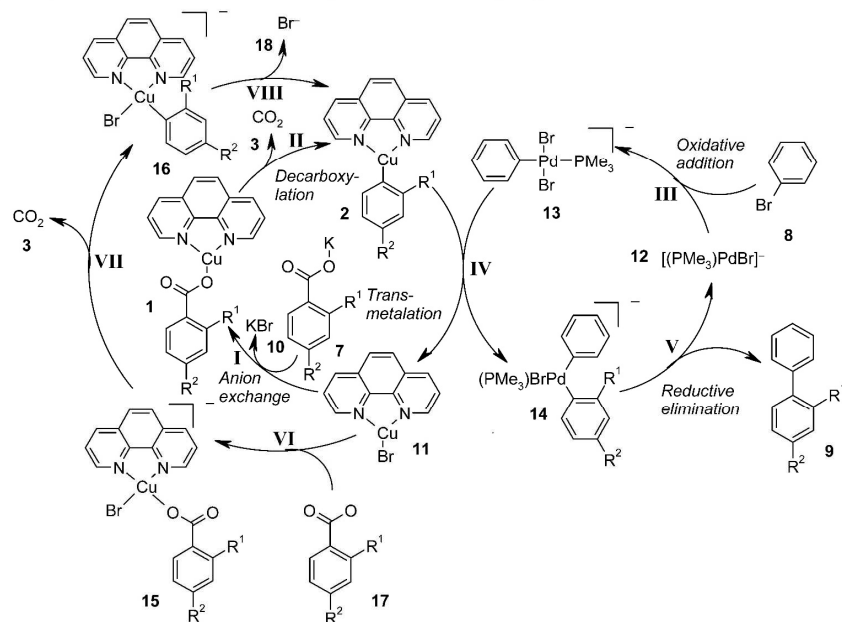
MODEL SYSTEM

We herein investigate the decarboxylative coupling of bromobenzene (**8**) with (a) potassium 2-fluorobenzoate (**7a**) as an example of a highly reactive arenecarboxylate and (b) potassium 4-fluorobenzoate (**7b**) as an example of an arenecarboxylate with low reactivity (Scheme 5).

The catalyst system employed in the calculations of these representative model reactions is composed of 1,10-phenanthroline copper(I) bromide, which is known to display a substantially greater decarboxylation activity than simple copper(I) salts,² and an anionic Pd(0) bromide catalyst with the simplified but still reasonably realistic ligand PMe_3 .

Comparative studies performed upfront, in combination with related literature studies, confirmed that the catalytic cycle

Scheme 6. Catalytic Cycles Calculated for Decarboxylative Cross-Couplings



shown in Scheme 6 is a realistic mechanistic model. For example, computational studies of Suzuki-type couplings led to the conclusion that catalytic cycles starting from various Pd(0) species, each of which may be present in solution, will have comparable energy profiles also in couplings with other carbon nucleophiles.²⁴ Among them, a pathway starting from $[(\text{PMe}_3)_2\text{PdOAc}]^-$ (6) (Figure 1) had proven to be the most advantageous overall. It thus appeared to be reasonable to use an analogous cycle based on similar structural units as a starting point for computing the cycle of the Pd-catalyst in the decarboxylative cross-coupling. For the Cu-catalyst, two different catalytic cycles were computed, both starting from 1,10-phenanthroline copper(I) bromide. The first solely involves neutral species, whereas in the second, an additional bromide is bound to copper during the decarboxylation step. This was calculated to find a possible explanation for the profound influence of bromide ions on the decarboxylation of non-*ortho*-substituted benzoates.

Both variants of the catalyst cycle were successfully calculated. Minima with reasonable structures and energies could be found for all intermediates, and transition states connecting these intermediates could be located. The computational studies led us to conclude that decarboxylative cross-couplings follow a neutral pathway consisting of the anion exchange (step I) and the decarboxylation step (step II) at the copper catalyst, the oxidative addition (step III) of the bromobenzene to the Pd catalyst, the transmetalation process (step IV) between the resulting palladium and copper species, and the reductive elimination (step V) of the biaryl product with regeneration of the Pd catalyst. Subsequently, the computational study of an anionic variant of the Cu-cycle is presented, which starts with the coordination (step VI) of the carboxylate to the copper catalyst, followed by decarboxylation (step VII) and bromide decoordination (step VIII). This alternative cycle was found to be less favorable.

COMPUTATIONAL METHOD

All calculations were performed with use of the Gaussian 03 or Gaussian 09 software packages.³⁰ The B3LYP exchange-correlation functional³¹ was used in all cases. For the geometry optimizations, the polarized split-valence 6-31+G(d) basis set³² was employed for all atoms except Cu and Pd, where a scalar-relativistic effective core potential³³ replaced 10 (Cu) or 28 (Pd) core electrons, together with the valence basis sets³³ in double- ζ quality. Spherical basis functions (SD, 7F) were used in all cases. In contrast to our previous studies,^{21c,22} some of the species investigated are anionic, so that diffuse basis functions were included in the basis set. Note that the valence basis sets for Cu and Pd already contain diffuse functions from the outset.

All geometries of minima (intermediates) and transition states were fully optimized for isolated (gas-phase) molecules. To locate the transition states, we first performed a relaxed potential energy surface scan in which the reaction coordinate was kept fixed at several defined distances, while all other degrees of freedom were optimized. In these scans, a series of structures were optimized in which the reaction coordinate was increased stepwise. The structure with the highest energy was then used as a starting point for the synchronous transit-guided quasi-Newton method³⁴ to locate the transition state with a molecular Hessian of exactly one negative eigenvalue. To identify the minima connected to the transition states thus identified, the intrinsic reaction coordinate (IRC)³⁵ was followed downhill for 10 points in both directions and the two resulting molecular geometries were used as starting points for subsequent geometry optimizations. Sometimes, additional intermediates were discovered this way. In these cases, the process described above was repeated until the reaction pathway was complete. For each molecular structure (intermediate or transition state), the calculated electronic energy (but not the molecular structure and harmonic vibrational frequencies) was improved by a single-point calculation in which the 6-31+G(d) basis (for all atoms except Cu and Pd) was replaced by the better polarized valence triple- ζ type 6-311+G(2d,p).³⁶ For Cu and Pd, the *d* functions of the original basis sets were decontracted slightly from [411] to [3111], and a single set of *f* functions (taken from the def2-TZVP basis sets,³⁷ $\eta_f(\text{Cu}) = 2.233$, $\eta_f(\text{Pd}) = 1.24629$) was added for both elements.

The above calculations provided electronic energies under vacuum (E_{tot}). To model the reaction energies more closely resembling

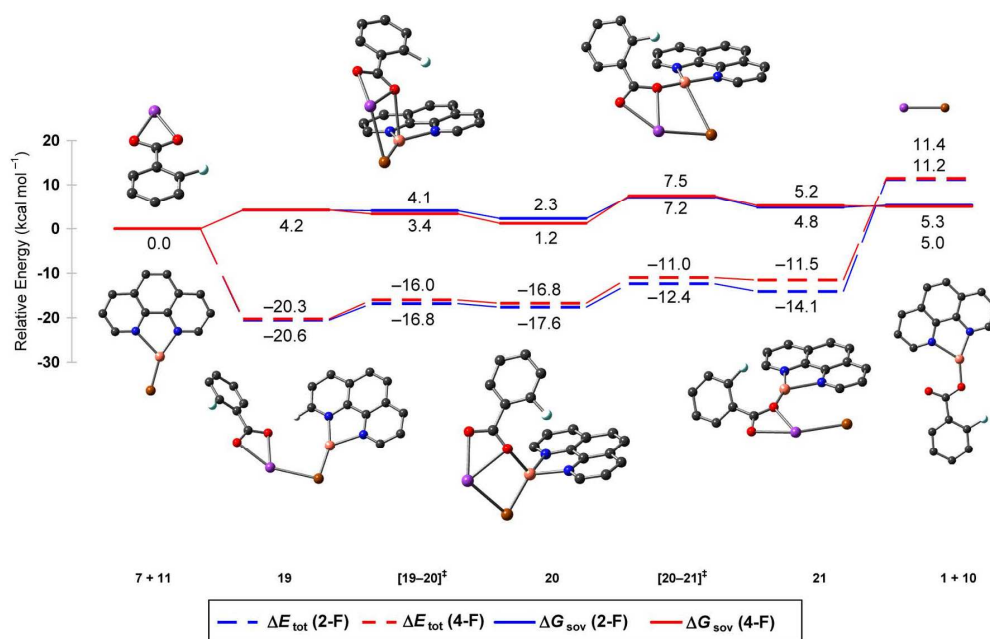


Figure 2. B3LYP/6-31+G(d) optimized structures for the anion exchange of potassium 2-fluorobenzoate and phenanthroline copper(I) bromide; hydrogens are omitted for clarity. Energy and solution Gibbs energy profiles overlaid for 2- and 4-fluorobenzoate. Color code: C, black; H, white; Br, brown; Cu, orange; F, turquoise; K, purple; N, blue; O, red.

experimental conditions, further terms were added, namely zero-point vibrational energy, thermal corrections to the energy, solvation and entropic effects, as well as empirical dispersion corrections. This way, an approximation to the Gibbs energy in solution (G_{solv}) was obtained.

Solvent effects were included by estimating the Gibbs energy of solvation for all intermediates and transition states using the conductor-like polarizable continuum model³⁸ (CPCM) of Gaussian 09, which is an implementation of the conductor-like screening solvation model³⁹ (COSMO). This model is particularly well-suited for polar solvents such as *N*-methyl-2-pyrrolidone (NMP, $\epsilon = 32.55$), which is the most effective solvent for decarboxylative cross-couplings.

To calculate the zero-point vibrational energies, the harmonic frequencies calculated (with the small basis) were scaled by a factor of 0.9613 as suggested by Wong.⁴⁰ The thermal correction to the Gibbs energy of each component depends on its concentration in the solution. Note that in the Gaussian program one has to specify the concentration as a pressure value, using the ideal gas law $p_i = RTn_i/V$, where p_i is the pressure, R the gas constant, T the absolute temperature, n_i the molar quantity, and V the reaction volume. Typical experiments, as modeled in our calculations, involve approximately 1 mmol of starting material and product in a reaction volume of 2 mL, which corresponds to a pressure of 1,844,115 Pa (18.2 atm) at a reaction temperature of 443 K. The amount of catalyst is lower by a factor of 20, so that we used a pressure of 101,325 Pa (1 atm) for all species involving Cu and/or Pd. The experimental solubility data of CO_2 in NMP⁴¹ show that under the experimental conditions, the molar fraction of CO_2 /NMP is clearly less than 0.01, most likely about 0.001 when extrapolating temperature and pressure, which implies that most of the CO_2 leaves the NMP solution. The resulting CO_2 concentration in the reaction mixture corresponds to a partial pressure of 101,325 Pa (1 atm) for an ideal gas. Because of the ideal gas approximation, the molar Gibbs energy for a given temperature T and pressure p was computed from the results for $p_0 = 1$ atm as $G(T, p) = G(T, p_0) + RT \ln(p/p_0)$.

For any sequence of elementary steps that involve a single species, the reaction profile does not depend on the concentration. These changes if association and dissociation steps are involved. These

considerations are relevant in this context because we have two coupled catalytic cycles. Reducing the catalyst load (both Cu and Pd) reduces the reaction rate of the steps involving only Cu or only Pd linearly, while the transmetalation step is affected quadratically. Therefore, the relative rates of the transmetalation compared to the other elementary steps depend on the catalyst load, with lower loads disfavoring the transmetalation. This is taken into account in our Gibbs energy profiles.

It is known that standard DFT methods neglect or severely underestimate London dispersion interactions.⁴² A robust and numerically inexpensive way to cure this deficiency is to add an empirical dispersion correction that sums up the contribution of all atom pairs. We used Grimme's D3 parametrization⁴³ and calculated the dispersion correction for all minima and transition states. These values are included in our final solution Gibbs energies G_{solv} . This correction significantly lowers the Gibbs energy of an encounter complex with respect to the two fragments, but also lowers the Gibbs energy of a tight transition state with respect to a loose intermediate.

Note that the solvation model as used in our calculations does not include nonelectrostatic solute–solvent interactions: in a numerical experiment, we found zero contributions when we set the dielectric constant to zero. This means that the loss of solute–solvent dispersion interaction upon formation of an adduct, which is a consequence of reducing the surface of the solute(s), is not taken into account. Therefore, we think that the dispersion interaction in solution is somewhat overestimated in our calculations, although the combination of empirical dispersion and solvent corrections has been reported to work well.⁴⁴

In the Supporting Information, the electronic energies (with and without solvation), the calculated Gibbs energies at 298 and 443 K (at 1 and 18.2 atm), the empirical dispersion corrections, and the final solution Gibbs energy including empirical dispersion corrections G_{solv} are documented. The diagrams in this paper contain the electronic energy E_{tot} (since molecular geometries and vibrational frequencies are obtained at this level) and solution Gibbs energy G_{solv} profiles including empirical dispersion corrections (which govern the reactivity). Throughout the text, all bond lengths are given in Å and

relative energies are expressed in kcal mol⁻¹. All ball-and-stick models are rendered with GaussView 5.⁴⁵

MODELING THE CATALYTIC CYCLE BY DFT

Anion Exchange. In the anion exchange step, the potassium benzoate (7a/b) reacts with the phenanthroline copper bromide catalyst **11** to afford the corresponding phenanthroline copper benzoate (**1a/b**) along with potassium bromide (**10**). The energy and solution Gibbs energy profiles for the model substrates, 2- and 4-fluorobenzoate are depicted in Figure 2, along with the optimized structures for the *o*-fluoro derivatives.

The anion exchange starts with the formation of an encounter complex **19** between the substrates **7** and **11**. This process is exothermic in the gas phase ($\Delta_r E_{\text{tot}} = -20.6$ kcal mol⁻¹) but endergonic by $\Delta_r G_{\text{sov}} = 4.2$ kcal mol⁻¹. This difference has two origins. First, entropy is lost when forming the adduct, even more so because the copper catalyst **11** is present only in low concentration compared to the substrate **7**. This entropy loss strongly contributes to the increase in Gibbs energy at the elevated reaction temperature (170 °C). Second, solvation disfavors adduct formation, since the combined solvation energies for **7** and **11** are larger than that for the adduct **19**. In the adduct, the C(2)–H bond of the 1,10-phenanthroline points toward one of the carboxylate oxygens, resulting in a short C–H...O (2.03 Å) and a long K–Br distance (3.26 Å). A Cu–O bond has not formed at this stage. The K–O bond is slightly elongated to 2.64 Å compared to 2.55 Å in **7**. Also, the Cu–Br bond is slightly increased to 2.30 Å compared to 2.26 Å in **11**.

Bringing a carboxylic oxygen closer to the copper center leads to the transition state [**19**–**20**][‡]. This process has a very small barrier ($\Delta^\ddagger E_{\text{tot}} = 3.8$ kcal mol⁻¹). The coordination sphere of the copper is distorted trigonal planar, with the bromine atom only slightly out of the plane formed by the phenanthroline backbone. The atoms Cu, Br, K, and O form an almost planar 4-membered ring. The K–Br (3.16 Å) and Cu–O (*ortho*: 2.77 Å) bonds are long, and the K–O (2.64 Å) and Cu–Br bonds (2.33 Å) are short. The forward motion along the reaction coordinate derived from the normal mode of the imaginary frequency (21 i cm⁻¹) is dominated by the shortening of the Cu–O distance. At the same time, the bromine atom moves out of the plane of the phenanthroline ligand.

In intermediate **20**, the copper atom is now in an almost tetrahedral environment. The K–Br (3.11 Å) and Cu–O (2.15 Å) bonds are further shortened and the K–O (2.66 Å) and Cu–Br bonds (2.41 Å) are elongated.

In the second phase of the anion exchange, a bromide leaves the copper center and eventually forms KBr. Stretching the Cu–Br bond leads to the transition state [**20**–**21**][‡]. The activation barrier is rather low ($\Delta^\ddagger E_{\text{tot}} = 5.2$ kcal mol⁻¹, $\Delta^\ddagger G_{\text{sov}} = 4.9$ kcal mol⁻¹). The copper is in a distorted trigonal planar environment with the oxygen atom only slightly out of the plane of the phenanthroline backbone. The K–Br (3.04 Å) and Cu–O (1.91 Å) bonds are rather short, whereas the K–O (2.71 Å) and Cu–Br bonds are long (3.50 Å). The forward motion along the reaction coordinate derived from the normal mode of the imaginary frequency (21 i cm⁻¹) is dominated by the elongation of the Cu–Br bond and the motion of the oxygen atom into the plane of the phenanthroline ligand.

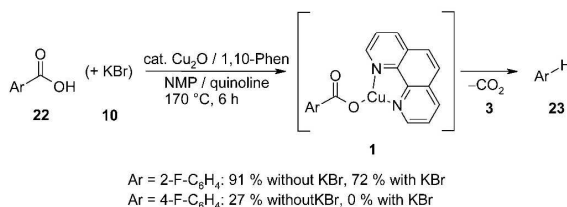
In the subsequent intermediate **21**, the Cu–Br bond is now fully broken while the K–Br (3.04 Å) and Cu–O (1.91 Å)

bond lengths remain almost unchanged and the K–O bond is slightly elongated (2.74 Å).

For the *o*-fluoro model system, intermediate **21** finally dissociates into KBr (**10**) and the product of the anion exchange, the phenanthroline copper 2-fluorobenzoate (**1a**) that decarboxylates subsequently. Cleaving the K–O bond requires some energy ($\Delta_r E_{\text{tot}} = 25.3$ kcal mol⁻¹), but the entropically favorable dissociation into two solvated molecules makes this step only slightly endergonic ($\Delta_r G_{\text{sov}} = 0.5$ kcal mol⁻¹). The copper atom in **1a** is coordinated to only one of the carboxylate oxygens by a short bond (Cu–O: 1.89 Å) in a distorted trigonal planar environment. The nitrogen donor atoms of the phenanthroline ligand transfer sufficient electron density to the copper(I) cation so that this coordination mode is preferred, while for the electron-poor potassium cation, a coordination to both oxygen atoms is favorable (structure **7**).

The calculations further revealed that for 4-fluorobenzoate, the energy profile of the anion exchange is almost identical with that of the 2-fluorobenzoate (Figure 2, see also the Supporting Information). This result came as a surprise since decarboxylative cross-couplings of aryl halides with 2-fluorobenzoates are well-documented, while the analogous reactions of 4-fluorobenzoates have not yet been achieved. Only aryl electrophiles with noncoordinating groups such as triflates can be coupled with non-*ortho*-substituted benzoates. To rationalize these experimental findings, the salt metathesis of copper(I) halides with potassium benzoates had been postulated to be favorable for *ortho*-substituted derivatives, but unfavorable for non-*ortho*-substituted benzoates. This hypothesis was supported by protodecarboxylation experiments in which benzoic acids (**22**) were converted to the corresponding arenes (**23**) in the presence of a phenanthroline copper system according to Scheme 7. In the absence of

Scheme 7. Influence of Halides on Protodecarboxylations



halides, this reaction proceeded well both for *ortho*- and non-*ortho*-substituted benzoic acids. Upon the addition of a halide salt, the decarboxylation of non-*ortho*-substituted benzoic acids was fully suppressed, whereas the reactivity of the *ortho*-substituted benzoic acids remained high.⁵

In a series of control experiments, similar observations were made also for the decarboxylation of the two fluorobenzoic acid isomers. The addition of 1 equiv of potassium bromide only slightly reduced the yield of the protodecarboxylation of 2-fluorobenzoic acid (**22a**) from 91% to 72% yield in the presence of potassium bromide. 4-Fluorobenzoic acid (**22b**) gave only 27% even in the absence of bromide ions, and when potassium bromide was added, the decarboxylation was completely suppressed.⁴⁶

According to our present DFT studies, the salt exchange between the copper bromide species **11** and the fluorobenzoate isomers (**7a** and **7b**) is energetically very similar. It is slightly endergonic (*ortho*: $\Delta_r G_{\text{sov}} = 5.3$ kcal mol⁻¹; *para*: $\Delta_r G_{\text{sov}} = 5.0$

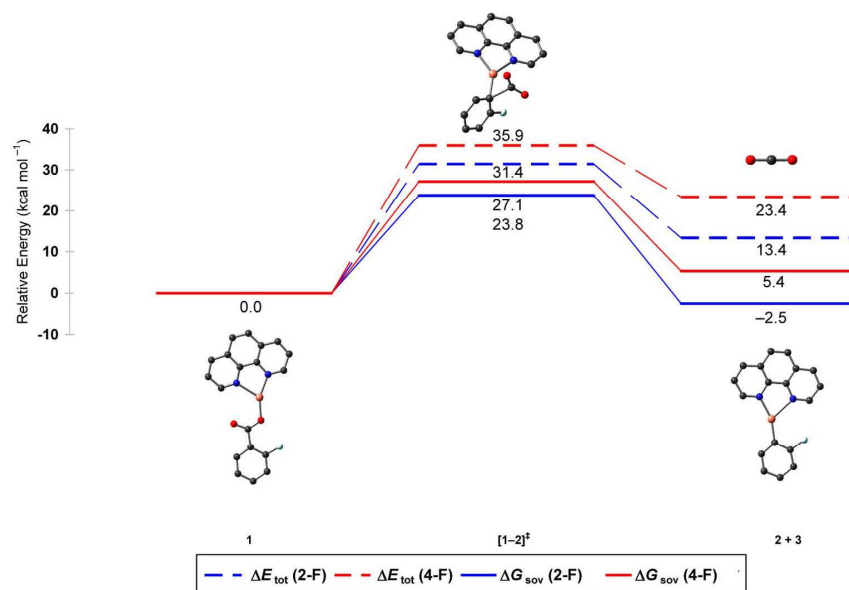


Figure 3. B3LYP/6-31+G(d) optimized structures for the decarboxylation of phenanthroline copper 2-fluorobenzoate; hydrogens are omitted for clarity. Energy and solution Gibbs energy profiles overlaid for 2- and 4-fluorobenzoate. Color code: C, black; Cu, orange; F, turquoise; N, blue; O, red.

kcal mol⁻¹) with low activation barriers. These calculations do not provide any rationale for the hypothesis that the presence of bromide ions suppresses the formation specifically of copper 4-fluorobenzoate complexes, so that the unique reactivity of *ortho*-substituted benzoates must have another reason. A precipitation of KBr, which would not be taken into account by the DFT calculations, is not observed in the experiment.

We therefore carefully explored alternative geometries for the salt exchange product phenanthroline copper 2-fluorobenzoate (**1a**), in which the carboxylate oxygen and the *o*-fluorine would both coordinate to the copper, potentially resulting in a more stable structure. This might be expected to lead to a substantially less endergonic anion exchange step for potassium 2-fluorobenzoate compared to 4-fluorobenzoate. However, no minima for complexes with chelating coordination were found.

We also investigated whether the energy profile is affected by leaving out the potassium counterion in the calculations. The resulting energy barriers are twice as high, and again, no differences of any potential consequence were found between 2- and 4-fluorobenzoates. The energy profiles along with the optimized structures can be found in Figure S1 in the Supporting Information.

Overall, the calculations do not support the previously postulated explanation for the effect of halide ions on the decarboxylation of non-*ortho*-substituted carboxylates. A possible explanation is that the additional bromide ions do not have an effect on the difference in reactivity of the *ortho*- and *para*-substituted benzoates in the anion exchange step but in the decarboxylation step that will be discussed in the next section. The presence of excess bromide salt shifts the equilibrium of the anion exchange step to the side of the copper bromide so that less copper carboxylate is available. This reduces the efficiency of the entire protodecarboxylation process. Since the decarboxylation of *ortho*-substituted benzoates requires less energy than that of non-*ortho*-

substituted benzoates, high conversions of *ortho*-substituted benzoic acids can be achieved at temperatures where non-*ortho*-substituted derivatives do not decarboxylate.

Decarboxylation. The decarboxylation step has already been the subject of previous DFT investigations,^{21c,22} because it was initially believed to be the only rate-determining step. We have now reinvestigated it using the high-quality basis set with diffuse functions detailed above, included solvent effects, dispersion interactions, and taken into account the concentrations and reaction temperatures.

The extrusion of carbon dioxide from phenanthroline copper 2-fluorobenzoate (**1**) was found to proceed via a concerted mechanism involving only one transition state ([**1-2**][‡], Figure 3). An extensive search did not reveal any further intermediates, such as π - or η^2 -bound arene-copper complexes.

In the copper 2-fluorobenzoate **1a**, all atoms are coplanar. The two nitrogen-copper bond lengths of the phenanthroline ligand are slightly different (2.0 and 2.2 Å), which indicates that this ligand geometry is not ideal for Cu^I. The decarboxylation step can be viewed as a substitution of the carboxylate group by the copper center in a concerted fashion. The activation barrier for the extrusion of CO₂ from 2-fluorobenzoate is relatively high ($\Delta^\ddagger E_{\text{tot}} = 31.4$ kcal mol⁻¹, $\Delta^\ddagger G_{\text{sov}} = 23.8$ kcal mol⁻¹), but within a realistic range for a reaction that requires a temperature of 160 °C. In the transition state [**1a-2a**][‡], the copper atom is in a distorted tetrahedral environment formed by the two phenanthroline nitrogens, the 2-fluorophenyl and the CO₂ carbons. The Cu-N bonds have similar lengths (ca. 2.1 Å). The fluorophenyl moiety binds to both the copper and the CO₂ carbon via its C(1) carbon. The aryl-CO₂ bond is short (1.94 Å) while the aryl-copper bond is relatively long (2.02 Å), which is indicative for a relatively early transition state. The forward motion along the reaction coordinate derived from the normal mode of the imaginary frequency (229

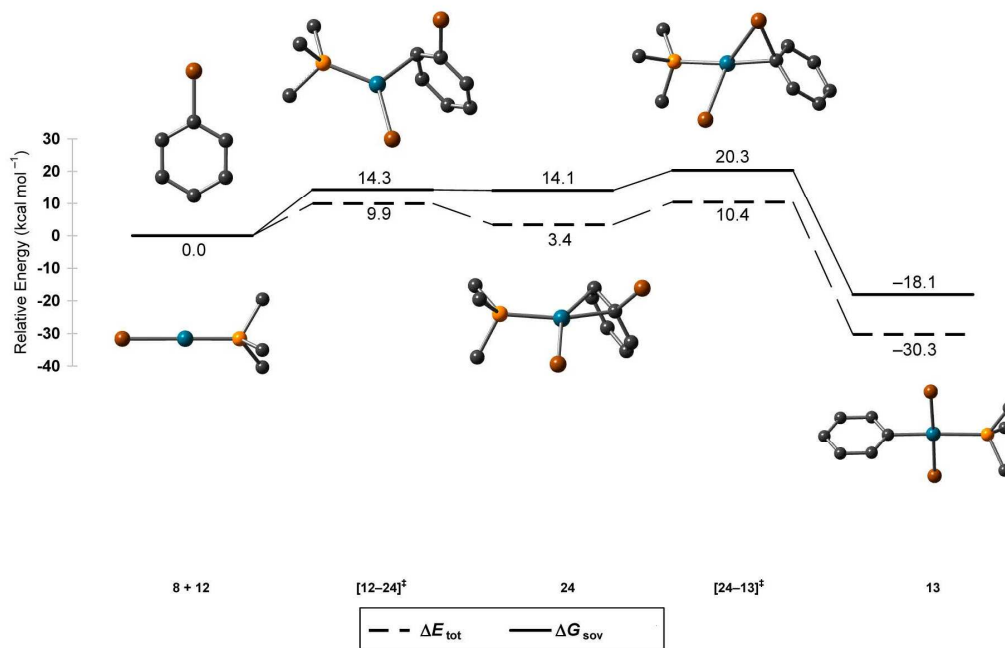


Figure 4. B3LYP/6-31+G(d) optimized structures for the oxidative addition of bromobenzene to $[\text{Pd}(\text{PMe}_3)\text{Br}]^-$; hydrogens are omitted for clarity. Color code: C, black; Br, brown; P, yellow; Pd, green.

i cm^{-1}) is dominated by the elongation of the aryl- CO_2 bond with a concomitant contraction of the aryl-copper bond.

The IRC calculation reveals that the transition state directly leads to the decarboxylation product **2a**. The 2-fluorophenyl ring remains in the plane of the phenanthroline backbone. A weak interaction between a fluorine lone pair and the hydrogen at C(2) of the phenanthroline scaffold, which are separated by a distance of only 2.30 Å, additionally stabilizes this geometry. The phenanthroline coordination is even more asymmetrical than prior to decarboxylation, with Cu-N bonds of 2.0 and 2.4 Å, respectively.

Overall, the decarboxylation of 2-fluorobenzoate is moderately endothermic ($\Delta_r E_{\text{tot}} = 13.4 \text{ kcal mol}^{-1}$). Whereas in the previous, simplified calculations, the decarboxylation had come out endergonic, the present, more refined calculations predict it to be exergonic ($\Delta_r G_{\text{sov}} = -2.5 \text{ kcal mol}^{-1}$) at the calculated reaction temperature of $T = 443.15 \text{ K}$. Among other effects, the entropy gained by releasing CO_2 contributes more strongly to the Gibbs energy because we take into account the higher reaction temperature.

The pathway for the decarboxylation of 4-fluorobenzoate is slightly different. The activation barrier for the extrusion of CO_2 is considerably higher ($\Delta^\ddagger E_{\text{tot}} = 35.9 \text{ kcal mol}^{-1}$, $\Delta^\ddagger G_{\text{sov}} = 27.1 \text{ kcal mol}^{-1}$), which is in good agreement with the experimental findings that the protodecarboxylation of non-*ortho*-substituted benzoic acids requires higher temperatures and longer reaction times than that of *ortho*-substituted derivatives.^{21c} In contrast to the decarboxylation of 2-fluorobenzoate, the transition state originating from 4-fluorobenzoate [**1b-2b**] ‡ has a long aryl- CO_2 bond (2.06 Å) and a short aryl-copper bond (1.98 Å). This is indicative of a later transition state, which suggests that the decarboxylation is more endergonic for this isomer. The formation of **2b** is indeed strongly endothermic ($\Delta_r E_{\text{tot}} = 23.4 \text{ kcal mol}^{-1}$), but

due to the entropically favorable liberation of CO_2 , it is only slightly endergonic ($\Delta_r G_{\text{sov}} = 5.4 \text{ kcal mol}^{-1}$). The structure of the decarboxylation product **2a** differs from that for the *ortho*-derivative **2a** in that the 4-fluorophenyl ring is rotated out of the plane of the phenanthroline backbone at an angle of 55.7° , which may be caused by the absence of a hydrogen-fluorine interaction. Overall, the decarboxylation of non-*ortho*-substituted benzoates is both kinetically and thermodynamically significantly less favorable than the analogous reaction of *ortho*-substituted benzoates, a result that is in perfect agreement with experimental observations of protodecarboxylations.^{21c}

Oxidative Addition. The catalytic cycle of palladium starts with the oxidative addition of the aryl halide to a Pd^0 species. When starting from the anionic palladium monophosphine complex $[\text{Pd}(\text{PMe}_3)\text{Br}]^-$ (**12**), this reaction step proceeds with particular ease (Figure 4). Upon bringing the bromobenzene (**8**) closer to the palladium center, an η^2 - π -complex (**24**) forms via the transition state [**12-24**] ‡ . The activation barrier for this step is rather low for a process in which a bond forms between two separately solubilized molecules ($\Delta^\ddagger E_{\text{tot}} = 9.9 \text{ kcal mol}^{-1}$, $\Delta^\ddagger G_{\text{sov}} = 14.3 \text{ kcal mol}^{-1}$). This difference stems from entropy and solvation as discussed above. In the transition state, a bond between the palladium and the C(2) atom of bromobenzene has already formed (Pd-C(2): 2.31 Å), and the previously linear Br-Pd-P bond is bent at an angle of 125.4° . The forward motion along the reaction coordinate derived from the normal mode of the imaginary frequency (62 i cm^{-1}) is dominated by the shortening of the Pd-C(1) and Pd-C(2) distances with simultaneous decrease of the Br-Pd-P angle.

The IRC calculation leads to intermediate **24**, in which the palladium atom is coordinated almost symmetrically to the π -bond between C(1) and C(2) (Pd-C(1): 2.11 Å; Pd-C(2): 2.18 Å). The C-Br bond is slightly elongated from 1.92 to 2.00 Å, and the Br-Pd-P angle has decreased to 90.8° .

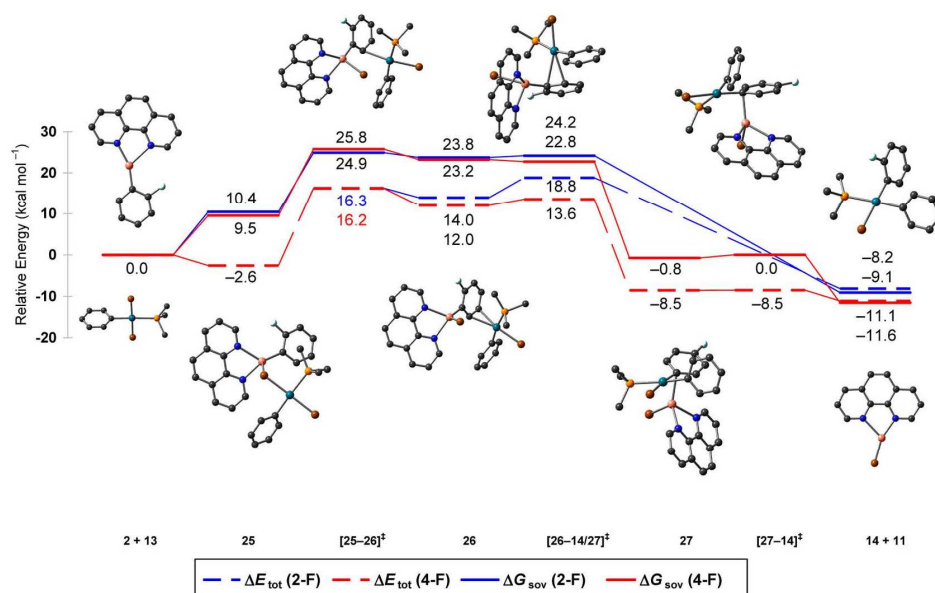


Figure 5. B3LYP/6-31+G(d) optimized structures for the transmetalation of the phenanthroline copper 2-fluorophenyl complex (**2**) with $[\text{Pd}(\text{PMe}_3)(\text{Ph})\text{Br}_2]^-$ (**13**); hydrogens are omitted for clarity. Energy and solution Gibbs energy profiles overlaid for the 2- and 4-fluorophenyl derivative. Color code: C, black; Br, brown; Cu, orange; F, turquoise; N, blue; P, yellow; Pd, green.

Further shortening of the Pd–C(1) bond leads to another transition state $[\mathbf{24}-\mathbf{13}]^\ddagger$, that has a Pd–C(1) bond length of 2.03 Å, and in which a Pd–Br bond is starting to form (2.89 Å). The C–Br bond is elongated to 2.22 Å. The forward motion along the reaction coordinate derived from the normal mode of the imaginary frequency (126 i cm^{-1}) is dominated by the movement of the palladium atom into the plane of the aromatic ring, resulting in a shortening of the Pd–C(1) bond, while the bromine moves out of this plane with concomitant elongation of the C–Br bond. The activation barrier for this step is rather low ($\Delta^\ddagger E_{\text{tot}} = 7.0 \text{ kcal mol}^{-1}$, $\Delta^\ddagger G_{\text{solv}} = 6.2 \text{ kcal mol}^{-1}$).

In the final oxidative addition product, the trimethylphosphino(phenyl)dibromopalladate **13**, the palladium is in a slightly distorted square-planar environment with the two bromine ligands *trans* to each other. The Pd–Br(1) and Pd–Br(2) bonds have almost the same lengths (2.54 and 2.52 Å), and the Pd–C distance amounts to 2.03 Å.

The overall oxidative addition process is strongly exothermic ($\Delta_r E_{\text{tot}} = -30.3 \text{ kcal mol}^{-1}$), and although two molecules are converted to one product, it remains exergonic ($\Delta_r G_{\text{solv}} = -18.1 \text{ kcal mol}^{-1}$). Under the reaction conditions of the decarboxylative coupling, the oxidative addition can be expected to proceed very smoothly.

Transmetalation. In the transmetalation step, the phenanthroline copper 2- or 4-fluorophenyl complex **2**, obtained by decarboxylation of copper 2- or 4-fluorophenyl benzoate, has to approach the palladium complex **13**, formed by the oxidative addition, in order to transfer the fluorophenyl group to the palladium center. One would expect to find that the actual transmetalation step would be preceded by the formation of an energetically favorable adduct between **2** and **13**, which would explain that this entropically unfavorable step takes place even at the low experimental concentrations of the two species.

We first sought for attractive interactions between **2a** and **13** by positioning the two fragments close to each other at various

angles and orientations. Whereas no energetically favorable interaction was found, e.g., when approaching the palladium and the π -system of the fluorophenyl ring, bringing palladium complex **13** into close proximity to the copper atom in **2a** via its bromine ligand results in the formation of a stable adduct (**25a**, Figure 5). The formation of a long Cu–Br(1) bond (2.82 Å) makes this step energetically favorable ($\Delta_r E_{\text{tot}} = -2.6 \text{ kcal mol}^{-1}$), which makes up for some of the high entropic hurdle and loss of solvation energy associated with forming an adduct at high reaction temperatures. In the present case, the amount of entropy lost is $33.4 \text{ cal K}^{-1} \text{ mol}^{-1}$, which at 443 K increases $\Delta_r G_{\text{solv}}$ by $14.8 \text{ kcal mol}^{-1}$. The dispersion interaction additionally stabilizes the adduct by $13.1 \text{ kcal mol}^{-1}$, whereas $9.1 \text{ kcal mol}^{-1}$ solvation energy is lost. Together, these factors turn a slightly exothermic step into a moderately endergonic one ($\Delta_r G_{\text{solv}} = 10.4 \text{ kcal mol}^{-1}$). The additional Cu–Br(1) bond changes the coordination environment at the copper center from a coordinatively unsaturated distorted trigonal planar arrangement to a distorted tetrahedral geometry ($\angle \text{Cu} - \text{Br} - \text{Pd} = 108.8^\circ$). The formation of the loose Cu–Br(1) contact (2.82 Å) does not lead to a significant elongation of the Pd–Br(1) bond (2.53 Å), and the geometry of the palladium fragment remains almost unchanged. The fluorophenyl group is bent outward slightly, but is not twisted. A transit scan from **25** with a stepwise elongation of the Cu–Br(1) bond revealed that in the gas phase, the encounter complex **25** is formed without a barrier.

Adduct **25** was found to be the entry point to a transmetalation pathway in which the bromine ligand is transferred from palladium to copper prior to transfer of the fluorophenyl group in the opposite direction. A search for alternative transmetalation pathways in which, for example, the transfer of the fluorophenyl group from Cu to Pd precedes that of the bromine ligand from Pd to Cu, did not yield any results.

This was to be expected in the absence of attractive interactions between the fluorophenyl group and the copper.

Shortening the Cu–Br(1) bond of **25a** to 2.54 Å leads to an energetically reasonable transition state $[25a-26a]^\ddagger$ ($\Delta^\ddagger E_{\text{tot}} = 18.9 \text{ kcal mol}^{-1}$, $\Delta^\ddagger G_{\text{sov}} = 14.5 \text{ kcal mol}^{-1}$). In $[25a-26a]^\ddagger$, the palladium is coordinated to the C(2) carbon of the fluorophenyl group over a rather long bond (2.59 Å), while the Pd–Br(1) bond is almost broken (3.65 Å). The tetrahedral environment at the copper is now more symmetrical than in adduct **25a**. The forward motion along the reaction coordinate derived from the normal mode of the imaginary frequency (30 i cm^{-1}) is dominated by the elongation of the Pd–Br(1) bond with a simultaneous shortening of the Pd–C(2) and Pd–C(3) distances. The IRC calculation confirms that this transition state leads to intermediate **26a**, in which the palladium atom is coordinated to the C(2)–C(3) π -bond in an almost symmetrical fashion (Pd–C(2): 2.48 Å; Pd–C(3): 2.52 Å). The Cu–Br(1) bond is slightly shortened to 2.51 Å. Intermediate **26a** is almost as high in energy as the transition state.

Starting from **25a**, no trajectory could be found along which the palladium would directly attack the C(1) carbon of the fluorophenyl group, so that the transfer of the bromine and of the fluorophenyl group would occur in a single step. This finding corresponds well with those for several oxidative addition and transmetalation pathways of other aromatic substrates, which also have been found to involve the intermediate formation of π -complexes to the C(2)–C(3) bond of the arene rings.^{24b,47}

Shortening the Pd–C(1) distance leads to a transition state $[26a-14a]^\ddagger$ across a rather low activation barrier ($\Delta^\ddagger E_{\text{tot}} = 4.8 \text{ kcal mol}^{-1}$, $\Delta^\ddagger G_{\text{sov}} = 0.4 \text{ kcal mol}^{-1}$). In $[26a-14a]^\ddagger$, the palladium atom has shifted to the C(1)–C(2) π -bond of the fluorophenyl group. The Pd–C(1) bond is slightly longer than the Pd–C(2) bond (Pd–C(1): 2.82 Å; Pd–C(2): 2.60 Å). The copper atom remains in the plane of the fluorophenyl ring, and the Cu–C(1) bond has the same length as in **26a** (1.96 Å). The distance between the copper and palladium atoms is reduced to only 3.30 Å. The forward motion along the reaction coordinate derived from the normal mode of the imaginary frequency (59 i cm^{-1}) is dominated by a lengthening of the Pd–C(2) bond with concomitant shortening of the Pd–C(1) and Cu–Pd bonds, resulting in the transfer of the fluorophenyl group from copper to palladium.

At first sight, it seemed counterintuitive that the copper atom would remain in the plane of the arene ring in transition state $[26a-14a]^\ddagger$, and that the Cu–C(1) bond length would not significantly contribute to the normal mode corresponding to the imaginary frequency. We would have expected a transition state structure in which the copper would already have moved out of the plane of the fluorophenyl ring and the Cu–C(1) bond would already have been elongated. We therefore investigated the pathway from $[26a-14a]^\ddagger$ to the transmetalation products **14a** + **11** in some detail by IRC calculations, followed by geometry optimizations. On the way downhill, we came across regions of the potential energy surface with molecular geometries meeting our above expectations, but found no stationary points. Instead, this process confirmed that the transition state $[26a-14a]^\ddagger$ indeed connects intermediate **26a** with the transmetalation products **14a** + **11**. The somewhat surprising structural features of the transition state are a consequence of its being very early, which conforms to the Hammond postulate.⁴⁸ Aryl transfer and separation into two fragments occur simultaneously in this final phase of the

transmetalation, which is therefore quite exothermic ($\Delta E_{\text{tot}} = -22.2 \text{ kcal mol}^{-1}$) and even more exergonic ($\Delta G_{\text{sov}} = -32.9 \text{ kcal mol}^{-1}$), because of the substantial gain in entropy and solvation energy.

The products of the transmetalation are the regenerated phenanthroline copper bromide catalyst **11**, which was already described in the anion exchange chapter, and the square-planar *cis*-diaryl palladium complex **14a**. Its Pd–C(1) bond length is further shortened to 2.04 Å, which is almost the same as that of the Pd–C(1') bond of 2.05 Å. Overall, the entire transmetalation starting from **2a** and **13** and leading to **11** and **14a** is moderately exothermic ($\Delta E_{\text{tot}} = -8.2 \text{ kcal mol}^{-1}$) and exergonic ($\Delta G_{\text{sov}} = -9.1 \text{ kcal mol}^{-1}$).

The reaction pathway for the transfer of the 4-fluorophenyl group from the aryl copper complex **2b** to the palladium complex **13** is different from that of the 2-fluorophenyl complex **2a**. Both the geometries and the energies of several structures involved are markedly different. Moreover, an additional intermediate is involved in the transmetalation for the 4-fluorophenyl derivative.

Adduct **25b** and the first transition state $[25b-26b]^\ddagger$ have closely related structural features and relative energies to their *ortho*-regioisomers. Compared to **26a**, intermediate **26b** is lower in energy by $-2.0 \text{ kcal mol}^{-1}$ and the Gibbs energy is lower by $-0.6 \text{ kcal mol}^{-1}$. According to our calculations, this can be attributed to the energy of solvation and explained with greater structural differences between these intermediates. After elongation of the Pd–Br contact in $[25-26]^\ddagger$, the 4-fluorophenyl group rotates around the Cu–C bond, which does not occur with the 2-fluorophenyl group. The structures of **26a** and **26b** provided in the Supporting Information are displayed with the fluorophenyl groups and coordinated palladium fragments in the same orientation. In **26a**, the phenanthroline points to the left and the bromine to the right of the copper. In **26b**, the phenanthroline points downward and the bromine upward. The Cu–Br bond in **26b** is somewhat longer (2.60 Å) than in $[25b-26b]^\ddagger$ (2.52 Å). The Pd–C(2) bond in **26b** is shorter by ca. 0.2 Å compared to the Pd–C(3) bond (Pd–C(2): 2.41 Å; Pd–C(3): 2.60 Å).

The energetic hurdle between **26b** and the transition state $[26b-27]^\ddagger$ amounts to $\Delta^\ddagger E_{\text{tot}} = 1.6 \text{ kcal mol}^{-1}$. This barrier is only one-third as high as that for the *ortho*-substituted derivative and can again be attributed to structural differences. The Pd–C(2) bond is slightly shorter (2.46 Å) than in $[26a-14a]^\ddagger$ (2.60 Å), and the distance between copper and palladium of 3.55 Å in $[26b-27]^\ddagger$ is longer compared to 3.30 Å in $[26a-14a]^\ddagger$.

In contrast to the *ortho*-intermediate, **26b** does not lead to the transmetalation products **14b** + **11** in a single step. It involves an additional intermediate **27** in which the palladium fragment is in a nearly square-planar environment. The palladium atom has almost moved into the plane of the fluorophenyl ring, and the Pd–C(1) bond has shortened to 2.10 Å. The copper atom has moved below the plane of the fluorophenyl ring but is still connected to its *ipso* carbon over a very long Cu–C(1) bond (2.32 Å). The Pd–C(1)–Cu angle of 77.8° is very small, so that the two transition metals are in close proximity to each other. The Pd–Cu distance is as short as 2.77 Å, which is smaller than the sum of their van der Waals radii (3.03 Å).⁴⁹ Completing the transmetalation from intermediate **27** requires only little activation energy (transition state $[27-14b]^\ddagger$; $\Delta^\ddagger E_{\text{tot}} = 0.0 \text{ kcal mol}^{-1}$, $\Delta^\ddagger G_{\text{sov}} = 0.8 \text{ kcal mol}^{-1}$), so that the existence or nonexistence of the intermediate virtually has

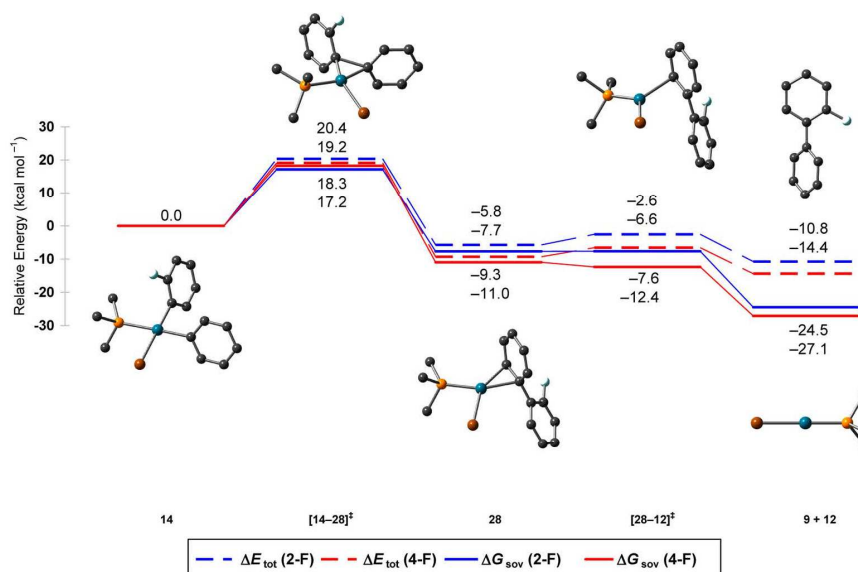


Figure 6. B3LYP/6-31+G(d) optimized structures for the reductive elimination of $[\text{Pd}(\text{PMe}_3)(2\text{-F-Ph})(\text{Ph})\text{Br}]^-$; hydrogens are omitted for clarity. Energy and solution Gibbs energy profiles overlaid for the 2- and 4-fluorophenyl derivative. Color code: C, black; Br, brown; F, turquoise; P, yellow; Pd, green.

no effect on the reactivity. Still, we invested some effort in finding a corresponding intermediate for the *ortho*-case. Thus, the optimized structure **27** was transformed into its *ortho*-derivative by replacing F by H and either of the two *o*-hydrogens by fluorine. However, for either of these structures, new geometry optimizations directly led to the transmetalation products. The existence of the intermediate **27** for the *para*- but not the *ortho*-case may be explained with electronic effects due to the fluorine substituent. The mesomeric effects of the fluorine substituent are comparable for the *ortho*- and *para*-positions, but the inductive effect on the *ipso* carbon of the fluorine in the *ortho*-position is certainly higher due to the smaller number of interjacent σ -bonds. In the 4-fluorophenyl ring, the electron-donating mesomeric effect of the fluorine predominates over the inductive effect and pushes sufficient electron density into the *ipso*-carbon to bind both transition metals simultaneously and lending stability to intermediate **27**. Contrarily, in the 2-fluorophenyl ring, the short-range electron-withdrawing inductive effect outweighs the mesomeric effect. The *ipso*-carbon thus lacks the electron density required to coordinate to palladium and copper at the same time.

Intermediate **27** features the shortest Pd–Cu distance (2.77 Å) observed in all these calculations. This begs the question whether there is an interaction or even a bond between copper and palladium. This is very difficult to answer with DFT calculations. Methods such as the analysis of the natural bond order (NBO), the bond critical point (BCP), or the shared electron number (SEN) with DFT are often regarded as inconclusive. Therefore, we looked for literature on bimetallic complexes with similarly short copper–palladium distances in which metal–metal interactions and bonds are discussed.

Kawamura et al. crystallized $[\text{Pd}_3(\text{S}_2\text{CN}^{\text{Pr}})_6\text{Cu}_2][\text{PF}_6]_2$ and found slightly longer Pd–Cu distances of 2.864(4) and 2.896(4) Å.⁵⁰ Their XPS binding studies suggest weak Pd–Cu bonding interactions. However, the authors were unable to prove the existence of direct Pd–Cu bonding. Peng and

Rohmer crystallized $[\text{Cu}_2\text{Pd}(\text{dpa})_4\text{Cl}_2]$ (dpa = dipyridylamine) with somewhat shorter Pd–Cu distances of 2.4971(3) and 2.5022(3) Å.⁵¹ For this complex, magnetic susceptibility measurements revealed an antiferromagnetic coupling between the two Cu^{II} metal centers connected to the Pd atom, which could be confirmed by powder EPR experiments, DFT calculations, and wave function theory calculations.⁵² Osakada et al. observed Pd–Cu distances of 2.462(1) and 2.632(1) Å in crystallized $[\text{Pd}(\mu\text{-CuI})(\text{Pd}(\text{dmpe}))_3(\mu_3\text{-GePh}_2)_3]$.⁵³ ^1H and $^{13}\text{C}\{^1\text{H}\}$ NMR experiments of the complex at various temperatures revealed that Cu forms a stable Pd–Cu bond to the core palladium and a labile Pd–Cu bond to one edge palladium. Because interactions or even bonds between copper and palladium could be proven for these complexes, which all possess short Pd–Cu distances in the same range as our intermediate **27**, we believe that attractive interactions between the copper and palladium atoms are at play also in the transmetalation step of decarboxylative cross-couplings.

Overall, our DFT results show that the transmetalation process is exothermic (*ortho*: $\Delta_r E_{\text{tot}} = -8.2 \text{ kcal mol}^{-1}$; *para*: $\Delta_r E_{\text{tot}} = -11.1 \text{ kcal mol}^{-1}$) as well as exergonic (*ortho*: $\Delta_r G_{\text{sov}} = -9.1 \text{ kcal mol}^{-1}$; *para*: $\Delta_r G_{\text{sov}} = -11.6 \text{ kcal mol}^{-1}$). However, the process starts with the formation of a bimetallic adduct that is endergonic (*ortho*: $\Delta_r G_{\text{sov}} = 10.4 \text{ kcal mol}^{-1}$; *para*: $\Delta_r G_{\text{sov}} = 9.5 \text{ kcal mol}^{-1}$). Furthermore, the transmetalation faces high activation barriers for its transition states that we will compare with those for the other elementary steps at the end of this section.

Reductive Elimination. In the reductive elimination step, the biaryl product **9** is liberated from the square-planar *cis*-diarylpalladium complex **14**, regenerating the initial palladium catalyst **12** (Figure 6). Both for the *ortho*- and the *para*-substituted model compounds, the overall process is moderately exothermic (*ortho*: $\Delta_r E_{\text{tot}} = -10.8 \text{ kcal mol}^{-1}$; *para*: $\Delta_r E_{\text{tot}} = -14.4 \text{ kcal mol}^{-1}$) and strongly exergonic (*ortho*: $\Delta_r G_{\text{sov}} =$

Scheme 8. Anionic Reaction Pathways Investigated for the Anion Exchange, Decarboxylation, and Adduct Formation

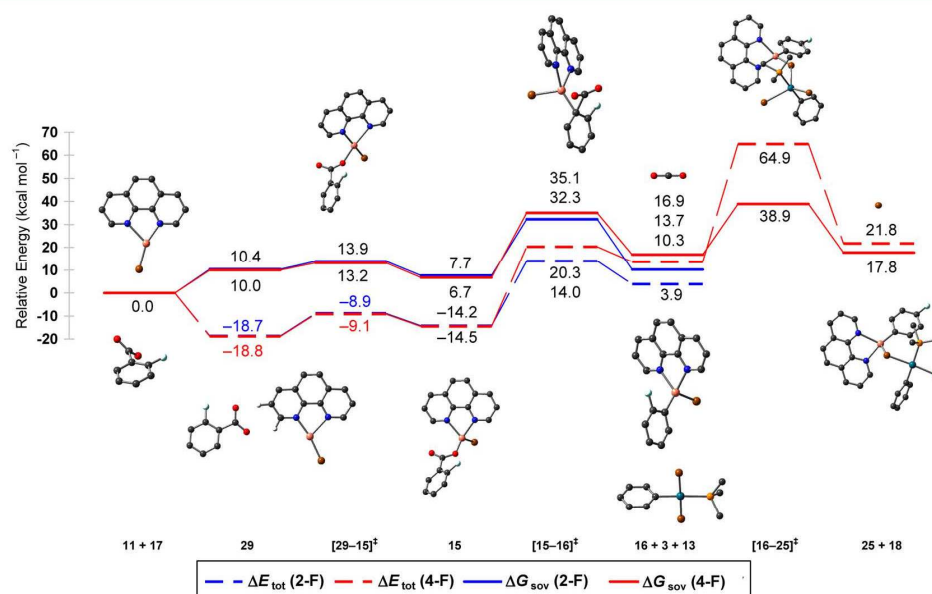
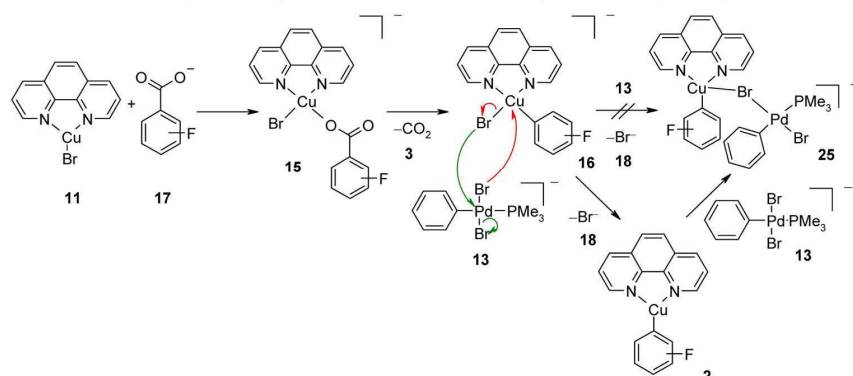


Figure 7. B3LYP/6-31+G(d) optimized structures for the anionic reaction pathway for anion exchange, decarboxylation, and adduct formation; hydrogens are omitted for clarity. Energy and solution Gibbs energy profiles overlaid for 2- and 4-fluorobenzoate. Color code: C, black; Br, brown; Cu, orange; F, turquoise; N, blue; O, red; P, yellow; Pd, green.

$-24.5 \text{ kcal mol}^{-1}$; *para*: $\Delta_{\text{r}}G_{\text{sov}} = -27.1 \text{ kcal mol}^{-1}$), since two molecules form from one.

Starting from **14a**, a first transition state $[14\text{a}-28\text{a}]^{\ddagger}$ was found by reducing the C(1) and C(1') distance between the two aromatic rings in the square-planar complex to 1.88 \AA . The barrier for its formation is comparatively low ($\Delta^{\ddagger}E_{\text{tot}} = 20.4 \text{ kcal mol}^{-1}$, $\Delta^{\ddagger}G_{\text{sov}} = 17.2 \text{ kcal mol}^{-1}$). The Pd–C bond lengths and the P–Pd–Br angle remain almost unchanged (Pd–C(1): 2.07 \AA ; Pd–C(1'): 2.11 \AA ; P–Pd–Br: 88.6°). The forward motion along the reaction coordinate derived from the normal mode of the imaginary frequency (306 i cm^{-1}) is dominated by a shortening of the aryl–aryl bond, while the angle between the planes of the aromatic rings is reduced.

An IRC calculation revealed that transition state $[14\text{a}-28\text{a}]^{\ddagger}$ connects structure **14a** with intermediate **28a**. In **28a**, the aryl–aryl bond is fully formed with a final length of 1.49 \AA , but the palladium remains η^2 -coordinated to the C(1')–C(2') bond of

the biaryl product (Pd–C(1'): 2.25 \AA ; Pd–C(2'): 2.17 \AA ; P–Pd–Br: 94.7°).

The energy barrier for the release of the Pd(0) catalyst **12** is very low ($\Delta^{\ddagger}E_{\text{tot}} = 3.2 \text{ kcal mol}^{-1}$, $\Delta^{\ddagger}G_{\text{sov}} = 0.03 \text{ kcal mol}^{-1}$). In the transition state $[28\text{a}-12\text{a}]^{\ddagger}$, which was found by increasing the distance between palladium and the phenyl ring, the palladium atom remains coordinated to C(2') over a distance of 2.35 \AA , and the P–Pd–Br angle has increased to 126.1° . The forward motion along the reaction coordinate derived from the normal mode of the imaginary frequency (54 i cm^{-1}) is dominated by a lengthening of the Pd–C bond with simultaneous opening of the P–Pd–Br angle (Pd–C(2'): 2.35 \AA ; P–Pd–Br: 126.1°).

A further IRC calculation showed that this transition state connects directly to the linear anionic monophosphine palladium complex **12** and the biaryl **9a**. In **9a**, the angle between the planes of the two aromatic rings amounts to 44.3° .

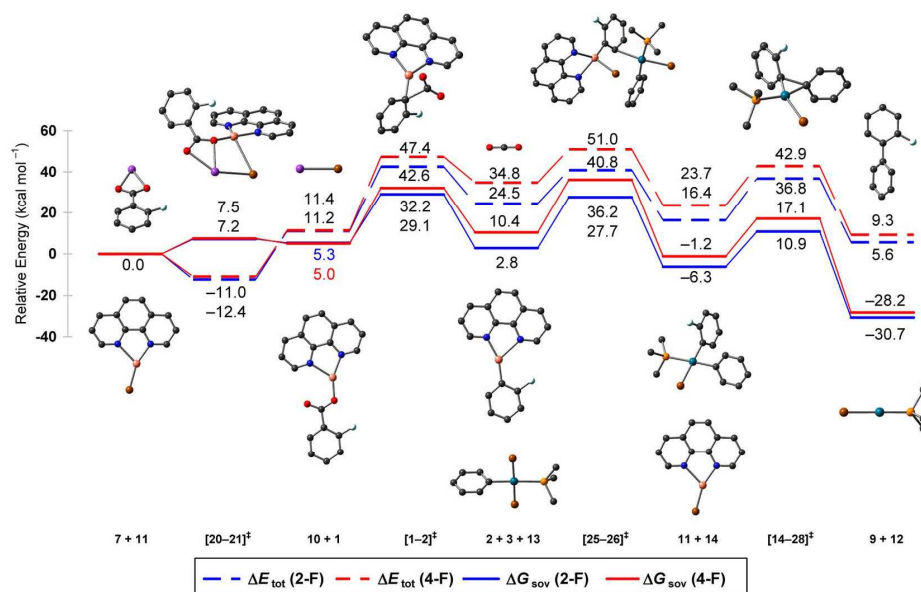


Figure 8. B3LYP/6-31+G(d) optimized structures for the simplified reaction profile; hydrogens are omitted for clarity. Energy and solution Gibbs energy profiles overlaid for the 2- and 4-fluorophenyl derivative. Color code: C, black; Br, brown; Cu, orange; F, turquoise; K, purple; N, blue; O, red; P, yellow; Pd, green.

As can be seen in Figure 6, the reaction pathway for the 4-fluorophenyl derivative is almost identical with that for the 2-derivative. The main activation barrier ($\Delta^\ddagger E_{\text{tot}} = 19.2$ kcal mol⁻¹, $\Delta^\ddagger G_{\text{soy}} = 18.3$ kcal mol⁻¹) and the imaginary frequency of the transition state $[14b-28b]^\ddagger$ (316 i cm⁻¹) are almost identical with those for the 2-derivative. In biaryl **9b**, the dihedral angle is slightly smaller than in **9a** (41.4° versus 44.3°), since the *o*-hydrogen requires less space than the fluorine atom.

Anionic Copper Cycle. In the transformations discussed above, all Cu^I intermediates were neutral and tricoordinated. An alternative pathway can be envisaged in which the carboxylate anion adds to copper complex **11** leading to a tetracoordinate anionic copper species, which after extrusion of CO₂ undergoes the transmetalation (Scheme 8). In this alternative pathway, the equivalent to the anion exchange step would be the coordination of the carboxylate **17** to the copper complex **11**. The resulting anionic copper complex **15** would decarboxylate to the anionic copper complex **16**. Complex **16** would then react with the palladium catalyst **13** in an associative substitution reaction to give adduct **25**, which would be the starting point for the transmetalation process. Alternatively to this associative pathway, one could also imagine that the bromide would decoordinate from **16** to give the fluorophenyl copper phenanthroline complex **2**, which would associate with **13** to give the adduct **25**. The energy and solution Gibbs energy profiles for the anionic pathway (**11** → **15** → **16** → **25**) are shown in Figure 7.

The formation of adduct **15a** from 2-fluorobenzoate **17a** and the copper complex **11** is exothermic ($\Delta_r E_{\text{tot}} = -14.2$ kcal mol⁻¹) in the gas phase and proceeds via an encounter complex **29a** and a transition state $[29a-15a]^\ddagger$. Due to the loss of entropy and solvation energy, this step is endergonic ($\Delta_r G_{\text{soy}} = 7.7$ kcal mol⁻¹), with a barrier ($\Delta^\ddagger G_{\text{soy}} = 13.9$ kcal mol⁻¹) that is higher than in the neutral anion exchange pathway (see Figure 2).

The anionic copper complex **15a** can then directly decarboxylate via transition state $[15a-16a]^\ddagger$, instead of first releasing the bromine ligand. The Gibbs activation energy of $\Delta^\ddagger G_{\text{soy}} = 24.6$ kcal mol⁻¹ is higher than that for the decarboxylation of the neutral phenanthroline copper 2-fluorobenzoate **1a** ($\Delta^\ddagger G_{\text{soy}} = 23.8$ kcal mol⁻¹).

Two pathways are imaginable for the associative substitution reaction of the anionic copper complex **16** with the palladium catalyst **13** each leading to formation of a bromine bridge between the two metals. One of the Pd-bound bromide ligands may attack the copper center and replace its bromide (red arrows, Scheme 8), or conversely the Cu-bound bromide may attack the palladium center with loss of a Pd-bound bromide (green arrows). For the first pathway, we were unable to find any feasible pathway in our DFT calculations. For the second, a transition state $[16b-25b]^\ddagger$ could be located only for the *p*-fluoro-substituted derivative. The activation barrier is very high ($\Delta^\ddagger E_{\text{tot}} = 51.2$ kcal mol⁻¹, $\Delta^\ddagger G_{\text{soy}} = 22.0$ kcal mol⁻¹). For the *ortho*-derivative **16a**, the only pathway we found required dissociation of the bromide. This dissociation of bromide is thermodynamically downhill for both the *ortho*- and the *para*-derivative (**16a/16b**), and leads to the phenanthroline copper fluorophenyl complex **2a/2b**, so that the neutral pathway is re-entered. When similar calculations were performed with potassium ions, we found direct elimination of KBr and a direct re-entry into the neutral pathway. Overall, the anionic complexes **15a/b** do not open up a pathway with a low energy profile that is more favorable for *ortho*- than for non-*ortho*-substituted benzoates and could explain why the former substrates react more readily in decarboxylative couplings.

Summary Assessment of the Catalytic Cycle. Improving a catalyst based on theoretical modeling requires a recipe for extracting the catalyst efficiency from the plethora of energetic data obtained in the calculations. The energetic span concept by Amatore and Jutand⁵⁴ says that the largest possible

rate and, correspondingly, the highest turnover number of the catalytic cycle is obtained for the lowest Gibbs energy span, which is the Gibbs energy difference between the highest transition state and lowest intermediate of the entire cycle. This concept has been refined by Kozuch and Shaik⁵⁵ by taking into account overall exergonicity. In our case, the situation is more complicated because of the two intertwined catalytic cycles, which join and separate at the transmetalation. The approximation behind the energy span concept is that the concentration c_i of a catalyst intermediate i is given by $c_i = c_0 \exp(-\Delta G_i/RT)$, where c_0 is the overall catalyst concentration and ΔG_i the Gibbs energy of i with respect to the most stable intermediate, where most of the catalyst is trapped. Both our calculated energy profile and our experience with related catalytic reactions tell us that the palladium catalyst is capable of providing the oxidative addition product **13** at a much faster rate than the cross-coupling proceeds, and according to our calculations, the oxidative addition is exergonic ($\Delta_r G = -18.1$ kcal mol⁻¹). Therefore, we can simplify the kinetic model by assuming that the stationary concentration of **13** is given by the overall amount of palladium catalyst. In other words, we consider a reaction with a single catalytic cycle in which one of the educts is **13** at its catalytic concentration, instead of the aryl bromide **8** at a stoichiometric concentration. We then apply the energetic span concept to the energy profile derived from this single cycle, which involves four steps (anion exchange, CO₂ extrusion, transmetalation, reductive elimination). Since none of these steps feature an intermediate lower in Gibbs energy than either their educts or their products, we need only consider a single effective activation energy given by the highest transition state of each step. This resulting simplified energy diagram is shown in Figure 8.

The energy barriers of this simplified reaction profile with the highest barrier at $\Delta^\ddagger G_{\text{sov}} = 36.2$ kcal mol⁻¹ are consistent with a reaction that takes place at temperatures around 160 °C.

For the *ortho*-case, the largest Gibbs energy span, which represents the apparent activation energy of the overall cycle, is between the starting materials (**7a** + **11**) and the decarboxylation transition state [**1a-2a**][‡] (29.1 kcal mol⁻¹). For the *para*-case, the largest Gibbs energy span is between the starting materials (**7b** + **11**) and the transmetalation transition state [**25b-26b**][‡] (36.2 kcal mol⁻¹). This implies that for the *ortho*-case, the decarboxylation transition state and for the *para*-case, the transmetalation transition state is the rate-limiting transition state. Considering each step individually, one would come to a different conclusion since for the *ortho*-case, the barrier is lower in the decarboxylation (23.8 kcal mol⁻¹) compared to the transmetalation (24.9 kcal mol⁻¹), whereas for the *para*-case the barrier is higher in the decarboxylation (27.1 kcal mol⁻¹) than in the transmetalation (25.8 kcal mol⁻¹). This contrast stems from the exergonicity/endergonicity of the decarboxylation step as its products are the starting point for the subsequent transmetalation. For the *ortho*-case the decarboxylation is exergonic by -2.5 kcal mol⁻¹ which decreases the starting point and the highest transition state of the transmetalation, while for the *para*-case the decarboxylation is endergonic by 5.4 kcal mol⁻¹, which increases the starting point and the highest transition state of the transmetalation, which explains the outcome of the overall reaction profile. For the *ortho*-case the difference between the heights of the decarboxylation (29.1 kcal mol⁻¹) and transmetalation transition state (27.7 kcal mol⁻¹) lies within the inaccuracy of the computational method. It is safe to say that the

decarboxylation and the transmetalation are so similar in energy that it probably depends on the individual substrate which of these two steps will be rate-determining.

As discussed above, the reason for the high overall barrier of the transmetalation is the entropic penalty associated with forming an adduct of two species present only in catalytic amounts, together with a loss in solvation energy. The accuracy of some contributions to the activation energy such as solvent effects is difficult to assess. However, such systematic errors are likely to cancel out when calculating the *para/ortho* difference in the Gibbs energy span. This difference is considerable (7.1 kcal mol⁻¹), and agrees with the experimental observation that 4-fluorobenzoate is substantially less reactive than its *ortho*-isomer. Interestingly, the largest contribution to this difference stems from the exer-/endergonicity of the decarboxylation step, where the difference between *para* and *ortho* is $\Delta\Delta_r G_{\text{sov}} = 7.6$ kcal mol⁻¹.

Based on this profile, it can also be understood why the presence of halide anions can affect the reaction rate. The presence of excess bromide shifts the equilibrium of the anion exchange step to the side of the copper bromide so that less copper carboxylate is available. If for a given substrate the decarboxylation is the rate-determining step in a decarboxylative cross-coupling, the presence of excess bromide should have a similar effect, because it increases the energy span between **7** + **11** and [**1-2**][‡] + **10** by about 3 kcal mol⁻¹.

Experimental Studies. The above DFT studies suggest that the transmetalation is rate-limiting for substrates that decarboxylate comparatively easily. Bidentate ligands designed to bridge the two metals and bring them into close spatial proximity can be expected to facilitate this step. To test this hypothesis, we first searched for a benzoic acid that decarboxylates with particular ease. We performed a series of protodecarboxylation experiments in which various benzoic acids **22** were heated to 100 °C in the presence of 5 mol % Cu₂O and 10 mol % 1,10-phenanthroline (Table 1). No

Table 1. Protodecarboxylation of Benzoic Acids^a

entry	carboxylic acid	R	t/h	product	yield/%
1	22a	2-F	6	23	3
2	22b	4-F	6	23	0
3	22c	2-NO ₂	6	30	64
4	22d	4-NO ₂	6	30	0
5	22c	2-NO ₂	24	30	99

^aReaction conditions: 0.5 mmol of carboxylic acid, 5 mol % Cu₂O, 10 mol % 1,10-Phen, 2.0 mL of NMP, 100 °C, GC yield after calibration.

conversion was observed at this low temperature for most carboxylic acids tested, including 2- and 4-fluorobenzoic acid (**22a** or **22b**) (entries 1 and 2). However, 2-nitrobenzoic acid (**22c**) was smoothly converted into nitrobenzene (**30**) in near-quantitative yield (entry 5).

It could thus be expected that the decarboxylation is not the rate-limiting step in a decarboxylative cross-coupling of 2-nitrobenzoic acid (**22c**) at 100 °C. We next performed various decarboxylative couplings at this temperature. Among all aryl electrophiles tested, triflates were the sole substrates to provide

Table 2. Decarboxylative Cross-Couplings with Monodentate and Bridging Ligands^a

entry	carboxylate	R	temp/°C	L	product	yield/%
1	7c	2-NO ₂	100	P(<i>p</i> -Tol) ₃	32c	9
2	7d	4-NO ₂	100	P(<i>p</i> -Tol) ₃	32d	0
3 ^b	7c	2-NO ₂	170	P(<i>p</i> -Tol) ₃	32c	84 (91) ^{7a}
4	7c	2-NO ₂	100	L1	32c	0
5	7c	2-NO ₂	100	L2	32c	0
6	7c	2-NO ₂	100	L3	32c	0
7	7c	2-NO ₂	100	L4	32c	40
8 ^c	7c	2-NO ₂	100	L4	32c	88

^aReaction conditions: 0.5 mmol of potassium carboxylate, 1 mmol of triflate, 5 mol % Cu₂O, 10 mol % 1,10-Phen, 2 mol % PdL₂, 6 mol % L, 2.0 mL of NMP, 100 °C, 24 h, GC yield after calibration. ^b1 mmol of potassium carboxylate, 2 mmol of triflate, 5 mol % Cu₂O, 10 mol % 1,10-Phen, 2 mol % PdL₂, 6 mol % P(*p*-Tol)₃, 4.0 mL of NMP, 170 °C, 1 h, GC yield after calibration, isolated yield in parentheses. ^c0.75 mmol of potassium carboxylate, 0.5 mmol of triflate, 5 mol % Cu₂O, 10 mol % 1,10-Phen, 3 mol % Pd(acac)₂, 6 mol % L4, 4.0 mL of NMP, 100 °C, 24 h, GC yield after calibration.

the coupling products in small amounts. For this reason, we investigated the coupling of 4-chlorophenyl triflate (**31**) with several potassium nitrobenzoates **7** as the model systems. With the best known catalyst system (Table 2), no conversion was observed in the coupling of potassium 4-nitrobenzoate (**7d**) with 4-chlorophenyl triflate (**31**) (entry 2), and potassium 2-nitrobenzoate (**7c**) gave less than 10% of 4-chloro-2'-nitrobiphenyl (**32c**) (entry 1). According to the literature, cross-couplings of aryl triflates with potassium benzoates with Cu/Pd systems and monodentate *p*-tolylphosphine have to be performed at 170 °C to give high yields.^{7a,b}

We then replaced the *p*-tolylphosphine ligand by various bidentate P,N-ligands (Figure 9).^{9,56} Among these, the

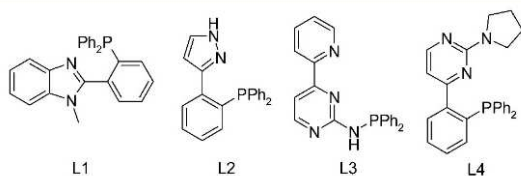


Figure 9. Bidentate P,N-ligands.

aminopyrimidinyl phosphines, especially ligand L4, developed by Thiel et al. in the context of other coupling reactions were most effective (entry 7).^{56c} After slight modifications to the reaction conditions, the coupling product **32c** was detected in high yield (88%) already at 100 °C (entry 8).

Lowering the reaction temperature by as much as 70 °C is a decisive improvement over the state of the art, which we attribute to the ability of this ligand to bring copper and palladium into close proximity and thus assist the transmetalation step. The presence of bimetallic Cu–Pd complexes was confirmed by ESI-MS investigations of the reaction mixture, suggesting that their formation is no longer rate-determining.⁵⁸ Further experimental studies with the bidentate ligands, including the structural investigation of Cu/Pd adducts detected by ESI-MS, are underway. We are convinced that the concept of bringing the two metals together by bridging ligands will allow reaching new levels of efficiency in decarboxylative couplings of activated benzoates.

Conclusions and Outlook. The geometries and energies of all starting materials, products, intermediates, and transition states of the catalytic cycle were calculated for the decarboxylative cross-coupling of potassium 2- and 4-fluorobenzoate with bromobenzene in the presence of a catalyst system consisting of copper(I)/1,10-phenanthroline and the anionic monophosphine palladium complex [Pd(PMe₃)Br][−]. Among all pathways investigated, a catalytic cycle via neutral copper complexes was found to be most favorable. It consists of a carboxylate–bromide exchange at the copper center to give an uncharged copper carboxylate, followed by a decarboxylation step in which an organocopper species is generated. A palladium species that has been formed by oxidative addition of the aryl electrophile to a low-valent palladium(0) species accepts the aryl group from the copper in the subsequent transmetalation step, which links the catalytic cycles of the copper and palladium catalysts. The resulting diarylpalladium species undergoes reductive elimination, releasing the biaryl product and regenerating the palladium(0) species (Scheme 6).

Based on realistic assumptions on the inherent accuracy of these calculations, the energetic span model cannot unambiguously decide whether the decarboxylation or the transmetalation is rate-determining. This implies that depending on the substrate, either step can pose the main limitation in the catalyst performance. This is in sharp contrast to the current opinion that it is only the decarboxylation step that needs to be addressed in the catalyst improvement. The calculations also do not support the hypothesis that the difference in reactivity between *ortho*- and non-*ortho*-substituted carboxylates in the reaction with aryl halides is caused by the anion exchange step. The low reactivity of the latter is probably caused by the higher barrier of the decarboxylation process, which is further increased in relation to the starting material if excess halide salt is present.

In the transmetalation, the electronic activation energy is not overly high. It is the free energy loss in the initial adduct formation that makes it difficult. This result suggests that future research aimed at further improving the catalyst should also target the transmetalation and not only the decarboxylation step. This was confirmed by an experimental study, in which

the reaction temperature of a decarboxylative coupling was lowered by 70 °C by a P,N-ligand designed to facilitate adduct formation between copper and palladium. In combination with these experimental findings, the mechanistic studies presented herein are likely to induce a paradigm shift in the development of more active catalyst generations for decarboxylative cross-coupling reactions.

■ ASSOCIATED CONTENT

● Supporting Information

Energies, graphical representations, geometrical parameters and Cartesian coordinates of all DFT-optimized structures. This material is available free of charge via the Internet at <http://pubs.acs.org>.

■ AUTHOR INFORMATION

Corresponding Author

goossen@chemie.uni-kl.de; vanwullen@chemie.uni-kl.de

Notes

The authors declare no competing financial interest.

■ ACKNOWLEDGMENTS

We thank W. R. Thiel for help with the DFT calculations and for providing P,N-ligands, K. Goßen for help proofreading the manuscript, and M. F. Grünberg for technical assistance. We also thank the DFG (GO 853/5-2 and SFB-TRR 88 “3Met”) and Landesgraduiertenförderung Rheinland-Pfalz (fellowship to A.F.) for funding.

■ REFERENCES

- (1) (a) Nilsson, M. *Acta Chem. Scand.* **1966**, *20*, 423–426. (b) Nilsson, M.; Ullenius, C. *Acta Chem. Scand.* **1968**, *22*, 1998–2002. (c) Chodowska-Palicka, J.; Nilsson, M. *Acta Chem. Scand.* **1970**, *24*, 3353–3361. (d) Shimizu, I.; Yamada, T.; Tsuji, J. *Tetrahedron Lett.* **1980**, *21*, 3199–3202. (e) Tsuji, J.; Yamada, T.; Minami, I.; Yuhara, M.; Nisar, M.; Shimizu, I. *J. Org. Chem.* **1987**, *52*, 2988–2995. (f) Myers, A. G.; Tanaka, D.; Mannion, M. R. *J. Am. Chem. Soc.* **2002**, *124*, 11250–11251. (g) Tanaka, D.; Myers, A. G. *Org. Lett.* **2004**, *6*, 433–436. (h) Tanaka, D.; Romeril, S. P.; Myers, A. G. *J. Am. Chem. Soc.* **2005**, *127*, 10323–10333.
- (2) Goossen, L. J.; Deng, G.; Levy, L. M. *Science* **2006**, *313*, 662–664.
- (3) (a) Rudolphi, F.; Song, B.; Goossen, L. J. *Adv. Synth. Catal.* **2011**, *353*, 337–342. (b) Collet, F.; Song, B.; Rudolphi, F.; Goossen, L. J. *Eur. J. Org. Chem.* **2011**, 6486–6501.
- (4) (a) Goossen, L. J.; Rudolphi, F.; Oppel, C.; Rodríguez, N. *Angew. Chem.* **2008**, *120*, 3085–3088; *Angew. Chem., Int. Ed.* **2008**, *47*, 3043–3045. (b) Grünberg, M. F.; Goßen, L. J. *J. Organomet. Chem.* **2013**, *744*, 140–143.
- (5) Goossen, L. J.; Rodríguez, N.; Melzer, B.; Linder, C.; Deng, G.; Levy, L. M. *J. Am. Chem. Soc.* **2007**, *129*, 4824–4833.
- (6) Goossen, L. J.; Zimmermann, B.; Knauber, T. *Angew. Chem.* **2008**, *120*, 7211–7214; *Angew. Chem., Int. Ed.* **2008**, *47*, 7103–7106.
- (7) (a) Goossen, L. J.; Rodríguez, N.; Linder, C. *J. Am. Chem. Soc.* **2008**, *130*, 15248–15249. (b) Goossen, L. J.; Linder, C.; Rodríguez, N.; Lange, P. P. *Chem.—Eur. J.* **2009**, *15*, 9336–9349. (c) Goossen, L. J.; Lange, P. P.; Rodríguez, N.; Linder, C. *Chem.—Eur. J.* **2010**, *16*, 3906–3909.
- (8) Goossen, L. J.; Rodríguez, N.; Lange, P. P.; Linder, C. *Angew. Chem.* **2010**, *122*, 1129–1132; *Angew. Chem., Int. Ed.* **2010**, *49*, 1111–1114.
- (9) Song, B.; Knauber, T.; Goossen, L. J. *Angew. Chem.* **2013**, *125*, 3026–3030; *Angew. Chem., Int. Ed.* **2013**, *52*, 2954–2958.
- (10) Shang, R.; Fu, Y.; Wang, Y.; Xu, Q.; Yu, H. Z.; Liu, L. *Angew. Chem.* **2009**, *121*, 9514–9518; *Angew. Chem., Int. Ed.* **2009**, *48*, 9350–9354.

- (11) Sun, Z. M.; Zhao, P. *Angew. Chem.* **2009**, *121*, 6854–6858; *Angew. Chem., Int. Ed.* **2009**, *48*, 6726–6730.
- (12) Weaver, J. D.; Recio, A., III; Grenning, A. J.; Tunge, J. A. *Chem. Rev.* **2010**, *111*, 1846–1913.
- (13) (a) Peschko, C.; Winkhofer, C.; Steglich, W. *Chem.—Eur. J.* **2000**, *6*, 1147–1152. (b) Forgione, P.; Brochu, M. C.; St-Onge, M.; Thesen, K. H.; Bailey, M. D.; Bilodeau, F. *J. Am. Chem. Soc.* **2006**, *128*, 11350–11351. (c) Bilodeau, F.; Brochu, M. C.; Guimond, N.; Thesen, K. H.; Forgione, P. *J. Org. Chem.* **2010**, *75*, 1550–1560. (d) Miyasaka, M.; Fukushima, A.; Satoh, T.; Hirano, K.; Miura, M. *Chem.—Eur. J.* **2009**, *15*, 3674–3677. (e) Miyasaka, M.; Hirano, K.; Satoh, T.; Miura, M. *Adv. Synth. Catal.* **2009**, *351*, 2683–2688. (f) Arroyave, F. A.; Reynolds, J. R. *Org. Lett.* **2010**, *12*, 1328–1331.
- (14) (a) Moon, J.; Jeong, M.; Nam, H.; Ju, J.; Moon, J. H.; Jung, H. M.; Lee, S. *Org. Lett.* **2008**, *10*, 945–948. (b) Moon, J.; Jang, M.; Lee, S. *J. Org. Chem.* **2009**, *74*, 1403–1406. (c) Kim, H.; Lee, P. H. *Adv. Synth. Catal.* **2009**, *351*, 2827–2832. (d) Park, K.; Bae, G.; Moon, J.; Choe, Y.; Song, K. H.; Lee, S. *J. Org. Chem.* **2010**, *75*, 6244–6251. (e) Zhang, W.-W.; Zhang, X.-G.; Li, J.-H. *J. Org. Chem.* **2010**, *75*, 5259–5264. (f) Zhao, D.; Gao, C.; Su, X.; He, Y.; You, J.; Xue, Y. *Chem. Commun.* **2010**, 46, 9049–9051. (g) Park, K.; Bae, G.; Park, A.; Kim, Y.; Choe, J.; Song, K. H.; Lee, S. *Tetrahedron Lett.* **2011**, *52*, 576–580. (h) Park, A.; Park, K.; Kim, Y.; Lee, S. *Org. Lett.* **2011**, *5*, 944–947.
- (15) Shang, R.; Fu, Y.; Li, J. B.; Zhang, S. L.; Guo, Q. X.; Liu, L. *J. Am. Chem. Soc.* **2009**, *131*, 5738–5739.
- (16) Yin, L.; Kanai, M.; Shibasaki, M. *J. Am. Chem. Soc.* **2009**, *131*, 9610–9611.
- (17) (a) Zhang, S. L.; Fu, Y.; Shang, R.; Guo, Q. X.; Liu, L. *J. Am. Chem. Soc.* **2010**, *132*, 638–646. (b) Hu, P.; Kan, J.; Su, W. P.; Hong, M. C. *Org. Lett.* **2009**, *11*, 2341–2344. (c) Fu, Z.; Huang, S.; Su, W.; Hong, M. *Org. Lett.* **2010**, *12*, 4992–4995. (d) Sun, Z.-M.; Zhang, J.; Zhao, P. *Org. Lett.* **2010**, *12*, 992–995. (e) Goossen, L. J.; Zimmermann, B.; Knauber, T. *Beilstein J. Org. Chem.* **2010**, *6*, 43–51.
- (18) (a) Voutchkova, A.; Coplin, A.; Leadbeater, N. E.; Crabtree, R. H. *Chem. Commun.* **2008**, 6312–6314. (b) Wang, C. Y.; Piel, I.; Glorius, F. *J. Am. Chem. Soc.* **2009**, *131*, 4194–4195. (c) Cornella, J.; Lu, P.; Larrosa, I. *Org. Lett.* **2009**, *11*, 5506–5509. (d) Zhang, F.; Greaney, M. F. *Angew. Chem.* **2010**, *122*, 2828–2831; *Angew. Chem., Int. Ed.* **2010**, *49*, 2768–2771.
- (19) (a) Gledhill, A. P.; McCall, C. J.; Threadgill, M. D. *J. Org. Chem.* **1986**, *51*, 3196–3201. (b) Huang, W. H.; Wang, M. L.; Yue, H. *Synthesis* **2008**, 1342–1344. (c) Bi, H.-P.; Zhao, L.; Liang, Y.-M.; Li, C.-J. *Angew. Chem.* **2009**, *121*, 806–809; *Angew. Chem., Int. Ed.* **2009**, *48*, 792–795. (d) Bi, H.-P.; Chen, W.-W.; Liang, Y.-M.; Li, C.-J. *Org. Lett.* **2009**, *11*, 3246–3249.
- (20) (a) Duan, Z. Y.; Ranjit, S.; Zhang, P. F.; Liu, X. G. *Chem.—Eur. J.* **2009**, *15*, 3666–3669. (b) Jia, W.; Jiao, N. *Org. Lett.* **2010**, *12*, 2000–2003. (c) Ranjit, S.; Duan, Z.; Zhang, P.; Liu, X. *Org. Lett.* **2010**, *12*, 4134–4136.
- (21) (a) President’s Information Technology Advisory Committee. *Computational Science: Ensuring America’s Competitiveness*; Arlington, VA, 2005. (b) Mpourmpakis, G.; Vlachos, D. G. *MRS Bull.* **2011**, *36*, 211–215. and references therein (c) Goossen, L. J.; Rodríguez, N.; Linder, C.; Lange, P. P.; Fromm, A. *ChemCatChem* **2010**, *2*, 430–442. (d) Dudnik, A. S.; Xia, Y.; Li, Y.; Gevorgyan, V. *J. Am. Chem. Soc.* **2010**, *132*, 7645–7655.
- (22) Goossen, L. J.; Thiel, W. R.; Rodríguez, N.; Linder, C.; Melzer, B. *Adv. Synth. Catal.* **2007**, *349*, 2241–2246.
- (23) (a) Braga, A. A. C.; Ujaque, G.; Maseras, F. *Organometallics* **2006**, *25*, 3647–3658. and references therein (b) Kozuch, S.; Shaik, S.; Jutand, A.; Amatore, C. *Chem.—Eur. J.* **2004**, *10*, 3072–3080. (c) Kozuch, S.; Amatore, C.; Jutand, A.; Shaik, S. *Organometallics* **2005**, *24*, 2319–2330.
- (24) (a) Goossen, L. J.; Koley, D.; Hermann, H.; Thiel, W. *J. Am. Chem. Soc.* **2005**, *127*, 11102–11114. (b) Goossen, L. J.; Koley, D.; Hermann, H.; Thiel, W. *Organometallics* **2006**, *25*, 54–67.

- (25) Keith, J. A.; Behenna, D. C.; Mohr, J. T.; Ma, S.; Marinescu, S. C.; Oxgaard, J.; Stoltz, B. M.; Goddard, W. A., III *J. Am. Chem. Soc.* **2007**, *129*, 11876–11877.
- (26) Shang, R.; Xu, Q.; Jiang, Y.-Y.; Wang, Y.; Liu, L. *Org. Lett.* **2010**, *12*, 1000–1003.
- (27) Xie, H.; Lin, F.; Lei, Q.; Fang, W. *Organometallics* **2013**, *32*, 6957–6968.
- (28) Hackenberger, D.; Song, B.; Grünberg, M. F.; Farsadpour, S.; Taghizadeh Ghoochany, L.; Menges, F.; Burkhardt, L.; Niedner-Schatteburg, G.; Thiel, W. R.; Goossen, L. J., *unpublished results*.
- (29) Recently, related studies have investigated the transfer of an aryl group from palladium to gold: Perez-Temprano, M. H.; Casares, J. A.; de Lera, A. R.; Alvarez, R.; Espinet, P. *Angew. Chem., Int. Ed.* **2012**, *51*, 4917–4920.
- (30) (a) Gaussian 03, Revision E.01; Gaussian, Inc.: Wallingford, CT, 2004. (b) Gaussian 09, Revision D.01; Gaussian, Inc.: Wallingford, CT, 2013; for full citations see the Supporting Information.
- (31) (a) Stephens, P. J.; Devlin, F. J.; Chabalowski, C. F.; Frisch, M. J. *J. Phys. Chem.* **1994**, *98*, 11623–11627. (b) Becke, A. D. *J. Chem. Phys.* **1993**, *98*, 5648–5652. (c) Becke, A. D. *Phys. Rev. A* **1988**, *38*, 3098–3100. (d) Lee, C.; Yang, W.; Parr, R. G. *Phys. Rev. B* **1988**, *37*, 785–789.
- (32) (a) Ditchfield, R.; Hehre, W. J.; Pople, J. A. *J. Chem. Phys.* **1971**, *54*, 724–728. (b) Hehre, W. J.; Ditchfield, R.; Pople, J. A. *J. Chem. Phys.* **1972**, *56*, 2257–2261. (c) Hariharan, P. C.; Pople, J. A. *Theor. Chim. Acta* **1973**, *28*, 213–222. (d) Clark, T.; Chandrasekhar, J.; Spitznagel, G. W.; Schleyer, P. v. R. *J. Comput. Chem.* **1983**, *4*, 294–301. (e) Rassolov, V. A.; Pople, J. A.; Ratner, M. A.; Windus, T. L. *J. Chem. Phys.* **1998**, *109*, 1223–1229. (f) Binning, R. C., Jr.; Curtiss, L. A. *J. Comput. Chem.* **1990**, *11*, 1206–1216. (g) Dunning, T. H. *J. Chem. Phys.* **1977**, *66*, 1382–1383.
- (33) (a) Dolg, M.; Wedig, U.; Stoll, H.; Preuss, H. *J. Chem. Phys.* **1987**, *86*, 866–872. (b) Andrae, D.; Häußermann, U.; Dolg, M.; Stoll, H.; Preuss, H. *Theor. Chim. Acta* **1990**, *77*, 123–141.
- (34) (a) Peng, C.; Schlegel, H. B. *Isr. J. Chem.* **1994**, *33*, 449–454. (b) Peng, C.; Ayala, P. Y.; Schlegel, H. B.; Frisch, M. J. *J. Comput. Chem.* **1996**, *17*, 49–56.
- (35) (a) Fukui, K. *Acc. Chem. Res.* **1981**, *14*, 363–368. (b) Hratchian, H. P.; Schlegel, H. B. In *Theory and Applications of Computational Chemistry: The First 40 Years*; Dykstra, C. E., Frenking, G., Kim, K. S., Scuseria, G., Eds.; Elsevier: Amsterdam, The Netherlands, 2005; pp 195–249. (c) Hratchian, H. P.; Schlegel, H. B. *J. Chem. Phys.* **2004**, *120*, 9918–9924. (d) Hratchian, H. P.; Schlegel, H. B. *J. Chem. Theory Comput.* **2005**, *1*, 61–69.
- (36) (a) Krishnan, R.; Binkley, J. S.; Seeger, R.; Pople, J. A. *J. Chem. Phys.* **1980**, *72*, 650–654. (b) Curtiss, L. A.; McGrath, M. P.; Blaudeau, J.-P.; Davis, N. E.; Binning, R. C.; Radom, L. *J. Chem. Phys.* **1995**, *103*, 6104–6113. (c) Blaudeau, J.-P.; McGrath, M. P.; Curtiss, L. A.; Radom, L. *J. Chem. Phys.* **1997**, *107*, 5016–5021.
- (37) Weigend, F.; Ahlrichs, R. *Phys. Chem. Chem. Phys.* **2005**, *7*, 3297–3305.
- (38) (a) Barone, V.; Cossi, M. *J. Phys. Chem. A* **1998**, *102*, 1995–2001. (b) Cossi, M.; Rega, N.; Scalmani, G.; Barone, V. *J. Comput. Chem.* **2003**, *24*, 669–681.
- (39) (a) Klamt, A.; Schüürmann, G. *J. Chem. Soc., Perkin Trans. 2* **1993**, 799–805. (b) Schäfer, A.; Klamt, A.; Sattel, D.; Lohrenz, J. C. W.; Eckert, F. *Phys. Chem. Chem. Phys.* **2000**, *2*, 2187–2193.
- (40) Wong, M. W. *Chem. Phys. Lett.* **1996**, *256*, 391–399.
- (41) Murrieta-Guevara, F.; Romero-Martinez, A.; Trejo, A. *Fluid Phase Equilib.* **1988**, *44*, 105–115.
- (42) Johnson, E. R.; Mackie, I. D.; DiLabio, G. A. *J. Phys. Org. Chem.* **2009**, *22*, 1127–1135.
- (43) Grimme, S.; Antony, J.; Ehrlich, S.; Krieg, H. *J. Chem. Phys.* **2010**, *132*, 154104.
- (44) Riley, K. E.; Vondrasek, J.; Hobza, P. *Phys. Chem. Chem. Phys.* **2007**, *9*, 5555–5560.
- (45) GaussView 5.0.8; Gaussian, Inc.: Wallingford, CT, 2008.
- (46) See the Supporting Information for details.
- (47) (a) Goossen, L. J.; Koley, D.; Hermann, H.; Thiel, W. *Chem. Commun.* **2004**, 2141–2143. (b) Goossen, L. J.; Koley, D.; Hermann, H.; Thiel, W. *Organometallics* **2005**, *24*, 2398–2410.
- (48) Hammond, G. S. *J. Am. Chem. Soc.* **1955**, *77*, 334–338.
- (49) Bondi, A. J. *Phys. Chem.* **1964**, *68*, 441–451.
- (50) Ebihara, M.; Tokoro, K.; Maeda, M.; Ogami, M.; Imaeda, K.; Sakurai, K.; Masuda, H.; Kawamura, T. *J. Chem. Soc., Dalton Trans.* **1994**, 3621–3635.
- (51) Liu, L. P.-C.; Lee, G.-H.; Peng, S.-M.; Bénard, M.; Rohmer, M.-M. *Inorg. Chem.* **2007**, *46*, 9602–9608.
- (52) Maynau, D.; Bolvin, H.; Van den Heuvel, W.; Bénard, M.; Rohmer, M.-M.; Ben Amor, N. C. R. *Chim.* **2012**, *15*, 170–175.
- (53) Tanabe, M.; Ishikawa, N.; Chiba, M.; Ide, T.; Osakada, K.; Tanase, T. *J. Am. Chem. Soc.* **2011**, *133*, 18598–18601.
- (54) Amatore, C.; Jutand, A. *J. Organomet. Chem.* **1999**, *576*, 254–278.
- (55) Kozuch, S.; Shaik, S. *Acc. Chem. Res.* **2011**, *44*, 101–110.
- (56) (a) Sun, Y.; Hienzsch, A.; Grasser, J.; Herdtweck, E.; Thiel, W. *J. Organomet. Chem.* **2006**, *691*, 291–298. (b) Sarcher, C.; Farsadpour, S.; Taghizadeh Ghoochany, L.; Sun, Y.; Thiel, W. R.; Roesky, P. W. *Dalton Trans.* **2014**, *43*, 2397–2405. (c) Farsadpour, S.; Taghizadeh Ghoochany, L.; Sun, Y.; Thiel, W. R. *Eur. J. Inorg. Chem.* **2011**, *29*, 4603–4609.

Wie aus der Publikation hervorgeht, war eine zentrale Entdeckung der DFT-Studien, dass abhängig vom eingesetzten Benzoat sowohl die Decarboxylierung als auch die Transmetallierung geschwindigkeitsbestimmend sein können. Dies stand im Gegensatz zu der bisherigen Annahme, dass alleinig die Decarboxylierung geschwindigkeitsbestimmend ist. Gleichzeitig lieferten diese Befunde eine mögliche Erklärung für die Diskrepanz zwischen der Temperatur, die für eine effiziente Protodecarboxylierung der *ortho*-Nitrobenzoesäure notwendig ist und den im Vergleich dazu höheren Reaktionstemperaturen für die decarboxylierende Kreuzkupplung dieses Substrats (siehe Abschnitt 5.1.1.1).

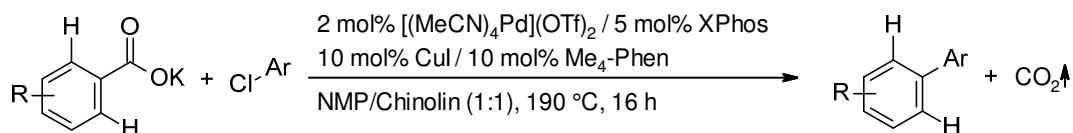
Dem aus den separat berechneten Teilschritten erhaltenen Energieprofil für den Gesamtprozess lag die Vereinfachung zugrunde, dass man einen monozyklischen anstelle eines bizyklischen Mechanismus annehmen kann. Dies sollte zulässig sein, da die oxidative Addition bereitwillig abläuft, sodass **5.1.1-13**, das Produkt der oxidativen Addition von Brombenzol (**5.1.1-8**) an den Palladium-Katalysator, als Edukt in einer stationären Konzentration, die der der Palladium-Katalysatorbeladung entspricht, angenommen werden kann. Die Anwendung des Energiespannenmodells^[145,146] auf das Gesamtenergieprofil (Energiespanne zwischen den Edukten **5.1.1-7 + 11** und dem höchsten Übergangszustand) brachte schließlich hervor, dass für die *ortho*-substituierte Säure der Übergangszustand der Decarboxylierung der geschwindigkeitsbestimmende Übergangszustand ist, während im Fall der *para*-substituierten Säure der Übergangszustand der Transmetallierung diese Stellung einnimmt. Im Gegensatz dazu lieferte ein Vergleich der einzelnen Teilschritte, also die jeweilige Betrachtung der Energiespanne zwischen der Gibbs-Energie eines Intermediats und der Gibbs-Energie des nachfolgenden Übergangszustands, ein anderes Ergebnis. So weist im Fall der *ortho*-substituierten Säure die Transmetallierung die höhere Barriere auf und im Fall der *para*-substituierten Säure die Decarboxylierung. Da insbesondere für die *ortho*-substituierte Säure der Unterschied der Gibbs-Energien zwischen dem Übergangszustand der Decarboxylierung und dem der Transmetallierung recht gering ist ($\Delta\Delta G_{\text{sov}} = 1.4 \text{ kcal}\cdot\text{mol}^{-1}$), sollte es für jedes individuelle Substrat unterschiedlich sein, welcher der beiden Schritte letztlich geschwindigkeitsbestimmend ist. Diese Ergebnisse stellen einen Paradigmenwechsel in der Entwicklung decarboxylierender Kreuzkupplungen dar, da nun ebenfalls die gezielte Verbesserung der Transmetallierung in den Fokus der Optimierungsarbeiten rückt, während bislang der Fokus auf der Optimierung des Decarboxylierungsschritts lag.

Maßgeblich für den Einfluss der entropisch ungünstigen Transmetallierung war die Entdeckung, dass diesem Schritt die Bildung eines Cu-Pd-Addukts vorausgeht. Diese

Adduktbildung ist leicht exotherm aber stark endergonisch, wodurch sie einen großen Teil der Gesamtaktivierungsbarriere darstellt. Aufbauend auf diesen Befunden wurde die Hypothese aufgestellt, dass durch die Verwendung verbrückender Liganden, die in der Lage sind, Kupfer und Palladium gleichzeitig zu koordinieren, um diese so in räumliche Nähe zueinander zu bringen, die Transmetallierung erleichtert werden sollte. Da dieser Schritt bei Benzoaten, die vergleichsweise bereitwillig decarboxylieren, gemäß den neuen Erkenntnissen als geschwindigkeitsbestimmend anzunehmen ist, wurde letztlich geschlussfolgert, dass so eine Reaktionsführung bei milderen Reaktionstemperaturen ermöglicht werden sollte. Wie im Manuskript beschrieben, konnte nachfolgend ein bimetallisches Cu/Pd-Katalysatorsystem unter Verwendung eines bidentaten Aminopyrimidinylphosphanliganden entwickelt werden, welches die decarboxylierende Kreuzkupplung von Kalium-2-nitrobenzoat mit 4-Chlorphenyltriflat bei einer Reaktionstemperatur von nur 100 °C ermöglicht. Dies stellt einen wichtigen Schritt bei der Entwicklung Cu/Pd-katalysierter decarboxylierender Kreuzkupplungen dar, um zukünftig das hohe synthetische Potential dieses Reaktionskonzepts besser ausschöpfen zu können und dieses als Alternative zu klassischen Kreuzkupplungen noch attraktiver zu gestalten.

Neben den zuvor diskutierten Befunden brachten die DFT-Rechnungen auch neue Erkenntnisse hinsichtlich des Einflusses von Halogenidionen im Falle nicht-*ortho*-substituierter Benzoate. So konnten die Rechnungen die bisher angenommene Erklärung für den Einfluss von Halogenidionen auf die Salzmetathese im Falle nicht-*ortho*-substituierter Benzoate nicht stützen, sondern brachten ähnliche Energieprofile für *ortho*- und *para*-substituierte Substrate hervor. Dahingegen bestätigten sie die ungünstige Gleichgewichtslage der Salzmetathese in Gegenwart von Halogenidionen, welche substratabhängig Einfluss auf die Reaktionsrate nimmt.

Geleitet von der Vorhersage, dass die bisherigen Limitierungen nicht intrinsischer Natur sind, wurde schließlich geschlussfolgert, dass nur mit einer holistischen Katalysatoroptimierung die Restriktion auf *ortho*-substituierte Benzoate in der Kupplung mit Arylchloriden überwunden werden kann.^[147] Auch diesen Hinweisen wurde in unserer Arbeitsgruppe schließlich erfolgreich nachgegangen. Mit einer Katalysatorkombination aus CuI, [(MeCN)₄Pd](OTf)₂, 3,4,7,8-Tetramethyl-1,10-phenanthrolin und XPhos ist nun das volle Spektrum an Benzoaten unabhängig von deren Substitutionsmuster für die decarboxylierende Kreuzkupplung zugänglich (Schema 27).^[147]



Schema 27: Decarboxylierende Kreuzkupplung mit Arylchloriden ohne aktivierende ortho-Substituenten.

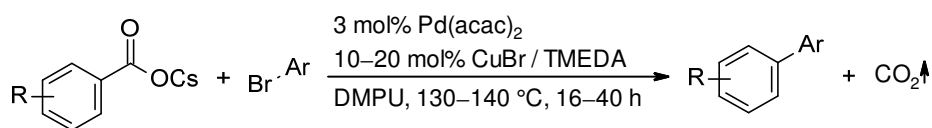
Gelänge es, auch für diese Transformation mit bidentaten Liganden die Transmetallierung zu erleichtern, so sollte schon bald auch in diesem Fall eine Reaktionsführung bei deutlich niedrigeren Temperaturen möglich sein.^[147]

5.1.2 Decarboxylierende Kreuzkupplungen bei 100–120 °C mit bidentaten Liganden

5.1.2.1 Hintergrund

Wie schon aus Abschnitt 5.1.1.1 hervorgeht, stellen die hohen Reaktionstemperaturen eine enorme Einschränkung der praktischen Anwendbarkeit der Cu/Pd-katalysierten decarboxylierenden Kreuzkupplung dar. Daher ist die Entwicklung verbesserter Katalysatoren ein wichtiger Schritt, um diese Reaktion als Alternative zu klassischen Kreuzkupplungen noch attraktiver zu gestalten.

Noch während der Durchführung der zuvor beschriebenen Studien konnten auch von Cahiez *et al.* erste Fortschritte hin zu einer Cu/Pd-katalysierten decarboxylierenden Kreuzkupplung bei vergleichsweise milden Temperaturen erzielt werden.^[148] Die Autoren beschrieben ein Katalysatorsystem bestehend aus Pd(acac)₂, CuBr und TMEDA als Ligand, welches die Kupplung *ortho*-substituierter Caesiumbenzoate mit Arylbromiden bei 130–140 °C in DMPU als Lösungsmittel ermöglicht (Schema 28). Zudem wurde demonstriert, dass für die Kupplung von Kalium-2-nitrobenzoat mit Brombenzol bei 120 °C mit diesem Katalysatorsystem moderate Ausbeuten erzielt werden können (22% in NMP bzw. 40% in DMPU).



Schema 28: Decarboxylierende Kreuzkupplung nach Cahiez *et al.*

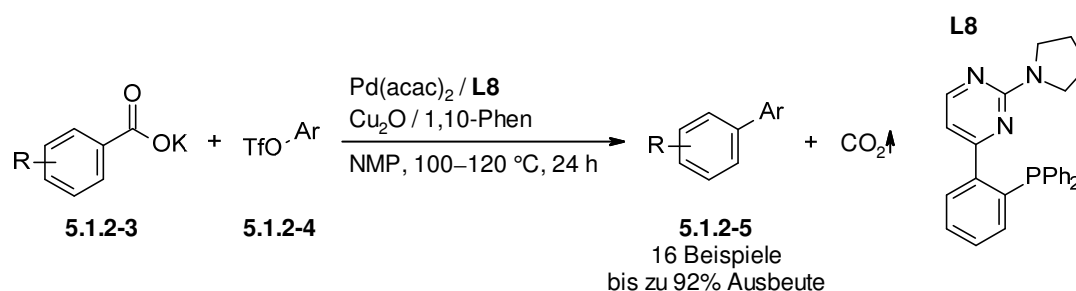
Neben dem bereits diskutierten Ag/Pd-basierten Katalysatorsystem für die decarboxylierende Kreuzkupplung bei 130 °C^[84] sind ferner lediglich monometallisch-katalysierte decarboxylierende Kreuzkupplungen von hoch aktivierten polyfluorierten Benzoaten bei Reaktionstemperaturen ab 120 °C möglich (Abschnitt 3.2.2.3).^[87–89] Daneben können

ausgewählte Heteroarylcarbonsäuren bei Temperaturen zwischen 130 °C und 140 °C in Gegenwart stöchiometrischer Mengen an Kupfer- oder Silbersalzen umgesetzt werden (Abschnitt 3.2.2.4).^[100,101]

In Anbetracht dieses relativ begrenzten Spektrums an Methoden sind die aus den DFT-Rechnungen erhaltenen Erkenntnisse sowie das daraus hervorgegangene Katalysatorsystem für die decarboxylierende Kreuzkupplung bei 100 °C eine wichtige Neuerung. Detailliertere Informationen hinsichtlich der Möglichkeiten und Grenzen, die das neue Katalysatorsystem bietet, sind daher von generellem Interesse.

5.1.2.2 Entwicklung und Untersuchung des neuen Katalysatorsystems

Die in *J. Am. Chem. Soc.* **2014**, *136*, 10007–10023 gezeigten Ergebnisse ergänzend, wurde die detaillierte Katalysatoroptimierung für die Cu/Pd-katalysierte decarboxylierende Kreuzkupplung von *ortho*-Nitrobenzoaten mit Aryltriflaten bei 100–120 °C unter Verwendung der *P,N*-Liganden (Schema 29) separat als „Full Paper“ publiziert.



Schema 29: Cu/Pd-Katalysierte decarboxylierende Kreuzkupplung bei 100–120 °C.

Dabei wurde die Anwendungsbreite des neuen Katalysatorsystems anhand der Synthese einer Vielzahl an Biarylen demonstriert. Zudem lieferten ESI-MS-Studien Hinweise darauf, dass die verwendeten Liganden bimetallische Cu/Pd-Spezies ausbilden können.

Beiträge der Autoren: Die nachfolgende Veröffentlichung entstand im Rahmen eines Kooperationsprojekts. Herr Dr. Bingrui Song begann mit der Entwicklung des Katalysatorsystems und den Optimierungsarbeiten zur decarboxylierenden Kreuzkupplung. Diese Arbeiten wurden zunächst von Herr Dr. Matthias Grünberg und dann eigenständig von mir fortgeführt sowie von mir fertiggestellt. Die Protodecarboxylierungsstudien wurden von mir mit Unterstützung von Herr Grünberg bearbeitet. Die Untersuchungen zur Anwendungsbreite der Reaktion wurde von mir durchgeführt. Weiterhin synthetisierte ich einen Palladium-Komplex des verwendeten Liganden. Herr Dr. Harald Kelm führte die

Kristallstrukturanalyse dieses Komplexes durch. Die ESI-MS-Studien unter Verwendung des Palladium-Komplexes wurden in Zusammenarbeit mit Herrn Dr. Fabian Menges aus dem Arbeitskreis von Herrn Prof. Dr. Gereon Niedner-Schatteburg durchgeführt. Die Liganden wurden von Herrn Prof. Dr. Werner R. Thiel zur Verfügung gestellt. Herr Dr. Saeid Farsadpour synthetisierte die Liganden und Herr Cedric Groß sowie Herr Timm Wolff unterstützten ihn dabei. Ich verfasste das Manuskript unter Verwendung der durch die jeweiligen Kooperationspartner angefertigten Passagen zur Ligandsynthese, zur Kristallstruktur und zu den ESI-MS-Studien und überarbeitete es mit Herrn Prof. Dr. L. J. Gooßen. Ich wertete die analytischen Daten zu den Katalyseexperimenten aus und erstellte die „Supporting Information“. Die Synthesevorschriften samt der analytischen Daten zu den Liganden sowie ergänzende Informationen zu den ESI-MS-Studien und zur Röntgenstrukturanalyse wurden von den jeweiligen Kooperationspartnern zur Verfügung gestellt.

Anmerkung zu den Arbeiten in Kapitel 5.1: Große Teile der Katalysatoroptimierung, der Untersuchungen zur Anwendungsbreite, der ESI-MS-Studien sowie die Synthese des Pd-Komplexes wurden im Rahmen meiner Diplomarbeit^[149] durchgeführt. Diese Arbeiten setzte ich im Rahmen der Doktorarbeit fort. So erfolgten weitere Katalyseversuche unter Variation verschiedener Parameter, weiterführende Untersuchungen zur Anwendungsbreite und Protodecarboxylierungsstudien. Weiterhin wurden ergänzende ESI-MS-Untersuchungen durchgeführt und ich synthetisierte einen neue *P,N*-Liganden. Ebenso wurden die Manuskripte im Rahmen der Doktorarbeit angefertigt.

Die detaillierte Katalysatoroptimierung, die Untersuchungen zur Anwendungsbreite sowie die ESI-MS-Studien zur Identifizierung bimetallischer Cu/Pd-Spezies werden im nachfolgenden Manuskript diskutiert. Dieses wurde in *ChemCatChem* veröffentlicht, für die vorliegende Arbeit angepasst und mit Erlaubnis des Verlags beigelegt:

"Reprinted (adapted) with permission from D. Hackenberger, B. Song, M. F. Grünberg, S. Farsadpour, F. Menges, H. Kelm, C. Groß, T. Wolff, G. Niedner-Schatteburg, W. R. Thiel, L. J. Gooßen, *ChemCatChem* **2015**, 7, 3579–3588: *Bimetallic Cu/Pd Catalysts with Bridging Aminopyrimidinyl Phosphines for Decarboxylative Cross-Coupling Reactions at Moderate Temperature*. Copyright 2015 WILEY-VCH Verlag GmbH & Co. KGaA, Weinheim."

JOHN WILEY AND SONS LICENSE TERMS AND CONDITIONS

This Agreement between Ms. Dagmar Hackenberger ("You") and John Wiley and Sons ("John Wiley and Sons") consists of your license details and the terms and conditions provided by John Wiley and Sons and Copyright Clearance Center.

License Number	4116370169422
License date	May 26, 2017
Licensed Content Publisher	John Wiley and Sons
Licensed Content Publication	ChemCatChem
Licensed Content Title	Bimetallic Cu/Pd Catalysts with Bridging Aminopyrimidinyl Phosphines for Decarboxylative Cross-Coupling Reactions at Moderate Temperature
Licensed Content Author	Dagmar Hackenberger, Bingrui Song, Matthias F. Grünberg, Saeid Farsadpour, Fabian Menges, Harald Kelm, Cedric Groß, Timm Wolff, Gereon Niedner-Schatteburg, Werner R. Thiel, Lukas J. Gooßen
Licensed Content Date	Sep 17, 2015
Licensed Content Pages	10
Type of use	Dissertation/Thesis
Requestor type	Author of this Wiley article
Format	Print and electronic
Portion	Full article
Will you be translating?	No

Bimetallic Cu/Pd Catalysts with Bridging Aminopyrimidinyl Phosphines for Decarboxylative Cross-Coupling Reactions at Moderate Temperature

Dagmar Hackenberger,^[a] Bingrui Song,^[a] Matthias F. Grünberg,^[a] Saeid Farsadpour,^[b] Fabian Menges,^[c] Harald Kelm,^[b] Cedric Groß,^[b] Timm Wolff,^[b] Gereon Niedner-Schatteburg,^{*,[c]} Werner R. Thiel,^{*,[b]} and Lukas J. Gooßen^{*,[a]}

A bimetallic catalyst system is presented that enables the decarboxylative cross-coupling of triflates with carboxylate salts at only 100 °C, which is 70 °C lower than with previous Cu/Pd-based systems. The new protocol allows the coupling of a broad range of aryl triflates with various substituted 2-nitrobenzoates in good to excellent yields. The key feature of the

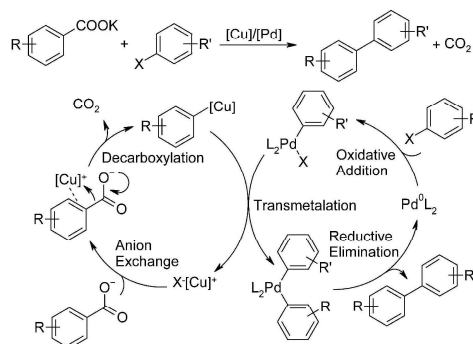
catalyst system is a bidentate P,N-ligand designed to bridge the Pd and Cu centres and thereby facilitating the rate-determining transmetalation step. Mass spectrometry (ESI-MS) studies support the ability of the aminopyrimidinyl phosphine to simultaneously coordinate copper and palladium.

Introduction

In the last decades, decarboxylative cross-coupling reactions have been established as a powerful methodology for the regioselective formation of C–C and C–heteroatom bonds.^[1] The advantage of this reaction type is that it draws on stable and readily available carboxylic acids as the coupling partners. Decarboxylative Heck-type reactions,^[2] allylations,^[3] redox-neutral cross-couplings,^[4] oxidative couplings,^[5] homo-couplings,^[6] C–H arylations,^[7] as well as Chan–Evans–Lam-type reactions^[8] have recently been disclosed.

Our key contribution to this rapidly expanding field was the development of redox-neutral decarboxylative cross-coupling reactions mediated by Cu/Pd bimetallic catalyst systems.^[4a] Within the coordination sphere of a Cu-based decarboxylation catalyst, the carbon nucleophile is generated by extrusion of CO₂ from the carboxylate and is then transferred to the Pd

centre, where coupling with the carbon electrophile takes place (Scheme 1). Bimetallic Cu/Pd systems proved to have a particularly broad substrate scope and high functional-group tolerance for both coupling partners.^[9] However, their practical applicability is still limited by the relatively high reaction temperatures, which usually exceed 150 °C.



Scheme 1. Mechanism of decarboxylative cross-coupling reactions.

Over the last years, some progress has been achieved in lowering the reaction temperature of decarboxylative cross-coupling reactions. Cahiez et al. reported that with tetramethylethylenediamine (TMEDA) as the copper ligand and *N,N'*-dimethylpropyleneurea (DMPU) as the reaction solvent, pre-formed caesium 2-nitrobenzoates can be coupled with aryl bromides at 120–140 °C.^[10] Similarly activated aromatic carboxylates were coupled with alkenyl bromides and chlorides at 130 °C.^[11] At the same temperature, particularly reactive polyfluoroben-

[a] D. Hackenberger, Dr. B. Song, Dr. M. F. Grünberg, Prof. Dr. L. J. Gooßen
Fachbereich Chemie—Organische Chemie
TU Kaiserslautern
Erwin-Schrödinger-Str., Geb. 54, 67663 Kaiserslautern (Germany)
Fax: (+49) 631-205-3921
E-mail: goossen@chemie.uni-kl.de

[b] Dr. S. Farsadpour, Dr. H. Kelm, C. Groß, T. Wolff, Prof. Dr. W. R. Thiel
Fachbereich Chemie—Anorganische Chemie
TU Kaiserslautern
Erwin-Schrödinger-Str., Geb. 54, 67663 Kaiserslautern (Germany)
Fax: (+49) 631-205-4676
E-mail: thiel@chemie.uni-kl.de

[c] Dr. F. Menges, Prof. Dr. G. Niedner-Schatteburg
Fachbereich Chemie—Physikalische Chemie
TU Kaiserslautern
Erwin-Schrödinger-Str., Geb. 52, 67663 Kaiserslautern (Germany)
Fax: (+49) 631-205-2750
E-mail: gns@chemie.uni-kl.de

Supporting Information for this article is available on the WWW under <http://dx.doi.org/10.1002/cctc.201500769>.

zoates can be decarboxylatively coupled with monometallic copper or palladium catalysts.^[12]

DFT calculations have guided the discovery of a silver-based catalyst system that promotes the protodecarboxylation of *ortho*-substituted benzoates at only 120 °C.^[13] Consequently, Ag/Pd catalyst systems allow decarboxylative cross-coupling of these carboxylates with aryl triflates at 130 °C.^[14]

Up to that point, the decarboxylation had been considered to be the sole rate-determining step; therefore, all efforts were directed at optimising the decarboxylation catalyst. Recent, extensive DFT calculations of Cu/Pd-catalysed decarboxylative cross-coupling reactions revealed, however, that the transmetalation step may also become rate-determining.^[15] The electronic activation energy of the transmetalation step is much lower than that of the decarboxylation step, but the free-energy loss during the Cu/Pd adduct formation preceding the actual aryl-group transfer is so high that the transmetalation step becomes strongly endergonic. For certain *ortho*-substituted substrates, the transmetalation will be rate-determining.

This leads to a paradigm shift in the development of decarboxylative coupling catalysts. Now, the most promising approach to lower the reaction temperature of decarboxylative couplings consists of facilitating Pd/Cu adduct formation by employing bidentate ligands designed to bridge the two metals and bring them into close spatial proximity.

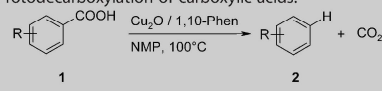
Results and Discussion

To probe the effect of bridging ligands on the transmetalation step, a test reaction needed to be identified in which this step alone was rate-determining.

Thus, a series of protodecarboxylation experiments were performed aimed at identifying substrates that decarboxylate so easily at 100 °C that the decarboxylation step will not be rate-determining in a decarboxylative coupling. Various benzoic acids **1** were heated to 100 °C in the presence of a catalyst system consisting of 5 mol% Cu₂O and 10 mol% 1,10-phenanthroline (1,10-Phen) (Table 1). As expected, most carboxylic acids tested were inert at such low temperatures with this standard decarboxylation catalyst (entries 2–7). However, 2-nitrobenzoic acid (**1a**) and 2,6-difluorobenzoic acid (**1e**) decarboxylated smoothly to give the corresponding arenes (entries 10,11) and even for the heterocyclic carboxylic acid **1f** reasonable protodecarboxylation could be achieved.

The decarboxylative coupling of potassium 2-nitrobenzoate (**3a**) with 4-chlorophenyl triflate (**4a**) was investigated next (Table 2). Triflates had previously been shown to give the best performance in coupling reactions at moderate temperatures.^[14] However, the state-of-the-art catalyst system (2 mol% PdI₂, 6 mol% P(*p*-Tol)₃, 5 mol% Cu₂O, 10 mol% 1,10-Phen), which gave high yields of the desired 4-chloro-2'-nitrobiphenyl product (**5aa**) at 170 °C,^[9c] was almost ineffective at 100 °C (Table 2, entries 1,2). Variation of the phosphine ligand confirmed P(*p*-Tol)₃ to be the optimal monodentate ligand. Even with high-performance ligands, such as John-Phos and X-Phos, no conversion was obtained.

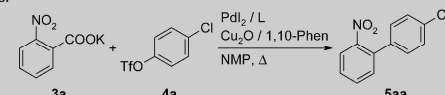
Table 1. Protodecarboxylation of carboxylic acids.^[a]



Entry	Carboxylic acid	R	t [h]	Product	Yield [%]
1	1a	2-NO ₂	6	2a	64
2	1a'	4-NO ₂	6	2a	0
3	1b	2-F	6	2b	3
4	1b'	4-F	6	2b	0
5	1c	2-OMe	6	2c	0
6	1c'	4-OMe	6	2c	0
7	1d	2,6-OMe	6	2d	0
8	1e	2,6-F	6	2e	57
9 ^[b]	1f	–	6	2f	7
10	1a	2-NO ₂	24	2a	99
11	1e	2,6-F	24	2e	96
12 ^[b]	1f	–	24	2f	24

[a] Reaction conditions: 0.5 mmol carboxylic acid, 5 mol% Cu₂O, 10 mol% 1,10-Phen, 2 mL NMP, 100 °C. GC yields with *n*-tetradecane as internal standard. 1,10-Phen = 1,10-phenanthroline; NMP = *N*-methyl-2-pyrrolidone. [b] **1f** = 3-Chloro-benzo[*b*]thiophene-2-carboxylic acid, **2f** = benzo[*b*]thiophene.

Table 2. Decarboxylative cross-coupling with monodentate and P,N-ligands.^[a]



Entry	L	T [°C]	Yield [%]
1	P(<i>p</i> -Tol) ₃	170	84 (91) ^[b,9c]
2	P(<i>p</i> -Tol) ₃	100	9 ^[c]
3	John-Phos	100	0 ^[c]
4	X-Phos	100	0 ^[c]
5	L1	100	50
6	L2	100	37
7	L3	100	48
8	L4	100	49
9	L5	100	45
10	L6	100	29
11	L7	100	28
12	L8	100	65
13	L9	100	60

[a] Reaction conditions: 0.3 mmol scale, **3a/4a** = 1.5:1, 2 mol% PdI₂, 6 mol% L, 5 mol% Cu₂O, 10 mol% 1,10-Phen, 2 mL NMP, 100 °C, 24 h. GC yields with *n*-tetradecane as internal standard. [b] 1 mmol scale, **3a/4a** = 1:2, 5 mol% Cu₂O, 10 mol% 1,10-Phen, 2 mol% PdI₂, 6 mol% P(*p*-Tol)₃, 4 mL NMP, 170 °C, 1 h. GC yield with *n*-tetradecane as internal standard, isolated yield in parentheses. [c] 0.5 mmol scale, **3a/4a** = 1:2.

Next, it was investigated whether ligands able to bring copper and palladium into close spatial proximity, and thereby facilitate the transmetalation, would be superior to the above monodentate ligands. An overview of the ligands investigated in this context is provided in Figure 1. The modular synthesis of pyrimidine-based bidentate ligands **L1**–**L9** allows the simple and broad variation of their molecular structures. In preceding investigations, ligands carrying a pyrimidin-4-yl unit have proved to have pronounced effects on the catalytic activity de-

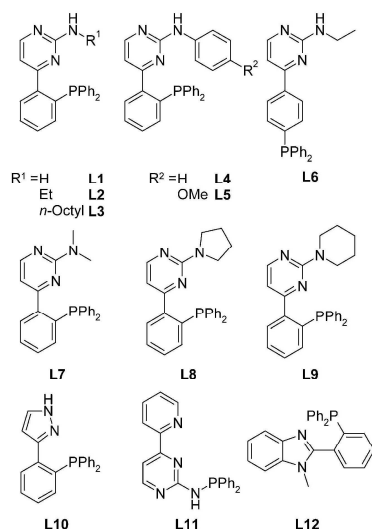
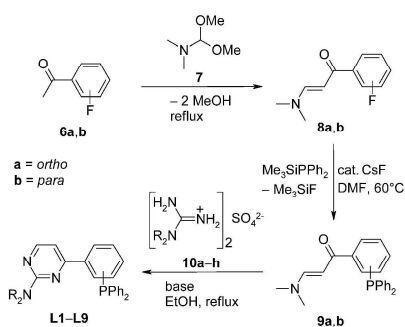


Figure 1. P,N-Ligands for the decarboxylative cross-coupling reaction.

pending on the nature of the amino group in the 2-position. This may be attributed to a C–H activation process in the 5-position of the pyrimidine ring, leading to ligands with a carbanionic nature.^[16]

The ligands were prepared starting from the fluoride-functionalised acetophenones **6a,b**, which underwent condensation with *N,N*-dimethylformamide dimethyl acetal **7** to yield the corresponding aminopropenones **8a,b**.^[17] These aminopropenones were then converted to the phosphine-functionalised aminopropenones **9a,b** in high yields by a fluoride-catalysed P–C coupling reaction.^[18] Further condensation of **9a,b** with the guanidinium salts **10a–h** in ethanol under basic conditions led to ligands **L1–L9** in good to excellent yields (Scheme 2). Cyclisation of **9a** with hydrazine provides the pyrazole-functionalised ligand **L10**.^[19]

Ligand **L11** was synthesised from 2-(2-aminopyrimidin-4-yl)-pyridine by reaction with Ph₂PCl in the presence of a base.^[20] The benzimidazolyl phosphine ligand **L12** was synthesised through a sequence of cyclisation, alkylation and phosphonation reactions starting from 2-bromobenzoic acid and 1,2-phenylenediamine.^[9f]



Scheme 2. Synthesis of the aminopyrimidinyl phosphine ligands.

nylenediamine.^[9f] The P,N-ligands were evaluated in the test reaction between potassium 2-nitrobenzoate (**3a**) and 4-chlorophenyl triflate (**4a**) at 100 °C. Most of the aminopyrimidinyl phosphines **L1–L9** showed higher catalytic activity than the optimal monodentate ligand P(*p*-Tol)₃ (Table 2), whereas ligands with a different backbone (**L10–L12**) were ineffective.^[15] Among the aminopyrimidinyl phosphines tested, **L1**, which bears a primary amino group, was more active than ligands substituted with secondary amino groups (**L2–L6**). Among the latter, electron-rich residues on the secondary amino nitrogen (**L2, L3, L5**) were beneficial. Ligand **L6**, in which the PPh₂ group is *para* to the pyrimidinyl ring, is less effective than the corresponding *ortho*-substituted derivative **L2**. Tertiary amino groups with acyclic amino groups (**L7**) led to moderate yields, but ligands with cyclic amine substituents (**L8** and **L9**), particularly **L8**, featuring a pyrrolidine group, showed the highest catalytic activity overall.

The reaction conditions were systematically optimised with the most effective bridging ligand **L8** (Table 3). Slightly increasing the amount of palladium from 2 to 3 mol % led to a decisive increase in the yields (entry 1). Among the palladium sources tested, Pd(acac)₂ (acac = acetylacetonate) was the most effective, resulting in an 88% yield of the desired product (entries 2–7). Further experiments showed that although Cu₂O is the most effective copper pre-catalyst, several other copper salts may also be used (entries 8–10).

1,10-Phenanthroline has the optimal properties as a copper-stabilising ligand. The use of phenanthrolines substituted with either electron-donating or -withdrawing substituents reduced the yields (entries 11, 12). In the absence of a stabilising ligand,

 Table 3. Optimisation of decarboxylative cross-coupling at moderate temperatures.^[a]

Entry	[Pd]	[Cu]	L'	Yield [%]
1	PdI ₂	Cu ₂ O	1,10-Phen	84
2	Pd(acac) ₂	Cu ₂ O	1,10-Phen	88
3	Pd(F ₆ -acac) ₂	Cu ₂ O	1,10-Phen	70
4	PdBr ₂	Cu ₂ O	1,10-Phen	72
5	Pd(OAc) ₂	Cu ₂ O	1,10-Phen	80
6	[Allyl]PdCl ₂	Cu ₂ O	1,10-Phen	77
7 ^[c]	[Pd(L8)]	Cu ₂ O	1,10-Phen	73
8	Pd(acac) ₂	CuBr ^[b]	1,10-Phen	80
9	Pd(acac) ₂	CuCl ^[b]	1,10-Phen	82
10	Pd(acac) ₂	[Cu(MeCN) ₄]BF ₄ ^[b]	1,10-Phen	74
11	Pd(acac) ₂	Cu ₂ O	NO ₂ -Phen	9
12	Pd(acac) ₂	Cu ₂ O	Me ₄ -Phen	66
13	Pd(acac) ₂	Cu ₂ O	–	16
14	Pd(acac) ₂	–	–	0
15	–	Cu ₂ O	1,10-Phen	0
16 ^[d]	Pd(acac) ₂	Cu ₂ O	1,10-Phen	23

[a] Reaction conditions: 0.3 mmol scale, **3a/4a** = 1.5:1, 3 mol % [Pd], 6 mol % **L8**, 5 mol % [Cu], 10 mol % L', 2 mL NMP, 100 °C, 24 h. GC yields with *n*-tetradecane as internal standard. NO₂-Phen = 5-nitro-1,10-phenanthroline; Me₄-Phen = 3,4,7,8-tetramethyl-1,10-phenanthroline. [b] 10 mol % [Cu]. [c] No additional amount of **L8** was added. vs = 1,3-divinyl-1,1,3,3-tetramethyldisiloxane. [d] 90 °C.

the transformation still led to 16% yield (entry 13). Further control experiments confirmed that the decarboxylative coupling requires both copper and palladium to proceed (entries 14, 15). Furthermore, the catalyst is still active even at 90 °C (entry 16). A solvent screening revealed that *N*-methyl-2-pyrrolidone (NMP) is the best solvent for the reaction. Mixtures of NMP with other polar solvents such as dimethylformamide (DMF), dimethyl sulfoxide (DMSO) or 2-methoxyethyl ether (diglyme) or in quinoline resulted in lower yields. Mesitylene was ineffective, probably because of the poor solubility of the benzoate in this non-polar solvent (see the Supporting Information).

Having found an effective reaction protocol, the scope of the reaction with regard to the electrophilic coupling partner was investigated. As can be seen from the examples in Table 4,

Table 4. Scope with regard to the electrophilic coupling partner.^[a]

Product	Yield [%]	Product	Yield [%]
	80 14 ^[b] 34 ^[b,c]		66
	58 90 ^[c]		66
	54 ^[c]		68 ^[c]
	92 ^[c]		75 ^[c]
	70 ^[c]		80 ^[c]
	81 ^[c]		

[a] Reaction conditions: 0.75 mmol **3a**, 0.50 mmol **4**, 3 mol% Pd(acac)₂, 6 mol% **L8**, 5 mol% Cu₂O, 10 mol% 1,10-Phen, 4 mL NMP, 100 °C, 24 h. Isolated yields from two identical runs. [b] 1-bromo-4-chlorobenzene was used as electrophile, GC yield with *n*-tetradecane as internal standard. [c] 120 °C.

various aryl triflates **4** with alkyl, halide, acyl or keto substituents were coupled in reasonable yields with potassium 2-nitrobenzoate (**3a**). After increasing the reaction temperature to 120 °C, less reactive substrates bearing, for example, ester or ether groups were converted in high yields; the same transformations at 100 °C did not proceed well. Beside aromatic triflates, vinyl triflate **4k** was also smoothly converted into the corresponding product **5ak** at 120 °C. Moreover, 1-bromo-4-

chlorobenzene was converted into the corresponding biaryl **5aa**, albeit in low yield.

The scope of the reaction with regard to the carboxylate coupling partner was investigated by using 4-chlorophenyl triflate (**4a**) as the electrophile. As illustrated in Table 5, various

Table 5. Scope with regard to the carboxylate.^[a]

Product	Yield [%]	Product	Yield [%]
	73		59
	70		75
	31 ^[b]		

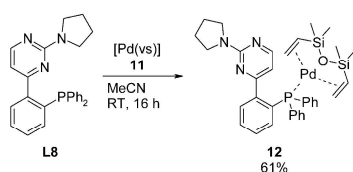
[a] Reaction conditions: 0.75 mmol **3**, 0.50 mmol **4a**, 3 mol% Pd(acac)₂, 6 mol% **L8**, 5 mol% Cu₂O, 10 mol% 1,10-Phen, 4 mL NMP, 100 °C, 24 h. Isolated yields from two identical runs. [b] 120 °C.

substituted 2-nitrobenzoates **3** were successfully converted into the corresponding biaryls in high yields at 100 °C. The coupling of the heterocyclic carboxylate **3f** took place only when the temperature was increased to 120 °C. Potassium 2,6-difluorobenzoate gave only small amounts of the desired biaryl, presumably as a result of the low solubility of this substrate in NMP at 100 °C.

As expected, only activated benzoates were successfully converted because these are the only substrates to decarboxylate sufficiently at the given temperature to make the transmetalation step rate-determining. In contrast, no conversion was observed in the coupling of 2-fluoro-, penta-fluoro-, 2-trifluoromethyl-, 2-methoxy-, 2-cyano- and 2,6-dimethoxy-substituted benzoates with 4-chlorophenyl triflate (**4a**).

Mechanistic studies were performed to elucidate the nature of the catalytic species and to investigate whether the ligand is indeed able to coordinate to both Pd and Cu. Based on previous mechanistic studies, it can be assumed that Pd enters the catalytic cycle as a Pd⁰-phosphine complex. To obtain structural information on this species, we added the olefin-stabilised Pd⁰ complex 1,3-divinyl-1,1,3,3-tetramethyldisiloxane palladium(0) ([Pd(vs)]) (**11**) in 2,4,6,8-tetramethyl-cyclotetrasiloxane (TMCTS) to ligand **L8** in acetonitrile and crystallised the resulting complex, which proved to be active in the decarboxylative cross-coupling reaction (Table 3, entry 7), from diethyl ether/acetonitrile at –20 °C (Scheme 3).

Single crystals suitable for X-ray structural analysis were obtained. The palladium atom is coordinated by the phosphorous



Scheme 3. Synthesis of palladium complex 12.

atom and the two C=C bonds of the vs ligand in a trigonal-planar coordination mode. The Pd–P bond length (2.320 Å) and the Pd–D bond lengths (D=mid points of the C=C bonds; 2.062 and 2.065 Å) are in the typical range for other reported structures.^[21] The C=C bonds lie exactly in the coordination plane. The bond lengths are slightly lengthened (1.394 and 1.397 Å) compared with an uncoordinated C=C bond length (1.34 Å), indicating a weak back-bonding for the Pd atom. The three bond angles D1–Pd–D2: 132.53°, D1–Pd–P: 114.00° and D2–Pd–P: 113.42° show that the trigonal-planar geometry is highly distorted. The five-membered ring in the backbone of **L8** adapts two slightly different conformations with the same probability as depicted in Figure 2.

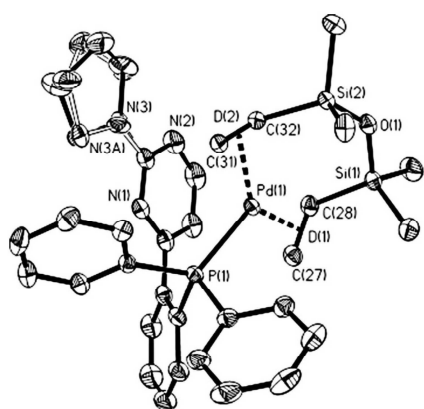


Figure 2. Perspective view of complex 12 showing 50% thermal ellipsoids. Hydrogen atoms are omitted for the purpose of clarity. Relevant distances [Å] and angles [°]: Pd(1)–P(1) 2.3203(4), Pd(1)–D1 2.062(6), Pd(1)–D2 2.065(6), C(27)–C(28) 1.394(2), C(31)–C(32) 1.397(2), P(1)–Pd(1)–D1 113.42 (0.20), P(1)–Pd(1)–D2 114.00(0.20), D1–Pd1–D2 132.53(0.29).

Upon addition of $[\text{Cu}(\text{MeCN})_4]\text{BF}_4$ **13** to an acetonitrile solution of complex **12**, a yellowish solution formed. However, all attempts to crystallise a bimetallic complex from this solution failed. The non-polar palladium complex **12** crystallised from polar solvents, whereas the polar copper complex **13** precipitated from non-polar solvents, both crystallisation processes shifting the equilibrium to monometallic species. We thus investigated an equimolar mixture of ligand **L8**, $[\text{Pd}(\text{vs})]$ (**11**), and $[\text{Cu}(\text{MeCN})_4]\text{BF}_4$ (**13**) in acetonitrile by ESI-MS.

The resulting mass spectra exhibit an intense peak at approximately 472 m/z (most abundant mass), which was assigned to a $[\text{Cu}(\text{L8})]^+$ complex (Figure 3 and Figure S1a). The high abundance of this complex provides evidence for the

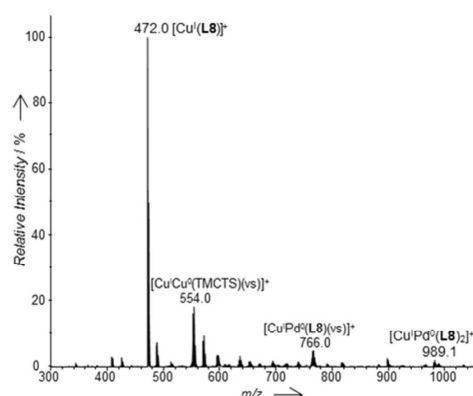


Figure 3. Mass spectrum of a solution of ligand **L8**, $[\text{Pd}(\text{vs})]$ (**11**) and $[\text{Cu}(\text{MeCN})_4]\text{BF}_4$ (**13**) in acetonitrile (see Figure S1 for details and simulations of isotopic distributions).

ability of the ligand to bind copper ions in solution. Several smaller signals could also be assigned to bimetallic species by comparing their mass and isotopic distribution with simulated patterns. Most interesting are the signals at approximately 766 and 989 m/z , which correspond to the heterobimetallic Cu/Pd species $[\text{CuPd}^0(\text{L8})(\text{vs})]^+$ and $[\text{CuPd}^0(\text{L8})_2]^+$ (Figure S1c, d). The isotope signals corresponding to the latter complex are partially overlaid by a second mass signal at approximately 981 m/z with an unknown composition. The peak at approximately 554 m/z was assigned to the bimetallic copper complex $[\text{CuCu}^0(\text{TMCTS})(\text{vs})]^+$ (Figure S1b).

Equimolar amounts of nitrogen donor ligands were then added to a mixture of ligand **L8**, $[\text{Pd}(\text{vs})]$ (**11**) and $[\text{Cu}(\text{MeCN})_4]\text{BF}_4$ (**13**) in acetonitrile to investigate their influence on the abundance of heterobimetallic complexes. We had expected to see bimetallic complexes with additionally coordinated nitrogen ligands. However, no such species were detected when adding either pyridine or triethylamine. Instead, the mass spectral intensity of the peaks at approximately $m/z = 766$ for $[\text{CuPd}^0(\text{L8})(\text{vs})]^+$, and 989 for $[\text{CuPd}^0(\text{L8})_2]^+$ strongly increased. The latter was no longer overlaid by the unassigned signal at approximately 981 m/z . Additional peaks detected at approximately 881 and 580 m/z are likely to represent $[\text{Cu}(\text{L8})_2]^+$ and the bimetallic complex $[\text{CuPd}^0(\text{L8})]^+$, respectively (Figure 4 and Figure S2b, d). Thus, the presence of nitrogen donor ligands has a critical effect on the composition of the species detected in the mass spectrum.

We assume that the influence of these additives results from the basicity of the molecules. The fact that the composition of the solution has such a strong influence on the detected signals suggests that bimetallic adducts are already present in solution, rather than that their detection is a consequence of the spray process. However, a detailed understanding on the observed effect remains to be achieved.

Added 1,10-phenanthroline, the optimal ligand for decarboxylative couplings, also affects the composition of the solution of **L8**, $[\text{Pd}(\text{vs})]$ (**11**) and $[\text{Cu}(\text{MeCN})_4]\text{BF}_4$ (**13**) in acetonitrile, but in a different way (Figure 5).

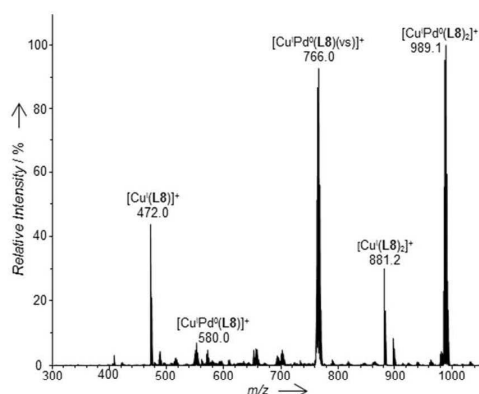


Figure 4. Mass spectrum of a solution of ligand **L8**, [Pd(vs)] (**11**), [Cu(MeCN)₄]BF₄ (**13**) and pyridine in acetonitrile (see Figure S2 for details and simulations of isotopic distributions).

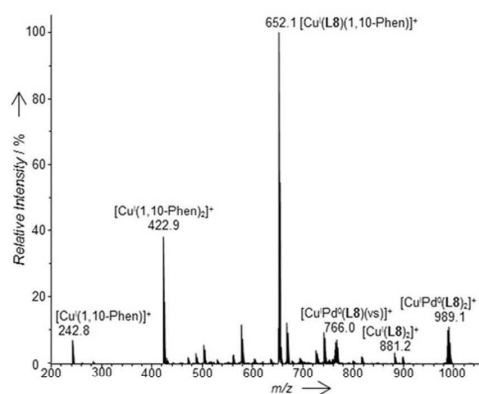


Figure 5. Mass spectrum of a solution of ligand **L8**, [Pd(vs)] (**11**), [Cu(MeCN)₄]BF₄ (**13**) and 1,10-phenanthroline in acetonitrile (see Figure S3 for details and simulations of isotopic distributions).

The intensities of the signals at approximately 989, 881 and 766 *m/z* are low, and the signal at 472 *m/z* corresponding to [Cu(L8)]⁺ is missing altogether. Instead, a strong signal at 652 *m/z* was recorded that can be assigned to a [Cu(L8)(1,10-Phen)]⁺ complex (Figure S3 c). Two additional signals were detected at 243 and 423 *m/z*, and assigned to the monometallic 1,10-phenanthroline copper species [Cu(1,10-Phen)]⁺ and [Cu(1,10-Phen)₂]⁺ (Figure S3 a,b). The large abundance of these three Cu/phenanthroline-containing complexes shows that phenanthroline coordinates more strongly to Cu than ligand **L8**. Unfortunately, no signals were detected resulting from a bimetallic Cu/Pd species bearing both ligands (Figure 2, and Figure 3). It is unclear whether such complexes are not present in solution, or whether they decompose during the spray process.

On the basis of these ESI-MS experiments, it appears likely that bimetallic Pd⁰/Cu^I complexes with ligand **L8** are present in solution, but especially in the presence of phenanthroline, they are unlikely to form exclusively. Instead, they appear to be

present in low quantities, along with monometallic Pd/phosphine and Cu/phenanthroline complexes. This would be in agreement with the proposed mechanism in which the temporary formation of Pd/Cu adducts is facilitated, but the two metals do not stay together throughout the catalytic cycle.

It would certainly be possible to design P,N-ligands with a nitrogen subunit that coordinates so strongly to copper that Cu/Pd complexes would prevail in solution. However, we expect that such rigid coordination of both metals would hamper the individual catalytic cycles of each metal owing to steric crowding. Therefore, a P,N-ligand that coordinates to Pd throughout, and is able to facilitate temporary Pd/Cu adduct formation by reversibly coordinating to the copper centre with its nitrogen binding site, might be the optimal design for efficient catalytic turnover. Further experimental studies with a broader range of P,N-ligands are clearly needed to elucidate this aspect.

Conclusions

The use of a potentially bridging aminopyrimidinyl phosphine ligand with a bimetallic Cu/Pd-based catalyst system allows decarboxylative cross-coupling of aryl triflates with aromatic carboxylate salts to be performed at only 100 °C.

The P,N-ligand, which is able to simultaneously coordinate Cu and Pd, lowers the reaction temperature by more than 50 °C in comparison with monodentate phosphine ligands. This is an important milestone in the evolution of decarboxylative cross-coupling reactions as a synthetic alternative to traditional coupling reactions.

DFT studies have previously revealed that for activated carboxylic acids, the transmetalation rather than the decarboxylation step should be rate-determining. The potential bridging ligand should facilitate the formation of adducts between the two metals and, thus, facilitate the transmetalation step. However, it is unlikely to strongly affect other reaction steps. The decisive effect of the rationally designed P,N-ligand on the reaction temperatures, thus, confirms the predictions by the DFT calculations.

In combination with high-performance decarboxylation catalysts, the use of such bridging P,N-ligands could soon allow inexpensive decarboxylative couplings to be performed at the low temperature of traditional couplings of preformed organometallic reagents.

Experimental Section

General methods

Chemicals and solvents were either purchased (puriss p.a.) from commercial suppliers or purified by standard procedures prior to use.^[22] Reactions were performed in oven-dried glassware, under a nitrogen atmosphere, containing a Teflon-coated stirrer bar and dry septum. Triflates were saturated with argon to exclude atmospheric oxygen and solvents were degassed by three freeze-pump-thaw cycles. All reactions were monitored by GC using *n*-tetradecane as an internal standard. Response factors of the products with regard to *n*-tetradecane were obtained experimentally by analysing known quantities of the substances. GC analyses were per-

formed by using an HP-5 capillary column (phenyl methyl siloxane, 30 m×320×0.25, 100/2.3–30–300/3, 2 min at 60 °C, heating rate 30 °C min⁻¹, 3 min at 300 °C). Column chromatography was performed by using a Combi Flash Companion Chromatography System and Reveleris packed columns (12 g). NMR spectra were recorded on Bruker Avance 600, Avance 400 or Avance 200 at ambient temperature using CDCl₃, CD₃OD, [D₆]DMSO or D₂O as solvent, with proton, carbon, and phosphorus resonances at 600/400/200, 151/101/50, and 243/162 MHz respectively. Mass spectral data were acquired on a Varian GC-MS Saturn 2100 T. ESI-MS data were acquired on a Bruker Esquire 6000. Sample solutions at concentrations of approximately 1×10⁻⁴ M were continuously infused into the ESI chamber at a flow rate of 2 μL min⁻¹ by using a syringe pump. Nitrogen was used as the drying gas at a flow rate of 3.0 to 4.0 L min⁻¹ at 300 °C and the solutions were sprayed at a nebuliser pressure of 4 psi with the electrospray needle held at 4.5 kV. CHN elemental analysis was performed with a Hanau Elemental Analyzer vario Micro cube. Melting points were measured on a Mettler FP 61 and infrared spectra on a PerkinElmer Spectrum 100 ATR-FTIR. The X-ray crystallographic data was collected on a Gemini S Ultra single crystal CCD diffractometer from Agilent equipped with a CryojetHT-temperature system.

General procedure for the protodecarboxylation experiments

An oven-dried vessel was charged with the carboxylic acid **1a-f** (0.50 mmol), copper(I) oxide (3.61 mg, 25.0 μmol) and 1,10-phenanthroline (9.10 mg, 50.0 μmol). The vessel was flushed with three alternating vacuum and nitrogen purge cycles and degassed NMP (2 mL) was added through a syringe. The resulting mixture was stirred at 100 °C for the given time. The reaction mixture was then allowed to cool to RT, *n*-tetradecane (50 μL) was added through a syringe and the mixture was diluted with ethyl acetate (4 mL). A sample of the reaction mixture (0.25 mL) was dissolved in ethyl acetate (2 mL), washed with a saturated solution of bicarbonate (2 mL), dried over MgSO₄ and analysed by GC.

Published synthesis of precursors and ligands

The precursors **9a,b**^[18] and the ligands **L1**, **L2**, **L7**, **L8** and **L9**^[16a] as well as **L10**,^[19] **L11**^[20] and **L12**^[9f] were synthesised according to procedures published in the literature. The analytical data matched those reported in the literature.

Ligand synthesis

4-(1-Diphenylphosphinophenyl)-2-octylaminopyrimidine (L3): Aminopropenone **9a** (2.35 g, 6.50 mmol) and *N*-octylguanidinium sulfate **10c** (2.73 g, 13.00 mmol) were suspended in dry EtOH (80 mL). After addition of KOH (0.67 g, 13.0 mmol), the mixture was heated at reflux for 48 h. After removal of the solvent under reduced pressure, the residue was dissolved in a mixture of water and CH₂Cl₂. The layers were separated and the aqueous layer was extracted with CH₂Cl₂ (15 mL). The combined organic layers were dried over anhydrous MgSO₄ and the solvent was removed under reduced pressure. Recrystallisation of the crude material from ethanol afforded **L3** (2.37 g, 5.07 mmol, 78%). M.p. 78–79 °C; ¹H NMR ([D₆]DMSO, 400 MHz): δ = 0.82 (brs, 3H), 1.00–1.50 (brs, 14H), 2.61–3.00 (brs, 2H), signal not observed: NH, 6.66 (d, ³J_{HH} = 4.9 Hz, 1H), 6.98 (dd, ³J_{HH} = 7.0, 3.9 Hz, 1H), 7.12–7.23 (m, 4H), 7.30–7.35 (m, 6H), 7.37 (t, ³J_{HH} = 7.6 Hz, 1H), 7.48 (t, ³J_{HH} = 7.5 Hz, 1H), 7.60 (m,

1H), 8.20 ppm (d, ³J_{HH} = 5.0 Hz, 1H); ¹³C NMR ([D₆]DMSO, 101 MHz): δ = 13.9, 22.0, 26.3, 28.7, 28.8, 28.9, 31.2, 40.2, 108.9, 128.35, 128.41, 129.0 (d, ³J_{CP} = 16.8 Hz, 129.09, 129.13, 133.2 (d, ²J_{CP} = 19.9 Hz), 134.5, 135.5 (d, ¹J_{CP} = 20.3 Hz), 138.2 (d, ¹J_{CP} = 12.3 Hz), 144.5, 157.9, 161.5, 166.1 ppm; ³¹P NMR ([D₆]DMSO, 162 MHz): δ = -12.0 ppm; elemental analysis: calcd (%) for C₃₀H₃₄N₃P (467.59): C 77.06, H 7.33, N 8.99; found: C 77.08, H 7.71, N 8.74.

4-(1-Diphenylphosphinophenyl)-2-phenylaminopyrimidine (L4): Sodium ethoxide (0.98 g, 14.4 mmol), *N*-phenylguanidinium sulfate **10d** (2.65 g, 7.19 mmol) and aminopropenone **9a** (2.35 g, 6.54 mmol) were dissolved in dry EtOH (32 mL). The mixture was heated at reflux for 48 h. After removal of the solvent under reduced pressure the residue was dissolved in a mixture of water and dichloromethane. The layers were separated and the aqueous layer was extracted three times with dichloromethane (20 mL). The combined organic layers were dried over anhydrous MgSO₄ and the solvent was removed under reduced pressure. The crude product was recrystallized from ethanol and then purified by column chromatography (dichloromethane/methanol gradient) to remove some of phosphine oxide, leading to a relatively high loss of yield. A second recrystallization from ethanol afforded **L4** (50.0 mg, 0.12 mmol, 2%). M.p. 149–150 °C; ¹H NMR (CDCl₃, 400 MHz): δ = 6.62 (s, 1H), 6.83–6.95 (m, 2H), 6.97–7.06 (m, 1H), 7.11–7.32 (m, 10H), 7.32–7.46 (m, 4H), 7.56–7.65 (m, 1H), 8.30 ppm (d, ³J_{HH} = 5.2 Hz, 1H); ¹³C NMR (CDCl₃, 101 MHz): δ = 111.3, 119.1, 122.5, 128.6, 128.6, 128.7, 128.9, 129.1, 129.8, 133.9 (d, ²J_{CP} = 20.0 Hz), 135.5, 136.9 (d, ²J_{CP} = 20.0 Hz), 139.0 (d, ¹J_{CP} = 9.8 Hz), 143.0 (²J_{CP} = 22.1 Hz), 157.4, 158.6, 166.5 ppm, ³¹P NMR (CDCl₃, 162 MHz): δ = -9.42 ppm; elemental analysis: calcd (%) for C₂₈H₂₂N₃P (431.47): C 77.94, H 5.14, N 9.74; found: C 77.77, H 5.02, N 9.70.

4-(1-Diphenylphosphinophenyl)-2-(4-methoxyphenyl)aminopyrimidine (L5): Ligand **L5** was synthesised according to the procedure described for **L4** from *N*-(4-methoxyphenyl)guanidinium sulfate **10e**. Yield: 1.05 g, 2.27 mmol, 82%. M.p. 122–123 °C; ¹H NMR ([D₆]DMSO, 400 MHz): δ = 3.69 (s, 3H), 6.71–6.79 (m, 3H), 7.04 (dd, ³J_{HH} = 7.3, 3.9 Hz, 1H), 7.16–7.23 (m, 4H), 7.33–7.39 (m, 6H), 7.43 (t, ³J_{HH} = 7.5 Hz, 1H), 7.51 (t, ³J_{HH} = 7.4 Hz, 1H), 7.55–7.61 (m, 3H), 8.33 (d, ³J_{HH} = 4.9 Hz, 1H), 9.13–9.26 ppm (brs, NH); ¹³C NMR ([D₆]DMSO, 101 MHz): δ = 55.12, 111.9 (d, ⁴J_{CP} = 5.1 Hz), 113.6, 120.5, 120.6, 128.7, 128.7, 128.8, 129.2 (d, ³J_{CP} = 8.0 Hz), 129.4, 129.4, 133.3 (d, ²J_{CP} = 20.1 Hz), 134.2, 135.2 (d, ¹J_{CP} = 18.9 Hz), 137.3 (d, ¹J_{CP} = 12.4 Hz), 144.4 (d, ²J_{CP} = 25.8 Hz), 154.1, 157.6, 159.6, 166.6 ppm (d, ³J_{CP} = 3.5 Hz); ³¹P NMR ([D₆]DMSO, 162 MHz): δ = -13.0 ppm; elemental analysis: calcd (%) for C₂₉H₂₄N₃OP (461.49): C 75.47, H 5.24, N 9.11; found: C 75.29, H 5.30, N 9.07.

4-(4-Diphenylphosphinophenyl)-2-ethylaminopyrimidine (L6): 1-Ethylguanidinium sulfate **10b** (2.35 g, 8.62 mmol) was added in one portion to a suspension of sodium methoxide (0.77 g, 14.2 mmol) in dry oxygen-free ethanol (25 mL) and the mixture was heated at reflux for 4 h. The aminopropenone **9b** (2.00 g, 5.56 mmol) was then added and the resulting mixture was heated at reflux for another 16 h. After cooling to RT, the mixture was stirred for 6 h and the solvent was removed under reduced pressure, producing an orange solid. This residue was dissolved in ether (30 mL) and the organic phase was extracted with water (3×10 mL) until a pH of approximately 5.0–5.5 was reached. The aqueous layer was extracted with ether (2×10 mL) and the combined organic phases were dried over MgSO₄ and concentrated under reduced pressure to give an orange solid (1.41 g, 3.66 mmol, 66%). The solid was purified by MPLC to give the desired product **L7** as a colourless solid (0.59 g, 1.56 mmol, 28%). M.p. 109–110 °C; ¹H NMR (CDCl₃, 400 MHz): δ = 1.17 (t, 3H), 3.38–3.46 (m, 2H), 5.24

(brs, 1 H, N-H), 6.84 (d, $^3J_{\text{HH}} = 5.2$ Hz, 1 H), 7.25–7.32 (m, 12 H), 7.98 (d, $^3J_{\text{HH}} = 7.7$ Hz, 2 H), 8.23 ppm (d, $^3J_{\text{HH}} = 5.2$ Hz, 1 H); ^{13}C NMR (CDCl_3 , 101 MHz): $\delta = 15.1, 36.4, 106.4, 127.0$ (d, $^3J_{\text{CP}} = 6.7$ Hz), 128.7 (d, $^3J_{\text{CP}} = 7.1$ Hz), 129.0, 133.8 (d, $^2J_{\text{CP}} = 18.9$ Hz), 133.9 (d, $^2J_{\text{CP}} = 22.4$ Hz), 137.0 (d, $^1J_{\text{CP}} = 11.1$ Hz), 138.0, 140.5 (d, $^1J_{\text{CP}} = 12.9$ Hz), 158.7, 162.9, 164.3 ppm; ^{31}P NMR (CDCl_3 , 162 MHz): $\delta = -4.2$ ppm; IR: $\tilde{\nu} = 3251$ (s), 3055 (m), 2972 (m), 1683 (w), 1578 (s), 1556 (s), 1433 (m), 1417 (s), 1340 (m), 1186 (w), 1154 (w), 1090 (m), 851 (w), 801 (s), 747 (s), 694 (s), 667 (s), 514 cm^{-1} (s); elemental analysis: calcd (%) for $\text{C}_{24}\text{H}_{22}\text{N}_3\text{P}$ (383.43): C 75.18, H 5.75, N 10.96; found: C 75.03, H 5.73, N 11.06.

General procedure for the biaryl synthesis

An oven-dried 20 mL vessel was charged with potassium carboxylate **3** (0.75 mmol), copper(I) oxide (3.61 mg, 25.0 μmol , 5 mol%), palladium(II) acetylacetonate (4.57 mg, 15.0 μmol , 3 mol%), ligand **L8** (12.3 mg, 30 μmol , 6 mol%) and 1,10-phenanthroline (9.10 mg, 50 μmol , 10 mol%) inside a glovebox. NMP (4 mL) and triflate **4** (0.5 mmol) were added inside the glovebox and the resulting mixture was stirred at the given temperature for 24 h outside of the glovebox under a dry atmosphere of nitrogen. After the reaction was complete, the mixture was allowed to cool to RT, diluted with aqueous HCl (1 N, 20 mL) and extracted with ethyl acetate (3 \times 20 mL). The combined organic layers were washed with water and brine, dried over MgSO_4 , filtered and the volatiles were removed under reduced pressure. The residue was purified by column chromatography (SiO_2 , ethyl acetate/hexane gradient) yielding the corresponding biaryl **5**. The isolated yield was determined by combining two identical 0.5 mmol scale reactions.

4-Chloro-2'-nitrobiphenyl (5aa): Compound **5aa** was prepared following the general procedure from potassium 2-nitrobenzoate (**3a**) (154 mg, 0.75 mmol) and 4-chlorophenyl triflate (**4a**) (130 mg, 0.5 mmol) at 100 °C in 4 mL of NMP. After combining two identical 0.5 mmol scale reactions, compound **5aa** was isolated as a yellow oil (186 mg, 80%). The analytical data (NMR, GC-MS) matched those reported in the literature^[9d, 23] [CAS: 6271-80-3].

3-Acetyl-2'-nitrobiphenyl (5ab): Compound **5ab** was prepared following the general procedure from potassium 2-nitrobenzoate (**3a**) (154 mg, 0.75 mmol) and 3-acetylphenyl triflate (**4b**) (134 mg, 0.5 mmol) at 100 °C in 4 mL of NMP. After combining two identical 0.5 mmol scale reactions, compound **5ab** was isolated as a colourless solid (158 mg, 66%; M.p. 103–104 °C). The analytical data (NMR, GC-MS) matched those reported in the literature^[9d] [CAS: 1195761-01-3].

3,5-Dimethyl-2'-nitrobiphenyl (5ac): Compound **5ac** was prepared following the general procedure from potassium 2-nitrobenzoate (**3a**) (154 mg, 0.75 mmol) and 3,5-dimethylphenyl triflate (**4c**) (127 mg, 0.5 mmol) at 100 °C and at 120 °C in 4 mL of NMP. After combining two identical 0.5 mmol scale reactions, compound **5ac** was isolated as an orange oil (132 mg, 58% (100 °C); 204 mg, 90% (120 °C)). The analytical data (NMR, GC-MS) matched those reported in the literature^[9d, 24] [CAS: 51839-09-9].

3-Formyl-2'-nitrobiphenyl (5ad): Compound **5ad** was prepared following the general procedure from potassium 2-nitrobenzoate (**3a**) (154 mg, 0.75 mmol) and 3-formylphenyl triflate (**4d**) (127 mg, 0.5 mmol) at 100 °C in 4 mL of NMP. After combining two identical 0.5 mmol scale reactions, compound **5ad** was isolated as a colourless solid (150 mg, 66%, M.p. 80–81 °C). The analytical data (NMR, GC-MS) matched those reported in the literature^[9d] [CAS: 1181294-97-2].

3-Chloro-2'-nitrobiphenyl (5ae): Compound **5ae** was prepared following the general procedure from potassium 2-nitrobenzoate (**3a**) (154 mg, 0.75 mmol) and 3-chlorophenyl triflate (**4e**) (130 mg, 0.5 mmol) at 120 °C in 4 mL of NMP. After combining two identical 0.5 mmol scale reactions, compound **5ae** was isolated as a yellow oil (126 mg, 54%). The analytical data (NMR) matched those reported in the literature^[14] [CAS: 951-22-4].

Ethyl 2'-nitrobiphenyl-2-carboxylate (5af): Compound **5af** was prepared following the general procedure from potassium 2-nitrobenzoate (**3a**) (154 mg, 0.75 mmol) and 2-trifluoromethylsulfonyloxy benzoic acid ethyl ester (**4f**) (149 mg, 0.5 mmol) at 120 °C in 4 mL of NMP. After combining two identical 0.5 mmol scale reactions, compound **5af** was isolated as a yellow oil (184 mg, 68%). The analytical data (NMR) matched those reported in the literature^[14] [CAS: 72256-33-8].

4-Methyl-2'-nitrobiphenyl (5ag): Compound **5ag** was prepared following the general procedure from potassium 2-nitrobenzoate (**2a**) (154 mg, 0.75 mmol) and 4-methylphenyl triflate (**4g**) (138 mg, 0.5 mmol) at 120 °C in 4 mL of NMP. After combining two identical 0.5 mmol scale reactions, compound **5ag** was isolated as an orange oil (197 mg, 92%). The analytical data (NMR, GC-MS) matched those reported in the literature^[9d, 25] [CAS: 70680-21-6].

1-(2'-Nitrophenyl)naphthalene (5ah): Compound **5ah** was prepared following the general procedure from potassium 2-nitrobenzoate (**3a**) (154 mg, 0.75 mmol) and 1-naphthyl triflate (**4h**) (138 mg, 0.5 mmol) at 120 °C in 4 mL of NMP. After combining two identical 0.5 mmol scale reactions, compound **5ah** was isolated as an orange solid (188 mg, 75%) [CAS: 5415-59-8]. M.p. 93–94 °C; ^1H NMR (200 MHz, CDCl_3): $\delta = 8.10$ (dd, $^3J_{\text{HH}} = 8.0, 1.5$ Hz, 1 H), 7.98–7.88 (m, 2 H), 7.77–7.56 (m, 2 H), 7.56–7.40 (m, 5 H), 7.40–7.34 ppm (m, 1 H); ^{13}C NMR (101 MHz, CDCl_3): $\delta = 149.8, 135.5, 135.3, 133.4, 133.1, 132.5, 131.4, 128.6, 128.5, 128.5, 126.6, 126.0, 126.0, 125.2, 124.8, 124.2$ ppm; IR: $\tilde{\nu} = 3053$ (w), 2852 (w), 1612 (w), 1520 (vs), 1337 (s), 858 (w), 800 (m), 791 (w), 779 (vs), 750 (s), 715 (m), 697 (m), 663 cm^{-1} (w); MS, m/z (%): 249 (14) [M^+], 248 (100), 232 (25), 220 (10), 204 (17), 202 (10), 50 (6); elemental analysis: calcd (%) for $\text{C}_{16}\text{H}_{11}\text{NO}_2$ (265.31): C 77.10, H 4.45, N 5.62; found: C 77.06, H 4.61, N 5.61.

2-Methyl-2'-nitrobiphenyl (5ai): Compound **5ai** was prepared following the general procedure from potassium 2-nitrobenzoate (**3a**) (154 mg, 0.75 mmol) and 2-methylphenyl triflate (**4i**) (120 mg, 0.5 mmol) at 120 °C in 4 mL of NMP. After combining two identical 0.5 mmol scale reactions, compound **5ai** was isolated as an orange solid (150 mg, 70%, m.p. 63–64 °C). The analytical data (NMR, GC-MS) matched those reported in the literature^[9d, 26] [CAS: 67992-12-5].

4-Methoxy-2'-nitrobiphenyl (5aj): Compound **5aj** was prepared following the general procedure from potassium 2-nitrobenzoate (**3a**) (154 mg, 0.75 mmol) and 4-methoxyphenyl triflate (**4j**) (128 mg, 0.5 mmol) at 120 °C in 4 mL of NMP. After combining two identical 0.5 mmol scale reactions, compound **5aj** was isolated as an orange solid (184 mg, 80%, m.p. 58–59 °C). The analytical data (NMR, GC-MS) matched those reported in the literature^[9d, 23] [CAS: 20013-55-2].

1-(2'-Nitrophenyl)-3,4-dihydronaphthalene (5ak): Compound **5ak** was prepared following the general procedure from potassium 2-nitrobenzoate (**3a**) (154 mg, 0.75 mmol) and 3,4-dihydronaphthalen-1-yl triflate (**4k**) (139 mg, 0.5 mmol) at 120 °C in 4 mL of NMP. After combining two identical 0.5 mmol scale reactions, compound **5ak** was isolated as a yellow solid (204 mg, 81%). M.p. 83–84 °C;

¹H NMR (200 MHz, CDCl₃): δ = 7.98 (dd, ³J_{HH} = 8.1, 1.2 Hz, 1H), 7.71–7.58 (m, 1H), 7.53 (dd, ³J_{HH} = 7.7, 1.6 Hz, 1H), 7.49–7.39 (m, 1H), 7.25–7.14 (m, 2H), 7.14–6.99 (m, 1H), 6.61 (d, ³J_{HH} = 7.3 Hz, 1H), 6.03 (t, ³J_{HH} = 4.6 Hz, 1H), 2.91 (brs, 2H), 2.54–2.35 ppm (m, 3H); ¹³C NMR (101 MHz, CDCl₃): δ = 149.2, 136.6, 135.9, 135.7, 134.2, 132.9, 132.4, 128.3, 128.0, 127.7, 127.4, 126.4, 124.23, 123.6, 27.8, 23.4 ppm; IR: $\tilde{\nu}$ = 3072 (w), 3022 (w), 2930 (w), 2853 (w), 1516 (vs), 1489 (m), 1346 (vs), 1270 (m), 1152 (w), 1041 (w), 848 (m), 787 (s), 768 (s), 753 (vs), 738 cm^{−1} (vs). MS, *m/z* (%): 250 (36) [M⁺], 233 (31), 216 (19), 207 (19), 206 (100), 204 (17), 50 (17); elemental analysis: calcd (%) for C₁₆H₁₃NO₂ (251.29): C 76.48, H 5.21, N 5.57; found: C 76.30, H 5.35, N 5.69.

4-Chloro-5'-methyl-2'-nitrobiphenyl (5ba): Compound **5ba** was prepared following the general procedure from potassium 5-methyl-2-nitrobenzoate (**3b**) (164 mg, 0.75 mmol) and 4-chlorophenyl triflate (**4a**) (130 mg, 0.5 mmol) at 100 °C in 4 mL of NMP. After combining two identical 0.5 mmol scale reactions, compound **5ba** was isolated as a yellow oil (180 mg, 73%). The analytical data (NMR) matched those reported in the literature^[14] [CAS: 70690-00-5].

4,5'-Dichloro-2'-nitrobiphenyl (5ca): Compound **5ca** was prepared following the general procedure from potassium 5-chloro-2-nitrobenzoate (**3c**) (180 mg, 0.75 mmol) and 4-chlorophenyl triflate (**4a**) (130 mg, 0.5 mmol) at 100 °C in 4 mL of NMP. After combining two identical 0.5 mmol scale reactions, compound **5ca** was isolated as a yellow solid (158 mg, 59%). M.p. 93–94 °C; ¹H NMR (400 MHz, CDCl₃): δ = 7.88 (d, ³J_{HH} = 8.8 Hz, 1H), 7.49 (dd, ³J_{HH} = 8.7, 2.4 Hz, 1H), 7.45–7.40 (m, 3H), 7.27–7.23 ppm (m, 2H); ¹³C NMR (101 MHz, CDCl₃): δ = 147.2, 138.7, 137.1, 135.0, 134.7, 131.8, 129.1, 129.1, 128.6, 125.8 ppm; IR: $\tilde{\nu}$ = 3084 (w), 3053 (w), 2845 (w), 1605 (w), 1524 (s), 1509 (s), 1339 (vs), 1081 (m), 1012 (m), 859 (s), 829 (vs), 821 (vs), 799 (m), 756 cm^{−1} (s); MS, *m/z* (%): 268 (62) [M⁺], 267 (19), 266 (100), 238 (25), 232 (31), 175 (29), 150 (20); elemental analysis: calcd (%) for C₁₂H₇Cl₂NO₂ (268.10): C 53.76, H 2.63, N 5.22; found: C 53.90, H 2.76, N 5.19.

4-Chloro-5'-methoxy-2'-nitrobiphenyl (5da): Compound **5da** was prepared following the general procedure from potassium 5-methoxy-2-nitrobenzoate (**3d**) (176 mg, 0.75 mmol) and 4-chlorophenyl triflate (**4a**) (130 mg, 0.5 mmol) at 100 °C in 4 mL of NMP. After combining two identical 0.5 mmol scale reactions, compound **5da** was isolated as a yellow solid (184 mg, 70%, m.p. 118–119 °C). The analytical data (NMR, GC-MS) matched those reported in the literature^[4a] [CAS: 911217-07-7].

4-Chloro-4',5'-dimethoxy-2'-nitrobiphenyl (5ea): Compound **5ea** was prepared following the general procedure from potassium 4,5-dimethoxy-2-nitrobenzoate (**3e**) (199 mg, 0.75 mmol) and 4-chlorophenyl triflate (**4a**) (130 mg, 0.5 mmol) at 100 °C in 4 mL of NMP. After combining two identical 0.5 mmol scale reactions, compound **5ea** was isolated as a yellow solid (220 mg, 75%). M.p. 146–147 °C; ¹H NMR (400 MHz, CDCl₃): δ = 7.58 (s, 1H), 7.43–7.38 (m, 2H), 7.25–7.20 (m, 2H), 6.74 (s, 1H), 4.00 (s, 3H), 3.96 ppm (s, 3H); ¹³C NMR (101 MHz, CDCl₃): δ = 152.4, 148.3, 140.8, 136.8, 134.0, 130.2, 129.4, 128.7, 113.4, 107.9, 45.5 ppm; IR: $\tilde{\nu}$ = 3072 (w), 2962 (w), 2833 (w), 1498 (s), 1488 (vs), 1332 (s), 1282 (vs), 1268 (s), 1220 (vs), 1089 (s), 1023 (s), 1013 (m), 844 (s), 822 (m), 791 (vs), 757 cm^{−1} (m); MS, *m/z* (%): 294 (31) [M⁺], 293 (16), 292 (100), 258 (18), 197 (13), 125 (13), 43 (62); elemental analysis: calcd (%) for C₁₄H₁₂ClNO₄ (293.71): C 57.25, H 4.12, N 4.77; found: C 57.45, H 4.40, N 4.95.

3-Chloro-2-(4'-chlorophenyl)benzo[b]thiophene (5fa): Compound **5fa** was prepared following the general procedure from potassium 3-chlorobenzo[b]thiophene-2-carboxylate (**3f**) (188 mg, 0.75 mmol)

and 4-chlorophenyl triflate (**4a**) (130 mg, 0.5 mmol) at 120 °C in 4 mL of NMP. After combining two identical 0.5 mmol scale reactions, compound **5fa** was isolated as a colourless solid (86 mg, 31%). M.p. 97–98 °C; ¹H NMR (400 MHz, CDCl₃): δ = 7.89 (d, ³J_{HH} = 8.0 Hz, 1H), 7.82 (d, ³J_{HH} = 8.0 Hz, 1H), 7.77–7.72 (m, 1H), 7.53–7.41 ppm (m, 4H); ¹³C NMR (101 MHz, CDCl₃): δ = 137.7, 136.7, 134.9, 134.8, 130.8, 130.5, 128.9, 125.7, 125.2, 122.3, 117.1 ppm; IR: $\tilde{\nu}$ = 3058 (w), 1522 (w), 1486 (w), 1434 (w), 1400 (w), 1301 (w), 1251 (w), 1098 (w), 1012 (w), 984 (w), 899 (m), 828 (m), 820 (s), 750 cm^{−1} (vs); MS, *m/z* (%): 281 (13), 279 (81) [M⁺], 278 (100), 208 (19), 163 (8), 49 (6), 44 (6); elemental analysis: calcd (%) for C₁₄H₈Cl₂S (279.19): C 60.23, H 2.89, S 11.49; found: C 60.19, H 3.10, S 11.19.

Synthesis of palladium(0) complex 12

1,3-divinyl-1,1,3,3-tetramethyldisiloxane palladium(0) (**11**) in 2,4,6,8-tetramethylcyclotetrasiloxane (1 M, 250 μ L, 250 μ mol) was added to a solution of **L8** (102 mg, 250 μ mol) in MeCN (8 mL). The solution was stirred at RT for 16 h and a colourless solid formed. The solid was filtered off and washed with MeCN (2 \times 1 mL). The complex was recrystallised from a solution of the crude product in Et₂O (0.5 mL) and MeCN (1.5 mL) at −20 °C yielding **12** as colourless crystals (107 mg, 61%). M.p. 293–294 °C (decomposed); ¹H NMR (600 MHz, CDCl₃): δ = 8.07 (d, ³J_{HH} = 5.0 Hz, 1H), 7.55 (dd, ³J_{HH} = 7.2, 4.3 Hz, 1H), 7.48 (t, ³J_{HH} = 7.5 Hz, 1H), 7.42 (t, ³J_{HH} = 8.2 Hz, 4H), 7.38–7.29 (m, 7H), 7.25 (t, ³J_{HH} = 7.8 Hz, 1H), 6.36 (d, ³J_{HH} = 5.0 Hz, 1H), 3.37 (brs, 2H), 3.14 (dd, ³J_{HH} = 16.1, 4.7 Hz, 2H), 2.84 (dd, ³J_{HH} = 12.3, 6.5 Hz, 2H), 2.62–2.54 (m, 2H), 2.43 (brs, 2H), 1.81 (brs, 2H), 1.59 (brs, 2H), 0.23 (s, 6H), −0.23 ppm (s, 6H); ¹³C NMR (101 MHz, CDCl₃): δ = 167.1 (d, ³J_{CP} = 3.6 Hz), 159.1, 156.6, 144.4 (d, ¹J_{CP} = 17.3 Hz), 138.6 (d, ¹J_{CP} = 28.2 Hz), 134.9 (d, ²J_{CP} = 21.8 Hz), 134.8, 134.7, 132.9, 130.3 (d, ²J_{CP} = 6.4 Hz), 129.2, 128.8, 128.5 (d, ³J_{CP} = 4.5 Hz), 127.8, 127.7, 108.6, 68.6, 66.8, 66.7, 45.9, 25.3, 1.4, −1.2 ppm; ³¹P NMR (243 MHz, CDCl₃): δ = 25.3 ppm; IR: $\tilde{\nu}$ = 3051 (w), 3036 (w), 2957 (w), 2184 (w), 1569 (m), 1558 (m), 1543 (m), 1510 (m), 1478 (m), 1431 (w), 1339 (w), 1317 (m), 1247 (m), 1210 (w), 1090 (w), 998 (s), 837 (m), 781 (vs), 770 (vs), 740 cm^{−1} (s); ESI-MS, *m/z* (%): 702 [M+H]⁺; elemental analysis: calcd (%) for C₃₄H₄₂N₂OPPdSi₂ (733.35): C 58.15, H 6.03, N 5.98, found: C 58.20, H 5.94, N 5.96. Crystal data for **12**: C₃₄H₄₂N₂OPPdSi₂; *M* = 702.26 g mol^{−1}; *T* = 150(2) K; triclinic; *P*1̄; *a* = 10.5752(3) Å, *b* = 10.9336(4) Å, *c* = 15.6717(6) Å; α = 89.765(3)°, β = 88.537(3)°, γ = 68.120(3)°; *V* = 1680.94(10) Å³; *Z* = 2; ρ_{calcd} = 1.387 mg m^{−3}; $\mu(\text{MoK}\alpha)$ = 0.702 mm^{−1} (λ = 0.71023 Å); 18112 reflections collected; independent reflections 9757; refinement converged to *R* = 0.0324, *wR*₂ = 0.0696 (*I* > 2 σ (*I*)), 429 Parameters and 12 restraints; min./max. residual electron density = +0.586 and −0.695 e Å^{−3}. CCDC 1033628 contains the supplementary crystallographic data for this paper. These data can be obtained free of charge from The Cambridge Crystallographic Data Centre

Acknowledgements

We thank the DFG (SFB-TRR 88 “3MET”) and the Stipendienstiftung Rheinland-Pfalz (fellowship to D. H.) for funding and Dr. K. Gooßen for help with the preparation of the manuscript.

Keywords: bridging ligands • carboxylic acids • copper • cross-coupling • palladium

- [1] a) W. I. Dzik, P. P. Lange, L. J. Gooßen, *Chem. Sci.* **2012**, *3*, 2671–2678; b) J. Cornella, I. Larrosa, *Synthesis* **2012**, *44*, 653–676; c) N. Rodríguez, L. J. Gooßen, *Chem. Soc. Rev.* **2011**, *40*, 5030–5048; d) L. J. Gooßen, N. Rodríguez, K. Gooßen, *Angew. Chem. Int. Ed.* **2008**, *47*, 3100–3120; *Angew. Chem.* **2008**, *120*, 3144–3164.
- [2] a) A. G. Myers, D. Tanaka, M. R. Mannion, *J. Am. Chem. Soc.* **2002**, *124*, 11250–11251; b) L. J. Gooßen, J. Paetzold, L. Winkel, *Synlett* **2002**, 1721–1723; c) P. Hu, J. Kan, W. Su, M. Hong, *Org. Lett.* **2009**, *11*, 2341–2344; d) Z.-M. Sun, P. Zhao, *Angew. Chem. Int. Ed.* **2009**, *48*, 6726–6730; *Angew. Chem.* **2009**, *121*, 6854–6858; e) L. J. Gooßen, B. Zimmermann, T. Knauber, *Beilstein J. Org. Chem.* **2010**, *6*, 43–51.
- [3] a) J. D. Weaver, A. Recio, A. J. Grenning, J. A. Tunge, *Chem. Rev.* **2011**, *111*, 1846–1913; b) M. F. Grünberg, L. J. Gooßen, *J. Organomet. Chem.* **2013**, *744*, 140–143.
- [4] a) L. J. Gooßen, G. Deng, L. M. Levy, *Science* **2006**, *313*, 662–664; b) L. J. Gooßen, N. Rodríguez, B. Melzer, C. Linder, G. Deng, L. M. Levy, *J. Am. Chem. Soc.* **2007**, *129*, 4824–4833; c) P. Forgiione, M.-C. Brochu, M. St-Onge, K. H. Thesen, M. D. Bailey, F. Bilodeau, *J. Am. Chem. Soc.* **2006**, *128*, 11350–11351; d) J.-M. Becht, C. Catala, C. Le Drian, A. Wagner, *Org. Lett.* **2007**, *9*, 1781–1783; e) R. Shang, Y. Fu, J.-B. Li, S.-L. Zhang, Q.-X. Guo, L. Liu, *J. Am. Chem. Soc.* **2009**, *131*, 5738–5739; f) R. Shang, Z.-W. Yang, Y. Wang, S.-L. Zhang, L. Liu, *J. Am. Chem. Soc.* **2010**, *132*, 14391–14393; g) R. Shang, D.-S. Ji, L. Chu, Y. Fu, L. Liu, *Angew. Chem. Int. Ed.* **2011**, *50*, 4470–4474; *Angew. Chem.* **2011**, *123*, 4562–4566; h) P. Y. Yeung, K. H. Chung, F. Y. Kwong, *Org. Lett.* **2011**, *13*, 2912–2915.
- [5] a) H.-P. Bi, L. Zhao, Y.-M. Liang, C.-J. Li, *Angew. Chem. Int. Ed.* **2009**, *48*, 792–795; *Angew. Chem.* **2009**, *121*, 806–809; b) J. Zhou, G. Wu, M. Zhang, X. Jie, W. Su, *Chem. Eur. J.* **2012**, *18*, 8032–8036.
- [6] a) J. Cornella, H. Lahlali, I. Larrosa, *Chem. Commun.* **2010**, *46*, 8276–8278; b) K. Xie, S. Wang, Z. Yang, J. Liu, A. Wang, X. Li, Z. Tan, C.-C. Guo, W. Deng, *Eur. J. Org. Chem.* **2011**, 5787–5790; c) P. Hu, Y. Shang, W. Su, *Angew. Chem. Int. Ed.* **2012**, *51*, 5945–5949; *Angew. Chem.* **2012**, *124*, 6047–6051.
- [7] a) C. Wang, I. Piel, F. Glorius, *J. Am. Chem. Soc.* **2009**, *131*, 4194–4195; b) J. Cornella, P. Lu, I. Larrosa, *Org. Lett.* **2009**, *11*, 5506–5509; c) A. Voutchkova, A. Coplin, N. E. Leadbeater, R. H. Crabtree, *Chem. Commun.* **2008**, 6312–6314; d) H. Yang, P. Sun, Y. Zhu, H. Yan, L. Lu, X. Qu, T. Li, J. Mao, *Chem. Commun.* **2012**, *48*, 7847–7849.
- [8] S. Bhadra, W. I. Dzik, L. J. Goossen, *J. Am. Chem. Soc.* **2012**, *134*, 9938–9941.
- [9] a) L. J. Gooßen, F. Rudolphi, C. Oppel, N. Rodríguez, *Angew. Chem. Int. Ed.* **2008**, *47*, 3043–3045; *Angew. Chem.* **2008**, *120*, 3085–3088; b) L. J. Gooßen, B. Zimmermann, T. Knauber, *Angew. Chem. Int. Ed.* **2008**, *47*, 7103–7106; *Angew. Chem.* **2008**, *120*, 7211–7214; c) L. J. Gooßen, N. Rodríguez, C. Linder, *J. Am. Chem. Soc.* **2008**, *130*, 15248–15249; d) L. J. Gooßen, C. Linder, N. Rodríguez, P. P. Lange, *Chem. Eur. J.* **2009**, *15*, 9336–9349; e) L. J. Gooßen, N. Rodríguez, P. P. Lange, C. Linder, *Angew. Chem. Int. Ed.* **2010**, *49*, 1111–1114; *Angew. Chem.* **2010**, *122*, 1129–1132; f) B. Song, T. Knauber, L. J. Gooßen, *Angew. Chem. Int. Ed.* **2013**, *52*, 2954–2958; *Angew. Chem.* **2013**, *125*, 3026–3030.
- [10] G. Cahiez, A. Moyeux, O. Gager, M. Poizat, *Adv. Synth. Catal.* **2013**, *355*, 790–796.
- [11] J. Tang, L. J. Gooßen, *Org. Lett.* **2014**, *16*, 2664–2667.
- [12] a) R. Shang, Y. Fu, Y. Wang, Q. Xu, H.-Z. Yu, L. Liu, *Angew. Chem. Int. Ed.* **2009**, *48*, 9350–9354; *Angew. Chem.* **2009**, *121*, 9514–9518; b) R. Shang, Q. Xu, Y.-Y. Jiang, Y. Wang, L. Liu, *Org. Lett.* **2010**, *12*, 1000–1003.
- [13] L. J. Gooßen, N. Rodríguez, C. Linder, P. P. Lange, A. Fromm, *ChemCatChem* **2010**, *2*, 430–442.
- [14] L. J. Gooßen, P. P. Lange, N. Rodríguez, C. Linder, *Chem. Eur. J.* **2010**, *16*, 3906–3909.
- [15] A. Fromm, C. van Wüllen, D. Hackenberger, L. J. Gooßen, *J. Am. Chem. Soc.* **2014**, *136*, 10007–10023.
- [16] a) S. Farsadpour, L. T. Ghoochany, Y. Sun, W. R. Thiel, *Eur. J. Inorg. Chem.* **2011**, 4603–4609; b) L. Wang, S. Shylesh, D. Dehe, T. Philippi, G. Dörr, A. Seifert, Z. Zhou, M. Hartmann, R. N. Klupp Taylor, M. Jia, S. Ernst, W. R. Thiel, *ChemCatChem* **2012**, *4*, 395–400; c) L. Taghizadeh Ghoochany, C. Kerner, S. Farsadpour, F. Menges, Y. Sun, G. Niedner-Schatteburg, W. R. Thiel, *Eur. J. Inorg. Chem.* **2013**, 4305–4317.
- [17] A.-K. Pleier, H. Glas, M. Grosche, P. Sirsch, W. R. Thiel, *Synthesis* **2001**, 0055–0062.
- [18] A. Reis, D. Dehe, S. Farsadpour, I. Munstein, Y. Sun, W. R. Thiel, *New J. Chem.* **2011**, *35*, 2488–2495.
- [19] Y. Sun, A. Hienzsich, J. Grasser, E. Herdtweck, W. R. Thiel, *J. Organomet. Chem.* **2006**, *691*, 291–298.
- [20] C. Sarcher, S. Farsadpour, L. T. Ghoochany, Y. Sun, W. R. Thiel, P. W. Roesky, *Dalton Trans.* **2014**, 2397–2405.
- [21] a) J. Krause, K.-J. Haack, K.-R. Pörschke, *Chem. Commun.* **1998**, 1291–1292; b) M. J.-L. Tschan, J.-M. López-Valbuena, Z. Freixa, H. Launay, H. Hagen, J. Benet-Buchholz, P. W. N. M. van Leeuwen, *Organometallics* **2011**, *30*, 792–799; c) M. J.-L. Tschan, E. J. García-Suárez, Z. Freixa, H. Launay, H. Hagen, J. Benet-Buchholz, P. W. N. M. van Leeuwen, *J. Am. Chem. Soc.* **2010**, *132*, 6463–6473.
- [22] W. L. F. Armarego, *Purification of Laboratory Chemicals*, Elsevier/Butterworth-Heinemann, Amsterdam, Boston, **2009**.
- [23] F.-X. Felpin, E. Fouquet, C. Zakrib, *Adv. Synth. Catal.* **2009**, *351*, 649–655.
- [24] L. Caron, L.-C. Campeau, K. Fagnou, *Org. Lett.* **2008**, *10*, 4533–4536.
- [25] L. Wang, Y. Zhang, L. Liu, Y. Wang, *J. Org. Chem.* **2006**, *71*, 1284–1287.
- [26] R. Rodríguez González, L. Liguori, A. Martínez Carrillo, H.-R. Bjørsvik, *J. Org. Chem.* **2005**, *70*, 9591–9594.

Received: July 9, 2015

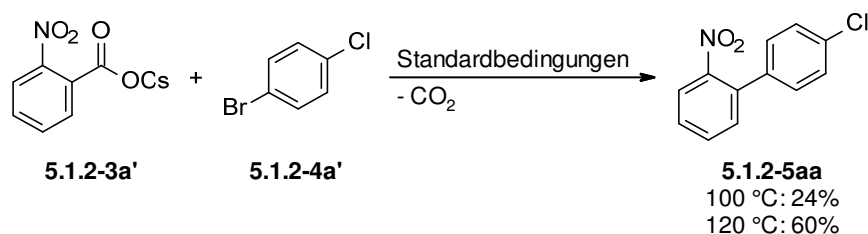
Revised: July 21, 2015

Published online on September 17, 2015

Ergänzend zu den im Manuskript aufgeführten Resultaten werden nachfolgend weiterführende Ergebnisse beschrieben.

Untersuchungen mit Aryl- und Alkenylbromiden als elektrophile Kupplungspartner

Wie im Manuskript diskutiert, konnten in der Reaktion mit Arylbromiden unter den Bedingungen für die decarboxylierende Kreuzkupplung bei 100 °C bzw. 120 °C nur geringe Ausbeuten erhalten werden. In Anlehnung an die Arbeiten von Cahiez *et al.*^[148] wurde weiterhin überprüft, ob sich für die Kupplung dieser Substrate bessere Ausbeuten mit Caesiumbenzoaten erzielen lassen (Schema 30). Während im Fall von Kalium-2-nitrobenzoat bei 100 °C lediglich eine Ausbeute von 14% erzielt werden konnte, wurden im Fall des entsprechenden Caesiumbenzoats **5.1.2-3a'** 24% an **5.1.2-5aa** gebildet und bei 120 °C konnte die Ausbeute von 34% auf 60% gesteigert werden.



Schema 30: Decarboxylierende Kreuzkupplung mit Caesium-2-nitrobenzoat (5.1.2-3a').

Cahiez *et al.* postulierten, dass die guten Ausbeuten unter Verwendung von Caesiumbenzoaten ausschließlich auf eine bessere Löslichkeit dieser Substrate, die gerade bei niedrigen Reaktionstemperaturen an Bedeutung gewinnt, zurückzuführen ist.^[148] Aus der Kupplung mit Aryltriflaten sowie einem im nachfolgenden Absatz diskutierten Protokoll für die Kupplung von Alkenylbromiden^[76] ist hingegen bekannt, dass Kaliumbenzoate bei 100 °C bzw. 120 °C in NMP bzw. einer Lösungsmittelmischung aus NMP und Mesitylen vollständig umsetzbar sind. Daher sollte die Löslichkeit im vorliegenden Fall nicht der alleinige Grund für die gesteigerte Reaktivität sein und ein zusätzlicher Einfluss der in der Reaktionslösung vorliegenden Caesiumionen auf die Effizienz der Reaktion kann an dieser Stelle nicht ausgeschlossen werden.

Zeitgleich zu diesen Studien wurde in unserer Arbeitsgruppe ein Protokoll für die Cu/Pd-katalysierte decarboxylierende Kreuzkupplung von *ortho*-substituierten Kaliumbenzoaten mit Alkenylbromiden entwickelt.^[76] Dabei ermöglicht ein Katalysatorsystem bestehend aus Pd(F₆-acac)₂ mit P(1-Naph)₃ als Ligand und CuI in Kombination mit 1,10-Phenanthrolin die Darstellung einer Vielzahl an Arylalkenen in sehr guten Ausbeuten bei

einer Reaktionstemperatur von 130 °C. Weiterhin zeigt das Katalysatorsystem auch bei 120 °C noch eine sehr hohe Effizienz. Das in diesen Arbeiten verwendete Modellsubstrat 1-Bromcyclohexen (**5.1.2-4l**) konnte auch unter den hier beschriebenen Standardbedingungen der decarboxylierenden Kreuzkupplung bei 100 °C umgesetzt werden, lieferte jedoch nur geringe Ausbeuten (Tabelle 1, Eintrag 1). In einem Lösungsmittelgemisch aus NMP und Mesitylen (1:3), welches sich im Protokoll bei 130 °C als ideal erwies, wurden 6% an **5.1.2-5al** detektiert (Eintrag 2). Die gleiche Reaktionsführung unter Verwendung von Caesium-2-nitrobenzoat (**5.1.2-3a'**) lieferte hingegen 21% an **5.1.2-5al** (Eintrag 3), was in diesem Fall vermutlich auf eine bessere Löslichkeit des Benzoats in dem vergleichsweise unpolaren Lösungsmittelgemisch zurückgeführt werden kann. Ähnliche Ausbeuten ließen sich zudem unter den Standardbedingungen bei 120 °C erzielen (Eintrag 4).

Tabelle 1: Decarboxylierende Kreuzkupplung mit 1-Bromcyclohexen.

Eintrag	M	Lösungsmittel	T (°C)	5.1.2-5al (%)
1	K ⁺	NMP	100	11
2	K ⁺	NMP/Mes (1:3)	"	6
3	Cs ⁺	"	"	21
4	K ⁺	NMP	120	24

Reaktionsbedingungen: **5.1.2-3** (0.75 mmol), **5.1.2-4l** (0.5 mmol), Cu₂O (5 mol%), 1,10-Phen (10 mol%), Pd(acac)₂ (3 mol%), **L8** (6 mol%), Lösungsmittel (4 mL), Δ, 24 h. GC-Ausbeuten mit *n*-Tetradecan als interner Standard.

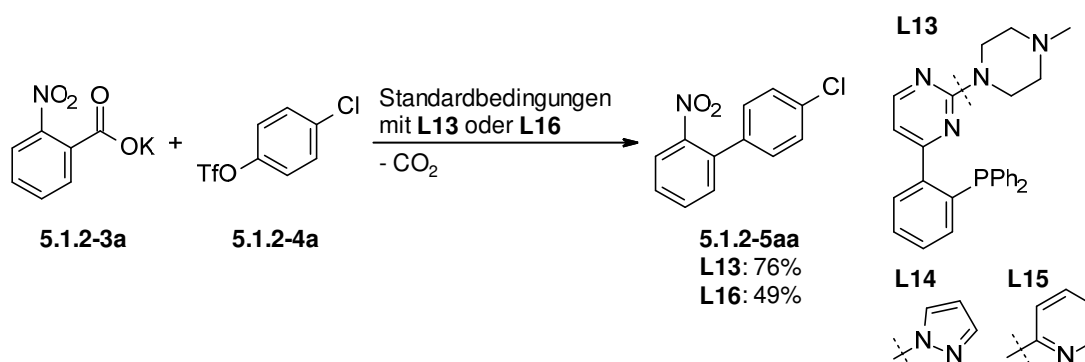
Die vorliegenden Resultate verdeutlichen, dass das neue Protokoll prinzipiell nicht auf die Kupplung von Aryltriflaten beschränkt ist. Dennoch sind weitere Optimierungsarbeiten notwendig, um auch für die Bromide eine effiziente Kupplung bei 100 °C zu realisieren. Dabei ist die Untersuchung verbesserter Ligandensysteme abermals ein vielversprechender Ansatzpunkt.

Darstellung und Untersuchung weiterer *P,N*-Liganden

Basierend auf den bisherigen Erkenntnissen sollte das Spektrum der *P,N*-Liganden um weitere Vertreter mit optimierten Donoreinheiten für die Katalysatormetalle ergänzt und die neuen Liganden in der Cu/Pd-katalysierten decarboxylierenden Kreuzkupplung bei 100 °C

getestet werden. Es sollten neue Strukturen identifiziert werden, die nach Möglichkeit eine verbesserte Koordination an die Katalysatormetalle gewährleisten und dadurch zu einer verbesserten Cu–Pd-Adduktbildung führen, was letztlich idealerweise in einer gesteigerten Katalysatoraktivität resultiert.

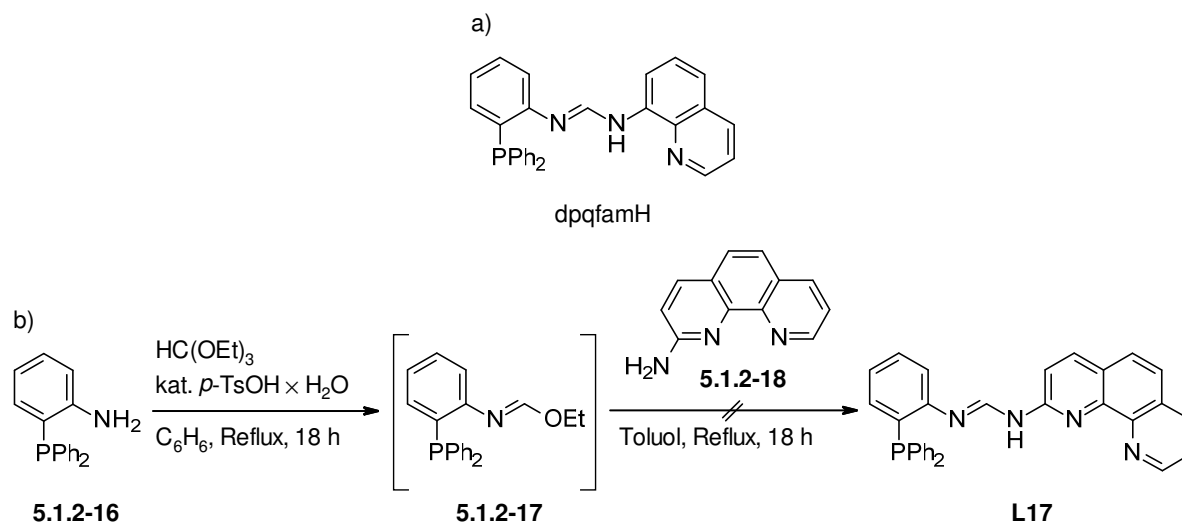
Zunächst sollte eine Variation der *N*-Donoreinheit des Substituenten am Pyrimidinring der Pyrimidinylphosphane vorgenommen werden. Eine Variante des Liganden **L9** mit einer zusätzlichen *N*-Donoreinheit repräsentiert der *N*-Methylpiperazinyl-substituierte Pyrimidinylphosphanligand **L13**. Dieser wurde von Herrn Julian Menges im Rahmen seiner Diplomarbeit^[150] analog zu der im Manuskript beschriebenen Pyrimidinylphosphansynthese^[151,152] dargestellt. In der Modellreaktion von **5.1.2-3a** mit **5.1.2-4a** konnten unter Verwendung von **L13** eine Ausbeute von 76% erzielt werden (Schema 31). Zwar ist ein maßgeblicher Einfluss des zusätzlichen Heteroatoms nicht zu beobachten, doch verdeutlichen diese Ergebnisse erneut, dass Pyrimidinylphosphane mit zyklischen tertiären Aminosubstituenten eine besonders hohe Aktivität in der vorliegenden Transformation aufweisen.



Schema 31: Decarboxylierende Kreuzkupplung bei 100 °C mit **L13** und **L16**.

In den Arbeiten von Herrn Menges bestand weiterhin die Aufgabe, einen Pyrazolyl- und einen Pyridyl-substituierten Pyrimidinylphosphanliganden zu synthetisieren (Schema 31).^[150] Jedoch konnte die Synthese des Pyrazolyl-substituierten Liganden **L14** nicht realisiert werden und der Pyridyl-substituierte Vertreter **L15** wurde in nur geringen Ausbeuten erhalten, sodass diese nicht für Katalyseexperimente zur Verfügung gestellt werden konnten.

Da der Ligand **L15** eine effiziente Koordination analog zu Bipyridinen, die sich ebenso wie Phenanthroline als *N*-Liganden für den Kupfer-Katalysator in decarboxylierenden Kreuzkupplungen eignen, erwarten lässt, wurde diese Strukturuntereinheit in einer weiteren Ligandsynthese erneut aufgegriffen. So wurde der Ligand **L16**, welcher neben dem Pyridylsubstituenten eine im Vergleich zu den bislang verwendeten Pyrimidinylphosphanen



Schema 33: a) *dpqfamH*; b) Angestrebte Synthese des Liganden **L17**.

Im Rahmen dieser Arbeit konnte **L17** jedoch nicht isoliert werden. Eine ^{31}P -NMR-spektroskopische Analyse der Reaktionsmischung zeigte eine komplexe Produktmischung anhand derer sich keine Aussage über eine mögliche Bildung des Liganden treffen lies. Dennoch bleibt die Darstellung von **L17** ein attraktives Synthesziel. Interessant wäre es, bimetallische Cu/Pd-Komplexe des Liganden zu synthetisieren, um diese sowie den Liganden selbst in der decarboxylierenden Kreuzkupplung bei 100 °C zu testen. Im Erfolgsfall könnte die zugrundeliegende Synthesestrategie außerdem einen einfachen Aufbau anderer Derivate zulassen.

5.2 Decarboxylierende Kreuzkupplungen heteroaromatischer Carbonsäuren

Die hier beschriebenen Arbeiten entstammen einem Kooperationsprojekt mit Pfizer Inc. und wurden beratend von Herrn Dr. David C. Blakemore und Herrn Dr. Brian O'Neill unterstützt.

5.2.1 Hintergrund

2-Arylpyridine sind wichtige Struktureinheiten in einer Vielzahl von Naturstoffen, Pharmaka und Funktionsmaterialien.^[155–160] Beispiele sind die in Abbildung 1 dargestellte Polyarylpyridinstruktur, ein fluoreszierender Chemosensor, das Pyridin-verbrückte Analogon zu Combretastatin-A4 sowie Streptonigrin aus *Streptomyces flocculus*, beides Antitumor-Mittel.

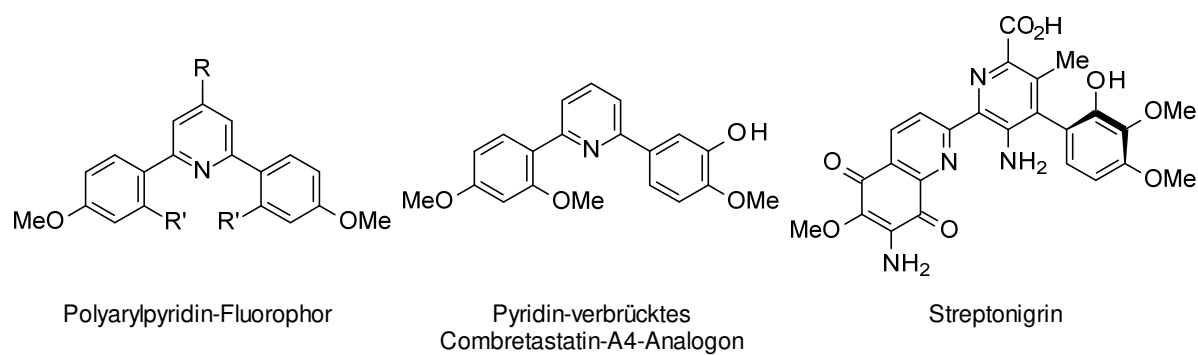
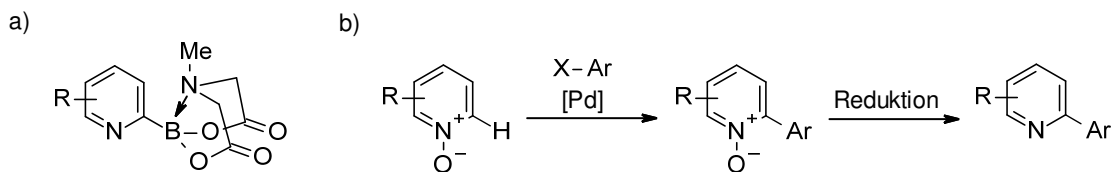


Abbildung 1: 2-Arylpyridine in Funktionsmaterialien, Natur- und Wirkstoffen.

Zwar haben sich Übergangsmetall-katalysierte Kreuzkupplungen präformierter Organometallverbindungen in den vergangenen Jahrzehnten als wertvolle Methode zur Darstellung verschiedenster Struktur motive etabliert,^[3] doch ist die Synthese von 2-Arylpyridinen ausgehend von 2-Pyridylorganometallverbindungen, wie beispielsweise Boronsäurederivaten, mit enormen Schwierigkeiten verbunden. So sind diese Substrate oft schwer zugänglich und instabil.^[104] Zudem neigen sie im Verlauf der Reaktion zu Protodemetallierung und weisen eine vergleichsweise langsame Transmetallierung auf, wodurch diese Reaktionen oft mit geringer Effizienz ablaufen.^[104,161]

Entscheidende Fortschritte auf dem Gebiet der 2-Arylpyridinsynthese konnten mit der Entwicklung stabilerer Arylboronsäurederivate erzielt werden.^[104,161–163] Hervorzuheben sind die von Burke beschriebenen luftstabilen 2-Pyridyl-MIDA-boronate (Schema 34, a), die effizient in Palladium-katalysierten Suzuki-Kupplungen umgesetzt werden können.^[162,163] Um die mit Kupplungen präformierter Organometallverbindungen einhergehenden Probleme zu überwinden (siehe auch Abschnitt 3.2.2.1), haben sich in den vergangenen Jahren zudem *ortho*-C–H-Arylierungen von Pyridin-*N*-oxiden als alternative Syntheseroute etabliert

(Schema 34, b).^[104,164–168] Diese zeigen jedoch in manchen Fällen Selektivitätsprobleme und erfordern einen zusätzlichen Reduktionsschritt im Anschluss an die Arylierung.



Schema 34: a) 2-Pyridyl-MIDA-boronate; b) *ortho*-Arylierung von Pyridin-N-oxiden.

Wie bereits in Abschnitt 3.2.2.4 diskutiert, wurden 2-Arylpyridinsynthesen, die auf decarboxylierenden Kreuzkupplungen von Pyridin-2-carbonsäuren mit Aryl- und Heteroaryl bromiden basieren, von den Gruppen um Wu und Stoltz beschrieben.^[102,103] Zwar stellen diese Protokolle eine willkommene Alternative zu den oben vorgestellten Methoden dar, doch lässt sich aufgrund der vergleichsweise geringen Ausbeuten sowie den relativ hohen Katalysatorbeladungen beziehungsweise den hohen Reaktionstemperaturen annehmen, dass das synthetische Potential dieser Varianten noch nicht vollends ausgeschöpft ist. Verbesserte Reaktionsprotokolle, welche die Kupplung von Pyridin-2-carbonsäuren mit hoher Effizienz unter milden Reaktionsbedingungen ermöglichen und zudem das Substratspektrum der existierenden Protokolle ergänzen, wären somit höchst erstrebenswert.

Die Ergebnisse der zwei nachfolgenden Unterkapitel wurden mit Herrn Philip Weber zu gleichen Teilen erarbeitet. Herr Jie Tang unterstützte uns bei diesen Arbeiten. Eine Erklärung zur Arbeitsteilung in Abschnitt 5.2.4 folgt dort und die in Abschnitt 5.2.5 diskutierten Arbeiten wurden von mir durchgeführt.

5.2.2 Protodecarboxylierung von Pyridin-2-carbonsäure

Um ein besseres Verständnis für die Reaktivität von Pyridin-2-carbonsäuren zu erhalten, wurden zunächst Protodecarboxylierungsstudien durchgeführt. In Anlehnung an die Arbeiten von Wu und Stoltz^[102,103] wurden dabei zunächst Kupfer-basierte Decarboxylierungskatalysatoren untersucht (Tabelle 2). Die Umsetzung von Pyridin-2-carbonsäure (**5.2.2-1**) in Gegenwart eines Katalysatorsystems aus Cu₂O und 1,10-Phenanthrolin bei 190 °C in NMP lieferte das gewünschte Produkt **5.2.2-2** in 82% Ausbeute (Eintrag 1). Eine Erhöhung der Katalysatorbeladung hatte keinen Einfluss auf die Ausbeute (Eintrag 2) und Lösungsmittelgemische aus NMP und Mesitylen oder Chinolin zeigten geringere oder ähnliche Effizienz verglichen mit reinem NMP (Einträge 3 und 4). Während die Wahl des

Phenanthrolinliganden nur einen geringen Einfluss zeigte (Einträge 5–7), erwiesen sich Kupferhalogenide als weniger geeignet (Einträge 8–10). Eine Variation der Reaktionstemperatur zeigte, dass sich selbst bei 160 °C noch eine vergleichsweise gute Ausbeute erzielen lässt (Einträge 11 und 12). Dahingegen war bei 140 °C eine deutlich geringere Ausbeute beobachtbar und bei 120 °C wurde kein Produkt gebildet (Einträge 13 und 14).

Tabelle 2: Protodecarboxylierungsstudien in Gegenwart eines Kupfer-Katalysators.

c1ccncc1C(=O)O
 $\xrightarrow[\text{NMP, } \Delta, 24 \text{ h}]{[\text{Cu}] / \text{N-Ligand}}$
c1ccncc1 + CO₂↑

5.2.2-1
5.2.2-2

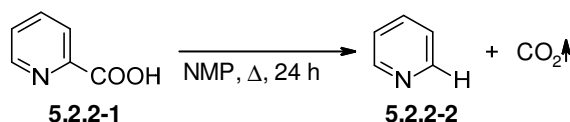
Eintrag	T (°C)	[Cu]	N-Ligand	5.2.2-2 (%)
1	190	Cu ₂ O	1,10-Phen	82
2 ^[a]	"	"	"	79
3 ^[b]	"	"	"	66
4 ^[c]	"	"	"	77
5	"	"	Ph ₂ -Phen	75
6	"	"	Me ₄ -Phen	80
7	"	"	2,2'-Bipyridin	75
8	"	CuCl	1,10-Phen	56
9	"	CuBr	"	63
10	"	CuI	"	62
11	180	Cu ₂ O	"	75
12	160	"	"	78
13	140	"	"	36
14	120	"	"	n.d.

Reaktionsbedingungen: **5.2.2-1** (0.5 mmol), [Cu] (5 mol%), N-Ligand (10 mol%), NMP (2 mL), Δ, 24 h. GC-Ausbeuten mit *n*-Dodecan als interner Standard. [a] Cu₂O (10 mol%), 1,10-Phen (20 mol%). [b] NMP/Mes (3:1, 2 mL). [c] NMP/Chinolin (3:1, 2 mL).

Kontrollexperimente zeigten, dass die Protodecarboxylierung der Pyridin-2-carbonsäure auch ohne Zusatz eines Katalysators abläuft (Tabelle 3). Die Ausbeuten entsprechen dabei mindestens etwa zwei Dritteln der Ausbeuten mit Katalysator (Tabelle 2) und es wird eine analoge Temperaturabhängigkeit beobachtet. Daraus lässt sich schließen, dass die Metall-

katalysierte Reaktion vergleichsweise langsam abläuft und einen geringeren Einfluss auf die in Tabelle 2 gezeigten Gesamtausbeuten hat.

Tabelle 3: Metall-freie Protodecarboxylierung von Pyridin-2-carbonsäure.



Eintrag	T (°C)	5.2.2-2 (%)
1	190	69
2	180	43
3	160	50
4	140	21
5	120	n.d.

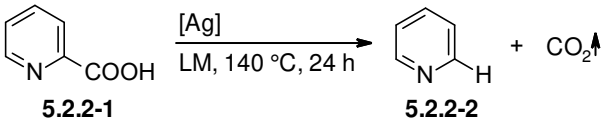
Reaktionsbedingungen: **5.2.2-1** (0.5 mmol), NMP (2 mL), Δ , 24 h. GC-Ausbeuten mit *n*-Dodecan als interner Standard.

Die Metall-freie Decarboxylierung von Pyridin-2-carbonsäuren ist seit langem bekannt und wird sich in der sogenannten Hammick-Reaktion zu Nutze gemacht. Dabei reagiert das intermediär gebildete Carben mit Carbonylverbindungen zu sekundären oder tertiären Alkoholen.^[169,170] In diesem Zusammenhang wurden Protokolle beschrieben, die diese Reaktion selbst bei 100 °C effizient ermöglichen.^[171] Im vorliegenden Fall eröffnet die Metall-freie Reaktionsvariante einen unerwünschten alternativen Reaktionspfad, der eine kontrollierte Reaktionsführung erschwert.

Larrosa und Mitarbeiter beschrieben ein Protokoll zur Silber-katalysierten Protodecarboxylierung von Heteroarylcarbonsäuren bei 120 °C in DMSO.^[172] Dabei konnten Pyridindicarbonsäuren selektiv in 2-Position decarboxyliert werden. Darauf basierend wurden nachfolgend Protodecarboxylierungsexperimente unter Verwendung von Silbersalzen durchgeführt, um zu überprüfen, ob sich auf diese Weise bessere Umsätze bei niedrigeren Temperaturen erzielen lassen (Tabelle 4). Während mit Ag₂O in NMP bei 140 °C eine nur geringe Ausbeute erzielt wurde (Eintrag 1), die mit der der Metall-freien Variante vergleichbar war (siehe Tabelle 3), zeigten die übrigen Silbersalze eine deutliche Aktivität und lieferten Ausbeuten von bis zu 48% (Einträge 2–4). Die Variation des Lösungsmittels unter Verwendung von Ag₂CO₃ zeigte in Übereinstimmung mit den Arbeiten von Larrosa,^[172] dass sich die Säure in DMSO quantitativ umsetzen lässt (Eintrag 5). DMF und Lösungsmittelgemische aus DMSO und NMP oder Mesitylen führten ebenfalls zu gesteigerten Ausbeuten, wenn auch in deutlich

geringerem Maße. Dahingegen lieferte DMAc ähnliche Resultate wie NMP und in Mesitylen war eine nur geringe Produktbildung beobachtbar (Einträge 6–10).

Tabelle 4: Protodecarboxylierungsstudien in Gegenwart von Silber-Katalysatoren.



c1ccncc1C(=O)O $\xrightarrow[\text{LM, 140 °C, 24 h}]{[\text{Ag}]}$ c1ccncc1 + CO₂↑
5.2.2-1 **5.2.2-2**

Eintrag	[Ag]	Lösungsmittel	5.2.2-2 (%)
1	Ag ₂ O	NMP	16
2	Ag ₂ CO ₃	"	40
3 ^[a]	AgOAc	"	45
4 ^[a]	AgTFA	"	48
5	Ag ₂ CO ₃	DMSO	99
6	"	DMF	54
7	"	DMAc	42
8	"	Mes	10
9 ^[b]	"	DMSO/NMP (1:1)	65
10 ^[b]	"	DMSO/Mes (1:1)	60

Reaktionsbedingungen: **5.2.2-1** (0.5 mmol), [Ag] (10 mol%), Lösungsmittel (2 mL), 140 °C, 24 h. GC-Ausbeuten mit *n*-Dodecan als interner Standard. [a] [Ag] (20 mol%). [b] Lösungsmittel (1 mL), 16 h.

Kontrollexperimente zeigten, dass in DMSO auch ohne Ag₂CO₃ sehr gute Ausbeuten an **5.2.2-2** erzielt werden können (Tabelle 5) und somit die Wahl des Lösungsmittels zu einer effizienteren Metall-freien Protodecarboxylierung führt (Eintrag 2). Eine Variation der Reaktionstemperatur zeigt zudem, dass diese selbst bei 120 °C noch abläuft. Es sei anzumerken, dass in den Arbeiten von Larrosa ein Metall-freier Reaktionspfad nicht geprüft und diskutiert wurde.^[172]

Tabelle 5: Kontrollexperimente zur Protodecarboxylierung in DMSO.

$ \begin{array}{ccc} \text{Pyridine-2-carboxylic acid (5.2.2-1)} & \xrightarrow{\text{DMSO, } \Delta, 16 \text{ h}} & \text{Pyridine-2-carbaldehyde (5.2.2-2)} + \text{CO}_2\uparrow \\ \text{5.2.2-1} & & \text{5.2.2-2} \end{array} $				
Eintrag	[M]	5.2.2-2 (%)		
		140 °C	130 °C	120 °C
1	Ag ₂ CO ₃	99	50	9
2	-	80	51	21

Reaktionsbedingungen: **5.2.2-1** (0.5 mmol), [M] (10 mol%), DMSO (1 mL), Δ , 16 h. GC-Ausbeuten mit *n*-Dodecan als interner Standard.

Abschließend wurde untersucht, ob sich die Reaktion in DMSO durch Zusatz eines Liganden zugunsten des Metall-katalysierten Reaktionspfads beeinflussen lässt. Um einen Effekt des Liganden beobachten zu können, wurde dabei die Reaktionszeit auf 4 h verkürzt (Tabelle 6).

Tabelle 6: Protodecarboxylierung in DMSO unter Variation des Liganden.

$ \begin{array}{ccc} \text{Pyridine-2-carboxylic acid (5.2.2-1)} & \xrightarrow[\text{DMSO, 140 °C, 4 h}]{\text{Ag}_2\text{CO}_3 / \text{Ligand}} & \text{Pyridine-2-carbaldehyde (5.2.2-2)} + \text{CO}_2\uparrow \\ \text{5.2.2-1} & & \text{5.2.2-2} \end{array} $		
Eintrag	Ligand	5.2.2-2 (%)
1	-	24
2	1,10-Phen	12
3	Ph ₂ -Phen	11
4	Me ₄ -Phen	9
5	NO ₂ -Phen	22
6	2,2'-Bipyridin	22
7	Pyridin	14 ^[a]
8	Lutidin	19
9	PPh ₃	13
10	bisSO	40
11 ^[b]	"	Spuren
12 ^[c]	-	29

Reaktionsbedingungen: **5.2.2-1** (0.5 mmol), Ag₂CO₃ (10 mol%), Ligand (20 mol%), DMSO (1 mL), 140 °C, 4 h. GC-Ausbeuten mit *n*-Dodecan als interner Standard. [a] Die Ausbeute an **5.2.2-2** wurde um die als Ligand eingesetzte Menge an Pyridin korrigiert. [b] In NMP (1 mL). [c] Ohne Ag₂CO₃.

Es zeigte sich, dass der Zusatz verschiedener *N*- oder *P*-Liganden keinen positiven Einfluss auf die Reaktion hat. Stattdessen wurden tendenziell geringer Ausbeuten verglichen mit der Reaktion ohne Ligand beobachtet (Einträge 1–9). Lediglich in Gegenwart eines bis-Sulfoxid-Liganden war eine höhere Ausbeute beobachtbar (Eintrag 10), die sowohl über der Ausbeute im Fall der Ligand-freien Reaktion als auch über der Ausbeute ohne den Silber-Katalysator lag (Eintrag 12).

Die in diesem Abschnitt diskutierten Ergebnisse verdeutlichen die Schwierigkeiten, die mit der Decarboxylierung von Pyridin-2-carbonsäuren einhergehen. Zur erfolgreichen Nutzung dieser Substrate in decarboxylierenden Kreuzkupplungen gilt es somit, eine Metall-freie Protodecarboxylierung zu unterdrücken, die Metall-katalysierte Variante möglichst effizient zu gestalten sowie eine Protonolyse der aus der Decarboxylierung entstehenden 2-Pyridylorganometallspezies zu vermeiden.

5.2.3 Decarboxylierende Kreuzkupplung von Pyridin-2-carbonsäure

Nachfolgend wurde nun die decarboxylierende Kreuzkupplung der Pyridin-2-carbonsäure untersucht. Dabei sollten zunächst Kupfer/Palladium-basierte Katalysatorsysteme überprüft werden. Als Modellsystem diente die Reaktion von Kalium-2-pyridincarboxylat (**5.2.3-1a**) mit Brombenzol (**5.2.3-2a**). Das Kaliumsalz anstelle der freien Säure wurde gewählt, um die Anwesenheit von Protonen zu vermeiden und so eine unerwünschte Protodecarboxylierung möglichst zu minimieren. Ein Katalysatorsystem bestehend aus PdI₂, PPh₃, Cu₂O und 1,10-Phenanthrolin, welches in ähnlicher Form in den Arbeiten von Stoltz verwendet wurde,^[103] lieferte bei 190 °C das gewünschte Kupplungsprodukt **5.2.3-3aa** in 31% Ausbeute neben 26% des Protodecarboxylierungsprodukts Pyridin (**5.2.3-4**) sowie 6% an Biphenyl (**5.2.3-5a**), welches aus der Homokupplung des Arylbromids resultiert (Tabelle 7, Eintrag 1). Eine höhere Katalysatorbeladung beeinflusste weder die Produktbildung noch die Bildung der Nebenprodukte maßgeblich (Einträge 2 und 3). Die Variation der Kupfer-Quelle zeigte, dass CuBr und CuI weniger effizient sind (Einträge 4 und 5), was mit den Beobachtungen aus den Protodecarboxylierungsstudien übereinstimmt. CuCl lieferte hingegen zu Cu₂O vergleichbare Produktausbeuten (Eintrag 6). In allen Fällen war jedoch ein vergleichsweise höherer Einfluss der unerwünschten Protodecarboxylierung zu beobachten. Ein Silber-basierter Decarboxylierungskatalysator erwies sich unter diesen Bedingungen als ungeeignet (Eintrag 7) und bei einer Reaktionstemperatur von 170 °C war ein deutlich geringerer Umsatz beobachtbar (Eintrag 8). Ein Kontrollexperiment ohne Cu₂O und 1,10-Phenanthrolin zeigte, dass unter

diesen Bedingungen die Bildung von **5.2.3-3aa** ausbleibt, während die Bildung von **5.2.3-4** sogar leicht ansteigt (Eintrag 9).

Tabelle 7: Variation des Decarboxylierungskatalysators.

$ \begin{array}{c} \text{Pyridine-2-COOK} + \text{BrPh} \xrightarrow[\text{NMP, 190 °C, 24 h, -CO}_2]{\text{PdI}_2 / \text{PPh}_3, [\text{M}] / \text{N-Ligand}} \text{Pyridine-2-Ph} + \text{Pyridine} + \text{Ph-Ph} \\ \text{5.2.3-1a} \quad \text{5.2.3-2a} \quad \quad \quad \text{5.2.3-3aa} \quad \text{5.2.3-4} \quad \text{5.2.3-5a} \end{array} $					
Eintrag	[M] (mol%)	N-Ligand (mol%)	5.2.3-3aa (%)	5.2.3-4 (%)	5.2.3-5a (%)
1	Cu ₂ O (5)	1,10-Phen (10)	31	26	6
2	Cu ₂ O (10)	1,10-Phen (20)	35	27	Spuren
3	Cu ₂ O (15)	1,10-Phen (30)	33	29	6
4 ^[a]	CuI (10)	1,10-Phen (10)	17	43	6
5 ^[a]	CuBr (10)	"	20	50	5
6 ^[a]	CuCl (10)	"	30	41	4
7	Ag ₂ CO ₃ (5)	-	9	4	Spuren
8 ^[b]	Cu ₂ O (5)	1,10-Phen (10)	6	11	Spuren
9	-	-	n.d.	36	6

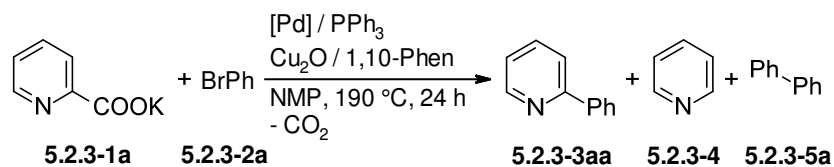
Reaktionsbedingungen: **5.2.3-1a** (0.5 mmol), **5.2.3-2a** (1 mmol), [M], N-Ligand, PdI₂ (5 mol%), PPh₃ (15 mol%), NMP (2 mL), 190 °C, 24 h. GC-Ausbeuten mit *n*-Tetradecan als interner Standard. [a] [M] (10 mol%). [b] 170 °C.

Insgesamt zeigte sich, dass unter den gewählten Bedingungen selbst bei 190 °C nur mäßige Umsätze erzielt werden können und dass die Protodecarboxylierung als Nebenreaktion den größten Einfluss hat. Während die Protodecarboxylierung der freien Säure auch bei Temperaturen von 160 °C noch in zufriedenstellender Effizienz erfolgte, wenn auch unter deutlichem Einfluss des Metall-freien Reaktionspfades, war im vorliegenden Fall schon bei 170 °C ein nur geringer Umsatz zu beobachten.

Basierend auf diesen Ergebnissen wurde untersucht, ob sich durch Variation anderer Reaktionsparameter bessere Ausbeuten und Selektivitäten erzielen lassen. Eine Variation der Palladium-Vorstufe zeigte, dass unter den Palladiumhalogeniden PdCl₂ und PdBr₂ am effizientesten sind (Tabelle 8, Einträge 1–3), wobei im letztgenannten Fall deutlich mehr Pyridin (**5.2.3-4**) gebildet wurde. Die übrigen geprüften Palladium-Vorstufen erwiesen sich

hingegen als weniger geeignet (Einträge 4–7) und eine Verringerung der Katalysatorbeladung an Palladium und PPh₃ führt ebenfalls zu einem deutlich geringeren Umsatz (Eintrag 8).

Tabelle 8: Variation der Palladium-Vorstufe.



Eintrag	[Pd]	5.2.3-3aa (%)	5.2.3-4 (%)	5.2.3-5a (%)
1	PdI ₂	31	23	Spuren
2	PdCl ₂	44	33	5
3	PdBr ₂	36	13	Spuren
4	Pd(OAc) ₂	22	26	8
5	Pd(acac) ₂	17	30	7
6	Pd(F ₆ -acac) ₂	15	22	6
7	Pd(COD)Cl ₂	22	28	5
8 ^[a]	PdCl ₂	17	10	Spuren

Reaktionsbedingungen: **5.2.3-1a** (0.5 mmol), **5.2.3-2a** (1 mmol), Cu₂O (5 mol%), 1,10-Phen (10 mol%), [Pd] (5 mol%), PPh₃ (15 mol%), NMP (2 mL), 190 °C, 24 h. GC-Ausbeuten mit *n*-Tetradecan als interner Standard. [a] [Pd] (3 mol%), PPh₃ (12 mol%).

Anschließend wurde der Einfluss verschiedener *N*-Liganden überprüft (Tabelle 9). Dabei zeigte sich, dass mit dem bisher verwendeten 1,10-Phenanthrolin die besten Resultate erzielt werden können (Eintrag 1). Elektronenreichere Derivate führten zu einer etwas geringeren Ausbeute an **5.2.3-3aa**, während in Gegenwart eines elektronenärmeren Vertreters nur noch 5% des Kreuzkupplungsprodukts **5.2.3-3aa** detektiert wurden (Einträge 2–4). Die Protodecarboxylierung lag in diesen Fällen bei 20–30%, sodass die Umsätze insgesamt geringer waren. 2,2'-Bipyridin sowie Pyridine und Chinuclidin, welche sich in den Arbeiten von Stoltz als vorteilhaft zeigten,^[103] erwiesen sich ebenfalls als unterlegen (Einträge 5–9) und ein Kontrollexperiment ohne *N*-Ligand lieferte dazu vergleichbare Resultate (Eintrag 10).

Tabelle 9: Variation des *N*-Liganden.

$ \begin{array}{c} \text{Pyridine-2-COOK} + \text{BrPh} \xrightarrow[\text{- CO}_2]{\text{PdCl}_2 / \text{PPh}_3, \text{Cu}_2\text{O} / \text{N-Ligand}, \text{NMP}, 190^\circ\text{C}, 24 \text{ h}} \text{Pyridine-2-Ph} + \text{Pyridine} + \text{Ph-Ph} \\ \text{5.2.3-1a} \quad \text{5.2.3-2a} \quad \quad \quad \text{5.2.3-3aa} \quad \text{5.2.3-4} \quad \text{5.2.3-5a} \end{array} $				
Eintrag	<i>N</i> -Ligand	5.2.3-3aa (%)	5.2.3-4 (%)	5.2.3-5a (%)
1	1,10-Phen	44	33	5
2	Me ₄ -Phen	30	20	4
3	Ph ₂ -Phen	33	30	6
4	NO ₂ -Phen	5	28	4
5	2,2'-Bipyridin	34	18	4
6 ^[a]	Pyridin	26	33 ^[b]	7
7 ^[a]	2,6-Lutidin	26	36	6
8 ^[a]	DMAP	28	29	7
9 ^[a]	Chinuclidin	28	33	7
10	-	27	19	5

Reaktionsbedingungen: **5.2.3-1a** (0.5 mmol), **5.2.3-2a** (1 mmol), Cu₂O (5 mol%), *N*-Ligand (10 mol%), PdCl₂ (5 mol%), PPh₃ (15 mol%), NMP (2 mL), 190 °C, 24 h. GC-Ausbeuten mit *n*-Tetradecan als interner Standard. [a] *N*-Ligand (30 mol%). [b] Die Ausbeute an **5.2.3-4** wurde um die als Ligand eingesetzte Menge an Pyridin korrigiert.

In Übereinstimmung mit den Arbeiten von Wu und Stoltz zeigten die Liganden PPh₃ und BINAP die höchste Aktivität,^[102,103] wenn auch gleichzeitig größere Mengen an Pyridin aus der unerwünschten Protodecarboxylierung detektiert wurden (Tabelle 10, Einträge 1 und 4). Andere Triaryl-basierte oder elektronenreiche, sterisch anspruchsvolle *P*-Liganden erwiesen sich als weniger effizient.

Tabelle 10: Variation des *P*-Liganden.

$ \begin{array}{c} \text{Pyridine-2-COOK} + \text{BrPh} \xrightarrow[\text{NMP, 190 °C, 24 h, -CO}_2]{\text{PdCl}_2 / \text{P-Ligand, Cu}_2\text{O / 1,10-Phen}} \text{Pyridine-2-Ph} + \text{Pyridine} + \text{Ph-Ph} \\ \text{5.2.3-1a} \quad \text{5.2.3-2a} \quad \quad \quad \text{5.2.3-3aa} \quad \text{5.2.3-4} \quad \text{5.2.3-5a} \end{array} $				
Eintrag	<i>P</i> -Ligand	5.2.3-3aa (%)	5.2.3-4 (%)	5.2.3-5a (%)
1	PPh ₃	44	33	5
2	P(<i>o</i> -Tol) ₃	12	22	4
3	P(<i>p</i> -Tol) ₃	23	31	4
4	BINAP	37	37	Spuren
5	JohnPhos	19	33	Spuren
6	SPhos	16	20	4
7	XPhos	21	30	4

Reaktionsbedingungen: **5.2.3-1a** (0.5 mmol), **5.2.3-2a** (1 mmol), Cu₂O (5 mol%), 1,10-Phen (10 mol%), PdCl₂ (5 mol%), *P*-Ligand (15 mol%), NMP (2 mL), 190 °C, 24 h. GC-Ausbeuten mit *n*-Tetradecan als interner Standard.

Ein Lösungsmittelscreening zeigte schließlich, dass mit einem unpolareneren Lösungsmittelgemisch aus NMP und Mesitylen im Volumenverhältnis 1:1 die Ausbeute an **5.2.3-3aa** auf 61% gesteigert werden kann. Dies bei gleichzeitiger Verminderung der Protodecarboxylierung (Tabelle 11, Eintrag 2). Mit anderen Lösungsmittelverhältnissen war ebenfalls weniger Protodecarboxylierung zu beobachten. Gleichzeitig konnte aber auch weniger des Kreuzkupplungsprodukts **5.2.3-3aa** detektiert werden (Einträge 3 und 4). Mischungen aus NMP und Chinolin lieferten verglichen dazu schlechtere Resultate (Einträge 5–7) und ein gesteigerter Gesamtumsatz war in keinem der Fälle zu beobachten.

Tabelle 11: Variation des Lösungsmittels.

$ \begin{array}{c} \text{Pyridine-2-COOK} + \text{BrPh} \xrightarrow[\text{- CO}_2]{\text{PdCl}_2 / \text{PPh}_3, \text{Cu}_2\text{O} / 1,10\text{-Phen}, \text{LM}, 190^\circ\text{C}, 24\text{ h}} \text{Pyridine-2-Ph} + \text{Pyridine} + \text{Ph-Ph} \\ \text{5.2.3-1a} \quad \text{5.2.3-2a} \quad \quad \quad \text{5.2.3-3aa} \quad \text{5.2.3-4} \quad \text{5.2.3-5a} \end{array} $				
Eintrag	Lösungsmittel	5.2.3-3aa (%)	5.2.3-4 (%)	5.2.3-5a (%)
1	NMP	44	33	5
2	NMP/Mes (1:1)	61	14	5
3	NMP/Mes (3:1)	53	20	4
4	NMP/Mes (1:3)	41	17	5
5	NMP/Chinolin (1:1)	43	28	5
6	NMP/Chinolin (3:1)	49	35	4
7	NMP/Chinolin (1:3)	33	32	4

Reaktionsbedingungen: **5.2.3-1a** (0.5 mmol), **5.2.3-2a** (1 mmol), Cu₂O (5 mol%), 1,10-Phen (10 mol%), PdCl₂ (5 mol%), PPh₃ (15 mol%), NMP (2 mL), 190 °C, 24 h. GC-Ausbeuten mit *n*-Tetradecan als interner Standard.

Ergänzend zu den vorhergegangenen Untersuchungen wurden zusätzliche Palladiumchloridkomplexe und kationische Palladiumspezies sowie elektronenarme Phosphane untersucht (Tabelle 12). Unter den verwendeten Palladium-Vorstufen lieferte keine bessere Resultate als PdCl₂ und mit (MeCN)₄Pd(BF₄)₂ waren zudem wieder erhöhte Mengen an Pyridin detektierbar (Einträge 1–6). Ebenso konnte mit den elektronenärmeren Phosphanen die Ausbeute nicht gesteigert werden (Einträge 7–9)

Tabelle 12: Ergänzende Experimente unter Variation der Palladium-Quelle und des P-Liganden.

$ \begin{array}{c} \text{Pyridine-2-COOK} + \text{BrPh} \xrightarrow[\text{- CO}_2]{\text{[Pd] / P-Ligand, Cu}_2\text{O / 1,10-Phen, NMP/Mes, 190 }^\circ\text{C, 24 h}} \text{Ph-Pyridine} + \text{Pyridine} + \text{Ph-Ph} \\ \text{5.2.3-1a} \quad \text{5.2.3-2a} \quad \quad \quad \text{5.2.3-3aa} \quad \text{5.2.3-4} \quad \text{5.2.3-5a} \end{array} $					
Eintrag	[Pd]	P-Ligand	5.2.3-3aa (%)	5.2.3-4 (%)	5.2.3-5a (%)
1	PdCl ₂	PPh ₃	61	14	5
2	(PPh ₃) ₂ PdCl ₂	"	49	n.d.	4
3	(PCy ₃) ₂ PdCl ₂	"	36	13	3
4	(MeCN) ₂ PdCl ₂	"	40	8	6
5	(MeCN) ₄ Pd(BF ₄) ₂	"	31	34	8
6	(MeCN) ₄ Pd(OTs) ₂	"	50	17	6
7	PdCl ₂	P(<i>p</i> -CF ₃ C ₆ H ₄) ₃	42	16	7
8	"	P(<i>p</i> -FC ₆ H ₄) ₃	40	8	4
9	"	P(2-Furyl) ₃	30	25	4

Reaktionsbedingungen: **5.2.3-1a** (0.5 mmol), **5.2.3-2a** (1 mmol), Cu₂O (5 mol%), 1,10-Phen (10 mol%), [Pd] (5 mol%), P-Ligand (15 mol%), NMP/Mes (1:1, 2 mL), 190 °C, 24 h. GC-Ausbeuten mit *n*-Tetradecan als interner Standard.

Um auszuschließen, dass die vermeintlich hohe Effizienz von PPh₃ auf eine unerwünschte Nebenreaktion dieses Liganden mit dem Substrat zurückgeht, die ebenfalls das gewünschte Kupplungsprodukt liefert, wurde nachfolgend *p*-Bromtoluol (**5.2.3-2b**) als Kupplungspartner gewählt (Tabelle 13). Tatsächlich ging dies mit enormen Ausbeuteverlusten einher, sodass das Kupplungsprodukt **5.2.3-3ab** in lediglich 35% Ausbeute erhalten wurde. Als Nebenprodukte wurden Pyridin (**5.2.3-4**) sowie das Homokupplungsprodukt **5.2.3-5b** neben 15% an Phenylpyridin (**5.2.3-3aa'**) detektiert (Eintrag 1). Somit bestätigte sich, dass eine C–P-Bindungsspaltung am Liganden mit einer Übertragung des Phenylrests auf den Pyridylrest für die erhöhten Ausbeuten verantwortlich war. Es ist anzunehmen, dass aufgrund dieser Hintergrundreaktion auch die Ausbeuten in den Arbeiten von Stoltz mit einem Fehler behaftet sind.^[103] Unter Verwendung von PdI₂ wurden ähnliche Resultate erhalten (Eintrag 2). Dabei waren 13% an Phenylpyridin (**5.2.3-3aa'**) detektierbar. In Gegenwart des Liganden BINAP, welcher zuvor ebenfalls gute Ausbeuten lieferte, wurde das unerwünschte Nebenprodukt ebenfalls gebildet (Eintrag 3). Dagegen waren beispielsweise mit CyJohnPhos ähnliche

Mengen an **5.2.3-3ab** zugänglich und es wurden keinerlei Nebenprodukte, die aus einer Hintergrundreaktion des Liganden resultieren könnten, detektiert (Eintrag 4).

Tabelle 13: Vergleichsexperimente mit *p*-Bromtoluol als Kupplungspartner.

$ \begin{array}{c} \text{Pyridine-2-COOK} + \text{Br}(p\text{-Tol}) \xrightarrow[\text{NMP/Mes, 190 °C, 24 h}]{\text{[Pd] / P-Ligand, Cu}_2\text{O / 1,10-Phen}} \\ \text{5.3.2-1a} \quad \text{5.3.2-2b} \quad \quad \quad \text{5.3.2-3ab} + \text{5.3.2-4} + p\text{-Tol-}p\text{-Tol} + \text{5.3.2-3aa'} \\ \text{- CO}_2 \end{array} $						
Eintrag	[Pd]	P-Ligand	5.2.3-3ab (%)	5.2.3-4 (%)	5.2.3-5b (%)	5.2.3-3aa' (%)
1	PdCl ₂	PPh ₃	35	19	5	15
2	PdI ₂	"	34	24	6	13
3	PdCl ₂	BINAP	32	9	5	12
4	PdI ₂	CyJohnPhos	29	25	4	-

Reaktionsbedingungen: **5.2.3-1a** (0.5 mmol), **5.2.3-2b** (1 mmol), Cu₂O (5 mol%), 1,10-Phen (10 mol%), [Pd] (5 mol%), P-Ligand (12 mol%), NMP/Mes (1:1, 2 mL), 190 °C, 24 h. GC-Ausbeuten mit *n*-Tetradecan als interner Standard.

Eine Variation der Katalysatorbeladung unter Verwendung von PPh₃ zeigte schließlich, dass durch Erhöhung der Menge an PdCl₂ auf 7.5 mol% und PPh₃ auf 18 mol% die Produktausbeute an **5.2.3-3ab** leicht gesteigert werden kann (Tabelle 14, Einträge 1 und 2).

Tabelle 14: Variation der Katalysatorbeladung.

$ \begin{array}{c} \text{Pyridine-2-COOK} + \text{Br}(p\text{-Tol}) \xrightarrow[\text{NMP/Mes, 190 °C, 24 h}]{\text{PdCl}_2 / \text{PPh}_3, \text{Cu}_2\text{O / 1,10-Phen}} \\ \text{5.3.2-1a} \quad \text{5.3.2-2b} \quad \quad \quad \text{5.3.2-3ab} + \text{5.3.2-4} + p\text{-Tol-}p\text{-Tol} + \text{5.3.2-3aa'} \\ \text{- CO}_2 \end{array} $						
Eintrag	Cu ₂ O / 1,10-Phen (mol%)	PdCl ₂ / PPh ₃ (mol%)	5.2.3-3ab (%)	5.2.3-4 (%)	5.2.3-5b (%)	5.2.3-3aa' (%)
1	5/10	5/12	35	19	5	15
2	5/10	7.5/18	39	7	5	32
3	5/10	10/24	28	10	5	42
4	7.5/15	5/12	31	9	7	14
5	10/20	5/12	53	3	13	10

Reaktionsbedingungen: **5.2.3-1a** (0.5 mmol), **5.2.3-2b** (1 mmol), Cu₂O, 1,10-Phen, PdCl₂, PPh₃, NMP/Mes (1:1, 2 mL), 190 °C, 24 h. GC-Ausbeuten mit *n*-Tetradecan als interner Standard.

Während eine weitere Erhöhung der Katalysatorbeladung schließlich zu geringeren Ausbeuten hinsichtlich **5.2.3-3ab** führte (Eintrag 3), nahm die Bildung des unerwünschten Phenylpyridins **5.2.3-3aa'** in deutlicherem Maße stetig zu. Dies ging interessanterweise mit einer leichten Umsatzsteigerung einher. Im Gegensatz dazu führte eine höhere Beladung an Cu₂O und 1,10-Phenanthrolin zu einer deutlich gesteigerten Ausbeute an **5.2.3-3ab** (Eintrag 5). Zwar wurde vergleichsweise mehr des Biaryls **5.2.3-5b** gebildet, doch konnte die Protodecarboxylierung sowie die Entstehung von **5.2.3-3aa'** verringert werden.

Neben den Experimenten mit Kupfer/Palladium-basierten Katalysatorsystemen bei 190 °C wurde überprüft, ob sich mit einem Silber/Palladium-basierten System in DMSO decarboxylierende Kreuzkupplungen von Kalium-2-picolinat bei niedrigeren Temperaturen realisieren lassen. Als Kupplungspartner wurde dabei *p*-Tolyltriflat gewählt. Eine stichprobenartige Variation verschiedener Reaktionsparameter bei 140 °C zeigte jedoch an dieser Stelle keine Hinweise auf die Realisierbarkeit der Reaktion unter diesen Bedingungen. So wurde die Bildung von **5.2.3-3ab** nicht beobachtet und selbst die Protodecarboxylierung von **5.2.3-1a** erfolgte lediglich in geringem Maße.

Die Untersuchungen zur Kupplung des Kalium-2-picolinats wurden an diesem Punkt eingestellt. Aufgrund der geringen Umsätze und Ausbeuten wurde anschließend untersucht, ob ein aktivierender Substituent in *ortho*-Position zur Carboxygruppe einen positiven Einfluss auf die Reaktivität des Substrats hat.

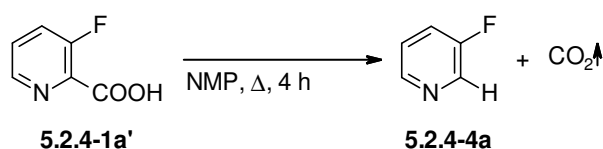
5.2.4 Decarboxylierende Kreuzkupplung 3-substituierter Pyridin-2-carbonsäuren

In weiterführenden Arbeiten wurde untersucht, ob ein elektronenziehender Substituent *ortho* zur Carboxygruppe einen ähnlichen Einfluss wie im Fall von Benzoesäuren ausübt und somit zu einer erleichterten Decarboxylierung führt,^[143] die letztlich eine effizientere Kreuzkupplung ermöglicht.

Zunächst wurden Protodecarboxylierungsstudien durchgeführt, in denen 3-Fluorpyridin-2-carbonsäure (**5.2.4-1a'**) sowohl in Gegenwart als auch in Abwesenheit eines Kupfer-basierten Decarboxylierungskatalysators bei verschiedenen Temperaturen zur Reaktion gebracht wurde (Tabelle 15). Es zeigte sich, dass **5.2.4-1a'** unter den gewählten Bedingungen selbst bei 100 °C noch effizient decarboxyliert werden kann (Eintrag 3) und dass die Reaktion erst bei Temperaturen unter 60 °C zum Erliegen kommt (Eintrag 8). Während die Anwesenheit des Katalysators im Fall der unsubstituierten Picolinsäure einen positiven Einfluss auf die Umsetzung hatte, war ein solcher Effekt für dieses Substrat nicht beobachtbar. Somit zeigt der

ortho-Substituent zwar eine aktivierende Wirkung, doch macht diese den Decarboxylierungskatalysator obsolet und erschwert damit eine kontrollierte Reaktionsführung.

Tabelle 15: Protodecarboxylierung von 3-Fluorpyridin-2-carbonsäure.



Eintrag	T (°C)	5.2.4-4a (%)	
		mit Cu ₂ O / 1,10-Phen	ohne Cu ₂ O / 1,10-Phen
1	180	92	95
2	160	99	95
3	140	96	90
4	120	86	91
5	100	82	91
6	80	65	69
7	60	14	12
8	40	n.d.	n.d.

Reaktionsbedingungen: **5.2.4-1a'** (0.5 mmol), Cu₂O (5 mol%), 1,10-Phen (10 mol%), NMP (2 mL), Δ, 4 h. ¹⁹F-NMR-Ausbeuten mit 1,4-Difluorbenzol als interner Standard.

Im Anschluss an die Protodecarboxylierungsstudien wurde schließlich überprüft, ob durch Verwendung des Fluor-substituierten Picolinats **5.2.4-1a** auch in der decarboxylierenden Kreuzkupplung verbesserte Umsätze erzielt werden können (Tabelle 16). Als Kupplungspartner wurde 1-Brom-4-fluorbenzol (**5.2.4-2a**) gewählt, um alle Edukte und Produkte mittels quantitativer ¹⁹F-NMR-Analytik untersuchen zu können. Unter den zuvor in der Kupplung von Kalium-2-picolinat verwendeten Bedingungen konnte bei 190 °C eine Produktausbeute an **5.2.4-3aa** von 68% neben 30% des unerwünschten Arylierungsprodukts **5.2.4-3ab'**, welches aus der Nebenreaktion mit dem Phosphanliganden resultiert, detektiert werden (Eintrag 1). Auch bei 170 °C und 150 °C wurde das substituierte Picolinat nahezu vollständig umgesetzt (Einträge 2 und 3). Selbst bei einer Reaktionstemperatur von 130 °C ließen sich moderate Ausbeuten erzielen (Eintrag 4) und erst bei 110 °C war das Katalysatorsystem nur noch wenig aktiv (Eintrag 5). Eine Protodecarboxylierung war nicht oder nur in geringem Maße zu beobachten, sodass insbesondere eine Metall-freie

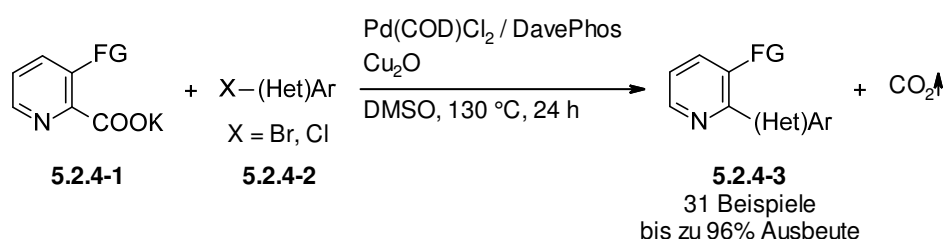
Reaktionsvariante die Effizienz der decarboxylierenden Kreuzkupplung nicht beeinflussen sollte.

Tabelle 16: Decarboxylierende Kreuzkupplung von Kalium-3-fluorpicolinat (**5.2.4-3aa**).

Eintrag	T (°C)	5.2.4-3aa (%)	5.2.4-3ab' (%)	5.2.4-4a (%)
1	190	68	30	n.d.
2	170	66	27	5
3	150	73	25	Spuren
4	130	49	20	n.d.
5	110	9	5	n.d.

Reaktionsbedingungen: **5.2.4-1a** (0.5 mmol), **5.2.4-2a** (1.0 mmol), Cu₂O (5 mol%), 1,10-Phen (10 mol%), PdCl₂ (5 mol%), PPh₃ (15 mol%), NMP/Mes (1:1, 2 mL), Δ, 24 h. ¹⁹F-NMR-Ausbeuten mit 1,4-Difluorbenzol als interner Standard.

Basierend auf diesen Ergebnissen wurde anschließend ein bimetallisches Cu/Pd-Katalysatorsystem optimiert, welches die decarboxylierende Kreuzkupplung 3-substituierter Picolinate mit Aryl- und Heteroarylhalogeniden bei 130 °C ermöglicht (Schema 35).



Schema 35: Decarboxylierende Kreuzkupplung 3-substituierter Picolinate.

Die Anwendungsbreite wurde anhand der Synthese einer Vielzahl an Arylpyridinen demonstriert. Weiterhin konnte der synthetische Nutzen von 2-Aryl-3-fluorpyridinen als Ausgangsverbindung für weitere Funktionalisierungen *via* nukleophiler aromatischer Substitution gezeigt werden.

Beiträge der Autoren: Die Bearbeitung dieses Projekts erfolgte zusammen mit Herrn Philip Weber. Die Protodecarboxylierungsexperimente der 3-Fluorpyridin-2-carbonsäure wurden von mir ausgeführt und die Studien zur Kupplung des Kalium-3-fluorpyridin-2-carboxylats in Abhängigkeit von der Temperatur erfolgten gemeinschaftlich. Ich optimierte die Reaktion und die Untersuchung der Anwendungsbreite erfolgte gemeinsam. Weiterhin wurden die nukleophilen aromatischen Substitutionen von mir durchgeführt. Ich verfasste das Manuskript und überarbeitete es mit Herrn Prof. Dr. L. J. Goossen. Herr Weber unterstützte mich bei der Auswertung der analytischen Daten ebenso wie beim Erstellen der „Supporting Information“.

Die Katalysatoroptimierung, die Untersuchungen zur Anwendungsbreite sowie die weitere Funktionalisierung der 2-Aryl-3-fluorpyridine sind in der nachfolgenden Publikation aufgeführt. Diese wurde im *Journal of Organic Chemistry* veröffentlicht, für die vorliegende Arbeit angepasst und mit Erlaubnis des Verlags beigelegt:

"Reprinted (adapted) with permission from D. Hackenberger, P. Weber, D. C. Blakemore, L. J. Goossen, *J. Org. Chem.* **2017**, 82, 3917–3925: *Synthesis of 3-Substituted 2-Arylpyridines via Cu/Pd-Catalyzed Decarboxylative Cross-Coupling of Picolinic Acids with (Hetero)Aryl Halides*. Copyright 2017 American Chemical Society."

Synthesis of 3-Substituted 2-Arylpyridines via Cu/Pd-Catalyzed Decarboxylative Cross-Coupling of Picolinic Acids with (Hetero)Aryl Halides

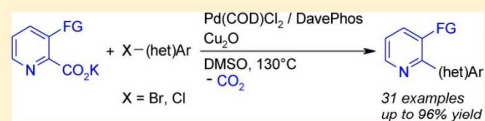
Dagmar Hackenberger,[†] Philip Weber,[†] David C. Blakemore,[‡] and Lukas J. Goossen^{*,†}

[†]Fakultät für Chemie und Biochemie, Ruhr Universität Bochum, Universitätsstr. 150, 44801 Bochum, Germany

[‡]Pfizer Inc., Eastern Point Road, Groton, Connecticut 06340, United States

Supporting Information

ABSTRACT: A decarboxylative cross-coupling of 3-substituted picolinic acids with (hetero)aryl halides is presented. In the presence of catalytic Cu₂O and Pd(1,5-cyclooctadiene)Cl₂ with 2-dicyclohexylphosphino-2'-(*N,N*-dimethylamino)biphenyl as the ligand, both electron-rich and electron-deficient aryl bromides and chlorides as well as heteroaryl bromides were successfully coupled with various picolinate salts under mild conditions in yields up to 96%. This protocol provides an efficient entry to 2-(hetero)arylpyridines, an attractive substance class in drug discovery.



Within the last decades, decarboxylative cross-coupling reactions have emerged as a powerful methodology for the regioselective formation of C–C and C–heteroatom bonds.^{1–3} The key advantage of this reaction type is that it draws on stable and readily available carboxylic acids as the coupling partners. As a result, a steadily growing number of atom-economic and waste-minimized protocols including decarboxylative Heck-type reactions,^{4–7} redox-neutral cross-couplings,^{8–11} allylations,^{12,13} oxidative couplings,^{14,15} C–H arylations,^{16–19} Chan–Evans–Lam-type reactions,²⁰ and photoredox-induced couplings have recently been disclosed.^{21,22}

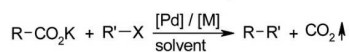
In redox-neutral decarboxylative cross-couplings, carboxylic acids are used as the source of carbon nucleophiles in place of sensitive and costly organometallic reagents. In this reaction variant, a Cu^I or Ag^I catalyst mediates the extrusion of CO₂ to form the carbon nucleophile, which is then transmetalated to a Pd complex, where the coupling with the carbon electrophile takes place (Scheme 1). Bimetallic Cu/Pd systems proved to

coupled even with monometallic catalyst systems.^{26,27} In contrast, pyridinecarboxylic acids belong to the most challenging substrates in decarboxylative couplings. 3-Pyridinecarboxylic acids can be converted under standard conditions but tend to give low yields,²⁸ whereas 4-pyridinecarboxylic acids require customized catalyst systems.²⁹ Arguably, the coupling of 2-pyridinecarboxylic acids poses the greatest challenge due to the instability of the 2-metallapyridines³⁰ and their tendency toward protodecarboxylation even in the absence of a metal catalyst (see the Supporting Information, Table S1).^{31–36} In order to allow a regioselective cross-coupling step, the unwanted protodecarboxylation, which starts at 120 °C, needs to be suppressed, and the high activation barrier of the metal-mediated decarboxylation pathway has to be lowered (Scheme 2).

Several dedicated catalyst systems have been designed specifically for decarboxylative couplings of 2-pyridinecarboxylates. Wu and Stoltz disclosed bimetallic Cu/Pd catalyst systems that allow decarboxylative cross-couplings of picolinic acid with (hetero)aryl bromides, albeit in only moderate yields at temperatures as high as 190 °C or with high catalyst loadings (Scheme 3, (1)).^{35,36} Hoarau et al. used an indirect strategy for their coupling that involves the protection/activation of the picolinic acids by upfront conversion into the *N*-oxides (Scheme 3, (2)).³⁸ Stoichiometric amounts of a silver or copper salt along with the palladium catalyst were still required to obtain reasonable yields. This protocol follows a mechanism that is related to the direct arylation of pyridine *N*-oxides.^{39–42}

To date, the importance of the 2-arylpyridine structural unit remains in stark contrast to the lack of effective and flexible tools for its preparation. 2-Aryl-3-fluoropyridines, in particular,

Scheme 1. Redox-Neutral Decarboxylative Cross-Couplings^a



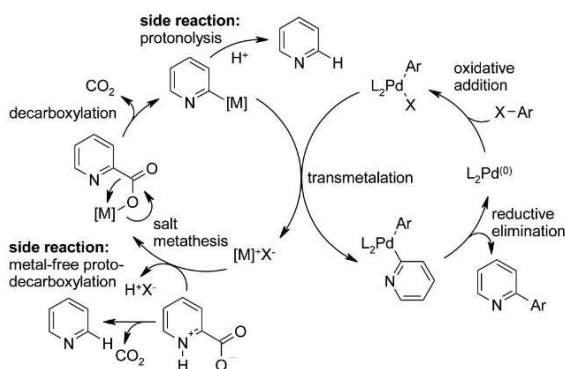
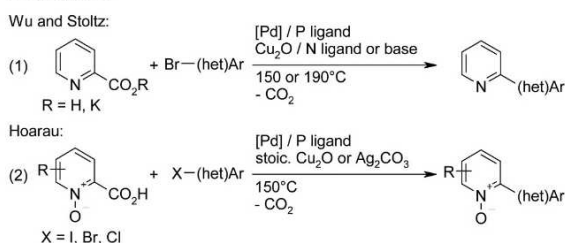
^aM = Cu, Ag; R = (hetero)aryl, vinyl, acyl; R' = (hetero)aryl, alkenyl; X = I, Br, Cl, OTf, OTs, OMs.

have a particularly broad scope with regard to both coupling partners.^{8,23,24} Various aromatic carboxylates have successfully been coupled with a broad range of (hetero)aryl halides and pseudohalides, and key limitations such as the restriction to benzoates bearing electron-withdrawing *ortho*-substituents have recently been overcome with customized catalyst systems.²⁵

Among the heterocyclic carboxylates, five-membered ring heteroarenes such as oxazole-, thiazole-, pyrrole-, thiophene-, and furancarboxylic acids react with particular ease and can be

Received: January 9, 2017

Published: March 16, 2017

Scheme 2. Competing Reaction Pathways in the Coupling of 2-Pyridinecarboxylic Acids^{36,37}

Scheme 3. Decarboxylative Cross-Coupling of Picolinic Acid Derivatives


would be interesting pharmacophores and, in addition, could be used as synthetic hubs for further derivatization via nucleophilic

aromatic fluorine substitution.^{43–50} The C–H arylation of *N*-oxides would likely give mixtures of regioisomers and require subsequent reduction.^{40,51} Suzuki–Miyaura couplings are challenging for this substrate class because of the instability of some heterocyclic boronates, particularly the 2-pyridyl derivatives.^{30,52} Data from the Pfizer internal electronic laboratory notebook shows that of 358 reactions attempted using pyridine-2-boronates, only 28 experiments, corresponding to <8% of examples, achieved a yield of at least 20%.⁵³ A decarboxylative cross-coupling of 3-fluoropicolinic acid appeared to be the most promising and versatile approach to directing the formation of the new bond between the nitrogen atom and the fluorine substituent.

In search of an efficient and generally applicable protocol for the synthesis of 3-fluoro-2-arylpyridines, the utility of various literature protocols was investigated in the coupling of potassium 3-fluoropicolinate (**1a**) with 1-bromo-4-fluorobenzene (**2a**). ¹⁹F NMR was employed to determine yields and selectivity for cross-coupling versus protodecarboxylation. When restricting the catalyst loading to a maximum of 10 mol % of copper/5 mol % of palladium and the temperature to 130 °C, the desired product was obtained in low yields. The best result was obtained using a catalyst system consisting of Cu₂O/1,10-phenanthroline and PdCl₂/PPh₃, which had previously been optimized for similar transformations (Table 1, entry 1).^{35,36} A decisive increase in yield was observed when switching the solvent from NMP to DMSO (entry 2). Only a 1:1 mixture of NMP/mesitylene gave comparable results, whereas other solvents such as DMF, DMAc, or mesitylene were inferior for this substrate combination (see the Supporting Information, Table S2). Systematic variation of the palladium source showed Pd(COD)Cl₂ to be the most effective, with a yield increased to 74% yield (entries 3–5). In investigations of

Table 1. Optimization of the Reaction Conditions^a

entry	[M]	N ligand	[Pd]	P ligand	3aa (%)	4a (%)
1 ^b	Cu ₂ O	phen	PdCl ₂	PPh ₃	19	trace
2	Cu ₂ O	phen	PdCl ₂	PPh ₃	60	7
3	Cu ₂ O	phen	Pd(COD)Cl ₂	PPh ₃	74	8
4	Cu ₂ O	phen	PdI ₂	PPh ₃	54	11
5	Cu ₂ O	phen	Pd(acac) ₂	PPh ₃	67	9
6 ^c	CuCl	phen	Pd(COD)Cl ₂	PPh ₃	66	nd
7	Ag ₂ CO ₃	phen	Pd(COD)Cl ₂	PPh ₃	66	10
8	Cu ₂ O	Me ₄ -phen	Pd(COD)Cl ₂	PPh ₃	83	nd
9	Cu ₂ O	NO ₂ -phen	Pd(COD)Cl ₂	PPh ₃	49	17
10	Cu ₂ O	Me ₄ -phen	Pd(COD)Cl ₂	P(<i>p</i> -Tol) ₃	84	trace
11	Cu ₂ O	Me ₄ -phen	Pd(COD)Cl ₂	BINAP	75	nd
12	Cu ₂ O	Me ₄ -phen	Pd(COD)Cl ₂	PCy ₃	28	trace
13	Cu ₂ O	Me ₄ -phen	Pd(COD)Cl ₂	CyJohnPhos	82	10
14	Cu ₂ O	Me ₄ -phen	Pd(COD)Cl ₂	DavePhos	92	7
15	Cu ₂ O	–	Pd(COD)Cl ₂	DavePhos	93	trace
16	–	–	Pd(COD)Cl ₂	DavePhos	7	32
17	Cu ₂ O	–	–	–	nd	nd

^aReaction conditions: **1a** (0.5 mmol), **2a** (1.0 mmol), [M] (5 mol %), N ligand (10 mol %), [Pd] (5 mol %), P ligand (15 mol %), DMSO (2 mL), 130 °C, 24 h; ¹⁹F NMR yield with 1,4-difluorobenzene as internal standard; NO₂-phen = 5-nitro-1,10-phenanthroline, Tol = tolyl, BINAP = 2,2'-bis(diphenylphosphino)-1,1'-binaphthyl, CyJohnPhos = (2-biphenyl)dicyclohexylphosphine, DavePhos = 2-dicyclohexylphosphino-2'-(*N,N*-dimethylamino)biphenyl; nd = not detected. ^bIn NMP (2 mL). ^c10 mol % of [M] was used.

silver- and copper-based decarboxylation catalysts, Cu₂O was identified as the most efficient in combination with 3,4,7,8-tetramethyl-1,10-phenanthroline (Me₄-phen) (entries 6–9). The choice of the phosphine ligand was similarly critical (entries 10–14). Not only did the phosphine affect the yields, but in addition, undesired P–C bond cleavage resulted in aryl group transfer to the pyridine with formation of hard-to-separate 2-arylpyridine byproducts. Because the quality of pharmacological structure–activity relationships is strongly affected by such structurally related impurities, a key criterion for the choice of the phosphine ligand was its stability under the reactions conditions. In this respect, DavePhos turned out to be most effective. Notably, with this ligand, the optimal yield and selectivity was obtained in the absence of Me₄-phen (entry 15). Control experiments confirmed that both Pd and Cu are essential components of the catalyst system (entries 16 and 17).

In the presence of 5 mol % of Pd(COD)Cl₂, 15 mol % of DavePhos, and 5 mol % of Cu₂O, the desired product was formed in 93% yield within 24 h at 130 °C in DMSO. This optimized protocol is applicable to the coupling of **1a** with a broad range of aryl bromides substituted in the *ortho*-, *meta*-, or *para*-position (Table 2). Common functionalities including

Table 2. Scope with Regard to the Electrophilic Coupling Partner^a

$\text{hetAr-COOK} + \text{X-(het)Ar} \xrightarrow[\text{DMSO, 130}^\circ\text{C, 24 h}]{\text{Pd(COD)Cl}_2 / \text{DavePhos, Cu}_2\text{O}} \text{hetAr-C(het)Ar} + \text{CO}_2$	
1a	2, X = Br, Cl
3aa , R = F, X = Br 86%, X = Cl 48%	3al , R = CF ₃ , X = Br 96%, X = Cl 61%
3ab , R = H, X = Br 74%, X = Cl 51%	3am , R = OMe, X = Br 97%, X = Cl 61%
3ac , R = Me, X = Br 52%, X = Cl 50%	3an , R = <i>t</i> Bu, X = Br 53%, X = Cl 65% ^b
3ad , R = OMe, X = Br 80%, X = Cl 82%	3ao , X = Br 90%
3ae , R = CF ₃ , X = Br 92%, X = Cl 82%	3ap , X = Br 74%
3af , R = Cl, X = Br 71%	
3ag , R = CO ₂ Et, X = Br 92%, X = Cl 59%	
3ah , R = Ph, X = Br 81%	
3ai , R = Ac, X = Br 47%	
3aj , R = CN, X = Br 82%	
3ak , R = NO ₂ , X = Br 88%	
3aq , X = Br 37% ^c	3ar , X = Br 62%
3as , X = Br 56%	3at , R = H, X = Br 63%, R = Ac, X = Br 31%
3av , X = Br 51%	

^aReaction conditions: **1a** (0.5 mmol), **2** (1.0 mmol), Cu₂O (5 mol %), Pd(COD)Cl₂ (5 mol %), DavePhos (15 mol %), DMSO (2 mL), 130 °C, 24 h. Yields of isolated products. ^b**1a** (0.5 mmol), **2** (1.0 mmol), Cu₂O (5 mol %), phen (10 mol %), PdCl₂ (5 mol %), CyJohnPhos (15 mol %), NMP/mesitylene (1:1, 2 mL), 150 °C, 24 h. Yield of isolated products. ^c**1a** (0.75 mmol), **2** (0.5 mmol).

ether, ester, carbonyl, trifluoromethyl, cyano, and nitro groups are tolerated. Heteroaryl bromides were also found to be suitable coupling partners. We were pleased to find that aryl chlorides, which are available in greater structural diversity and are less expensive, but less reactive, were smoothly converted without further adjustments to the catalyst or conditions. As the main side reactions, homocoupling of the excess aryl halide and protodecarboxylation of the picolinic acid were observed.

Having thus established a versatile protocol for our synthetic needs, we briefly investigated whether this catalyst system is advantageous also for other heteroaromatic carboxylates (Table 3). 3-Acetylpycolinate was also converted in moderate yield,

Table 3. Scope with Regard to the Carboxylate^a

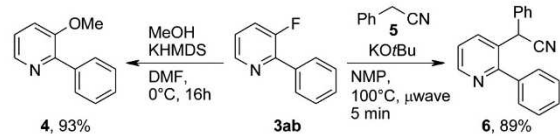
$\text{hetAr-COOK} + \text{Br-Ar'} \xrightarrow[\text{DMSO, 130}^\circ\text{C, 24 h}]{\text{Pd(COD)Cl}_2 / \text{DavePhos, Cu}_2\text{O}} \text{hetAr-C-Ar'} + \text{CO}_2$	
1	2a , Ar' = 4-FC ₆ H ₄
3ba , 52%	3ca , 17%
3da , 61% ^b	3ea , 70% ^c
3fa , R = F, 37% ^d	3ga , 64% ^c
3fb , R = H, 40% ^d	3ha , 36%, 75% ^e
3fd , R = OMe, 28% ^d	3ia , 21% ^c

^aReaction conditions: **1** (0.5 mmol), **2a** (1.0 mmol), Cu₂O (5 mol %), Pd(COD)Cl₂ (5 mol %), DavePhos (15 mol %), DMSO (2 mL), 130 °C, 24 h. Yields of isolated products. ^bAg₂CO₃ (5 mol %) was used instead of Cu₂O. ^c**1** (0.5 mmol), **2** (1.0 mmol), Cu₂O (5 mol %), phen (10 mol %), PdCl₂ (5 mol %), CyJohnPhos (15 mol %), NMP/mesitylene (1:1, 2 mL), 150 °C, 24 h. Yields of isolated products. ^d**1f** (0.5 mmol), **2** (1.0 mmol), Cu₂O (5 mol %), Pd(COD)Cl₂ (5 mol %), DavePhos (15 mol %), NMP/mesitylene (1:1, 2 mL), 190 °C, 24 h. Yields of isolated products.

whereas the yield was low for 3-piperidylpicolinate. 3-Chloropicolinate (**1d**) was converted most effectively using a silver-based decarboxylation catalyst, which is in line with observations made for *ortho*-chloro-substituted benzoates.²⁴ Slightly modified reaction conditions (5 mol % of PdCl₂, 15 mol % of CyJohnPhos, 5 mol % of Cu₂O, and 10 mol % of phen in 2 mL of NMP/mesitylene (1:1) at 150 °C) were necessary to efficiently convert 3-methoxypicolinate (**1e**). Remarkably, picolinic acids devoid of substituents in the 3-position could only be converted at 190 °C. This indicates that a substituent *ortho* to the carboxylate facilitates decarboxylation not only for benzoates but also for picolines. Picolinic acids substituted in another position of the heteroaromatic ring (4-Cl, 5-F, 6-F/Cl/OMe) did not react under our reaction conditions, again underlining the unique reactivity of pyridines substituted in the 3-position. Further studies revealed that five-membered heteroaromatic carboxylates, including *N*-methylpyrazole, thiazole, or benzothiophene derivatives, can also be converted in reasonable yields using the new catalyst system. As side products, homocoupling products of the aryl halides were detected along with unreacted starting materials.

In order to demonstrate the utility of the 2-aryl-3-fluoropyridines as synthetic hubs for further derivatization via nucleophilic aromatic fluorine substitution, **3ab** was applied in a C–O and a C–C bond formation (Scheme 4). Reaction of **3ab**

Scheme 4. Derivatization of **3ab**



with methanol, which can also be replaced by more complex alcohols, in the presence of potassium bis(trimethylsilyl)amide (KHMDS)⁴⁵ gave the desired product **4**, and treatment of **3ab** in the presence of nitrile **5** and potassium *tert*-butoxide under microwave conditions furnished compound **6**,⁴⁴ both in good yield.

In conclusion, an efficient protocol for the Cu/Pd-catalyzed decarboxylative cross-coupling of picolinic acid derivatives with (hetero)aryl bromides and chlorides has been developed, which gives convenient access to otherwise hard to synthesize 3-substituted arylpyridines. It draws on stable picolinate salts as the source of the nucleophile, proceeds at reasonable temperatures, and requires only catalytic amounts of transition metals.

EXPERIMENTAL SECTION

General Remarks. Chemicals and solvents were either purchased (puriss. p.A.) from commercial suppliers or purified by standard procedures prior to use.⁵⁴ All reactions were performed in oven-dried glassware under an argon atmosphere containing a Teflon-coated stirrer bar and dry septum. Microwave-assisted reactions were performed in sealed microwave vessels using the Biotage Initiator 2.5 EXP microwave system (external IR sensor) with the Initiator Remote Viewer reaction monitoring software. Solvents and liquid reagents were degassed with argon. Reactions were monitored by ¹⁹F NMR using 1,4-difluorobenzene as an internal standard or by GC using dodecane as an internal standard. Response factors of the products with regard to dodecane were obtained experimentally by analyzing known quantities of the substances. GC analyses were carried out using a capillary column (phenyl methyl siloxane, 30 m × 320 × 0.25, 100/2.3–30–300/3, 2 min at 60 °C, heating rate 30 °C min^{−1}, 3 min at 300 °C). Column chromatography was performed on a flash chromatography machine. NMR spectra were recorded at ambient temperature using CDCl₃ or DMSO-*d*₆ as solvent, with proton, carbon, and fluorine resonances at 400/300/200/250, 151/101/75/63/50, and 377/235/41 MHz, respectively. Mass spectral data were acquired on a GC-MS and on a GC-HRMS with a TOF mass analyzer. The ionization was achieved by EI. Infrared spectra were recorded on a FT-IR spectrometer with an ATR sampling accessory. Melting points were measured on a melting point apparatus.

General Procedure for the Synthesis of Potassium Carboxylate Salts. A 250 mL round-bottomed flask was charged with the carboxylic acid (20.0 mmol) and ethanol (20 mL). A solution of potassium *tert*-butoxide (2.24 g, 20.0 mmol) in ethanol (20 mL) was added dropwise over 1 h. After complete addition, the reaction mixture was stirred for another 1 h at rt. A gradual formation of a precipitate was observed. The resulting solid was collected by filtration, washed sequentially with ethanol (2 × 10 mL) and diethyl ether (10 mL), and dried in vacuum to provide the corresponding potassium carboxylate. If after the addition of the potassium *tert*-butoxide solution a formation of a precipitate was not observed, the solution was concentrated in vacuum. The resulting solid was collected by filtration, washed with diethyl ether (10 mL), and dried in vacuum to provide the corresponding potassium carboxylate.

General Procedure for the Biaryl Synthesis. Method A. An oven-dried 20 mL vessel was charged with copper(I) oxide (3.61 mg, 25.0 μmol, 5 mol %), dichloro(1,5-dicyclooctadienyl)palladium(II) (7.13 mg, 25.0 μmol, 5 mol %), DavePhos (29.5 mg, 75 μmol, 15 mol %), and the potassium carboxylate **1** (0.50 mmol). DMSO (2 mL) and the aryl halide **2** (1 mmol) were added, and the resulting mixture was stirred at 130 °C under a dry atmosphere of argon. After 24 h, the mixture was allowed to cool to rt, washed with distilled water (20 mL), and extracted with ethyl acetate (3 × 20 mL). The combined organic layers were washed with brine, dried over MgSO₄, filtered, and the volatiles were removed under reduced pressure. The residue was purified by column chromatography (SiO₂, cyclohexane/ethyl acetate gradient) yielding the corresponding biaryl **3**.

Method B. An oven-dried 20 mL vessel was charged with copper(I) oxide (3.61 mg, 25.0 μmol, 5 mol %), palladium(II) chloride (4.44 mg, 25.0 μmol, 5 mol %), 1,10-phenanthroline (9.01 mg, 50 μmol, 10 mol %), CyJohnPhos (26.3 mg, 75 μmol, 15 mol %), and the potassium carboxylate **1** (0.50 mmol). NMP/mesitylene (2 mL, 1/1) and the aryl bromide **2** (1 mmol) were added, and the resulting mixture was stirred at 150 °C under a dry atmosphere of argon. After 24 h, the mixture was allowed to cool to rt, washed with distilled water (20 mL), and extracted with ethyl acetate (3 × 20 mL). The combined organic layers were washed with brine, dried over MgSO₄, filtered, and the volatiles were removed under reduced pressure. The residue was purified by column chromatography (SiO₂, cyclohexane/ethyl acetate gradient) yielding the corresponding biaryl **3**.

3-Fluoro-2-(4-fluorophenyl)pyridine (3aa) [CAS: 511522-74-0]. Compound **3aa** was prepared following method A from potassium 3-fluoro-2-pyridinecarboxylate **1a** (90.5 mg, 0.50 mmol) and 1-bromo-4-fluorobenzene **2a** (177 mg, 1.0 mmol). **3aa** was isolated (SiO₂, cyclohexane/ethyl acetate = 6/1) as a colorless solid (82 mg, 86%). Compound **3aa** was prepared following method A from potassium 3-fluoro-2-pyridinecarboxylate **1a** (90.5 mg, 0.50 mmol) and 1-chloro-4-fluorobenzene **2a'** (133 mg, 1.0 mmol). **3aa** was isolated (SiO₂, cyclohexane/ethyl acetate = 6/1) as a colorless solid (45 mg, 48%); mp 63–64 °C; ¹H NMR (CDCl₃, 400 MHz) δ 8.49–8.54 (m, 1H), 7.96–8.03 (m, 2H), 7.50 (ddd, 1H, *J* = 11.0, 8.3, 1.5 Hz), 7.25–7.31 (m, 1H), 7.14–7.22 (m, 2H); ¹³C NMR (CDCl₃, 75 MHz) δ 163.4 (d, *J*_{C–F} = 249.3 Hz), 157.4 (d, *J*_{C–F} = 259.8 Hz), 145.4 (d, *J*_{C–F} = 5.5 Hz), 145.2 (d, *J*_{C–F} = 10.5 Hz), 131.4 (dd, *J*_{C–F} = 5.5, 3.3 Hz), 130.7 (dd, *J*_{C–F} = 8.6, 6.4 Hz), 124.2 (d, *J*_{C–F} = 19.9 Hz), 128.4 (d, *J*_{C–F} = 4.4 Hz), 115.4 (d, *J*_{C–F} = 21.6 Hz); ¹⁹F NMR (CDCl₃, 377 MHz) δ −112.1, −123.0; IR ν 3048, 3021, 1603, 1516, 1447, 1227, 833, 756 cm^{−1}; MS *m/z* (%) 191.0 (100) [M]⁺, 190 (58), 172 (16), 170 (10), 74 (12), 50 (16); HRMS (EI) *m/z* [M]⁺ calcd for C₁₁H₇F₂N 191.0547; found 191.0548.

3-Fluoro-2-phenylpyridine (3ab) [CAS: 1214342-78-5]. Compound **3ab** was prepared following method A from potassium 3-fluoro-2-pyridinecarboxylate **1a** (90.5 mg, 0.50 mmol) and bromobenzene **2b** (159 mg, 1.0 mmol). **3ab** was isolated (SiO₂, cyclohexane/ethyl acetate = 9/1) as a colorless solid (64 mg, 74%). Compound **3ab** was prepared following method A from potassium 3-fluoro-2-pyridinecarboxylate **1a** (90.5 mg, 0.50 mmol) and chlorobenzene **2b'** (113 mg, 1.0 mmol). **3ab** was isolated (SiO₂, cyclohexane/ethyl acetate = 9/1) as a colorless solid (44 mg, 71%); mp 48–49 °C; ¹H NMR (CDCl₃, 400 MHz) δ 8.50–8.58 (m, 1H), 7.93–8.04 (m, 2H), 7.42–7.55 (m, 4H), 7.25–7.31 (m, 1H); ¹³C NMR (CDCl₃, 101 MHz) δ 157.5 (d, *J*_{C–F} = 258.9 Hz), 146.2 (d, *J*_{C–F} = 10.9 Hz), 145.4 (d, *J*_{C–F} = 5.5 Hz), 135.3 (d, *J*_{C–F} = 5.4 Hz), 129.2, 128.8 (d, *J*_{C–F} = 5.4 Hz), 128.4, 124.1 (d, *J*_{C–F} = 20.0 Hz), 123.4 (d, *J*_{C–F} = 3.6 Hz); ¹⁹F NMR (CDCl₃, 377 MHz) δ −123.0; IR ν 3064, 1596, 1431, 1250, 1188, 798 cm^{−1}; MS *m/z* (%) 173 (100) [M]⁺, 172 (78), 145 (11), 125 (11), 51 (13), 50 (23); HRMS (EI) *m/z* [M]⁺ calcd for C₁₁H₈FN 173.0641; found 173.0639.

3-Fluoro-2-(4-methylphenyl)pyridine (3ac). Compound **3ac** was prepared following methods A and B, respectively, from potassium 3-fluoro-2-pyridinecarboxylate **1a** (90.5 mg, 0.50 mmol) and 1-bromo-4-methylbenzene **2c** (175 mg, 1.0 mmol). **3ac** was isolated (SiO₂, cyclohexane/ethyl acetate = 9/1) as a colorless solid (48 mg, 52% (method A); 79 mg, 84% (method B)). Compound **3ac** was

prepared following method A from potassium 3-fluoro-2-pyridinecarboxylate **1a** (90.5 mg, 0.50 mmol) and 1-chloro-4-methylbenzene **2c'** (129 mg, 1.0 mmol). **3ac** was isolated (SiO₂, cyclohexane/ethyl acetate = 9/1) as a colorless solid (47 mg, 50%); mp 51–52 °C; ¹H NMR (CDCl₃, 400 MHz) δ 8.45–8.58 (m, 1H), 7.90 (dd, 2H, *J* = 8.3, 1.5 Hz), 7.47 (ddd, 1H, *J* = 11.0, 8.3, 1.0 Hz), 7.31 (d, 2H, *J* = 8.3 Hz), 7.20–7.27 (m, 1H), 2.43 (s, 3H); ¹³C NMR (CDCl₃, 101 MHz) δ 157.4 (d, *J*_{C–F} = 259.8 Hz), 146.2 (d, *J*_{C–F} = 10.9 Hz), 145.2 (d, *J*_{C–F} = 5.4 Hz), 139.2, 132.5 (d, *J*_{C–F} = 5.4 Hz), 129.1, 128.6 (d, *J*_{C–F} = 6.4 Hz), 123.9 (d, *J*_{C–F} = 20.9 Hz), 123.0 (d, *J*_{C–F} = 3.6 Hz), 21.3; ¹⁹F NMR (CDCl₃, 377 MHz) δ –123.0; IR ν 3050, 3027, 2921, 1596, 1444, 1405, 1251, 1187, 1106 cm^{–1}; MS, *m/z* (%) 187 (100) [M]⁺, 186 (60), 185 (17), 91 (12), 63 (10), 50 (11); HRMS (EI) *m/z* [M]⁺ calcd for C₁₁H₁₀FN 187.0797; found 187.0796.

3-Fluoro-2-(4-methoxyphenyl)pyridine (3ad) [CAS: 847226-10-2]. Compound **3ad** was prepared following method A from potassium 3-fluoro-2-pyridinecarboxylate **1a** (90.5 mg, 0.50 mmol) and 1-bromo-4-methoxybenzene **2d** (187 mg, 1.0 mmol). **3ad** was isolated (SiO₂, cyclohexane/ethyl acetate = 9/1) as a yellow oil (82 mg, 80%). Compound **3ad** was prepared following method A from potassium 3-fluoro-2-pyridinecarboxylate **1a** (90.5 mg, 0.50 mmol) and 1-chloro-4-methoxybenzene **2d'** (145 mg, 1.0 mmol). **3ad** was isolated (SiO₂, cyclohexane/ethyl acetate = 9/1) as a yellow oil (83 mg, 82%); ¹H NMR (CDCl₃, 400 MHz) δ 8.45–8.53 (m, 1H), 7.97 (dd, 2H, *J* = 8.8, 1.5 Hz), 7.46 (ddd, 1H, *J* = 11.3, 8.3, 1.3 Hz), 7.18–7.25 (m, 1H), 6.97–7.07 (m, 2H), 3.88 (s, 3H); ¹³C NMR (CDCl₃, 101 MHz) δ 160.4, 157.3 (d, *J*_{C–F} = 259.8 Hz), 145.8 (d, *J*_{C–F} = 10.0 Hz), 145.2 (d, *J*_{C–F} = 5.5 Hz), 130.1 (d, *J*_{C–F} = 5.5 Hz), 127.9 (d, *J*_{C–F} = 5.4 Hz), 123.9 (d, *J*_{C–F} = 20.9 Hz), 122.7 (d, *J*_{C–F} = 4.5 Hz), 113.8, 55.3; ¹⁹F NMR (CDCl₃, 377 MHz) δ –123.2; IR ν 3064, 3006, 2838, 1611, 1513, 1436, 1307, 1245, 1175, 1023 cm^{–1}; MS, *m/z* (%) 203 (100) [M]⁺, 188 (54), 160 (35), 159 (22); HRMS (EI) *m/z* [M]⁺ calcd for C₁₂H₁₀FNO 203.0746; found 203.0745.

3-Fluoro-2-[4-(trifluoromethyl)phenyl]pyridine (3ae) [CAS: 1261805-54-2]. Compound **3ae** was prepared following method A from potassium 3-fluoro-2-pyridinecarboxylate **1a** (90.5 mg, 0.50 mmol) and 1-bromo-4-(trifluoromethyl)benzene **2e** (227 mg, 1.0 mmol). **3ae** was isolated (SiO₂, cyclohexane/ethyl acetate = 9/1) as a colorless oil (111 mg, 92%). Compound **3ae** was prepared following method A from potassium 3-fluoro-2-pyridinecarboxylate **1a** (90.5 mg, 0.50 mmol) and 1-chloro-4-(trifluoromethyl)benzene **2e'** (184 mg, 1.0 mmol). **3ae** was isolated (SiO₂, cyclohexane/ethyl acetate = 9/1) as a colorless oil (99 mg, 82%); ¹H NMR (CDCl₃, 250 MHz) δ 8.51–8.61 (m, 1H), 8.13 (d, 2H, *J* = 8.1 Hz), 7.75 (d, 2H, *J* = 8.4 Hz), 7.46–7.60 (m, 1H), 7.30–7.38 (m, 1H); ¹³C NMR (CDCl₃, 151 MHz) δ 157.8 (d, *J*_{C–F} = 260.8 Hz), 145.6, 144.5 (d, *J*_{C–F} = 9.7 Hz), 138.6, 131.0 (q, *J*_{C–F} = 33.3 Hz), 129.1 (d, *J*_{C–F} = 6.9 Hz), 125.4 (q, *J*_{C–F} = 4.2 Hz), 124.6, 124.43, 124.37 (q, *J*_{C–F} = 273.3 Hz); ¹⁹F NMR (CDCl₃, 377 MHz) δ –62.7, –122.5; IR ν 3067, 1619, 1597, 1446, 1406, 1323, 1252, 1163, 1114, 1068, 1016 cm^{–1}; MS, *m/z* (%) 241 (100) [M]⁺, 222 (19), 221 (17), 172 (27), 68 (15), 50 (12); HRMS (EI) *m/z* [M]⁺ calcd for C₁₂H₇F₃N 241.0515; found 241.0519.

2-(4-Chlorophenyl)-3-fluoropyridine (3af) [CAS: 1233702-02-7]. Compound **3af** was prepared following method A from 3-fluoro-2-pyridinecarboxylate **1a** (90.5 mg, 0.50 mmol) and 1-chloro-4-bromobenzene **2f** (191 mg, 1.0 mmol). **3af** was isolated (SiO₂, cyclohexane/ethyl acetate = 9/1) as a colorless solid (73 mg, 71 mmol); mp 74–75 °C; ¹H NMR (CDCl₃, 400 MHz) δ 8.52 (d, 1H, *J* = 4.5 Hz), 7.95 (dd, 2H, *J* = 8.5, 1.3 Hz), 7.41–7.55 (m, 3H), 7.24–7.33 (m, 1H); ¹³C NMR (CDCl₃, 101 MHz) δ 157.5 (d, *J*_{C–F} = 260.7 Hz), 145.3, 144.9 (d, *J*_{C–F} = 10.0 Hz), 135.4, 133.6, 130.1 (d, *J*_{C–F} = 5.5 Hz), 128.7, 124.3 (d, *J*_{C–F} = 20.9 Hz), 123.8; ¹⁹F NMR (CDCl₃, 377 MHz) δ –123.0; IR ν 3048, 3016, 1599, 1497, 1445, 1398, 1254, 1190, 1092 cm^{–1}; MS, *m/z* (%) 209 (33) [M]⁺, 208 (16), 207 (100) [M]⁺, 172 (55), 145 (10), 75 (7), 50 (9); HRMS (EI) *m/z* [M]⁺ calcd for C₁₁H₇³⁵ClFN 207.0251; found 207.0249.

4-(3-Fluoro-2-pyridinyl)benzoic Acid Ethyl Ester (3ag) [CAS: 1246461-83-5]. Compound **3ag** was prepared following method A from 3-fluoro-2-pyridinecarboxylate **1a** (90.5 mg, 0.50 mmol) and 4-bromobenzoic acid ethyl ester **2g** (231 mg, 1.0 mmol). **3ag**

was isolated (SiO₂, cyclohexane/ethyl acetate = 9/1) as a yellow oil (113 mg, 92%). Compound **3ag** was prepared following method A from 3-fluoro-2-pyridinecarboxylate **1a** (90.5 mg, 0.50 mmol) and 4-chlorobenzoic acid ethyl ester **2g'** (188 mg, 1.0 mmol). **3ag** was isolated (SiO₂, cyclohexane/ethyl acetate = 9/1) as a yellow oil (72 mg, 59%); ¹H NMR (CDCl₃, 400 MHz) δ 8.51–8.59 (m, 1H), 8.11–8.21 (m, 2H), 8.01–8.10 (m, 2H), 7.52 (ddd, 1H, *J* = 10.9, 8.4, 1.0 Hz), 7.30–7.35 (m, 1H), 4.42 (q, 2H, *J* = 7.1 Hz), 1.43 (t, 3H, *J* = 7.2 Hz); ¹³C NMR (CDCl₃, 101 MHz) δ 166.3, 157.8 (d, *J*_{C–F} = 261.6 Hz), 145.6 (d, *J*_{C–F} = 5.4 Hz), 145.0 (d, *J*_{C–F} = 10.9 Hz), 139.4 (d, *J*_{C–F} = 5.5 Hz), 130.8, 129.6, 128.7 (d, *J*_{C–F} = 6.4 Hz), 124.3 (d, *J*_{C–F} = 25.4 Hz), 124.2, 61.1, 14.3; ¹⁹F NMR (CDCl₃, 377 MHz) δ –122.1; IR ν 3064, 2984, 1711, 1443, 1402, 1367, 1267, 1186, 1095, 1016 cm^{–1}; MS, *m/z* (%) 245 (59) [M]⁺, 217 (47), 201 (16), 200 (100), 172 (27), 125 (10); HRMS (EI) *m/z* [M]⁺ calcd for C₁₄H₁₂FNO₂ 245.0852; found 245.0847.

2-[1,1'-Biphenyl]-4-yl-3-fluoropyridine (3ah). Compound **3ah** was prepared following method A from potassium 3-fluoro-2-pyridinecarboxylate **1a** (90.5 mg, 0.50 mmol) and 4-bromo-1,1'-biphenyl **2h** (259 mg, 1.0 mmol). **3ah** was isolated (SiO₂, cyclohexane/ethyl acetate = 9/1) as a colorless solid (100 mg, 81%); mp 97–98 °C; ¹H NMR (CDCl₃, 400 MHz) δ 8.52–8.59 (m, 1H), 8.09 (dd, 2H, *J* = 8.4, 1.6 Hz), 7.72–7.77 (m, 2H), 7.64–7.71 (m, 2H), 7.45–7.56 (m, 3H), 7.36–7.42 (m, 1H), 7.28–7.32 (m, 1H); ¹³C NMR (CDCl₃, 101 MHz) δ 156.3 (d, *J*_{C–F} = 259.8 Hz), 145.7 (d, *J*_{C–F} = 10.1 Hz), 145.2 (d, *J*_{C–F} = 5.5 Hz), 142.0, 140.5, 134.0 (d, *J*_{C–F} = 5.5 Hz), 129.2 (d, *J*_{C–F} = 6.4 Hz), 128.8, 127.6, 127.17, 127.15, 124.3 (d, *J*_{C–F} = 20.9 Hz), 123.4 (d, *J*_{C–F} = 3.6 Hz); ¹⁹F NMR (CDCl₃, 377 MHz) δ –122.7; IR ν 3062, 3024, 1594, 1485, 1440, 1397, 1246 cm^{–1}; MS, *m/z* (%) 249 (100) [M]⁺, 248 (23), 51 (8), 50 (10), 44 (8); HRMS (EI) *m/z* [M]⁺ calcd for C₁₇H₁₂FN 249.0954; found 249.0938.

1-[4-(3-Fluoro-2-pyridinyl)phenyl]ethanone (3ai). Compound **3ai** was prepared following method A from potassium 3-fluoro-2-pyridinecarboxylate **1a** (90.5 mg, 0.50 mmol) and 1-(4-bromophenyl)ethanone **2i** (203 mg, 1.0 mmol). **3ai** was isolated (SiO₂, cyclohexane/ethyl acetate = 6/1) as a colorless solid (50 mg, 47%); mp 88–89 °C; ¹H NMR (CDCl₃, 200 MHz) δ 8.57 (dt, 1H, *J*_d = 4.5, *J*_t = 1.5 Hz), 8.03–8.15 (m, 4H), 7.47–7.60 (m, 1H), 7.28–7.38 (m, 1H), 2.66 (s, 3H); ¹³C NMR (CDCl₃, 50 MHz) δ 197.8, 157.8 (d, *J*_{C–F} = 261.6 Hz), 145.6 (d, *J*_{C–F} = 5.1 Hz), 144.8 (d, *J*_{C–F} = 10.2 Hz), 139.6 (d, *J*_{C–F} = 5.9 Hz), 137.2, 128.9 (d, *J*_{C–F} = 6.2 Hz), 128.4, 124.34 (d, *J*_{C–F} = 20.9 Hz), 124.30 (d, *J*_{C–F} = 4.0 Hz), 26.7; ¹⁹F NMR (CDCl₃, 377 MHz) δ –122.1; IR ν 3078, 3009, 1674, 1603, 1443, 1400, 1246 cm^{–1}; MS, *m/z* (%) 215 (17) [M]⁺, 201 (14), 200 (100), 172 (30); HRMS (EI) *m/z* [M]⁺ calcd for C₁₃H₁₀FNO 215.0746; found 215.0741.

4-(3-Fluoro-2-pyridinyl)benzonitrile (3aj) [CAS: 1352794-83-2]. Compound **3aj** was prepared following method A from potassium 3-fluoro-2-pyridinecarboxylate **1a** (90.5 mg, 0.50 mmol) and 4-bromobenzonitrile **2j** (184 mg, 1.0 mmol). **3aj** was isolated (SiO₂, cyclohexane/ethyl acetate = 6/1) as a colorless solid (81 mg, 82%); mp 124–125 °C; ¹H NMR (CDCl₃, 75 MHz) δ 8.57 (dt, 1H, *J*_d = 4.4, *J*_t = 1.6 Hz), 8.10–8.17 (m, 2H), 7.74–7.81 (m, 2H), 7.55 (ddd, 1H, *J* = 11.1, 8.3, 1.3 Hz), 7.32–7.40 (m, 1H); ¹³C NMR (CDCl₃, 75 MHz) δ 157.8 (d, *J*_{C–F} = 262.0 Hz), 145.7 (d, *J*_{C–F} = 5.5 Hz), 143.9 (d, *J*_{C–F} = 9.9 Hz), 139.5 (d, *J*_{C–F} = 5.5 Hz), 132.2 (d, *J*_{C–F} = 0.7 Hz), 129.3 (d, *J*_{C–F} = 6.6 Hz), 124.8 (d, *J*_{C–F} = 4.0 Hz), 124.6 (d, *J*_{C–F} = 20.9 Hz), 118.7, 112.7 (d, *J*_{C–F} = 1.1 Hz); ¹⁹F NMR (CDCl₃, 377 MHz) δ –121.9; IR ν 3061, 2226, 1605, 1595, 1441, 1402, 1248, 1099 cm^{–1}; MS, *m/z* (%) 198 (100) [M]⁺, 197 (56), 50 (8); HRMS (EI) *m/z* [M]⁺ calcd for C₁₂H₇FN₂ 198.0593; found 198.0585.

3-Fluoro-2-(4-nitrophenyl)pyridine (3ak). Compound **3ak** was prepared following method A from potassium 3-fluoro-2-pyridinecarboxylate **1a** (90.5 mg, 0.50 mmol) and 1-bromo-4-nitrobenzene **2k** (204 mg, 1.0 mmol). **3ak** was isolated (SiO₂, cyclohexane/ethyl acetate = 9/1) as a colorless solid (96 mg, 88%); mp 140–141 °C; ¹H NMR (CDCl₃, 200 MHz) δ 8.59 (dt, 1H, *J*_d = 4.5 Hz, *J*_t = 1.5 Hz), 8.30–8.40 (m, 2H), 8.16–8.26 (m, 2H), 7.51–7.63 (m, 1H), 7.34–7.45 (m, 1H); ¹³C NMR (CDCl₃, 50 MHz) δ 157.9 (d, *J*_{C–F} = 262.0), 148.0, 145.8 (d, *J*_{C–F} = 5.5 Hz), 143.4 (d, *J*_{C–F} = 9.9 Hz), 141.3 (d, *J*_{C–F} = 5.9 Hz), 129.6 (d, *J*_{C–F} = 6.6 Hz), 125.0 (d, *J*_{C–F} = 4.4 Hz),

124.6 (d, J_{C-F} = 20.5 Hz), 123.5; ^{19}F NMR (CDCl_3 , 377 MHz) δ -121.6; IR ν 3076, 1593, 1514, 1440, 1342, 1188, 1103 cm^{-1} ; MS m/z (%) 218 (100) $[\text{M}]^+$, 188 (38), 172 (35), 160 (19), 145 (20), 125 (17), 44 (15); HRMS (EI) m/z $[\text{M}]^+$ calcd for $\text{C}_{11}\text{H}_7\text{FN}_2\text{O}_2$ 218.0492; found 218.0486.

3-Fluoro-2-[3-(trifluoromethyl)phenyl]pyridine (3al) [CAS: 1261634-22-3]. Compound **3al** was prepared following method A from potassium 3-fluoro-2-pyridinecarboxylate **1a** (90.5 mg, 0.50 mmol) and 1-bromo-3-(trifluoromethyl)benzene **2l** (227 mg, 1.0 mmol). **3al** was isolated (SiO_2 , cyclohexane/ethyl acetate = 9/1) as a colorless oil (116 mg, 96%); ^1H NMR (CDCl_3 , 400 MHz) δ 8.49–8.61 (m, 1H), 8.30 (s, 1H), 8.19 (d, 1H, J = 7.8 Hz), 7.71 (d, 1H, J = 8.0 Hz), 7.62 (t, 1H, J = 7.8 Hz), 7.54 (ddd, J = 11.0, 8.3, 1.3 Hz), 7.29–7.39 (m, 1H); ^{13}C NMR (CDCl_3 , 101 MHz): 157.6 (d, J_{C-F} = 261.6 Hz), 145.6 (d, J_{C-F} = 5.4 Hz), 144.5 (d, J_{C-F} = 10.9 Hz), 136.0 (d, J_{C-F} = 5.5 Hz), 131.8–132.1 (m), 130.9 (q, J_{C-F} = 31.8 Hz), 128.9, 125.7–125.9 (m), 125.5–125.7 (m), 124.4 (d, J_{C-F} = 20.9 Hz), 124.2 (d, J_{C-F} = 4.5 Hz), 123.9 (q, J_{C-F} = 273.4 Hz); ^{19}F NMR (CDCl_3 , 377 MHz) δ -62.6, -122.8; IR ν 3071, 1597, 1444, 1421, 1334, 1303, 1252, 1163, 1119, 1074 cm^{-1} ; MS, m/z (%) 241 (100) $[\text{M}]^+$, 222 (20), 221 (19), 172 (25), 69 (16), 50 (12); HRMS (EI) m/z $[\text{M}]^+$ calcd for $\text{C}_{12}\text{H}_7\text{F}_3\text{N}$ 241.0515; found 241.0503.

3-Fluoro-2-(3-methoxyphenyl)pyridine (3am) [CAS: 1269225-56-0]. Compound **3am** was prepared following method A from 3-fluoropyridinecarboxylate **1a** (90.5 mg, 0.50 mmol) and 1-bromo-3-methoxybenzene **2m** (191 mg, 1.0 mmol). **3am** was isolated (SiO_2 , cyclohexane/ethyl acetate = 6/1) as an orange oil (99 mg, 97%). Compound **3am** was prepared following method A from 3-fluoropyridinecarboxylate **1a** (90.5 mg, 0.50 mmol) and 1-chloro-3-methoxybenzene **2m'** (145 mg, 1.0 mmol). **3am** was isolated (SiO_2 , cyclohexane/ethyl acetate = 6/1) as an orange oil (62 mg, 61%); ^1H NMR (CDCl_3 , 400 MHz) δ 8.52–8.54 (m, 1H), 7.54–7.60 (m, 2H), 7.50 (ddd, 1H, J = 11.0, 8.3, 1.5 Hz), 7.41 (t, 1H, J = 7.9 Hz), 7.26–7.30 (m, 1H), 6.98–7.03 (m, 1H), 3.89 (s, 3H); ^{13}C NMR (CDCl_3 , 101 MHz) δ 159.7, 157.5 (d, J_{C-F} = 260.4 Hz), 146.0 (d, J_{C-F} = 10.3 Hz), 145.3 (d, J_{C-F} = 5.1 Hz), 136.6 (d, J_{C-F} = 5.1 Hz), 129.4, 124.1 (d, J_{C-F} = 21.3 Hz), 123.5 (d, J_{C-F} = 3.7 Hz), 121.3 (d, J_{C-F} = 7.3 Hz), 115.4, 113.8 (d, J_{C-F} = 5.1 Hz), 55.3; ^{19}F NMR (CDCl_3 , 377 MHz) δ -122.4; IR ν 3068, 2935, 2836, 1585, 1463, 1439, 1417, 1288, 1253, 1229 cm^{-1} ; MS, m/z (%) 203 (97) $[\text{M}]^+$, 202 (100), 174 (39), 173 (27), 172 (46), 159 (14); HRMS (EI) m/z $[\text{M}]^+$ calcd for $\text{C}_{12}\text{H}_{10}\text{FNO}$ 203.0746; found 203.0744.

2-[3-(tert-Butyl)phenyl]-3-fluoropyridine (3an). Compound **3an** was prepared following method A from 3-fluoro-2-pyridinecarboxylate **1a** (90.5 mg, 0.50 mmol) and 1-bromo-3-(1,1-dimethylethyl)benzene **2n** (213 mg, 1.0 mmol). **3an** was isolated (SiO_2 , cyclohexane/ethyl acetate = 9/1) as a colorless liquid (61 mg, 53%); ^1H NMR (CDCl_3 , 400 MHz) δ 8.54 (dt, 1H, J_d = 4.5 Hz, J_t = 1.5 Hz), 8.00 (d, 1H, J = 1.5 Hz), 7.76 (dq, 1H, J_d = 7.5 Hz, J_q = 1.6 Hz), 7.40–7.53 (m, 3H), 7.23–7.30 (m, 1H), 1.40 (s, 9H); ^{13}C NMR (CDCl_3 , 101 MHz) δ 157.5 (d, J_{C-F} = 262.5 Hz), 151.3, 146.8 (d, J_{C-F} = 10.9 Hz), 145.1 (d, J_{C-F} = 5.4 Hz), 134.7 (d, J_{C-F} = 4.5 Hz), 128.1, 126.4, 126.0 (d, J_{C-F} = 5.4 Hz), 125.8 (d, J_{C-F} = 4.5 Hz), 124.1 (d, J_{C-F} = 20.9 Hz), 123.3 (d, J_{C-F} = 3.6 Hz), 34.8, 31.3; ^{19}F NMR (CDCl_3 , 377 MHz) δ -122.9; IR ν 3064, 2963, 2868, 1596, 1438, 1409, 1364, 1249 cm^{-1} ; MS, m/z (%) 229 (28) $[\text{M}]^+$, 215 (15), 214 (100), 199 (11), 185 (10), 43 (15); HRMS (EI) m/z $[\text{M}]^+$ calcd for $\text{C}_{15}\text{H}_{16}\text{FN}$ 229.1267; found 229.1285.

3-Fluoro-2-(5-methoxy-2-methylphenyl)pyridine (3ao). Compound **3ao** was prepared following method A from potassium 3-fluoro-2-pyridinecarboxylate **1a** (90.5 mg, 0.50 mmol) and 1-bromo-4-methoxy-2-methylbenzene **2o** (207 mg, 1.0 mmol). **3ao** was isolated (SiO_2 , cyclohexane/ethyl acetate = 9/1) as a yellow oil (98 mg, 90%); ^1H NMR (CDCl_3 , 400 MHz) δ 8.41–8.47 (m, 1H), 7.36–7.45 (m, 1H), 7.19–7.29 (m, 2H), 6.74–6.81 (m, 2H), 3.78 (s, 3H), 2.20 (s, 3H); ^{13}C NMR (CDCl_3 , 101 MHz) δ 159.9, 157.0 (d, J_{C-F} = 256.1 Hz), 148.1 (d, J_{C-F} = 14.5 Hz), 145.1 (d, J_{C-F} = 5.4 Hz), 138.3, 131.1 (d, J_{C-F} = 1.8 Hz), 127.6 (d, J_{C-F} = 3.6 Hz), 123.3 (d, J_{C-F} = 2.7 Hz), 123.2 (d, J_{C-F} = 14.5 Hz), 115.7, 111.2, 55.2, 19.9; ^{19}F NMR (CDCl_3 , 377 MHz) δ -121.2; IR ν 3061, 3002, 2930, 2835, 1608,

1575, 1507, 1436, 1283, 1240, 1185 cm^{-1} ; MS, m/z (%) 217 (67) $[\text{M}]^+$, 216 (28), 198 (77), 197 (100), 183 (25), 182 (24), 154 (23); HRMS (EI) m/z $[\text{M}]^+$ calcd for $\text{C}_{13}\text{H}_{12}\text{FNO}$ 217.0903; found 217.0901.

3-Fluoro-2-(1-naphthalenyl)pyridine (3ap). Compound **3ap** was prepared following method A from potassium 3-fluoro-2-pyridinecarboxylate **1a** (90.5 mg, 0.50 mmol) and 2-bromonaphthalene **2p** (213 mg, 1.0 mmol). **3ap** was isolated (SiO_2 , cyclohexane/ethyl acetate = 9/1) as a colorless solid (82 mg, 74%); mp 93–94 °C; ^1H NMR (CDCl_3 , 400 MHz) δ 8.59–8.68 (m, 1H), 7.89–8.03 (m, 2H), 7.76 (d, 1H, J = 8.0 Hz), 7.56–7.69 (m, 3H), 7.46–7.56 (m, 2H), 7.37–7.45 (m, 1H); ^{13}C NMR (CDCl_3 , 101 MHz) δ 157.5 (d, J_{C-F} = 257.9 Hz), 147.4 (d, J_{C-F} = 14.5 Hz), 145.4 (d, J_{C-F} = 5.4 Hz), 133.7, 132.8 (d, J_{C-F} = 3.6 Hz), 131.2, 129.5, 128.4, 127.9 (d, J_{C-F} = 1.0 Hz), 126.5, 125.9, 125.2 (d, J_{C-F} = 1.8 Hz), 125.1, 123.9 (d, J_{C-F} = 3.6 Hz), 123.6 (d, J_{C-F} = 20.0 Hz); ^{19}F NMR (CDCl_3 , 377 MHz) δ -120.3; IR ν 3047, 3010, 1592, 1561, 1447, 1395, 1341, 1253, 1201 cm^{-1} ; MS, m/z (%) 223 (34) $[\text{M}]^+$, 222 (100), 221 (7), 111 (8), 50 (9); HRMS (EI) m/z $[\text{M}]^+$ calcd for $\text{C}_{15}\text{H}_{10}\text{FN}$ 223.0797; found 223.0785.

3-Fluoro-2,2'-bipyridine (3aq) [CAS: 1863378-49-7]. Compound **3aq** was prepared following method A from potassium 3-fluoro-2-pyridinecarboxylate **1a** (136 mg, 0.75 mmol) and 2-bromopyridine **2q** (80 mg, 0.48 mmol). **3aq** was isolated (SiO_2 , cyclohexane/ethyl acetate = 1/1) as a colorless oil (32 mg, 37%); ^1H NMR (CDCl_3 , 200 MHz) δ 8.81 (d, 1H, J = 4.8 Hz), 8.59 (dt, 1H, J_d = 4.5 Hz, J_t = 1.5 Hz), 7.94–8.04 (m, 1H), 7.77–7.89 (m, 1H), 7.48–7.62 (m, 1H), 7.31–7.41 (m, 2H); ^{13}C NMR (CDCl_3 , 101 MHz) δ 158.0 (d, J_{C-F} = 264.3 Hz), 153.5 (d, J_{C-F} = 6.4 Hz), 149.6, 145.5 (d, J_{C-F} = 5.5 Hz), 144.8 (d, J_{C-F} = 9.1 Hz), 136.7, 124.9 (d, J_{C-F} = 3.6 Hz), 124.7 (d, J_{C-F} = 20.9 Hz), 124.2 (d, J_{C-F} = 5.4 Hz), 123.6; ^{19}F NMR (CDCl_3 , 377 MHz) δ -122.5; IR ν 3059, 3011, 1585, 1454, 1422, 1256, 1196, 802 cm^{-1} ; MS, m/z (%) 174 (100) $[\text{M}]^+$, 173 (33), 147 (20), 146 (20), 76 (15), 51 (26), 50 (25); HRMS (EI) m/z $[\text{M}]^+$ calcd for $\text{C}_{10}\text{H}_7\text{FN}_2$ 174.0593; found 174.0597.

3-(3-Fluoro-2-pyridinyl)quinoline (3ar). Compound **3ar** was prepared following method A from potassium 3-fluoro-2-pyridinecarboxylate **1a** (90.5 mg, 0.50 mmol) and 3-bromoquinoline **2r** (104 mg, 0.50 mmol). **3ar** was isolated (SiO_2 , cyclohexane/ethyl acetate = 4/1) as a colorless solid (70 mg, 62%); mp 138–139 °C; ^1H NMR (CDCl_3 , 200 MHz) δ 9.57 (s, 1H), 8.77–8.82 (m, 1H), 8.59–8.65 (m, 1H), 8.18 (d, 1H, J = 8.3 Hz), 7.95 (dd, 1H, J = 8.1, 1.5 Hz), 7.72–7.84 (m, 1H), 7.52–7.66 (m, 2H), 7.31–7.43 (m, 1H); ^{13}C NMR (CDCl_3 , 50 MHz) δ 158.0 (d, J_{C-F} = 261.3 Hz), 150.3 (d, J_{C-F} = 6.6 Hz), 148.0, 145.8 (d, J_{C-F} = 5.1 Hz), 143.6 (d, J_{C-F} = 11.0 Hz), 136.0 (d, J_{C-F} = 7.0 Hz), 130.2, 129.3, 128.6, 128.2 (d, J_{C-F} = 5.9 Hz), 127.5, 126.9, 124.3 (d, J_{C-F} = 16.8 Hz), 124.1 (d, J_{C-F} = 4.0 Hz); ^{19}F NMR (CDCl_3 , 377 MHz) δ -122.3; IR ν 3061, 3038, 1595, 1410, 1344, 1113 cm^{-1} ; MS, m/z (%) 224 (100) $[\text{M}]^+$, 223 (45), 205 (10), 122 (10), 76 (10), 50 (14); HRMS (EI) m/z $[\text{M}]^+$ calcd for $\text{C}_{14}\text{H}_9\text{FN}_2$ 224.0750; found 224.0739.

3-Fluoro-2-(3-thienyl)pyridine (3as). Compound **3as** was prepared following method A from potassium 3-fluoro-2-pyridinecarboxylate **1a** (90.5 mg, 0.50 mmol) and 3-bromothiophene **2s** (168 mg, 1.0 mmol). **3as** was isolated (SiO_2 , cyclohexane/ethyl acetate = 9/1) as a colorless oil (50 mg, 56%); ^1H NMR (CDCl_3 , 200 MHz) δ 8.46 (dt, 1H, J_d = 4.5 Hz, J_t = 1.6 Hz), 8.04–8.12 (m, 1H), 7.86 (dt, 1H, J_d = 5.1 Hz, J_t = 1.3 Hz), 7.36–7.53 (m, 2H), 7.14–7.25 (m, 1H); ^{13}C NMR (CDCl_3 , 50 MHz) δ 156.8 (d, J_{C-F} = 260.5 Hz), 145.1 (d, J_{C-F} = 4.8 Hz), 142.1 (d, J_{C-F} = 11.0 Hz), 136.9 (d, J_{C-F} = 6.2 Hz), 127.6 (d, J_{C-F} = 4.8 Hz), 126.2 (d, J_{C-F} = 11.0 Hz), 125.3 (d, J_{C-F} = 1.5 Hz), 123.7 (d, J_{C-F} = 20.5 Hz), 122.7 (d, J_{C-F} = 4.0 Hz); ^{19}F NMR (CDCl_3 , 377 MHz) δ -121.4; IR ν 3113, 3065, 3021, 1597, 1454, 1440, 1206, 1099 cm^{-1} ; MS, m/z (%) 179 (100) $[\text{M}]^+$, 178 (26), 160 (37), 135 (10), 107 (10), 45 (11); HRMS (EI) m/z $[\text{M}]^+$ calcd for $\text{C}_9\text{H}_6\text{FNS}$ 179.0205; found 179.0208.

3-Fluoro-2-(2-thienyl)pyridine (3at). Compound **3at** was prepared following method A from potassium 3-fluoropyridinecarboxylate **1a** (90.5 mg, 0.50 mmol) and 2-bromothiophene **2t** (166 mg, 1.0 mmol). **3at** was isolated (SiO_2 , cyclohexane/ethyl acetate = 9/1) as a colorless solid (56 mg, 63%); mp 43–44 °C; ^1H NMR (CDCl_3 , 200

MHz) δ 8.41 (dt, 1H, $J_d = 4.9$ Hz, $J_t = 1.6$ Hz), 7.80–7.86 (m, 1H), 7.38–7.53 (m, 2H), 7.12–7.23 (m, 2H); ^{13}C NMR (CDCl_3 , 50 MHz) δ 155.7 (d, $J_{\text{C-F}} = 263.1$ Hz), 145.0 (d, $J_{\text{C-F}} = 4.8$ Hz), 141.3 (d, $J_{\text{C-F}} = 11.3$ Hz), 139.8 (d, $J_{\text{C-F}} = 7.7$ Hz), 128.2 (d, $J_{\text{C-F}} = 2.2$ Hz), 128.1 (d, $J_{\text{C-F}} = 5.5$ Hz), 127.9 (d, $J_{\text{C-F}} = 7.3$ Hz), 123.6 (d, $J_{\text{C-F}} = 19.4$ Hz), 122.6 (d, $J_{\text{C-F}} = 4.0$ Hz); ^{19}F NMR (CDCl_3 , 377 MHz) δ -120.7; IR ν 3123, 3082, 1597, 1449, 1362, 1260, 1204, 1101 cm^{-1} ; MS, m/z (%) 179 (100) [$\text{M}]^+$, 178 (13), 135 (17), 134 (8), 107 (10), 45 (14); HRMS (EI) m/z [$\text{M}]^+$ calcd for $\text{C}_9\text{H}_6\text{FNS}$ 179.0205; found 179.0200.

1-[5-(3-Fluoro-2-pyridinyl)-2-thienyl]ethanone (3au). Compound **3au** was prepared following method A from potassium 3-fluoro-2-pyridinecarboxylate **1a** (90.5 mg, 0.50 mmol) and 1-(5-bromo-2-thienyl)ethanone **2u** (207 mg, 1.0 mmol). **3au** was isolated (SiO_2 , cyclohexane/ethyl acetate = 9/1) as a yellow solid (34 mg, 31%); mp 146–147 °C; ^1H NMR (CDCl_3 , 200 MHz) δ 8.44 (dt, 1H, $J_d = 4.5$ Hz, $J_t = 1.6$ Hz), 7.76–7.82 (m, 1H), 7.69–7.74 (m, 1H), 7.43–7.55 (m, 1H), 7.22–7.32 (m, 1H), 2.59 (s, 3H); ^{13}C NMR (CDCl_3 , 75 MHz) δ 190.7, 156.4 (d, $J_{\text{C-F}} = 262.6$ Hz), 147.0 (d, $J_{\text{C-F}} = 7.7$ Hz), 145.4 (d, $J_{\text{C-F}} = 5.0$ Hz), 144.9 (d, $J_{\text{C-F}} = 3.3$ Hz), 140.1 (d, $J_{\text{C-F}} = 11.1$ Hz), 133.0 (d, $J_{\text{C-F}} = 2.2$ Hz), 128.3 (d, $J_{\text{C-F}} = 12.2$ Hz), 124.3 (d, $J_{\text{C-F}} = 3.3$ Hz), 124.1 (d, $J_{\text{C-F}} = 18.2$ Hz), 26.9; ^{19}F NMR (CDCl_3 , 377 MHz) δ -119.4; IR ν 3121, 3063, 2920, 2850, 1646, 1425, 1273, 1259 cm^{-1} ; MS, m/z (%) 221 (42) [$\text{M}]^+$, 207 (14), 206 (100), 178 (23), 134 (17), 107 (9); HRMS (EI) m/z [$\text{M}]^+$ calcd for $\text{C}_{11}\text{H}_8\text{FNO}$ 221.0311; found 221.0304.

3-Fuoro-2-(5-benzofuranyl)pyridine (3av). Compound **3av** was prepared following method A from potassium 3-fluoro-2-pyridinecarboxylate **1a** (90.5 mg, 0.50 mmol) and 5-bromobenzofuran **2v** (203 mg, 1.0 mmol). **3av** was isolated (SiO_2 , cyclohexane/ethyl acetate = 9/1) as a yellow solid (54 mg, 51%); mp 81–82 °C; ^1H NMR (CDCl_3 , 200 MHz) δ 8.50–8.58 (m, 1H), 8.23 (t, 1H, $J = 1.5$ Hz), 7.91–8.00 (m, 1H), 7.44–7.70 (m, 3H), 7.21–7.32 (m, 1H), 6.86 (dd, 1H, $J = 2.3$, 1.0 Hz); ^{13}C NMR (CDCl_3 , 75 MHz) δ 157.4 (d, $J_{\text{C-F}} = 259.8$ Hz), 155.4, 146.5 (d, $J_{\text{C-F}} = 10.5$ Hz), 145.6, 145.3 (d, $J_{\text{C-F}} = 5.5$ Hz), 130.3 (d, $J_{\text{C-F}} = 5.5$ Hz), 127.6, 125.3 (d, $J_{\text{C-F}} = 5.5$ Hz), 124.1 (d, $J_{\text{C-F}} = 20.5$ Hz), 123.0 (d, $J_{\text{C-F}} = 3.9$ Hz), 122.0 (d, $J_{\text{C-F}} = 6.1$ Hz), 111.3, 107.0; ^{19}F NMR (CDCl_3 , 41 MHz) δ -120.7; IR ν 3156, 3125, 3042, 3013, 1597, 1443, 1192, 1024 cm^{-1} ; MS, m/z (%) 213 (100) [$\text{M}]^+$, 212 (14), 185 (17), 184 (13); HRMS (EI) m/z [$\text{M}]^+$ calcd for $\text{C}_{13}\text{H}_8\text{FNO}$ 213.0590; found 213.0585.

1-[2-(4-Fluorophenyl)-3-pyridinyl]ethanone (3ba) [CAS: 280573-47-9]. Compound **3ba** was prepared following method A from potassium 3-acetyl-2-pyridinecarboxylate **1b** (102 mg, 0.50 mmol) and 1-bromo-4-fluorobenzene **2a** (177 mg, 1.1 μL , 1.0 mmol). **3ba** was isolated (SiO_2 , cyclohexane/ethyl acetate = 2/1) as an orange oil (56 mg, 52%); ^1H NMR (CDCl_3 , 250 MHz) δ 8.75 (dd, 1H, $J = 4.8$, 1.7 Hz), 7.86 (dd, 1H, $J = 7.7$, 1.7 Hz), 7.51–7.61 (m, 2H), 7.35 (dd, 1H, $J = 7.7$, 4.9 Hz), 7.11–7.22 (m, 2H), 2.11 (s, 3H); ^{13}C NMR (CDCl_3 , 63 MHz) δ 203.3, 163.6 (d, $J_{\text{C-F}} = 250.0$ Hz), 156.0, 150.9, 136.2, 136.2, 135.8 (d, $J_{\text{C-F}} = 3.7$ Hz), 131.0 (d, $J_{\text{C-F}} = 8.3$ Hz), 122.0, 115.8 (d, $J_{\text{C-F}} = 22.1$ Hz), 30.2; ^{19}F NMR (CDCl_3 , 235 MHz) δ -111.7; IR ν 3046, 2922, 2853, 1686, 1510, 1425, 1221, 843 cm^{-1} ; MS, m/z (%) 215 (42) [$\text{M}]^+$, 214 (26), 200 (100), 172 (45), 145 (20), 43 (43); HRMS (EI) m/z [$\text{M}]^+$ calcd for $\text{C}_{13}\text{H}_{10}\text{FNO}$ 215.0746; found 215.0742.

3-(1-Piperidinyl)-2-(4-fluorophenyl)pyridine (3ca). Compound **3ca** was prepared following method A from potassium 3-(1-piperidinyl)-2-pyridinecarboxylate **1c** (122 mg, 0.50 mmol) and 1-bromo-4-fluorobenzene **2a** (177 mg, 1.1 μL , 1.0 mmol). **3ca** was isolated (SiO_2 , cyclohexane/ethyl acetate = 9/1) as a brown oil (22 mg, 17%); ^1H NMR (CDCl_3 , 200 MHz) δ 8.30 (dd, 1H, $J = 4.5$, 1.5 Hz), 7.95–8.08 (m, 2H), 7.34 (dd, 1H, $J = 8.3$, 1.5 Hz), 7.04–7.21 (m, 3H), 2.78 (m, 4H), 1.44–1.64 (m, 6H); ^{13}C NMR (CDCl_3 , 50 MHz) δ 162.5 (d, $J_{\text{C-F}} = 246.6$ Hz), 151.3, 147.9, 142.7, 136.6 (d, $J_{\text{C-F}} = 3.7$ Hz), 130.3 (d, $J_{\text{C-F}} = 8.1$ Hz), 126.0, 122.5, 114.9 (d, $J_{\text{C-F}} = 21.2$ Hz), 52.3, 25.9, 23.9; ^{19}F NMR (CDCl_3 , 41 MHz) δ -114.4 IR ν 3060, 2935, 2854, 1602, 1573, 1507, 1432, 1219 cm^{-1} ; MS, m/z (%) 256 (100) [$\text{M}]^+$, 255 (39), 199 (15), 160 (17), 159 (7), 145 (8); HRMS (EI) m/z [$\text{M}]^+$ calcd for $\text{C}_{16}\text{H}_{17}\text{FN}_2$ 256.1376; found 256.1365.

3-Chloro-2-(4-fluorophenyl)pyridine (3da) [CAS: 847226-00-0]. Compound **3da** was prepared following method A from potassium 3-chloro-2-pyridinecarboxylate **1d** (97.8 mg, 0.50 mmol) and 1-bromo-4-fluorobenzene **2a** (177 mg, 1.1 μL , 1.0 mmol) in the presence of Ag_2CO_3 (6.96 mg, 25 μmol , 5 mol %) instead of Cu_2O . **3da** was isolated (SiO_2 , cyclohexane/ethyl acetate = 9/1) as a colorless solid (63 mg, 49%); mp 80–81 °C; ^1H NMR (CDCl_3 , 300 MHz) δ 8.59 (dd, 1H, $J = 4.7$, 1.6 Hz), 7.71–7.83 (m, 3H), 7.12–7.26 (m, 3H); ^{13}C NMR (CDCl_3 , 50 MHz) δ 163.1 (d, $J_{\text{C-F}} = 248.1$ Hz), 155.5, 147.6, 138.2, 134.2 (d, $J_{\text{C-F}} = 3.3$ Hz), 131.3 (d, $J_{\text{C-F}} = 8.4$ Hz), 130.1, 123.1, 115.0 (d, $J_{\text{C-F}} = 22.0$ Hz); ^{19}F NMR (CDCl_3 , 41 MHz) δ -112.6; IR ν 3044, 1599, 1574, 1513, 1432, 1402, 1161, 848 cm^{-1} ; MS, m/z (%) 209 (30) [$\text{M}]^+$, 208 (12), 207 (73) [$\text{M}]^+$, 173 (12), 172 (100), 145 (20), 43 (20); HRMS (EI) m/z [$\text{M}]^+$ calcd for $\text{C}_{11}\text{H}_7^{35}\text{ClFN}$ 207.0251; found 207.0237; [$\text{M}]^+$ calcd for $\text{C}_{11}\text{H}_7^{37}\text{ClFN}$ 209.0222; found 209.0211.

2-(4-Fluorophenyl)-3-methoxypyridine (3ea) [CAS: 1214324-71-6]. Compound **3ea** was prepared following method B from potassium 3-methoxy-2-pyridinecarboxylate **1e** (95.6 mg, 0.50 mmol) and 1-bromo-4-fluorobenzene **2a** (177 mg, 1.1 μL , 1.0 mmol). **3ea** was isolated (SiO_2 , cyclohexane/ethyl acetate = 6/1) as a colorless oil (71 mg, 70%); ^1H NMR (CDCl_3 , 400 MHz) δ 8.31 (dd, 1H, $J = 4.6$, 1.4 Hz), 7.90–7.97 (m, 2H), 7.28–7.32 (m, 1H), 7.22–7.26 (m, 1H), 7.09–7.17 (m, 2H), 3.88 (s, 3H); ^{13}C NMR (CDCl_3 , 101 MHz) δ 162.8 (d, $J_{\text{C-F}} = 247.0$ Hz), 153.4, 147.0, 141.3, 133.7 (d, $J_{\text{C-F}} = 2.7$ Hz), 131.2 (d, $J_{\text{C-F}} = 8.2$ Hz), 122.9, 118.5, 114.8 (d, $J_{\text{C-F}} = 20.9$ Hz), 55.4; ^{19}F NMR (CDCl_3 , 377 MHz) δ -113.7; IR ν 3061, 3006, 2942, 2839, 1601, 1508, 1430, 1266, 1220, 1196, 1158, 1125, 1013 cm^{-1} ; MS, m/z (%) 203 (71) [$\text{M}]^+$, 202 (100), 174 (14), 173 (18), 172 (32), 133 (28), 50 (12); HRMS (EI) m/z [$\text{M}]^+$ calcd for $\text{C}_{12}\text{H}_{10}\text{FNO}$ 203.0746; found 203.0744.

2-(4-Fluorophenyl)-pyridine (3fa) [CAS: 58861-53-3]. Compound **3fa** was prepared following method A in NMP/mesitylene (2 mL, 1/1) at 190 °C from potassium 2-pyridinecarboxylate **1f** (81.4 mg, 0.50 mmol) and 1-bromo-4-fluorobenzene **2a** (177 mg, 1.1 μL , 1.0 mmol). **3fa** was isolated (SiO_2 , cyclohexane/ethyl acetate = 9/1) as a colorless solid (32 mg, 37%); mp 39–40 °C; ^1H NMR (CDCl_3 , 300 MHz) δ 8.73–8.63 (m, 1H), 8.06–7.94 (m, 2H), 7.81–7.65 (m, 2H), 7.26–7.12 (m, 3H); ^{13}C NMR (CDCl_3 , 101 MHz) δ 163.5 (d, $J_{\text{C-F}} = 248.5$ Hz), 156.5, 149.7, 136.8, 135.6 (d, $J_{\text{C-F}} = 3.3$ Hz), 128.7 (d, $J_{\text{C-F}} = 8.4$ Hz), 122.0, 120.2, 115.6 (d, $J_{\text{C-F}} = 21.6$ Hz); ^{19}F NMR (CDCl_3 , 41 MHz) δ -112.0; IR ν 3055, 3011, 1600, 1584, 1509, 1464, 1433, 1219, 1099 cm^{-1} ; MS, m/z (%) 173 (100) [$\text{M}]^+$, 146 (9), 51 (11); HRMS (EI) m/z [$\text{M}]^+$ calcd for $\text{C}_{11}\text{H}_8\text{FN}$ 173.0641; found 173.0640.

2-Phenylpyridine (3fb) [CAS: 1008-89-5].^{35,56} Compound **3fb** was prepared following method A in NMP/mesitylene (2 mL, 1/1) at 190 °C from potassium 2-pyridinecarboxylate **1f** (81.4 mg, 0.50 mmol) and bromobenzene **2b** (159 mg, 1.06 μL , 1.0 mmol). **3fb** was isolated (SiO_2 , cyclohexane/ethyl acetate = 9/1) as a colorless liquid (31 mg, 40%); ^1H NMR (CDCl_3 , 200 MHz) δ 8.72 (dt, 1H, $J_d = 4.8$, $J_t = 1.4$ Hz), 8.06–7.95 (m, 2H), 7.83–7.70 (m, 2H), 7.55–7.37 (m, 3H), 7.30–7.21 (m, 1H); ^{13}C NMR (CDCl_3 , 50 MHz) δ 157.5, 149.6, 139.4, 136.8, 129.0, 128.7, 126.9, 122.1, 120.6; MS, m/z (%) 155 (100) [$\text{M}]^+$.

2-(4-Methoxyphenyl)-pyridine (3fd) [CAS: 5957-90-4].^{35,56} Compound **3fd** was prepared following method A in NMP/mesitylene (2 mL, 1/1) at 190 °C from potassium 2-pyridinecarboxylate **1f** (81.4 mg, 0.50 mmol) and bromo-4-methoxybenzene **2d** (187 mg, 1.26 μL , 1.0 mmol). **3fd** was isolated (SiO_2 , cyclohexane/ethyl acetate = 4/1) as a colorless oil (26 mg, 28%); ^1H NMR (CDCl_3 , 200 MHz) δ 8.67 (dt, 1H, $J_d = 4.7$ Hz, $J_t = 1.5$ Hz), 8.01–7.92 (m, 2H), 7.78–7.63 (m, 2H), 7.19 (dd, 1H, $J = 6.6$, 4.9, 1.9 Hz), 7.06–6.96 (m, 2H), 3.88 (s, 3H); ^{13}C NMR (CDCl_3 , 50 MHz) δ 160.5, 157.1, 149.4, 136.7, 131.9, 128.2, 121.4, 119.8, 114.1, 55.3; MS, m/z (%) 185 (100) [$\text{M}]^+$.

5-(4-Fluorophenyl)-1-methyl-1H-pyrazole (3ga) [CAS: 689251-78-3]. Compound **3ga** was prepared following method B from potassium 1-methyl-1H-pyrazole-5-carboxylate **1g** (82.1 mg, 0.50 mmol) and 1-bromo-4-fluorobenzene **2a** (177 mg, 1.1 μL , 1.0 mmol). **3ga** was isolated (SiO_2 , cyclohexane/ethyl acetate = 6/1) as a colorless liquid (56 mg, 64%); ^1H NMR (CDCl_3 , 250 MHz) δ 7.51 (d,

^1H , $J = 1.9$ Hz), 7.34–7.44 (m, 2H), 7.08–7.21 (m, 2H), 6.28 (d, ^1H , $J = 1.9$ Hz), 3.87 (s, 3H); ^{13}C NMR (CDCl_3 , 50 MHz) δ 162.8 (d, $J_{\text{C-F}} = 248.1$ Hz), 142.5, 138.5, 130.6 (d, $J_{\text{C-F}} = 3.7$ Hz), 126.9 (d, $J_{\text{C-F}} = 8.1$ Hz), 115.7 (d, $J_{\text{C-F}} = 22.0$ Hz), 106.1, 37.3; ^{19}F NMR (CDCl_3 , 235 MHz) δ -112.8; IR ν 3103, 3063, 2947, 1605, 1545, 1493, 1223, 839 cm^{-1} ; MS, m/z (%) 176 (100) [$\text{M}]^+$, 175 (39), 148 (16), 133 (13), 121 (16), 109 (9); HRMS (EI) m/z [$\text{M}]^+$ calcd for $\text{C}_{10}\text{H}_9\text{FN}_2$ 176.0750; found 176.0740.

5-(4-Fluorophenyl)-4-methylthiazole (3ha) [CAS: 623577-48-0]. Compound **3ha** was prepared following methods A and B, respectively, from potassium 4-methyl-5-thiazolecarboxylate **1h** (90.6 mg, 0.50 mmol) and 1-bromo-4-fluorobenzene **2a** (177 mg, 1.11 μL , 1.0 mmol). **3ha** was isolated (SiO_2 , cyclohexane/ethyl acetate = 6/1) as a yellow solid (35 mg, 36% (method A); 72 mg, 75% (method B)): mp 35–36 $^\circ\text{C}$; ^1H NMR (CDCl_3 , 250 MHz) δ 8.68 (s, 1H), 7.35–7.46 (m, 2H), 7.05–7.18 (m, 2H), 2.51 (s, 3H); ^{13}C NMR (CDCl_3 , 50 MHz) δ 162.4 (d, $J_{\text{C-F}} = 248.5$ Hz), 150.2, 148.6 (d, $J_{\text{C-F}} = 0.7$ Hz), 131.0 (d, $J_{\text{C-F}} = 8.0$ Hz), 130.8, 127.9 (d, $J_{\text{C-F}} = 3.3$ Hz), 115.7 (d, $J_{\text{C-F}} = 22.0$ Hz), 15.9; ^{19}F NMR (CDCl_3 , 235 MHz) δ -113.5; IR ν 3096, 3042, 2922, 1603, 1497, 1240, 831 cm^{-1} ; MS, m/z (%) 193 (100) [$\text{M}]^+$, 192 (9), 166 (24), 165 (24), 133 (19), 122 (11); HRMS (EI) m/z [$\text{M}]^+$ calcd for $\text{C}_{10}\text{H}_8\text{FNS}$ 193.0361; found 193.0352.

2-(4-Fluorophenyl)-benzo[*b*]thiophene (3ia) [CAS: 936734-96-2]. Compound **3ia** was prepared following method B from potassium benzo[*b*]thiophene-2-carboxylate **1i** (108 mg, 0.50 mmol) and 1-bromo-4-fluorobenzene **2a** (177 mg, 1.11 μL , 1.0 mmol). **3ia** was isolated (SiO_2 , cyclohexane) as a colorless solid (24 mg, 21%): mp 181–182 $^\circ\text{C}$; ^1H NMR (CDCl_3 , 250 MHz) δ 7.75–7.89 (m, 2H), 7.63–7.75 (m, 2H), 7.48 (s, 1H), 7.28–7.43 (m, 2H), 7.06–7.21 (m, 2H); ^{13}C NMR (CDCl_3 , 50 MHz) δ 162.8 (d, $J_{\text{C-F}} = 248.1$ Hz), 143.1, 140.7, 139.5, 130.6, 128.2 (d, $J_{\text{C-F}} = 8.1$ Hz), 124.6, 124.4, 123.5, 122.2, 119.4 (d, $J_{\text{C-F}} = 1.5$ Hz), 115.9 (d, $J_{\text{C-F}} = 21.6$ Hz); ^{19}F NMR (CDCl_3 , 235 MHz) δ -113.4; IR ν 3061, 1593, 1431, 1233, 818 cm^{-1} ; MS, m/z (%) 228 (100) [$\text{M}]^+$, 196 (8), 183 (12), 40 (9); HRMS (EI) m/z [$\text{M}]^+$ calcd for $\text{C}_{14}\text{H}_8\text{FS}$ 228.0409; found 228.0397.

Synthesis of 3-Methoxy-2-phenylpyridine (4) [CAS: 53698-49-0]. To a solution of methanol (17.6 mg, 22 μL , 0.55 mmol) and **3ab** (86.6 mg, 0.5 mmol) in dry DMF (5 mL) at 0 $^\circ\text{C}$ was added dropwise dry KHMDS (0.5 M in toluene, 1.1 mL, 0.55 mmol). The reaction was allowed to warm to rt overnight and then quenched with saturated aqueous NaHCO_3 (10 mL). The aqueous layer was extracted with ethyl acetate (3 \times 20 mL). The combined organic layers were washed with brine, dried over MgSO_4 , filtered, and the volatiles were removed under reduced pressure. The residue was purified by column chromatography (SiO_2 , cyclohexane/ethyl acetate = 6/1), yielding **4** as colorless oil (86 mg, 93%): ^1H NMR (CDCl_3 , 200 MHz) δ 8.33 (dd, ^1H , $J = 4.3$, 1.8 Hz), 7.96–7.86 (m, 2H), 7.51–7.32 (m, 3H), 7.30–7.19 (m, 2H), 3.87 (s, 3H); ^{13}C NMR (CDCl_3 , 50 MHz) δ 153.6, 148.2, 141.3, 137.7, 129.4, 128.3, 128.0, 122.9, 118.5, 55.5; MS, m/z (%) 185 (61) [$\text{M}]^+$, 184 (100), 154 (33).

Synthesis of 2-Phenyl-2-(3-(2-phenylpyridyl)acetonitrile (6). A 20 mL microwave vessel was charged with **3ab** (86.6 mg, 0.5 mmol) and potassium *tert*-butoxide (318 mg, 2.75 mmol). NMP (1 mL) and benzyliocyanide **5** (293 mg, 290 μL , 2.5 mmol) were added, and the mixture was heated at 100 $^\circ\text{C}$ in the microwave for 5 min. The mixture was allowed to cool to rt, washed with distilled water (20 mL), and extracted with ethyl acetate (3 \times 20 mL). The combined organic layers were washed with brine, dried over MgSO_4 , filtered, and the volatiles were removed under reduced pressure. The residue was purified by column chromatography (SiO_2 , *n*-pentane/diethyl ether = 2/3), yielding compound **6** as colorless oil (120 mg, 89%): ^1H NMR (CDCl_3 , 200 MHz) δ 8.69 (dd, ^1H , $J = 4.8$, 1.5 Hz), 7.85 (dd, ^1H , $J = 8.0$, 1.6 Hz), 7.53–7.42 (m, 5H), 7.41–7.28 (m, 4H), 7.18–7.06 (m, 2H), 5.44 (s, 1H); ^{13}C NMR (CDCl_3 , 50 MHz) δ 158.5, 149.3, 138.7, 137.3, 135.2, 130.1, 129.2, 128.9, 128.8, 128.7, 128.3, 127.4, 123.1, 119.4, 38.9; IR ν 3051, 2910, 2241, 1564, 1492, 1435 cm^{-1} ; MS, m/z (%) 270.15 (89) [$\text{M}]^+$, 269.15 (100); HRMS (EI) m/z [$\text{M}]^+$ calcd for $\text{C}_{19}\text{H}_{14}\text{N}_2$ 270.1157; found 270.1146.

■ ASSOCIATED CONTENT

Supporting Information

The Supporting Information is available free of charge on the ACS Publications website at DOI: 10.1021/acs.joc.7b00046.

Full optimization table and copies of ^1H , ^{13}C , and ^{19}F NMR spectra of all products (PDF)

■ AUTHOR INFORMATION

Corresponding Author

*E-mail: lukas.goossen@rub.de.

ORCID

Lukas J. Goossen: 0000-0002-2547-3037

Notes

The authors declare no competing financial interest.

■ ACKNOWLEDGMENTS

We thank Brian T. O'Neill for helpful discussions, the DFG (SFB/TRR-88 "3MET" and EXC/1069 "RESOLV"), and the Stipendienstiftung Rheinland-Pfalz (fellowship to D.H.) for financial support.

■ REFERENCES

- (1) Dzik, W. I.; Lange, P. P.; Goossen, L. J. *Chem. Sci.* **2012**, *3*, 2671–2678.
- (2) Cornella, J.; Larrosa, I. *Synthesis* **2012**, *44*, 653–676.
- (3) Maiti, D.; Patra, T. *Chem. - Eur. J.* **2017**, DOI: 10.1002/chem.201604496.
- (4) Myers, A. G.; Tanaka, D.; Mannion, M. R. *J. Am. Chem. Soc.* **2002**, *124*, 11250–11251.
- (5) Hu, P.; Kan, J.; Su, W.; Hong, M. *Org. Lett.* **2009**, *11*, 2341–2344.
- (6) Tang, J.; Hackenberger, D.; Goossen, L. J. *Angew. Chem., Int. Ed.* **2016**, *55*, 11296–11299.
- (7) Agasti, S.; Dey, A.; Maiti, D. *Chem. Commun.* **2016**, *52*, 12191–12194.
- (8) Goossen, L. J.; Deng, G.; Levy, L. M. *Science* **2006**, *313*, 662–664.
- (9) Becht, J.-M.; Catala, C.; Le Drian, C.; Wagner, A. *Org. Lett.* **2007**, *9*, 1781–1783.
- (10) Shang, R.; Fu, Y.; Li, J.-B.; Zhang, S.-L.; Guo, Q.-X.; Liu, L. *J. Am. Chem. Soc.* **2009**, *131* (16), 5738–5739.
- (11) Shang, R.; Yang, Z.-W.; Wang, Y.; Zhang, S.-L.; Liu, L. *J. Am. Chem. Soc.* **2010**, *132*, 14391–14393.
- (12) Weaver, J. D.; Recio, A.; Grenning, A. J.; Tunge, J. A. *Chem. Rev.* **2011**, *111*, 1846–1913.
- (13) Behenna, D. C.; Liu, Y.; Yurino, T.; Kim, J.; White, D. E.; Virgil, S. C.; Stoltz, B. M. *Nat. Chem.* **2012**, *4*, 130–133.
- (14) Bi, H.-P.; Zhao, L.; Liang, Y.-M.; Li, C.-J. *Angew. Chem., Int. Ed.* **2009**, *48*, 792–795.
- (15) Zhou, J.; Wu, G.; Zhang, M.; Jie, X.; Su, W. *Chem. - Eur. J.* **2012**, *18*, 8032–8036.
- (16) Wang, C.; Piel, I.; Glorius, F. *J. Am. Chem. Soc.* **2009**, *131*, 4194–4195.
- (17) Cornella, J.; Lu, P.; Larrosa, I. *Org. Lett.* **2009**, *11*, 5506–5509.
- (18) Voutchkova, A.; Coplin, A.; Leadbeater, N. E.; Crabtree, R. H. *Chem. Commun.* **2008**, *47*, 6312–6314.
- (19) Pichette Drapeau, M.; Goossen, L. J. *Chem. - Eur. J.* **2016**, *22*, 18654–18677.
- (20) Bhadra, S.; Dzik, W. I.; Goossen, L. J. *J. Am. Chem. Soc.* **2012**, *134*, 9938–9941.
- (21) Zuo, Z.; Ahneman, D. T.; Chu, L.; Terrett, J. A.; Doyle, A. G.; MacMillan, D. W. C. *Science* **2014**, *345*, 437–440.
- (22) Noble, A.; McCarver, S. J.; MacMillan, D. W. C. *J. Am. Chem. Soc.* **2015**, *137*, 624–627.
- (23) Song, B.; Knauber, T.; Goossen, L. J. *Angew. Chem., Int. Ed.* **2013**, *52*, 2954–2958.

- (24) Goossen, L. J.; Lange, P. P.; Rodríguez, N.; Linder, C. *Chem. - Eur. J.* **2010**, *16*, 3906–3909.
- (25) Tang, J.; Biafora, A.; Goossen, L. J. *Angew. Chem., Int. Ed.* **2015**, *54*, 13130–13133.
- (26) Forgione, P.; Brochu, M.-C.; St-Onge, M.; Thesen, K. H.; Bailey, M. D.; Bilodeau, F. J. *Am. Chem. Soc.* **2006**, *128*, 11350–11351.
- (27) Zhang, F.; Greaney, M. F. *Org. Lett.* **2010**, *12*, 4745–4747.
- (28) Goossen, L. J.; Rodríguez, N.; Linder, C. J. *Am. Chem. Soc.* **2008**, *130*, 15248–15249.
- (29) He, R.-T.; Wang, J.-F.; Wang, H.-F.; Ren, Z.-G.; Lang, J.-P. *Dalton Trans.* **2014**, *43*, 9786.
- (30) Campeau, L.-C.; Fagnou, K. *Chem. Soc. Rev.* **2007**, *36*, 1058–1068.
- (31) Lu, P.; Sanchez, C.; Cornella, J.; Larrosa, I. *Org. Lett.* **2009**, *11*, 5710–5713.
- (32) Dupuy, S.; Nolan, S. P. *Chem. - Eur. J.* **2013**, *19*, 14034–14038.
- (33) Toy, X. Y.; Roslan, I. I. B.; Chuah, G. K.; Jaenicke, S. *Catal. Sci. Technol.* **2014**, *4*, 516–523.
- (34) Baruah, D.; Konwar, D. *Catal. Commun.* **2015**, *69*, 68–71.
- (35) Li, X.; Zou, D.; Leng, F.; Sun, C.; Li, J.; Wu, Y.; Wu, Y. *Chem. Commun.* **2013**, *49*, 312–314.
- (36) Haley, C. K.; Gilmore, C. D.; Stoltz, B. M. *Tetrahedron* **2013**, *69*, 5732–5736.
- (37) Fromm, A.; van Wüllen, C.; Hackenberger, D.; Goossen, L. J. *J. Am. Chem. Soc.* **2014**, *136*, 10007–10023.
- (38) Rouchet, J.-B.; Schneider, C.; Spitz, C.; Lefèvre, J.; Dupas, G.; Fruit, C.; Hoarau, C. *Chem. - Eur. J.* **2014**, *20*, 3610–3615.
- (39) Campeau, L.-C.; Rousseaux, S.; Fagnou, K. J. *Am. Chem. Soc.* **2005**, *127*, 18020–18021.
- (40) Campeau, L.-C.; Stuart, D. R.; Leclerc, J.-P.; Bertrand-Laperle, M.; Villemure, E.; Sun, H.-Y.; Lasserre, S.; Guimond, N.; Lecavallier, M.; Fagnou, K. J. *Am. Chem. Soc.* **2009**, *131*, 3291–3306.
- (41) Ackermann, L.; Fenner, S. *Chem. Commun.* **2011**, *47*, 430–432.
- (42) Tan, Y.; Barrios-Landeros, F.; Hartwig, J. F. *J. Am. Chem. Soc.* **2012**, *134*, 3683–3686.
- (43) Caron, S.; Ghosh, A. In *Practical Synthetic Organic Chemistry*; Caron, S., Ed.; John Wiley & Sons, Inc.: Hoboken, NJ, 2011; pp 237–253.
- (44) Cherng, Y.-J. *Tetrahedron* **2002**, *58*, 4931–4935.
- (45) Henderson, A. S.; Medina, S.; Bower, J. F.; Galan, M. C. *Org. Lett.* **2015**, *17*, 4846–4849.
- (46) Ribas, X. *C–H and C–X Bond Functionalization: Transition Metal Mediation*; Royal Society of Chemistry: Cambridge, UK, 2013.
- (47) Buckley, H. L.; Wang, T.; Tran, O.; Love, J. A. *Organometallics* **2009**, *28*, 2356–2359.
- (48) Sun, A. D.; Love, J. A. *Org. Lett.* **2011**, *13*, 2750–2753.
- (49) Lu, F.; Sun, H.; Du, A.; Feng, L.; Li, X. *Org. Lett.* **2014**, *16*, 772–775.
- (50) Senaweera, S.; Weaver, J. D. *J. Am. Chem. Soc.* **2016**, *138*, 2520–2523.
- (51) Sun, H.-Y.; Gorelsky, S. I.; Stuart, D. R.; Campeau, L.-C.; Fagnou, K. J. *Org. Chem.* **2010**, *75*, 8180–8189.
- (52) Billingsley, K. L.; Buchwald, S. L. *Angew. Chem., Int. Ed.* **2008**, *47*, 4695–4698.
- (53) Blakemore, D. *Synthetic Methods in Drug Discovery*; Royal Society of Chemistry: Cambridge, UK, 2016; Vol. 1, pp 1–69.
- (54) Armarego, W. L. F. *Purification of Laboratory Chemicals*, 6th ed.; Elsevier/Butterworth-Heinemann: Amsterdam, 2009.
- (55) Moreno-Mañas, M.; Pleixats, R. *Synlett* **2006**, *2006*, 3001–3004.
- (56) Ackermann, L.; Althammer, A. *Org. Lett.* **2006**, *8*, 3457–3460.
- (57) Lemire, A.; Grenon, M.; Pourashraf, M.; Charette, A. B. *Org. Lett.* **2004**, *6*, 3517–3520.

5.2.5 Decarboxylierende Kreuzkupplung von Pyrimidin-2-carbonsäure

Neben den zuvor beschriebenen Studien sollte weiterhin überprüft werden, ob sich Pyrimidin-2-carbonsäure als Substrat in decarboxylierenden Kreuzkupplungen eignet. Als Modellsubstrate dienten Kalium-2-pyrimidincarboxylat (**5.2.5-1**) und 1-Brom-4-fluorbenzol (**5.2.5-2**), die in Gegenwart des zuvor für die Kupplung der Pyridin-2-carbonsäure genutzten Katalysatorsystems umgesetzt wurden. Dabei wurde zunächst der Einfluss des Lösungsmittels untersucht (Tabelle 17).

Tabelle 17: Einfluss des Lösungsmittels und der Lösungsmittelmenge.

Eintrag	T (°C)	Lösungsmittel	5.2.5-3 (%)
1	190	NMP (2 mL)	20
2	"	Chinolin (2 mL)	36
3	"	NMP/Chinolin (1:1, 2 mL)	36
4	"	Chinolin/Mes (1:1, 2 mL)	26
5	"	NMP/Mes (1:1, 2 mL)	41 / 40 ^[a]
6 ^[a]	"	NMP/Mes (1:1, 3 mL)	39
7 ^[a]	"	NMP/Mes (1:1, 1 mL)	27
8	170	NMP/Mes (1:1, 2 mL)	15

Reaktionsbedingungen: **5.2.5-1** (0.5 mmol), **5.2.5-2** (1.0 mmol), Cu₂O (5 mol%), 1,10-Phen (10 mol%), PdCl₂ (5 mol%), PPh₃ (15 mol%), Lösungsmittel, 190 °C, 24 h. ¹⁹F-NMR-Ausbeuten mit 1,4-Difluorbenzol als interner Standard. [a] Mit CyJohnPhos als *P*-Ligand.

Wie auch in den vorhergehenden Studien bei 190 °C erwies sich eine 1:1 Mischung aus NMP und Mesitylen im Vergleich zu anderen Kombinationen aus NMP, Chinolin und Mesitylen oder reinem NMP beziehungsweise Chinolin als besonders geeignet (Einträge 1–5). Als Nebenprodukt wurde das aus der Homokupplung von **5.2.5-2** resultierende Biaryl erhalten, dies in allen Fällen jedoch in Ausbeuten von ≤ 5%. Qualitative GC/GC-MS-Analysen zeigten weiterhin, dass auch in diesen Fällen das unerwünschte Arylierungsprodukt, welches aus der C–P-Bindungsspaltung des Phosphans resultiert, gebildet wird. Daraufhin wurde PPh₃ durch CyJohnPhos ersetzt. In dieser Reaktion ließ sich eine zu PPh₃ vergleichbare Ausbeute erzielen (Eintrag 5), während keinerlei Nebenprodukte aus der Reaktion des Liganden mit dem Substrat

detektiert wurden. Dies steht im Einklang mit den Beobachtungen, die mit diesem Liganden in den Studien in Abschnitt 5.2.3 gemacht wurden. Da sich **5.2.5-1** selbst im optimalen Lösungsmittelgemisch bei 190 °C nicht vollständig löste, wurde die Lösungsmittelmenge erhöht, was allerdings keine Auswirkung auf die Ausbeute hatte (Eintrag 6). Eine Verringerung der Lösungsmittelmenge führte hingegen zu einer schlechteren Ausbeute (Eintrag 7). Auch bei 170 °C wurde eine nur geringe Menge an **5.2.5-3** detektiert (Eintrag 8), sodass für die weiteren Untersuchungen die Reaktionstemperatur von 190 °C beibehalten wurde.

Eine Variation der Palladium-Vorstufe zeigte, dass mit Ausnahme von PdI₂, Pd(OAc)₂ und Pd(F₆-acac)₂, die zu geringeren Umsätzen führten, alle übrigen Palladium-Quellen ähnliche Resultate liefern (Tabelle 18). Lediglich mit Pd(COD)Cl₂ konnte auch in diesem Fall die Ausbeute leicht gesteigert werden, sodass das gewünschte Produkt in 52% detektiert wurde (Eintrag 4). Ein Experiment in der Labormikrowelle zeigte weiterhin, dass sich unter diesen Bedingungen eine Ausbeute von 45% bei einer Reaktionszeit von 1 h erzielen lässt.

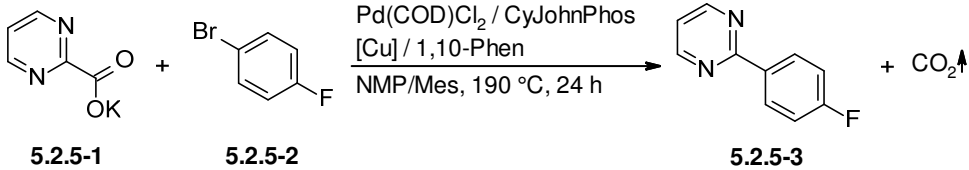
Tabelle 18: Variation der Palladium-Quelle.

Eintrag	[Pd]	5.2.5-3 (%)
1	PdCl ₂	40
2	PdBr ₂	40
3	PdI ₂	26
4	Pd(COD)Cl ₂	52 / 45 ^[a]
5	Pd(OAc) ₂	21
6	White-Katalysator	41
7	Pd(acac) ₂	36
8	Pd(TFA) ₂	38
9	Pd(F ₆ -acac) ₂	28

Reaktionsbedingungen: **5.2.5-1** (0.5 mmol), **5.2.5-2** (1.0 mmol), Cu₂O (5 mol%), 1,10-Phen (10 mol%), [Pd] (5 mol%), CyJohnPhos (15 mol%), NMP/Mes (1:1, 2 mL), 190 °C, 24 h. ¹⁹F-NMR-Ausbeuten mit 1,4-Difluorbenzol als interner Standard. [a] Reaktionsführung in der Labormikrowelle, 50 °C (5 min) → 190 °C (1 h).

Weitere Experimente brachten hervor, dass sich neben Cu₂O auch Kupfer(I)-halogenide in der vorliegenden Transformation anwenden lassen (Tabelle 19). Dabei zeigte CuI die höchste Aktivität (Eintrag 4) und lieferte eine Ausbeute von 58%.

Tabelle 19: Variation der Kupfer-Quelle.

		
5.2.5-1	5.2.5-2	5.2.5-3
Eintrag	[Cu]	5.2.5-3 (%)
1	Cu ₂ O	52
2	CuCl	45
3	CuBr	46
4	CuI	58

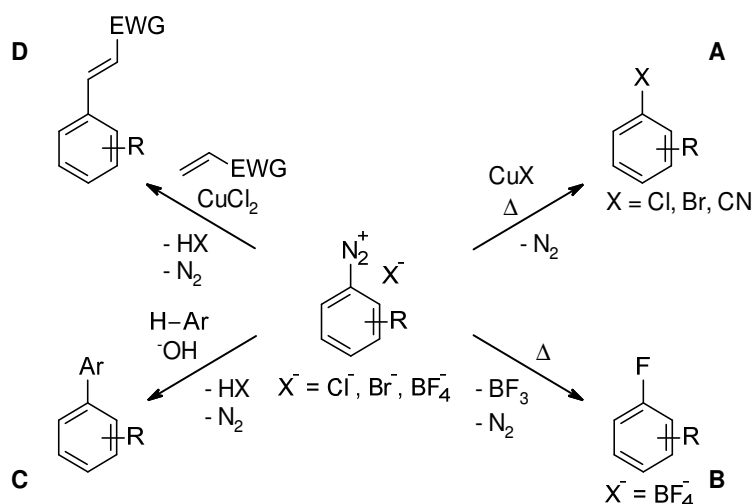
Reaktionsbedingungen: **5.2.5-1** (0.5 mmol), **5.2.5-2** (1.0 mmol), [Cu] (5 mol%), 1,10-Phen (10 mol%), Pd(COD)Cl₂ (5 mol%), CyJohnPhos (15 mol%), NMP/Mes (1:1, 2 mL), 190 °C, 24 h. ¹⁹F-NMR-Ausbeuten mit 1,4-Difluorbenzol als interner Standard.

Basierend auf diesen Ergebnissen könnte in zukünftigen Arbeiten der Einfluss von verschiedenen Liganden untersucht werden. Dies sollte weiterhin von Vergleichsexperimenten in der Labormikrowelle begleitet werden. Wenn es dadurch gelingen würde, auch zufriedenstellende Ausbeuten bei niedrigeren Temperaturen zu erhalten, könnte zudem ein breiteres Spektrum an Lösungsmitteln beziehungsweise Lösungsmittelgemischen getestet werden, in denen eine bessere Löslichkeit des Substrats gegebenenfalls gesteigerte Ausbeuten ermöglicht.

5.3 Iridium-katalysierte *ortho*-Arylierung mit Aryldiazoniumsalzen

5.3.1 Hintergrund

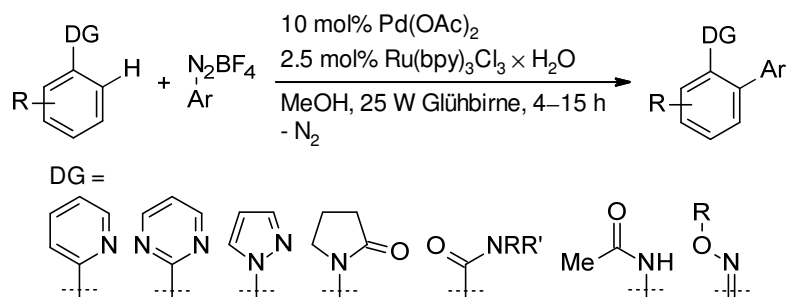
Aryldiazoniumsalze, die sich in großer struktureller Vielfalt ausgehend von kostengünstigen Anilinen darstellen lassen,^[173] sind bedeutende Substrate in der organischen Synthesechemie.^[173–176] Bekannte Namensreaktion, bei denen die Diazoniumsalze unter Extrusion von N₂ reagieren, gehen auf Entdeckungen Ende des 19. bis Mitte des 20. Jahrhunderts zurück (Schema 36).^[174] Dazu zählen beispielsweise die Sandmeyer-Reaktion (**A**)^[177,178] und die Balz-Schiemann-Reaktion (**B**).^[179] Reaktionen unter Funktionalisierung von C–H-Bindungen sind die Gomberg-Bachmann-Reaktion (**C**),^[180] als intramolekulare Variante bereits zuvor von Pschorr beschrieben,^[181] sowie die Meerwein-Arylierung (**D**).^[182]



Schema 36: Bekannte Namensreaktionen mit Aryldiazoniumsalzen.

Insbesondere im Hinblick auf die Arylierungen haben die letzten Jahrzehnte eine Vielzahl moderner Varianten dieser Reaktionen, beispielsweise unter Verwendung photokatalytischer Methoden, hervorgebracht.^[175,183–188] Daneben werden Aryldiazoniumsalze auch als Substrate in Übergangsmetall-katalysierten Kupplungsreaktionen verwendet.^[189] Dabei können die dediazotierenden Reaktionen der Aryldiazoniumsalze sowohl auf einer homolytischen als auch auf einer heterolytischen Bindungsspaltung beruhen.^[175,190] Damit dienen sie als Quelle für Arylradikale oder Arylkationen und bieten eine Alternative zu Arylhalogeniden sowie -sulfonaten.^[175,189] Sie ermöglichen weiterhin eine Reaktionsführung unter vergleichsweise milden Reaktionsbedingungen und gewährleisten eine hohe Chemo Selektivität der Kupplung.^[175]

Aufgrund der genannten Eigenschaften stellen Aryldiazoniumsalze auch attraktive Substrate für dirigierte *ortho*-C–H-Arylierungen dar. Pionierarbeiten auf diesem Gebiet wurden von der Gruppe um Sanford geleistet, die Aryldiazoniumsalze in Palladium/Ruthenium-katalysierten Photoredox-*ortho*-Arylierungen mit Stickstoff- und/oder Sauerstoff-basierten dirigierenden Gruppen umsetzten (Schema 37).^[191,192] Dabei sind die Produkte unter äußerst milden Bedingungen in guten bis sehr guten Ausbeuten zugänglich. Nachteilig an diesem Verfahren ist, dass ein vierfacher Überschuss an Diazoniumsalz benötigt wird.

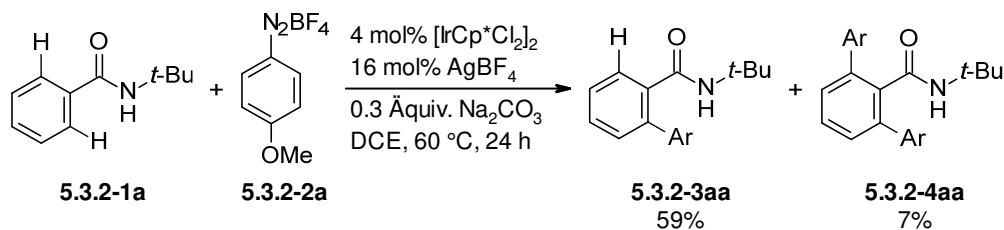


Schema 37: Photoredox-*ortho*-Arylierung mit Diazoniumsalzen.

Besonders im Hinblick auf die *ortho*-Arylierung von Benzoesäuren wäre eine Variante mit Aryldiazoniumsalzen als Kupplungspartner synthetisch wertvoll. So würde eine Alternative zu den bisher beschriebenen Kupplungen mit Arylhalogeniden, Arylboronsäuren beziehungsweise -boronaten oder (Hetero-)Arenen, die häufig bei hohen Temperaturen ablaufen und oftmals den Einsatz stöchiometrischer Mengen an Silbersalzen und/oder Oxidationsmitteln erfordern, geschaffen werden.^[33,39]

5.3.2 Amid-dirigierte *ortho*-Arylierung

Ausgangspunkt der Arbeiten war die Entdeckung von Herrn Dr. Liangbin Huang, dass sich Benzoessäure-*tert*-butylamid (**5.3.2-1a**) mit 4-Methoxybenzoldiazoniumtetrafluorborat (**5.3.2-2a**) in Gegenwart eines Iridium/Silber-basierten Katalysators, ein System welches in ähnlicher Form für *ortho*-Amidierungen mit Aziden unter Extrusion von N₂ beschrieben wurde,^[193–195] *ortho*-arylieren lässt. Dabei wurde eine Ausbeute von 59% des monoarylierten Produkts **5.3.2-3aa** neben 7% des diarylierten Derivats **5.3.2-4aa** erhalten (Schema 38 und Tabelle 20, Eintrag 1).



Schema 38: Iridium-katalysierte Amid-dirigierte *ortho*-Arylierung mit Diazoniumsalzen.

Im Vergleich dazu war das in den Arbeiten von Sanford beschriebene Katalysatorsystem basierend auf Palladium und Ruthenium für ähnliche Substrate weniger effizient. So wurden mit Benzamid sowie mit *N*-Methyl- und *N,N*-Dimethylbenzamid Ausbeuten von 25%, 38% beziehungsweise 8% erhalten.^[192]

Benzamide sind leicht aus Benzoesäuren und deren Derivaten zugänglich^[15] und eine effiziente *ortho*-Arylierung dieser Substrate mit Aryldiazoniumsalzen würde ebenso wie für den Fall der Benzoesäuren diskutiert eine willkommene Alternative zu bestehenden Verfahren darstellen.^[196–203] Daher wurde im Folgenden zunächst die Reaktion von **5.3.2-1a** mit **5.3.2-2a** näher untersucht und optimiert.

Basierend auf der Entdeckung von Herrn Huang wurden die nachfolgend diskutierten Optimierungsarbeiten eigenständig von mir durchgeführt.

Zu Beginn der Optimierungsarbeiten wurde ein Lösungsmittelscreening durchgeführt. Dieses zeigte, dass die Reaktion statt in DCE auch in DCM oder Aceton durchgeführt werden kann (Tabelle 20, Einträge 2 und 3), wobei im letzteren Fall geringe Mengen an Anisol (**5.3.2-5a**), welches aus der Protodediazotierung des Diazoniumsalzes resultiert, detektiert wurden. Die übrigen getesteten Lösungsmittel erwiesen sich allesamt als ineffizient und führten in den meisten Fällen lediglich zu einer gesteigerten Protodediazotierung von **5.3.2-2a** (Einträge 4–9). Da halogenierte Lösungsmittel aus ökologischer Sicht bedenklich sind,^[204,205] wurden die folgenden Studien mit Aceton als Solvens durchgeführt. Weitere Experimente zeigten, dass die Lösungsmittelmenge einen entscheidenden Einfluss auf die Produktausbeute hat. So wurden mit 2 mL statt 1 mL Aceton lediglich 26% **5.3.2-3aa** neben 30% **5.3.2-5a** erhalten (Eintrag 10). Weiterhin wurde in einem Kontrollexperiment bei 50 °C nur eine geringe Menge an **5.3.2-3aa** detektiert (Eintrag 11). Da das Lösungsmittel der Wahl keine Reaktionsführung bei höheren Temperaturen zulässt, wurde die Reaktionstemperatur von 60 °C beibehalten.

Tabelle 20: Lösungsmittelscreening für die ortho-Arylierung von tert-Butylbenzamid.

5.3.2-1a	5.3.2-2a	5.3.2-3aa	5.3.2-4aa	5.3.2-5a
Eintrag	Lösungsmittel	5.3.2-3aa (%)	5.3.2-4aa (%)	5.3.2-5a (%)
1 ^[a]	DCE	59	7	n.d.
2	DCM	60	9	n.d.
3	Aceton	58	8	9
4	MeCN	Spuren	n.d.	16
5	DMF	"	"	99
6	THF	"	"	88
7	Tol	"	"	Spuren
8	MeOH	"	"	76
9	H ₂ O	"	"	5
10 ^[b]	Aceton	26	Spuren	30
11 ^[c]	"	6	n.d.	21

Reaktionsbedingungen: **5.3.2-1a** (0.5 mmol), **5.3.2-2a** (0.5 mmol), [IrCp*Cl₂]₂ (4 mol%), AgBF₄ (16 mol%), Na₂CO₃ (0.3 Äquiv.), Lösungsmittel (1 mL), 60 °C, 16 h. GC-Ausbeuten mit *n*-Tetradecan als interner Standard. [a] Mit 0.5 Äquiv. Base wurden unter diesen Bedingungen 63% **5.3.2-3aa** und 15% **5.3.2-4aa** und mit 0.2 Äquiv. Base 52% **5.3.2-3aa** und 5% **5.3.2-4aa** detektiert. [b] 2 mL Aceton. [c] 50 °C.

Nachfolgend wurde die Katalysatorbeladung variiert. Dies zeigte, dass die Menge an [IrCp*Cl₂]₂ und AgBF₄ problemlos auf 3 mol% und 12 mol% reduziert werden kann (Tabelle 21, Eintrag 2). Zudem konnte die Ausbeute mit AgOTf anstelle von AgBF₄ leicht gesteigert werden (Eintrag 6). Die gebildete Menge an **5.3.2-4aa** blieb dabei nahezu unverändert. Während ähnliche Resultate auch mit AgSbF₆ erzielt werden konnten (Eintrag 4), erwiesen sich die übrigen Silbersalze als ineffizient (Einträge 5, 7 und 8).

Tabelle 21: Variation der Katalysatorbeladung und der Silber-Quelle.

5.3.2-1a	5.3.2-2a	5.3.2-3aa	5.3.2-4aa	5.3.2-5a
Eintrag	[Ag]	5.3.2-3aa (%)	5.3.2-4aa (%)	5.3.2-5a (%)
1 ^[a]	AgBF ₄	58	8	9
2	"	64	10	4
3 ^[b]	"	12	n.d.	34
4	AgSbF ₆	67	7	5
5	AgPF ₆	12	n.d.	34
6	AgOTf	70	11	4
7	AgOAc	Spuren	n.d.	42
8	Ag ₂ CO ₃	6	n.d.	37

Reaktionsbedingungen: **5.3.2-1a** (0.5 mmol), **5.3.2-2a** (0.5 mmol), [IrCp*Cl₂]₂ (3 mol%), [Ag] (12 mol%), Na₂CO₃ (0.3 Äquiv.), Aceton (1 mL), 60 °C, 16 h. GC-Ausbeuten mit *n*-Tetradecan als interner Standard. [a] [IrCp*Cl₂]₂ (4 mol%), [Ag] (16 mol%). [b] [IrCp*Cl₂]₂ (2 mol%), [Ag] (8 mol%).

Basierend auf diesen Ergebnissen wurden schließlich verschiedene Basen in der Reaktion von **5.3.2-1a** mit **5.3.2-2a** getestet (Tabelle 22). Dabei zeigte sich, dass mit Na₂CO₃ und Li₂CO₃ ähnlich gute Ausbeuten zu erzielen sind (Einträge 1 und 2). K₂CO₃ und Cs₂CO₃ erwiesen sich als nicht geeignet für diese Transformation und führten lediglich zu mehr Protodediazotierung (Einträge 3 und 4), wohingegen mit CaCO₃ moderate Ausbeuten von 55% an **5.3.2-3aa** erreicht wurden (Eintrag 5). Acetat-, Fluorid- und Phosphatbasen zeigten ebenfalls nur mäßige Umsätze, wobei in Gegenwart von K₃PO₃ vergleichsweise viel Protodediazotierung zu beobachten war (Einträge 6–10).

Tabelle 22: Variation der Base.

Eintrag	Base	5.3.2-3aa (%)	5.3.2-4aa (%)	5.3.2-5a (%)
1	Na ₂ CO ₃	70	11	4
2	Li ₂ CO ₃	69	8	Spuren
3	K ₂ CO ₃	11	n.d.	25
4	Cs ₂ CO ₃	Spuren	n.d.	39
5	CaCO ₃	55	4	Spuren
6	NaOAc	43	n.d.	9
7	LiOAc	47	Spuren	9
8	LiF	35	n.d.	Spuren
9	CsF	44	Spuren	Spuren
10	K ₃ PO ₄	25	Spuren	39

Reaktionsbedingungen: **5.3.2-1a** (0.5 mmol), **5.3.2-2a** (0.5 mmol), [IrCp*Cl₂]₂ (3 mol%), AgOTf (12 mol%), Base (0.3 Äquiv.), Aceton (1 mL), 60 °C, 16 h. GC-Ausbeuten mit *n*-Tetradecan als interner Standard.

Die Ausbeute konnte letztlich durch Erhöhung der Menge an AgOTf gesteigert werden. Dabei wurde das gewünschte Produkt **5.3.2-3aa** in 83% Ausbeute neben 7% des diarylierten Benzamids **5.3.2-4aa** erhalten (Tabelle 23, Eintrag 3). Kontrollexperimente zeigten, dass sowohl Iridium als auch Silber für eine erfolgreiche Umsetzung anwesend sein müssen (Einträge 4 und 5).

Tabelle 23: Variation der Silber-Menge und Kontrollexperimente.

Eintrag	AgOTf (mol%)	5.3.2-3aa (%)	5.3.2-4aa (%)	5.3.2-5a (%)
1	12	70	11	4
2	20	80	9	n.d.
3	30	83	7	n.d.
4 ^[a]	-	n.d.	n.d.	n.d.
5 ^[b]	16	n.d.	n.d.	17

Reaktionsbedingungen: **5.3.2-1a** (0.5 mmol), **5.3.2-2a** (0.5 mmol), [IrCp*Cl₂]₂ (3 mol%), AgOTf, Na₂CO₃ (0.3 Äquiv.), Aceton (1 mL), 60 °C, 16 h. GC-Ausbeuten mit *n*-Tetradecan als interner Standard. [a] [IrCp*Cl₂]₂ (4 mol%). [b] Ohne [IrCp*Cl₂]₂, AgBF₄ statt AgOTf.

In weiteren Kontrollexperimenten wurde überprüft, ob die hier gezeigte *ortho*-Arylierung auch durch andere Übergangsmetall-Katalysatoren vermittelt werden kann (Tabelle 24). Dabei erwiesen sich jedoch mit Ausnahme des bisher verwendeten [IrCp*Cl₂]₂ alle Katalysatoren als inaktiv.

Tabelle 24: Überprüfung anderer Übergangsmetall-Katalysatoren.

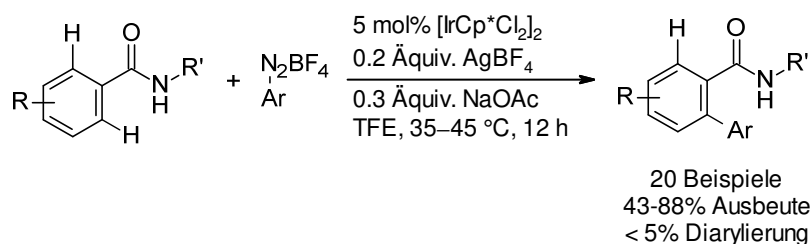
Eintrag	[M]	5.3.2-3aa (%)	5.3.2-4aa (%)	5.3.2-5a (%)
1	[IrCp*Cl ₂] ₂	70	11	4
2	Ir(COD)(acac)	Spuren	n.d.	28
3	[RhCp*Cl ₂] ₂	"	"	27
4	[Ru(<i>p</i> -cym)Cl ₂] ₂	"	"	41
5	Pd(OAc) ₂	"	"	32

Reaktionsbedingungen: **5.3.2-1a** (0.5 mmol), **5.3.2-2a** (0.5 mmol), [M] (3 mol%), AgOTf (12 mol%), Base (0.3 Äquiv.), Aceton (1 mL), 60 °C, 16 h. GC-Ausbeuten mit *n*-Tetradecan als interner Standard.

Zusammenfassend konnte im Rahmen der bis dahin durchgeführten Optimierungsarbeiten ein Katalysatorsystem bestehend aus $[\text{IrCp}^*\text{Cl}_2]_2$, AgOTf und Na_2CO_3 entwickelt werden, welches erfolgreich die *ortho*-Arylierung von Benzoessäure-*tert*-butylamid **5.3.2-1a** mit 4-Methoxybenzoldiazoniumtetrafluorborat **5.3.2-2a** vermittelt. Dabei sind Produktausbeuten von bis zu 83% möglich.

5.3.3 Alternative Iridium-katalysierte C-H-Arylierung von Benzamiden mit Aryldiazoniumsalzen

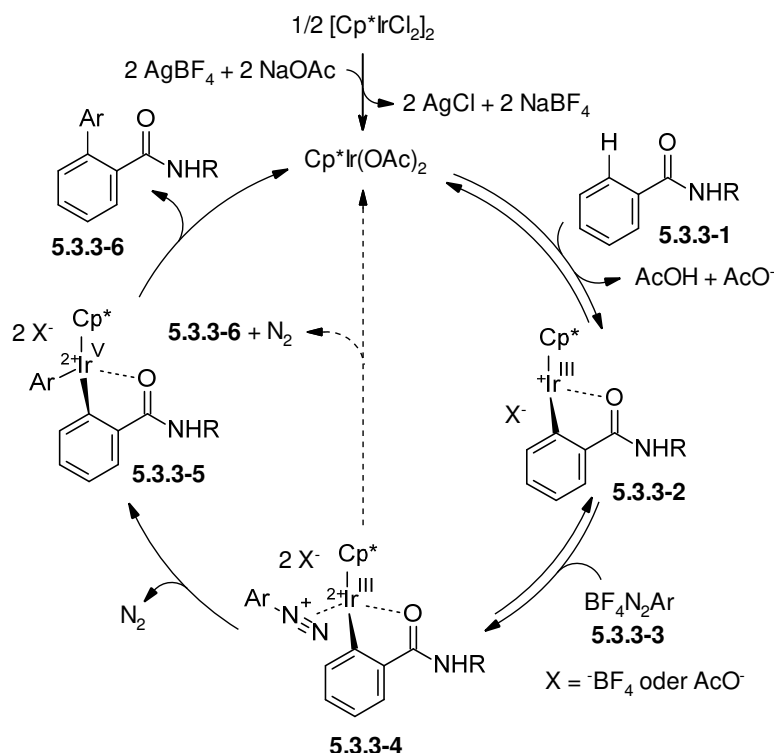
Gegen Ende der im vorigen Abschnitt diskutierten Optimierungsarbeiten wurde von Chang und Mitarbeitern ein Manuskript veröffentlicht, in dem ein ähnliches Protokoll für die Iridium-katalysierte *ortho*-Arylierung von Benzamiden mit Aryldiazoniumsalzen beschrieben wird (Schema 39).^[206] Dabei dient ebenfalls $[\text{IrCp}^*\text{Cl}_2]_2$ in Kombination mit AgBF_4 als Katalysator neben NaOAc als Base. Unter diesen Bedingungen lassen sich diverse Benzamide mit vorwiegend elektronenarmen Aryldiazoniumsalzen unter milden Bedingungen in guten Ausbeuten umsetzen.



Schema 39: *ortho*-Arylierung von Benzamiden mit Aryldiazoniumsalzen nach Chang et al.

Zwar lässt sich die Reaktion bei geringeren Reaktionstemperaturen durchführen, doch sind höhere Iridium-Katalysatorbeladungen und Trifluorethanol als Lösungsmittel notwendig. Während die Reaktion ebenfalls in DCE oder DCM durchführbar ist, war ein getestetes Katalysatorsystem in ökologisch unbedenklicherem Aceton interessanterweise inaktiv.^[206]

Basierend auf DFT-Rechnungen und experimentellen mechanistischen Studien schlugen die Autoren einen Reaktionsmechanismus vor, der in vereinfachter Form in Schema 40 dargestellt ist.^[206] Dieser sollte in ähnlicher Form für die im Rahmen der eigenen Arbeiten durchgeführte Transformation anzunehmen sein.

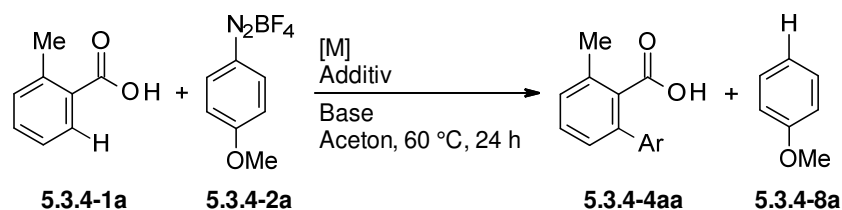


Schema 40: Vorgeschlagener Mechanismus für die *ortho*-Arylierung von Benzamiden mit Aryldiazoniumsalzen nach Chang et al.

Ausgehend von $[\text{IrCp}^*\text{Cl}_2]_2$ entsteht zunächst der aktive Katalysator $\text{Cp}^*\text{Ir}(\text{OAc})_2$. In einer konzertierten Deprotonierung und Metallierung wird anschließend die cyclometallierte Ir(III)-Spezies **5.3.3-2** gebildet. Eine side-on-Koordination des Diazoniumsalzes mit nachfolgender oxidativer Addition unter N_2 -Extrusion liefert schließlich eine Ir(V)-Spezies **5.3.3-5**. Dabei wird die Bildung letzterer als geschwindigkeitsbestimmend angenommen. Im abschließenden Schritt wird in einer reduktiven Eliminierung schließlich das Produkt **5.3.3-6** freigesetzt, wodurch sich der Katalysezyklus schließt. Ein alternativer Mechanismus, in dem die Produktbildung und -freisetzung konzertiert in einem redox-neutralen Schritt ausgehend von Komplex **5.3.3-4** erfolgen, wird von den Autoren allerdings nicht ausgeschlossen.^[206]

5.3.4 Carboxylat-dirigierte *ortho*-Arylierung

Nachfolgend wurde schließlich überprüft, ob sich das Konzept auch auf Benzoesäuren übertragen lässt. Um eine unerwünschte Diarylierung zu unterbinden, wurde 2-Methylbenzoesäure **5.3.4-1a** als Modells substrat gewählt. Zunächst wurde **5.3.4-1a** mit 4-Methoxybenzoldiazoniumtetrafluorborat **5.3.4-2a** in Gegenwart verschiedener Übergangsmetall-Katalysatoren und stöchiometrischer Mengen Ag_2CO_3 umgesetzt (Tabelle 25). Als Lösungsmittel wurde Aceton beibehalten.

Tabelle 25: Optimierung der *ortho*-Arylierung von Benzoesäuren mit Aryldiazoniumsalzen.


Eintrag	[M]	Additiv (Äquiv.)	Base (Äquiv.)	5.3.4-4aa (%)	5.3.4-8a (%)
1	[RhCp*Cl ₂] ₂	Ag ₂ CO ₃ (1)	-	n.d.	18
2 ^[a]	Pd(OAc) ₂	"	-	n.d.	14
3	[Ru(<i>p</i> -cym)Cl ₂] ₂	"	-	n.d.	20
4	[IrCp*Cl ₂] ₂	"	-	80	n.d.
5	"	Ag ₂ CO ₃ (0.5)	-	74	"
6	"	Ag ₂ CO ₃ (0.3)	-	55	"
7	"	Ag ₂ CO ₃ (0.15)	-	21	"
8	"	"	Li ₂ CO ₃ (1)	74	"
9	"	"	Li ₂ CO ₃ (0.5)	82 (83)	"
10	"	"	Li ₂ CO ₃ (0.3)	76	"
11	"	"	Li ₂ CO ₃ (0.15)	50	"
12 ^[b]	"	"	Li ₂ CO ₃ (0.5)	59	"
13 ^[c]	"	"	"	24	16

Reaktionsbedingungen: **5.3.4-1a** (0.5 mmol), **5.3.4-2a** (0.5 mmol), [M] (3 mol%), Additiv, Base, Aceton (1 mL), 60 °C, 24 h. GC-Ausbeuten nach Veresterung mit K₂CO₃ (2 Äquiv.) und MeI (5 Äquiv.) in MeCN und *n*-Tetradecan als interner Standard. Isolierte Ausbeuten in Klammern. [a] [M] (6 mol%). [b] [M] (2 mol%). [c] [M] (1 mol%).

In Übereinstimmung mit den vorhergehenden Studien zur *ortho*-Arylierung von *N*-tert-Butylbenzamid, war unter den getesteten Katalysatoren nur [IrCp*Cl₂]₂ aktiv in dieser Transformation und lieferte das gewünschte Produkt **5.3.4-4aa** bereits in 80% Ausbeute (Einträge 1–4). Weitere Untersuchungen zeigten, dass die Menge an Ag₂CO₃ auf nur 0.15 Äquiv. reduziert werden kann, wenn zusätzlich eine Carbonatbase zugesetzt wird (Einträge 5–11). Allerdings ist die Wahl von Li₂CO₃ als Base entscheidend. So konnten mit anderen Alkalimetallcarbonaten nur geringe Umsätze erzielt werden (siehe hierzu auch Tabelle 26, Einträge 8–11). Das beste Resultat ließ sich mit 3 mol% [IrCp*Cl₂]₂, 0.15 Äquiv. Ag₂CO₃ und 0.5 Äquiv. Li₂CO₃ erzielen. Dabei konnte das Produkt in 83% Ausbeute isoliert

werden (Eintrag 9). Weitere Experimente zeigten, dass in Gegenwart von 2 mol% des Iridium-Katalysators eine noch moderate Ausbeute erhalten werden kann (Eintrag 12), während mit 1 mol% des Katalysators nur noch ein geringer Umsatz zu verzeichnen war (Eintrag 13). Als einziges Nebenprodukt wurde Anisol **5.3.4-8a**, welches aus der Protodediazotierung des Diazoniumsalzes resultiert, neben nicht umgesetzter Benzoesäure **5.3.4-1a** in Form des Methylesters detektiert.

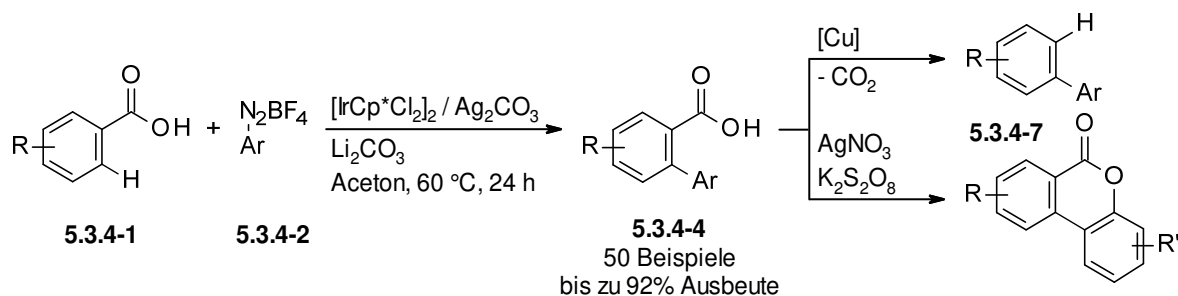
Tabelle 26: Variation der Silber-Quelle und der Base.

	5.3.4-1a	5.3.4-2a	5.3.4-4aa	5.3.4-8a
Eintrag	Additiv	Base	5.3.4-4aa (%)	5.3.4-8a (%)
1	Ag ₂ CO ₃	Li ₂ CO ₃	76	n.d.
2 ^[a]	AgOAc	"	71	Spuren
3 ^[a]	AgOTf	"	64	"
4 ^[a]	AgPF ₆	"	50	"
5 ^[a]	AgSbF ₆	"	64	"
6 ^[a]	AgF	"	59	"
7 ^[a]	AgBF ₄	"	62	"
8 ^[b]	Ag ₂ CO ₃	Na ₂ CO ₃	4	47
9		K ₂ CO ₃	6	34
10	"	Cs ₂ CO ₃	Spuren	37
11	"	CaCO ₃	33	19
12	"	NaOAc	Spuren	34
13	"	LiOAc	21	29
14	"	LiF	25	35
15	"	CsF	Spuren	31
16	"	K ₃ PO ₄	19	33

Reaktionsbedingungen: **5.3.4-1a** (0.5 mmol), **5.3.4-2a** (0.5 mmol), [IrCp*Cl₂]₂ (3 mol%), Additiv (0.15 Äquiv.), Base (0.3 Äquiv.), Aceton (1 mL), 60 °C, 24 h. GC-Ausbeuten nach Veresterung mit K₂CO₃ (2 Äquiv.) und MeI (5 Äquiv.) in MeCN und *n*-Tetradecan als interner Standard. [a] Additiv (0.3 Äquiv.). [b] Base (0.5 Äquiv.).

Im Rahmen dieser Arbeiten wurde weiterhin eine Variation der Silber-Quelle und der Base durchgeführt (Tabelle 26). Dabei zeigte sich, dass mit AgOAc ähnlich gute Resultate wie mit Ag₂CO₃ erzielt werden können, während bei den übrigen Silbersalzen etwas geringere Ausbeuten zu verzeichnen waren (Einträge 1–7). Wie bereits diskutiert, waren andere Carbonate als Li₂CO₃ ineffizient in dieser Transformation (Einträge 8–11). Ebenso wurden in Gegenwart von Acetat-, Fluorid- oder Phosphatbasen nur geringe Ausbeuten erzielt (Einträge 12–16) und es war deutlich mehr Protodediazotierung zu verzeichnen.

Zusammenfassend wurde somit ein Katalysatorsystem bestehend aus [IrCp*Cl₂]₂ und Ag₂CO₃ mit Li₂CO₃ als Base entwickelt, welches die *ortho*-Arylierung von Benzoesäuren mit Aryldiazoniumsalzen unter milden Reaktionsbedingungen ermöglicht (Schema 41).



Schema 41: Iridium-katalysierte *ortho*-Arylierung von Benzoesäuren mit Aryldiazoniumsalzen.

Die Anwendbarkeit dieses Protokolls wurde nachfolgend anhand der Synthese einer Vielzahl divers funktionalisierter Biaryl-2-carboxylate in guten bis sehr guten Ausbeuten demonstriert. Daneben war es möglich, das Protokoll mit einer Protodecarboxylierung bzw. mit einer oxidativen Zyklisierung zu praktischen Eintopf-Verfahren zu kombinieren.

Beiträge der Autoren: Die Bearbeitung dieses Projekts erfolgte zusammen mit Herrn Dr. Liangbin Huang, der die vorliegende Reaktion entdeckte. Die Katalysatoroptimierung wurden größtenteils von mir durchgeführt. Herr Huang und ich untersuchten die Anwendungsbreite gleichberechtigt und realisierten ebenso die Eintopf-Verfahren. Während Herr Huang das im Anschluss an die Publikation diskutierte Konkurrenzexperiment mit dem Arylketon durchführte, erfolgten die Studien zu den Konkurrenzexperimenten mit dem Benzamid durch mich. Das Manuskript verfasste Herr Huang und überarbeitete es zusammen mit Herrn Prof. Dr. L. J. Gooßen. Herr Huang und ich werteten die analytischen Daten aus und erstellten die „Supporting Information“ gemeinsam.

Eine Zusammenfassung der Katalysatoroptimierung und weitere Kontrollexperimente, die Untersuchungen zur Anwendungsbreite sowie die Eintopf-Verfahren werden in der nachfolgenden Publikation diskutiert. Diese wurde in *Angewandte Chemie* veröffentlicht, für die vorliegende Arbeit angepasst und mit Erlaubnis des Verlags beigelegt:

"Reprinted (adapted) with permission from L. Huang, D. Hackenberger, L. J. Gooßen, *Angew. Chem. Int. Ed.* **2015**, 54, 12607–12611: *Iridium-Catalyzed ortho-Arylation of Benzoic Acids with Arenediazonium Salts*. Copyright 2015 WILEY-VCH Verlag GmbH & Co. KGaA, Weinheim."

JOHN WILEY AND SONS LICENSE TERMS AND CONDITIONS

This Agreement between Ms. Dagmar Hackenberger ("You") and John Wiley and Sons ("John Wiley and Sons") consists of your license details and the terms and conditions provided by John Wiley and Sons and Copyright Clearance Center.

License Number	4116360263550
License date	May 26, 2017
Licensed Content Publisher	John Wiley and Sons
Licensed Content Publication	Angewandte Chemie International Edition
Licensed Content Title	Iridium-Catalyzed ortho-Arylation of Benzoic Acids with Arenediazonium Salts
Licensed Content Author	Liangbin Huang, Dagmar Hackenberger, Lukas J. Gooßen
Licensed Content Date	Sep 3, 2015
Licensed Content Pages	5
Type of use	Dissertation/Thesis
Requestor type	Author of this Wiley article
Format	Print and electronic
Portion	Full article
Will you be translating?	No

C–H Activation

International Edition: DOI: 10.1002/anie.201505769
German Edition: DOI: 10.1002/ange.201505769

Iridium-Catalyzed *ortho*-Arylation of Benzoic Acids with Arenediazonium Salts

Liangbin Huang, Dagmar Hackenberger, and Lukas J. Goossen*

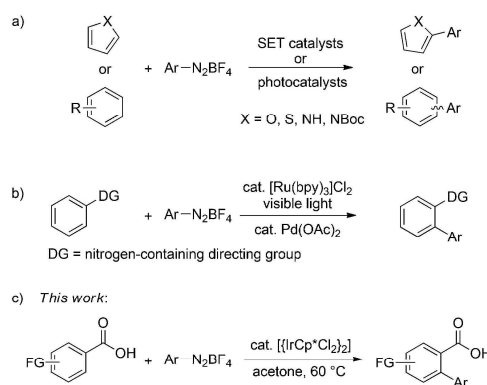
Abstract: In the presence of catalytic $[\text{IrCp}^*\text{Cl}_2]_2$ and Ag_2CO_3 , Li_2CO_3 as the base, and acetone as the solvent, benzoic acids react with arenediazonium salts to give the corresponding diaryl-2-carboxylates under mild conditions. This C–H arylation process is generally applicable to diversely substituted substrates, ranging from extremely electron-rich to electron-poor derivatives. The carboxylate directing group is widely available and can be removed tracelessly or employed for further derivatization. Orthogonality to halide-based cross-couplings is achieved by the use of diazonium salts, which can be coupled even in the presence of iodo substituents.

The design of efficient synthetic routes to construct biaryls is of great importance due to the prevalence of this structural unit in pharmaceuticals, agrochemicals, and functional materials.^[1] Established methods to access this substructure include the Ullmann reaction, catalytic cross-couplings of preformed organometallic reagents, and decarboxylative couplings.^[2,3]

C–H Arylating reactions have been studied extensively as an alternative to these intrinsically regioselective couplings since in principle, they do not require prefunctionalization steps. The regioselectivity of the C–H arylation can be controlled by various directing groups.^[4] However, these often need to be introduced and later removed in additional reaction steps, increasing the complexity of the overall synthetic sequence.

The use of carboxylates as directing groups represents a tremendous advance in this area.^[5] Benzoic acids are widely available in great structural diversity, and after *ortho*-arylation, the carboxylate group can be removed tracelessly,^[6] or converted into other functionalities via decarboxylative cross-couplings.^[7] However, the low coordinating ability of this group poses substantial challenges with regard to the reactivity and selectivity of the C–H activating step. Substantial progress in this field has been made by the groups of Yu,^[8] Daugulis,^[9] Larrosa,^[6d,f,10] Su,^[6g] and others,^[6h,11] who developed transformations based on aryl halides, arylboronic acids, and (hetero)arenes as the aryl sources. The limitations of these approaches are the high reaction temperatures, the cost of the substrates, the restriction to specific substrates and substitution patterns, and the use of stoichiometric silver salts as halide scavengers and/or oxidants.

We believe that this field could benefit significantly from the use of arenediazonium salts as aryl electrophiles, because these are readily available from low-cost anilines in great structural diversity, and their intrinsic reactivity is high even at low temperatures.^[12] The use of diazonium salts in C–H arylating reactions was pioneered by Pschorr^[13] and Gomberg and Bachmann.^[14] Modern versions of such nondirected (hetero)arylations were reported by the groups of Heinrich, König, Felpin, and Martín, respectively (Scheme 1 a).^[15] The



Scheme 1. Direct C–H arylation of (hetero)arenes with arenediazonium salts.

only *ortho*-directed arylations were disclosed by Sanford, who used pyridine and other nitrogen-based directing groups in a photoredox/palladium-catalyzed reaction (Scheme 1 b).^[16] and Chang and co-workers, who employed *tert*-butyl amides to arylate electron-poor arenediazonium salts.^[17]

In order to probe whether a C–H arylation of benzoic acids with arenediazonium salts could be directed into the *ortho* position of the weakly coordinating carboxylate group, we treated 2-methylbenzoic acid (**1a**) with 4-methoxybenzenediazonium tetrafluoroborate (**2a**) (Table 1).^[18] At the desired low reaction temperature of 60 °C, many state-of-the-art catalysts widely employed in *ortho*-arylations, including $[\text{RhCp}^*\text{Cl}_2]_2$,^[19] $\text{Pd}(\text{OAc})_2$,^[8,9] and $[\text{Ru}(p\text{-cym})\text{Cl}_2]_2$,^[20] were inactive in this challenging transformation (entries 1–3).^[4] $[\text{IrCp}^*\text{Cl}_2]_2/\text{Ag}_2\text{CO}_3$, a system similar to that employed in C–H aminations, alkenylation, and alkynylations,^[21] was the only catalyst to give the desired 2-arylbenzoic acid **3**. After some optimization, we managed to achieve high yields even with the ecofriendly solvent acetone (entry 4), which sets this apart from many other C–H activating reactions that

[*] Dr. L. Huang, D. Hackenberger, Prof. Dr. L. J. Goossen
FB Chemie-Organische Chemie
Technische Universität Kaiserslautern
Erwin-Schrödinger-Strasse Geb. 54, 67663 Kaiserslautern (Germany)
E-mail: goossen@chemie.uni-kl.de

Supporting information for this article is available on the WWW under <http://dx.doi.org/10.1002/anie.201505769>.

Table 1: Optimization of the *ortho*-arylation conditions.^[a]

Entry	Catalyst	Additive (equiv)	Base (equiv)	Yield [%] ^[b]
1	{[RhCp*Cl ₂] ₂ }	Ag ₂ CO ₃ (1.0)	–	n.d.
2	Pd(OAc) ₂	Ag ₂ CO ₃ (1.0)	–	n.d.
3	{[Ru(<i>p</i> -cym)Cl ₂] ₂ }	Ag ₂ CO ₃ (1.0)	–	n.d.
4	{[IrCp*Cl ₂] ₂ }	Ag ₂ CO ₃ (1.0)	–	80
5	{[IrCp*Cl ₂] ₂ }	Ag ₂ CO ₃ (0.15)	–	21
6	{[IrCp*Cl ₂] ₂ }	Ag ₂ CO ₃ (0.15)	Li ₂ CO ₃ (1.0)	74
7	{[IrCp*Cl ₂] ₂ }	Ag ₂ CO ₃ (0.15)	Li ₂ CO ₃ (0.5)	82 (83)
8	{[IrCp*Cl ₂] ₂ }	Ag ₂ CO ₃ (0.15)	Li ₂ CO ₃ (0.3)	76
9	{[IrCp*Cl ₂] ₂ }	–	Li ₂ CO ₃ (0.5)	n.d.
10	{[IrCp*Cl ₂] ₂ }	Tl ₂ CO ₃ (0.15)	Li ₂ CO ₃ (0.5)	10
11	–	Ag ₂ CO ₃ (0.15)	Li ₂ CO ₃ (0.5)	n.d.
12	[Ir(cod)(acac)]	Ag ₂ CO ₃ (0.15)	Li ₂ CO ₃ (0.5)	n.d.
13 ^[c]	{[IrCp*Cl ₂] ₂ }	Ag ₂ CO ₃ (0.15)	Li ₂ CO ₃ (0.5)	73
14 ^[d]	{[IrCp*Cl ₂] ₂ }	Ag ₂ CO ₃ (0.15)	Li ₂ CO ₃ (0.5)	78 (83)

[a] Reaction conditions: **1a** (0.5 mmol), **2a** (0.5 mmol), catalyst (3 mol %), Ag₂CO₃, base, and 1 mL acetone, 60 °C, 24 h. [b] GC yields after esterification with K₂CO₃ (2 equiv) and MeI (5 equiv) in MeCN with tetradecane as the internal standard; yields of isolated products are given in parentheses. [c] 0.6 mmol **1a**. [d] **2a** 0.6 mmol.

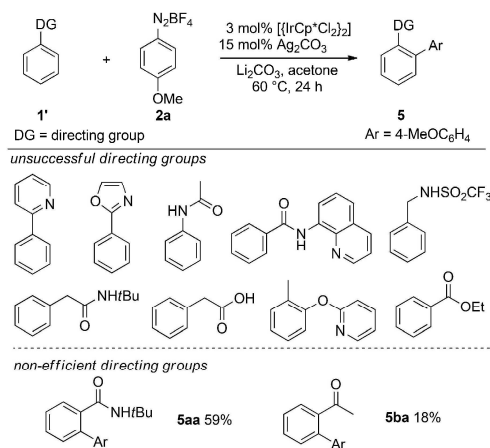
are restricted to ecologically questionable halogenated solvents such as DCE and HFIP.^[17,21c–f,h,i]

The amount of silver carbonate can be reduced to catalytic quantities if another carbonate base is added (entries 5–8). In this context, Li₂CO₃ is particularly effective. Some silver is required to open up coordination sites at the iridium by removing coordinated chloride, and in its absence, no product is formed. Interestingly, the reaction did not proceed well when thallium carbonate was used as a halide abstractor, indicating that the role of the silver might be more complex (entries 9 and 10). No reaction occurred with iridium(I) complexes (entry 12).^[22]

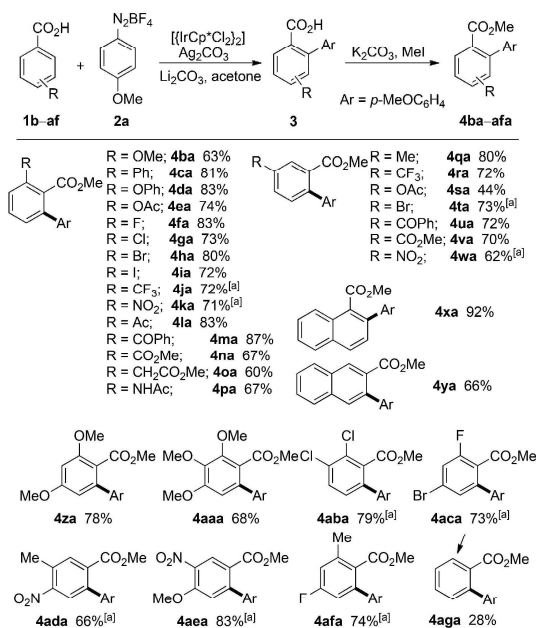
Substrates **1a** and **2a** are best employed in a 1:1 ratio. Excess diazonium salt does not improve the yields, and excess benzoic acid slightly lowers the yield (entries 13 and 14).

Under these optimal conditions, the free carboxylate is not only the simplest and thus most desirable, but also the most effective directing group. Other widely employed, but more complex directing groups were found to be inactive in this context. These include methylene carboxylates and amides and even the strongly coordinating pyridine, NHAc, and Daugulis amide groups (Scheme 2). Weakly coordinating groups such as carboxamides and ketones gave low to moderate yields. This is in agreement with a report by Chang et al.,^[17] which appeared recently. Their arylation of benzoic acid *tert*-butyl amides remained limited to certain electron-deficient diazonium salts, even though fluorinated solvents and higher iridium catalyst loadings were used.

Regioselective monoarylation occurs for *meta*-substituted benzoic acids selectively at the less hindered *ortho*-position (**4qa–wa**, Scheme 3). Various functional groups are tolerated

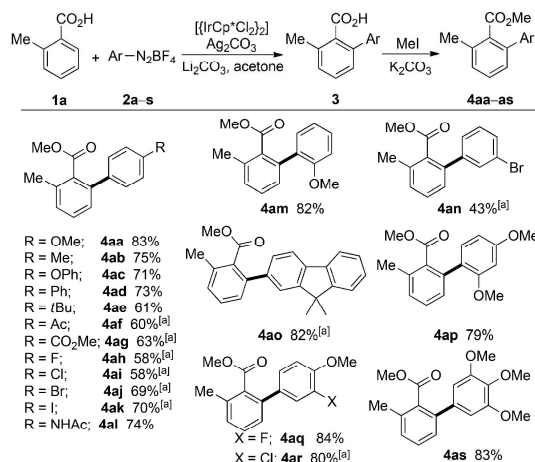


Scheme 2. Screening of other directing groups for the selective *ortho*-arylation with diazonium salts. Reaction conditions: **1'** (0.5 mmol), **2a** (0.5 mmol), {[IrCp*Cl₂]₂} (3 mol %), Ag₂CO₃ (0.15 equiv), Li₂CO₃ (0.5 equiv), acetone (1 mL), 60 °C, 24 h. Yields of isolated products are given.



Scheme 3. Substrate scope of benzoic acids. Reaction conditions: **1b–af** (1 mmol), **2a** (1 mmol), {[IrCp*Cl₂]₂} (3 mol %), Ag₂CO₃ (0.15 equiv), Li₂CO₃ (0.5 equiv), acetone (2 mL), 60 °C, 24 h. Yields of isolated products are given. [a] AgOTf (0.2 equiv), AgOAc (0.3 equiv), Li₂CO₃ (0.3 equiv).

including methoxy, halo, ester, acyl, carboxylate, and even acetamino groups. The tolerance of the latter functionality is particularly remarkable and opens up opportunities for



Scheme 4. Direct C–H arylation of benzoic acid with various arenediazonium salts. Reaction conditions: **1a** (1 mmol), **2a–s** (1 mmol), $[\text{IrCp}^*\text{Cl}_2]_2$ (3 mol %), Ag_2CO_3 (0.15 equiv), Li_2CO_3 (0.5 equiv), acetone (2 mL), 60 °C, 24 h. Yields of isolated products are given. [a] AgOTf (0.2 equiv), AgOAc (0.3 equiv), Li_2CO_3 (0.3 equiv).

orthogonal difunctionalizations, since acetamido groups are powerful directing groups in combination with other catalysts.^[16] The tolerance of bromo and iodo groups demonstrates the orthogonality of the present transformation to traditional cross-coupling processes. Unsubstituted benzoic acid gives a nearly 1:1 ratio of mono- to di-arylation product (**4aga**). Interestingly, doubly *meta*-substituted benzoic acids show no conversion, illustrating how strongly steric factors influence this reaction. Cinnamic acid did not show any conversion to the C–H arylation product.^[17]

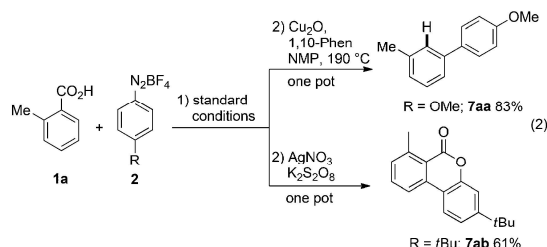
The reaction is also widely applicable with regard to the diazonium salt coupling partner (Scheme 4). *ortho*-Toluic acid was successfully coupled both with electron-rich and electron-deficient aromatic diazonium salts. A wealth of functional groups is tolerated in the *para*, *ortho*, or *meta* positions. Even reactive iodo substituents do not give rise to unwanted side products. Protodediazotization is the only significant side reaction occasionally observed. Unfortunately, heteroarene diazonium salts could not yet be converted.

Control experiments confirmed that aryl triflates, tosylates, and halides are inactive as carbon electrophiles under the reaction conditions. However, C–H arylation can alternatively be achieved with diaryliodonium salt electrophiles [Eq. (1)].

The products in Schemes 3 and 4 were converted into the corresponding esters to simplify chromatographic purification, but the carboxylic acid can also be isolated in unmodified form. Optional in situ protodecarboxylation directly

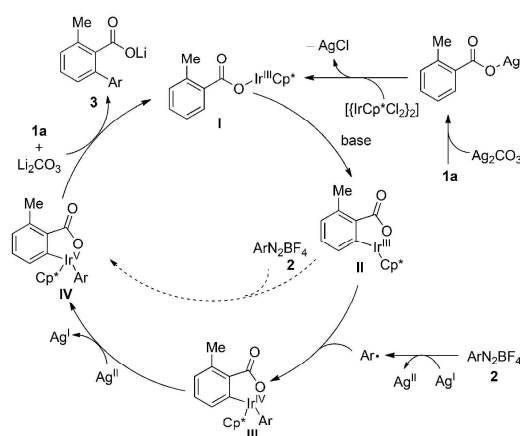


leads to the parent biaryl, whereas oxidative cyclization furnishes structurally interesting lactones [Eq. (2)].^[23] Both these reactions can be combined with the arylation in convenient one-pot protocols.



The addition of stoichiometric amounts of TEMPO as a radical scavenger shuts down the reaction, which suggests single-electron-transfer processes may be involved (see the Supporting Information).

A plausible catalytic cycle for this process is outlined in Scheme 5.^[17] The catalytically active species **I** is generated by replacing a chloride with a benzoate ligand at the Ir^{III} precursor. In the presence of the carbonate base, the cyclo-



Scheme 5. Proposed mechanism for Ir^{III}-catalyzed *ortho*-arylation of benzoic acids with arenediazonium salts.

metalated Ir^{III} complex **II** is likely to form and may be converted directly to the Ir^V species **IV** by oxidative addition of the diazonium salt. However, the oxidation of Cp*Ir^{III} complexes is known to be difficult via two-electron processes,^[24] so this may also be a stepwise process involving one-electron-transfer steps. This would explain the influence of the radical scavenger and the difference between silver and thallium cocatalysts.^[25] The biaryl product **3** is released via reductive elimination and salt metathesis with a benzoate substrate, regenerating the Ir^{III} species **I**. In-depth mechanistic studies are underway to fully clarify the reaction pathway.

In conclusion, the carboxylate-directed *ortho*-arylation of benzoic acids with arenediazonium salts allows the convenient synthesis of a wide variety of diaryl carboxylates under remarkably mild conditions. In the presence of a $\text{Cp}^*\text{Ir}^{\text{III}}$ catalyst, simple carboxylates are the most efficient directing groups, so that even substrates with functionalities that act as powerful directing groups with other catalysts selectively yield *ortho*-aryl benzoates. The carboxylate may then be utilized as a leaving group in various decarboxylative couplings. The use of diazonium salts as electrophiles, rare in C–H activations, makes this process orthogonal to aryl halide couplings.

Experimental Section

An oven-dried 20 mL vessel was charged with $[\text{IrCp}^*\text{Cl}_2]_2$ (23.9 mg, 0.03 mmol, 3 mol %), Ag_2CO_3 (41.2 mg, 0.15 mmol, 15 mol %), Li_2CO_3 (40 mg, 0.50 mmol, 50 mol %), the benzoic acid **1** (1 mmol), and the arenediazonium salt **2** (1 mmol). After the vessel had been flushed with three alternating vacuum and nitrogen purge cycles, degassed acetone (2 mL) was added via syringe. The resulting mixture was stirred at 60 °C for 24 h. After the reaction was complete, the mixture was allowed to cool to room temperature. MeCN (3 mL), K_2CO_3 (414 mg, 3 mmol), and MeI (310 μL , 5 mmol) were added and the mixture was stirred at 50 °C for another 2 h. The mixture was allowed to cool to room temperature. Brine (20 mL) was added and the resulting mixture was extracted with ethyl acetate (3×20 mL). The combined organic layers were dried over MgSO_4 and filtered, and the volatiles were removed under reduced pressure. The residue was purified by column chromatography (SiO_2 , ethyl acetate/hexane gradient) yielding the diarylbenzoic acid in the form of its methyl ester.

Acknowledgements

We thank Umicore for donating chemicals, the DFG (SFB/TRR-88, “3MET”), the Alexander von Humboldt Foundation (fellowship to L.H.), and the Stipendienstiftung Rheinland-Pfalz (fellowship to D.H.) for financial support.

Keywords: benzoic acid · biaryl synthesis · C–H arylation · diazonium salts · iridium

How to cite: *Angew. Chem. Int. Ed.* **2015**, *54*, 12607–12611
Angew. Chem. **2015**, *127*, 12798–12802

- [1] D. A. Horton, G. T. Bourne, M. L. Smythe, *Chem. Rev.* **2003**, *103*, 893–930.
- [2] a) *Synthesis of Biaryls* (Ed.: I. Cepanec), Elsevier Science, Oxford, **2004**, pp. 1–349; b) P. E. Fanta, *Chem. Rev.* **1946**, *38*, 139–196; c) G. Bringmann, R. Walter, R. Weirich, *Angew. Chem. Int. Ed. Engl.* **1990**, *29*, 977–991; *Angew. Chem.* **1990**, *102*, 1006–1019; d) C. C. Johansson Seechurn, M. O. Kitching, T. J. Colacot, V. Snieckus, *Angew. Chem. Int. Ed.* **2012**, *51*, 5062–5085; *Angew. Chem.* **2012**, *124*, 5150–5174; e) N. Miyaura, A. Suzuki, *Chem. Rev.* **1995**, *95*, 2457–2483; f) V. B. Phapale, D. J. Cárdenas, *Chem. Soc. Rev.* **2009**, *38*, 1598–1607; g) E. Negishi, *Acc. Chem. Res.* **1982**, *15*, 340–348; h) W. I. Dzik, P. P. Lange, L. J. Gooßen, *Chem. Sci.* **2012**, *3*, 2671–2678.
- [3] Selected references for biaryl formation: a) C.-L. Sun, Z.-J. Shi, *Chem. Rev.* **2014**, *114*, 9219–9280; b) L. T. Ball, G. C. Lloyd-Jones, C. A. Russell, *Science* **2012**, *337*, 1644–1648.
- [4] a) L. Ackermann, R. Vicente, A. R. Kapdi, *Angew. Chem. Int. Ed.* **2009**, *48*, 9792–9826; *Angew. Chem.* **2009**, *121*, 9976–10011; b) H. Bonin, M. Sauthier, F.-X. Felpin, *Adv. Synth. Catal.* **2014**, *356*, 645–671; c) I. Hussain, T. Singh, *Adv. Synth. Catal.* **2014**, *356*, 1661–1696; d) G. P. Chiusoli, M. Catellani, M. Costa, E. Motti, N. Della Ca', G. Maestri, *Coord. Chem. Rev.* **2010**, *254*, 456–469.
- [5] a) K. M. Engle, T.-S. Mei, M. Wasa, J.-Q. Yu, *Acc. Chem. Res.* **2012**, *45*, 788–802; b) Y.-H. Zhang, B.-F. Shi, J.-Q. Yu, *Angew. Chem. Int. Ed.* **2009**, *48*, 6097–6100; *Angew. Chem.* **2009**, *121*, 6213–6216; c) R. Giri, J.-Q. Yu, *J. Am. Chem. Soc.* **2008**, *130*, 14082–14083; d) T.-S. Mei, R. Giri, N. Maugel, J.-Q. Yu, *Angew. Chem. Int. Ed.* **2008**, *47*, 5215–5219; *Angew. Chem.* **2008**, *120*, 5293–5297.
- [6] a) P. Mamone, G. Danoun, L. J. Gooßen, *Angew. Chem. Int. Ed.* **2013**, *52*, 6704–6708; *Angew. Chem.* **2013**, *125*, 6836–6840; b) S. Bhadra, W. I. Dzik, L. J. Gooßen, *Angew. Chem. Int. Ed.* **2013**, *52*, 2959–2962; *Angew. Chem.* **2013**, *125*, 3031–3035; c) S. Mochida, K. Hirano, T. Satoh, M. Miura, *Org. Lett.* **2010**, *12*, 5776–5779; d) J. Cornella, M. Righi, I. Larrosa, *Angew. Chem. Int. Ed.* **2011**, *50*, 9429–9432; *Angew. Chem.* **2011**, *123*, 9601–9604; e) J. Luo, S. Preciado, I. Larrosa, *J. Am. Chem. Soc.* **2014**, *136*, 4109–4112; f) J. Luo, S. Preciado, I. Larrosa, *Chem. Commun.* **2015**, *51*, 3127–3130; g) Y. Zhang, H. Zhao, M. Zhang, W. Su, *Angew. Chem. Int. Ed.* **2015**, *54*, 3817–3821; *Angew. Chem.* **2015**, *127*, 3888–3892; h) X. Qin, D. Sun, Q. You, Y. Cheng, J. Lan, J. You, *Org. Lett.* **2015**, *17*, 1762–1765.
- [7] a) L. J. Gooßen, G. Deng, L. M. Levy, *Science* **2006**, *313*, 662–664; b) A. Fromm, C. van Willen, D. Hackenberger, L. J. Gooßen, *J. Am. Chem. Soc.* **2014**, *136*, 10007–10023; c) P. P. Lange, L. J. Gooßen, P. Podmore, T. Underwood, N. Sciammetta, *Chem. Commun.* **2011**, *47*, 3628–3630; d) L. J. Goossen, T. Knauber, *J. Org. Chem.* **2008**, *73*, 8631–8634.
- [8] a) R. Giri, N. Maugel, J.-J. Li, D.-H. Wang, S. P. Breazzano, L. B. Saunders, J.-Q. Yu, *J. Am. Chem. Soc.* **2007**, *129*, 3510–3511; b) D.-H. Wang, T.-S. Mei, J.-Q. Yu, *J. Am. Chem. Soc.* **2008**, *130*, 17676–17677; c) K. M. Engle, P. S. Thuy-Boun, M. Dang, J.-Q. Yu, *J. Am. Chem. Soc.* **2011**, *133*, 18183–18193.
- [9] H. A. Chiong, Q.-N. Pham, O. Daugulis, *J. Am. Chem. Soc.* **2007**, *129*, 9879–9884.
- [10] C. Arroniz, A. Ironmonger, G. Rassias, I. Larrosa, *Org. Lett.* **2013**, *15*, 910–913.
- [11] a) H. Gong, H. Zeng, F. Zhou, C.-J. Li, *Angew. Chem. Int. Ed.* **2015**, *54*, 5718–5721; *Angew. Chem.* **2015**, *127*, 5810–5813; b) X. Qin, X. Li, Q. Huang, H. Liu, D. Wu, Q. Guo, J. Lan, R. Wang, J. You, *Angew. Chem. Int. Ed.* **2015**, *54*, 7167–7170; *Angew. Chem.* **2015**, *127*, 7273–7276; c) Z. Wu, S. Chen, C. Hu, Z. Li, H. Xiang, X. Zhou, *ChemCatChem* **2013**, *5*, 2839–2842.
- [12] a) C. Galli, *Chem. Rev.* **1988**, *88*, 765–792; b) A. Roglans, A. Pla-Quintana, M. Moreno-Mañas, *Chem. Rev.* **2006**, *106*, 4622–4643; c) F. Mo, G. Dong, Y. Zhang, J. Wang, *Org. Biomol. Chem.* **2013**, *11*, 1582–1593; d) L. He, G. Qiu, Y. Gao, J. Wu, *Org. Biomol. Chem.* **2014**, *12*, 6965–6971; e) D. P. Hari, B. König, *Angew. Chem. Int. Ed.* **2013**, *52*, 4734–4743; *Angew. Chem.* **2013**, *125*, 4832–4842.
- [13] R. Pschorr, *Ber. Dtsch. Chem. Ges.* **1896**, *29*, 496–501.
- [14] M. Gomberg, W. E. Bachmann, *J. Am. Chem. Soc.* **1924**, *46*, 2339–2343.
- [15] a) D. P. Hari, P. Schroll, B. König, *J. Am. Chem. Soc.* **2012**, *134*, 2958–2961; b) A. Wetzel, V. Ehrhardt, M. R. Heinrich, *Angew. Chem. Int. Ed.* **2008**, *47*, 9130–9133; *Angew. Chem.* **2008**, *120*, 9270–9273; c) F. P. Crisóstomo, T. Martín, R. Carrillo, *Angew. Chem. Int. Ed.* **2014**, *53*, 2181–2185; *Angew. Chem.* **2014**, *126*, 2213–2217; d) A. Honraedt, M.-A. Raux, E. L. Grognet, D. Jacquemin, F.-X. Felpin, *Chem. Commun.* **2014**, *50*, 5236–5238.
- [16] D. Kalyani, K. B. McMurtrey, S. R. Neufeldt, M. S. Sanford, *J. Am. Chem. Soc.* **2011**, *133*, 18566–18569.

- [17] K. Shin, S.-W. Park, S. Chang, *J. Am. Chem. Soc.* **2015**, *137*, 8584–8592.
- [18] See also Table S2 in the Supporting Information.
- [19] This catalyst was also used for double C–H activating dehydrogenative couplings: a) J. Wencel-Delord, C. Nimphius, H. Wang, F. Glorius, *Angew. Chem. Int. Ed.* **2012**, *51*, 13001–13005; *Angew. Chem.* **2012**, *124*, 13175–13180; b) J. Wencel-Delord, C. Nimphius, F. W. Patureau, F. Glorius, *Angew. Chem. Int. Ed.* **2012**, *51*, 2247–2251; *Angew. Chem.* **2012**, *124*, 2290–2294; c) N. Kuhl, M. N. Hopkinson, F. Glorius, *Angew. Chem. Int. Ed.* **2012**, *51*, 8230–8234; *Angew. Chem.* **2012**, *124*, 8354–8358; d) Y. Shang, X. Jie, H. Zhao, P. Hu, W. Su, *Org. Lett.* **2014**, *16*, 416–419; e) X. Qin, H. Liu, D. Qin, Q. Wu, J. You, D. Zhao, Q. Guo, X. Huang, J. Lan, *Chem. Sci.* **2013**, *4*, 1964–1969; f) J. Dong, Z. Long, F. Song, N. Wu, Q. Guo, J. Lan, J. You, *Angew. Chem. Int. Ed.* **2013**, *52*, 580–584; *Angew. Chem.* **2013**, *125*, 608–612; g) M. Itoh, K. Hirano, T. Satoh, Y. Shibata, K. Tanaka, M. Miura, *J. Org. Chem.* **2013**, *78*, 1365–1370; h) K. Morimoto, M. Itoh, K. Hirano, T. Satoh, Y. Shibata, K. Tanaka, M. Miura, *Angew. Chem. Int. Ed.* **2012**, *51*, 5359–5362; *Angew. Chem.* **2012**, *124*, 5455–5458.
- [20] L. Ackermann, *Chem. Rev.* **2011**, *111*, 1315–1345.
- [21] a) K. Ueura, T. Satoh, M. Miura, *J. Org. Chem.* **2007**, *72*, 5362–5367; b) K. L. Engelman, Y. Feng, E. A. Ison, *Organometallics* **2011**, *30*, 4572–4577; c) J. Ryu, J. Kwak, K. Shin, D. Lee, S. Chang, *J. Am. Chem. Soc.* **2013**, *135*, 12861–12868; d) H. Kim, K. Shin, S. Chang, *J. Am. Chem. Soc.* **2014**, *136*, 5904–5907; e) J. Kim, S. Chang, *Angew. Chem. Int. Ed.* **2014**, *53*, 2203–2207; *Angew. Chem.* **2014**, *126*, 2235–2239; f) T. Kang, Y. Kim, D. Lee, Z. Wang, S. Chang, *J. Am. Chem. Soc.* **2014**, *136*, 4141–4144; g) Y. Quan, Z. Xie, *J. Am. Chem. Soc.* **2014**, *136*, 15513–15516; h) F. Xie, Z. Qi, S. Yu, X. Li, *J. Am. Chem. Soc.* **2014**, *136*, 4780–4787; i) D. Lee, S. Chang, *Chem. Eur. J.* **2015**, *21*, 5364–5368; j) C. Suzuki, K. Hirano, T. Satoh, M. Miura, *Org. Lett.* **2015**, *17*, 1597–1600; k) D. A. Frasco, C. P. Lilly, P. D. Boyle, E. A. Ison, *ACS Catal.* **2013**, *3*, 2421–2429; l) Y. Xia, Z. Liu, S. Feng, Y. Zhang, J. Wang, *J. Org. Chem.* **2015**, *80*, 223–236.
- [22] a) K.-I. Fujita, M. Nonogawa, R. Yamaguchi, *Chem. Commun.* **2004**, 1926–1927; b) B. Join, T. Yamamoto, K. Itami, *Angew. Chem. Int. Ed.* **2009**, *48*, 3644–3647; *Angew. Chem.* **2009**, *121*, 3698–3701.
- [23] For selected examples for the functionalization of 2-phenylbenzoic acid, see a) Y. Wang, A. V. Gulevich, V. Gevorgyan, *Chem. Eur. J.* **2013**, *19*, 15836–15840; b) C. Wang, S. Rakshit, F. Glorius, *J. Am. Chem. Soc.* **2010**, *132*, 14006–14008; c) J. Gallardo-Donaire, R. Martin, *J. Am. Chem. Soc.* **2013**, *135*, 9350–9353; d) D.-B. Zhou, G.-W. Wang, *Org. Lett.* **2015**, *17*, 1260–1263; e) T. Fukuyama, S. Maetani, K. Miyagawa, I. Ryu, *Org. Lett.* **2014**, *16*, 3216–3219.
- [24] L. S. Park-Gehrke, J. Freudenthal, W. Kaminsky, A. G. DiPasquale, J. M. Mayer, *Dalton Trans.* **2009**, 1972–1983.
- [25] a) M. C. Lehman, D. R. Pahls, J. M. Meredith, R. D. Sommer, D. M. Heinekey, T. R. Cundari, E. A. Ison, *J. Am. Chem. Soc.* **2015**, *137*, 3574–3584; b) J. Kan, S. Huang, J. Lin, M. Zhang, W. Su, *Angew. Chem. Int. Ed.* **2015**, *54*, 2199–2203; *Angew. Chem.* **2015**, *127*, 2227–2231.

Received: June 23, 2015
Published online: September 3, 2015

Anmerkung zu Scheme 5: Der vorgeschlagene Mechanismus der Reaktion wurde stark vereinfacht dargestellt. Auf eine Angabe der genauen Koordinationssphäre beziehungsweise von Komplex-Ladungen wurde der Übersichtlichkeit halber verzichtet.

Ergänzend zu den im Manuskript beschriebenen Resultaten werden nachfolgend weiterführende Ergebnisse diskutiert.

Konkurrenzexperimente

Im Verlauf dieser Arbeiten wurden außerdem Konkurrenzexperimente mit Acetophenon (**5.3.4-1b'**) und *N*-*tert*-Butylbenzamid (**5.3.4-1a'**), die sich ebenfalls, wenn auch weniger effizient, unter den neuen Bedingungen *ortho*-arylieren lassen, durchgeführt (Tabelle 27). Dabei wurden äquimolare Mengen der Carbonsäure, des Ketons bzw. des Amids und des Diazoniumsalzes unter den Standardbedingungen zur Reaktion gebracht.

Tabelle 27: Konkurrenzexperimente.

CC1=CC=C(C(=O)O)C=C1 + COc1ccc([N+]#N)cc1 + CC1=CC=C(C(=O)N)C=C1
 $\xrightarrow[\text{Li}_2\text{CO}_3, \text{Aceton}, 60^\circ\text{C}, 24\text{ h}]{[\text{IrCp}^*\text{Cl}_2]_2, \text{Ag}_2\text{CO}_3}$
CC1=CC=C(C(=O)O)C(=C1)Ar + CC1=CC=C(C(=O)N)C(=C1)Ar

5.3.4-1a **5.3.4-2a** **5.3.4-1'** **5.3.4-4aa** **5.3.4-5**

DG = CC(=O)C oder CC(=O)N

Eintrag	DG	Li ₂ CO ₃ (Äquiv.)	5.3.4-4aa (%)	5.3.4-5 (%)
1	Keton	0.5	78	n.d.
2	Amid	0.3	43	39
3	"	0.5	61	24
4	"	0.8	67	16
5	"	1	64	6
6	"	1.5	50	Spuren

Reaktionsbedingungen: **5.3.4-1a** (0.5 mmol), **5.3.4-2a** (0.5 mmol), **5.3.4-1a'** oder **5.3.4-1b'** (0.5 mmol), [IrCp*Cl₂]₂ (3 mol%), Ag₂CO₃ (0.15 Äquiv.), Li₂CO₃, Aceton (1 mL), 60 °C, 24 h. GC-Ausbeuten nach Veresterung mit K₂CO₃ (2 Äquiv.) und MeI (5 Äquiv.) in MeCN und *n*-Tetradecan als interner Standard.

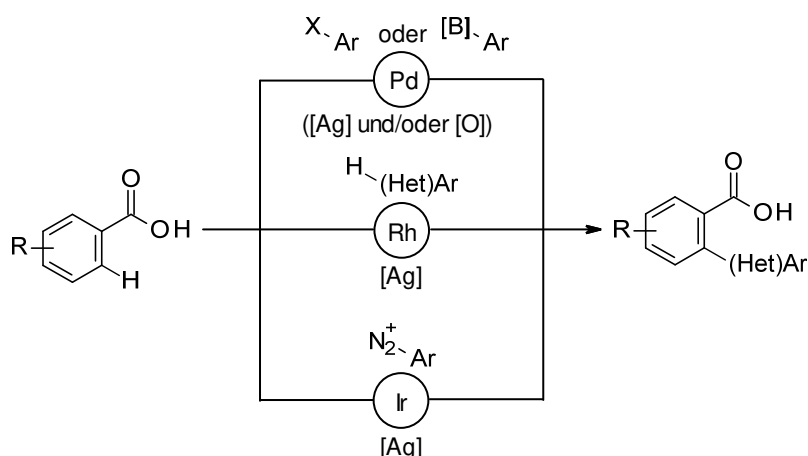
In beiden Fällen zeigte sich, dass die Carbonsäure unter den gewählten Bedingungen die deutlich effizientere dirigierende Gruppe ist. Dabei wurde im Fall des Ketons kein Arylierungsprodukt detektiert (Eintrag 1), während sich bei gleichzeitiger Umsetzung der Säure und des Amids eine Produktverteilung im Verhältnis 3:1 ergab (Eintrag 3). Durch Erhöhung

der Basenmenge ließ sich die Arylierung des Amids einschränken, wobei überstöchiometrische Mengen Base zu geringeren Ausbeuten führten (Einträge 4–6). Könnten Bedingungen identifiziert werden, die die Arylierung der Carbonsäure in Gegenwart des Amids mit höchster Effizienz ermöglichen und gleichzeitig die Arylierung des Amids unterbinden, würde sich bei Substraten mit beiden dirigierenden Gruppen die Möglichkeit zur orthogonalen Difunktionalisierung bieten. Damit könnte das synthetische Potential dieser Methode abermals demonstriert werden.

5.4 Ruthenium-katalysierte *ortho*-Arylierung von Benzoesäuren

5.4.1 Hintergrund

Wie bereits in Abschnitt 3.2.3.1 beschrieben, hat seit den Pionierarbeiten von Daugulis *et al.* zur Carboxylat-dirigierten *ortho*-Arylierung von Benzoesäuren mit Arylhalogeniden eine stetige Weiterentwicklung dieses Reaktionskonzepts stattgefunden. Dabei basieren die katalytischen Systeme ebenso wie bei den oxidativen Kupplungen mit Arylboronsäuren oder -boronaten auf Palladium, meist in Kombination mit Silbersalzen und/oder stöchiometrischen Mengen eines Oxidationsmittels.^[33,39] Der Einsatz von Rhodium-basierten Katalysatorsystemen in Kombination mit stöchiometrischen Mengen an Silbersalzen hat dehydrierende *ortho*-C–H-Arylierungen hervorgebracht^[132–134] und Aryldiazoniumsalze können mit einem Katalysatorsystem bestehend aus Iridium und Silber als elektrophile Kupplungspartner genutzt werden (Abschnitt 5.3.4, Schema 42).



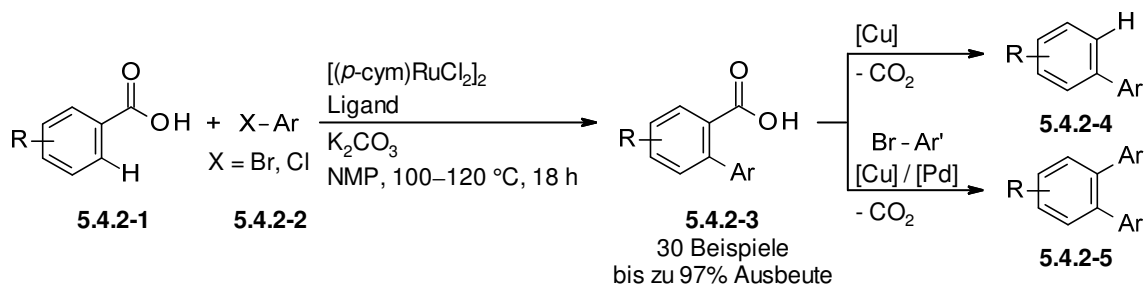
Schema 42: *ortho*-Arylierungen von Benzoesäuren in Gegenwart von Pd, Rh oder Ir.

Protokolle für Carboxylat-dirigierte *ortho*-C–H-Arylierungen basierend auf kostengünstigeren Ruthenium-Katalysatoren^[207] wurden bisher nicht beschrieben, wäre aber aus ökonomischer Sicht eine Verbesserung. Zwar existiert eine Vielzahl an Ruthenium-katalysierten C–H-Funktionalisierungen, darunter auch *ortho*-Arylierungen mit beispielsweise Arylbromiden oder -chloriden unter Verwendung stark koordinierender dirigierender Gruppen,^[108,208] doch sind im Hinblick auf Carboxylat-dirigierte Varianten lediglich Fujiwara-Moritani-Reaktionen und Hydroarylierungen von Alkenen oder Alkinen bekannt.^[108,138–140,142,208,209]

5.4.2 Ruthenium-katalysierte *ortho*-C–H-Arylierung mit Arylchloriden und -bromiden

Ausgangspunkt der Arbeiten war die Entdeckung von Herrn Agostino Biafora, dass sich Benzoessäuren in Gegenwart eines Ruthenium-Katalysators und einer Carbonatbase in NMP bei 100–120 °C mit Aryliodiden *ortho*-arylieren lassen. Eine nähere Untersuchung dieser Reaktion erfolgte von Herrn Florian Belitz unter Betreuung von Herrn Biafora im Rahmen eines Forschungspraktikums.

Darauf basierend wurde ein Protokoll für die Ruthenium-katalysierte *ortho*-Arylierung von Benzoessäuren mit Arylbromiden sowie Arylchloriden entwickelt (Schema 43).



Schema 43: Ruthenium-katalysierte *ortho*-Arylierung von Benzoessäuren.

Die Anwendungsbreite dieser Verfahren konnte anhand der Synthese einer Vielzahl an Biaryl-2-carboxylaten in guten bis sehr guten Ausbeuten demonstriert werden. Weiterhin gelang es, diese Verfahren mit einer Kupfer-katalysierten Protodecarboxylierung sowie erstmals mit einer Kupfer/Palladium-katalysierten decarboxylierenden Kreuzkupplung zu einem Eintopf- bzw. einem sequenziellen Eintopf-Verfahren zu kombinieren. Mechanistische Studien lieferten zudem nähere Informationen über den Ablauf dieser Reaktion.

Beiträge der Autoren: Die Bearbeitung dieses Projekts erfolgte zusammen mit Herrn Agostino Biafora, Herrn Thilo Krause und Herrn Florian Belitz. Herr Biafora und Herr Belitz optimierten die Reaktion. Diese Optimierungsarbeiten wurden später von Herrn Krause und gegen Ende von mir unterstützt. Die Untersuchung der Anwendungsbreite erfolgte gleichberechtigt. Weiterhin wurden die Eintopf-Verfahren zu gleichen Teilen von Herrn Biafora, Herrn Krause und mir entwickelt. Herr Biafora führte die mechanistischen Studien durch und verfasste das Manuskript, welches von Herrn Prof. Dr. L. J. Gooßen überarbeitet wurde. Herr Biafora, Herr Krause und ich werteten die analytischen Daten gemeinsam aus und erstellten die „Supporting Information“.

Die Katalysatoroptimierung, die Untersuchungen zur Anwendungsbreite, die Entwicklung der Eintopf-Verfahren sowie die mechanistischen Studien sind in der nachfolgenden Publikation aufgeführt. Diese wurde in *Angewandte Chemie* veröffentlicht, für die vorliegende Arbeit angepasst und mit Erlaubnis des Verlags beigelegt:

"Reprinted (adapted) with permission from A. Biafora, T. Krause, D. Hackenberger, F. Belitz, L. J. Gooßen, *Angew. Chem. Int. Ed.* **2016**, 55, 14752–14755: *ortho*-C–H Arylation of Benzoic Acids with Aryl Bromides and Chlorides Catalyzed by Ruthenium. Copyright 2016 WILEY-VCH Verlag GmbH & Co. KGaA, Weinheim."

JOHN WILEY AND SONS LICENSE TERMS AND CONDITIONS

This Agreement between Ms. Dagmar Hackenberger ("You") and John Wiley and Sons ("John Wiley and Sons") consists of your license details and the terms and conditions provided by John Wiley and Sons and Copyright Clearance Center.

License Number	4116361091001
License date	May 26, 2017
Licensed Content Publisher	John Wiley and Sons
Licensed Content Publication	Angewandte Chemie International Edition
Licensed Content Title	<i>ortho</i> -C–H Arylation of Benzoic Acids with Aryl Bromides and Chlorides Catalyzed by Ruthenium
Licensed Content Author	Agostino Biafora, Thilo Krause, Dagmar Hackenberger, Florian Belitz, Lukas J. Gooßen
Licensed Content Date	Oct 21, 2016
Licensed Content Pages	4
Type of use	Dissertation/Thesis
Requestor type	Author of this Wiley article
Format	Print and electronic
Portion	Full article
Will you be translating?	No

C–H Activation

International Edition: DOI: 10.1002/anie.201607270
German Edition: DOI: 10.1002/ange.201607270

ortho-C–H Arylation of Benzoic Acids with Aryl Bromides and Chlorides Catalyzed by Ruthenium

Agostino Biafora, Thilo Krause, Dagmar Hackenberger, Florian Belitz, and Lukas J. Goossen*

Abstract: A system consisting of catalytic amounts of $[(p\text{-cym})\text{RuCl}_2]_2/\text{PEt}_3\text{HBF}_4$, K_2CO_3 as the base, and NMP as the solvent efficiently mediates the ortho-C–H arylation of benzoic acids with aryl bromides at 100°C . Replacing the phosphine ligand with the amino acid DL-pipecolinic acid enables the analogous transformation with aryl chlorides. The key advantage of this broadly applicable transformation is the use of an inexpensive ruthenium catalyst in combination with simple carboxylates as directing groups, which can either be tracelessly removed or used as anchor points for decarboxylative ipso substitutions.

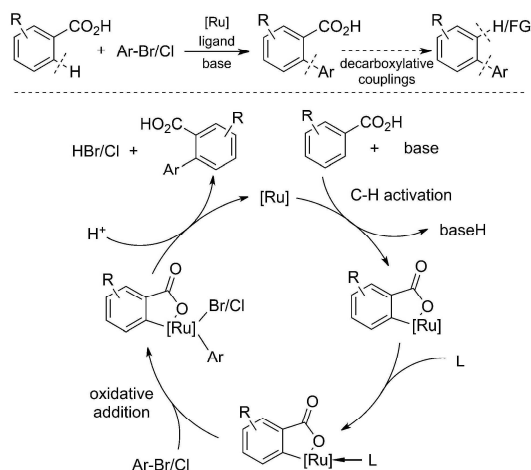
Biaryls are ubiquitous in pharmaceuticals, agrochemicals, and functional materials, and efficient methods to access these substructures are constantly sought after.^[1] Traditionally, these structures are accessed by cross-coupling of preformed organometallic reagents with aryl halides^[2] or by oxidative or reductive couplings of prefunctionalized substrates.^[3]

The discovery of directing groups that efficiently control the regioselectivity of C–H arylations has recently revolutionized this field, enabling the regiospecific introduction of aryl groups in unfunctionalized positions.^[4] However, this great conceptual advantage is often offset by the structural complexity of the required directing groups.^[5] Their introduction and subsequent removal adds several steps to the overall synthetic process. Only recently, abundant functional groups with low coordinating ability, such as carboxylates, have successfully been used as directing groups for ortho-C–H arylations.^[6] The key benefit of carboxylate groups is that they can be tracelessly removed by protodecarboxylation or utilized as leaving groups in a rapidly growing number of decarboxylative coupling reactions, with formation of C–C, C–O, C–N, C–S, C–P, and C–halogen bonds, for example.^[7]

The development of transformations based on carboxylate directing groups is highly challenging. The low σ -donating ability of the carboxylate limits their ability to direct metal centers to one specific C–H bond and reduces the activity of

the resulting metallacycle towards aryl electrophiles. ortho Arylations of benzoic acids were first reported by the groups of Daugulis,^[8] Larrosa,^[9] Su,^[10] and Yu,^[11] who employed expensive palladium catalysts.^[12] With aryl iodides, these transformations proceeded smoothly even at room temperature.^[10] The conversion of aryl bromides is possible only under rather harsh conditions, and the coupling of aryl chlorides has thus far required such high temperatures that selective monoarylation could not be achieved.^[8] With arenediazonium salts as electrophiles, ortho arylation proceeds under mild conditions, but requires expensive iridium catalysts.^[13] Oxidative arylations have been reported with expensive aryl boronic acids and a limited set of heteroarenes as arylating agents.^[14]

Despite the remarkable progress achieved in this highly topical area, a broadly applicable carboxylate-directed C–H arylation that is based on readily available aryl bromides or chlorides and the use of a reasonably priced catalyst^[15] has not yet been described. Ackermann and co-workers as well as our group have recently demonstrated that simple and affordable ruthenium catalysts efficiently promote regioselective hydroarylations of carboxylates.^[16] We reasoned that the addition of electron-rich ligands might activate the intermediary ruthenacycle towards oxidative insertion into Ar–Br or Ar–Cl bonds by increasing its electron density, as outlined in Scheme 1. This hypothesis was supported by results of Dixneuf,^[17] Larrosa,^[18] Ackermann,^[19] and others,^[20] who demonstrated that ruthenium catalysts can activate aryl chlorides or bromides, and the observations by Daugulis,^[8] Dixneuf,^[21]



Scheme 1. Carboxylate-directed C–H arylation of arenes with aryl electrophiles assisted by electron-rich ligands.

[*] A. Biafora, F. Belitz
FB Chemie-Organische Chemie, TU Kaiserslautern
Erwin-Schrödinger-Strasse Geb. 54, 67663 Kaiserslautern (Germany)
T. Krause, D. Hackenberger, Prof. Dr. L. J. Goossen
Fakultät Chemie und Biochemie
Ruhr Universität Bochum
Universitätsstrasse 150, 44801 Bochum (Germany)
E-mail: lukas.goossen@rub.de

Supporting information and the ORCID identification number(s) for the author(s) of this article can be found under:
<http://dx.doi.org/10.1002/anie.201607270>.

and Ackermann^[22,19b] that such processes are facilitated by electron-rich phosphine and amino acid ligands.

To confirm our hypothesis, we chose the reaction of 2-methylbenzoic acid (**1a**) and bromobenzene (**2a**) as a model system and investigated various catalysts and conditions (Table 1). Encouragingly, traces of the desired product **3a** were detected when [(*p*-cym)RuCl₂]₂ was used as

Table 1: Optimization of the *ortho* arylation reaction.^[a]

Entry	Catalyst	PhX	Base	Ligand	Yield ^[b] [%]
1	[(<i>p</i> -cym)RuCl ₂] ₂	PhBr	GuanCO ₃	–	trace
2	[(<i>p</i> -cym)RuCl ₂] ₂	PhBr	K ₂ CO ₃	–	13
3	[(<i>p</i> -cym)RuCl ₂] ₂	PhBr	K ₂ CO ₃	PPh ₃	35
4	[(C ₆ H ₅)RuCl ₂] ₂	PhBr	K ₂ CO ₃	PPh ₃	34
5	[(C ₆ Me ₆)RuCl ₂] ₂	PhBr	K ₂ CO ₃	PPh ₃	0
6	[(<i>p</i> -cym)Ru] ₂	PhBr	K ₂ CO ₃	PPh ₃	35
7	[(<i>p</i> -cym)RuCl ₂] ₂	PhBr	K ₂ CO ₃	PPhCy ₂	59
8	[(<i>p</i> -cym)RuCl ₂] ₂	PhBr	K ₂ CO ₃	PCy ₃	76
9	[(<i>p</i> -cym)RuCl ₂] ₂	PhBr	K ₂ CO ₃	P ^t Pr ₃	80
10	[(<i>p</i> -cym)RuCl ₂] ₂	PhBr	K ₂ CO ₃	PMMe ₃ ·HBF ₄	73
11	[(<i>p</i> -cym)RuCl ₂] ₂	PhBr	K ₂ CO ₃	PEt ₃ ·HBF ₄	90
12 ^[c]	[(<i>p</i> -cym)RuCl ₂] ₂	PhBr	K ₂ CO ₃	PEt ₃ ·HBF ₄	93 (93)
13 ^[c]	[(<i>p</i> -cym)RuCl ₂] ₂	PhCl	K ₂ CO ₃	PEt ₃ ·HBF ₄	12
14 ^[d]	[(<i>p</i> -cym)RuCl ₂] ₂	PhCl	K ₂ CO ₃	PEt ₃ ·HBF ₄	12/75 ^[e]
15 ^[d]	[(<i>p</i> -cym)RuCl ₂] ₂	PhCl	K ₂ CO ₃	L-proline	47
16 ^[d]	[(<i>p</i> -cym)RuCl ₂] ₂	PhCl	K ₂ CO ₃	D,L-pipecolinic acid	80 (75)

[a] Reaction conditions: **1a** (1 equiv), **2a** (4 equiv), [Ru] (4 mol %), ligand (8 mol %), base (1.1 equiv), NMP (3 mL), 100 °C, 18 h, N₂ atmosphere. [b] Yields of the corresponding methyl esters determined by GC analysis after esterification with K₂CO₃ (2 equiv) and MeI (5 equiv) in NMP using *n*-tetradecane as the internal standard; yields of isolated products are given in parentheses. [c] PhX (1 equiv). [d] 120 °C. [e] After 48 h. Cy = cyclohexyl, GuanCO₃ = guanidine carbonate, NMP = *N*-methylpyrrolidone, *p*-cym = *para*-cymene.

the catalyst in combination with guanidine carbonate at 120 °C (entry 1), conditions that had been highly effective for our hydroarylation reaction.^[16b] A major increase in yield was achieved upon switching to potassium carbonate as the base (entry 2). As anticipated, the yields improved substantially upon addition of a phosphine ligand (entry 3). Systematic variation of the ruthenium precursor confirmed that [(*p*-cym)RuCl₂]₂ is the optimal precatalyst (entries 4–6). The nature of the ligand had a decisive influence on the reaction outcome. Among the ligands tested, electron-rich alkyl phosphines turned out to be superior. The best yields were achieved with triethylphosphine (entry 11), which can be conveniently administered in the form of its HBF₄ salt. After optimization of the reaction conditions (4 mol % [(*p*-cym)RuCl₂]₂, 8 mol % PEt₃·HBF₄, and 1.1 equiv K₂CO₃ in 3 mL NMP at 100 °C), high yields were obtained even when using only one equivalent of the aryl bromide (entry 12). NMP is uniquely effective as the solvent (see the Supporting Information).

When chlorobenzene was used as the electrophile, only modest yields were observed under these conditions (entry 13), even upon increasing the temperature to 120 °C (entry 14). Once again, the ligand turned out to be the decisive factor in the reaction development. Phosphine ligands were almost ineffective whereas amino acids strongly promoted the desired transformation (entry 15). After increasing the amount of aryl chloride, the monoarylated product **3a** was obtained in 80 % yield. Although pipecolinic acid is a more efficient ligand than PEt₃·HBF₄, the latter gave high yields when the reaction time was extended to 48 h, indicating that the reaction proceeds through a similar mechanism for aryl chlorides and bromides. Control experiments revealed that the optimal system for aryl chlorides is less effective for aryl bromides (33 % yield, see the Supporting Information).

With effective methods in hand for the conversion of both aryl bromides and chlorides, we investigated the scope of the transformation. The model substrate 2-methylbenzoic acid (**1a**) was successfully coupled with various aryl bromides using method A (Table 2). Electron-rich and electron-poor substrates reacted similarly, and common functional groups, such as CF₃, CN, ester, halo, keto, alkyl, and methoxy moieties as well as unprotected phenolic and benzylic hydroxy groups,

Table 2: Substrate scope of the direct arylation with various aryl bromides and chlorides.^[a]

1a	Ar-X	3a
	X = Br, 2a–2r X = Cl, 2a'–2n'	
3aa	R = OMe, X = Br 82% X = Cl 72%	
3ab	R = Me, X = Cl 55%	
3ac	R = NHAc, X = Br 93%	
3ad	R = CO ₂ Et, X = Br 83%	
3ae	R = OH, X = Br 52% ^[b]	
3af	R = COPh, X = Br 81%	
3ag	R = Cl, X = Br 61%	
3ah	R = OMe, X = Br 87%	
3ai	R = CF ₃ , X = Br 71%	
3aj	R = ^t Bu, X = Br 79%	
3ak	R = CN, X = Br 52%	
3al	R = CN, X = Br 52%	
3am	X = Br 40%	
3an	X = Cl 68% ^[d]	
3ao	X = Br 85% ^[c]	
3ap	X = Br 52%	
3aq	X = Br 86%	
3ar	X = Br 68%	

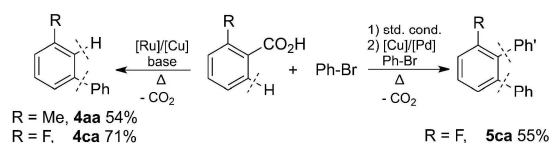
[a] Reaction conditions: Method A: **1a** (0.5 mmol), ArBr (0.5 mmol), [(*p*-cym)RuCl₂]₂ (4 mol %), PEt₃·HBF₄ (8 mol %), K₂CO₃ (1.1 equiv), NMP (3 mL), 100 °C, 18 h, N₂ atmosphere. Method B: **1a** (0.5 mmol), ArCl (0.75 mmol), [(*p*-cym)RuCl₂]₂ (4 mol %), D,L-pipecolinic acid (8 mol %), K₂CO₃ (1.1 equiv), NMP (3 mL), 120 °C, 18 h. Yields of the corresponding methyl esters after esterification with K₂CO₃ (2 equiv) and MeI (5 equiv) in NMP. [b] Isolated as the methyl ether. [c] ArBr (1.5 equiv). [d] Isolated as the free acid.

were tolerated in the *para* or *meta* position. *ortho* Substituents led to only moderate yields. It is noteworthy that under these conditions, aryl halides bearing functional groups that would be expected to be more efficient directing groups smoothly reacted with the *ortho* position of the carboxylates. This opens up welcome opportunities for polyfunctionalization. Products **3aa** and **3ab** demonstrate that comparable yields were achieved starting from aryl chlorides using method B (4 mol % [(*p*-cym)RuCl₂]₂, 8 mol % DL-pipecolinic acid, 1.1 equiv K₂CO₃ in 3 mL NMP at 120 °C).

The scope with regard to the aromatic carboxylate was investigated with bromobenzene (**2a**) and chlorobenzene (**2a'**; Table 3). Benzoic acids bearing electron-donating or electron-withdrawing substituents, including methoxy, halo, and acyl groups, were smoothly coupled. Heterocyclic carboxylates were also successfully converted into the desired products. Unwanted double arylation could not be suppressed with unsubstituted or *para*-substituted benzoic acids. However, a substituent in the 3-position was sufficient to direct the arylation to the 6-position exclusively. This regioselectivity towards the less hindered *ortho* position was also observed with fused (hetero)aromatic quinoline 6-carboxylic acid (**1i**) and 2-naphthylcarboxylic acid (**1i**). A particularly remarkable example is the coupling of 2-acetamidobenzoic acid with **2a**. The new bond is selectively formed in the *ortho* position of the benzoic acid rather than in the *ortho* position of the amide

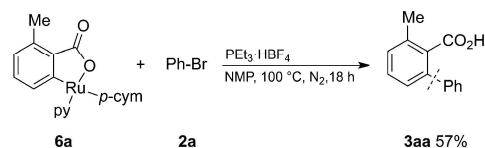
despite the C–H directing ability of the latter, which by far exceeds that of carboxylic acids in related C–H functionalizations. Four additional examples demonstrate that method B permits the coupling of aryl chlorides in comparable yields.

We next probed whether the biaryl synthesis could also be combined with concomitant protodecarboxylation.^[23] The examples in Scheme 2 demonstrate that this process does not even require an additional reaction step. By simply adding a copper catalyst to the reaction medium and increasing the temperature to 190 °C, the corresponding biaryl products **4** were formed in good yields. The *ortho* arylation can also be combined with decarboxylative cross-couplings,^[24] as demonstrated by the synthesis of terphenyl **5ca** in 55 % non-optimized yield.



Scheme 2. *ortho* Arylations followed by decarboxylative reactions.

To shed light on the mechanism proposed in Scheme 1, we synthesized *ortho*-ruthenated toluate **6a**. The stoichiometric reaction of **6a** and PEt₃·HBF₄ with bromobenzene (**2a**) yielded **3aa** in 57 % yield (Scheme 3), which supports the intermediacy of an *ortho*-metalated species in the catalytic cycle. In the presence of only pyridine as the ligand, no product formation was observed, which confirmed the necessity for a suitable ligand (see the Supporting Information). In-depth mechanistic studies are underway to fully clarify the reaction pathway.



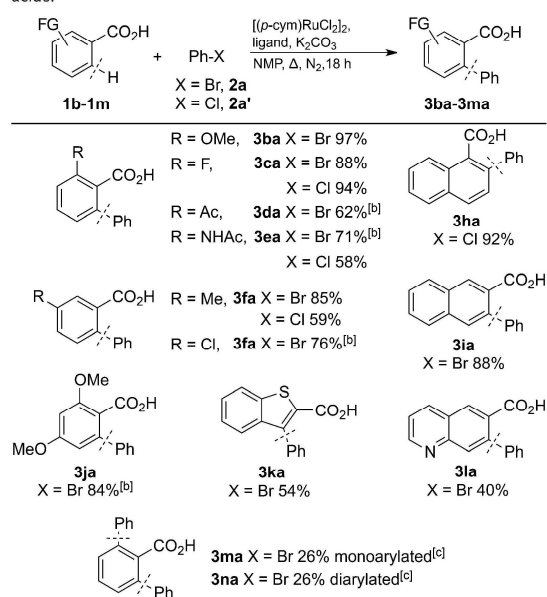
Scheme 3. Stoichiometric reaction of the *ortho*-ruthenated toluate **6a**.

In conclusion, we have shown that cost-effective ruthenium complexes are at least as effective and broadly applicable as state-of-the-art palladium systems for catalyzing the synthetically useful *ortho* arylation of benzoic acids. In combination with subsequent decarboxylative *ipso* substitutions, they promise to open up new perspectives for sustainable, regioselective arene (di)functionalization.

Experimental Section

An oven-dried 20 mL vessel was charged with [Ru(*p*-cym)Cl₂]₂ (12.2 mg, 0.02 mmol, 4 mol %), triethylphosphonium tetrafluoroborate (8.3 mg, 0.04 mmol, 8 mol %, method A) or DL-pipecolinic acid (5.2 mg, 0.04 mmol, 8 mol %, method B), K₂CO₃ (76 mg, 0.55 mmol, 1.1 equiv), and benzoic acid **1** (0.50 mmol). After the vessel had been subjected to three alternating vacuum and nitrogen purge cycles, NMP (3 mL) and the aryl halide **2** (0.50 mmol, method A; 0.75 mmol, method B) were added via syringe. The resulting mixture was stirred at 100 °C for 18 h. After the reaction was complete, the mixture was

Table 3: Substrate scope of the direct arylation with various benzoic acids.^[a]



[a] Reaction conditions: Method A: **1** (0.5 mmol), **2a** (0.75 mmol), [(*p*-cym)RuCl₂]₂ (4 mol %), PEt₃·HBF₄ (8 mol %), K₂CO₃ (1.1 equiv), NMP (3 mL), 100 °C, 18 h. Method B: **1** (0.5 mmol), **2a'** (0.75 mmol), [(*p*-cym)RuCl₂]₂ (4 mol %), DL-pipecolinic acid (8 mol %), K₂CO₃ (1.1 equiv), NMP (3 mL), 120 °C, 18 h. Yields of the corresponding methyl esters after esterification with K₂CO₃ (2 equiv) and MeI (5 equiv) in NMP. [b] ArBr (1 equiv). [c] Yield determined by GC analysis.

allowed to cool to room temperature. NMP (2 mL), K_2CO_3 (207 mg, 3 equiv), and MeI (156 μ L, 5 equiv) were added, and the mixture was stirred at 60 °C for 2 h. The mixture was allowed to cool to room temperature, ethyl acetate (20 mL) was added, and the resulting mixture was washed with water, aqueous LiCl solution (20%), and brine (20 mL each). The organic layer was dried over $MgSO_4$, filtered, and the volatiles were removed under reduced pressure. The residue was purified by column chromatography (SiO_2 , ethyl acetate/hexane gradient), yielding the corresponding biaryl.

Acknowledgements

We thank Umicore for donating chemicals, the DFG (SFB/TRR-88, "3MET" and EXC/1069 "RESOLV") and the Stipendienstiftung Rheinland-Pfalz (fellowship to D.H.) for financial support and Joachim Hower for technical assistance with the ESI-MS measurements. We thank Prof. Dr. Daniel J. Weix (University of Rochester) for agreeing to coordinate publication.

Keywords: aryl halides · benzoic acids · biaryls · C–H arylation · ruthenium

How to cite: *Angew. Chem. Int. Ed.* **2016**, *55*, 14752–14755
Angew. Chem. **2016**, *128*, 14972–14975

- [1] D. A. Horton, G. T. Bourne, M. L. Smythe, *Chem. Rev.* **2003**, *103*, 893–930.
- [2] a) G. Bringmann, R. Walter, R. Weirich, *Angew. Chem. Int. Ed. Engl.* **1990**, *29*, 977–991; *Angew. Chem.* **1990**, *102*, 1006–1019; b) J. Hassan, M. Sévignon, C. Gozzi, E. Schulz, M. Lemaire, *Chem. Rev.* **2002**, *102*, 1359–1470; c) V. B. Phapale, D. J. Cárdenas, *Chem. Soc. Rev.* **2009**, *38*, 1598–1607; d) P. E. Fanta, *Chem. Rev.* **1946**, *38*, 139–196; e) N. Miyaura, A. Suzuki, *Chem. Rev.* **1995**, *95*, 2457–2483; f) E. Negishi, *Acc. Chem. Res.* **1982**, *15*, 340–348.
- [3] a) L. K. G. Ackerman, M. M. Lovell, D. J. Weix, *Nature* **2015**, *524*, 454–457; b) M. Amatore, C. Gosmini, *Angew. Chem. Int. Ed.* **2008**, *47*, 2089–2092; *Angew. Chem.* **2008**, *120*, 2119–2122; c) *Synthesis of Biaryls* (Ed.: I. Cepanec), Elsevier Science, Oxford, **2004**, pp. 1–349; d) C. C. C. Johansson Seechurn, M. O. Kitching, T. J. Colacot, V. Snieckus, *Angew. Chem. Int. Ed.* **2012**, *51*, 5062–5085; *Angew. Chem.* **2012**, *124*, 5150–5174; e) C.-L. Sun, Z.-J. Shi, *Chem. Rev.* **2014**, *114*, 9219–9280; f) L. T. Ball, G. C. Lloyd-Jones, C. A. Russell, *Science* **2012**, *337*, 1644–1648.
- [4] a) L. Ackermann, R. Vicente, A. Kapdi, *Angew. Chem. Int. Ed.* **2009**, *48*, 9792–9826; *Angew. Chem.* **2009**, *121*, 9976–10011; b) X. Chen, K. M. Engle, D.-H. Wang, J.-Q. Yu, *Angew. Chem. Int. Ed.* **2009**, *48*, 5094–5115; *Angew. Chem.* **2009**, *121*, 5196–5217; c) J. A. Labinger, J. E. Bercaw, *Nature* **2002**, *417*, 507–514.
- [5] a) H. Bonin, M. Sauthier, F.-X. Felpin, *Adv. Synth. Catal.* **2014**, *356*, 645–671; b) I. Hussain, T. Singh, *Adv. Synth. Catal.* **2014**, *356*, 1661–1696; c) G. P. Chiusoli, M. Catellani, M. Costa, E. Motti, N. Della Ca', G. Maestri, *Coord. Chem. Rev.* **2010**, *254*, 456–469; d) M. Zhang, Y. Zhang, X. Jie, H. Zhao, G. Li, W. Su, *Org. Chem. Front.* **2014**, *1*, 843–895.
- [6] a) S. De Sarkar, W. Liu, S. I. Kozhushkov, L. Ackermann, *Adv. Synth. Catal.* **2014**, *356*, 1461–1479; b) K. M. Engle, T.-S. Mei, M. Wasa, J.-Q. Yu, *Acc. Chem. Res.* **2012**, *45*, 788–802; c) Z. Chen, B. Wang, J. Zhang, W. Yu, Z. Liu, Y. Zhang, *Org. Chem. Front.* **2015**, *2*, 1107–1295; d) P. Nareddy, F. Jordan, S. E. Brenner-Moyer, M. Szostak, *ACS Catal.* **2016**, *6*, 4755–4759; e) *C–H Activation* (Eds.: J.-Q. Yu, L. Ackermann, Z. Shi), Springer, Heidelberg, **2010**; f) P. H. Dixneuf, H. Doucet, *C–H Bond Activation and Catalytic Functionalization I*, Springer, Heidelberg, **2015**; g) P. H. Dixneuf, H. Doucet, *C–H Bond Activation and Catalytic Functionalization II*, Springer, Heidelberg, **2016**.
- [7] a) W. I. Dzik, P. P. Lange, L. J. Gooßen, *Chem. Sci.* **2012**, *3*, 2671–2678; b) N. Rodríguez, L. J. Goossen, *Chem. Soc. Rev.* **2011**, *40*, 5030–5048; c) L. J. Goossen, F. Collet, K. Goossen, *Isr. J. Chem.* **2010**, *50*, 617–629; d) L. J. Gooßen, N. Rodríguez, K. Gooßen, *Angew. Chem. Int. Ed.* **2008**, *47*, 3100–3120; *Angew. Chem.* **2008**, *120*, 3144–3164.
- [8] H. A. Chiong, Q.-N. Pham, O. Daugulis, *J. Am. Chem. Soc.* **2007**, *129*, 9879–9884.
- [9] a) J. Luo, S. Preciado, I. Larrosa, *J. Am. Chem. Soc.* **2014**, *136*, 4109–4112; b) J. Cornella, M. Righi, I. Larrosa, *Angew. Chem.* **2011**, *123*, 9601–9604.
- [10] C. Zhu, Y. Zhang, J. Kan, H. Zhao, W. Su, *Org. Lett.* **2015**, *17*, 3418–3421.
- [11] M. Wasa, B. T. Worrell, J.-Q. Yu, *Angew. Chem. Int. Ed.* **2010**, *49*, 1275–1277; *Angew. Chem.* **2010**, *122*, 1297–1299.
- [12] D.-H. Wang, T.-S. Mei, J.-Q. Yu, *Synfacts* **2009**, 0436–0436.
- [13] L. Huang, D. Hackenberger, L. J. Gooßen, *Angew. Chem. Int. Ed.* **2015**, *54*, 12607–12611; *Angew. Chem.* **2015**, *127*, 12798–12802.
- [14] a) D.-H. Wang, T.-S. Mei, J.-Q. Yu, *J. Am. Chem. Soc.* **2008**, *130*, 17676–17677; b) Y. Zhang, H. Zhao, M. Zhang, W. Su, *Angew. Chem. Int. Ed.* **2015**, *54*, 3817–3821; *Angew. Chem.* **2015**, *127*, 3888–3892.
- [15] See the Johnson Matthey Precious Metals Management homepage for the monthly average prices of palladium, iridium, rhodium, and ruthenium between 22nd June 2015 and 22nd July 2016 under <http://www.platinum.matthey.com/prices/price-charts>, **2016**. Last accessed 22nd July 2016.
- [16] a) N. Y. P. Kumar, A. Bechtoldt, K. Raghuvanshi, L. Ackermann, *Angew. Chem. Int. Ed.* **2016**, *55*, 6929–6932; *Angew. Chem.* **2016**, *128*, 7043–7046; b) L. Huang, A. Bialora, G. Zhang, V. Bragoni, L. J. Gooßen, *Angew. Chem. Int. Ed.* **2016**, *55*, 6933–6937; *Angew. Chem.* **2016**, *128*, 7047–7051.
- [17] I. Özdemir, S. Demir, B. Çetinkaya, C. Goulaouen, F. Maseras, C. Bruneau, P. H. Dixneuf, *J. Am. Chem. Soc.* **2008**, *130*, 1156–1157.
- [18] M. Simonetti, G. J. P. Perry, X. C. Cambeiro, F. Juliá-Hernández, J. N. Arokianathar, I. Larrosa, *J. Am. Chem. Soc.* **2016**, *138*, 3596–3606.
- [19] a) L. Ackermann, *Org. Process Res. Dev.* **2015**, *19*, 260–269; b) J. Li, S. Warratz, D. Zell, S. De Sarkar, E. E. Ishikawa, L. Ackermann, *J. Am. Chem. Soc.* **2015**, *137*, 13894–13901; c) L. Ackermann, *Org. Lett.* **2005**, *7*, 3123–3125.
- [20] a) P. B. Arockiam, C. Bruneau, P. H. Dixneuf, *Chem. Rev.* **2012**, *112*, 5879–5918; b) G.-F. Zha, H.-L. Qin, E. A. B. Kantchev, *RSC Adv.* **2016**, *6*, 30875–30885; c) S. Oi, S. Fukita, N. Hirata, N. Watanuki, S. Miyano, Y. Inoue, *Org. Lett.* **2001**, *3*, 2579–2581; d) S. Oi, Y. Ogino, S. Fukita, Y. Inoue, *Org. Lett.* **2002**, *4*, 1783–1785; e) H. Grounds, J. C. Anderson, B. Hayter, A. J. Blake, *Organometallics* **2009**, *28*, 5289–5292.
- [21] P. B. Arockiam, C. Fischmeister, C. Bruneau, P. H. Dixneuf, *Green Chem.* **2013**, *15*, 67–71.
- [22] J. Hubrich, L. Ackermann, *Eur. J. Org. Chem.* **2016**, 3700–3704.
- [23] L. J. Gooßen, N. Rodríguez, C. Linder, P. P. Lange, A. Fromm, *ChemCatChem* **2010**, *2*, 430–442.
- [24] L. J. Goossen, N. Rodríguez, B. Melzer, C. Linder, G. Deng, L. M. Levy, *J. Am. Chem. Soc.* **2007**, *129*, 4824–4833.

Received: July 27, 2016

Revised: September 2, 2016

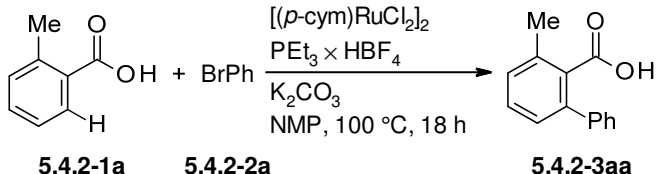
Published online: October 21, 2016

Nachfolgend werden zusätzlich zu den im Manuskript beschriebenen Resultaten weitere Ergebnisse diskutiert.

Kontrollexperimente

Ergänzend zu der in der Publikation diskutierten Reaktionsoptimierung enthält Tabelle 28 weitere Kontrollexperimente. So zeigte eine Variation der Base, dass sich mit Na₂CO₃ oder Cs₂CO₃ ähnlich gute Ausbeuten erzielen lassen wie mit K₂CO₃ (Eintrag 2), während sich Li₂CO₃ oder GuaCO₃ als nicht geeignet erwiesen (Eintrag 3). Weiterhin lieferte ein Experiment mit einer geringeren Basenmenge ebenfalls schlechtere Resultate (Eintrag 4). Unter den optimalen Reaktionsbedingungen war statt in NMP lediglich in DMSO eine *ortho*-Arylierung möglich (Einträge 5 und 6). Während die Zugabe von 1 Äquiv. Wasser zur Reaktion keinen negativen Einfluss zeigte (Eintrag 7), wurde in einer Reaktion ohne Luftausschluss kein Produkt gebildet (Eintrag 8). Zudem erwiesen sich ein Iridium- oder ein Palladium-Katalysator als ungeeignet unter den vorliegenden Bedingungen (Eintrag 9).

Tabelle 28: Einfluss verschiedener Parameter auf die Ru-katalysierte *ortho*-Arylierung.

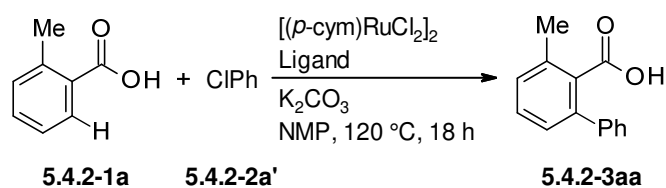
		
Eintrag	Abweichung von den Standardbedingungen	5.4.2-3aa (%)
1	-	93
2	Na ₂ CO ₃ oder Cs ₂ CO ₃ statt K ₂ CO ₃	84
3	Li ₂ CO ₃ oder GuaCO ₃ statt K ₂ CO ₃	13 / n.d.
4	0.5 Äquiv. K ₂ CO ₃ statt 1.1 Äquiv. K ₂ CO ₃	60
5	DMSO als Lösungsmittel	25
6	<i>t</i> -AmylOH, DMF, Tol oder Dioxan als Lösungsmittel	n.d.
7	Zusatz von 1 Äquiv. H ₂ O	89
8	Nicht unter Schutzgasatmosphäre	n.d.
9	[IrCp*Cl ₂] ₂ oder Pd(OAc) ₂ statt [(<i>p</i> -cym)RuCl ₂] ₂	n.d.

Reaktionsbedingungen: 5.4.2-1a (0.5 mmol), 5.4.2-2a (0.5 mmol), [(*p*-cym)RuCl₂]₂ (4 mol%), PEt₃ × HBF₄ (8 mol%), K₂CO₃ (1.1 Äquiv.), 100 °C, NMP (3 mL), 18 h. GC-Ausbeuten nach Veresterung mit K₂CO₃ (2 Äquiv.) und MeI (5 Äquiv.) in NMP und *n*-Tetradecan als interner Standard.

Ligandenscreening für die Kupplung der Arylchloride

Nach der Optimierung der Reaktionsbedingungen für die Arylbromide wurde überprüft, ob sich Arylchloride ebenfalls als Substrate für diese Transformation eignen. Unter den Standardbedingungen wurde das Arylierungsprodukt jedoch nur in einer Ausbeute von 12% erhalten (Tabelle 29, Eintrag 1) und selbst bei 120 °C mit 4 Äquiv. an Chlorbenzol (**5.4.2-2a'**) war keine bessere Ausbeute zu verzeichnen (Eintrag 2). Weiterhin erwiesen sich Phosphanliganden, die in der Kupplung mit Arylbromiden ebenfalls gute Resultate zeigten, in der Transformation mit Chlorbenzol als gänzlich ineffizient (Einträge 3–5). Selbst ein Experiment ohne Ligand lieferte im Vergleich zu den letztgenannten Reaktionen ein geringfügig besseres Ergebnis (Eintrag 6). Da die Effizienz von Aminosäuren als Liganden in Carboxylat-dirigierten C–H-Funktionalisierungen in den vergangenen Jahren bereits mehrfach demonstriert werden konnte,^[41,210–215] wurden diese im Folgenden in der vorliegenden Reaktion getestet. Während mit L-Ala-OH und DL-Phe-OH ebenfalls nur geringe Ausbeuten erzielt wurden (Einträge 7 und 8), ermöglichten DL-Val-OH und L-Ile-OH leicht verbesserte Ausbeuten (Einträge 9 und 11). Mit der zyklischen Aminosäure L-Pro-OH konnte weiterhin eine Ausbeute von 47% an **5.4.2-3aa** erhalten werden (Eintrag 13). Interessanterweise waren die *N*-geschützten Derivate der Aminosäuren weniger aktiv (Einträge 10, 12 und 14), was vermutlich auf eine weniger effiziente Koordination an das Katalysatormetall zurückzuführen ist. Die Untersuchung von Liganden, die eine strukturelle Ähnlichkeit zu Prolin aufweisen, zeigte schließlich, dass mit DL-Pipecolinsäure das gewünschte Produkt in 80% Ausbeute zugänglich ist (Eintrag 16). Zwar führte eine Verringerung der eingesetzten Menge an Chlorbenzol von 4 Äquiv. auf 1 Äquiv. zu einer geringeren Ausbeute (Einträge 17 und 18), doch konnte bei einer Reaktionstemperatur von 140 °C auch unter diesen Bedingungen eine gute Ausbeute erzielt werden (Eintrag 19).

Tabelle 29: Ligandenscreening für die Ru-katalysierte ortho-Arylierung mit Arylchloriden.



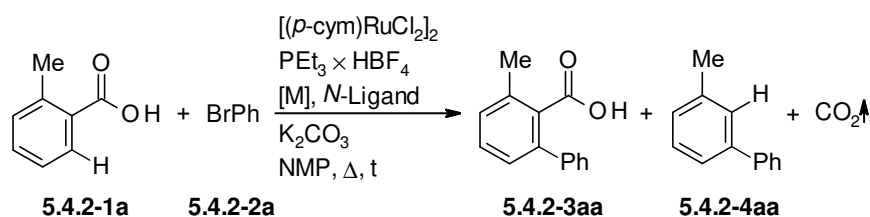
Eintrag	Ligand	5.4.2-3aa (%)
1 ^[a]	PEt ₃ × HBF ₄	12
2	"	12
3	PCy ₃	Spuren
4	PPh ₃	"
5	Pi-Pr ₃	"
6	-	7
7	L-Ala-OH	11
8	DL-Phe-OH	16
9	DL-Val-OH	24
10	N-Cbz-DL-Val-OH	18
11	L-Ile-OH	26
12	N-Cbz-Ile-OH	18
13	L-Pro-OH	47
14	N-Boc-L-Pro-OH	18
15	L-Pyroglutaminsäure	Spuren
16	DL-Pipecolinsäure	80
17 ^[b]	"	57
18 ^[c]	"	32
19 ^[d]	"	80

Reaktionsbedingungen: **5.4.2-1a** (0.5 mmol), **5.4.2-2a'** (2.0 mmol), [(p-cym)RuCl₂]₂ (4 mol%), Ligand (8 mol%), K₂CO₃ (1.1 Äquiv.), 120 °C, NMP (3 mL), 18 h. GC-Ausbeuten nach Veresterung mit K₂CO₃ (2 Äquiv.) und MeI (5 Äquiv.) in NMP und *n*-Tetradecan als interner Standard. [a] **5.4.2-2a'** (0.5 mmol), 100 °C. [b] **5.4.2-2a'** (1.0 mmol). [c] **5.4.2-2a'** (0.5 mmol). [d] **5.4.2-2a'** (0.5 mmol), 140 °C.

Optimierung der sequenziellen ortho-Arylierung/Protodecarboxylierung

Um eine Sequenz aus *ortho*-Arylierung und Protodecarboxylierung zu realisieren, wurden verschiedene Varianten der Reaktionsführung getestet (Tabelle 30). Zunächst wurde das Standardkatalysatorsystem mit Cu₂O kombiniert. Nach Ablauf der Reaktionszeit bei 100 °C wurde die Reaktionsmischung weitere 12 h bei 170 °C gerührt. Dabei wurden 76% **5.4.2-3aa** neben lediglich 9% des Protodecarboxylierungsprodukts **5.4.2-4aa** detektiert (Eintrag 1). Ähnliche Resultate wurden in einer Standardreaktion bei 170 °C in Gegenwart von Cu₂O erhalten (Eintrag 2). Zwar erfolgte die gewünschte Protodecarboxylierung in diesen Fällen nur in geringem Maße, doch wurden sehr gute Gesamtausbeuten an aryliertem Produkt erhalten, was darauf hinweist, dass der zugesetzte Kupfer-Katalysator die Arylierung nicht negativ beeinflusst. Die Zugabe des Kupfer-Katalysators nach Beendigung der *ortho*-Arylierung und anschließendem Rühren bei 180 °C lieferte ebenfalls nur geringe Mengen an **5.4.2-4aa** (Eintrag 3). Dahingegen konnte in einer Reaktion bei 180 °C, in der der Kupfer-Katalysator zu Beginn zugesetzt wurde, 46% des Biaryls **5.4.2-4aa** erhalten werden (Eintrag 4). Kontrollexperimente zeigten, dass unter diesen Bedingungen nicht auf Cu₂O verzichtet werden kann (Eintrag 5), Ruthenium eine Protodecarboxylierung also nicht vermittelt, die Menge an Cu₂O jedoch wenig Einfluss auf die Ausbeute an **5.4.2-4aa** hat (Einträge 6 und 7). In einer Reaktion mit dem Kupfer-Katalysator und 1,10-Phenanthrolin wurden nur Spuren des *ortho*-arylierten Produkts **5.4.2-3aa** gebildet und Biaryl **5.4.2-4aa** wurde nicht detektiert (Eintrag 8). Dies ist vermutlich darauf zurückzuführen, dass der Ligand den Ruthenium-Katalysator inhibiert. Weiterhin erfolgte die Protodecarboxylierung bei späterer Zugabe des Liganden nur in geringem Maße (Einträge 9–11). Andere Decarboxylierungskatalysatoren wie CuBr und Ag₂O erwies sich als weniger geeignet (Einträge 12–15). Letztlich konnte die Ausbeute durch Erhöhung der Temperatur auf 190 °C gesteigert werden. Das gewünschte Produkt **5.4.2-4aa** wurde in einer Ausbeute von 51% neben 23% des nicht decarboxylierten Derivats **5.4.2-3aa** isoliert (Eintrag 16). Im Fall der *ortho*-Fluorbenzoesäure **5.4.2-1c** konnten 71% an **5.4.2-4ca** neben 13% an **5.4.2-3ca** erhalten werden (Eintrag 17).

Tabelle 30: Optimierung der sequenziellen ortho-Arylierung/Protodecarboxylierung.

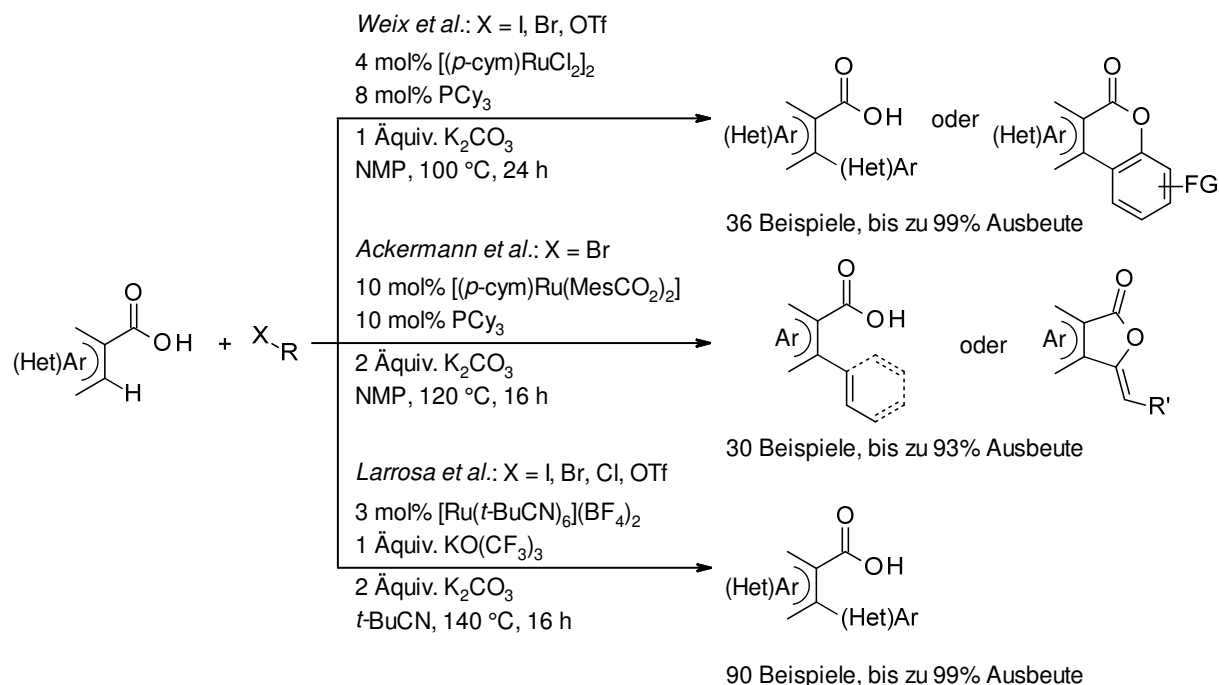


Eintrag	[M] (mol%)	T (°C)	N-Ligand	t (h)	5.4.2-3aa (%)	5.4.2-4aa (%)
1	Cu ₂ O (10)	100 → 170	-	18 + 12	76	9
2	"	170	-	18	70	10
3 ^[a]	"	100 → 180	-	18 + 12	87	4
4	"	180	-	18	41	46
5	-	"	-	"	73	10
6	Cu ₂ O (20)	"	-	"	37	51
7	Cu ₂ O (50)	"	-	"	40	44
8	Cu ₂ O (10)	"	1,10-Phen	"	Spuren	n.d.
9 ^[b]	"	100 → 180	"	18 + 12	77	9
10 ^[c]	"	"	"	"	87	Spuren
11 ^[c]	"	"	Pyridin	"	67	20
12	CuBr (20)	180	-	18	49	32
13	Ag ₂ O (10)	"	-	"	45	33
14 ^[d]	"	100 → 180	-	18 + 12	69	4
15	"	160	-	18	68	11
16	"	190	-	18	19 (23)	61 (54)
17 ^[e]	"	"	-	"	10 (13)	63 (71)

Reaktionsbedingungen: **5.4.2-1a** (0.5 mmol), **5.4.2-2a** (0.5 mmol), [(p-cym)RuCl₂]₂ (4 mol%), PEt₃ × HBF₄ (8 mol%), K₂CO₃ (1.1 Äquiv.), [M], N-Ligand (20 mol%), NMP (3 mL), 18 h gefolgt von 12 h jeweils bei der angegebenen Temperatur oder 18 h bei der angegebenen Temperatur. GC-Ausbeuten nach Veresterung mit K₂CO₃ (2 Äquiv.) und MeI (5 Äquiv.) in NMP und *n*-Tetradecan als interner Standard. Isolierte Ausbeuten in Klammern. [a] Cu₂O wurde nach 18 h zugesetzt. [b] Cu₂O und 1,10-Phen wurden nach 18 h zugesetzt. [c] N-Ligand wurden nach 18 h zugesetzt. [d] Ag₂O wurde nach 18 h zugesetzt. [e] 2-Fluorbenzoesäure (**5.4.2-1c**) statt **5.4.2-1a**.

5.4.3 Alternative Protokolle

Zeitgleich mit den zuvor beschriebenen Arbeiten publizierten die Gruppen um Weix, Ackermann und Larrosa ebenfalls Protokolle zur Ruthenium-katalysierten *ortho*-Arylierung von Benzoessäuren (Schema 44).^[216–218]



Schema 44: Alternative Protokolle zur Ruthenium-katalysierten *ortho*-Arylierung.

Die dort beschriebenen Katalysatorsysteme, die im Fall von Weix und Ackermann recht ähnlich zu unserem System sind, ermöglichen die vorliegende Transformation mit vergleichbarer Effizienz. Zudem ergänzen sie das Substratspektrum insbesondere um weitere (hetero-)aromatische Carbonsäuren und (Hetero-)Arylhalogenide sowie um Kupplungen mit Alkenyl- und Alkinylbromiden. Weiterhin wurde gezeigt, dass sich Aryltriflate ebenfalls unter den beschriebenen Bedingungen in befriedigenden Ausbeuten umsetzen lassen (PhOTf, 58% bzw. 57%).^[216,218] Ein Beispiel für die Kupplung eines Arylchlorids wurde lediglich in den Arbeiten von Larrosa beschrieben. Dabei konnten jedoch nur geringe Ausbeuten (PhCl, 13%) erzielt werden.^[218]

5.5 Decarboxylierende Mizoroki-Heck-Reaktion von Arylhalogeniden mit Zimtsäuren zur Synthese von 1,1-Diarylklenen

5.5.1 Hintergrund

1,1-Disubstituierte Alkene sind weit verbreitete Strukturuntereinheiten in einer Vielzahl an Naturstoffen oder biologisch aktiven Substanzen.^[219–224] Beispiele sind die aus *Emericella rugulosa* isolierbaren Prenylxanthone, die antimalariaaktiven 1,2,4-Trioxane sowie Bexaroten, ein Wirkstoff gegen Krebs (Abbildung 2).

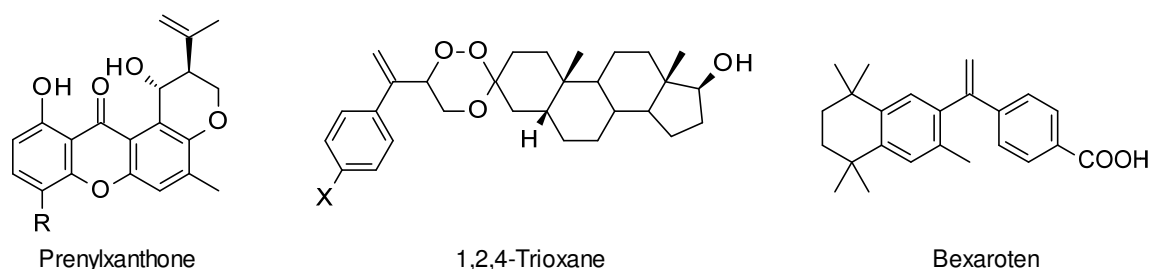
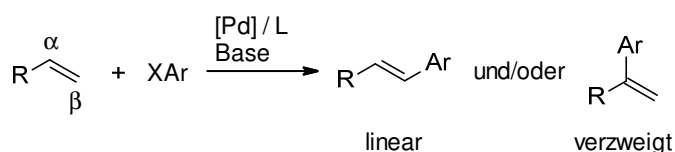


Abbildung 2: 1,1-Disubstituierte Alkene in Natur- und Wirkstoffen.

Eine attraktive Methode zur Darstellung solcher Strukturen stellt die Palladium-katalysierte Arylierung von Olefinen, die sogenannte Mizoroki-Heck-Reaktion, dar (Schema 45).^[225,226] Generell kann diese Reaktion zwei regioisomere Produkte hervorbringen, doch sind seit ihrer Entdeckung Anfang der 1970er Jahre enorme Fortschritte erzielt worden, sodass heute eine Vielzahl an Protokollen zur regioselektiven C–C-Bindungsknüpfung zur Verfügung steht.^[227–229]



Schema 45: Mizoroki-Heck-Reaktion.

Die selektive Synthese verzweigter (1,1-disubstituierter) Alkene gelingt beispielsweise ausgehend von elektronenreichen Vinylethern ($\text{R} = \text{OR}'$) oder Vinylamiden ($\text{R} = \text{N}(\text{COR}')\text{R}''$) und Arylhalogeniden oder -pseudohalogeniden.^[230–235] Alternativ ist dies auch ausgehend von Arylboronsäuren unter oxidativen Bedingungen möglich.^[236] Ebenso existieren redox-neutrale und oxidative Verfahren, die selektiv den Zugang zu verzweigten Alkenen ausgehend von einfachen Olefinen ($\text{R} = \text{Alkyl}$) gewährleisten.^[237–241] Dabei sind neben Palladium-katalysierten Reaktionen auch Nickel-katalysierte Varianten bekannt.^[242–244] Im Vergleich dazu reagieren Styrole ($\text{R} = \text{Ar}$) bevorzugt zu den linearen (1,2-disubstituierten) Produkten.^[228,229,245,246] So

existiert neben wenigen intramolekularen Varianten nur ein Protokoll,^[247,248] welches selektiv 1,1-Diarylalkene ausgehend von Styrolen zugänglich macht.^[249] Das Katalysatorsystem besteht aus Pd(dba)₂, dem sterisch anspruchsvollen Liganden 1,1'-Bis[di(1-naphthyl)phosphanyl]ferrocen (dnfpf) und Urotropin als Base. Als Elektrophile dienen Aryltriflate.

Einen alternativen Weg zu 1,1-Diarylalkenen würde sich über eine Heck-Reaktion von Zimtsäuren mit nachfolgender Protodecarboxylierung bieten. Damit würde man indirekt über eine Arylierung in β -Position zur Carboxygruppe, deren Durchführbarkeit bereits von Botella und Nájera demonstriert wurde,^[250] zum 1,1-diarylierten Produkt gelangen. Gemäß dem Fall, dass die Arylierung der Zimtsäure mit einer Aktivierung einhergeht, die eine Protodecarboxylierung begünstigt, sollte sich zudem ein Reaktionsmodus ähnlich dem von Carbonsäuren als abfallenden dirigierenden Gruppen realisieren lassen.

5.5.2 Selektivitätsumkehr in Heck-Reaktionen durch Carboxylate als abfallende dirigierende Gruppen

Um zu überprüfen, ob eine Arylierung der Zimtsäure in β -Position zu einer Aktivierung führt, die schließlich eine Decarboxylierung begünstigt, wurden zunächst Protodecarboxylierungsstudien durchgeführt. Dabei wurden Zimtsäure (**5.5.2-1a'**) und β -Tolylzimtsäure (**5.5.2-4aa**) jeweils bei verschiedenen Temperaturen in Gegenwart eines Kupfer-basierten Decarboxylierungskatalysators umgesetzt (Tabelle 31).

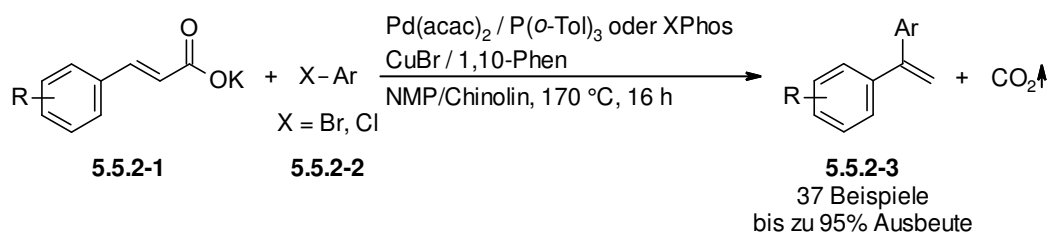
Tabelle 31: Protodecarboxylierungsstudien mit Zimtsäure und β -Tolylzimtsäure.

5.5.2-1a' oder 5.5.2-4aa		5.5.2-7a oder 5.5.2-3aa	
Eintrag	T (°C)	5.5.2-7a (R = H, %)	5.5.2-3aa (R = <i>p</i> -Tol %)
1	130	Spuren	95
2	140	31	93
3	150	63	91
4	170	70	99

Reaktionsbedingungen: **5.5.2-1a'** oder **5.5.2-4aa** (0.3 mmol), Cu₂O (5 mol%), 1,10-Phen (10 mol%), NMP (1 mL), 16 h. GC-Ausbeuten mit *n*-Tetradecan als interner Standard.

Die Experimente zeigten, dass β -Tolylzimtsäure unter den gewählten Bedingungen bereits bei 130 °C nahezu quantitativ protodecarboxyliert (Eintrag 1, R = *p*-Tol). Im Fall der Zimtsäure wurden hingegen nur Spuren des gewünschten Produkts detektiert und erst bei höheren Temperaturen waren bessere Umsätze zu verzeichnen (Einträge 1–4, R = H). Damit sollte es prinzipiell möglich sein, die Carboxygruppe als abfallende dirigierende Gruppe zu nutzen. Zudem sollte sich aufgrund dieser Reaktivitätsunterschiede eine decarboxylierende Kreuzkupplung der Zimtsäure^[64,83] weitestgehend unterbinden lassen, sofern die Heck-Reaktion letzterer mit vergleichsweise höherer Effizienz realisiert werden kann.

Basierend auf diesen Studien wurde ein bimetallisches Cu/Pd-Katalysatorsystem entwickelt, welches eine decarboxylierende Mizoroki-Heck-Reaktion von Zimtsäuren mit Arylhalogeniden zur Darstellung von 1,1-diarylierten Alkenen ermöglicht (Schema 46). Dabei dirigiert die Carboxylatgruppe die Palladium-katalysierte Arylierung in β -Position und wird anschließend rückstandslos über eine Kupfer-katalysierte Protodecarboxylierung entfernt. Somit fungiert die Carboxylatgruppe in dieser Transformation als abfallende dirigierende Gruppe und eröffnet einen Reaktionspfad, der die traditionellen 1,2-selektiven Heck-Reaktionen von Styrolen komplementiert.



Schema 46: Decarboxylierende Mizoroki-Heck-Reaktion von Zimtsäuren mit Arylhalogeniden.

Die Praktikabilität dieses Verfahrens wurde anhand der Synthese einer Vielzahl divers funktionalisierter 1,1-Diarylalkene in guten bis sehr guten Ausbeuten demonstriert. Zudem gelang die Kombination dieser Transformation mit einer klassischen Heck-Reaktion ausgehend von Methylacrylat zu einem praktischen Eintopf-Verfahren. Mit einer Reihe an Kontrollexperimenten konnte außerdem mehr Klarheit über den Mechanismus dieser Reaktion erhalten werden.

Beiträge der Autoren: Die Bearbeitung dieses Projekts erfolgte zusammen mit Herrn Jie Tang, der die initiale Katalysatoroptimierung vornahm. Herr Tang und ich stellten die Optimierungsarbeiten zusammen fertig und untersuchten die Anwendungsbreite gemeinschaftlich. Ich führte das Ligandenscreening für die Kupplung der Arylchloride sowie

die Protodecarboxylierungsexperimente aus, während Herr Tang die mechanistischen Studien durchführte. Das Eintopf-Verfahren wurde gleichberechtigt entwickelt. Das Manuskript wurde von Herrn Tang mit meiner Unterstützung verfasst und von Herrn Prof. Dr. L. J. Goossen überarbeitet. Herr Tang und ich werteten die analytischen Daten gemeinsam aus und erstellten die „Supporting Information“.

Die Protodecarboxylierungsstudien, die Katalysatoroptimierung, die Untersuchungen zur Anwendungsbreite, die Entwicklung des Eintopf-Verfahrens sowie die mechanistischen Studien sind in der nachfolgenden Publikation aufgeführt. Diese wurde in *Angewandte Chemie* veröffentlicht, für die vorliegende Arbeit angepasst und mit Erlaubnis des Verlags beigelegt:

"Reprinted (adapted) with permission from J. Tang, D. Hackenberger, L. J. Goossen, *Angew. Chem. Int. Ed.* **2016**, 55, 11296–11299: *Branched Arylalkenes from Cinnamates: Selectivity Inversion in Heck Reactions by Carboxylates as Deciduous Directing Groups*. Copyright 2016 WILEY-VCH Verlag GmbH & Co. KGaA, Weinheim."

JOHN WILEY AND SONS LICENSE TERMS AND CONDITIONS

This Agreement between Ms. Dagmar Hackenberger ("You") and John Wiley and Sons ("John Wiley and Sons") consists of your license details and the terms and conditions provided by John Wiley and Sons and Copyright Clearance Center.

License Number	4116360850664
License date	May 26, 2017
Licensed Content Publisher	John Wiley and Sons
Licensed Content Publication	Angewandte Chemie International Edition
Licensed Content Title	Branched Arylalkenes from Cinnamates: Selectivity Inversion in Heck Reactions by Carboxylates as Deciduous Directing Groups
Licensed Content Author	Jie Tang, Dagmar Hackenberger, Lukas J. Goossen
Licensed Content Date	Aug 3, 2016
Licensed Content Pages	4
Type of use	Dissertation/Thesis
Requestor type	Author of this Wiley article
Format	Print and electronic
Portion	Full article
Will you be translating?	No

Cross-Coupling

International Edition: DOI: 10.1002/anie.201605744
German Edition: DOI: 10.1002/ange.201605744

Branched Arylalkenes from Cinnamates: Selectivity Inversion in Heck Reactions by Carboxylates as Deciduous Directing Groups

Jie Tang, Dagmar Hackenberger, and Lukas J. Goossen*

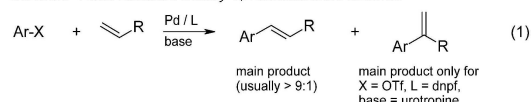
Abstract: A decarboxylative Mizoroki–Heck coupling of aryl halides with cinnamic acids has been developed in which the carboxylate group directs the arylation into its β -position before being tracelessly removed through protodecarboxylation. In the presence of a copper/palladium catalyst, both electron-rich and electron-deficient aryl bromides and chlorides bearing numerous functionalities were successfully coupled with broadly available cinnamates, with selective formation of 1,1-disubstituted alkenes. This reaction concept, in which the carboxylate acts as a deciduous directing group, ideally complements traditional 1,2-selective Heck reactions of styrenes.

1,1-Disubstituted alkenes are prevalent in natural^[1] and synthetic products^[2] with a wide spectrum of applications. Traditional syntheses of this substructure, such as Wittig or Peterson olefinations,^[3] arylations of alkynes,^[4] olefin metathesis,^[5] and transition-metal-catalyzed cross-coupling reactions of preformed α -metalated vinylarenes^[6] or 2-alkenyl electrophiles,^[7] are limited in scope, waste-intensive, and/or require multistep syntheses of starting materials.

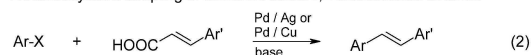
The selective synthesis of 1,1-diarylalkenes from widely available aryl (pseudo)halides by Heck-type reactions would be a welcome alternative.^[8] However, electronic and steric factors usually determine the regiochemical outcome of the carbopalladation for simple hydrocarbons,^[9–12] so that 1,2-diarylalkenes are obtained from styrenes [Scheme 1, Eq. (1)].^[13] Only in very few cases has this selectivity been successfully shifted towards the 1,1-diarylalkenes: Zou et al. reported that aryl triflates react with selected styrenes with formation of 1,1-diarylalkenes when using a urotropine base and the exceptionally bulky 1,1'-bis[di(1-naphthyl)phosphino]ferrocene (dnfpf) ligand.^[14]

As a result of the wealth of methods for their preparation, cinnamic acids are more widely available in greater structural diversity than styrenes, and are, thus, more attractive starting materials.^[15] In Heck coupling reactions with aryl halides, the carboxylate group should direct the carbopalladation into its β -position,^[16] thereby leading to the intermediate formation of diarylacrylic acids. Their in situ conversion into the desired

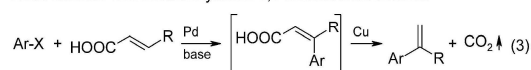
Mizoroki–Heck reaction: mostly 1,2-disubstituted alkenes



Decarboxylative coupling of cinnamic acids: 1,2-disubstituted alkenes



Heck reaction with decarboxylation: 1,1-disubstituted alkenes



Scheme 1. Synthesis of substituted alkenes.

1,1-diarylalkenes might be accomplished by an added copper or silver decarboxylation catalyst [Eq. (3)]. However, this attractive approach seemed to be out of reach, because the same catalyst combination is known to effectively promote a decarboxylative cross-coupling with formation of 1,2-diarylalkenes [Eq. (2)].^[17]

The utility of carboxylates as directing groups that are tracelessly cleavable in situ has been demonstrated for example, for C–H hydroxylations,^[18] amidations,^[19] (hydro)-arylations,^[20] and alkoxylation.^[21] Ideally, the carboxylate will act as a deciduous rather than a removable directing group, staying in place for only just as long as it is required to direct the metal catalyst into the α -position, but is destabilized by the newly formed bond to an extent that it is shed directly afterwards.

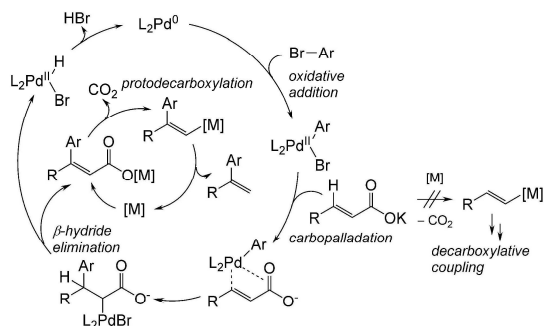
To switch the reaction of cinnamic acids with aryl halides from a decarboxylative coupling pathway to the desired Heck pathway, with the carboxylate acting as a deciduous directing group, it is critical to identify a catalyst system that a) promotes the carbopalladation of cinnamic acids with unprecedented efficiency and b) efficiently mediates the decarboxylation of diarylacrylic acids, but c) does not promote the decarboxylation of cinnamates, thus blocking decarboxylative cross-coupling (Scheme 2).

Prerequisite (a) already represented a substantial hurdle because the reactivity of the electron-rich cinnamate salts formed under the basic conditions of a Heck process is low. The Nájera and Fujiwara research groups found that cinnamic acids gave unsatisfactory yields (42%) even under optimized conditions, whereas the corresponding alkyl cinnamates reacted quantitatively.^[22] However, these literature results demonstrate that both oxidative addition and carbopalladation should take place at temperatures below those required for most decarboxylative coupling reactions.

To probe whether prerequisites (b) and (c) could be fulfilled, we performed decarboxylation studies, and were

[*] J. Tang, D. Hackenberger, Prof. Dr. L. J. Goossen
FB Chemie-Organische Chemie
Technische Universität Kaiserslautern
Erwin-Schrödinger-Strasse, Geb. 54
67663 Kaiserslautern (Germany)
E-mail: goossen@chemie.uni-kl.de
Homepage: <http://www.chemie.uni-kl.de/goossen>

Supporting information and the ORCID identification number(s) for the author(s) of this article can be found under <http://dx.doi.org/10.1002/anie.201605744>.



Scheme 2. Mechanistic outline for the envisioned process.

delighted to find that an additional aryl group strongly activates the substrates towards CO_2 extrusion. Thus, β -tolylcinnamic acid underwent almost quantitative protodecarboxylation at 130°C in the presence of a Cu_2O catalyst, whereas under the same conditions, cinnamic acid showed $<5\%$ conversion after 16 h (see Table S1 in the Supporting Information).

These preliminary experiments served to define a starting point for the rational development of a catalyst. We chose the reaction of potassium cinnamate **1a** with 4-bromotoluene (**2a**) as a model to systematically investigate the influence of Heck and decarboxylation catalysts on the reaction outcome under various conditions (Table 1). Subjecting substrates **1a** and **2a** to classical Mizoroki–Heck conditions (Table 1, entry 1) led to only low conversion being observed, mostly to the non-decarboxylated Heck product **4aa**, along with decarboxylative cross-coupling product **5aa**. However, when copper(I) bromide was added, the selectivity for the branched product **4aa** increased sharply, which indicates that the soft Lewis acid CuBr promotes the carbometalation step more strongly than the decarboxylation (entry 2). The addition of Lewis acids, such as $\text{Sc}(\text{OTf})_3$, facilitated the Heck coupling reaction even more strongly, but the selectivity was lower (entries 2 and 3). This finding suggests that the role of the copper is mainly that of a soft Lewis acid. Lower yields were observed starting from preformed copper cinnamate, which speaks against the intermediacy of these compounds in the transformation (entry 4). In the presence of Ag_2CO_3 , **5aa** was formed as the main product (entry 5). Increasing the temperature led to preferential formation of decarboxylated product **3aa** over **4aa**, without reducing the selectivity for the branched over the linear product **5aa** (entries 6 and 7).

Systematic variation of the phosphine ligand revealed that the moderately electron-donating, sterically demanding ligand tri-*o*-tolylphosphine was most effective and gave greater than 10:1 selectivity for **3aa** at full conversion (entries 8–12). $\text{Pd}(\text{acac})_2$ was found to be the optimal Pd precursor (entries 13–16). Among the Cu sources, copper halides and CuBr , in particular, were most effective (entries 17 and 18). A solvent mixture of NMP and quinoline gave the best results (entries 19 and 20).

The addition of potassium acetate is required when starting directly from cinnamic acid, whereas stronger bases retard the reaction (entries 21–23). Control experiments

Table 1: Optimization of the reaction conditions.^[a]

		[Pd] / Ligand		[M] / phen		Yield [%]		
		1a		2a		3aa	4aa	5aa
Entry	[Pd]	Ligand	[M]			3aa	4aa	5aa
1 ^[b]	$\text{Pd}(\text{acac})_2$	PPh_3	–			4	12	10
2 ^[b]	$\text{Pd}(\text{acac})_2$	PPh_3	CuBr			2	23	4
3 ^[b]	$\text{Pd}(\text{acac})_2$	PPh_3	$\text{Sc}(\text{OTf})_3$			6	40	12
4 ^[b,c]	$\text{Pd}(\text{acac})_2$	PPh_3	–			5	<1	<1
5 ^[b]	$\text{Pd}(\text{acac})_2$	PPh_3	Ag_2CO_3			6	<1	12
6 ^[d]	$\text{Pd}(\text{acac})_2$	PPh_3	CuBr			28	9	7
7	$\text{Pd}(\text{acac})_2$	PPh_3	CuBr			73	<1	12
8	$\text{Pd}(\text{acac})_2$	Cy_3P	CuBr			76	<1	12
9	$\text{Pd}(\text{acac})_2$	(<i>p</i> -tol) $_3\text{P}$	CuBr			76	<1	14
10	$\text{Pd}(\text{acac})_2$	BINAP	CuBr			78	<1	13
11	$\text{Pd}(\text{acac})_2$	Johnphos	CuBr			77	<1	11
12	$\text{Pd}(\text{acac})_2$	(<i>o</i> -tol) $_3\text{P}$	CuBr			92	<1	8
13	PdCl_2	(<i>o</i> -tol) $_3\text{P}$	CuBr			83	<1	13
14	PdBr_2	(<i>o</i> -tol) $_3\text{P}$	CuBr			82	<1	12
15	$\text{Pd}(\text{TFA})_2$	(<i>o</i> -tol) $_3\text{P}$	CuBr			86	<1	14
16	$\text{Pd}(\text{dba})_2$	(<i>o</i> -tol) $_3\text{P}$	CuBr			88	<1	12
17	$\text{Pd}(\text{acac})_2$	(<i>o</i> -tol) $_3\text{P}$	CuCl			90	<1	10
18	$\text{Pd}(\text{acac})_2$	(<i>o</i> -tol) $_3\text{P}$	Cu_2O			75	<1	10
19 ^[e]	$\text{Pd}(\text{acac})_2$	(<i>o</i> -tol) $_3\text{P}$	CuBr			25	<1	11
20 ^[f]	$\text{Pd}(\text{acac})_2$	(<i>o</i> -tol) $_3\text{P}$	CuBr			42	<1	7
21 ^[g]	$\text{Pd}(\text{acac})_2$	(<i>o</i> -tol) $_3\text{P}$	CuBr/KOAc			88	<1	12
22 ^[g]	$\text{Pd}(\text{acac})_2$	(<i>o</i> -tol) $_3\text{P}$	$\text{CuBr/K}_2\text{CO}_3$			43	<1	15
23 ^[g]	$\text{Pd}(\text{acac})_2$	(<i>o</i> -tol) $_3\text{P}$	$\text{CuBr/K}_2\text{CO}_3$			<1	<1	<1
24	$\text{Pd}(\text{acac})_2$	(<i>o</i> -tol) $_3\text{P}$	–			6	<1	16
25	–	–	CuBr			<1	<1	<1

[a] Reaction conditions: **1a** (0.60 mmol), **2a** (0.5 mmol), [M] (10 mol %), 1,10-phenanthroline (10 mol %), [Pd] (2 mol %), P ligand (5 mol %), 3 mL solvent (NMP/quinoline (1:1)), 170°C , 16 h. Yields were determined by GC analysis after esterification with MeI using *n*-tetradecane as an internal standard. For abbreviations see Ref. [23]. [b] 130°C .

[c] Copper cinnamate was used instead of **1a**. [d] 150°C . [e] In NMP.

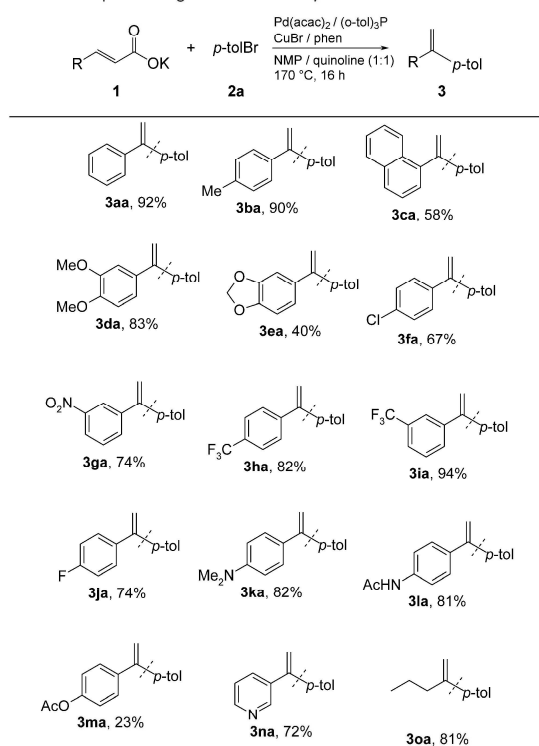
[f] In NMP/mesitylene (1:1). [g] Starting from cinnamic acid.

confirmed that neither the Pd nor the Cu catalyst alone are able to mediate this transformation (entries 24 and 25).

We next investigated the scope of the optimized procedure (2 mol % $\text{Pd}(\text{acac})_2$, 5 mol % (*o*-tol) $_3\text{P}$, 5 mol % Cu_2O , 10 mol % 1,10-phenanthroline, NMP/quinoline (1:1), 170°C , 16 h) with regard to the α,β -unsaturated carboxylic acids.

Both electron-rich and electron-poor cinnamic acids reacted smoothly with 4-bromotoluene (**2a**; Table 2). Common functionalities, such as halo, ester, ether, carbonyl, and even nitro and amino groups, were tolerated. The reaction also proceeded well with heterocyclic and alkyl-substituted allylic acids.

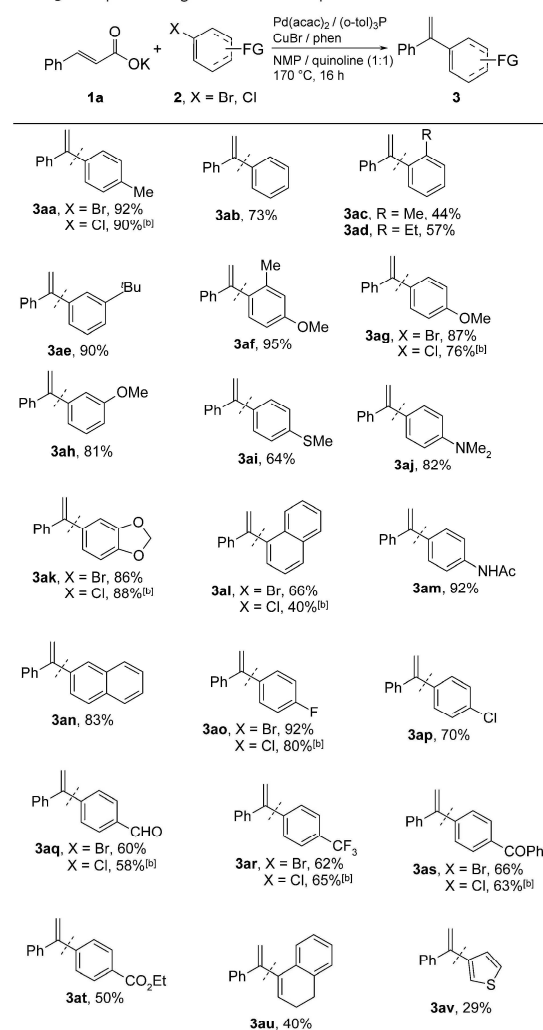
The reaction is also widely applicable with regard to the electrophilic coupling partner (Table 3). *ortho*-, *meta*-, and *para*-substituted aryl bromides bearing sensitive functionalities including ether, ester, carbonyl, thioether, and tertiary amino groups were successfully converted. Besides aryl bromides, alkenyl and heteroaryl bromides were successfully converted, although in somewhat lower yields. Changing the ligand to XPhos led to less expensive, but also less reactive, aryl chlorides also being converted in high yields.

Table 2: Scope with regard to the carboxylates.^[a]


[a] Reaction conditions: **1** (1.20 mmol), **2a** (1.00 mmol), CuBr (10 mol %), 1,10-phenanthroline (10 mol %), Pd(acac)₂ (2 mol %), (o-tol)₃P (5 mol %), 3 mL of solvent (NMP/quinoline (1:1)), 170 °C, 16 h. Yields of isolated products.

The new decarboxylative Heck process was successfully combined with a traditional Heck reaction into a convenient one-pot synthesis of unsymmetrically substituted 1,1-diarylalkenes from two different aryl bromides and methyl acrylate. In the first step, a cinnamate salt was synthesized from the corresponding aryl bromide and methyl acrylate by a Mizoroki-Heck reaction followed by hydrolysis of the methyl cinnamate. Subsequently, without solvent change or isolation of intermediates, a decarboxylative Heck coupling reaction furnishes the 1,1-diarylethylene in 62 % yield (Scheme 3).

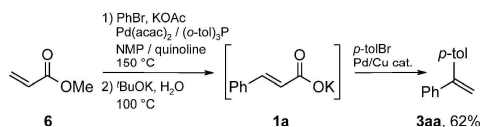
A series of experiments was performed to shed more light on the reaction mechanism (see the Supporting Information). The reaction occurred smoothly in the presence of the radical scavenger 2,2,6,6-tetramethylpiperidinyloxy (TEMPO), thus suggesting that neither coupling nor decarboxylation proceed through a radical pathway.^[24] The reaction of styrene with 4-bromotoluene (**2a**) yielded the linear product **4aa** with high selectivity, which rules out a reaction pathway involving protodecarboxylation followed by a Heck reaction. When the reaction was performed with the deuterium-labeled starting material potassium (*E*)-3-(3,4-dimethoxyphenyl)-2-propenoate-3-*d* (**D-1d**), only 20 % of the deuterium was incorporated in the original position of the carboxylate group. This

 Table 3: Scope with regard to the electrophiles.^[a]


[a] Reaction conditions: **1a** (1.20 mmol), **2** (1.00 mmol), CuBr (10 mol %), 1,10-phenanthroline (10 mol %), Pd(acac)₂ (2 mol %), (o-tol)₃P (5 mol %), 3 mL of solvent (NMP/quinoline (1:1)), 170 °C, 16 h. Yields of isolated products. [b] **1a** (0.60 mmol), **2** (0.5 mmol), CuBr (10 mol %), 1,10-phenanthroline (10 mol %), Pd(acac)₂ (2 mol %), XPhos (5 mol %), 3 mL of solvent (NMP/quinoline (1:1)), 170 °C, 16 h. Yields of isolated products. FG = functional group.

indicates that the Heck coupling and decarboxylation steps occur in a separate rather than concerted fashion.

In conclusion, the decarboxylative Heck reaction disclosed herein opens up a convenient route to the synthesis of unsymmetrical 1,1-disubstituted alkenes from widely available precursors. Key advantages are the good regiochemical control, which is complementary to that of traditional Heck reactions, the use of cinnamates as the source of the vinyl group, and the excellent functional group tolerance. In this process, the carboxylate controls the regiochemistry of C–C



Scheme 3. One-pot synthesis of 1,1-diarylethenes from methyl acrylate.

bond formation and is subsequently shed, thus acting as a deciduous directing group.

Acknowledgments

We thank the DFG (SFB/TRR88 “3MET”), the Chinese Scholarship Council (fellowship to J.T.), and the Stipendienstiftung Rheinland-Pfalz (fellowship to D.H.) for financial support.

Keywords: alkenes · carboxylic acids · copper · Heck reaction · palladium

How to cite: *Angew. Chem. Int. Ed.* **2016**, *55*, 11296–11299
Angew. Chem. **2016**, *128*, 11466–11470

- [1] a) P. Moosophon, S. Kanokmedhakul, K. Kanokmedhakul, K. Soyong, *J. Nat. Prod.* **2009**, *72*, 1442; b) V. Rukachaisirikul, A. Rodglin, Y. Sukpondma, S. Phongpaichit, J. Buatong, J. Sakayaroj, *J. Nat. Prod.* **2012**, *75*, 853; c) M. S. Ali, S. Mahmud, S. Perveen, V. U. Ahmad, G. H. Rizwani, *Phytochemistry* **1999**, *50*, 1385.
- [2] a) H. C. Kolb, M. S. VanNieuwenhze, K. B. Sharpless, *Chem. Rev.* **1994**, *94*, 2483; b) C. Singh, M. Hassam, V. P. Verma, A. S. Singh, N. K. Naikade, S. K. Puri, P. R. Maulik, R. Kant, *J. Med. Chem.* **2012**, *55*, 10662; c) S. P. Cook, A. Polara, S. J. Danishefsky, *J. Am. Chem. Soc.* **2006**, *128*, 16440; d) S. Poplata, A. Tröster, Y.-Q. Zou, T. Bach, *Chem. Rev.* **2016**, DOI: 10.1021/acs.chemrev.5b00723; e) S. J. Roseblade, A. Pfaltz, *Acc. Chem. Res.* **2007**, *40*, 1402.
- [3] a) B. E. Maryanoff, A. B. Reitz, *Chem. Rev.* **1989**, *89*, 863; b) D. J. Peterson, *J. Org. Chem.* **1968**, *33*, 780.
- [4] a) C. H. Oh, H. H. Jung, K. S. Kim, N. Kim, *Angew. Chem. Int. Ed.* **2003**, *42*, 805; *Angew. Chem.* **2003**, *115*, 829; b) D. P. Ojha, K. R. Prabhu, *Org. Lett.* **2016**, *18*, 432.
- [5] a) R. H. Grubbs, S. Chang, *Tetrahedron* **1998**, *54*, 4413; b) A. Fürstner, *Angew. Chem. Int. Ed.* **2000**, *39*, 3012; *Angew. Chem.* **2000**, *112*, 3140.
- [6] a) G. A. Molander, B. J. Rahn, D. C. Shubert, S. E. Bonde, *Tetrahedron Lett.* **1983**, *24*, 5449; b) A. Gavryushin, C. Kofink, G. Manolikakes, P. Knochel, *Tetrahedron* **2006**, *62*, 7521.
- [7] a) C.-L. Sun, Y. Wang, X. Zhou, Z.-H. Wu, B.-J. Li, B.-T. Guan, Z.-J. Shi, *Chem. Eur. J.* **2010**, *16*, 5844; b) J. Tang, L. J. Gooßen, *Org. Lett.* **2014**, *16*, 2664; c) A. L. Hansen, J.-P. Ebran, T. M. Gøsgsig, T. Skrydstrup, *Chem. Commun.* **2006**, 4137.
- [8] a) R. F. Heck, *Acc. Chem. Res.* **1979**, *12*, 146; b) W. Cabri, I. Candiani, *Acc. Chem. Res.* **1995**, *28*, 2.
- [9] a) M. Oestreich, *The Mizoroki-Heck Reaction*, Wiley, Hoboken, **2009**; b) I. P. Beletskaya, A. V. Cheprakov, *Chem. Rev.* **2000**, *100*, 3009.
- [10] a) W. Cabri, I. Candiani, A. Bedeschi, R. Santi, *J. Org. Chem.* **1992**, *57*, 3558; b) M.-P. Denieul, T. Skrydstrup, *Tetrahedron Lett.* **1999**, *40*, 4901; c) D. Tselikhovsky, S. L. Buchwald, *J. Am. Chem. Soc.* **2010**, *132*, 14048; d) L. F. Tietze, S. G. Stewart, M. E. Polomska, A. Modi, A. Zeeck, *Chem. Eur. J.* **2004**, *10*, 5233.
- [11] For Heck reactions or vinylations of other substrates that selectively yield 1,1-disubstituted alkenes, see a) Y. Yang, K. Cheng, Y. Zhang, *Org. Lett.* **2009**, *11*, 5606; b) C. Zheng, S. S. Stahl, *Chem. Commun.* **2015**, *51*, 12771; c) C. Zheng, D. Wang, S. S. Stahl, *J. Am. Chem. Soc.* **2012**, *134*, 16496; d) L. Qin, X. Ren, Y. Lu, Y. Li, J. (Steve) Zhou, *Angew. Chem. Int. Ed.* **2012**, *51*, 5915; *Angew. Chem.* **2012**, *124*, 6017; e) L. Qin, H. Hirao, J. (Steve) Zhou, *Chem. Commun.* **2013**, *49*, 10236; f) J. Ruan, J. Xiao, *Acc. Chem. Res.* **2011**, *44*, 614, g) J. Ruan, J. A. Iggo, N. G. Berry, J. Xiao, *J. Am. Chem. Soc.* **2010**, *132*, 16689; h) T. M. Gøsgsig, A. T. Lindhardt, M. Dekhane, J. Grouleff, T. Skrydstrup, *Chem. Eur. J.* **2009**, *15*, 5950; i) P. Hu, J. Kan, W. Su, M. Hong, *Org. Lett.* **2009**, *11*, 2341.
- [12] a) L. J. Gooßen, J. Paetzold, L. Winkel, *Synlett* **2002**, 1721; b) L. J. Gooßen, J. Paetzold, *Angew. Chem. Int. Ed.* **2002**, *41*, 1237; *Angew. Chem.* **2002**, *114*, 1285.
- [13] a) H. A. Dieck, R. F. Heck, *J. Am. Chem. Soc.* **1974**, *96*, 1133; b) A. F. Littke, G. C. Fu, *J. Am. Chem. Soc.* **2001**, *123*, 6989.
- [14] Y. Zou, L. Qin, X. Ren, Y. Lu, Y. Li, J. (Steve) Zhou, *Chem. Eur. J.* **2013**, *19*, 3504.
- [15] a) W. H. Perkin, *J. Chem. Soc.* **1868**, *21*, 181; b) W. H. Perkin, *J. Chem. Soc.* **1877**, *32*, 660; c) K. E. Kolb, K. W. Field, P. F. Schatz, *J. Chem. Educ.* **1990**, *67*, A304; d) Sigma Aldrich offers about 150 cinnamic acids, whereas only about 80 styrenes are available.
- [16] R. Giri, J.-Q. Yu, *J. Am. Chem. Soc.* **2008**, *130*, 14082.
- [17] a) L. J. Goossen, N. Rodríguez, B. Melzer, C. Linder, G. Deng, L. M. Levy, *J. Am. Chem. Soc.* **2007**, *129*, 4824; b) Z. Wang, Q. Ding, X. He, J. Wu, *Org. Biomol. Chem.* **2009**, *7*, 863; c) M. Yamashita, K. Hirano, T. Satoh, M. Miura, *Org. Lett.* **2010**, *12*, 592; d) L. J. Gooßen in *Inventing Reactions* (Ed.: L. J. Gooßen), Heidelberg, **2013**, pp. 121–141.
- [18] Y.-H. Zhang, J.-Q. Yu, *J. Am. Chem. Soc.* **2009**, *131*, 14654.
- [19] a) D. Lee, S. Chang, *Chem. Eur. J.* **2015**, *21*, 5364; b) K.-H. Ng, F.-N. Ng, W.-Y. Yu, *Chem. Commun.* **2012**, *48*, 11680.
- [20] a) Y. Zhang, H. Zhao, M. Zhang, W. Su, *Angew. Chem. Int. Ed.* **2015**, *54*, 3817; *Angew. Chem.* **2015**, *127*, 3888; b) J. Luo, S. Preciado, I. Larrosa, *J. Am. Chem. Soc.* **2014**, *136*, 4109; c) J. Cornella, M. Righi, I. Larrosa, *Angew. Chem. Int. Ed.* **2011**, *50*, 9429; *Angew. Chem.* **2011**, *123*, 9601; d) X. Qin, D. Sun, Q. You, Y. Cheng, J. Lan, J. You, *Org. Lett.* **2015**, *17*, 1762; e) H. A. Chiong, Q.-N. Pham, O. Daugulis, *J. Am. Chem. Soc.* **2007**, *129*, 9879; f) H. Gong, H. Zeng, F. Zhou, C.-J. Li, *Angew. Chem. Int. Ed.* **2015**, *54*, 5718; *Angew. Chem.* **2015**, *127*, 5810; g) K. M. Engle, T.-S. Mei, M. Wasa, J.-Q. Yu, *Acc. Chem. Res.* **2012**, *45*, 788; h) K. Ueura, T. Satoh, M. Miura, *Org. Lett.* **2007**, *9*, 1407; i) K. Ueura, T. Satoh, M. Miura, *J. Org. Chem.* **2007**, *72*, 5362; j) N. Y. P. Kumar, A. Bechtoldt, K. Raghuvanshi, L. Ackermann, *Angew. Chem. Int. Ed.* **2016**, *55*, 6929; *Angew. Chem.* **2016**, *128*, 7043; k) L. Huang, A. Biafora, G. Zhang, V. Bragioni, L. J. Gooßen, *Angew. Chem. Int. Ed.* **2016**, *55*, 6933; *Angew. Chem.* **2016**, *128*, 7047; l) L. Huang, D. Hackenberger, L. J. Gooßen, *Angew. Chem. Int. Ed.* **2015**, *54*, 12607; *Angew. Chem.* **2015**, *127*, 12798.
- [21] S. Bhadra, W. I. Dzik, L. J. Gooßen, *Angew. Chem. Int. Ed.* **2013**, *52*, 2959; *Angew. Chem.* **2013**, *125*, 3031.
- [22] a) L. Botella, C. Nájera, *J. Org. Chem.* **2005**, *70*, 4360; b) C. Jia, W. Lu, T. Kitamura, Y. Fujiwara, *Org. Lett.* **1999**, *1*, 2097.
- [23] phen = 1,10-phenanthroline; acac = acetylacetonate; BINAP = 2,2'-bis(diphenylphosphino)-1,1'-binaphthyl; Johnphos = (2-biphenyl)di-tert-butylphosphine; TFA = trifluoroacetate; dba = dibenzylideneacetone; NMP = N-methyl-2-pyrrolidone.
- [24] a) A. J. Borah, G. Yan, *Org. Biomol. Chem.* **2015**, *13*, 8094; b) J. Kan, S. Huang, J. Lin, M. Zhang, W. Su, *Angew. Chem. Int. Ed.* **2015**, *54*, 2199; *Angew. Chem.* **2015**, *127*, 2227.

Received: June 14, 2016

Published online: August 3, 2016

Ergänzend zu den im Manuskript beschriebenen Resultaten werden nachfolgend weitere Ergebnisse diskutiert.

Ligandenscreening für die Kupplung der Arylchloride

Im Anschluss an die in der Publikation beschriebenen Optimierungsarbeiten wurde überprüft, ob sich die Reaktion auf kostengünstigere aber auch unreaktivere Arylchloride übertragen lässt. Da sich unter den optimalen Bedingungen nur geringe Ausbeuten erzielen ließen (Tabelle 32, Eintrag 1), wurde erneut eine systematische Variation des Phosphanliganden durchgeführt. Dabei wurden elektronenreiche, sterisch anspruchsvolle Liganden vom Buchwald-Typ getestet, deren Effizienz in der Aktivierung von Arylchloriden bereits häufig demonstriert werden konnte.^[251] Die besten Resultate ließen sich mit dem Liganden XPhos erzielen (Eintrag 5). Wie der Publikation zu entnehmen ist, konnten unter diesen Bedingungen diverse Arylchloride mit Zimtsäure in guten bis sehr guten Ausbeuten zu den entsprechenden 1,1-Diarylalkenen umgesetzt werden.

Tabelle 32: Variation des Phosphanliganden in der Kupplung mit Arylchloriden.

$ \begin{array}{c} \text{Ph}-\text{CH}=\text{CH}-\text{C}(=\text{O})\text{OK} + \text{Cl}(p\text{-Tol}) \xrightarrow[\text{- CO}_2]{\begin{array}{l} \text{Pd}(\text{acac})_2 / P\text{-Ligand} \\ \text{CuBr} / 1,10\text{-Phen} \\ \text{NMP/Chinolin, 170 }^\circ\text{C, 16 h} \end{array}} \begin{array}{c} p\text{-Tol} \\ \\ \text{Ph}-\text{C}=\text{CH}_2 \end{array} + \text{Ph}-\text{CH}=\text{CH}-p\text{-Tol} \\ \text{5.5.2-1a} \quad \text{5.5.2-2a'} \quad \quad \quad \text{5.5.2-3aa} \quad \quad \text{5.5.2-5aa} \end{array} $			
Eintrag	P-Ligand	5.5.2-3aa (%)	5.5.2-5aa (%)
1	P(<i>o</i> -Tol) ₃	6	n.d.
2	JohnPhos	19	Spuren
3	SPhos	68	14
4	DavePhos	19	Spuren
5	XPhos	79	19
6	<i>t</i> -BuXPhos	20	Spuren

Reaktionsbedingungen: **5.5.2-1a** (0.60 mmol), **5.5.2-2a'** (0.50 mmol), CuBr (10 mol%), 1,10-Phen (10 mol%), Pd(acac)₂ (2 mol%), P-Ligand (5 mol%), NMP/Chinolin (1:1, 3mL), 170 °C, 16 h. GC-Ausbeuten mit *n*-Tetradecan als interner Standard.

Entwicklung des Eintopf-Verfahrens

Zur Realisierung des Eintopf-Verfahrens wurde zunächst getestet, ob sich Methylacrylat (**5.5.2-6**) unter Bedingungen möglichst ähnlich zu denen der Reaktion von Zimtsäuren mit Arylbromiden in einer Heck-Reaktion umsetzen lässt. Dies war insofern wichtig, als dass für

das Eintopf-Verfahren beispielsweise möglichst auf einen Lösungsmittelwechsel verzichtet werden sollte. So wurde Methylacrylat (**5.5.2-6**) in Gegenwart des $\text{Pd}(\text{acac})_2/\text{P}(o\text{-Tol})_3$ -Katalysators in NMP/Chinolin bei 150 °C unter Variation der Base mit Brombenzol (**5.5.2-2b**) umgesetzt (Tabelle 33).

Tabelle 33: Reaktion von Methylacrylat mit Brombenzol unter Variation der Base.

$ \begin{array}{c} \text{O} \\ \parallel \\ \text{CH}_2=\text{CH}-\text{C}-\text{OMe} \end{array} + \text{BrPh} \xrightarrow[\text{NMP/Chinolin, 150 °C, 16 h}]{\text{Pd}(\text{acac})_2 / \text{P}(o\text{-Tol})_3, \text{Base}} \begin{array}{c} \text{O} \\ \parallel \\ \text{Ph}-\text{CH}=\text{CH}-\text{C}-\text{OMe} \end{array} + \begin{array}{c} \text{Ph} \quad \text{O} \\ \diagup \quad \parallel \\ \text{Ph}-\text{C}=\text{CH}-\text{C}-\text{OMe} \end{array} $			
5.5.2-6	5.5.2-2b	5.5.2-1a''	5.5.2-4ab
Eintrag	Base	5.5.2-1a'' (%)	5.5.2-4ab (%)
1	KOt-Bu	n.d.	n.d.
2	NaOMe	n.d.	n.d.
3	KOH	39	4
4	K ₂ CO ₃	79	5
5	MeN(Cy) ₂	67	n.d.
6	KOAc	75	3
7 ^[a]	"	76	4

Reaktionsbedingungen: **5.5.2-6** (0.525 mmol), **5.5.2-2b** (0.50 mmol), $\text{Pd}(\text{acac})_2$ (2 mol%), $\text{P}(o\text{-Tol})_3$ (5 mol%), Base (1 Äquiv.), NMP/Chinolin (1:1, 3 mL), 150 °C, 16 h. GC-Ausbeuten mit *n*-Tetradecan als interner Standard. [a] Base (1.2 Äquiv.).

Während mit Alkoholatbasen keine Produktbildung beobachtet wurde (Einträge 1 und 2), konnten in Gegenwart von KOH oder *N,N*-Dicyclohexylmethylamin moderate Ausbeuten erzielt werden (Einträge 3 und 5). Die besten Resultate wurden mit K₂CO₃ und KOAc erzielt. Dabei wurde das gewünschte Produkt **5.5.2-1a''** in guten Ausbeuten neben geringen Mengen an diaryliertem Methylacrylat **5.5.2-4ab** detektiert (Einträge 4, 6 und 7).

Da aus den vorhergehenden Studien bekannt war, dass die decarboxylierende Heck-Reaktion ausgehend von der freien Zimtsäure in Gegenwart von K₂CO₃ gehemmt wird, wurde für die nachfolgende Kombination beider Arylierungen zum sequenziellen Eintopf-Verfahren die Variante in Gegenwart von KOAc gewählt. Aus einer stichprobenartigen Prüfung anderer Palladium-Quellen und Phosphanliganden ging zudem hervor, dass diese allesamt ähnliche Resultate liefern (Tabelle 34). Daher wurde das $\text{Pd}(\text{acac})_2/\text{P}(o\text{-Tol})_3$ -System beibehalten. Verknüpft wurden beide Verfahren durch die Hydrolyse des in der ersten Synthesestufe gebildeten Zimtsäuremethylesters in Gegenwart von KOt-Bu.

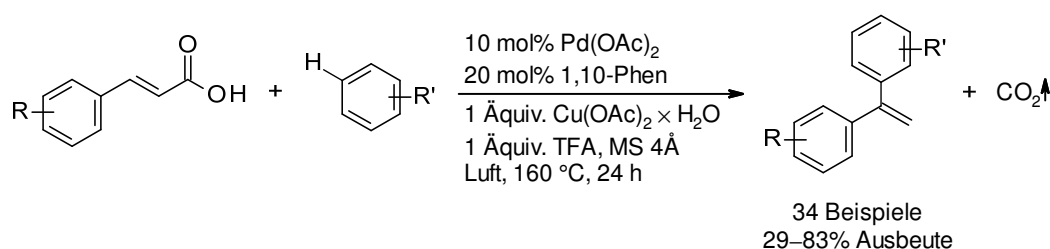
Tabelle 34: Variation der Palladium-Quelle und des Liganden.

$ \begin{array}{c} \text{CH}_2=\text{CH}-\text{C}(=\text{O})\text{OMe} + \text{BrPh} \xrightarrow[\text{NMP/Chinolin, 150 }^\circ\text{C, 16 h}]{[\text{Pd}] / P\text{-Ligand, KOAc}} \\ \text{5.5.2-6} \quad \text{5.5.2-2b} \quad \quad \quad \text{5.5.2-1a''} \quad \quad \text{5.5.2-4ab} \end{array} $				
Eintrag	[Pd]	P-Ligand	5.5.2-1a'' (%)	5.5.2-4ab (%)
1	Pd(acac) ₂	P(<i>o</i> -Tol) ₃	75	3
2	Pd(OAc) ₂	"	76	2
3	PdCl ₂	"	78	Spuren
4	Pd(dba) ₂	"	73	"
5	Pd(acac) ₂	PPh ₃	74	"
6	"	P(<i>p</i> -Tol) ₃	77	"

Reaktionsbedingungen: **5.5.2-6** (0.525 mmol), **5.5.2-2b** (0.50 mmol), [Pd] (2 mol%), P-Ligand (5 mol%), KOAc (1 Äquiv.), NMP/Chinolin (1:1, 3 mL), 150 °C, 16 h. GC-Ausbeuten mit *n*-Tetradecan als interner Standard.

5.5.3 1,1-Diarylalkene aus Zimtsäuren und Arenen

Kurz nach Veröffentlichung dieser Arbeiten publizierten Maiti und Mitarbeiter ein konzeptionell ähnliches Protokoll zur Darstellung von 1,1-Diarylalkenen ausgehend von Zimtsäuren und Arenen (Schema 47).^[252] Dabei handelt es sich um eine Fujiwara-Moritani-Reaktion,^[253,254] also eine dehydrierende Heck-Reaktion unter oxidativen Bedingungen, mit anschließender Protodecarboxylierung.



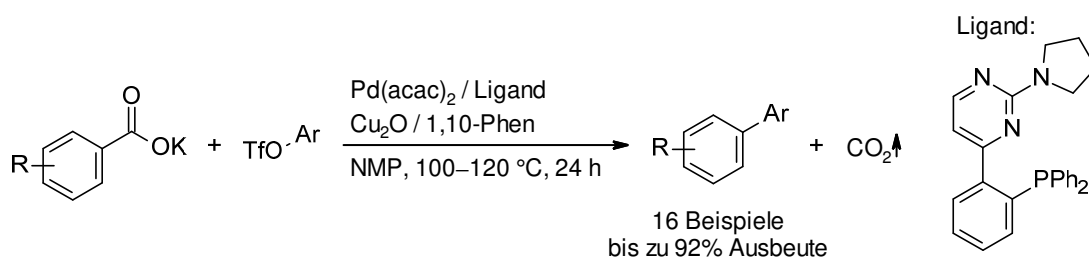
Schema 47: 1,1-Diarylalkensynthese nach Maiti et al.

Zwar bietet diese Variante den Vorteil, dass sie auf einer nachhaltigeren Funktionalisierung zweier C–H-Bindungen ohne Präfunktionalisierung beruht, doch führt die Umsetzung in vielen Fällen aufgrund der geringen Selektivität der C–H-Aktivierung zu Regioisomerengemischen. Zudem sind vergleichsweise hohe Katalysatorbeladung und stöchiometrische Kupfermengen notwendig.^[252]

6 Zusammenfassung und Ausblick

Im Rahmen dieser Arbeit wurden neue nachhaltige Methoden zur selektiven C–C-Bindungsknüpfung ausgehend von Carbonsäuren entwickelt. Dabei wurden insbesondere die Reaktionskonzepte der decarboxylierenden Biarylsynthese sowie der Carboxylat-dirigierten Arylierung verfolgt.

Geleitet von neuen Erkenntnissen aus detaillierten DFT-Studien wurde im ersten Projekt ein Katalysatorsystem entwickelt, welches die Kupfer/Palladium-katalysierte decarboxylierende Kreuzkupplung erstmals bei nur 100–120 °C ermöglicht (Schema 48). Aus den DFT-Studien ging hervor, dass für aktivierte Benzoate die Transmetallierung geschwindigkeitsbestimmend ist. Ferner wurde gezeigt, dass diesem Schritt die entropisch ungünstige Bildung eines Cu–Pd-Addukts vorausgeht, welche die Gesamtaktivierungsbarriere maßgeblich beeinflusst. Dies führte zur Voraussage, dass mit bidentate *P,N*-Liganden, die die Katalysatormetalle verbrückend koordinieren können, eine Verbesserung der Transmetallierung erzielt und so die Reaktionstemperatur herabgesetzt werden kann. Daraus ergab sich das Design des neuen Katalysatorsystems unter Verwendung der Aminopyrimidinylphosphanliganden, mit dem die Reaktionstemperatur im Vergleich zu ursprünglichen Protokollen bemerkenswerterweise um mehr als 50 °C abgesenkt werden konnte. Die Praktikabilität des neuen Katalysatorsystems wurde anhand der Synthese einer Vielzahl an Biarylen ausgehend von *ortho*-Nitrobenzoaten und Aryltriflaten demonstriert. Umfangreiche ESI-MS-Studien lieferten zudem deutliche Hinweise darauf, dass der verwendete Ligand tatsächlich bimetallische Kupfer/Palladium-Spezies ausbilden kann.

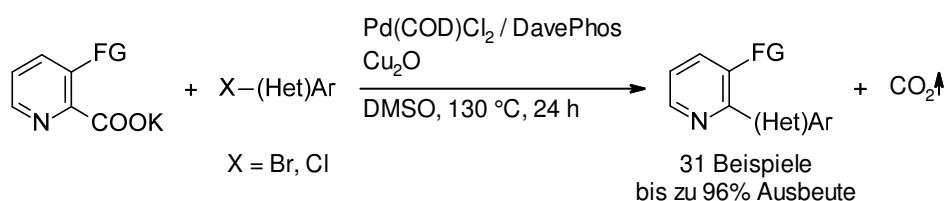


Schema 48: Cu/Pd-Katalysierte decarboxylierende Kreuzkupplung mit bidentaten Liganden.

Das rationale Design solcher effizienten Katalysatorsysteme, die die decarboxylierende Kreuzkupplung unter deutlich milderen Bedingungen ermöglichen, ist ein Schlüssel, um dieses Reaktionskonzept als Alternative zu klassischen Kreuzkupplungen zu etablieren. In zukünftigen Arbeiten könnten verbesserte Ligandensysteme entwickelt werden, um beispielsweise auch Arylhalogenide bei diesen Reaktionstemperaturen effizient mit

Carbonsäuren zu kuppeln. Daneben sollten leistungsstärkere Decarboxylierungskatalysatoren kombiniert mit den innovativen *P,N*-Liganden abermals Fortschritte hin zu niedrigeren Reaktionstemperaturen gewährleisten.

In einem zweiten Projekt wurden decarboxylierende Kreuzkupplungen mit einem der anspruchsvollsten Substrate für diese Transformation, der Pyridin-2-carbonsäure, untersucht. Studien zur Protodecarboxylierung zeigten, dass diese Reaktion von einer parallel zur Metallkatalysierten Reaktion ablaufenden, Metall-freien Variante dominiert wird. Während die Protodecarboxylierung der freien Säure schon bei einer Temperatur von 120 °C auftrat, war für die Umsetzung des entsprechenden Kaliumsalzes in der decarboxylierenden Kreuzkupplung eine Reaktionstemperatur von 190 °C notwendig. Das Kupplungsprodukt konnte nur in moderaten Ausbeuten erhalten werden und als unerwünschte Nebenreaktionen wurde hauptsächlich die Protodecarboxylierung sowie eine Arylierung durch den verwendeten Phosphanliganden beobachtet. Der Schlüssel zum Erfolg war schließlich die Einführung eines Fluorsubstituenten in *ortho*-Position zur Carboxygruppe der Pyridin-2-carbonsäure, welcher ebenso wie im Fall von Benzoesäuren einen aktivierenden Effekt ausübt. Daraufhin gelang es, ein bimetallisches Kupfer/Palladium-Katalysatorsystem zu entwickeln, welches die decarboxylierende Kreuzkupplung 3-substituierter Picolinate mit Aryl- und Heteroarylhalogeniden unter äußerst milden Bedingungen effizient ermöglicht. Die Anwendungsbreite des neuen Protokolls wurde anhand der Synthese zahlreicher Arylpyridine erfolgreich demonstriert (Schema 49).

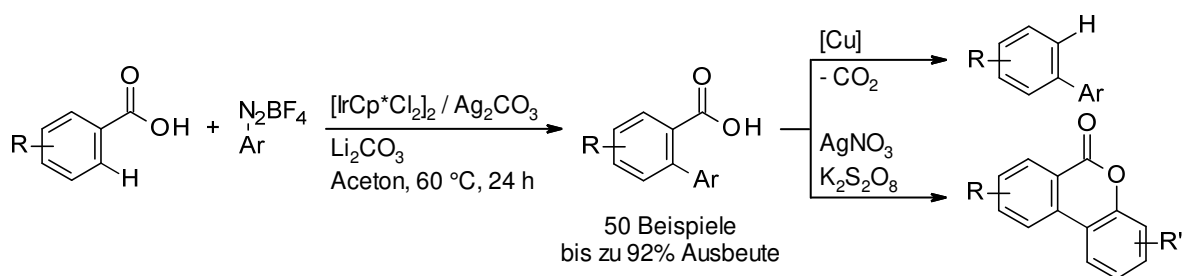


Schema 49: Decarboxylierende Kreuzkupplung 3-substituierter Picolinate.

Eine effiziente decarboxylierende Kreuzkupplung dieser Substrate macht interessante Molekülstrukturen auf einem nachhaltigen Weg zugänglich. Um zukünftig das volle Spektrum an Pyridin-2-carbonsäuren, insbesondere nicht-*ortho*-substituierte Vertreter, unter milden Bedingungen in hohen Ausbeuten kuppeln zu können, ist eine ganzheitliche Katalysatoroptimierung notwendig, die insbesondere darauf abzielt, die unerwünschten Nebenreaktionen zu unterbinden. Neue maßgeschneiderte Ligandensysteme könnten auch in diesem Fall ein vielversprechender Ansatzpunkt sein. Ein leistungsstarker Decarboxylierungskatalysator kombiniert mit einem darauf abgestimmten

Kreuzkupplungskatalysator könnte dann eine effiziente Umsetzung bei möglichst milden Reaktionstemperaturen gewährleisten.

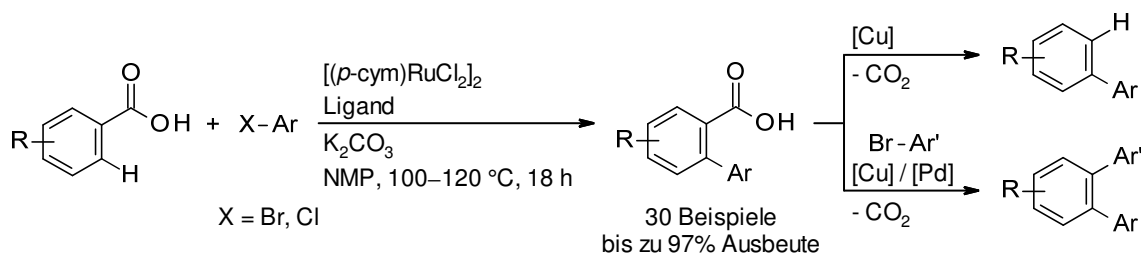
Neben den decarboxylierenden *ipso*-Arylierungen wurden auch neue Protokolle für Carboxylat-dirigierte *ortho*-Arylierungen von Benzoesäuren entwickelt. So gelang es im dritten Projekt erstmals, Aryldiazoniumsalze, die ausgehend von breit verfügbaren Anilinen leicht zugänglich sind, als Kupplungspartner zu nutzen. Dabei wurde mit einem Iridium-basierten Katalysatorsystem ein breites Spektrum an Biaryl-2-carboxylaten unter besonders milden Bedingungen in umweltverträglichem Aceton als Lösungsmittel zugänglich und auch Benzamide konnten unter diesen Bedingungen erfolgreich umgesetzt werden. Weiterhin wurde gezeigt, dass sich die Carboxygruppe im Anschluss an die Reaktion über eine Kupfer-vermittelte Protodecarboxylierung rückstandslos entfernen lässt und die *ortho*-arylierte Säure in einer oxidativen Zyklisierung zu einem Lacton umgesetzt werden kann (Schema 50).



Schema 50: Ir-Katalysierte *ortho*-Arylierung von Benzoesäuren mit Aryldiazoniumsalzen.

Der große Vorteil dieser Methode ist, dass durch die Verwendung von Aryldiazoniumsalzen neue orthogonale Kupplungen zu Arylhalogeniden unter milden Reaktionsbedingungen eröffnet werden. Diese könnten zukünftig beispielsweise auch in C(sp³)-H-Arylierungen von Carbonsäuren Anwendung finden.

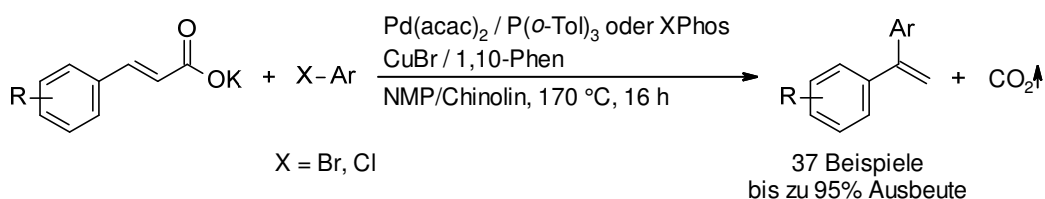
Im vierten Projekt wurde zudem ein Protokoll für die *ortho*-Arylierung von Benzoesäuren mit Arylhalogeniden entwickelt, welches auf einem kostengünstigen Ruthenium-Katalysator basiert. Während dieser kombiniert mit PEt₃ × HBF₄ die Kupplung von Arylbromiden ermöglichte, konnten Arylchloriden in Gegenwart der Aminosäure DL-Pipecolinsäure als Ligand umgesetzt werden. Die Praktikabilität beider Varianten wurde anhand der Synthese einer Vielzahl an Biaryl-2-carboxylaten demonstriert. Weiterhin gelang es, diese Verfahren mit einer Kupfer-katalysierten Protodecarboxylierung sowie erstmals mit einer Kupfer/Palladium-katalysierten decarboxylierenden *ipso*-Arylierung zu kombinieren (Schema 51).



Schema 51: Ru-Katalysierte *ortho*-Arylierung von Benzoesäuren.

Insbesondere die letztgenannte Reaktion stellt einen entscheidenden Fortschritt dar, da sie die Vorteile Carboxylat-dirigierter *ortho*-Funktionalisierungen und decarboxylierender Kreuzkupplungen vereint und so den Grundstein für eine Vielzahl neuer nachhaltiger Difunktionalisierungen von Carbonsäuren legt.

Im fünften Projekt wurde eine Kupfer/Palladium-katalysierte decarboxylierende Mizoroki-Heck-Reaktion von Zimtsäuren mit Arylhalogeniden erschlossen. Dabei dirigiert die Carboxylatgruppe die Arylierung in die β -Position der Säure. Durch die Bindungsknüpfung wird die C–COOH-Bindung destabilisiert, woraufhin eine Protodecarboxylierung erfolgt. Somit agiert die Carboxylatgruppe in dieser Reaktion als abfallende dirigierende Gruppe. Auf diese Weise sind schließlich 1,1-Diarylalkene zugänglich, was die vorliegende Transformation komplementär zu klassischen Mizoroki-Heck-Reaktionen von Styrolen macht. Die Anwendungsbreite des neuen Protokolls wurde anhand der Synthese einer Vielzahl von divers funktionalisierten 1,1-Diarylalkenen demonstriert (Schema 52). Zudem wurde die neue Transformation mit einer klassischen Heck-Reaktion ausgehend von Methylacrylat zu einem praktischen Eintopf-Verfahren kombiniert.



Schema 52: Decarboxylierende Mizoroki-Heck-Reaktion von Zimtsäuren mit Arylhalogeniden.

In weiterführenden Arbeiten könnte das Konzept auf andere Funktionalisierungen von Zimtsäuren in β -Position übertragen werden. Neben einem breiteren Spektrum an Elektrophilen könnten beispielsweise auch oxidative Kupplungen mit Boronsäuren oder oxidative Alkoxylierungen interessante Produkte liefern. Weiterhin würde eine Reaktionsvariante, welche die β -Arylierung mit einer decarboxylierenden *ipso*-Funktionalisierung kombiniert, komplexere Alkenen zugänglich machen.

7 Experimenteller Teil

7.1 Anmerkung

Dieser Teil der Arbeit besteht hauptsächlich aus den englischsprachigen „Supporting Information“ der Originalveröffentlichungen, die entsprechend angepasst und ergänzt wurden. Auf einen Anhang zu den in *J. Am. Chem. Soc.* **2014**, *136*, 10007–10023 publizierten DFT-Rechnungen wird im Rahmen dieser Arbeit verzichtet. Detaillierte Informationen zu den DFT-Rechnungen sind in der entsprechenden „Supporting Information“ auf dem Onlineportal des Journals frei zugänglich.

7.2 Allgemeine Arbeitstechniken

7.2.1 Chemikalien und Lösungsmittel

Kommerziell verfügbare Chemikalien wurden bei einer Reinheit von $\geq 95\%$ direkt eingesetzt oder andernfalls nach Standardverfahren aufgereinigt.^[255] Luft- und feuchtigkeitsempfindliche Substanzen wurden mit Standard-Schlenktechniken stets unter einer Stickstoff- oder Argonatmosphäre gelagert und gehandhabt. Die verwendeten Lösungsmittel wurden nach Standardverfahren getrocknet^[255] und unter Stickstoff- oder Argonatmosphäre über Molsieben (3 Å oder 4 Å) gelagert. Letztere wurden zuvor im Mikrowellenofen (2×2 min, 600 W) erhitzt und im Vakuum (10^{-3} mbar) abgekühlt. Soweit nicht anders angegeben, wurden flüssige Einsatzstoffe und Lösungsmittel vor der Reaktion mittels Durchleiten von Argon (20 min) von Sauerstoff befreit. Feststoffe wurden in der Regel an Luft eingewogen und im Ölpumpenvakuum (10^{-3} mbar) von Luft und Feuchtigkeit befreit.

7.2.2 Durchführung von Parallelreaktionen

Die Reihenversuche wurden in 20 mL Headspace-Vials für die Gaschromatographie durchgeführt und mit Aluminium-Bördekappen mit Teflon-beschichteten Butylgummisepten verschlossen. Letztere waren mit einer Sicherheitsperforation versehen, die bei einem Überdruck von > 0.5 bar ausreißt und so das Platzen der Gefäße verhindert. Die Temperierung der Reaktionsgefäße erfolgte in 8 cm hohen Aluminiumblöcken mit 7 cm tiefen, zylindrischen Bohrungen, deren Durchmesser dem der Reaktionsgefäße angepasst war. Eine weitere Bohrung gewährleistete die Aufnahme eines Temperaturfühlers. Der Durchmesser der Heizblöcke entsprach dem der Heizplatten gängiger Labor-Magnetrührer. Zum gleichzeitigen Evakuieren und Rückbefüllen mehrerer Reaktionsgefäße wurden mit der Schlenk-Linie verbundene

Vakuumverteiler verwendet, die mit jeweils zehn vakuumfeste 3 mm Teflonschläuchen mit Adaptern zur Anbringung von Luer-Lock-Spritzennadeln ausgestattet waren.

Zur Durchführung der Reihenversuche wurden die festen Einsatzstoffe an der Luft in die Reaktionsgefäße eingewogen. Letztere wurden mit 20 mm Magnet-Rührkernen ausgestattet und mit einer Septumkappe luftdicht verschlossen. Luft- und feuchtigkeitsempfindliche Substanzen wurden in einer Glovebox mit Stickstoff als Inertgas eingewogen. Die Gefäße wurden in die Bohrungen eines Aluminiumblocks eingesetzt und über die Spritzennadeln mit dem Vakuumverteiler verbunden. Die Reaktionsgefäße wurden dann dreimal hintereinander evakuiert und mit Stickstoff oder Argon rückbefüllt. Lösungsmittel, Stammlösungen oder flüssige Einsatzstoffe wurden anschließend mit Hilfe von Spritzen durch die Septen injiziert. Anschließend wurden die Spritzennadeln des Vakuumverteilers entfernt und der Aluminiumblock auf Reaktionstemperatur gebracht. Die angegebenen Temperaturen beziehen sich auf die Temperaturen des Heizblocks, welche erfahrungsgemäß $\pm 2\text{ }^{\circ}\text{C}$ von den Temperaturen in den Reaktionsgefäßen abweichen. Gerührt wurde mit etwa 450–500 Umdrehungen pro Minute.

Reaktionen in der Labormikrowelle wurden in einem *Initiator Mikrowellenreaktor* der Fa. *Biotage* in Reaktionsgefäßen der Größen 0.5–2.0 mL mit einem Teflon-beschichteten Rührkern durchgeführt. Die Steuerung erfolgte mit der Software-Version 2.5. Die Reaktionszeit begann mit Erreichen der Reaktionstemperatur. Die Messung der Reaktionstemperatur erfolgte über einen externen IR-Sensor, der die Temperatur an der Glaswand bestimmt. Eine Kühlung der Reaktionsgefäße durch einen Druckluftstrom erfolgte erst nach Ablauf der Reaktionszeit.

Nach Ablauf der Reaktionszeit und dem Abkühlen auf Raumtemperatur wurde der Überdruck in den Reaktionsgefäßen mittels einer Spritzennadel vorsichtig abgelassen und der Standard zugesetzt. Nach ausreichender Durchmischung wurde das Reaktionsgefäß schließlich vorsichtig geöffnet.

Zur GC-Analyse wurden die Reaktionsmischungen mit Ethylacetat (4 mL) verdünnt und gut durchmischt. Mit einer Einwegpipette wurden 0.25 mL der Reaktionsmischungen in 10 mL Rollrandgefäße überführt, in die vorher Ethylacetat (2 mL) und ein wässriges Extraktionsmedium (2 mL) gegeben wurden. Die Phasen wurden mit der Einwegpipette gut durchmischt und eine Phasentrennung abgewartet. Anschließend wurden 1.5 mL der organischen Phasen durch 0.3 mL trockenes Magnesiumsulfat in 2 mL GC-Probengläschen filtriert. Dabei dienten Einweg-Glaspipetten, die mit einem Wattepfropfen versehen waren, als Filter. Die so vorbereiteten Proben wurden schließlich gaschromatographisch untersucht. Die

Ausbeute der Reaktionen wurde durch Integration des Produktsignals im Vergleich zum internen Standard ermittelt. Responsefaktoren in Bezug auf den internen Standard wurde experimentell durch Analyse bekannter Menge des Produktes bestimmt.

Zur Bestimmung der Ausbeute mittels ^{19}F -NMR wurde 1 mL der Reaktionsmischungen durch Einweg-Glaspipetten, die mit einem Wattepfropfen versehen und mit 0.3 mL trockenem Magnesiumsulfat und 0.3 mL Celite gefüllt waren, in ein NMR-Röhrchen filtriert. Die so vorbereiteten Proben wurden schließlich mittels ^{19}F -NMR untersucht und die Ausbeute der Reaktionen durch Integration des Produktsignals im Vergleich zum internen Standard ermittelt.

Mit Hilfe der beschriebenen Versuchsaapparaturen war es möglich die Reihenversuche in einem Bruchteil der Zeit durchzuführen, die bei der Verwendung von Standardtechniken erforderlich gewesen wäre. Nur durch die Anwendung dieser Parallelisierungstechniken und durch die Verwendung eines elektronischen Laborjournals^[256] gelang es, die für die Entwicklung der neuen Methoden benötigte Zahl an Experimenten innerhalb kurzer Zeit durchzuführen und auszuwerten.

7.2.3 Analytische Methoden

7.2.3.1 Dünnschichtchromatographie

Es wurden Polyester-Fertigfolien POLYGRAM® mit 0.2 mm Kieselgel 60 F254 der Fa. *Macherey-Nagel* verwendet. Zur Detektion der Substanzen wurden Fluoreszenzlösungen bei 254 nm oder das Anfärben mit KMnO_4 -Lösung (3g KMnO_4 , 20 g K_2CO_3 , 15 g NaOH , 300 mL Wasser) genutzt.

7.2.3.2 Säulenchromatographie

Die Isolierung der Produkte wurde mit dem Combi Flash Companion-Chromatographie-System der Fa. *Isco-Systems* oder mit dem Reveleris X2-Chromatographie-System der Fa. *GRACE* vorgenommen. Als Säulen wurden die kommerziell erhältlichen Reveleris Silica-Säulen der Größe 12 g oder 24g der Fa. *GRACE* verwendet.

7.2.3.3 Gaschromatographie

Für GC-Analysen wurde ein *Hewlett Packard 6890* Gaschromatograph verwendet. Als Trägergas diente Stickstoff mit einer Flussrate von 44 mL/min (0.64 bar Druck). Die Injektortemperatur betrug 220 °C. Das Split-Verhältnis betrug 1:20. Zur Trennung wurde eine HP-5-Säule mit 5% Phenyl-Methyl-Siloxan (30 m × 320 µm × 1.0 µm) der Fa. *Agilent*

verwendet. Temperaturprogramm: Anfangstemperatur 60 °C (2 min), linearer Temperaturanstieg (30 °C min⁻¹) auf 300 °C, Endtemperatur 300 °C (13 min).

7.2.3.4 Massenspektrometrie

Massenspektren wurden an dem GC-MS *Saturn 2100 T* der Fa. *Varian* aufgenommen. Die hochauflösenden Massenspektren wurden in der Analytikabteilung des Fachbereichs Chemie der Technischen Universität Kaiserslautern an einem *GCT Premier* der Fa. *Waters* gemessen. Die Ionisation erfolgte per Elektronenstoßionisation. Weiterhin wurden Massenspektren an einem *Esquire 6000* der Fa. *Bruker* aufgenommen. Hier erfolgte die Ionisation per Elektrosprayionisation. Die angegebenen Intensitäten der Signale beziehen sich auf das Verhältnis zum intensivsten Peak. Für Fragmente mit einer Isotopenverteilung ist jeweils nur der intensivste Peak eines Isotopomers aufgeführt.

7.2.3.5 Infrarotspektroskopie

Infrarot-Schwingungsspektren wurden an einem *Spectrum 100* ATR-FTIR der Fa. *Perkin Elmer* gemessen. Alle Messungen erfolgten gegen Luft als Hintergrund in einem Bereich von 4000 bis 400 Wellenzahlen. Die Angabe der Schwingungsbanden erfolgt in Wellenzahlen (cm⁻¹).

7.2.3.6 Kernresonanzspektroskopie

¹H-NMR-, breitbandentkoppelte ¹³C-NMR-, ¹⁹F-NMR- und ³¹P-NMR-Spektren wurden bei Raumtemperatur größtenteils am FT-NMR-Spektrometer *Avance 400* der Fa. *Bruker* aufgenommen. Einzelne Messungen erfolgten weiterhin an den Geräten *Avance 200*, *Avance 300*, *Avance 600*, *DPX 200* und *DPX 250* der Fa. *Bruker* sowie am *Spinsolve* Benchtop-NMR der Fa. *Magritek*. ¹⁹F-NMR-Messungen zur Ausbeutenbestimmung wurden am *Spinsolve* Benchtop-NMR mit einer Fluorresonanz bei 41 MHz durchgeführt. Die chemischen Verschiebungen der Signale sind in Einheiten der δ -Skala (ppm) angegeben. Als interner Standard dienten die Resonanzsignale der Restprotonen des verwendeten deuterierten Lösungsmittels bei ¹H-Spektren bzw. die entsprechenden Resonanzsignale bei ¹³C-Spektren.^[257] Die Multiplizität der Signale wird durch folgende Abkürzungen wiedergegeben: brs = breites Singulett, s = Singulett, d = Dublett, dd = Dublett eines Dubletts, dt = Dublett eines Tripletts, t = Triplet, q = Quartett, m = Multiplett. Die Kopplungskonstanten *J* sind in Hertz [Hz] angegeben. Die Bearbeitung und Auswertung der Spektren erfolgte mit dem Programm *ACD-Labs 12.0* (Advanced Chemistry Development Inc.).

7.2.3.7 Schmelzpunkte

Schmelzpunkte wurden an einem *Mettler FP 61* mit optischem Sensor zur automatischen Erkennung des Schmelzpunktes gemessen.

7.2.3.8 Elementaranalyse

Elementaranalysen wurden an einem *Elemental Analyzer vario Micro cube* durch die Analytikabteilung des Fachbereichs Chemie der Technischen Universität Kaiserslautern gemessen.

7.2.3.9 Röntgenstrukturanalyse

Die Röntgenstrukturanalyse erfolgte am Diffraktometer *Oxford Diffraction Gemini S Ultra* bei 150 K unter Verwendung von MoK α -Strahlung.

7.3 Bimetallic Cu/Pd Catalysts with Bridging Aminopyrimidinyl Phosphines for Decarboxylative Cross-Coupling Reactions at Moderate Temperature

7.3.1 General remarks

Reaction media and liquid reactants were saturated with Argon to exclude atmospheric oxygen. NMP was degassed *via* three freeze-pump thaw cycles. The carboxylates and the triflates were prepared following the procedures below and were directly used.

7.3.2 General procedure for the protodecarboxylation experiments

An oven-dried vessel was charged with the carboxylic acid (0.50 mmol), copper(I) oxide (3.61 mg, 25.0 μ mol), and 1,10-phenanthroline (9.10 mg, 50 μ mol). After the vessel was flushed with 3 alternating vacuum and nitrogen purge cycles, degassed NMP (2 mL) was added *via* syringe. The resulting mixture was stirred at 100 °C for the given time. Then the reaction mixture was allowed to cool to RT, *n*-tetradecane (50 μ L) was added *via* syringe and the mixture was diluted with ethyl acetate (4 mL). A sample of the reaction mixture (0.25 mL) was dissolved in ethyl acetate (2 mL), washed with a saturated solution of bicarbonate (2 mL), dried over MgSO₄, and analyzed by GC.

7.3.3 Preparation of starting materials

General procedure for the synthesis of potassium carboxylate salts:

A 250 mL, two-necked, round-bottomed flask was charged with the carboxylic acid (20.0 mmol) and ethanol (20 mL). To this, a solution of potassium *tert*-butoxide (2.24 g, 20.0 mmol) in ethanol (20 mL) was added dropwise over 1 h. After complete addition, the

reaction mixture was stirred for another 1 h at RT. A gradual formation of a white precipitate was observed. The resulting solid was collected by filtration, washed sequentially with ethanol (2×10 mL) and cold ($0\text{ }^{\circ}\text{C}$) diethyl ether (10 mL), and dried in vacuum to provide the corresponding potassium salts of the carboxylic acids.

General procedure for the synthesis of aryl triflates:^[258]

To a solution of the corresponding phenol (20.0 mmol) in anhydrous CH_2Cl_2 (10 mL) was added pyridine (3.25 mL, 40.0 mmol) and the solution was cooled to $0\text{ }^{\circ}\text{C}$. A solution of trifluoromethanesulfonic anhydride (4.00 mL, 24.0 mmol) in anhydrous CH_2Cl_2 (12 mL) was added dropwise at this temperature and the mixture was allowed to warm slowly to RT with stirring. The mixture was then diluted with Et_2O (30 mL) and quenched with 10% aq. HCl. The aqueous layer was extracted with Et_2O (2×30 mL) and the combine organic layers were washed successively with aq. NaHCO_3 and brine (20 mL). After drying over MgSO_4 , the solvent was removed under reduced pressure and the residue was purified by Kugelrohr distillation to give the corresponding aryl triflate.

Procedure for the synthesis of the vinyl triflate:^[259]

A solution of alpha-tetralone (1.51 g, 10.0 mmol) in anhydrous CH_2Cl_2 (5 mL) was cooled to $0\text{ }^{\circ}\text{C}$ and 2,4,6-trimethylpyridine (1.90 mL, 20 mmol) was added. A solution of trifluoromethanesulfonic anhydride (2.70 mL, 20.0 mmol) in anhydrous CH_2Cl_2 (10 mL) was added dropwise at this temperature and the mixture was allowed to warm slowly to RT with stirring. Hexane (20 mL) was added and the mixture was filtrated through a pad of celite. The solids were washed with EtOAc (20 mL) and the combined organic layers were concentrated under reduced pressure. The residue was purified by column chromatography (SiO_2 , ethyl acetate/hexane gradient) yielding the vinyl triflate as a colorless oil (1.83 g, 66%). The analytical data matched those reported in literature.^[259,260]

7.3.4 Optimization of the Cu/Pd-catalyzed decarboxylative cross-coupling at $100\text{ }^{\circ}\text{C}$

General method:

Inside a glovebox an oven-dried 20 mL vessel was charged with the solid reagents. The solvent and the liquid reagents were added inside a glovebox and the resulting mixture was stirred at the given temperature for 24 h outside the glovebox under a dry atmosphere of nitrogen. The reaction mixture was allowed to cool to RT, *n*-tetradecane (50 μL) was added *via* syringe and the mixture was diluted with ethyl acetate (4 mL). A sample of the reaction mixture (0.25 mL) was dissolved in ethyl acetate (2 mL) and washed with aqueous HCl (1 N, 2 mL). The organic phase was filtered through a plug of NaHCO_3 / MgSO_4 and analyzed by GC.

Tabelle 35: Solvent screening.

5.1.2-3a	5.1.2-4a	5.1.2-5aa
Entry	solvent	5.1.2-5aa (%)
1	NMP	82
2	Mes	n.d.
3	quinoline	57
4	NMP/Mes (1:2)	8
5	NMP/Mes (2:1)	68
6	NMP/DMF (3:1)	73
7	NMP/DMSO (3:1)	67
8	NMP/diglyme (3:1)	53
9	NMP ^[a]	60

Reaction conditions: **5.1.2-3a** (0.45 mmol), **5.1.2-4a** (0.3 mmol), Pd(acac)₂ (2 mol%), **L8** (6 mol%), Cu₂O (5 mol%), 1,10-Phen (10 mol%), NMP (2 mL), 100 °C. GC yield with *n*-tetradecane as internal standard. [a] 2 equiv. of water were added to the reaction mixture.

Tabelle 36: Optimization of the reaction conditions.

5.1.2-3a	5.1.2-4a	5.1.2-5aa		
Entry	[Pd]	[Cu]	<i>N</i> -ligand	5.1.2-5aa (%)
1 ^[a]	PdI ₂	Cu ₂ O	1,10-Phen	65
2 ^[a]	Pd(acac) ₂	"	"	82
3	PdI ₂	"	"	84
4	Pd(acac) ₂	"	"	88
5	PdBr ₂	"	"	72
6	PdCl ₂	"	"	52
7	Pd(dba) ₂	"	"	75
8	Pd(F ₆ -acac) ₂	"	"	70

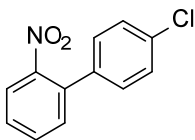
9	Pd(TFA) ₂	"	"	79
10	Pd(OAc) ₂	"	"	80
11	(allylPdCl) ₂	"	"	77
12	Pd(COD)Cl ₂	"	"	55
13 ^[b]	5.1.2-12	"	"	73
14	Pd(acac) ₂	CuBr ^[c]	"	80
15	"	CuCl ^[c]	"	82
16	"	[Cu(MeCN) ₄]BF ₄ ^[c]	"	74
17	"	Cu ₂ O	NO ₂ -Phen	9
18	"	"	Me ₄ -Phen	66
19	"	"	-	16
20	"	-	-	n.d.
21	-	Cu ₂ O	1,10-Phen	n.d.
22 ^[d]	Pd(acac) ₂	"	"	23
23 ^[b]	5.1.2-12	[Cu(MeCN) ₄]BF ₄ ^[c]	"	74
24 ^[b]	"	"	-	18

Reaction conditions: **5.1.2-3a** (0.45 mmol), **5.1.2-4a** (0.3 mmol), [Pd] (3 mol%), **L8** (6 mol%), [Cu] (5 mol%), *N*-ligand (10 mol%), NMP (2 mL), 100 °C, 24 h; GC yields with *n*-tetradecane as internal standard. [a] [Pd] (2 mol%). [b] No additional amount of **L8** was added. [c] [Cu] (10 mol%). [d] 90 °C.

7.3.5 General procedure for the biaryl synthesis

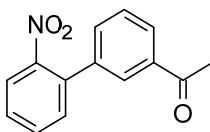
An oven-dried 20 mL vessel was charged with the potassium carboxylate **5.1.2-3** (0.75 mmol), copper(I) oxide (3.61 mg, 25.0 μmol, 5 mol%), palladium(II) acetylacetonate (4.57 mg, 15.0 μmol, 3 mol%), ligand **L8** (12.3 mg, 30.0 μmol, 6 mol%) and 1,10-phenanthroline (9.10 mg, 50.0 μmol, 10 mol%) inside the glovebox. NMP (4 mL) and the triflate **5.1.2-4** (0.5 mmol) were added inside a glovebox and the resulting mixture was stirred at the given temperature for 24 h outside the glovebox under a dry atmosphere of nitrogen. The mixture was allowed to cool to RT, diluted with aqueous HCl (1 N, 20 mL) and extracted with ethyl acetate (3 × 20 mL). The combined organic layers were washed with water and brine, dried over MgSO₄, filtered, and the volatiles were removed under reduced pressure. The residue was purified by column chromatography (SiO₂, ethyl acetate/hexane gradient) yielding the corresponding biaryl **5.1.2-5**. The isolated yield was determined by combining two identical 0.5 mmol scale reactions.

7.3.6 Synthesis and characterization of the corresponding products



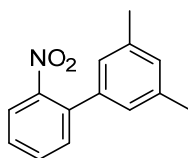
4-Chloro-2'-nitrobiphenyl (**5.1.2-5aa**) [CAS: 6271-80-3]: Compound **5.1.2-5aa** was prepared following the general procedure from potassium 2-nitrobenzoate (**5.1.2-3a**) (154 mg, 0.75 mmol) and 4-chlorophenyl triflate (**5.1.2-4a**) (130 mg, 0.5 mmol) at 100 °C in 4 mL of NMP. After combining two identical 0.5 mmol scale-reactions, compound **5.1.2-5aa** was isolated as a yellow oil (186 mg, 80%).

¹H-NMR (400 MHz, CDCl₃): δ = 7.88 (dd, J = 8.1, 1.2 Hz, 1 H), 7.63 (td, J_t = 7.6 Hz, J_d = 1.2 Hz, 1 H), 7.51 (td, J_t = 7.8 Hz, J_d = 1.2 Hz, 1 H), 7.43–7.38 (m, 3 H), 7.28–7.23 (m, 2 H) ppm; **¹³C-NMR** (101 MHz, CDCl₃): δ = 149.1, 135.9, 135.2, 134.5, 132.5, 131.8, 129.2, 128.9, 128.5, 124.3 ppm; **IR** (ATR): $\tilde{\nu}$ = 3067, 2867, 1521, 1472, 1348, 1089, 1006, 853, 782, 687 cm⁻¹; **MS** (EI, 70 eV), m/z (%): 234 (31) [M⁺], 233 (21), 232 (100), 170 (28), 152 (30), 141 (25), 114 (23); **elemental analysis**: calcd. (%) for C₁₂H₈ClNO₂: C 61.69, H 3.45, N 5.99; found: C 61.83, H 3.74, N 6.03.



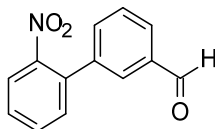
3-Acetyl-2'-nitrobiphenyl (**5.1.2-5ab**) [CAS: 1195761-01-3]: Compound **5.1.2-5ab** was prepared following the general procedure from potassium 2-nitrobenzoate (**5.1.2-3a**) (154 mg, 0.75 mmol) and 3-acetylphenyl triflate (**5.1.2-4b**) (134 mg, 0.5 mmol) at 100 °C in 4 mL of NMP. After combining two identical 0.5 mmol scale reactions, compound **5.1.2-5ab** was isolated as a colorless solid (158 mg, 66%).

¹H-NMR (200 MHz, CDCl₃): δ = 8.04–7.91 (m, 3 H), 7.72–7.63 (m, 1 H), 7.61–7.43 (m, 4 H), 2.46 (s, 3 H) ppm; **¹³C-NMR** (101 MHz, CDCl₃): δ = 197.5, 149.0, 138.1, 137.4, 135.5, 132.6, 132.5, 132.0, 128.9, 128.7, 128.1, 127.8, 124.4, 26.7 ppm; **IR** (ATR): $\tilde{\nu}$ = 3050, 1678, 1522, 1354, 1239, 1105, 855, 807, 784, 746, 693 cm⁻¹. **MS** (EI, 70 eV), m/z (%): 241 (11) [M⁺], 226 (15), 225 (100), 224 (9), 153 (9), 44 (24), 42 (18); **elemental analysis**: calcd. (%) for C₁₄H₁₁NO₃: C 69.70, H 4.60, N 5.81; found: C 69.66, H 4.81, N 5.73; **m.p.**: 103–104 °C.



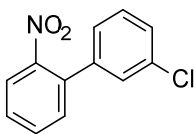
3,5-Dimethyl-2'-nitrobiphenyl (**5.1.2-5ac**) [CAS: 51839-09-9]: Compound **5.1.2-5ac** was prepared following the general procedure from potassium 2-nitrobenzoate (**5.1.2-3a**) (154 mg, 0.75 mmol) and 3,5-dimethylphenyl triflate (**5.1.2-4c**) (127 mg, 0.5 mmol) at 100 °C and at 120 °C in 4 mL of NMP. After combining two identical 0.5 mmol scale reactions, compound **5.1.2-5ac** was isolated as an orange oil (132 mg, 58% (100 °C); 204 mg, 90% (120 °C)).

¹H-NMR (400 MHz, CDCl₃): δ = 7.83 (dd, J = 8.1, 1.1 Hz, 1 H), 7.64–7.57 (m, 1 H), 7.49–7.42 (m, 2 H), 7.05 (s, 1 H), 6.95 (s, 2 H), 2.36 (s, 6 H) ppm; **¹³C-NMR** (101 MHz, CDCl₃): δ = 149.3, 138.3, 137.2, 136.6, 132.1, 131.9, 129.9, 127.9, 125.6, 123.9, 21.3 ppm; **IR** (ATR): $\tilde{\nu}$ = 3028, 2918, 1601, 1522, 1354, 1292, 1039, 997, 867, 850, 839, 780, 749, 697 cm⁻¹; **MS** (EI, 70 eV), m/z (%): 227 (3) [M⁺], 209 (16), 199 (16), 198 (100), 184 (21), 182 (27), 170 (17), 167 (14); **elemental analysis**: calcd. (%) for C₁₄H₁₃NO₂: C 73.99, H 5.77, N 6.16; found: C 73.87, H 5.84, N 6.17.



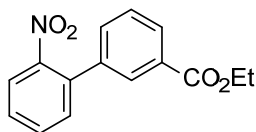
3-Formyl-2'-nitrobiphenyl (**5.1.2-5ad**) [CAS: 1181294-97-2]: Compound **5.1.2-5ad** was prepared following the general procedure from potassium 2-nitrobenzoate (**5.1.2-3a**) (154 mg, 0.75 mmol) and 3-formylphenyl triflate (**5.1.2-4d**) (127 mg, 0.5 mmol) at 100 °C in 4 mL of NMP. After combining two identical 0.5 mmol scale reactions, compound **5.1.2-5ad** was isolated as a colorless solid (150 mg, 66%).

¹H-NMR (400 MHz, CDCl₃): δ = 10.1 (s, 1 H), 7.46 (dd, J = 7.7, 1.3 Hz, 1 H), 7.64–7.54 (m, 3 H), 7.69 (td, J_t = 7.6 Hz, J_d = 1.2 Hz, 1 H), 7.86 (t, J = 1.4 Hz, 1 H), 7.94 (dt, J_d = 8.2 Hz, J_t = 1.2 Hz, 1 H), 7.97 (dd, J = 8.2, 1.2 Hz, 1 H) ppm; **¹³C-NMR** (101 MHz, CDCl₃): δ = 191.7, 148.9, 138.7, 136.7, 135.2, 133.8, 132.7, 132.0, 129.5, 129.3, 128.9, 124.5 ppm; **IR** (ATR): $\tilde{\nu}$ = 2837, 2738, 1687, 1581, 1570, 1514, 1351, 1183, 1165, 1144, 850, 798, 783, 750, 690 cm⁻¹; **MS** (EI, 70 eV), m/z (%): 227 (3) [M⁺], 209 (33), 182 (51), 170 (26), 154 (45), 152 (43), 115 (43), 44 (100); **elemental analysis**: calcd. (%) for C₁₃H₉NO₃: C 68.72, H 3.99, N 6.16; found: C 68.72, H 4.23, N 6.19; **m.p.**: 80–81 °C.



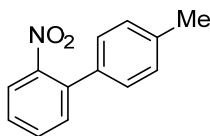
3-Chloro-2'-nitrobiphenyl (5.1.2-5ae) [CAS: 951-22-4]: Compound **5.1.2-5ae** was prepared following the general procedure from potassium 2-nitrobenzoate (**5.1.2-3a**) (154 mg, 0.75 mmol) and 3-chlorophenyl triflate (**5.1.2-4e**) (130 mg, 0.5 mmol) at 120 °C in 4 mL of NMP. After combining two identical 0.5 mmol scale reactions, compound **5.1.2-5ae** was isolated as a yellow oil (126 mg, 54%).

¹H-NMR (400 MHz, CDCl₃): δ = 7.92 (dd, *J* = 8.0, 1.3 Hz, 1 H), 7.63 (td, *J*_t = 7.5 Hz, *J*_d = 1.3 Hz, 1 H), 7.53 (td, *J*_t = 7.8 Hz, *J*_d = 1.4 Hz, 1 H), 7.45–7.33 (m, 4 H), 7.19 (dt, *J*_d = 7.2 Hz, *J*_t = 1.2 Hz, 1 H) ppm; **¹³C-NMR** (101 MHz, CDCl₃): δ = 148.9, 139.2, 135.0, 134.5, 132.5, 131.8, 129.8, 128.7, 128.4, 128.0, 126.1, 124.3 ppm; **IR** (ATR): $\tilde{\nu}$ = 3065, 2868, 1595, 1522, 1349, 1079, 1025, 854, 782, 746, 690 cm⁻¹; **MS** (EI, 70 eV), *m/z* (%): 234 (5) [M⁺], 206 (35), 204 (100), 170 (36), 168 (16), 152 (23), 114 (23), 50 (16); **elemental analysis**: calcd. (%) for C₁₂H₈ClNO₂: C 61.69, H 3.45, N 5.99; found: C 61.94, H 3.59, N 6.03.



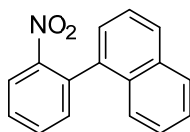
Ethyl 2'-nitrophenyl-3-carboxylate (5.1.2-5af) [CAS: 72256-33-8]: Compound **5.1.2-5af** was prepared following the general procedure from potassium 2-nitrobenzoate (**5.1.2-3a**) (154 mg, 0.75 mmol) and 2-trifluoromethylsulfonyloxy benzoic acid ethyl ester (**5.1.2-4f**) (149 mg, 0.5 mmol) at 120 °C in 4 mL of NMP. After combining two identical 0.5 mmol scale reactions, compound **5.1.2-5af** was isolated as a yellow oil (184 mg, 68%).

¹H-NMR (200 MHz, CDCl₃): δ = 8.14–8.09 (m, 2 H), 7.67–7.47 (m, 4 H), 7.31–7.22 (m, 2 H), 4.16–4.04 (m, 2 H), 1.07 (t, *J* = 7.2 Hz, 3 H) ppm; **¹³C-NMR** (101 MHz, CDCl₃): δ = 166.3, 148.1, 139.7, 137.5, 132.6, 132.0, 131.4, 130.6, 129.9, 128.9, 128.1, 128.0, 124.0, 60.9, 13.8 ppm; **IR** (ATR): $\tilde{\nu}$ = 3066, 2983, 1713, 1521, 1346, 1256, 1079, 854, 766, 746, 709, 700 cm⁻¹; **MS** (EI, 70 eV), *m/z* (%): 271 (3) [M⁺], 225 (29), 197 (100), 180 (14), 153 (17), 152 (14), 138 (10), 114 (9); **elemental analysis**: calcd. (%) for C₁₅H₁₃NO₄: C 66.41, H 4.83, N 5.16; found: C 66.48, H 4.85, N 5.12.



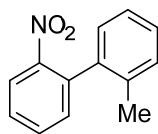
4-Methyl-2'-nitrobiphenyl (**5.1.2-5ag**) [CAS: 70680-21-6]: Compound **5.1.2-5ag** was prepared following the general procedure from potassium 2-nitrobenzoate (**5.1.2-2a**) (154 mg, 0.75 mmol) and 4-methylphenyl triflate (**5.1.2-4g**) (120 mg, 0.5 mmol) at 120 °C in 4 mL of NMP. After combining two identical 0.5 mmol scale reactions, compound **5.1.2-5ag** was isolated as an orange oil (197 mg, 92%).

¹H-NMR (400 MHz, CDCl₃): δ = 7.84 (dd, *J* = 8.1, 1.0 Hz, 1 H), 7.61 (td, *J*_t = 7.6 Hz, *J*_d = 1.2 Hz, 1 H), 7.50–7.43 (m, 2 H), 7.26–7.21 (m, 4 H), 2.41 (s, 3 H) ppm; **¹³C-NMR** (101 MHz, CDCl₃): δ = 149.4, 138.2, 136.3, 134.4, 132.2, 131.9, 129.4, 127.9, 127.7, 124.0, 21.2 ppm; **IR** (ATR): $\tilde{\nu}$ = 3061, 3027, 2921, 2867, 1521, 1475, 1353, 1284, 1275, 1007, 853, 818, 781, 748, 703 cm⁻¹; **MS** (EI, 70 eV), *m/z* (%): 213 (22) [M⁺], 212 (70), 196 (84), 185 (100), 168 (71), 165 (37), 156 (36), 115 (37); **elemental analysis**: calcd. (%) for C₁₃H₁₁NO₂: C 73.23, H 5.20, N 6.57; found: C 73.07, H 5.20, N 6.63.



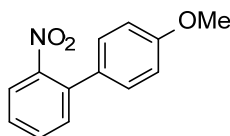
1-(2'-Nitrophenyl)naphthalene (**5.1.2-5ah**) [CAS: 5415-59-8]: Compound **5.1.2-5ah** was prepared following the general procedure from potassium 2-nitrobenzoate (**5.1.2-3a**) (154 mg, 0.75 mmol) and 1-naphthyl triflate (**5.1.2-4h**) (138 mg, 0.5 mmol) at 120 °C in 4 mL of NMP. After combining two identical 0.5 mmol scale reactions, compound **5.1.2-5ah** was isolated as an orange solid (188 mg, 75%).

¹H-NMR (200 MHz, CDCl₃): δ = 8.10 (dd, *J* = 8.0, 1.5 Hz, 1 H), 7.98–7.88 (m, 2 H), 7.77–7.56 (m, 2 H), 7.56–7.40 (m, 5 H), 7.40–7.34 (m, 1 H) ppm; **¹³C-NMR** (101 MHz, CDCl₃): δ = 149.8, 135.5, 135.3, 133.4, 133.1, 132.5, 131.4, 128.6, 128.5, 128.5, 126.6, 126.0, 126.0, 125.2, 124.8, 124.2 ppm; **IR** (ATR): $\tilde{\nu}$ = 3053, 2852, 1612, 1520, 1337, 858, 800, 791, 779, 750, 715, 697, 663 cm⁻¹; **MS** (EI, 70 eV), *m/z* (%): 249 (14) [M⁺], 248 (100), 232 (25), 220 (10), 204 (17), 202 (10), 50 (6); **elemental analysis**: calcd. (%) for C₁₆H₁₁NO₂: C 77.10, H 4.45, N 5.62; found: C 77.06, H 4.61, N 5.61; **m.p.**: 93–94 °C.



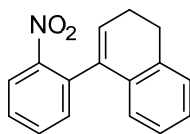
2-Methyl-2'-nitrobiphenyl (5.1.2-5ai) [CAS: 67992-12-5]: Compound **5.1.2-5ai** was prepared following the general procedure from potassium 2-nitrobenzoate (**5.1.2-3a**) (154 mg, 0.75 mmol) and 2-methylphenyl triflate (**5.1.2-4i**) (120 mg, 0.5 mmol) at 120 °C in 4 mL of NMP. After combining two identical 0.5 mmol scale reactions, compound **5.1.2-5ai** was isolated as an orange solid (150 mg, 70%).

¹H-NMR (200 MHz, CDCl₃): δ = 8.01 (dd, *J* = 8.0, 1.3 Hz, 1 H), 7.65 (td, *J*_t = 7.5 Hz, *J*_d = 1.4 Hz, 1 H), 7.58–7.48 (m, 1 H), 7.35 (dd, *J* = 7.5, 1.5 Hz, 1 H), 7.31–7.18 (m, 3 H), 7.11 (d, *J* = 7.1 Hz, 1 H), 2.12 (s, 3 H) ppm; **¹³C-NMR** (101 MHz, CDCl₃): δ = 149.1, 137.4, 136.5, 135.6, 132.5, 132.2, 130.0, 128.3, 128.2, 128.2, 125.7, 124.1, 19.9 ppm; **IR** (ATR): $\tilde{\nu}$ = 3013, 1518, 1471, 1349, 1266, 1006, 854, 772, 743, 727 cm⁻¹; **MS** (EI, 70 eV), *m/z* (%): 213 (20) [M⁺], 196 (21), 195 (93), 182 (100), 167 (24), 166 (61), 165 (42); **elemental analysis**: calcd. (%) for C₁₃H₁₁NO₂: C 73.23, H 5.20, N 6.57; found: C 73.09, H 5.35, N 6.62; **m.p.**: 63–64 °C.



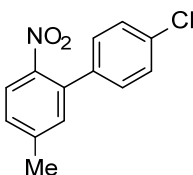
4-Methoxy-2'-nitrobiphenyl (5.1.2-5aj) [CAS: 20013-55-2]: Compound **5.1.2-5aj** was prepared following the general procedure from potassium 2-nitrobenzoate (**5.1.2-3a**) (154 mg, 0.75 mmol) and 4-methoxyphenyl triflate (**5.1.2-4j**) (128 mg, 0.5 mmol) at 120 °C in 4 mL of NMP. After combining two identical 0.5 mmol scale reactions, compound **5.1.2-5aj** was isolated as an orange solid (184 mg, 80%).

¹H-NMR (400 MHz, CDCl₃): δ = 7.81 (d, *J* = 8.3 Hz, 1 H), 7.60 (td, *J*_t = 5.0 Hz, *J*_d = 1.4 Hz, 1 H), 7.47–7.43 (m, 2 H), 7.28–7.25 (m, 2 H), 6.99–6.96 (m, 2 H), 3.86 (s, 3 H) ppm; **¹³C-NMR** (101 MHz, CDCl₃): δ = 159.6, 149.4, 135.8, 132.1, 131.9, 129.4, 127.7, 124.0, 114.2, 55.3 ppm; **IR** (ATR): $\tilde{\nu}$ = 3010, 2949, 2920, 2844, 1611, 1515, 1357, 1248, 1189, 1034, 854, 832, 784, 755, 728, 720 cm⁻¹; **MS** (EI, 70 eV), *m/z* (%): 229 (16) [M⁺], 228 (100), 212 (11), 184 (10), 146 (8), 140 (9), 139 (15); **elemental analysis**: calcd. (%) for C₁₃H₁₁NO₃: C 68.11, H 4.84, N 6.11; found: C 68.16, H 4.90, N 6.10; **m.p.**: 58–59 °C



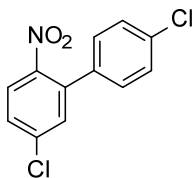
1-(2'-Nitrophenyl)-3,4-dihydronaphthalene (5.1.2-5ak): Compound **5.1.2-5ak** was prepared following the general procedure from potassium 2-nitrobenzoate (**5.1.2-3a**) (154 mg, 0.75 mmol) and 3,4-dihydronaphthalen-1-yl triflate (**5.1.2-4k**) (139 mg, 0.5 mmol) at 120 °C in 4 mL of NMP. After combining two identical 0.5 mmol scale reactions, compound **5.1.2-5ak** was isolated as a yellow solid (204 mg, 81%).

¹H-NMR (200 MHz, CDCl₃): δ = 7.98 (dd, *J* = 8.1, 1.2 Hz, 1 H), 7.71–7.58 (m, 1 H), 7.53 (dd, *J* = 7.7, 1.6 Hz, 1 H), 7.49–7.39 (m, 1 H), 7.25–7.14 (m, 2 H), 7.14–6.99 (m, 1 H), 6.61 (d, *J* = 7.3 Hz, 1 H), 6.03 (t, *J* = 4.6 Hz, 1 H), 2.91 (brs, 2 H), 2.54–2.35 (m, 3 H) ppm; **¹³C-NMR** (101 MHz, CDCl₃): δ = 149.2, 136.6, 135.9, 135.7, 134.2, 132.9, 132.4, 128.3, 128.0, 127.7, 127.4, 126.4, 124.23, 123.6, 27.8, 23.4 ppm; **IR** (ATR): $\tilde{\nu}$ = 3072, 3022, 2930, 2853, 1516, 1489, 1346, 1270, 1152, 1041, 848, 787, 768, 753, 738 cm⁻¹; **MS** (EI, 70 eV), *m/z* (%): 250 (36) [M⁺], 233 (31), 216 (19), 207 (19), 206 (100), 204 (17), 50 (17); **elemental analysis**: calcd. (%) for C₁₆H₁₃NO₂: C 76.48, H 5.21, N 5.57; found: C 76.30, H 5.35, N 5.69; **m.p.**: 83–84 °C.



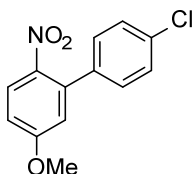
4-Chloro-5'-methyl-2'-nitrobiphenyl (5.1.2-5ba) [CAS: 70690-00-5]: Compound **5.1.2-5ba** was prepared following the general procedure from potassium 5-methyl-2-nitrobenzoate (**5.1.2-3b**) (164 mg, 0.75 mmol) and 4-chlorophenyl triflate (**5.1.2-4a**) (130 mg, 0.5 mmol) at 100 °C in 4 mL of NMP. After combining two identical 0.5 mmol scale reactions, compound **5.1.2-5ba** was isolated as a yellow oil (180 mg, 73%).

¹H-NMR (400 MHz, CDCl₃): δ = 7.84 (d, *J* = 8.3 Hz, 1 H), 7.42–7.38 (m, 2 H), 7.30 (dd, *J* = 8.3, 1.3 Hz, 1 H), 7.22–7.27 (m, 2 H), 7.19 (d, *J* = 1.3 Hz, 1 H), 2.47 (s, 3 H) ppm; **¹³C-NMR** (101 MHz, CDCl₃): δ = 146.7, 143.6, 136.3, 135.4, 134.2, 132.5, 129.2, 129.0, 128.8, 124.6, 21.4 ppm; **IR** (ATR): $\tilde{\nu}$ = 2975, 2861, 1905, 1610, 1586, 1517, 1344, 1089, 1014, 835, 829, 758 cm⁻¹; **MS** (EI, 70 eV), *m/z* (%): 248 (33) [M⁺], 246 (100), 218 (24), 212 (41), 184 (23), 165 (22), 156 (29); **elemental analysis**: calcd. (%) for C₁₃H₁₀ClNO₂: C 63.04, H 4.07, N 5.66; found: C 63.31, H 4.06, N 5.64.



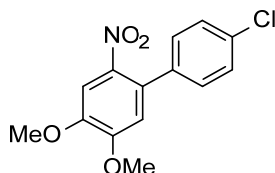
4,5'-Dichloro-2'-nitrobiphenyl (5.1.2-5ca): Compound **5.1.2-5ca** was prepared following the general procedure from potassium 5-chloro-2-nitrobenzoate (**5.1.2-3c**) (180 mg, 0.75 mmol) and 4-chlorophenyl triflate (**5.1.2-4a**) (130 mg, 0.5 mmol) at 100 °C in 4 mL of NMP. After combining two identical 0.5 mmol scale reactions, compound **5.1.2-5ca** was isolated as a yellow solid (158 mg, 59%).

¹H-NMR (400 MHz, CDCl₃): δ = 7.88 (d, *J* = 8.8 Hz, 1 H), 7.49 (dd, *J* = 8.7, 2.4 Hz, 1 H), 7.45–7.40 (m, 3 H), 7.27–7.23 (m, 2 H) ppm; **¹³C-NMR** (101 MHz, CDCl₃): δ = 147.2, 138.7, 137.1, 135.0, 134.7, 131.8, 129.1, 129.1, 128.6, 125.8 ppm; **IR** (ATR): $\tilde{\nu}$ = 3084, 3053, 2845, 1605, 1524, 1509, 1339, 1081, 1012, 859, 829, 821, 799, 756 cm⁻¹; **MS** (EI, 70 eV), *m/z* (%): 268 (62) [M⁺], 267 (19), 266 (100), 238 (25), 232 (31), 175 (29), 150 (20); **elemental analysis**: calcd. (%) for C₁₂H₇Cl₂NO₂: C 53.76, H 2.63, N 5.22; found: C 53.90, H 2.76, N 5.19; **m.p.**: 93–94°C.



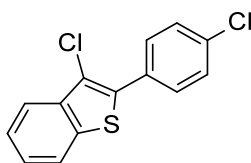
4-Chloro-5'-methoxy-2'-nitrobiphenyl (5.1.2-5da) [CAS: 911217-07-7]: Compound **5.1.2-5da** was prepared following the general procedure from potassium 5-methoxy-2-nitrobenzoate (**5.1.2-3d**) (176 mg, 0.75 mmol) and 4-chlorophenyl triflate (**5.1.2-4a**) (130 mg, 0.5 mmol) at 100 °C in 4 mL of NMP. After combining two identical 0.5 mmol scale reactions, compound **5.1.2-5da** was isolated as a yellow solid (184 mg, 70%).

¹H-NMR (400 MHz, CDCl₃): δ = 8.02 (d, *J* = 9.3 Hz, 1 H), 7.43–7.38 (m, 2 H), 7.28–7.22 (m, 2 H), 6.96 (dd, *J* = 9.0, 2.8 Hz, 1 H), 6.82 (d, *J* = 2.8 Hz, 1 H), 3.91 (s, 3 H) ppm; **¹³C-NMR** (101 MHz, CDCl₃): δ = 147.2, 138.7, 137.1, 135.0, 134.7, 131.8, 129.1, 129.1, 128.6, 125.8 ppm; **IR** (ATR): $\tilde{\nu}$ = 3089, 3013, 2979, 2840, 1611, 1579, 1512, 1501, 1346, 1297, 1216, 1180, 1089, 1023, 1010, 830, 820, 757, 739 cm⁻¹; **MS** (EI, 70 eV), *m/z* (%): 264 (39) [M⁺], 263 (18), 262 (100), 228 (36), 172 (24), 139 (23), 44 (56); **elemental analysis**: calcd. (%) for C₁₃H₁₀ClNO₃: C 59.22, H 3.82, N 5.31; found: C 59.26, H 3.81, N 5.31 **m.p.**: 118–119°C.



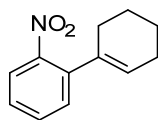
4-Chloro-4',5'-dimethoxy-2'-nitrobiphenyl (**5.1.2-5ea**) [CAS: 1810747-84-2]: Compound **5.1.2-5ea** was prepared following the general procedure from potassium 4,5-dimethoxy-2-nitrobenzoate (**5.1.2-3e**) (199 mg, 0.75 mmol) and 4-chlorophenyl triflate (**5.1.2-4a**) (130 mg, 0.5 mmol) at 100 °C in 4 mL of NMP. After combining two identical 0.5 mmol scale reactions, compound **5.1.2-5ea** was isolated as a yellow solid (220 mg, 75%).

¹H-NMR (400 MHz, CDCl₃): δ = 7.58 (s, 1 H), 7.43–7.38 (m, 2 H), 7.25–7.20 (m, 2 H), 6.74 (s, 1 H), 4.00 (s, 3 H), 3.96 (s, 3 H) ppm; **¹³C-NMR** (101 MHz, CDCl₃): δ = 152.4, 148.3, 140.8, 136.8, 134.0, 130.2, 129.4, 128.7, 113.4, 107.9, 45.5 ppm; **IR** (ATR): $\tilde{\nu}$ = 3072, 2962, 2833, 1498, 1488, 1332, 1282, 1268, 1220, 1089, 1023, 1013, 844, 822, 791, 757 cm⁻¹; **MS** (EI, 70 eV), *m/z* (%): 294 (31) [M⁺], 293 (16), 292 (100), 258 (18), 197 (13), 125 (13), 43 (62); **elemental analysis**: calcd. (%) for C₁₄H₁₂ClNO₄: C 57.25, H 4.12, N 4.77; found: C 57.45, H 4.40, N 4.95; **m.p.**: 146–147 °C.



3-Chloro-2-(4'-chlorophenyl)benzo[b]thiophene (**5.1.2-5fa**) [CAS: 1810747-85-3]: Compound **5.1.2-5fa** was prepared following the general procedure from potassium 3-chlorobenzo[b]thiophene-2-carboxylate (**5.1.2-3f**) (188 mg, 0.75 mmol) and 4-chlorophenyl triflate (**5.1.2-4a**) (130 mg, 0.5 mmol) at 120 °C in 4 mL of NMP. After combining two identical 0.5 mmol scale reactions, compound **5.1.2-5fa** was isolated as a colorless solid (86 mg, 31%).

¹H-NMR (400 MHz, CDCl₃): δ = 7.89 (d, *J* = 8.0 Hz, 1 H), 7.82 (d, *J* = 8.0 Hz, 1 H), 7.77–7.72 (m, 1 H), 7.53–7.41 (m, 4 H) ppm; **¹³C-NMR** (101 MHz, CDCl₃): δ = 137.7, 136.7, 134.9, 134.8, 130.8, 130.5, 128.9, 125.7, 125.2, 122.3, 117.1 ppm; **IR** (ATR): $\tilde{\nu}$ = 3058, 1522, 1486, 1434, 1400, 1301, 1251, 1098, 1012, 984, 899, 828, 820, 750 cm⁻¹; **MS** (EI, 70 eV), *m/z* (%): 281 (13), 279 (81) [M⁺], 278 (100), 208 (19), 163 (8), 49 (6), 44 (6); **elemental analysis**: calcd. (%) for C₁₄H₈Cl₂S: C 60.23, H 2.89, S 11.49; found: C 60.19, H 3.10, S 11.19; **m.p.**: 97–98 °C.

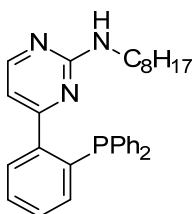


1-(1-Cyclohexen-1-yl)-2-nitrobenzene (**5.1.2-3al**) [CAS: 859219-19-5]: The screening reactions discussed in section 5.1.2 were performed following the procedure described in section 7.3.4.

MS (EI, 70 eV), *m/z* (%): 204 (3) [$M+H^+$], 186 (10), 158 (100), 146 (38), 130 (82), 115 (33), 92 (45), 91 (46), 77 (48); the MS data matched those reported in the literature.^[76]

7.3.7 Ligand synthesis

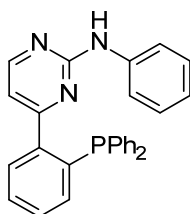
The precursors **5.1.2-9a,b**^[151] and the ligands 2-amino-4-(1-diphenyl-phosphino-phenyl)pyrimidine (**L1**), 4-(1-diphenylphosphinophenyl)-2-ethylaminopyrimidine (**L2**), 2-dimethylamino-4-(1-diphenylphosphinophenyl)pyrimidine (**L7**), 4-(1-diphenylphosphinophen-yl)-2-pyrrolidinylpyrimidine (**L8**), and 4-(1-diphenylphosphinophenyl)-2-piperidinylpyrimidine (**L9**)^[152] as well as diphenyl-(2-(3(5)-pyrazol-1-yl)phenyl)phosphine (**L10**),^[261] *N*-(diphenylphosphino)-4-(pyridin-2-yl)pyrimidin-2-amine (**L11**),^[262] and 2-(1-diphenylphosphinophenyl)-1-methylbenzimidazole (**L12**)^[70] were synthesized according to the procedures published in the literature. **L13** was synthesized and provided by Julian Menges.^[150]



4-(1-Diphenylphosphinophenyl)-2-octylaminopyrimidine (**L3**): Aminopropenone **5.1.2-9a** (2.35 g, 6.50 mmol) and *N*-octylguanidinium sulfate **5.1.2-10c** (2.73 g, 13.00 mmol) were suspended in dry EtOH (80 mL). After adding KOH (0.67 g, 13.0 mmol), the mixture was heated to reflux for 48 h. After removing the solvent under vacuum, the residue was dissolved in a mixture of water and CH₂Cl₂. The layers were separated and the aqueous layer was extracted with CH₂Cl₂ (15 mL). The combined organic layers were dried over anhydrous MgSO₄ and the solvent was removed under reduced pressure. Recrystallisation of the crude material from ethanol afforded **L3** (2.37 g, 5.07 mmol, 78%).

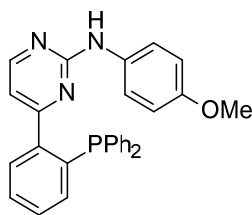
¹H-NMR (400 MHz, DMSO-*d*₆): δ = 0.82 (brs, 3 H), 1.00–1.50 (brs, 14 H), 2.61–3.00 (brs, 2 H), signal not observed: NH, 6.66 (d, *J* = 4.9 Hz, 1 H), 6.98 (dd, *J* = 7.0, 3.9 Hz, 1 H), 7.12–

7.23 (m, 4 H), 7.30–7.35 (m, 6 H), 7.37 (t, $J = 7.6$ Hz, 1 H), 7.48 (t, $J = 7.5$ Hz, 1 H), 7.60 (m, 1 H), 8.20 (d, $J = 5.0$ Hz, 1 H) ppm; $^{13}\text{C-NMR}$ (101 MHz, DMSO- d_6): $\delta = 13.9, 22.0, 26.3, 28.7, 28.8, 28.9, 31.2, 40.2, 108.9, 128.35, 128.41, 129.0$ (d, $J_{\text{C-P}} = 16.8$ Hz), 129.09, 129.13, 133.2 (d, $J_{\text{C-P}} = 19.9$ Hz), 134.5, 135.5 (d, $J_{\text{C-P}} = 20.3$ Hz), 138.2 (d, $J_{\text{C-P}} = 12.3$ Hz), 144.5, 157.9, 161.5, 166.1 ppm; $^{31}\text{P-NMR}$ (162 MHz, DMSO- d_6): $\delta = -12.0$ ppm; **elemental analysis**: calcd. (%) for $\text{C}_{30}\text{H}_{34}\text{N}_3\text{P}$: C 77.06, H 7.33, N 8.99; found C 77.08, H 7.71, N 8.74; **m.p.**: 78–79 °C.



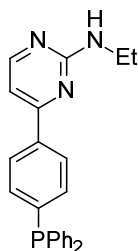
4-(1-Diphenylphosphinophenyl)-2-phenylaminopyrimidine (L4): Sodium ethoxide (0.98 g, 14.4 mmol), *N*-phenylguanidinium sulfate **5.1.2-10d** (2.65 g, 7.19 mmol) and the aminopropenone **5.1.2-9a** (2.35 g, 6.54 mmol) were dissolved in dry EtOH (32 mL). The mixture was heated to reflux for 48 h. After removing the solvent under reduced pressure the residue was dissolved in a mixture of water and dichloromethane. The layers were separated and the aqueous layer was extracted three times with dichloromethane (20 mL). The combined organic layers were dried over anhydrous MgSO_4 and the solvent was removed under reduced pressure. The crude product was recrystallized from ethanol and then purified by MPLC (dichloromethane/methanol gradient) to get rid of some phosphine oxide leading to a relatively high loss of yield. A second recrystallization from ethanol afforded **L4** (50.0 mg, 0.12 mmol, 2%).

$^1\text{H-NMR}$ (400 MHz, CDCl_3): $\delta = 6.62$ (s, 1 H), 6.83–6.95 (m, 2 H), 6.97–7.06 (m, 1 H), 7.11–7.32 (m, 10 H), 7.32–7.46 (m, 4 H), 7.56–7.65 (m, 1 H), 8.30 (d, $J = 5.2$ Hz, 1H) ppm; $^{13}\text{C-NMR}$ (101 MHz, CDCl_3): $\delta = 111.3, 119.1, 122.5, 128.6, 128.6, 128.7, 128.9, 129.1, 129.8, 133.9$ (d, $J_{\text{C-P}} = 20.0$ Hz), 135.5, 136.9 (d, $J_{\text{C-P}} = 20.0$ Hz), 139.0 (d, $J_{\text{C-P}} = 9.8$ Hz), 143.0 ($J_{\text{C-P}} = 22.1$ Hz), 157.4, 158.6, 166.5 ppm; $^{31}\text{P-NMR}$ (162 MHz, CDCl_3): $\delta = -9.42$ ppm; **elemental analysis**: calcd. (%) for $\text{C}_{28}\text{H}_{22}\text{N}_3\text{P}$: C 77.94, H 5.14, N 9.74; found: C 77.77, H 5.02, N 9.70; **m.p.**: 149–150 °C.



4-(1-Diphenylphosphinophenyl)-2-(4-methoxyphenyl)aminopyrimidine (L5): Ligand **L5** was synthesized according to the procedure described for **L4** from *N*-(4-methoxyphenyl)guanidinium sulfate **5.1.2-10e**. Yield: 1.05 g, 2.27 mmol, 82 %.

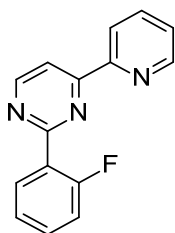
¹H-NMR (400 MHz, DMSO-*d*₆): δ = 3.69 (s, 3 H), 6.71–6.79 (m, 3 H), 7.04 (dd, J = 7.3, 3.9 Hz, 1 H), 7.16–7.23 (m, 4 H), 7.33–7.39 (m, 6 H), 7.43 (t, J = 7.5 Hz, 1 H), 7.51 (t, J = 7.4 Hz, 1 H), 7.55–7.61 (m, 3 H), 8.33 (d, J = 4.9 Hz, 1 H), 9.13–9.26 (brs) ppm; **¹³C-NMR** (101 MHz, DMSO-*d*₆): δ = 55.12, 111.9 (d, J_{C-P} = 5.1 Hz), 113.6, 120.5, 120.6, 128.7, 128.7, 128.8, 129.2 (d, J_{C-P} = 8.0 Hz), 129.4, 129.4, 133.3 (d, J_{C-P} = 20.1 Hz), 134.2, 135.2 (d, J_{C-P} = 18.9 Hz), 137.3 (d, J_{C-P} = 12.4 Hz), 144.4 (d, J_{C-P} = 25.8 Hz), 154.1, 157.6, 159.6, 166.6 (d, J_{C-P} = 3.5 Hz) ppm; **³¹P-NMR** (162 MHz, DMSO-*d*₆): δ = -13.0 ppm; **elemental analysis**: calcd. (%) for C₂₉H₂₄N₃OP: C 75.47, H 5.24, N 9.11; found: C 75.29, H 5.30, N 9.07; **m.p.**: 122–123°C.



4-(4-Diphenylphosphinophenyl)-2-ethylaminopyrimidine (L6): 1-Ethylguanidinium sulfate **5.1.2-10b** (2.35 g, 8.62 mmol) was added in one portion to a suspension of sodium methoxide (0.77 g, 14.2 mmol) in dry oxygen-free ethanol (25 mL) and the mixture was heated to reflux for 4 h. Then the aminopropenone **5.1.2-9b** (2.00 g, 5.56 mmol) was added and the resulting mixture was heated to reflux for another 16 h. After cooling to RT, the mixture was stirred for 6 h and the solvent was removed under reduced pressure, producing an orange solid. This residue was dissolved in ether (30 mL) and the organic phase was extracted with water (3 × 10 mL) until a pH of about 5.0–5.5 was reached. The aqueous layer was extracted with ether (2 × 10 mL) and the combined organic phases were dried over MgSO₄ and concentrated under reduced pressure to give an orange solid (1.41 g, 3.66 mmol, 66%). The solid was purified by MPLC to give the desired product **L6** as a colorless solid (0.59 g, 1.56 mmol, 28%).

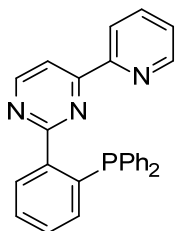
¹H-NMR (400 MHz, CDCl₃): δ = 1.17 (t, 3 H), 3.38–3.46 (m, 2 H), 5.24 (brs, 1 H), 6.84 (d, J = 5.2 Hz, 1 H), 7.25–7.32 (m, 12 H), 7.98 (d, J = 7.7 Hz, 2 H), 8.23 (d, J = 5.2 Hz, 1 H) ppm;

¹³C-NMR (101 MHz, CDCl₃): δ = 15.1, 36.4, 106.4, 127.0 (d, J_{C-P} = 6.7 Hz), 128.7 (d, J_{C-P} = 7.1 Hz), 129.0, 133.8 (d, J_{C-P} = 18.9 Hz), 133.9 (d, J_{C-P} = 22.4 Hz), 137.0 (d, J_{C-P} = 11.1 Hz), 138.0, 140.5 (d, J_{C-P} = 12.9 Hz), 158.7, 162.9, 164.3 ppm; **³¹P-NMR** (162 MHz, CDCl₃): δ = -4.2 ppm; **IR** (ATR): $\tilde{\nu}$ = 3251, 3055, 2972, 1683, 1578, 1556, 1433, 1417, 1340, 1186, 1154, 1090, 851, 801, 747, 694, 667, 514 cm⁻¹; **elemental analysis**: calcd. (%) for C₂₄H₂₂N₃P: C 75.18, H 5.75, N 10.96; found: C 75.03, H 5.73, N 11.06; **m.p.**: 109–110 °C.



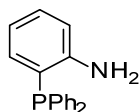
2-(2-Fluorophenyl)-4-(2-pyridinyl)-pyrimidine (5.1.2-15): An oven-dried 50 mL vessel was charged with 3-(dimethylamino)-1-(2-pyridinyl)-2-propen-1-one (**5.1.2-13**)^[263] (881 mg, 5 mmol), 2-fluorobenzamidine hydrochloride (**5.1.2-14**)^[264] (2.62 g, 15 mmol) and sodium methoxide (1.42 g, 25 mmol). After the vessel was flushed with 3 alternating vacuum and nitrogen purge cycles, dry oxygen-free ethanol (12 mL) was added *via* syringe. The resulting mixture was stirred at 80 °C for 12 h. After the mixture was cooled to RT the solids were removed by filtration and the filtrate was concentrated under reduced pressure. The residue was purified by column chromatography (SiO₂, ethyl acetate/hexane gradient) yielding **5.1.2-15** as yellow solid (1.02 g, 4.06 mmol, 81%).

¹H-NMR (400 MHz, CDCl₃): δ = 9.01 (d, J = 5.3 Hz, 1 H), 8.82–8.73 (m, 1 H), 8.66 (d, J = 7.8 Hz, 1 H), 8.31 (d, J = 5.0 Hz, 1 H), 8.22 (td, J_t = 7.8 Hz, J_d = 1.8 Hz, 1 H), 7.90 (td, J_t = 7.7 Hz, J_d = 1.8 Hz, 1 H), 7.54–7.41 (m, 2 H), 7.35–7.21 (m, 2 H) ppm; **¹³C-NMR** (101 MHz, CDCl₃): δ = 163.3 (d, J_{C-F} = 4.5 Hz), 162.6, 162.2 (d, J_{C-F} = 289.7 Hz), 158.3, 154.0, 149.5, 137.1, 131.9 (d, J_{C-F} = 2.7 Hz), 131.8 (d, J_{C-F} = 9.1 Hz), 126.5 (d, J_{C-F} = 9.1 Hz), 125.4, 124.1 (d, J_{C-F} = 3.6 Hz), 121.9, 116.9 (d, J_{C-F} = 22.7 Hz), 115.0 ppm; **¹⁹F-NMR** (376 MHz, CDCl₃): δ = -114.5 ppm; **IR** (ATR): $\tilde{\nu}$ = 3058, 3027, 3009, 1570, 1540, 1415, 1382, 1022, 995 cm⁻¹. **MS** (EI, 70 eV), m/z (%): 252 (18), 251 (100) [M⁺], 250 (14), 130 (14), 103 (40), 76 (12), 50 (12); **elemental analysis**: calcd. (%) for C₁₅H₁₀N₃F: C 71.70, H 4.01, N 16.72; found: C 71.70, H 4.11, N 16.74; **m.p.**: 98–99 °C.



2-(2-Diphenylphosphinophenyl)-4-(2-pyridinyl)-pyrimidine (L16): Under a dry atmosphere of argon, **5.1.2-15** (485 mg, 1.93 mmol) and CsF (296 mg, 1.93 mmol) were suspended in dry DMF. After dropwise addition of diphenyl(trimethylsilyl)phosphine (495 μ L, 1.93 mmol), the reaction mixture was stirred for 48 h at RT. The mixture was diluted with H₂O and CH₂Cl₂, the layers were separated and the aqueous layer was extracted with CH₂Cl₂ (3 \times 20 mL). The combined organic layers were washed with H₂O (3 \times 40 mL), dried over MgSO₄ and the solvent was removed in vacuo. The resulting yellow solid was washed with diethyl ether and recrystallized from ethanol. **L16** was obtained as a colorless solid (0.52 g, 1.25 mmol, 65%).

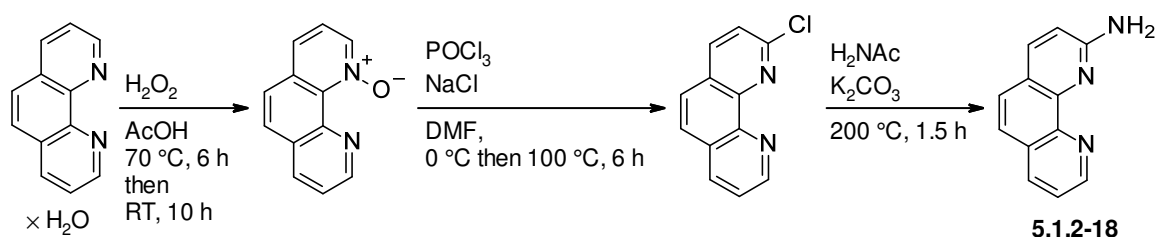
¹H-NMR (400 MHz, CDCl₃): δ = 8.89 (d, J = 5.1 Hz, 1 H), 8.69–8.62 (m, 1 H), 8.28 (ddd, J = 7.8, 4.3, 1.3 Hz, 1 H), 8.21 (d, J = 5.1 Hz, 1 H), 7.76 (dd, J = 8.0, 0.7 Hz, 1 H), 7.56–7.48 (m, 2 H), 7.38 (td, J_t = 7.5, J_d = 1.4 Hz, 1 H), 7.35–7.28 (m, 11 H), 7.13 (ddd, J = 7.8, 4.1, 1.0 Hz, 1 H) ppm; **¹³C-NMR** (101 MHz, CDCl₃): δ = 165.7, 162.2, 157.8, 153.8, 149.2, 134.6 (d, J_{C-P} = 20.5 Hz), 139.2 (d, J_{C-P} = 11.0 Hz), 137.0, 136.8 (d, J_{C-P} = 21.3 Hz), 135.3, 133.9 (d, J_{C-P} = 19.8 Hz), 130.5 (d, J_{C-P} = 3.7 Hz), 129.7, 128.7, 128.3, 128.2 (d, J_{C-P} = 7.3 Hz), 125.1, 122.4 (d, J_{C-P} = 2.2 Hz), 114.6 ppm; **³¹P-NMR** (162 MHz, CDCl₃): δ = -8.43 ppm; **IR** (ATR): $\tilde{\nu}$ = 3055, 3030, 3004, 1569, 1541, 1473, 1417, 1379, 1136, 995 cm⁻¹; **elemental analysis**: calcd. (%) for C₂₇H₂₀N₃P: C 77.69, H 4.83, N 10.07; found: C 77.43, H 4.86, N 10.13; **m.p.**: 150–151 °C.



(2-Aminophenyl)diphenylphosphine (5.1.5-16) [CAS: 65423-44-1]: An oven-dried Schlenk tube was charged with CuI (48.6 mg, 0.25 mmol, 5 mol%). After the vessel was flushed with 3 alternating vacuum and nitrogen purge cycles, anhydrous toluene (5 mL), diphenylphosphine (915 μ L, 5.00 mmol) and *N,N*-dimethylethylenediamine (188 μ L, 1.75 mmol, 35 mol%) were added. The mixture was stirred for 10 min at RT. 2-Iodoaniline (1.10 g, 5.00 mmol), Cs₂CO₃ (3.26 g, 10.0 mmol) and anhydrous toluene (5 mL) were added. The reaction mixture was stirred at 110 °C for 24 h. The resulting suspension was allowed to cool to RT, diluted with water (15 mL) and extracted with ethyl acetate (3 \times 20 mL). The combined organic phases were dried

over MgSO_4 , concentrated, and the residue was purified by column chromatography (SiO_2 , ethyl acetate/hexane gradient). **5.1.5-16** was isolated as a colorless solid (900 mg, 3.25 mmol, 65%).^[265,266]

$^1\text{H-NMR}$ (400 MHz, CDCl_3): δ = 7.40–7.30 (m, 10 H), 7.19 (ddd, J = 8.2, 7.0, 1.6 Hz, 1 H), 6.80–6.75 (m, 1 H), 6.74–6.67 (m, 2 H), 4.15 (brs, 2 H) ppm; **$^{31}\text{P-NMR}$** (162 MHz, CDCl_3): δ = -20.44 ppm; **MS** (EI, 70 eV), m/z (%): 278 (18), 277 (100) [M^+], 276 (74), 198 (42), 183 (12), 122 (9), 51 (10); the analytical data matched those reported in the literature.^[265,266]



1,10-Phenanthroline-*N*-oxide [CAS: 1891-19-6]: To a solution of 1,10-phenanthroline monohydrate (4.96 g, 25 mmol) in acetic acid (30 mL) was added H_2O_2 (30%, 3.2 mL). The mixture was stirred for 3 h at 70 °C, after which an additional portion of H_2O_2 (3.2 mL) was added. The mixture was stirred at 70 °C for another 3 h. The mixture was allowed to cool to RT, a third portion of H_2O_2 (2 mL) was added and the reaction mixture was stirred for 10 h. The solution was concentrated under reduced pressure to a total volume of approximately 10 mL. Water (35 mL) was added and the mixture was re-concentrated back to a volume of 10 mL. To the resulting oil solid K_2CO_3 (50.0 g) was added and the mixture was extracted (Soxhlet apparatus) with CHCl_3 (500 mL) for 3 h. To the CHCl_3 solution charcoal and MgSO_4 were added. The solids were filtered off and the solvent was removed under reduced pressure yielding the *N*-oxide as a greenish powder (1.70 g, 8.68 mmol, 35%).^[267]

$^1\text{H-NMR}$ (400 MHz, CDCl_3): δ = 9.31 (dd, J = 4.4, 1.9 Hz, 1 H), 8.74 (dd, J = 6.3, 1.3 Hz, 1 H), 8.23 (dd, J = 8.2, 1.9 Hz, 1 H), 7.83–7.78 (m, 1 H), 7.77–7.70 (m, 2 H), 7.66 (dd, J = 8.0, 1.5 Hz, 1 H), 7.46 (dd, J = 8.2, 6.2 Hz, 1 H) ppm; **$^{13}\text{C-NMR}$** (101 MHz, CDCl_3): δ = 150.0, 142.6, 140.8, 138.4, 135.8, 133.3, 129.0, 128.9, 126.5, 124.4, 123.1, 122.8 ppm; the analytical data matched those reported in the literature.^[267]

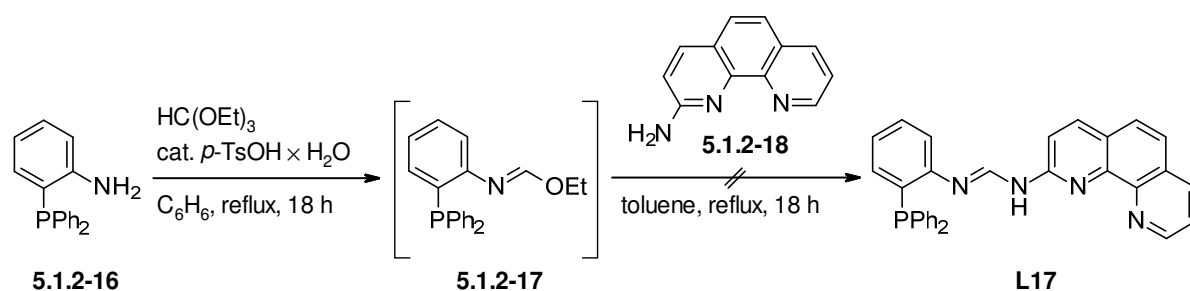
2-Chloro-1,10-phenanthroline [CAS: 7089-68-1]: To a mixture of 1,10-phenanthroline-*N*-oxide (1.47 g, 7.50 mmol) and NaCl (10.5 g, 45.0 mmol) in DMF (25 mL), POCl_3 (2.00 mL, 22.5 mmol) was added by syringe at 0 °C. Then, the reaction mixture was heated to 100 °C for 6 h. After cooling to RT, water (60 mL) was added and the mixture was basified with aq. ammonia and saturated with NaCl. The solids were filtered off and the resulting solution was

extracted with CHCl_3 (3×50 mL). The combined extracts were washed with brine (3×50 mL) and dried over MgSO_4 . The solution was concentrated under reduced pressure and the crude residue was purified by column chromatography (SiO_2 , ethyl acetate/hexane gradient) to afford the desired product as a yellow solid (899 mg, 4.19 mmol, 56%).^[267]

$^1\text{H-NMR}$ (400 MHz, CDCl_3): δ = 9.23 (dd, J = 4.3, 1.8 Hz, 1 H), 8.26 (dd, J = 8.0, 1.8 Hz, 1 H), 8.19 (d, J = 8.3 Hz, 1 H), 7.85–7.75 (m, 2 H), 7.68–7.60 (m, 2 H) ppm; **$^{13}\text{C-NMR}$** (101 MHz, CDCl_3): δ = 151.5, 150.8, 146.1, 145.1, 138.7, 136.0, 129.0, 127.2, 126.9, 125.7, 124.3, 123.4 ppm; **MS** (EI, 70 eV), m/z (%): 216 (36), 215 (17), 214 (100) [M^+], 179 (51), 75 (12), 50 (12), 44 (9); the analytical data matched those reported in the literature.^[267]

2-Amino-1,10-phenanthroline (5.1.2-18) [CAS: 22426-18-2]: A mixture of 2-chloro-1,10-phenanthroline (537 mg, 2.5 mmol), acetamide (2.95 g, 50 mmol) and K_2CO_3 (2.42 g, 17.5 mmol) was heated to 200 °C for 1.5 h. The mixture was allowed to cool to RT and water (20 mL) was added. The resulting mixture was extracted with CH_2Cl_2 (3×30 mL). The combined organic extracts were washed with brine (3×20 mL), dried over MgSO_4 and the solvent was removed under reduced pressure. The crude residue was recrystallized from ethyl acetate to give **5.1.2-18** as a yellow solid (90 mg, 0.46 mmol, 18%).^[267]

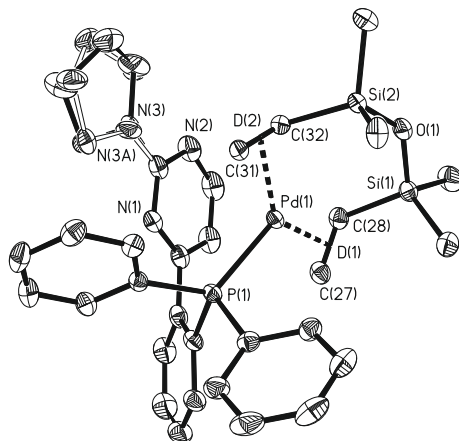
$^1\text{H-NMR}$ (400 MHz, CDCl_3): δ = 9.21 (dd, J = 4.4, 1.9 Hz, 1 H), 8.20 (dd, J = 8.2, 1.9 Hz, 1 H), 7.99 (d, J = 8.5 Hz, 1 H), 7.66 (d, J = 8.5 Hz, 1 H), 7.58–7.52 (m, 2 H), 6.91 (d, J = 8.5 Hz, 1 H), 5.12 (brs, 2 H) ppm; **$^{13}\text{C-NMR}$** (101 MHz, CDCl_3): δ = 157.7, 149.5, 145.7, 145.0, 138.1, 135.9, 129.2, 126.4, 122.8, 122.4, 121.9, 111.9 ppm; the analytical data matched those reported in the literature.^[267]



Envisioned synthesis of *N*-(2-(diphenylphosphino)phenyl)-*N'*-(2-phenanthrolinyl)formamidine (**L17**): A solution of **5.1.2-16** (693 mg, 2.50 mmol), triethyl orthoformate (850 μL , 5.00 mmol) and $p\text{-TsOH} \times \text{H}_2\text{O}$ (4.8 mg, 25 μmol , 10 mol%) in benzene (10 mL) was refluxed for 18 h. After cooling to RT, the mixture was concentrated under reduced pressure at RT. The residue was redissolved in toluene (2 mL) and **5.1.2-18** (89.8 mg, 0.46 mmol) was added to the solution. The mixture was refluxed for 18 h. After cooling to RT, the reaction mixture was concentrated

under reduced pressure at RT.^[154] All attempts to isolate **L17** (recrystallization from *i*-PrOH, column chromatography (SiO₂, ethyl acetate/hexane gradient)) failed so far. ³¹P-NMR analyses showed a complex set of signals, which did not allow for an unequivocal proof on the formation of **L17**.

7.3.8 Synthesis and characterization of the palladium complex



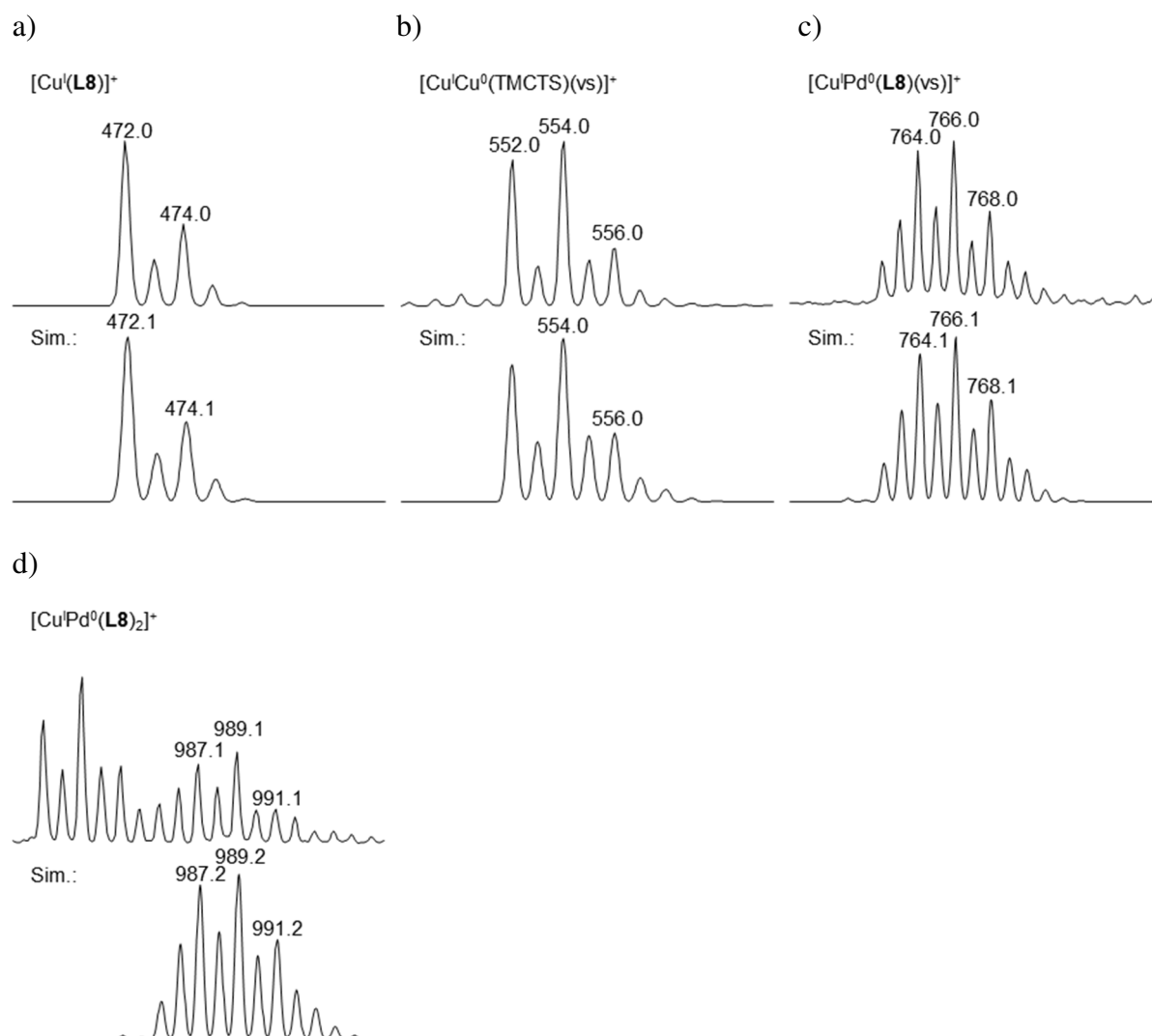
To a solution of **L8** (102 mg, 250 μ mol) in MeCN (8 mL) 1,3-divinyl-1,1,3,3-tetramethyldisiloxanepalladium(0) **5.1.2-11** in 2,4,6,8-tetramethylcyclotetrasiloxan (1 M, 250 μ L, 250 μ mol) was added. The solution was stirred at RT for 16 h whereupon a colorless solid formed. The solid was filtered off and washed with MeCN (2×1 mL). The complex was recrystallized from a saturated solution of the crude product in Et₂O and MeCN at -20 °C yielding **5.1.2-12** as colorless crystals (107 mg, 61%).

¹H-NMR (600 MHz, CDCl₃): δ = 8.07 (d, J = 5.0 Hz, 1 H), 7.55 (dd, J = 7.2, 4.3 Hz, 1 H), 7.48 (t, J = 7.5 Hz, 1 H), 7.42 (t, J = 8.2 Hz, 4 H), 7.38–7.29 (m, 7 H), 7.25 (t, J = 7.8 Hz, 1 H), 6.36 (d, J = 5.0 Hz, 1 H), 3.37 (brs, 2 H), 3.14 (dd, J = 16.1, 4.7 Hz, 2 H), 2.84 (dd, J = 12.3, 6.5 Hz, 2 H), 2.62–2.54 (m, 2 H), 2.43 (brs, 2 H), 1.81 (brs, 2 H), 1.59 (brs, 2 H), 0.23 (s, 6 H), -0.23 (s, 6 H) ppm; **¹³C-NMR** (101 MHz, CDCl₃): δ = 167.1 (d, J_{C-P} = 3.6 Hz), 159.1, 156.6, 144.4 (d, J_{C-P} = 17.3 Hz), 138.6 (d, J_{C-P} = 28.2 Hz), 134.9 (d, J_{C-P} = 21.8 Hz), 134.8, 134.7, 132.9, 130.3 (d, J_{C-P} = 6.4 Hz), 129.2, 128.8, 128.5 (d, J_{C-P} = 4.5 Hz), 127.8, 127.7, 108.6, 68.6, 68.6, 66.8, 66.7, 45.9, 25.3, 1.4, -1.2 ppm; **³¹P-NMR** (243 MHz, CDCl₃): δ = 25.3 ppm; **IR** (ATR): $\tilde{\nu}$ = 3051, 3036, 2957, 2184, 1569, 1558, 1543, 1510, 1478, 1431, 1339, 1317, 1247, 1210, 1090, 998, 837, 781, 770, 740 cm⁻¹; **ESI-MS**, m/z (%): 702 [M+H⁺]; **elemental analysis**: calcd. (%) for C₃₄H₄₂N₃OPPdSi₂: C 58.15, H 6.03, N 5.98; found: C 58.20, H 5.94, N 5.96; **m.p.**: 293–294 °C (decomposed).

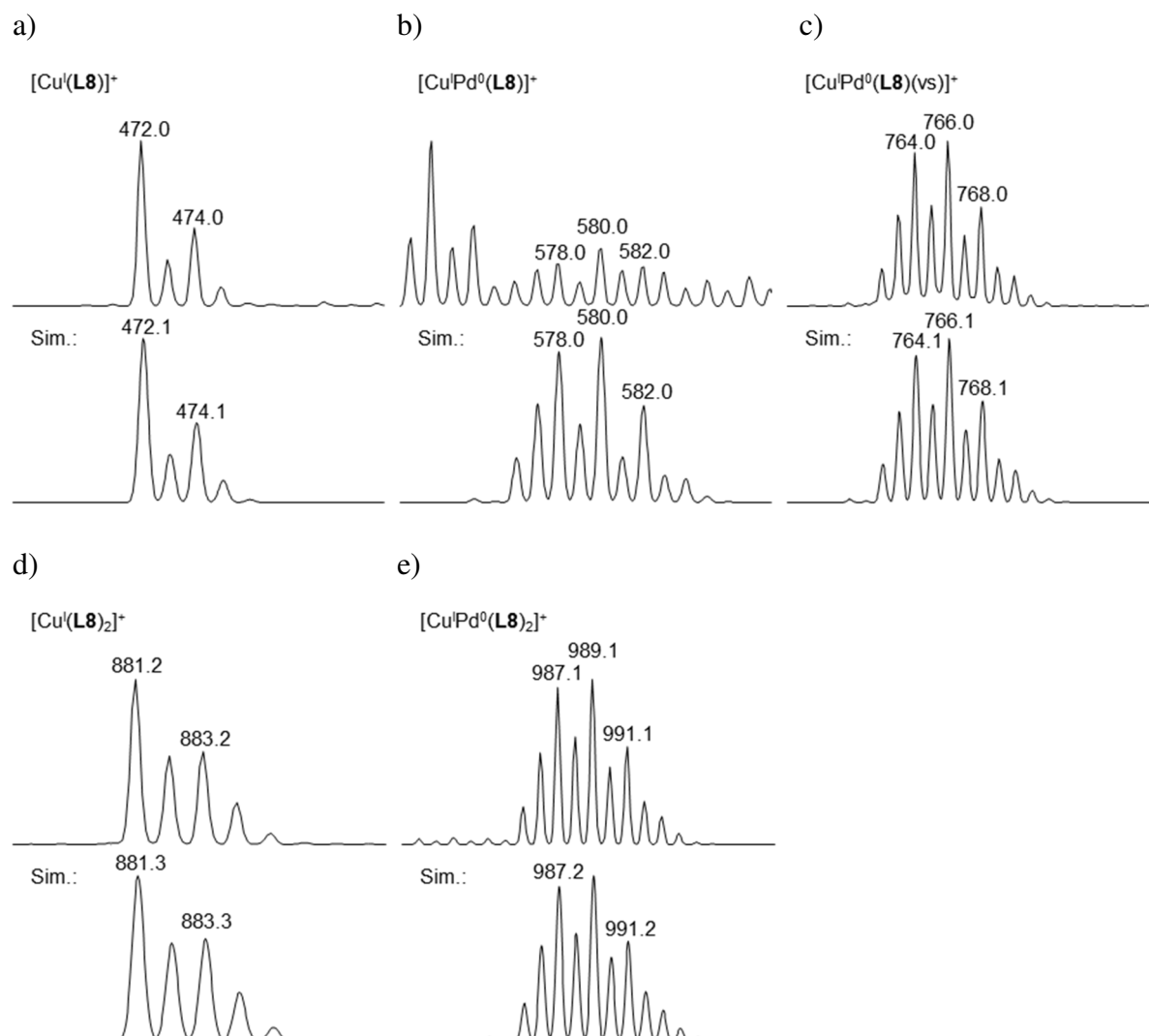
Crystal data for **5.1.2-12**: $C_{34}H_{42}N_3OPPdSi_2$; $M = 702.26 \text{ g mol}^{-1}$; $T = 150(2) \text{ K}$; triclinic; $P\bar{1}$; $a = 10.5752(3) \text{ \AA}$, $b = 10.9336(4) \text{ \AA}$, $c = 15.6717(6) \text{ \AA}$; $\alpha = 89.765(3)^\circ$, $\beta = 88.537(3)^\circ$, $\gamma = 68.120(3)^\circ$; $V = 1680.94(10) \text{ \AA}^3$; $Z = 2$; $\rho_{\text{calcd}} = 1.387 \text{ mgm}^{-1}$; $\mu(\text{MoK}\alpha) = 0.702 \text{ mm}^{-1}$ ($\lambda = 0.71023 \text{ \AA}$); 18112 reflections collected; independent reflections 9757; refinement converged to $R = 0.0324$, $wR_2 = 0.0696$ ($I > 2 \sigma(I)$), 429 Parameters and 12 restraints; min./max. residual electron density = $+0.586$ and $-0.695 \text{ e}^{-}\text{\AA}^{-3}$. CCDC 1033628 contains the supplementary crystallographic data. These data are available from the Cambridge Crystallographic Data Centre via www.ccdc.cam.ac.uk/data_request/cif.

7.3.9 Details and simulations of isotopic distributions of the ESI-MS studies

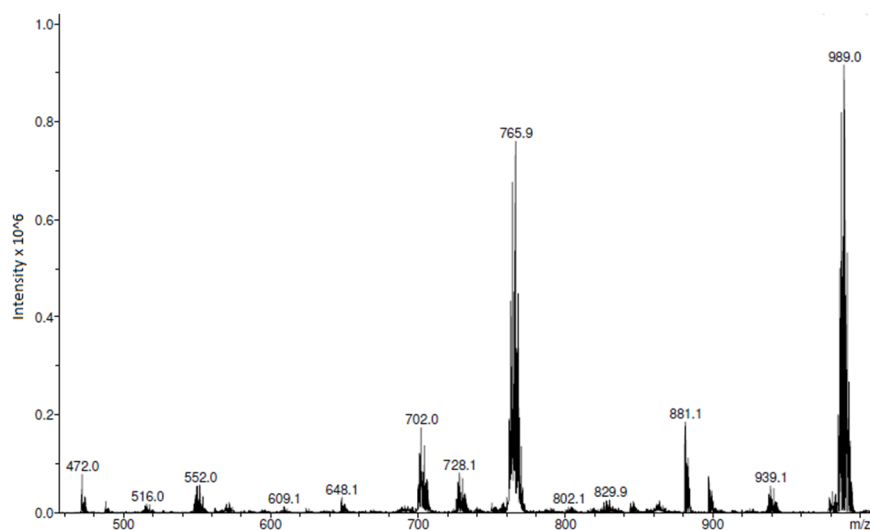
Details and simulations of isotopic distributions referring to Figure 3 in *ChemCatChem* **2015**, 7, 3579–3588:



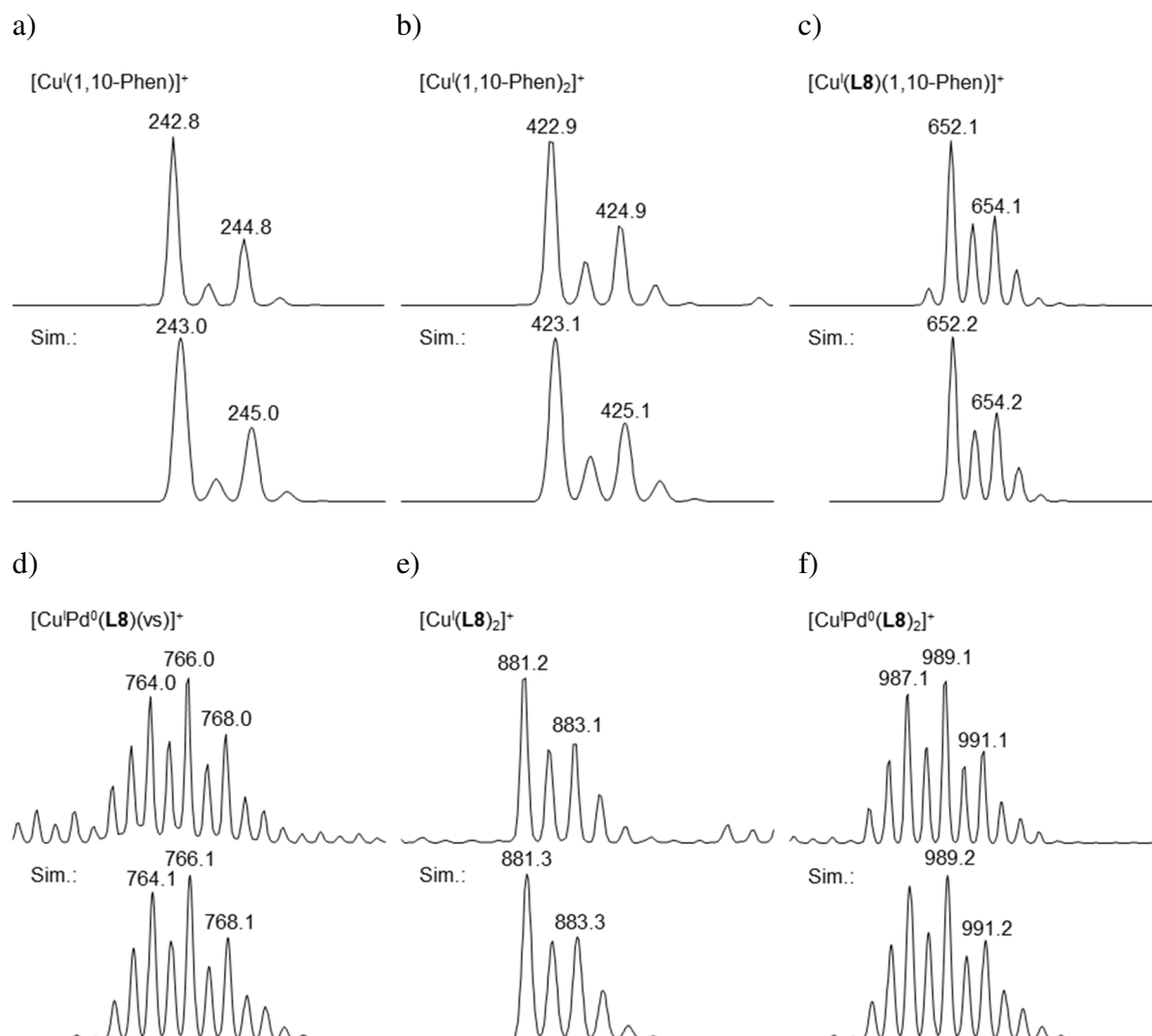
Details and simulations of isotopic distributions referring to Figure 4 in ChemCatChem **2015**, *7*, 3579–3588:



*Mass spectrum of a solution of ligand L8, $[\text{Pd}(\text{vs})]$ (**11**), $[\text{Cu}(\text{MeCN})_4]\text{BF}_4$ (**13**) and NEt_3 in acetonitrile:*



Details and simulations of isotopic distributions referring to Figure 5 in ChemCatChem **2015**, 7, 3579–3588:



7.4 Synthesis of 2-Arylpyridines *via* Cu/Pd-Catalyzed Decarboxylative Cross-Coupling of Picolinic Acids with (Hetero)Aryl Halides

7.4.1 General remarks

The reactions discussed in sections 5.2.2, 5.2.3 and 5.2.5 were performed in oven-dried glassware under a nitrogen atmosphere. The reaction discussed in section 5.2.4 were performed in oven-dried glassware under an argon atmosphere. The carboxylates were prepared from the corresponding carboxylic acids following the procedure below and were directly used.

7.4.2 General method for the catalyst screening in section 5.2.3 and 5.2.5 and the protodecarboxylation studies

An oven-dried 20 mL vessel was charged with the solid reagents. After the vessel was flushed with 3 alternating vacuum and nitrogen purge cycles, the solvent and the liquid reagents were added *via* syringe and the resulting mixture was stirred at the given temperature for the given time.

Work-up for GC analysis:

The reaction mixture was allowed to cool to RT. *n*-Tetradecane (50 μ L) was added *via* syringe and the mixture was diluted with ethyl acetate (4 mL). A sample of the reaction mixture (0.25 mL) was dissolved in ethyl acetate (2 mL), washed with brine (2 mL), dried over MgSO_4 , and analyzed by GC.

Work-up for ^{19}F -NMR analysis:

The reaction mixture was allowed to cool to RT and 1,4-difluorobenzene (30 μ L or 52 μ L) was added *via* syringe. A sample of the reaction mixture (1 mL) was filtered through a plug of Celite / MgSO_4 and analyzed by ^{19}F -NMR.

7.4.3 Preparation of starting materials

General procedure for the synthesis of potassium carboxylate salts:

A 250 mL round-bottomed flask was charged with the carboxylic acid (20.0 mmol) and ethanol (20 mL). A solution of potassium *tert*-butoxide (2.24 g, 20.0 mmol) in ethanol (20 mL) was added dropwise over 1 h. After complete addition, the reaction mixture was stirred for another 1 h at RT. A gradual formation of a precipitate was observed. The resulting solid was collected by filtration, washed sequentially with ethanol (2×10 mL) and diethyl ether (10 mL), and dried in vacuum to provide the corresponding potassium carboxylate. If after the addition of the potassium *tert*-butoxide solution a formation of a precipitate was not observed, the

solution was concentrated in vacuum. The resulting solid was collected by filtration, washed with diethyl ether (10 mL), and dried in vacuum to provide the corresponding potassium carboxylate.

7.4.4 Optimization of the decarboxylative cross-coupling of potassium 3-fluoropicolinate

General method:

An oven-dried 20 mL vessel was charged with the solid reagents. After the vessel was flushed with 3 alternating vacuum and argon purge cycles, the solvent and the liquid reagents were added *via* syringe and the resulting mixture was stirred at the given temperature for 24 h. The reaction mixture was allowed to cool to RT and 1,4-difluorobenzene (30 μ L) was added *via* syringe. A sample of the reaction mixture (1 mL) was filtered through a plug of Celite / MgSO_4 and analyzed by ^{19}F -NMR.

Tabelle 37: Optimization of the reaction conditions.

	5.2.4-1a	5.2.4-2a				5.2.4-3aa	5.2.4-4a
Entry	[M]	N-ligand	[Pd]	P-ligand	solvent	Yield (%)	
						5.2.4-3aa	4a
1	Cu_2O	1,10-Phen	PdCl_2	PPh_3	NMP/Mes	49	n.d.
2	"	"	"	"	NMP	19	trace
3	"	"	"	"	Mes	5	n.d.
4	"	"	"	"	DMF	35	trace
5	"	"	"	"	DMAc	36	9
6	"	"	"	"	DMSO	60	7
7	"	"	$\text{Pd}(\text{COD})\text{Cl}_2$	"	"	74	8
8	"	"	PdBr_2	"	"	51	14
9	"	"	PdI_2	"	"	54	11
10	"	"	$\text{Pd}(\text{OAc})_2$	"	"	49	23
11	"	"	$\text{Pd}(\text{TFA})_2$	"	"	53	6
12	"	"	$\text{Pd}(\text{acac})_2$	"	"	67	9

EXPERIMENTELLER TEIL

13	"	"	Pd(F ₆ -acac) ₂	"	"	30	31
14 ^[a]	CuCl	"	Pd(COD)Cl ₂	"	"	66	n.d.
15 ^[a]	CuBr	"	"	"	"	58	n.d.
16 ^[a]	CuI	"	"	"	"	71	8
17	Ag ₂ CO ₃	"	"	"	"	66	10
18	Ag ₂ O	"	"	"	"	52	30
19	Cu ₂ O	Me ₂ -Phen	"	"	"	62	n.d.
20	"	Me ₄ -Phen	"	"	"	83	n.d.
21	"	Ph ₂ -Phen	"	"	"	79	9
22	"	NO ₂ -Phen	"	"	"	49	17
23	"	2,2'-bipy	"	"	"	70	7
24	"	pyridine	"	"	"	72	6
25	"	Me ₄ -Phen	"	P(<i>p</i> -Tol) ₃	"	84	trace
26	"	"	"	P(<i>o</i> -Tol) ₃	"	78	7
27	"	"	"	PCy ₃	"	28	trace
28	"	"	"	P(2-Furyl) ₃	"	74	7
29	"	"	"	BINAP	"	75	n.d.
30	"	"	"	JohnPhos	"	41	8
31	"	"	"	SPhos	"	80	6
32	"	"	"	XPhos	"	74	11
33	"	"	"	CyJohnPhos	"	82	10
34	"	"	"	DavePhos	"	92	7
35	"	-	"	"	"	93	trace
36 ^[b]	"	-	"	"	"	64	12
37 ^[c]	"	-	"	"	"	23	7
38 ^[d]	"	-	"	"	"	18	5
39	-	-	"	"	"	7	32
40	Cu ₂ O	-	"	-	"	12	trace
41	"	-	-	-	"	n.d.	n.d.

Reaction conditions: **5.2.4-1a** (0.5 mmol), **5.2.4-2a** (1.0 mmol), [M] (5 mol%), *N*-ligand (10 mol%), [Pd] (5 mol%), *P*-ligand (15 mol%), solvent (2 mL), 130 °C, 24 h. ¹⁹F-NMR yield with 1,4-difluorobenzene as internal standard. [a] 10 mol% [M] was used. [b] 120 °C. [c] 110 °C. [d] 100 °C.

7.4.5 General procedure for the biaryl synthesis

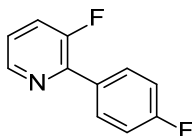
Method A:

An oven-dried 20 mL vessel was charged with copper(I) oxide (3.61 mg, 25.0 μ mol, 5 mol%), dichloro(1,5-dicyclooctadien)palladium(II) (7.13 mg, 25.0 μ mol, 5 mol%), DavePhos (29.5 mg, 75 μ mol, 15 mol%), and the potassium carboxylate **5.2.4-1** (0.50 mmol). DMSO (2 mL) and the aryl halide **5.2.4-2** (1 mmol) were added and the resulting mixture was stirred at 130 °C under a dry atmosphere of argon. After 24 h, the mixture was allowed to cool to RT, washed with distilled water (20 mL) and extracted with ethyl acetate (3 \times 20 mL). The combined organic layers were washed with brine, dried over MgSO₄, filtered, and the volatiles were removed under reduced pressure. The residue was purified by column chromatography (SiO₂, cyclohexane/ethyl acetate gradient) yielding the corresponding biaryl **5.2.4-3**.

Method B:

An oven-dried 20 mL vessel was charged with copper(I) oxide (3.61 mg, 25.0 μ mol, 5 mol%), palladium(II) chloride (4.44 mg, 25.0 μ mol, 5 mol%), 1,10-phenanthroline (9.01 mg, 50 μ mol, 10 mol%), CyJohnPhos (26.3 mg, 75 μ mol, 15 mol%), and the potassium carboxylate **5.2.4-1** (0.50 mmol). NMP/mesitylene (2 mL, 1:1) and the aryl bromide **5.2.4-2** (1 mmol) were added and the resulting mixture was stirred at 150 °C under a dry atmosphere of argon. After 24 h, the mixture was allowed to cool to RT, washed with distilled water (20 mL) and extracted with ethyl acetate (3 \times 20 mL). The combined organic layers were washed with brine, dried over MgSO₄, filtered, and the volatiles were removed under reduced pressure. The residue was purified by column chromatography (SiO₂, cyclohexane/ethyl acetate gradient) yielding the corresponding biaryl **5.2.4-3**.

7.4.6 Synthesis and characterization of the corresponding products

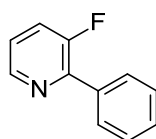


3-Fluoro-2-phenylpyridine (**5.2.4-3ab**) [CAS: 1214342-78-5]: Compound **5.2.4-3ab** was prepared following method A from potassium 3-fluoro-2-pyridinecarboxylate **5.2.4-1a** (90.5 mg, 0.50 mmol) and bromobenzene **5.2.4-2b** (159 mg, 1.06 mmol). **5.2.4-3ab** was isolated (SiO₂, cyclohexane/ethyl acetate = 9:1) as a colorless solid (64 mg, 74%).

Compound **5.2.4-3ab** was prepared following method A from potassium 3-fluoro-2-pyridinecarboxylate **5.2.4-1a** (90.5 mg, 0.50 mmol) and chlorobenzene **5.2.4-2b'** (113 mg,

102 μL , 1.0 mmol). **5.2.4-3ab** was isolated (SiO_2 , cyclohexane/ethyl acetate = 9:1) as a colorless solid (44 mg, 71%).

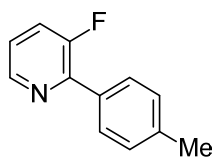
$^1\text{H-NMR}$ (400 MHz, CDCl_3): δ = 8.50–8.58 (m, 1 H), 7.93–8.04 (m, 2 H), 7.42–7.55 (m, 4 H), 7.25–7.31 (m, 1 H) ppm; **$^{13}\text{C-NMR}$** (101 MHz, CDCl_3): δ = 157.5 (d, $J_{\text{C-F}}$ = 258.9 Hz), 146.2 (d, $J_{\text{C-F}}$ = 10.9 Hz), 145.4 (d, $J_{\text{C-F}}$ = 5.5 Hz), 135.3 (d, $J_{\text{C-F}}$ = 5.4 Hz), 129.2, 128.8 (d, $J_{\text{C-F}}$ = 5.4 Hz), 128.4, 124.1 (d, $J_{\text{C-F}}$ = 20.0 Hz), 123.4 (d, $J_{\text{C-F}}$ = 3.6 Hz) ppm; **$^{19}\text{F-NMR}$** (377 MHz, CDCl_3): δ = -112.1, -123.0 ppm; **IR** (ATR): $\tilde{\nu}$ = 3064, 1596, 1431, 1250, 1188, 798 cm^{-1} ; **MS** (EI, 70 eV), m/z (%): 173 (100) [M^+], 172 (78), 145 (11), 125 (11), 51 (13), 50 (23); **HRMS** (EI-TOF), m/z : [M^+] calcd. for $\text{C}_{11}\text{H}_8\text{FN}$: 173.0641; found 173.0639; **m.p.**: 48–49 $^\circ\text{C}$.



3-Fluoro-2-phenylpyridine (**5.2.4-3ab**) [CAS: 1214342-78-5]: Compound **5.2.4-3ab** was prepared following method A from potassium 3-fluoro-2-pyridinecarboxylate **5.2.4-1a** (90.5 mg, 0.50 mmol) and bromobenzene **5.2.4-2b** (159 mg, 106 μL , 1.0 mmol). **5.2.4-3ab** was isolated (SiO_2 , cyclohexane/ethyl acetate = 9:1) as a colorless solid (64 mg, 74%).

Compound **5.2.4-3ab** was prepared following method A from potassium 3-fluoro-2-pyridinecarboxylate **5.2.4-1a** (90.5 mg, 0.50 mmol) and chlorobenzene **5.2.4-2b'** (113 mg, 102 μL , 1.0 mmol). **5.2.4-3ab** was isolated (SiO_2 , cyclohexane/ethyl acetate = 9:1) as a colorless solid (44 mg, 71%).

$^1\text{H-NMR}$ (400 MHz, CDCl_3): δ = 8.50–8.58 (m, 1 H), 7.93–8.04 (m, 2 H), 7.42–7.55 (m, 4 H), 7.25–7.31 (m, 1 H) ppm; **$^{13}\text{C-NMR}$** (101 MHz, CDCl_3): δ = 157.5 (d, $J_{\text{C-F}}$ = 258.9 Hz), 146.2 (d, $J_{\text{C-F}}$ = 10.9 Hz), 145.4 (d, $J_{\text{C-F}}$ = 5.5 Hz), 135.3 (d, $J_{\text{C-F}}$ = 5.4 Hz), 129.2, 128.8 (d, $J_{\text{C-F}}$ = 5.4 Hz), 128.4, 124.1 (d, $J_{\text{C-F}}$ = 20.0 Hz), 123.4 (d, $J_{\text{C-F}}$ = 3.6 Hz) ppm; **$^{19}\text{F-NMR}$** (377 MHz, CDCl_3): δ = -123.0 ppm; **IR** (ATR) : $\tilde{\nu}$ = 3064, 1596, 1431, 1250, 1188, 798 cm^{-1} ; **MS** (EI, 70 eV), m/z (%): 173 (100) [M^+], 172 (78), 145 (11), 125 (11), 51 (13), 50 (23); **HRMS** (EI-TOF), m/z : [M^+] calcd. for $\text{C}_{11}\text{H}_8\text{FN}$: 173.0641; found 173.0639; **m.p.**: 48–49 $^\circ\text{C}$.

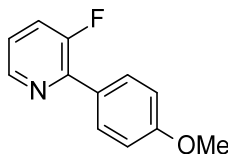


3-Fluoro-2-(4-methylphenyl)pyridine (**5.2.4-3ac**): Compound **5.2.4-3ac** was prepared following method A and B, respectively, from potassium 3-fluoro-2-pyridinecarboxylate

5.2.4-1a (90.5 mg, 0.50 mmol) and 1-bromo-4-methylbenzene **5.2.4-2c** (175 mg, 126 μ L, 1.0 mmol). **5.2.4-3ac** was isolated (SiO₂, cyclohexane/ethyl acetate = 9:1) as a colorless solid (48 mg, 52% (method A); 79mg. 84% (method B)).

Compound **5.2.4-3ac** was prepared following method A from potassium 3-fluoro-2-pyridinecarboxylate **5.2.4-1a** (90.5 mg, 0.50 mmol) and 1-chloro-4-methylbenzene **5.2.4-2c'** (129 mg, 121 μ L, 1.0 mmol). **5.2.4-3ac** was isolated (SiO₂, cyclohexane/ethyl acetate = 9:1) as a colorless solid (47 mg, 50%).

¹H-NMR (400 MHz, CDCl₃): δ = 8.45–8.58 (m, 1 H), 7.90 (dd, J = 8.3, 1.5 Hz, 2 H), 7.47 (ddd, J = 11.0, 8.3, 1.0 Hz, 1 H), 7.31 (d, J = 8.3 Hz, 2 H), 7.20–7.27 (m, 1 H), 2.43 (s, 3 H) ppm; **¹³C NMR** (101 MHz, CDCl₃): δ = 157.4 (d, J_{C-F} = 259.8 Hz), 146.2 (d, J_{C-F} = 10.9 Hz), 145.2 (d, J_{C-F} = 5.4 Hz), 139.2, 132.5 (d, J_{C-F} = 5.4 Hz), 129.1, 128.6 (d, J_{C-F} = 6.4 Hz), 123.9 (d, J_{C-F} = 20.9 Hz), 123.0 (d, J_{C-F} = 3.6 Hz), 21.3 ppm; **¹⁹F-NMR** (377 MHz, CDCl₃): δ = -123.0 ppm; **IR** (ATR): $\tilde{\nu}$ = 3050, 3027, 2921, 1596, 1444, 1405, 1251, 1187, 1106 cm⁻¹; **MS** (EI, 70 eV), m/z (%): 187 (100) [M⁺], 186 (60), 185 (17), 91 (12), 63 (10), 50 (11); **HRMS** (EI-TOF), m/z : [M⁺] calcd. for C₁₂H₁₀FN: 187.0797; found 187.0796; **m.p.**: 51–52 °C.

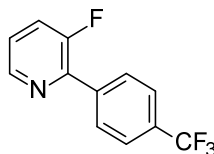


3-Fluoro-2-(4-methoxyphenyl)pyridine (**5.2.4-3ad**) [CAS: 847226-10-2]: Compound **5.2.4-3ad** was prepared following method A from potassium 3-fluoro-2-pyridinecarboxylate **5.2.4-1a** (90.5 mg, 0.50 mmol) and 1-bromo-4-methoxybenzene **5.2.4-2d** (187 mg, 126 μ L, 1.0 mmol). **5.2.4-3ad** was isolated (SiO₂, cyclohexane/ethyl acetate = 9:1) as a yellow oil (82 mg, 80%).

Compound **5.2.4-3ad** was prepared following method A from potassium 3-fluoro-2-pyridinecarboxylate **5.2.4-1a** (90.5 mg, 0.50 mmol) and 1-chloro-4-methoxybenzene **5.2.4-2d'** (145 mg, 125 μ L, 1.0 mmol). **5.2.4-3ad** was isolated (SiO₂, cyclohexane/ethyl acetate = 9:1) as a yellow oil (83 mg, 82%).

¹H-NMR (400 MHz, CDCl₃): δ = 8.45–8.53 (m, 1 H), 7.97 (dd, J = 8.8, 1.5 Hz, 2 H), 7.46 (ddd, J = 11.3, 8.3, 1.3 Hz, 1 H), 7.18–7.25 (m, 1 H), 6.97–7.07 (m, 2 H), 3.88 (s, 3 H) ppm; **¹³C-NMR** (101 MHz, CDCl₃): δ = 160.4, 157.3 (d, J_{C-F} = 259.8 Hz) 145.8 (d, J_{C-F} = 10.0 Hz) 145.2 (d, J_{C-F} = 5.5 Hz) 130.1 (d, J_{C-F} = 5.5 Hz) 127.9 (d, J_{C-F} = 5.4 Hz) 123.9 (d, J_{C-F} = 20.9 Hz) 122.7 (d, J_{C-F} = 4.5 Hz), 113.8, 55.3 ppm; **¹⁹F-NMR** (377 MHz, CDCl₃): δ = -123.2 ppm; **IR** (ATR): $\tilde{\nu}$ = 3064, 3006, 2838, 1611, 1513, 1436, 1307, 1245, 1175, 1023 cm⁻¹; **MS** (EI, 70 eV),

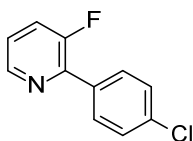
m/z (%): 203 (100) [M^+], 188 (54), 160 (35), 159 (22); **HRMS** (EI-TOF), m/z : [M^+] calcd. for $C_{12}H_{10}FNO$: 203.0746; found 203.0745.



3-Fluoro-2-[4-(trifluoromethyl)phenyl]pyridine (5.2.4-3ae) [CAS: 1261805-54-2]: Compound **5.2.4-3ae** was prepared following method A from potassium 3-fluoro-2-pyridinecarboxylate **5.2.4-1a** (90.5 mg, 0.50 mmol) and 1-bromo-4-(trifluoromethyl)benzene **5.2.4-2e** (227 mg, 142 μ L, 1.0 mmol). **5.2.4-3ae** was isolated (SiO_2 , cyclohexane/ethyl acetate = 9:1) as a colorless oil (111 mg, 92%).

Compound **5.2.4-3ae** was prepared following method A from potassium 3-fluoro-2-pyridinecarboxylate **5.2.4-1a** (90.5 mg, 0.50 mmol) and 1-chloro-4-(trifluoromethyl)benzene **5.2.4-2e'** (184 mg, 136 μ L, 1.0 mmol). **5.2.4-3ae** was isolated (SiO_2 , cyclohexane/ethyl acetate = 9:1) as a colorless oil (99 mg, 82%).

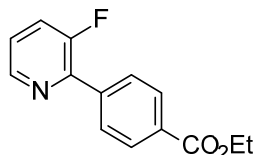
1H -NMR (250 MHz, $CDCl_3$): δ = 8.51–8.61 (m, 1 H), 8.13 (d, J = 8.1 Hz, 2 H), 7.75 (d, J = 8.4 Hz, 2 H), 7.46–7.60 (m, 1 H), 7.30–7.38 (m, 1 H) ppm; **^{13}C -NMR** (151 MHz, $CDCl_3$): δ = 157.8 (d, J_{C-F} = 260.8 Hz), 145.6, 144.5 (d, J_{C-F} = 9.7 Hz), 138.6, 131.0 (q, J_{C-F} = 33.3 Hz), 129.1 (d, J_{C-F} = 6.9 Hz), 125.4 (q, J_{C-F} = 4.2 Hz), 124.6, 124.43, 124.37 (q, J_{C-F} = 273.3 Hz) ppm; **^{19}F -NMR** (377 MHz $CDCl_3$): δ = -62.7, -122.5 ppm; **IR** (ATR): $\tilde{\nu}$ = 3067, 1619, 1597, 1446, 1406, 1323, 1252, 1163, 1114, 1068, 1016 cm^{-1} ; **MS** (EI, 70 eV), m/z (%): 241 (100) [M^+], 222 (19), 221 (17), 172 (27), 68 (15), 50 (12); **HRMS** (EI-TOF), m/z : [M^+] Calcd. for $C_{12}H_7F_4N$: 241.0515; found 241.0519.



2-(4-Chlorophenyl)-3-fluoropyridine (5.2.4-3af) [CAS: 1233702-02-7]: Compound **5.2.4-3af** was prepared following method A from 3-fluoro-2-pyridinecarboxylate **5.2.4-1a** (90.5 mg, 0.50 mmol) and 1-chloro-4-bromobenzene **5.2.4-2f** (191 mg, 1.0 mmol). **5.2.4-3af** was isolated (SiO_2 , cyclohexane/ethyl acetate = 9:1) as a colorless solid (73 mg, 71 mmol).

1H -NMR (400 MHz, $CDCl_3$): δ = 8.52 (d, J = 4.5 Hz, 1 H), 7.95 (dd, J = 8.5, 1.3 Hz, 2 H), 7.41–7.55 (m, 3 H), 7.24–7.33 (m, 1 H) ppm; **^{13}C -NMR** (101 MHz, $CDCl_3$): δ = 157.5 (d, J_{C-F} = 260.7 Hz), 145.3, 144.9 (d, J_{C-F} = 10.0 Hz), 135.4, 133.6, 130.1 (d, J_{C-F} = 5.5 Hz), 128.7, 124.3

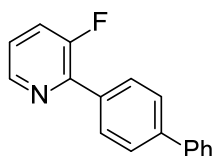
(d, $J_{\text{C-F}} = 20.9$ Hz), 123.8 ppm; $^{19}\text{F-NMR}$ (377 MHz, CDCl_3): $\delta = -123.0$ ppm; **IR** (ATR): $\tilde{\nu} = 3048, 3016, 1599, 1497, 1445, 1398, 1254, 1190, 1092$ cm^{-1} ; **MS** (EI, 70 eV), m/z (%): 209 (33) $[\text{M}^+]$, 208 (16), 207 (100) $[\text{M}]^+$, 172 (55), 145 (10), 75 (7), 50 (9); **HRMS** (EI-TOF), m/z : $[\text{M}^+]$ calcd. for $\text{C}_{11}\text{H}_7^{35}\text{ClFN}$: 207.0251; found 207.0249; **m.p.**: 74–75 °C.



4-(3-Fluoro-2-pyridinyl)benzoic acid ethyl ester (**5.2.4-3ag**) [CAS: 1246461-83-5]: Compound **5.2.4-3ag** was prepared following method A from 3-fluoro-2-pyridinecarboxylate **5.2.4-1a** (90.5 mg, 0.50 mmol) and 4-bromobenzoic acid ethyl ester **5.2.4-2g** (231 mg, 162 μL , 1.0 mmol). **5.2.4-3ag** was isolated (SiO_2 , cyclohexane/ethyl acetate = 9:1) as a yellow oil (113 mg, 92%).

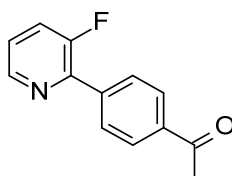
Compound **5.2.4-3ag** was prepared following method A from 3-fluoro-2-pyridinecarboxylate **5.2.4-1a** (90.5 mg, 0.50 mmol) and 4-chlorobenzoic acid ethyl ester **5.2.4-2g'** (188 mg, 158 μL , 1.0 mmol). **5.2.4-3ag** was isolated (SiO_2 , cyclohexane/ethyl acetate = 9:1) as a yellow oil (72 mg, 59%).

$^1\text{H-NMR}$ (400 MHz, CDCl_3): $\delta = 8.51\text{--}8.59$ (m, 1 H), 8.11–8.21 (m, 2 H), 8.01–8.10 (m, 2 H), 7.52 (ddd, $J = 10.9, 8.4, 1.0$ Hz, 1 H), 7.30–7.35 (m, 1 H), 4.42 (q, $J = 7.1$ Hz, 2 H), 1.43 (t, $J = 7.2$ Hz, 3 H) ppm; $^{13}\text{C-NMR}$ (101 MHz, CDCl_3): $\delta = 166.3, 157.8$ (d, $J_{\text{C-F}} = 261.6$ Hz), 145.6 (d, $J_{\text{C-F}} = 5.4$ Hz), 145.0 (d, $J_{\text{C-F}} = 10.9$ Hz), 139.4 (d, $J_{\text{C-F}} = 5.5$ Hz), 130.8, 129.6, 128.7 (d, $J_{\text{C-F}} = 6.4$ Hz), 124.3 (d, $J_{\text{C-F}} = 25.4$ Hz), 124.2, 61.1, 14.3 ppm; $^{19}\text{F-NMR}$ (377 MHz, CDCl_3): $\delta = -122.1$ ppm; **IR** (ATR): $\tilde{\nu} = 3064, 2984, 1711, 1443, 1402, 1367, 1267, 1186, 1095, 1016$ cm^{-1} ; **MS** (EI, 70 eV), m/z (%): 245 (59) $[\text{M}^+]$, 217 (47), 201 (16), 200 (100), 172 (27), 125 (10); **HRMS** (EI-TOF), m/z : $[\text{M}^+]$ calcd. for $\text{C}_{14}\text{H}_{12}\text{FNO}_2$: 245.0852; found 245.0847.



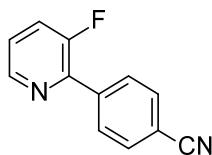
2-[1,1'-Biphenyl]-4-yl-3-fluoropyridine (**5.2.4-3ah**): Compound **5.2.4-3ah** was prepared following method A from potassium 3-fluoro-2-pyridinecarboxylate **5.2.4-1a** (90.5 mg, 0.50 mmol) and 4-bromo-1,1'-biphenyl **5.2.4-2h** (259 mg, 1.0 mmol). **5.2.4-3ah** was isolated (SiO_2 , cyclohexane/ethyl acetate = 9:1) as a colorless solid (100 mg, 81%).

¹H-NMR (400 MHz, CDCl₃): δ = 8.52–8.59 (m, 1 H), 8.09 (dd, J = 8.4, 1.6 Hz, 2 H), 7.72–7.77 (m, 2 H), 7.64–7.71 (m, 2 H), 7.45–7.56 (m, 3 H), 7.36–7.42 (m, 1 H), 7.28–7.32 (m, 1 H) ppm; **¹³C-NMR** (101 MHz, CDCl₃): δ = 156.3 (d, J_{C-F} = 259.8 Hz), 145.7 (d, J_{C-F} = 10.1 Hz), 145.2 (d, J_{C-F} = 5.5 Hz), 142.0, 140.5, 134.0 (d, J_{C-F} = 5.5 Hz), 129.2 (d, J_{C-F} = 6.4 Hz), 128.8, 127.6, 127.17, 127.15, 124.3 (d, J_{C-F} = 20.9 Hz), 123.4 (d, J_{C-F} = 3.6 Hz) ppm; **¹⁹F-NMR** (377 MHz, CDCl₃): δ = -122.7 ppm; **IR** (ATR): $\tilde{\nu}$ = 3062, 3024, 1594, 1485, 1440, 1397, 1246 cm⁻¹; **MS** (EI, 70 eV), m/z (%): 249 (100) [M⁺], 248 (23), 51 (8), 50 (10), 44 (8); **HRMS** (EI-TOF), m/z : [M⁺] calcd. for C₁₇H₁₂FN: 249.0954; found 249.0938; **m.p.**: 97–98 °C.



1-[4-(3-Fluoro-2-pyridinyl)phenyl]ethanone (5.2.4-3ai): Compound **5.2.4-3ai** was prepared following method A from potassium 3-fluoro-2-pyridinecarboxylate **5.2.4-1a** (90.5 mg, 0.50 mmol) and 1-(4-bromophenyl)ethanone **5.2.4-2i** (203 mg, 1.0 mmol). **5.2.4-3ai** was isolated (SiO₂, cyclohexane/ethyl acetate = 6:1) as a colorless solid (50 mg, 47%).

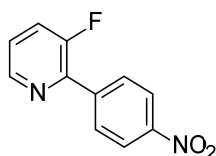
¹H-NMR (200 MHz, CDCl₃): δ = 8.57 (dt, J_d = 4.5, J_t = 1.5 Hz, 1 H), 8.03–8.15 (m, 4 H), 7.47–7.60 (m, 1 H), 7.28–7.38 (m, 1 H), 2.66 (s, 3 H) ppm; **¹³C-NMR** (50 MHz, CDCl₃): δ = 197.8, 157.8 (d, J_{C-F} = 261.6 Hz), 145.6 (d, J_{C-F} = 5.1 Hz), 144.8 (d, J_{C-F} = 10.2 Hz), 139.6 (d, J_{C-F} = 5.9 Hz), 137.2, 128.9 (d, J_{C-F} = 6.2 Hz), 128.4, 124.34 (d, J_{C-F} = 20.9 Hz), 124.30 (d, J_{C-F} = 4.0 Hz), 26.7 ppm; **¹⁹F-NMR** (377 MHz, CDCl₃): δ = -121.1 ppm; **IR** (ATR): $\tilde{\nu}$ = 3078, 3009, 1674, 1603, 1443, 1400, 1246 cm⁻¹; **MS** (EI, 70 eV), m/z (%): 215 (17) [M⁺], 201 (14), 200 (100), 172 (30); **HRMS** (EI-TOF), m/z : [M⁺] calcd. for C₁₃H₁₀FNO: 215.0746; found 215.0741; **m.p.**: 88–89 °C.



4-(3-Fluoro-2-pyridinyl)benzonitrile (5.2.4-3aj) [CAS: 1352794-83-2]: Compound **5.2.4-3aj** was prepared following method A from potassium 3-fluoro-2-pyridinecarboxylate **5.2.4-1a** (90.5 mg, 0.50 mmol) and 4-bromo-benzonitrile **5.2.4-2j** (184 mg, 1.0 mmol). **5.2.4-3aj** was isolated (SiO₂, cyclohexane/ethyl acetate = 6:1) as a colorless solid (81 mg, 82%).

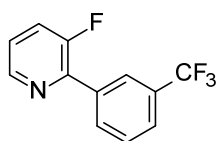
¹H-NMR (75 MHz, CDCl₃): δ = 8.57 (dt, J_d = 4.4, J_t = 1.6 Hz, 1 H), 8.10–8.17 (m, 2 H), 7.74–7.81 (m, 2 H), 7.55 (ddd, J = 11.1, 8.3, 1.3 Hz, 1 H), 7.32–7.40 (m, 1 H) ppm; **¹³C-NMR**

(75 MHz, CDCl₃): δ = 157.8 (d, J_{C-F} = 262.0 Hz), 145.7 (d, J_{C-F} = 5.5 Hz), 143.9 (d, J_{C-F} = 9.9 Hz), 139.5 (d, J_{C-F} = 5.5 Hz), 132.2 (d, J_{C-F} = 0.7 Hz), 129.3 (d, J_{C-F} = 6.6 Hz), 124.8 (d, J_{C-F} = 4.0 Hz), 124.6 (d, J_{C-F} = 20.9 Hz), 118.7, 112.7 (d, J_{C-F} = 1,1 Hz) ppm; **¹⁹F-NMR** (377 MHz, CDCl₃): δ = -121.9 ppm; **IR** (ATR): $\tilde{\nu}$ 3061, 2226, 1605, 1595, 1441, 1402, 1248, 1099 cm⁻¹; **MS** (EI, 70 eV), m/z (%): 198 (100) [M⁺], 197 (56), 50 (8); **HRMS** (EI-TOF), m/z : [M⁺] calcd. for C₁₂H₇FN₂: 198.0593; found 198.0585; **m.p.**: 124–125 °C.



3-Fluoro-2-(4-nitrophenyl)pyridine (5.2.4-3ak): Compound **5.2.4-3ak** was prepared following method A from potassium 3-fluoro-2-pyridinecarboxylate **5.2.4-1a** (90.5 mg, 0.50 mmol) and 1-bromo-4-nitrobenzene **5.2.4-2k** (204 mg, 1.0 mmol). **5.2.4-3ak** was isolated (SiO₂, cyclohexane/ethyl acetate = 9:1) as a colorless solid (96 mg, 88%).

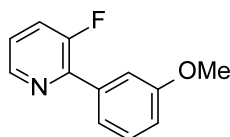
¹H-NMR (200 MHz, CDCl₃): δ = 8.59 (dt, J_d = 4.5 Hz, J_t = 1.5 Hz, 1 H), 8.30–8.40 (m, 2 H), 8.16–8.26 (m, 2 H), 7.51–7.63 (m, 1 H), 7.34–7.45 (m, 1 H) ppm; **¹³C-NMR** (50 MHz, CDCl₃): δ = 157.9 (d, J_{C-F} = 262.0), 148.0, 145.8 (d, J_{C-F} = 5.5 Hz), 143.4 (d, J_{C-F} = 9.9 Hz), 141.3 (d, J_{C-F} = 5.9 Hz), 129.6 (d, J_{C-F} = 6.6 Hz), 125.0 (d, J_{C-F} = 4.4 Hz), 124.6 (d, J_{C-F} = 20.5 Hz), 123.5 ppm; **¹⁹F-NMR** (CDCl₃, 377 MHz): δ = -121.6 ppm; **IR** (ATR): $\tilde{\nu}$ = 3076, 1593, 1514, 1440, 1342, 1188, 1103 cm⁻¹; **MS** (EI, 70 eV), m/z (%): 218 (100) [M⁺], 188 (38), 172 (35), 160 (19), 145 (20), 125 (17), 44 (15); **HRMS** (EI-TOF), m/z : [M⁺] calcd. for C₁₁H₇FN₂O₂: 218.0492; found 218.0486; **m.p.**: 140–141 °C.



3-Fluoro-2-[3-(trifluoromethyl)phenyl]pyridine (5.2.4-3al) [CAS: 1261634-22-3]: Compound **5.2.4-3al** was prepared following method A from potassium 3-fluoro-2-pyridinecarboxylate **5.2.4-1a** (90.5 mg, 0.50 mmol) and 1-bromo-3-(trifluoromethyl)benzene **5.2.4-2l** (227 mg, 141 μ L, 1.0 mmol). **5.2.4-3al** was isolated (SiO₂, cyclohexane/ethyl acetate = 9:1) as a colorless oil (116 mg, 96%).

¹H-NMR (400 MHz, CDCl₃): δ = 8.49–8.61 (m, 1 H), 8.30 (s, 1 H), 8.19 (d, J = 7.8 Hz, 1 H), 7.71 (d, J = 8.0 Hz, 1 H), 7.62 (t, J = 7.8 Hz, 1 H), 7.54 (ddd, J = 11.0, 8.3, 1.3 Hz, 1 H), 7.29–7.39 (m, 1 H) ppm; **¹³C-NMR** (101 MHz, CDCl₃): 157.6 (d, J_{C-F} = 261.6 Hz), 145.6 (d, J_{C-F} = 5.4 Hz), 144.5 (d, J_{C-F} = 10.9 Hz), 136.0 (d, J_{C-F} = 5.5 Hz), 131.8–132.1 (m), 130.9 (q,

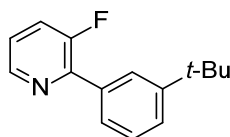
$J_{\text{C-F}} = 31.8$ Hz), 128.9, 125.7–125.9 (m), 125.5–125.7 (m), 124.4 (d, $J_{\text{C-F}} = 20.9$ Hz), 124.2 (d, $J_{\text{C-F}} = 4.5$ Hz), 123.9 (q, $J_{\text{C-F}} = 273.4$ Hz) ppm; ^{19}F -NMR (CDCl_3 , 377 MHz): $\delta = -62.6$, -122.8 ppm; **IR** (ATR): $\tilde{\nu} = 3071$, 1597, 1444, 1421, 1334, 1303, 1252, 1163, 1119, 1074 cm^{-1} ; **MS** (EI, 70 eV), m/z (%): 241 (100) [M^+], 222 (20), 221 (19), 172 (25), 69 (16), 50 (12); **HRMS** (EI-TOF), m/z : [M^+] calcd. for $\text{C}_{12}\text{H}_7\text{F}_4\text{N}$: 241.0515; found 241.0503.



3-Fluoro-2-(3-methoxyphenyl)pyridine (**5.2.4-3am**) [CAS: 1269225-56-0]: Compound **5.2.4-3am** was prepared following method A from 3-fluoropyridinecarboxylate **5.2.4-1a** (90.5 mg, 0.50 mmol) and 1-bromo-3-methoxybenzene **5.2.4-2m** (191 mg, 129 μL , 1.0 mmol). **5.2.4-3am** was isolated (SiO_2 , cyclohexane/ethyl acetate = 6:1) as an orange oil (99 mg, 97%).

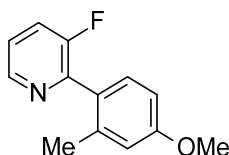
Compound **5.2.4-3am** was prepared following method A from 3-fluoropyridinecarboxylate **5.2.4-1a** (90.5 mg, 0.50 mmol) and 1-chloro-3-methoxybenzene **5.2.4-2m'** (145 mg, 125 μL , 1.0 mmol). **5.2.4-3am** was isolated (SiO_2 , cyclohexane/ethyl acetate = 6:1) as an orange oil (62 mg, 61%).

^1H -NMR (400 MHz, CDCl_3): $\delta = 8.52$ – 8.54 (m, 1 H), 7.54–7.60 (m, 2 H), 7.50 (ddd, $J = 11.0$, 8.3, 1.5 Hz, 1 H), 7.41 (t, $J = 7.9$ Hz, 1 H), 7.26–7.30 (m, 1 H), 6.98–7.03 (m, 1 H), 3.89 (s, 3 H) ppm; ^{13}C -NMR (101 MHz, CDCl_3): $\delta = 159.7$, 157.5 (d, $J_{\text{C-F}} = 260.4$ Hz), 146.0 (d, $J_{\text{C-F}} = 10.3$ Hz), 145.3 (d, $J_{\text{C-F}} = 5.1$ Hz), 136.6 (d, $J_{\text{C-F}} = 5.1$ Hz), 129.4, 124.1 (d, $J_{\text{C-F}} = 21.3$ Hz), 123.5 (d, $J_{\text{C-F}} = 3.7$ Hz), 121.3 (d, $J_{\text{C-F}} = 7.3$ Hz), 115.4, 113.8 (d, $J_{\text{C-F}} = 5.1$ Hz), 55.3 ppm; ^{19}F -NMR (377 MHz, CDCl_3): $\delta = -122.4$ ppm; **IR** (ATR): $\tilde{\nu} = 3068$, 2935, 2836, 1585, 1463, 1439, 1417, 1288, 1253, 1229 cm^{-1} ; **MS** (EI, 70 eV), m/z (%): 203 (97) [M^+], 202 (100), 174 (39), 173 (27), 172 (46), 159 (14); **HRMS** (EI-TOF), m/z : [M^+] calcd. for $\text{C}_{12}\text{H}_{10}\text{FNO}$: 203.0746; found 203.0744.



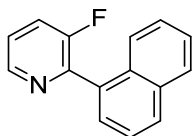
2-[3-(tert-Butyl)phenyl]-3-fluoropyridine (**5.2.4-3an**). Compound **5.2.4-3an** was prepared following method A and B, respectively, from 3-fluoro-2-pyridinecarboxylate **5.2.4-1a** (90.5 mg, 0.50 mmol) and 1-bromo-3-(1,1-dimethylethyl)benzene **5.2.4-2n** (213 mg, 170 μL , 1.0 mmol). **5.2.4-3an** was isolated (SiO_2 , cyclohexane/ethyl acetate = 9:1) as a colorless liquid (61 mg, 53% (method A), 75 mg, 65% (method B)).

¹H-NMR (400 MHz, CDCl₃): δ = 8.54 (dt, J_d = 4.5 Hz, J_t = 1.5 Hz, 1 H), 8.00 (d, J = 1.5 Hz, 1 H), 7.76 (dq, J_d = 7.5 Hz, J_q = 1.6 Hz, 1 H), 7.40–7.53 (m, 3 H), 7.23–7.30 (m, 1 H), 1.40 (s, 9 H) ppm; **¹³C-NMR** (101 MHz, CDCl₃): δ = 157.5 (d, J_{C-F} = 262.5 Hz), 151.3, 146.8 (d, J_{C-F} = 10.9 Hz), 145.1 (d, J_{C-F} = 5.4 Hz), 134.7 (d, J_{C-F} = 4.5 Hz), 128.1, 126.4, 126.0 (d, J_{C-F} = 5.4 Hz), 125.8 (d, J_{C-F} = 4.5 Hz), 124.1 (d, J_{C-F} = 20.9 Hz), 123.3 (d, J_{C-F} = 3.6 Hz), 34.8, 31.3 ppm; **¹⁹F-NMR** (377 MHz, CDCl₃): δ = -122.9 ppm; **IR** (ATR): $\tilde{\nu}$ = 3064, 2963, 2868, 1596, 1438, 1409, 1364, 1249 cm⁻¹; **MS** (EI, 70 eV), m/z (%): 229 (28) [M⁺], 215 (15), 214 (100), 199 (11), 185 (10), 43 (15); **HRMS** (EI-TOF) m/z : [M⁺] calcd. for C₁₅H₁₆FN: 229.1267; found 229.1285.



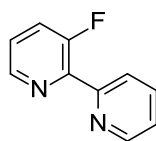
3-Fluoro-2-(5-methoxy-2-methylphenyl)pyridine (5.2.4-3ao): Compound **5.2.4-3ao** was prepared following method A from potassium 3-fluoro-2-pyridinecarboxylate **5.2.4-1a** (90.5 mg, 0.50 mmol) and 1-bromo-4-methoxy-2-methylbenzene **5.2.4-2o** (207 mg, 228 μ L, 1.0 mmol). **5.2.4-3ao** was isolated (SiO₂, cyclohexane/ethyl acetate = 9:1) as a yellow oil (98 mg, 90%).

¹H-NMR (400 MHz, CDCl₃): δ = 8.41–8.47 (m, 1 H), 7.36–7.45 (m, 1 H), 7.19–7.29 (m, 2 H), 6.74–6.81 (m, 2 H), 3.78 (s, 3 H), 2.20 (s, 3 H) ppm; **¹³C-NMR** (101 MHz, CDCl₃): δ = 159.9, 157.0 (d, J_{C-F} = 256.1 Hz), 148.1 (d, J_{C-F} = 14.5 Hz), 145.1 (d, J_{C-F} = 5.4 Hz), 138.3, 131.1 (d, J_{C-F} = 1.8 Hz), 127.6 (d, J_{C-F} = 3.6 Hz), 123.3 (d, J_{C-F} = 2.7 Hz), 123.2 (d, J_{C-F} = 14.5 Hz), 115.7, 111.2, 55.2, 19.9 ppm; **¹⁹F-NMR** (377 MHz, CDCl₃): δ = -121.2 ppm; **IR** (ATR): $\tilde{\nu}$ = 3061, 3002, 2930, 2835, 1608, 1575, 1507, 1436, 1283, 1240, 1185 cm⁻¹; **MS** (EI, 70 eV), m/z (%): 217 (67) [M⁺], 216 (28), 198 (77), 197 (100), 183 (25), 182 (24), 154 (23); **HRMS** (EI-TOF), m/z : [M⁺] calcd. for C₁₃H₁₂FNO: 217.0903; found 217.0901.



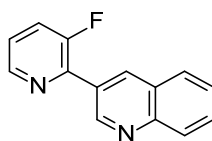
3-Fluoro-2-(1-naphthalenyl)pyridine (5.2.4-3ap): Compound **5.2.4-3ap** was prepared following method A from potassium 3-fluoro-2-pyridinecarboxylate **5.2.4-1a** (90.5 mg, 0.50 mmol) and 2-bromonaphthalene **5.2.4-2p** (213 mg, 1.0 mmol). **5.2.4-3ap** was isolated (SiO₂, cyclohexane/ethyl acetate = 9:1) as a colorless solid (82 mg, 74%).

¹H-NMR (400 MHz, CDCl₃): δ = 8.59–8.68 (m, 1 H), 7.89–8.03 (m, 2 H), 7.76 (d, J = 8.0 Hz, 1 H), 7.56–7.69 (m, 3 H), 7.46–7.56 (m, 2 H), 7.37–7.45 (m, 1 H) ppm; **¹³C-NMR** (101 MHz, CDCl₃): δ = 157.5 (d, $J_{\text{C-F}}$ = 257.9 Hz), 147.4 (d, $J_{\text{C-F}}$ = 14.5 Hz), 145.4 (d, $J_{\text{C-F}}$ = 5.4 Hz), 133.7, 132.8 (d, $J_{\text{C-F}}$ = 3.6 Hz), 131.2, 129.5, 128.4, 127.9 (d, $J_{\text{C-F}}$ = 1.0 Hz), 126.5, 125.9, 125.2 (d, $J_{\text{C-F}}$ = 1.8 Hz), 125.1, 123.9 (d, $J_{\text{C-F}}$ = 3.6 Hz), 123.6 (d, $J_{\text{C-F}}$ = 20.0 Hz) ppm; **¹⁹F-NMR** (377 MHz, CDCl₃): δ = -120.3 ppm; **IR** (ATR): $\tilde{\nu}$ = 3047, 3010, 1592, 1561, 1447, 1395, 1341, 1253, 1201 cm⁻¹; **MS** (EI, 70 eV), m/z (%): 223 (34) [M⁺], 222 (100), 221 (7), 111 (8), 50 (9); **HRMS** (EI-TOF), m/z : [M⁺] calcd. for C₁₅H₁₀FN: 223.0797; found 223.0785; **m.p.**: 93–94 °C.



3-Fluoro-2,2'-bipyridine (**5.2.4-3aq**) [CAS: 1863378-49-7]: Compound **5.2.4-3aq** was prepared following method A from potassium 3-fluoro-2-pyridinecarboxylate **5.2.4-1a** (136 mg, 0.75 mmol) and 2-bromopyridine **5.2.4-2q** (80 mg, 48 μ L, 0.5 mmol). **5.2.4-3aq** was isolated (SiO₂, cyclohexane/ethyl acetate = 1:1) as a colorless oil (32 mg, 37%).

¹H-NMR (200 MHz, CDCl₃): δ = 8.81 (d, J = 4.8 Hz, 1 H), 8.59 (dt, J_{d} = 4.5 Hz, J_{t} = 1.5 Hz, 1 H), 7.94–8.04 (m, 1 H), 7.77–7.89 (m, 1 H), 7.48–7.62 (m, 1 H), 7.31–7.41 (m, 2 H) ppm; **¹³C-NMR** (101 MHz, CDCl₃): δ = 158.0 (d, $J_{\text{C-F}}$ = 264.3 Hz), 153.5 (d, $J_{\text{C-F}}$ = 6.4 Hz), 149.6, 145.5 (d, $J_{\text{C-F}}$ = 5.5 Hz), 144.8 (d, $J_{\text{C-F}}$ = 9.1 Hz), 136.7, 124.9 (d, $J_{\text{C-F}}$ = 3.6 Hz), 124.7 (d, $J_{\text{C-F}}$ = 20.9 Hz), 124.2 (d, $J_{\text{C-F}}$ = 5.4 Hz), 123.6 ppm; **¹⁹F-NMR** (CDCl₃, 377 MHz): δ = -122.5 ppm; **IR** (ATR): $\tilde{\nu}$ = 3059, 3011, 1585, 1454, 1422, 1256, 1196, 802 cm⁻¹; **MS** (EI, 70 eV), m/z (%): 174 (100) [M⁺], 173 (33), 147 (20), 146 (20), 76 (15), 51 (26), 50 (25); **HRMS** (EI-TOF), m/z : [M⁺] calcd. for C₁₀H₇FN₂: 174.0593; found 174.0597.



3-(3-Fluoro-2-pyridinyl)quinoline (**5.2.4-3ar**). Compound **5.2.4-3ar** was prepared following method A from potassium 3-fluoro-2-pyridinecarboxylate **5.2.4-1a** (90.5 mg, 0.50 mmol) and 3-bromoquinoline **5.2.4-2r** (104 mg, 68 μ L, 0.50 mmol). **5.2.4-3ar** was isolated (SiO₂, cyclohexane/ethyl acetate = 4:1) as a colorless solid (70 mg, 62%).

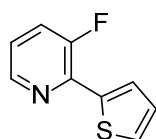
¹H-NMR (200 MHz, CDCl₃): δ = 9.57 (s, 1 H), 8.77–8.82 (m, 1 H), 8.59–8.65 (m, 1 H), 8.18 (d, J = 8.3 Hz, 1 H), 7.95 (dd, J = 8.1, 1.5 Hz, 1 H), 7.72–7.84 (m, 1 H), 7.52–7.66 (m, 2 H), 7.31–7.43 (m, 1 H) ppm; **¹³C-NMR** (50 MHz, CDCl₃): δ = 158.0 (d, $J_{\text{C-F}}$ = 261.3 Hz), 150.3

(d, $J_{\text{C-F}} = 6.6$ Hz), 148.0, 145.8 (d, $J_{\text{C-F}} = 5.1$ Hz), 143.6 (d, $J_{\text{C-F}} = 11.0$ Hz), 136.0 (d, $J_{\text{C-F}} = 7.0$ Hz), 130.2, 129.3, 128.6, 128.2 (d, $J_{\text{C-F}} = 5.9$ Hz), 127.5, 126.9, 124.3 (d, $J_{\text{C-F}} = 16.8$ Hz), 124.1 (d, $J_{\text{C-F}} = 4.0$ Hz) ppm; **^{19}F -NMR** (377 MHz, CDCl_3): $\delta = -122.3$ ppm; **IR** (ATR): $\tilde{\nu} = 3061, 3038, 1595, 1410, 1344, 1113$ cm^{-1} ; **MS** (EI, 70 eV), m/z (%): 224 (100) [M^+], 223 (45), 205 (10), 122 (10), 76 (10), 50 (14); **HRMS** (EI-TOF) m/z : [M^+] calcd. for $\text{C}_{14}\text{H}_9\text{FN}_2$: 224.0750; found 224.0739; **m.p.**: 138–139 °C.



3-Fluoro-2-(3-thienyl)pyridine (5.2.4-3as): Compound **5.2.4-3as** was prepared following method A from potassium 3-fluoro-2-pyridinecarboxylate **5.2.4-1a** (90.5 mg, 0.50 mmol) and 3-bromothiophene **5.2.4-2s** (168 mg, 97 μL , 1.0 mmol). **5.2.4-3as** was isolated (SiO_2 , cyclohexane/ethyl acetate = 9:1) as a colorless oil (50 mg, 56%).

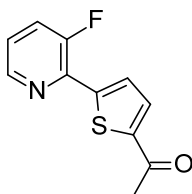
^1H -NMR (200 MHz, CDCl_3): $\delta = 8.46$ (dt, $J_d = 4.5$ Hz, $J_t = 1.6$ Hz, 1 H), 8.04–8.12 (m, 1 H), 7.86 (dt, $J_d = 5.1$ Hz, $J_t = 1.3$ Hz, 1 H), 7.36–7.53 (m, 2 H), 7.14–7.25 (m, 1 H) ppm; **^{13}C -NMR** (50 MHz, CDCl_3): $\delta = 156.8$ (d, $J_{\text{C-F}} = 260.5$ Hz), 145.1 (d, $J_{\text{C-F}} = 4.8$ Hz), 142.1 (d, $J_{\text{C-F}} = 11.0$ Hz), 136.9 (d, $J_{\text{C-F}} = 6.2$ Hz), 127.6 (d, $J_{\text{C-F}} = 4.8$ Hz), 126.2 (d, $J_{\text{C-F}} = 11.0$ Hz), 125.3 (d, $J_{\text{C-F}} = 1.5$ Hz), 123.7 (d, $J_{\text{C-F}} = 20.5$ Hz), 122.7 (d, $J_{\text{C-F}} = 4.0$ Hz) ppm; **^{19}F -NMR** (377 MHz, CDCl_3): $\delta = -121.4$ ppm; **IR** (ATR): $\tilde{\nu} = 3113, 3065, 3021, 1597, 1454, 1440, 1206, 1099$ cm^{-1} ; **MS** (EI, 70 eV), m/z (%): 179 (100) [M^+], 178 (26), 160 (37), 135 (10), 107 (10), 45 (11); **HRMS** (EI-TOF), m/z : [M^+] calcd. for $\text{C}_9\text{H}_6\text{FNS}$: 179.0205; found 179.0208.



3-Fluoro-2-(2-thienyl)pyridine (5.2.4-3at): Compound **5.2.4-3at** was prepared following method A from potassium 3-fluoropyridinecarboxylate **5.2.4-1a** (90.5 mg, 0.50 mmol) and 2-bromothiophene **5.2.4-2t** (166 mg, 99 μL , 1.0 mmol). **5.2.4-3at** was isolated (SiO_2 , cyclohexane/ethyl acetate = 9:1) as a colorless solid (56 mg, 63%).

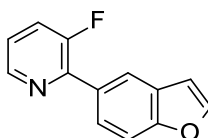
^1H -NMR (200 MHz, CDCl_3): $\delta = 8.41$ (dt, $J_d = 4.9$ Hz, $J_t = 1.6$ Hz, 1 H), 7.80–7.86 (m, 1 H), 7.38–7.53 (m, 2 H), 7.12–7.23 (m, 2 H) ppm; **^{13}C -NMR** (50 MHz, CDCl_3): $\delta = 155.7$ (d, $J_{\text{C-F}} = 263.1$ Hz), 145.0 (d, $J_{\text{C-F}} = 4.8$ Hz), 141.3 (d, $J_{\text{C-F}} = 11.3$ Hz), 139.8 (d, $J_{\text{C-F}} = 7.7$ Hz), 128.2 (d, $J_{\text{C-F}} = 2.2$ Hz), 128.1 (d, $J_{\text{C-F}} = 5.5$ Hz), 127.9 (d, $J_{\text{C-F}} = 7.3$ Hz), 123.6 (d, $J_{\text{C-F}} = 19.4$ Hz), 122.6 (d, $J_{\text{C-F}} = 4.0$ Hz) ppm; **^{19}F -NMR** (377 MHz, CDCl_3): $\delta = -120.7$ ppm; **IR** (ATR): $\tilde{\nu} =$

3123, 3082, 1597, 1449, 1362, 1260, 1204, 1101 cm^{-1} ; **MS** (EI, 70 eV), m/z (%): 179 (100) $[\text{M}^+]$, 178 (13), 135 (17), 134 (8), 107 (10), 45 (14); **HRMS** (EI-TOF) m/z : $[\text{M}]^+$ calcd. for $\text{C}_9\text{H}_6\text{FNS}$ 179.0205; found 179.0200; **m.p.**: 43–44 $^\circ\text{C}$.



1-[5-(3-Fluoro-2-pyridinyl)-2-thienyl]ethanone (**5.2.4-3au**). Compound **5.2.4-3au** was prepared following method A from potassium 3-fluoro-2-pyridinecarboxylate **5.2.4-1a** (90.5 mg, 0.50 mmol) and 1-(5-bromo-2-thienyl)ethanone **5.2.4-2u** (207 mg, 1.0 mmol). **5.2.4-3au** was isolated (SiO_2 , cyclohexane/ethyl acetate = 9:1) as a yellow solid (34 mg, 31%).

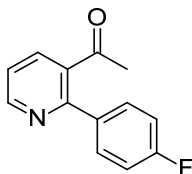
$^1\text{H-NMR}$ (200 MHz, CDCl_3): δ = 8.44 (dt, J_d = 4.5 Hz, J_t = 1.6 Hz, 1 H), 7.76–7.82 (m, 1 H), 7.69–7.74 (m, 1 H), 7.43–7.55 (m, 1 H), 7.22–7.32 (m, 1 H), 2.59 (s, 3 H) ppm; **$^{13}\text{C-NMR}$** (75 MHz, CDCl_3): δ = 190.7, 156.4 (d, $J_{\text{C-F}}$ = 262.6 Hz), 147.0 (d, $J_{\text{C-F}}$ = 7.7 Hz), 145.4 (d, $J_{\text{C-F}}$ = 5.0 Hz), 144.9 (d, $J_{\text{C-F}}$ = 3.3 Hz), 140.1 (d, $J_{\text{C-F}}$ = 11.1 Hz), 133.0 (d, $J_{\text{C-F}}$ = 2.2 Hz), 128.3 (d, $J_{\text{C-F}}$ = 12.2 Hz), 124.3 (d, $J_{\text{C-F}}$ = 3.3 Hz), 124.1 (d, $J_{\text{C-F}}$ = 18.2 Hz), 26.9 ppm; **$^{19}\text{F-NMR}$** (377 MHz, CDCl_3): δ = -119.4 ppm; **IR** (ATR): $\tilde{\nu}$ = 3121, 3063, 2920, 2850, 1646, 1425, 1273, 1259 cm^{-1} ; **MS** (EI, 70 eV), m/z (%): 221 (42) $[\text{M}^+]$, 207 (14), 206 (100), 178 (23), 134 (17), 107 (9); **HRMS** (EI-TOF), m/z : $[\text{M}^+]$ calcd. for $\text{C}_{11}\text{H}_8\text{FNOS}$: 221.0311; found 221.0304; **m.p.**: 146–147 $^\circ\text{C}$.



3-Fluoro-2-(5-benzofuranyl)pyridine (**5.2.4-3av**): Compound **5.2.4-3av** was prepared following method A from potassium 3-fluoro-2-pyridinecarboxylate **5.2.4-1a** (90.5 mg, 0.50 mmol) and 5-bromobenzofuran **5.2.4-2v** (203 mg, 1.0 mmol). **5.2.4-3av** was isolated (SiO_2 , cyclohexane/ethyl acetate = 9:1) as a yellow solid (54 mg, 51%).

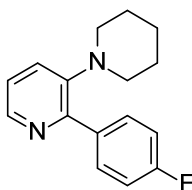
$^1\text{H-NMR}$ (200 MHz, CDCl_3): δ = 8.50–8.58 (m, 1 H), 8.23 (t, J = 1.5 Hz, 1 H), 7.91–8.00 (m, 1 H), 7.44–7.70 (m, 3 H), 7.21–7.32 (m, 1 H), 6.86 (dd, J = 2.3, 1.0 Hz, 1 H) ppm; **$^{13}\text{C-NMR}$** (75 MHz, CDCl_3): δ = 157.4 (d, $J_{\text{C-F}}$ = 259.8 Hz), 155.4, 146.5 (d, $J_{\text{C-F}}$ = 10.5 Hz), 145.6, 145.3 (d, $J_{\text{C-F}}$ = 5.5 Hz), 130.3 (d, $J_{\text{C-F}}$ = 5.5 Hz), 127.6, 125.3 (d, $J_{\text{C-F}}$ = 5.5 Hz), 124.1 (d, $J_{\text{C-F}}$ = 20.5 Hz), 123.0 (d, $J_{\text{C-F}}$ = 3.9 Hz), 122.0 (d, $J_{\text{C-F}}$ = 6.1 Hz), 111.3, 107.0 ppm; **$^{19}\text{F-NMR}$** (41 MHz, CDCl_3): δ = -120.7 ppm; **IR** (ATR): $\tilde{\nu}$ = 3156, 3125, 3042, 3013, 1597, 1443, 1192,

1024 cm^{-1} ; **MS** (EI, 70 eV), m/z (%): 213 (100) [M^+], 212 (14), 185 (17), 184 (13); **HRMS** (EI-TOF), m/z : [M^+] calcd. for $\text{C}_{13}\text{H}_8\text{FNO}$: 213.0590; found 213.0585; **m.p.**: 81–82 °C.



1-[2-(4-Fluorophenyl)-3-pyridinyl]ethanone (**5.2.4-3ba**) [CAS: 280573-47-9]: Compound **5.2.4-3ba** was prepared following method A from potassium 3-acetyl-2-pyridinecarboxylate **5.2.4-1b** (102 mg, 0.50 mmol) and 1-bromo-4-fluorobenzene **5.2.4-2a** (177 mg, 111 μL , 1.0 mmol). **5.2.4-3ba** was isolated (SiO_2 , cyclohexane/ethyl acetate = 2:1) as an orange oil (56 mg, 52%).

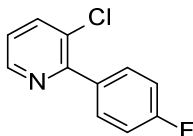
^1H -NMR (250 MHz, CDCl_3): δ = 8.75 (dd, J = 4.8, 1.7 Hz, 1 H), 7.86 (dd, J = 7.7, 1.7 Hz, 1 H), 7.51–7.61 (m, 2 H), 7.35 (dd, J = 7.7, 4.9 Hz, 1 H), 7.11–7.22 (m, 2 H), 2.11 (s, 3 H) ppm; **^{13}C -NMR** (63 MHz, CDCl_3): δ = 203.3, 163.6 (d, $J_{\text{C-F}}$ = 250.0 Hz), 156.0, 150.9, 136.2, 136.2, 135.8 (d, $J_{\text{C-F}}$ = 3.7 Hz), 131.0 (d, $J_{\text{C-F}}$ = 8.3 Hz), 122.0, 115.8 (d, $J_{\text{C-F}}$ = 22.1 Hz), 30.2 ppm; **^{19}F -NMR** (235 MHz, CDCl_3): δ = -111.7 ppm; **IR** (ATR): $\tilde{\nu}$ = 3046, 2922, 2853, 1686, 1510, 1425, 1221, 843 cm^{-1} ; **MS** (EI, 70 eV), m/z (%): 215 (42) [M^+], 214 (26), 200 (100), 172 (45), 145 (20), 43 (43); **HRMS** (EI-TOF), m/z : [M^+] calcd. for $\text{C}_{13}\text{H}_{10}\text{FNO}$ 215.0746; found 215.0742.



3-(1-Piperidinyl)-2-(4-fluorophenyl)pyridine (**5.2.4-3ca**): Compound **5.2.4-3ca** was prepared following method A from potassium 3-(1-piperidinyl)-2-pyridinecarboxylate **5.2.4-1c** (122 mg, 0.50 mmol) and 1-bromo-4-fluorobenzene **5.2.4-2a** (177 mg, 111 μL , 1.0 mmol). **5.2.4-3ca** was isolated (SiO_2 , cyclohexane/ethyl acetate = 9:1) as a brown oil (22 mg, 17%).

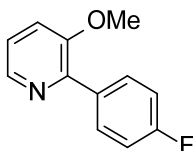
^1H -NMR (200 MHz, CDCl_3): δ = 8.30 (dd, J = 4.5, 1.5 Hz, 1 H), 7.95–8.08 (m, 2 H), 7.34 (dd, J = 8.3, 1.5 Hz, 1 H), 7.04–7.21 (m, 3 H), 2.78 (m, 4 H), 1.44–1.64 (m, 6 H) ppm; **^{13}C -NMR** (50 MHz, CDCl_3): δ = 162.5 (d, $J_{\text{C-F}}$ = 246.6 Hz), 151.3, 147.9, 142.7, 136.6 (d, $J_{\text{C-F}}$ = 3.7 Hz), 130.3 (d, $J_{\text{C-F}}$ = 8.1 Hz), 126.0, 122.5, 114.9 (d, $J_{\text{C-F}}$ = 21.2 Hz), 52.3, 25.9, 23.9 ppm; **^{19}F -NMR** (41 MHz, CDCl_3): δ = -114.4 ppm; **IR** (ATR): $\tilde{\nu}$ = 3060, 2935, 2854, 1602, 1573, 1507, 1432,

1219 cm^{-1} ; **MS** (EI, 70 eV), m/z (%): 256 (100) [M^+], 255 (39), 199 (15), 160 (17), 159 (7), 145 (8); **HRMS** (EI-TOF), m/z : [M^+] calcd. for $\text{C}_{16}\text{H}_{17}\text{FN}_2$: 256.1376; found 256.1365.



3-Chloro-2-(4-fluorophenyl)pyridine (**5.2.4-3da**) [CAS: 847226-00-0]: Compound **5.2.4-3da** was prepared following method A from potassium 3-chloro-2-pyridinecarboxylate **5.2.4-1d** (97.8 mg, 0.50 mmol) and 1-bromo-4-fluorobenzene **5.2.4-2a** (177 mg, 111 μL , 1.0 mmol) in the presence of Ag_2CO_3 (6.96 mg, 25 μmol , 5mol%) instead of Cu_2O . **5.2.4-3da** was isolated (SiO_2 , cyclohexane/ethyl acetate = 9:1) as a colorless solid (63 mg, 49%).

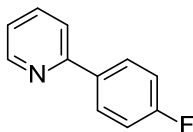
^1H -NMR (300 MHz, CDCl_3): δ = 8.59 (dd, J = 4.7, 1.6 Hz, 1 H), 7.71–7.83 (m, 3 H), 7.12–7.26 (m, 3 H) ppm; **^{13}C -NMR** (50 MHz, CDCl_3): δ = 163.1 (d, $J_{\text{C-F}}$ = 248.1 Hz), 155.5, 147.6, 138.2, 134.2 (d, $J_{\text{C-F}}$ = 3.3 Hz), 131.3 (d, $J_{\text{C-F}}$ = 8.4 Hz), 130.1, 123.1, 115.0 (d, $J_{\text{C-F}}$ = 22.0 Hz) ppm; **^{19}F -NMR** (41 MHz, CDCl_3): δ = -112.6 ppm; **IR** (ATR): $\tilde{\nu}$ = 3044, 1599, 1574, 1513, 1432, 1402, 1161, 848 cm^{-1} ; **MS** (EI, 70 eV), m/z (%): 209 (30) [M^+], 208 (12), 207 (73) [M^+], 173 (12), 172 (100), 145 (20), 43 (20); **HRMS** (EI-TOF), m/z : [M^+] calcd. for $\text{C}_{11}\text{H}_7^{35}\text{ClFN}$: 207.0251; found 207.0237; [M^+] calcd. for $\text{C}_{11}\text{H}_7^{37}\text{ClFN}$: 209.0222; Found 209.0211; **m.p.**: 80–81 $^\circ\text{C}$.



2-(4-Fluorophenyl)-3-methoxypyridine (**5.2.4-3ea**) [CAS: 1214324-71-6]: Compound **5.2.4-3ea** was prepared following method B from potassium 3-methoxy-2-pyridinecarboxylate **5.2.4-1e** (95.6 mg, 0.50 mmol) and 1-bromo-4-fluorobenzene **5.2.4-2a** (177 mg, 111 μL , 1.0 mmol). **5.2.4-3ea** was isolated (SiO_2 , cyclohexane/ethyl acetate = 6:1) as a colorless oil (71 mg, 70%).

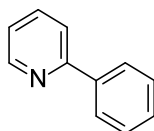
^1H -NMR (400 MHz, CDCl_3): δ = 8.31 (dd, J = 4.6, 1.4 Hz, 1 H), 7.90–7.97 (m, 2 H), 7.28–7.32 (m, 1 H), 7.22–7.26 (m, 1 H), 7.09–7.17 (m, 2 H), 3.88 (s, 3 H) ppm; **^{13}C -NMR** (101 MHz, CDCl_3): δ = 162.8 (d, $J_{\text{C-F}}$ = 247.0 Hz), 153.4, 147.0, 141.3, 133.7 (d, $J_{\text{C-F}}$ = 2.7 Hz), 131.2 (d, $J_{\text{C-F}}$ = 8.2 Hz), 122.9, 118.5, 114.8 (d, $J_{\text{C-F}}$ = 20.9 Hz), 55.4 ppm; **^{19}F -NMR** (377 MHz, CDCl_3): δ = -113.7 ppm; **IR** (ATR): $\tilde{\nu}$ = 3061, 3006, 2942, 2839, 1601, 1508, 1430, 1266, 1220, 1196, 1158, 1125, 1013 cm^{-1} ; **MS** (EI, 70 eV), m/z (%): 203 (71) [M^+], 202 (100), 174 (14), 173 (18),

172 (32), 133 (28), 50 (12); **HRMS** (EI-TOF), m/z : $[M^+]$ calcd. for $C_{12}H_{10}FNO$: 203.0746; found 203.0744.



2-(4-Fluorophenyl)-pyridine (5.2.4-3fa) [CAS: 58861-53-3]: Compound **5.2.4-3fa** was prepared following method A in NMP/mesitylene (2 mL, 1:1) at 190 °C from potassium 2-pyridinecarboxylate **5.2.4-1f** (81.4 mg, 0.50 mmol) and 1-bromo-4-fluorobenzene **5.2.4-2a** (177 mg, 111 μ L, 1.0 mmol). **5.2.4-3fa** was isolated (SiO₂, cyclohexane/ethyl acetate = 9:1) as a colorless solid (32 mg, 37%).

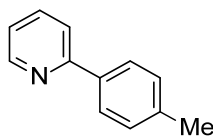
¹H-NMR (300 MHz, CDCl₃): δ = 8.73–8.63 (m, 1 H), 8.06–7.94 (m, 2 H), 7.81–7.65 (m, 2 H), 7.26–7.12 (m, 3 H) ppm; **¹³C-NMR** (101 MHz, CDCl₃): δ = 163.5 (d, J_{C-F} = 248.5 Hz), 156.5, 149.7, 136.8, 135.6 (d, J_{C-F} = 3.3 Hz), 128.7 (d, J_{C-F} = 8.4 Hz), 122.0, 120.2, 115.6 (d, J_{C-F} = 21.6 Hz) ppm; **¹⁹F-NMR** (41 MHz, CDCl₃): δ = -112.0 ppm; **IR** (ATR): $\tilde{\nu}$ = 3055, 3011, 1600, 1584, 1509, 1464, 1433, 1219, 1099 cm⁻¹, **MS** (EI, 70 eV), m/z (%): 173 (100) $[M^+]$, 146 (9), 51 (11); **HRMS** (EI-TOF), m/z : $[M^+]$ calcd. for $C_{11}H_8FN$: 173.0641; found 173.0640; **m.p.**: 39–40 °C.



2-Phenylpyridine (5.2.3-3aa und 5.2.4-3fb) [CAS: 1008-89-5]: The screening reactions in 5.2.3 were performed following the procedure described in section 7.4.2.

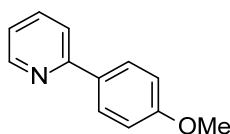
Compound **5.2.4-3fb** was prepared following method A in NMP/mesitylene (2 mL, 1:1) at 190 °C from potassium 2-pyridinecarboxylate **5.2.4-1f** (81.4 mg, 0.50 mmol) and bromobenzene **5.2.4-2b** (159 mg, 106 μ L, 1.0 mmol). **5.2.4-3fb** was isolated (SiO₂, cyclohexane/ethyl acetate = 9:1) as a colorless liquid (31 mg, 40%).

¹H-NMR (200 MHz, CDCl₃): δ = 8.72 (dt, J_d = 4.8, J_t = 1.4 Hz, 1 H), 8.06–7.95 (m, 2 H), 7.83–7.70 (m, 2 H), 7.55–7.37 (m, 3 H), 7.30–7.21 (m, 1 H) ppm; **¹³C-NMR** (50 MHz, CDCl₃): δ = 157.5, 149.6, 139.4, 136.8, 129.0, 128.7, 126.9, 122.1, 120.6 ppm; **MS** (EI, 70 eV), m/z (%): 155 (100) $[M^+]$; the analytical data matched those reported in the literature.^[102,268]



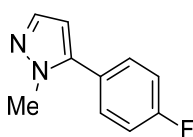
2-(4-Methylphenyl)-pyridine (**5.3.2-3ab**) [CAS: 4467-06-5]: The screening reactions in 5.2.3 were performed following the procedure described in section 7.4.2.

MS (EI, 70 eV), m/z (%): 169 (100) [M^+], 168 (68), 167 (30), 63 (10), 51 (14), 50 (12); the MS data matched those reported in the literature.^[269]



2-(4-Methoxyphenyl)-pyridine (**5.2.4-3fd**) [CAS: 5957-90-4]: Compound **5.2.4-3fd** was prepared following method A in NMP/mesitylene (2 mL, 1:1) at 190 °C from potassium 2-pyridinecarboxylate **5.2.4-1f** (81.4 mg, 0.50 mmol) and bromo-4-methoxybenzene **5.2.4-2d** (187 mg, 1.0 mmol). **5.2.4-3fd** was isolated (SiO₂, cyclohexane/ethyl acetate = 4:1) as a colorless oil (26 mg, 28%).

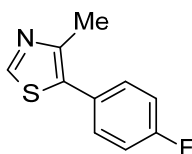
¹H-NMR (200 MHz, CDCl₃): δ = 8.67 (dt, J_d = 4.7 Hz, J_t = 1.5 Hz, 1 H), 8.01–7.92 (m, 2 H), 7.78–7.63 (m, 2 H), 7.19 (ddd, J = 6.6, 4.9, 1.9 Hz, 1 H), 7.06–6.96 (m, 2 H), 3.88 (s, 3 H) ppm; **¹³C-NMR** (50 MHz, CDCl₃): 160.5, 157.1, 149.4, 136.7, 131.9, 128.2, 121.4, 119.8, 114.1, 55.3 ppm; **MS** (EI, 70 eV), m/z (%): 185 (100) [M^+]; the analytical data matched those reported in the literature.^[102,270]



5-(4-Fluorophenyl)-1-methyl-1H-pyrazole (**5.2.4-3ga**) [CAS: 689251-78-3]: Compound **5.2.4-3ga** was prepared following method B from potassium 1-methyl-1H-pyrazole-5-carboxylate **5.2.4-1g** (82.1 mg, 0.50 mmol) and 1-bromo-4-fluorobenzene **5.2.4-2a** (177 mg, 1.0 mmol). **5.2.4-3ga** was isolated (SiO₂, cyclohexane/ethyl acetate = 6:1) as a colorless liquid (56 mg, 64%).

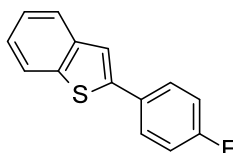
¹H-NMR (250 MHz, CDCl₃): δ = 7.51 (d, J = 1.9 Hz, 1 H), 7.34–7.44 (m, 2 H), 7.08–7.21 (m, 2 H), 6.28 (d, J = 1.9 Hz, 1 H), 3.87 (s, 3 H) ppm; **¹³C-NMR** (50 MHz, CDCl₃): δ = 162.8 (d, J_{C-F} = 248.1 Hz), 142.5, 138.5, 130.6 (d, J_{C-F} = 3.7 Hz), 126.9 (d, J_{C-F} = 8.1 Hz), 115.7 (d, J_{C-F} = 22.0 Hz), 106.1, 37.3 ppm; **¹⁹F-NMR** (CDCl₃, 235 MHz): δ = -112.8 ppm; **IR** (ATR): $\tilde{\nu}$ = 3103,

3063, 2947, 1605, 1545, 1493, 1223, 839 cm^{-1} ; **MS** (EI, 70 eV), m/z (%): 176 (100) [M^+], 175 (39), 148 (16), 133 (13), 121 (16), 109 (9); **HRMS** (EI-TOF), m/z : [M^+] calcd. for $\text{C}_{10}\text{H}_9\text{FN}_2$: 176.0750; found 176.0740.



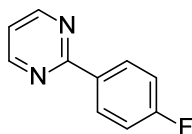
5-(4-Fluorophenyl)-4-methyl-thiazole (5.2.4-3ha) [CAS: 623577-48-0]: Compound **5.2.4-3ha** was prepared following method A and B, respectively, from potassium 4-methyl-5-thiazolecarboxylate **5.2.4-1h** (90.6 mg, 0.50 mmol) and 1-bromo-4-fluorobenzene **2a** (177 mg, 111 μL , 1.0 mmol). **5.2.4-3ha** was isolated (SiO_2 , cyclohexane/ethyl acetate = 6:1) as a yellow solid (35 mg, 36% (method A); 72 mg, 75% (method B)).

^1H -NMR (250 MHz, CDCl_3): δ = 8.68 (s, 1 H), 7.35–7.46 (m, 2 H), 7.05–7.18 (m, 2 H), 2.51 (s, 3 H) ppm; **^{13}C -NMR** (50 MHz, CDCl_3): δ = 162.4 (d, $J_{\text{C-F}}$ = 248.5 Hz), 150.2, 148.6 (d, $J_{\text{C-F}}$ = 0.7 Hz), 131.0 (d, $J_{\text{C-F}}$ = 8.0 Hz), 130.8, 127.9 (d, $J_{\text{C-F}}$ = 3.3 Hz), 115.7 (d, $J_{\text{C-F}}$ = 22.0 Hz), 15.9 ppm; **^{19}F -NMR** (235 MHz, CDCl_3): δ = -113.5 ppm; **IR** (ATR): $\tilde{\nu}$ = 3096, 3042, 2922, 1603, 1497, 1240, 831 cm^{-1} ; **MS** (EI, 70 eV), m/z (%): 193 (100) [M^+], 192 (9), 166 (24), 165 (24), 133 (19), 122 (11); **HRMS** (EI-TOF), m/z : [M^+] calcd. for $\text{C}_{10}\text{H}_8\text{FNS}$: 193.0361; found 193.0352; **m.p.**: 35–36 $^\circ\text{C}$.



2-(4-Fluorophenyl)-benzo[b]thiophene (5.2.4-3ia) [CAS: 936734-96-2]: Compound **5.2.4-3ia** was prepared following method B from potassium benzo[b]thiophene-2-carboxylate **5.2.4-1i** (108 mg, 0.50 mmol) and 1-bromo-4-fluorobenzene **5.2.4-2a** (177 mg, 111 μL , 1.0 mmol). **5.2.4-3ia** was isolated (SiO_2 , cyclohexane) as a colorless solid (24 mg, 21%).

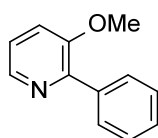
^1H -NMR (250 MHz, CDCl_3): δ = 7.75–7.89 (m, 2 H), 7.63–7.75 (m, 2 H), 7.48 (s, 1 H), 7.28–7.43 (m, 2 H), 7.06–7.21 (m, 2 H) ppm; **^{13}C -NMR** (50 MHz, CDCl_3): δ = 162.8 (d, $J_{\text{C-F}}$ = 248.1 Hz), 143.1, 140.7, 139.5, 130.6, 128.2 (d, $J_{\text{C-F}}$ = 8.1 Hz), 124.6, 124.4, 123.5, 122.2, 119.4 (d, $J_{\text{C-F}}$ = 1.5 Hz), 115.9 (d, $J_{\text{C-F}}$ = 21.6 Hz) ppm; **^{19}F -NMR** (235 MHz, CDCl_3): δ = -113.4 ppm; **IR** (ATR): $\tilde{\nu}$ = 3061, 1593, 1431, 1233, 818 cm^{-1} ; **MS** (EI, 70 eV), m/z (%): 228 (100) [M^+], 196 (8), 183 (12), 40 (9); **HRMS** (EI-TOF), m/z : [M^+] calcd. for $\text{C}_{14}\text{H}_9\text{FS}$: 228.0409; found 228.0397; **m.p.**: 181–182 $^\circ\text{C}$.



2-(4-Fluorophenyl)-pyrimidine (5.2.5-3) [CAS: 68049-17-2]: The screening reactions in 5.2.5 were performed following the procedure described in section 7.4.2.

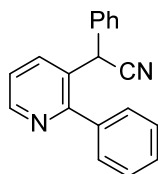
¹⁹F-NMR (377 MHz, CDCl₃): δ = -110.3 ppm; **MS** (EI, 70 eV), m/z (%): 175 (13), 174 (100) [M⁺], 173 (9), 147 (7), 122 (8), 121 (56), 94 (13); the NMR data matched those reported in the literature.^[271]

7.4.7 Nucleophilic aromatic fluorine substitutions



3-Methoxy-2-phenylpyridine (5.2.4-4) [53698-49-0]: To a solution of methanol (17.6 mg, 22 μ L, 0.55 mmol) and **5.2.4-3ab** (86.6 mg, 0.5 mmol) in dry DMF (5 mL) at 0 °C dry KHMDS (0.5 M in toluene, 1.1 mL, 0.55 mmol) was added dropwise. The reaction was allowed to warm to RT overnight and then quenched with sat. aq. NaHCO₃ (10 mL). The aqueous layer was extracted with ethyl acetate (3 \times 20 mL). The combined organic layers were washed with brine, dried over MgSO₄, filtered, and the volatiles were removed under reduced pressure. The residue was purified by column chromatography (SiO₂, cyclohexane/ethyl acetate = 6:1) yielding **5.2.4-4** as colorless oil (86 mg, 93%).^[272]

¹H-NMR (200 MHz, CDCl₃): δ = 8.33 (dd, J = 4.3, 1.8 Hz, 1 H), 7.96–7.86 (m, 2 H), 7.51–7.32 (m, 3 H), 7.30–7.19 (m, 2 H), 3.87 (s, 3 H) ppm; **¹³C-NMR** (50 MHz, CDCl₃): δ = 153.6, 148.2, 141.3, 137.7, 129.4, 128.3, 128.0, 122.9, 118.5, 55.5 ppm; **MS** (EI, 70 eV), m/z (%): 185 (61) [M]⁺, 184 (100), 154 (33); the analytical data matched those reported in the literature.^[273]



2-Phenyl-2-(3-(2-phenyl)pyridyl)acetonitrile (5.2.4-6): A 20 mL microwave vessel was charged with **5.2.4-3ab** (86.6 mg, 0.5 mmol) and potassium *tert*-butoxide (318 mg, 2.75 mmol). NMP (1 mL) and benzylnitrile **5.2.4-5** (293 mg, 290 μ L, 2.5 mmol) were added and the mixture was heated at 100 °C in the microwave for 5 min. The mixture was allowed to cool to

RT, washed with distilled water (20 mL) and extracted with ethyl acetate (3 × 20 mL). The combined organic layers were washed with brine, dried over MgSO₄, filtered, and the volatiles were removed under reduced pressure. The residue was purified by column chromatography (SiO₂, *n*-pentane/diethyl ether = 2:3) yielding compound **5.2.4-6** as colorless oil (120 mg, 89%).^[274]

¹H-NMR (200 MHz, CDCl₃): δ = 8.69 (dd, *J* = 4.8, 1.5 Hz, 1 H), 7.85 (dd, *J* = 8.0, 1.6 Hz, 1 H), 7.53–7.42 (m, 5 H), 7.41–7.28 (m, 4 H), 7.18–7.06 (m, 2 H), 5.44 (s, 1 H) ppm; **¹³C-NMR** (50 MHz, CDCl₃): δ = 158.5, 149.3, 138.7, 137.3, 135.2, 130.1, 129.2, 128.9, 128.8, 128.7, 128.3, 127.4, 123.1, 119.4, 38.9 ppm; **IR** (ATR): $\tilde{\nu}$ = 3051, 2910, 2241, 1564, 1492, 1435 cm⁻¹; **MS** (EI, 70 eV), *m/z* (%): 270 (89) [M⁺], 269 (100); **HRMS** (EI-TOF), *m/z*: [M⁺] calcd. for C₁₉H₁₄N₂: 270.1157; found 270.1146.

7.5 Iridium-Catalyzed *ortho*-Arylation of Benzoic Acids and Benzamides with Arenediazonium Salts

7.5.1 Preparation of starting materials

Synthesis of arenediazonium tetrafluoroborates:

In a 50 mL round-bottom flask, the aniline (10 mmol) was dissolved in absolute ethanol (30 mL) and an aqueous solution of HBF₄ (50%, 2.5 mL, 20 mmol) was added. *tert*-Butyl nitrite (2.7 mL, 20 mmol) was added dropwise to the solution at 0 °C. The reaction was stirred at RT for 1 h and diethyl ether (20 mL) was added to precipitate the arenediazonium tetrafluoroborate that was then filtered off and washed with diethyl ether (10 mL). The diazonium salt was recrystallized two times by dissolving it in acetone (10 mL) and precipitating it by adding diethyl ether (25 mL). The arenediazonium tetrafluoroborate was filtered off, washed with diethyl ether (2 × 10 mL), dried in vacuo (10⁻³ mbar) for 10 min and was then directly used.

7.5.2 General method for the catalyst screening

An oven-dried 20 mL vessel was charged with the solid reagents. After the vessel was flushed with 3 alternating vacuum and nitrogen purge cycles, the solvent and the liquid reagents were added *via* syringe and the resulting mixture was stirred at the given temperature for the given time. The reaction mixture was allowed to cool to RT and *n*-tetradecane (50 μL) was added *via* syringe.

Work-up with esterification:

K₂CO₃ (207 mg, 3 equiv.), MeI (156 µL, 5 equiv.) and MeCN (3 mL) were added and the mixture was stirred at 60 °C for 2 h. After the mixture was cool to RT, a sample of the reaction mixture (0.25 mL) was dissolved in ethyl acetate (2 mL), washed with water (2 mL), dried over MgSO₄, and analyzed by GC.

Work-up without esterification:

The mixture was diluted with ethyl acetate (3 mL). A sample of the reaction mixture (0.25 mL) was dissolved in ethyl acetate (2 mL), washed with water (2 mL), dried over MgSO₄, and analyzed by GC.

7.5.3 General procedure for the Ir-catalyzed ortho-arylation*Method A:*

An oven-dried 20 mL vessel was charged with [IrCp*Cl₂]₂ (23.9 mg, 0.03 mmol, 3 mol%), Ag₂CO₃ (41.2 mg, 0.15 mmol, 15 mol%), Li₂CO₃ (40 mg, 0.50 mmol, 50 mol%), the benzoic acid **5.3.4-1** (1.00 mmol) and the arenediazonium salt **5.3.4-2** (1.00 mmol). After the vessel was flushed with 3 alternating vacuum and nitrogen purge cycles, degassed acetone (2 mL) was added *via* syringe. The resulting mixture was stirred at 60 °C for 24 h. After the reaction was complete, the mixture was allowed to cool to RT. MeCN (3 mL), K₂CO₃ (414 mg, 3 equiv.) and MeI (310 µL, 5 equiv.) were added and the mixture was stirred at 50 °C for 2 h. The mixture was allowed to cool to RT, brine (20 mL) was added and the resulting mixture was extracted with ethyl acetate (3 × 20 mL). The combined organic layers were dried over MgSO₄, filtered, and the volatiles were removed under reduced pressure. The residue was purified by column chromatography (SiO₂, ethyl acetate/hexane gradient) yielding the corresponding biaryl.

Method A1:

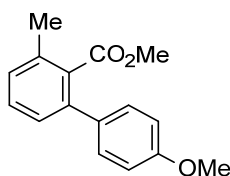
An oven-dried 20 mL vessel was charged with [IrCp*Cl₂]₂ (23.9 mg, 0.03 mmol, 3 mol%), Ag₂CO₃ (41.2 mg, 0.15 mmol, 15 mol%), Li₂CO₃ (40 mg, 0.50 mmol, 50 mol%), the benzoic acid **5.3.4-1** (1.00 mmol) and the arenediazonium salt **5.3.4-2** (1.20 mmol). After the vessel was flushed with 3 alternating vacuum and nitrogen purge cycles, degassed acetone (2 mL) was added *via* syringe. The resulting mixture was stirred at 60 °C for 24 h. After the reaction was complete, the mixture was allowed to cool to RT. MeCN (3 mL), K₂CO₃ (414 mg, 3 equiv.) and MeI (310 µL, 5 equiv.) were added and the mixture was stirred at 50 °C for 2 h. The mixture was allowed to cool to RT, brine (20 mL) was added and the resulting mixture was extracted with ethyl acetate (3 × 20 mL). The combined organic layers were dried over MgSO₄, filtered,

and the volatiles were removed under reduced pressure. The residue was purified by column chromatography (SiO₂, ethyl acetate/hexane gradient) yielding the corresponding biaryl.

Method B:

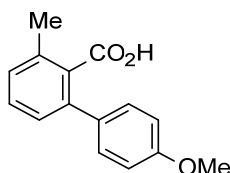
An oven-dried 20 mL vessel was charged with [IrCp*Cl₂]₂ (12 mg, 0.015 mmol, 3 mol%), AgOTf (26 mg, 0.10 mmol, 20 mol%), AgOAc (25 mg, 0.15 mmol, 30 mol%), Li₂CO₃ (11 mg, 0.15 mmol, 30 mol%), the benzoic acid **5.3.4-1** (0.50 mmol) and the arenediazonium salt **5.3.4-2** (0.50 mmol). After the vessel was flushed with 3 alternating vacuum and nitrogen purge cycles, degassed acetone (1 mL) was added *via* syringe. The resulting mixture was stirred at 60 °C for 24 h. After the reaction was complete, the mixture was allowed to cool to RT. MeCN (3 mL), K₂CO₃ (207 mg, 3 equiv.) and MeI (155 µL, 5 equiv.) were added and the mixture was stirred at 50 °C for 2 h. The mixture was allowed to cool to RT, brine (20 mL) was added and the resulting mixture was extracted with ethyl acetate (3 × 20 mL). The combined organic layers were dried over MgSO₄, filtered, and the volatiles were removed under reduced pressure. The residue was purified by column chromatography (SiO₂, ethyl acetate/hexane gradient) yielding the corresponding biaryl.

7.5.4 Synthesis and characterization of the corresponding products



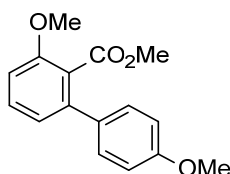
Methyl 4'-methoxy-3-methyl-[1,1'-biphenyl]-2-carboxylate (5.3.4-4aa) [CAS: 1097018-19-3]: Compound **5.3.4-4aa** was prepared following method A, starting from 2-methylbenzoic acid (138 mg, 1.00 mmol) and 4-methoxybenzenediazonium tetrafluoroborate (222 mg, 1.00 mmol). After purification, **5.3.4-4aa** was obtained as colorless solid (213 mg, 0.83 mmol, 83%).

¹H-NMR (400 MHz, CDCl₃): δ = 7.36–7.28 (m, 3 H), 7.19 (dd, *J* = 7.6 Hz, 2.8 Hz, 2 H), 6.95–6.91 (m, 2 H), 3.84 (s, 3 H), 3.63 (s, 3 H), 2.93 (s, 3 H) ppm; **¹³C-NMR** (101 MHz, CDCl₃): δ = 170.5, 159.0, 139.6, 135.3, 133.3, 133.1, 129.34, 129.30, 128.7, 127.2, 113.7, 55.2, 51.9, 19.7 ppm; **IR** (ATR): $\tilde{\nu}$ = 3002, 2969, 2945, 1726, 1439, 1247 cm⁻¹; **MS** (EI, 70 eV), *m/z* (%): 257 (16), 256 (100) [M⁺], 226 (8), 225 (55), 224 (48), 209 (13), 182 (8); **elemental analysis**: calcd. (%) for C₁₆H₁₆O₃: C 74.98, H 6.29; found: C 75.11, H 6.35; **m.p.**: 69–70 °C.



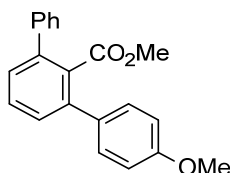
4'-Methoxy-3-methylbiphenyl-2-carboxylic acid (5.3.4-3aa) [CAS: 1261902-83-3]: Compound **5.3.4-3aa** was prepared following method A, starting from 2-methylbenzoic acid (138 mg, 1.00 mmol) and 4-methoxybenzenediazonium tetrafluoroborate (222 mg, 1.00 mmol). After the reaction was complete, the reaction mixture was allowed to cool to RT. The reaction mixture was diluted with ethyl acetate (20 mL) and extracted with aq. NaOH solution (3 × 20 mL). The aq. basic phase was acidified with HCl (pH 1–2) and afterwards extracted with ethyl acetate (3 × 20 mL). The combined organic layers were dried over MgSO₄, filtered, and the volatiles were removed under reduced pressure. The residue was purified by column chromatography (SiO₂, ethyl acetate/hexane gradient, 1% AcOH) yielding **5.3.4-3aa** as colorless solid (186 mg, 0.77 mmol, 77%).

¹H-NMR (400 MHz, CDCl₃): δ = 7.38–7.33 (m, 3 H), 7.20 (d, *J* = 7.6 Hz, 2 H), 6.95–6.91 (m, 2 H), 3.84 (s, 3 H), 2.45 (s, 3 H) ppm; **¹³C-NMR** (101 MHz, CDCl₃): δ = 174.9, 159.2, 139.7, 135.3, 133.0, 132.0, 129.7, 129.5, 128.8, 127.4, 113.8, 55.2, 19.9 ppm; **IR** (ATR): $\tilde{\nu}$ = 3009, 2970, 2940, 1738, 1690, 1515, 1460, 1366, 1292 cm⁻¹; **elemental analysis**: calcd. (%) for C₁₅H₁₄O₃: C 74.36, H 5.82; found: C 74.06, H 5.92; **m.p.**: 138–139 °C.



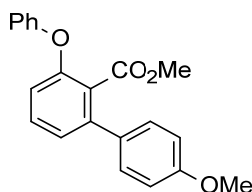
Methyl 3,4'-dimethoxy-[1,1'-biphenyl]-2-carboxylate (5.3.4-4ba) [CAS: 1809272-29-4]: Compound **5.3.4-4ba** was prepared following method A, starting from 2-methoxybenzoic acid (154 mg, 1.00 mmol) and 4-methoxybenzenediazonium tetrafluoroborate (222 mg, 1.00 mmol). After purification, **5.3.4-4ba** was obtained as beige solid (171 mg, 0.63 mmol, 63%).

¹H-NMR (400 MHz, CDCl₃): δ = 7.39 (t, *J* = 8.0 Hz, 1 H), 7.35–7.31 (m, 2 H), 6.97 (dd, *J* = 7.6, 0.4 Hz, 1 H), 6.98–6.90 (m, 3 H), 3.87 (s, 3 H), 3.83 (s, 3 H), 3.67 (s, 3 H) ppm; **¹³C-NMR** (101 MHz, CDCl₃): δ = 168.7, 159.1, 156.4, 140.8, 132.4, 130.4, 129.3, 122.9, 121.9, 113.8, 109.4, 56.0, 55.2, 52.2 ppm; **IR** (ATR): $\tilde{\nu}$ = 3009, 2970, 1725, 1366, 1231 cm⁻¹; **MS** (70 eV), *m/z* (%): 273 (18), 272 (100) [M⁺], 242 (12), 241 (73), 226 (11); **elemental analysis**: calcd. (%) for C₁₆H₁₆O₄: C 70.57, H 5.92; found: C 70.61, H 6.03; **m.p.**: 82–83 °C.



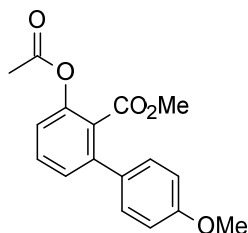
Methyl 4-methoxy-[1,1':3',1''-terphenyl]-2'-carboxylate (5.3.4-4ca) [CAS: 1809272-30-7]: Compound **5.3.4-4ca** was prepared following method A, starting from biphenyl-2carboxylic acid (202 mg, 1.00 mmol), 4-methoxybenzenediazonium tetrafluoroborate (222 mg, 1.00 mmol). After purification, **5.3.4-4ca** was obtained as orange solid (257 mg, 0.81 mmol, 81%).

¹H-NMR (400 MHz, CDCl₃): δ = 7.55–7.41 (m, 10 H), 7.03–7.01 (d, J = 8.4 Hz, 2 H), 3.87 (s, 3 H), 3.48 (s, 3 H) ppm; **¹³C-NMR** (100 MHz, CDCl₃): δ = 169.8, 159.0, 140.4, 140.1, 139.7, 132.62, 132.58, 129.3, 129.2, 128.7, 128.3, 128.2, 128.1, 127.3, 113.6, 55.0, 51.5 ppm; **IR** (ATR): $\tilde{\nu}$ = 3032, 2946, 2838, 1727, 1514, 1438, 1245 cm⁻¹; **MS** (EI, 70 eV), m/z (%): 319 (20), 318 (94) [M⁺], 288 (23), 287 (100), 255 (9), 244 (9), 215 (13); **elemental analysis**: calcd. (%) for C₂₁H₁₈O₃: C 79.23, H 5.70; found: C 79.01, H 5.68; **m.p.**: 87–88 °C.



Methyl 4'-methoxy-3-phenoxy-[1,1'-biphenyl]-2-carboxylate (5.3.4-4da) [CAS: 1809272-31-8]: Compound **5.3.4-4da** was prepared following method A, starting from 2-phenoxybenzoic acid (214 mg, 1.00 mmol) and 4-methoxybenzenediazonium tetrafluoroborate (222 mg, 1.00 mmol). After purification, **5.3.4-4da** was obtained as brown oil (278 mg, 0.83 mmol, 83%).

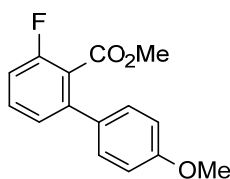
¹H-NMR (400 MHz, CDCl₃): δ = 7.44–7.41 (m, 2 H), 7.39–7.34 (m, 3 H), 7.16–7.10 (m, 4 H), 7.00–6.97 (m, 2 H), 6.89 (dd, J = 8.4 Hz, 0.8 Hz, 1 H), 3.84 (s, 3 H), 3.67 (s, 3 H) ppm; **¹³C-NMR** (101 MHz, CDCl₃): δ = 167.8, 159.2, 156.8, 154.2, 141.1, 131.9, 130.3, 129.6, 129.2, 125.5, 124.3, 123.5, 119.0, 116.8, 113.7, 55.0, 52.0 ppm; **IR** (ATR): $\tilde{\nu}$ = 3064, 2949, 1731, 1516, 1490, 1235, 1208, 1179 cm⁻¹; **MS** (EI, 70 eV), m/z (%): 335 (23), 334 (100) [M⁺], 304 (13), 303 (62), 287 (8), 271 (9); **elemental analysis**: calcd. (%) for C₂₁H₁₈O₄: C 75.43, H 5.43; found: C 75.33, H 5.47.



Methyl 3-acetoxy-4'-methoxy-[1,1'-biphenyl]-2-carboxylate (5.3.4-4ea) [CAS: 1809272-32-9]:

Compound **5.3.4-4ea** was prepared following method A, starting from acetylsalicylic acid (182 mg, 1.00 mmol) and 4-methoxybenzenediazonium tetrafluoroborate (222 mg, 1.00 mmol). After purification, **5.3.4-4ea** was obtained as brown solid (222 mg, 0.74 mmol, 74%).

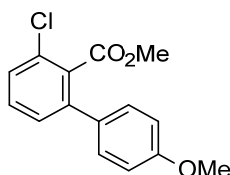
¹H-NMR (400 MHz, CDCl₃): δ = 7.39 (t, J = 8.0 Hz, 1 H), 7.23–7.22 (m, 1 H), 7.21–7.19 (m, 2 H), 7.04 (dd, J = 8.0 Hz, 1.2 Hz, 1 H), 6.88–6.84 (m, 2 H), 3.77 (s, 3 H), 3.55 (s, 3 H), 2.22 (s, 3 H) ppm; **¹³C-NMR** (101 MHz, CDCl₃): δ = 169.2, 167.2, 159.3, 148.2, 141.8, 132.1, 130.6, 129.3, 127.4, 126.0, 121.3, 113.8, 55.3, 52.2, 20.8 ppm; **IR** (ATR): $\tilde{\nu}$ = 1765, 1725, 1288, 1263, 1180 cm⁻¹; **MS** (EI, 70 eV), m/z (%): 300 (25) [M⁺], 258 (41), 227 (23), 226 (100), 198 (29), 183 (13), 155 (10); **elemental analysis**: calcd. (%) for C₁₇H₁₆O₅: C 67.99, H 5.37; found: C 67.77, H 5.41; **m.p.**: 95–96 °C.



Methyl 3-fluoro-4'-methoxy-[1,1'-biphenyl]-2-carboxylate (5.3.4-4fa) [CAS: 1809272-33-0]:

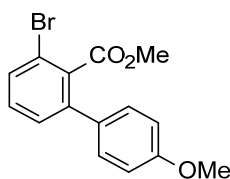
Compound **5.3.4-4fa** was prepared following method A, starting from 2-fluorobenzoic acid (142 mg, 1.00 mmol) and 4-methoxybenzenediazonium tetrafluoroborate (222 mg, 1.00 mmol). After purification, **5.3.4-4fa** was obtained as brown oil (218 mg, 0.83 mmol, 83%).

¹H-NMR (400 MHz, CDCl₃): δ = 7.40 (td, J = 8.1 Hz, 5.8 Hz, 1 H), 7.33–7.26 (m, 2 H), 7.16 (d, J = 7.6 Hz, 1 H), 7.09–7.05 (m, 1 H), 6.96–6.93 (m, 2 H), 3.82 (s, 3 H), 3.71 (s, 3 H) ppm; **¹³C-NMR** (101 MHz, CDCl₃): δ = 166.3, 159.3, 158.8 (d, J_{C-F} = 249.8 Hz), 141.9 (d, J_{C-F} = 2.7 Hz), 131.4 (d, J_{C-F} = 2.7 Hz), 131.0 (d, J_{C-F} = 9.1 Hz), 129.2, 125.2 (d, J_{C-F} = 3.6 Hz), 121.2 (d, J_{C-F} = 16.4 Hz), 114.0, 113.8, 55.0, 52.3 ppm; **IR** (ATR): $\tilde{\nu}$ = 3000, 2952, 1730, 1610, 1516, 1458, 1236 cm⁻¹; **MS** (EI, 70 eV), m/z (%): 261 (17), 260 (100) [M⁺], 229 (96), 209 (15), 186 (17), 181 (15), 157 (16); **elemental analysis**: calcd. (%) for C₁₅H₁₃FO₃: C 69.22, H 5.03; found: C 69.21, H 5.02.



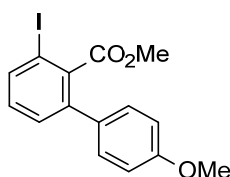
Methyl 3-chloro-4'-methoxy-[1,1'-biphenyl]-2-carboxylate (5.3.4-4ga) [CAS: 1809272-34-1]: Compound **5.3.4-4ga** was prepared following method A, starting from 2-chlorobenzoic acid (160 mg, 1.00 mmol) and 4-methoxybenzenediazonium tetrafluoroborate (222 mg, 1.00 mmol). After purification, **5.3.4-4ga** was obtained as yellow solid (203 mg, 0.73 mmol, 73%).

¹H-NMR (400 MHz, CDCl₃): δ = 7.40–7.36 (m, 2 H), 7.34–7.31 (m, 2 H), 7.29–7.27 (m, 1 H), 6.89–6.84 (m, 2 H), 3.85 (s, 3 H), 3.72 (s, 3 H) ppm; **¹³C-NMR** (101 MHz, CDCl₃): δ = 167.8, 159.5, 141.3, 133.0, 131.6, 131.0, 130.3, 129.4, 128.1, 127.8, 113.9, 55.3, 52.4 ppm; **IR** (ATR): $\tilde{\nu}$ = 3008, 2952, 1731, 1234, 1115 cm⁻¹; **MS** (EI, 70 eV), m/z (%): 278 (29), 276 (84) [M⁺], 247 (32), 246 (15), 245 (100), 210 (28), 139 (18); **elemental analysis**: calcd. (%) for C₁₅H₁₃ClO₃: C 65.11, H 4.74; found: C 65.05, H 4.81; **m.p.**: 72–73 °C.



Methyl 3-bromo-4'-methoxy-[1,1'-biphenyl]-2-carboxylate (5.3.4-4ha) [CAS: 1809272-35-2]: Compound **5.3.4-4ha** was prepared following method A, starting from 2-bromobenzoic acid (207 mg, 1.00 mmol) and 4-methoxybenzenediazonium tetrafluoroborate (222 mg, 1.00 mmol). After purification, **5.3.4-4ha** was obtained as black solid (259 mg, 0.80 mmol, 80%).

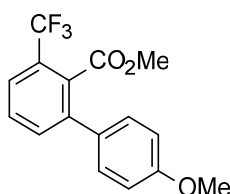
¹H-NMR (400 MHz, CDCl₃): δ = 7.55 (dd, J = 7.0 Hz, 1.8 Hz, 1 H), 7.35–7.29 (m, 4 H), 6.98–6.92 (m, 2 H), 3.84 (s, 3 H), 3.73 (s, 3 H) ppm; **¹³C-NMR** (100 MHz, CDCl₃): δ = 168.4, 159.5, 141.4, 135.1, 131.7, 131.0, 130.5, 129.4, 128.7, 119.5, 113.9, 55.2, 52.4 ppm; **MS** (EI, 70 eV), m/z (%): 323 (16), 322 (100), 321 (15) [M⁺], 320 (79), 291 (54), 289 (44), 210 (20); **IR** (ATR): $\tilde{\nu}$ = 3008, 2945, 2836, 1729, 1515, 1438, 1277, 1247 cm⁻¹; **HRMS** (EI-TOF), m/z : [M⁺] calcd. for C₁₅H₁₃BrO₃: 320.0048; found: 320.0057; **m.p.**: 90–91 °C.



Methyl 3-iodo-4'-methoxy-[1,1'-biphenyl]-2-carboxylate (5.3.4-4ia) [CAS: 1809272-36-3]: Compound **5.3.4-4ia** was prepared following method A, starting from 2-iodobenzoic acid

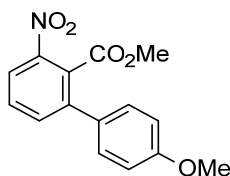
(248 mg, 1.00 mmol) and 4-methoxybenzenediazonium tetrafluoroborate (222 mg, 1.00 mmol). After purification, **5.3.4-4ia** was obtained as beige solid (266 mg, 0.72 mmol, 72%).

¹H-NMR (400 MHz, CDCl₃): δ = 7.80 (dd, J = 8.0 Hz, 1.2 Hz, 1 H), 7.34–7.30 (m, 3 H), 7.13 (t, J = 7.8 Hz, 1 H), 6.97–6.93 (m, 2 H), 3.83 (s, 3 H), 3.73 (s, 3 H) ppm; **¹³C-NMR** (101 MHz, CDCl₃): δ = 169.3, 159.3, 141.0, 139.1, 137.3, 131.7, 130.5, 129.3, 129.2, 113.7, 92.4, 55.1, 52.3 ppm; **IR** (ATR): $\tilde{\nu}$ = 3008, 2969, 2950, 1731, 1242 cm⁻¹; **MS** (EI, 70 eV), m/z (%): 369 (15), 368 (100) [M⁺], 338 (9), 337 (40), 210 (9); **HRMS** (EI-TOF), m/z : [M⁺] calcd. for C₁₅H₁₃IO₃: 367.9909; found: 367.9913; **m.p.**: 99–100 °C.



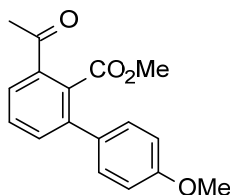
Methyl 4'-methoxy-3-(trifluoromethyl)-[1,1'-biphenyl]-2-carboxylate (**5.3.4-4ja**) [CAS: 1809272-37-4]: Compound **5.3.4-4ja** was prepared following method B, starting from 2-(trifluoromethyl)benzoic acid (97 mg, 0.50 mmol) and 4-methoxybenzenediazonium tetrafluoroborate (111 mg, 0.50 mmol). After purification, **5.3.4-4ja** was obtained as orange oil (111 mg, 0.36 mmol, 72%).

¹H-NMR (400 MHz, CDCl₃): δ = 7.69–7.64 (m, 1 H), 7.57–7.52 (m, 2 H), 7.32–7.28 (m, 2 H), 6.97–6.93 (m, 2 H), 3.84 (s, 3 H), 3.68 (s, 3 H) ppm; **¹³C-NMR** (101 MHz, CDCl₃): δ = 167.9, 159.5, 140.9, 133.5, 131.33, 131.25 (q, J_{C-F} = 1.8 Hz), 129.54, 129.45, 127.6 (q, J_{C-F} = 31.6 Hz), 124.5 (q, J_{C-F} = 4.8 Hz), 123.5 (q, J_{C-F} = 272.2 Hz), 113.8, 55.1, 52.4 ppm; **IR** (ATR): $\tilde{\nu}$ = 3008, 2953, 1737, 1518, 1327, 1278, 1247, 1129 cm⁻¹; **MS** (EI, 70 eV), m/z (%): 311 (16), 310 (100) [M⁺], 279 (18), 260 (8), 259 (35); **elemental analysis**: calcd. (%) for C₁₆H₁₃F₃O₃: C 61.94, H 4.22; found: C 62.18, H 4.38.



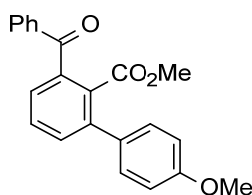
Methyl 4'-methoxy-3-nitro-[1,1'-biphenyl]-2-carboxylate (**5.3.4-4ka**) [CAS: 1809272-38-5]: Compound **5.3.4-4ka** was prepared following method B, starting from 2-nitrobenzoic acid (83.6 mg, 0.50 mmol) and 4-methoxybenzenediazonium tetrafluoroborate (111 mg, 0.50 mmol). After purification, **5.3.4-4ka** was obtained as orange solid (102 mg, 0.36 mmol, 71%).

¹H-NMR (400 MHz, CDCl₃): δ = 8.12 (dd, J = 8.4 Hz, 1.2 Hz, 1 H), 7.66 (dd, J = 7.6 Hz, 1.2 Hz, 1 H), 7.60 (t, J = 7.8 Hz, 1 H), 7.32–7.28 (m, 2 H), 6.97–6.93 (m, 2 H), 3.85 (s, 3 H), 3.75 (s, 3 H) ppm; **¹³C-NMR** (100 MHz, CDCl₃): δ = 166.6, 159.8, 146.2, 141.8, 135.8, 130.1, 129.8, 129.7, 128.9, 122.7, 114.0, 55.3, 53.0 ppm; **IR** (ATR): $\tilde{\nu}$ = 2955, 2919, 2849, 1733, 1531, 1351, 1289, 1255 cm⁻¹; **MS** (EI, 70 eV), m/z (%): 288 (16), 287 (100) [M⁺], 256 (37), 226 (26), 198 (9), 183 (12), 139 (13); **HRMS** (EI-TOF), m/z : [M⁺] calcd. for C₁₅H₁₃NO₅: 287.0794; found: 287.0792; **m.p.**: 105–106 °C.



Methyl 3-acetyl-4'-methoxy-[1,1'-biphenyl]-2-carboxylate (5.3.4-4la) [CAS: 1809272-39-6]: Compound **5.3.4-4la** was prepared following method A, starting from 2-acetylbenzoic acid (166 mg, 1.00 mmol) and 4-methoxybenzenediazonium tetrafluoroborate (222 mg, 1.00 mmol). After purification, **5.3.4-4la** was obtained as colorless solid (253 mg, 0.83 mmol, 83%).

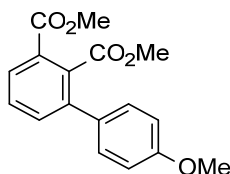
¹H-NMR (400 MHz, CDCl₃): δ = 7.67 (dd, J = 6.8 Hz, 2.4 Hz, 1 H), 7.40–7.35 (m, 2 H), 7.19–7.15 (m, 2 H), 6.83–6.78 (m, 2 H), 3.69 (s, 3 H), 3.58 (s, 3 H), 2.49 (s, 3 H) ppm; **¹³C-NMR** (101 MHz, CDCl₃): δ = 198.1, 169.7, 159.1, 140.4, 135.5, 134.1, 132.6, 131.3, 129.5, 129.0, 127.5, 113.5, 55.0, 52.0, 27.3 ppm; **IR** (ATR): $\tilde{\nu}$ = 3015, 2970, 2949, 1736, 1365, 1217 cm⁻¹; **MS** (EI, 70 eV), m/z (%): 285 (17), 284 (95) [M⁺], 270 (15), 269 (100), 253 (23), 237 (26), 42 (14); **elemental analysis**: calcd. (%) for C₁₇H₁₆O₄: C 71.82, H 5.67; found: C 71.93, H 5.72; **m.p.**: 85–86 °C.



Methyl 3-benzoyl-4'-methoxy-[1,1'-biphenyl]-2-carboxylate (5.3.4-4ma) [CAS: 1809272-40-9]: Compound **5.3.4-4ma** was prepared following procedure A, starting from 2-benzoylbenzoic acid (231 mg, 1.00 mmol) and 4-methoxybenzenediazonium tetrafluoroborate (222 mg, 1.00 mmol). After purification, **5.3.4-4ma** was obtained as brown solid (300 mg, 0.87 mmol, 87%).

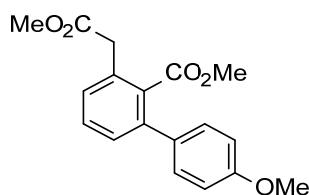
¹H-NMR (400 MHz, CDCl₃): δ = 7.85–7.83 (m, 2 H), 7.56–7.52 (m, 2 H), 7.51–7.42 (m, 4 H), 7.32–7.28 (m, 2 H), 6.96–6.92 (m, 2 H), 3.80 (s, 3 H), 3.45 (s, 3 H) ppm; **¹³C-NMR** (101 MHz,

CDCl₃): δ = 196.1, 168.7, 159.1, 140.9, 138.2, 136.6, 133.0, 132.6, 132.5, 131.8, 129.8, 129.2, 129.0, 128.2, 127.6, 113.6, 55.0, 51.9 ppm; **IR** (ATR): $\tilde{\nu}$ = 3072, 2947, 1734, 1664, 1447, 1237, 1184 cm⁻¹; **MS** (EI, 70 eV), m/z (%): 347 (24), 346 (100) [M⁺], 315 (48), 269 (35), 237 (13), 105 (21), 77 (20); **elemental analysis**: calcd. (%) for C₂₂H₁₈O₄: C 76.29, H 5.24; found: C 75.97, H 5.21; **m.p.**: 117–118 °C.



Dimethyl 4'-methoxy-[1,1'-biphenyl]-2,3-dicarboxylate (**5.3.4-4na**) [CAS: 19617-61-9]: Compound **5.3.4-4na** was prepared following method A, starting from methyl hydrogen phthalate (184 mg, 1.00 mmol) and 4-methoxybenzenediazonium tetrafluoroborate (222 mg, 1.00 mmol). After purification, **5.3.4-4na** was obtained as brown solid (202 mg, 0.67 mmol, 67%).

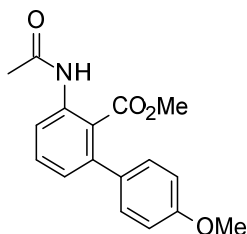
¹H-NMR (400 MHz, CDCl₃): δ = 7.85 (dd, J = 7.6 Hz, 1.6 Hz, 1 H), 7.42–7.33 (m, 2 H), 7.20–7.16 (m, 2 H), 6.82–7.80 (m, 2 H), 3.78 (s, 3 H), 3.70 (s, 3 H), 3.60 (s, 3 H) ppm; **¹³C-NMR** (100 MHz, CDCl₃): δ = 169.2, 166.0, 159.2, 140.0, 134.5, 134.1, 131.3, 129.5, 128.9, 128.3, 127.8, 113.6, 55.0, 52.3, 52.1 ppm; **IR** (ATR): $\tilde{\nu}$ = 3008, 2969, 2945, 1729, 1248 cm⁻¹. **MS** (EI, 70 eV), m/z (%): 301 (18), 300 (100) [M⁺], 270 (10), 269 (59), 238 (7), 237 (30), 209 (8); **elemental analysis**: calcd. (%) for C₁₇H₁₆O₅: C, 67.99; H, 5.37; found: C, 67.85; H, 5.40; **HRMS** (EI-TOF), m/z : [M⁺] calcd. for C₁₇H₁₆O₅: 300.0998; found: 300.1002; **m.p.**: 118–119 °C.



Methyl 4'-methoxy-3-(2-methoxy-2-oxoethyl)-[1,1'-biphenyl]-2-carboxylate (**5.3.4-4oa**) [CAS: 1809272-41-0]: Compound **5.3.4-4oa** was prepared following method A, starting from homophthalic acid (180 mg, 1.00 mmol) and 4-methoxybenzenediazonium tetrafluoroborate (222 mg, 1.00 mmol). After purification, **5.3.4-4oa** was obtained as brown solid (190 mg, 0.60 mmol, 60%).

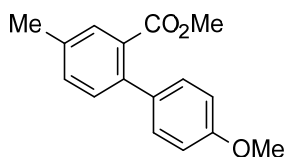
¹H-NMR (400 MHz, CDCl₃): δ = 7.29 (t, J = 7.6 Hz, 1 H), 7.20–7.14 (m, 4 H), 6.83–6.79 (m, 2 H), 3.70 (s, 3 H), 3.68 (s, 2 H), 3.56 (s, 3 H), 3.46 (s, 3 H) ppm; **¹³C-NMR** (101 MHz, CDCl₃):

δ = 171.2, 169.7, 158.9, 140.5, 133.1, 132.7, 132.0, 129.6, 129.2, 129.1, 128.8, 113.6, 55.0, 51.9, 51.7, 38.9 ppm; **IR** (ATR): $\tilde{\nu}$ = 3000, 2954, 2839, 1727, 1459, 1429, 1236 cm^{-1} ; **MS** (EI, 70 eV), m/z (%): 315 (19), 314 (100) [M^+], 283 (22), 282 (30), 255 (30), 254 (71), 239 (51); **elemental analysis**: calcd. (%) for $\text{C}_{18}\text{H}_{18}\text{O}_5$: C 68.78, H 5.77; found: C 68.80, H 5.82; **m.p.**: 75–76 °C.



Methyl 3-acetamido-4'-methoxy-[1,1'-biphenyl]-2-carboxylate (5.3.4-4pa) [CAS: 1809272-42-1]: Compound **5.3.4-4pa** was prepared following method A, starting from *N*-acetylanthranilic acid (181 mg, 1.00 mmol) and 4-methoxybenzenediazonium tetrafluoroborate (222 mg, 1.00 mmol). After purification, **5.3.4-4pa** was obtained as brown solid (201 mg, 0.67 mmol, 67%).

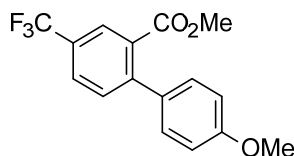
¹H-NMR (400 MHz, CDCl_3): δ = 9.19 (s, 1 H), 8.26 (d, J = 8.0 Hz, 1 H), 7.40 (t, J = 8.0 Hz, 1 H), 7.15 (d, J = 8.4 Hz, 2 H), 7.05 (d, J = 8.0 Hz, 1 H), 6.89–6.87 (d, J = 8.4 Hz, 2 H), 3.78 (s, 3 H), 3.44 (s, 3 H), 2.15 (s, 3 H) ppm; **¹³C-NMR** (101 MHz, CDCl_3): δ = 169.7, 168.4, 158.7, 142.1, 137.3, 133.8, 131.2, 128.8, 125.4, 120.0, 119.9, 113.5, 55.0, 51.8, 24.7 ppm; **IR** (ATR): $\tilde{\nu}$ = 3264, 2955, 2928, 1740, 1655, 1514, 1460, 1248 cm^{-1} ; **MS** (EI, 70 eV), m/z (%): 300 (15), 299 (74) [M^+], 257 (72), 226 (20), 225 (100), 210 (16), 43 (14); **elemental analysis**: calcd. (%) for $\text{C}_{17}\text{H}_{17}\text{NO}_4$: C 68.22, H 5.72, N 4.68; found: C 67.92, H 5.78, N 4.52; **m.p.**: 133–134 °C.



Methyl 4'-methoxy-4-methyl-[1,1'-biphenyl]-2-carboxylate (5.3.4-4qa) [CAS: 1809272-43-2]: Compound **5.3.4-4qa** was prepared following method A, starting from 3-methylbenzoic acid (138 mg, 1.00 mmol) and 4-methoxybenzenediazonium tetrafluoroborate (222 mg, 1.00 mmol). After purification, **5.3.4-4qa** was obtained as orange oil (205 mg, 0.80 mmol, 80%).

¹H-NMR (400 MHz, CDCl_3): δ = 7.66–7.65 (m, 1 H), 7.34 (dd, J = 8.0 Hz, 1.2 Hz, 1 H), 7.30–7.27 (m, 3 H), 6.99–6.95 (m, 2 H), 3.86 (s, 3 H), 3.70 (s, 3 H), 2.44 (s, 3 H) ppm; **¹³C-NMR** (100 MHz, CDCl_3): δ = 169.4, 158.7, 139.0, 136.4, 133.4, 131.8, 130.5, 120.0, 129.3, 124.1, 113.3, 55.0, 51.7, 20.7 ppm; **IR** (ATR): $\tilde{\nu}$ = 2949, 2836, 1716, 1610, 1489, 1434, 1289,

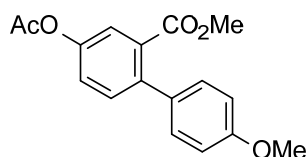
1239 cm^{-1} ; **MS** (EI, 70 eV), m/z (%): 257 (17), 256 (100) [M^+], 226 (9), 225 (52), 182 (8); **elemental analysis**: calcd. (%) for $\text{C}_{16}\text{H}_{16}\text{O}_3$: C 74.98, H 6.29; found: C 74.68, H 6.29.



Methyl 4'-methoxy-4-(trifluoromethyl)-[1,1'-biphenyl]-2-carboxylate (**5.3.4-4ra**)

[CAS: 1809272-44-3]: Compound **5.3.4-4ra** was prepared following method A, starting from 3-(trifluoromethyl)benzoic acid (194 mg, 1.00 mmol) and 4-methoxybenzenediazonium tetrafluoroborate (222 mg, 1.00 mmol). After purification, **5.3.4-4ra** was obtained as orange oil (222 mg, 0.72 mmol, 72%).

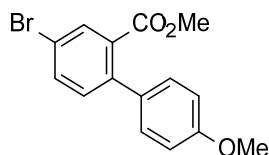
$^1\text{H-NMR}$ (400 MHz, CDCl_3): δ = 7.99 (d, J = 1.2 Hz, 1 H), 7.68 (dd, J = 8.0 Hz, 1.2 Hz, 1 H), 7.42 (d, J = 8.0 Hz, 1 H), 7.20–7.18 (m, 1 H), 7.18–7.16 (m, 1 H), 6.91–6.87 (m, 2 H), 3.79 (s, 3 H), 3.64 (s, 3 H) ppm; **$^{13}\text{C-NMR}$** (101 MHz, CDCl_3): δ = 168.1, 159.5, 145.5, 132.1, 131.34, 131.28, 129.41, 129.35 (q, $J_{\text{C-F}}$ = 33.6 Hz), 127.7 (q, $J_{\text{C-F}}$ = 3.6 Hz), 126.9 (q, $J_{\text{C-F}}$ = 3.6 Hz), 123.7 (q, $J_{\text{C-F}}$ = 272.5 Hz), 113.8, 55.3, 52.4 ppm; **IR** (ATR): $\tilde{\nu}$ = 2952, 1728, 1335, 1240 cm^{-1} ; **MS** (EI, 70 eV), m/z (%): 311 (18), 310 (100) [M^+], 280 (9), 279 (47); **elemental analysis**: calcd. (%) for $\text{C}_{16}\text{H}_{13}\text{F}_3\text{O}_3$: C 61.94, H 4.22; found: C 61.93, H 4.33.



Methyl 4-acetoxy-4'-methoxy-[1,1'-biphenyl]-2-carboxylate (**5.3.4-4sa**) [CAS: 1809272-45-4]:

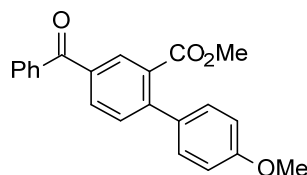
Compound **5.3.4-4sa** was prepared following method A, starting from 3-acetoxybenzoic acid (184 mg, 1.00 mmol) and 4-methoxybenzenediazonium tetrafluoroborate (222 mg, 1.00 mmol). After purification, **5.3.4-4sa** was obtained as brown solid (133 mg, 0.44 mmol, 44%).

$^1\text{H-NMR}$ (400 MHz, CDCl_3): δ = 7.45 (d, J = 2.8 Hz, 1 H), 7.24 (d, J = 8.4 Hz, 1 H), 7.15–7.09 (m, 3 H), 6.84–6.79 (m, 2 H), 3.71 (s, 3 H), 3.55 (s, 3 H), 2.20 (s, 3 H) ppm; **$^{13}\text{C-NMR}$** (101 MHz, CDCl_3): δ = 169.1, 167.9, 158.9, 149.1, 139.7, 132.6, 131.7, 131.4, 129.3, 124.3, 122.8, 113.4, 55.0, 51.9, 20.8 ppm; **IR** (ATR): $\tilde{\nu}$ = 2948, 2843, 1732, 1482, 1435, 1257, 1236, 1178 cm^{-1} ; **MS** (EI, 70 eV), m/z (%): 301 (7), 300 (43) [M^+], 259 (17), 258 (100), 227 (21), 43 (12); **elemental analysis**: calcd. (%) for $\text{C}_{17}\text{H}_{16}\text{O}_5$: C 67.99, H 5.37; found: C 67.78, H 5.41; **m.p.**: 81–82 $^{\circ}\text{C}$.



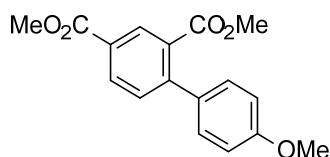
Methyl 4-bromo-4'-methoxy-[1,1'-biphenyl]-2-carboxylate (5.3.4-4ta) [CAS: 493028-86-7]: Compound **5.3.4-4ta** was prepared following method B, starting from 3-bromobenzoic acid (103 mg, 0.50 mmol) and 4-methoxybenzenediazonium tetrafluoroborate (111 mg, 0.50 mmol). After purification, **5.3.4-4ta** was obtained as yellow solid (117 mg, 0.37 mmol, 73%).

¹H-NMR (400 MHz, CDCl₃): δ = 7.85 (d, *J* = 2.0 Hz, 1 H), 7.54 (dd, *J* = 8.3 Hz, 2.2 Hz, 1 H), 7.18–7.14 (m, 2 H), 7.13–7.12 (m, 1 H), 6.88–6.84 (m, 2 H), 3.77 (s, 3 H), 3.61 (s, 3 H) ppm; **¹³C-NMR** (101 MHz, CDCl₃): δ = 167.9, 159.2, 140.9, 134.1, 132.5, 132.32, 132.30, 132.27, 129.3, 120.6, 113.6, 55.2, 52.2 ppm; **IR** (ATR): $\tilde{\nu}$ = 2949, 2835, 1722, 1517, 1468, 1434, 1278, 1234 cm⁻¹; **MS** (EI, 70 eV), *m/z* (%): 323 (18), 322 (100) [M⁺], 320 (98), 291 (36), 289 (39), 210 (58), 139 (24); **elemental analysis**: calcd. (%) for C₁₅H₁₃BrO₃: C 56.10, H 4.08; found: C 56.39, H 4.11; **m.p.**: 76–77 °C.



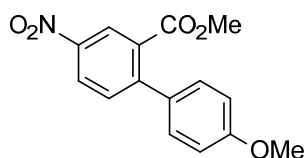
Methyl 4-benzoyl-4'-methoxy-[1,1'-biphenyl]-2-carboxylate (5.3.4-4ua) [CAS: 1809272-46-5]: Compound **5.3.4-4ua** was prepared following method A, starting from 3-benzoylbenzoic acid (229 mg, 1.00 mmol) and 4-methoxybenzenediazonium tetrafluoroborate (222 mg, 1.00 mmol). After purification, **5.3.4-4ua** was obtained as beige solid (250 mg, 0.72 mmol, 72%).

¹H-NMR (400 MHz, CDCl₃): δ = 8.08 (d, *J* = 1.6 Hz, 1 H), 7.78 (dd, *J* = 8.0 Hz, 2.0 Hz, 1 H), 7.68–7.66 (m, 2 H), 7.46–7.42 (m, 1 H), 7.34 (t, *J* = 7.8 Hz, 3 H), 7.15 (d, *J* = 8.4 Hz, 2 H), 6.81 (d, *J* = 8.8 Hz, 2 H), 3.67 (s, 3 H), 3.53 (s, 3 H) ppm; **¹³C-NMR** (101 MHz, CDCl₃): δ = 195.0, 168.4, 159.3, 145.5, 136.9, 135.6, 132.4, 132.13, 132.06, 131.2, 130.7, 130.5, 129.7, 129.2, 128.2, 113.5, 55.0, 52.0 ppm; **IR** (ATR): $\tilde{\nu}$ = 3059, 3023, 2942, 1725, 1647, 1599, 1258 cm⁻¹; **MS** (EI, 70 eV), *m/z* (%): 347 (28), 346 (100) [M⁺], 315 (14), 2 (38), 226 (8), 105 (33), 77 (13); **HRMS** (EI-TOF), *m/z*: [M⁺] calcd. for C₂₂H₁₈O₄: 346.1205; found: 346.1203; **m.p.**: 113–114 °C.



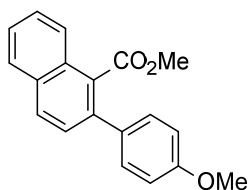
Dimethyl 4'-methoxy-[1,1'-biphenyl]-2,4-dicarboxylate (**5.3.4-4va**) [CAS: 99885-46-8]: Compound **5.3.4-4va** was prepared following method A, starting from methyl hydrogen isophthalate (186 mg, 1.00 mmol) and 4-methoxybenzenediazonium tetrafluoroborate (222 mg, 1.00 mmol). After purification, **5.3.4-4va** was obtained as grey solid (211 mg, 0.70 mmol, 70%).

¹H-NMR (400 MHz, CDCl₃): δ = 8.41 (d, J = 1.6 Hz, 1 H), 8.09 (dd, J = 8.4 Hz, 1.6 Hz, 1 H), 7.39 (d, J = 8.0 Hz, 1 H), 7.21–7.24 (m, 2 H), 6.90–6.92 (m, 2 H), 3.90 (s, 3 H), 3.79 (s, 3 H), 3.67 (s, 3 H) ppm; **¹³C-NMR** (101 MHz, CDCl₃): δ = 168.2, 165.8, 159.3, 146.0, 132.1, 131.7, 130.81, 130.78, 130.6, 129.2, 128.3, 113.5, 55.0, 52.0, 51.9 ppm; **IR** (ATR): $\tilde{\nu}$ = 3028, 3002, 2970, 1738, 1606, 1448, 1366, 1217, 1117, 1071, 1025 cm⁻¹; **m.p.**: 86–87 °C.^[275]



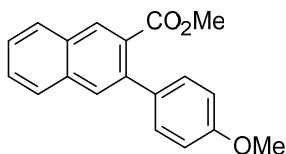
Methyl 4'-methoxy-4-nitro-[1,1'-biphenyl]-2-carboxylate (**5.3.4-4wa**) [CAS: 937601-71-3]: Compound **5.3.4-4wa** was prepared following method B, starting from 3-nitrobenzoic acid (84.4 mg, 5.00 mmol) and 4-methoxybenzenediazonium tetrafluoroborate (111 mg, 0.50 mmol). After purification, **5.3.4-4wa** was obtained as brown oil (250 mg, 0.31 mmol, 62%).

¹H-NMR (400 MHz, CDCl₃): δ = 8.55 (d, J = 2.4 Hz, 1 H), 8.24 (dd, J = 8.4 Hz, 2.4 Hz, 1 H), 7.46 (d, J = 8.4 Hz, 1 H), 7.20–7.17 (m, 2 H), 6.91–6.87 (m, 2 H), 3.78 (s, 3 H), 3.67 (s, 3 H) ppm; **¹³C-NMR** (101 MHz, CDCl₃): δ = 167.2, 160.0, 148.2, 146.2, 131.8, 131.7, 131.1, 129.4, 125.5, 125.1, 113.9, 55.2, 52.5 ppm; **IR** (ATR): $\tilde{\nu}$ = 3076, 2952, 2838, 1723, 1606, 1516, 1475, 1436, 1346, 1247 cm⁻¹; **MS** (EI, 70 eV), m/z (%): 288 (17), 287 (100) [M⁺], 257 (9), 256 (43), 226 (11), 210 (14), 139 (11).



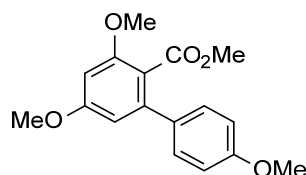
Methyl 2-(4-methoxyphenyl)-1-naphthoate (5.3.4-4xa) [CAS: 1415046-18-2]: Compound **5.3.4-4xa** was prepared following method A, starting from 1-naphthoic acid (176 mg, 1.00 mmol) and 4-methoxybenzenediazonium tetrafluoroborate (222 mg, 1.00 mmol). After purification, **5.3.4-4xa** was obtained as colorless solid (270 mg, 0.92 mmol, 92%).

¹H-NMR (400 MHz, CDCl₃): δ = 7.99 (d, J = 8.4 Hz, 1 H), 7.94 (d, J = 8.4 Hz, 1 H), 7.89 (d, J = 7.6 Hz, 1 H), 7.61–7.57 (m, 1 H), 7.55–7.51 (m, 2 H), 7.48–7.44 (m, 2 H), 7.03–6.99 (m, 2 H), 3.86 (s, 3 H), 3.78 (s, 3 H) ppm; **¹³C-NMR** (101 MHz, CDCl₃): δ = 170.2, 159.1, 137.5, 133.1, 132.0, 129.9, 129.8, 129.6, 128.0, 127.4, 127.3, 126.1, 124.8, 113.8, 55.1, 52.1 ppm; **IR** (ATR): $\tilde{\nu}$ = 2970, 2948, 1728, 1231 cm⁻¹; **MS** (EI, 70 eV), m/z (%): 293 (20), 292 (89) [M⁺], 262 (20), 261 (100), 218 (17), 189 (14); **HRMS** (EI-TOF), m/z : [M⁺] calcd. for C₁₉H₁₆O₃: 292.1099; found: 292.1097; **m.p.**: 117–118 °C.



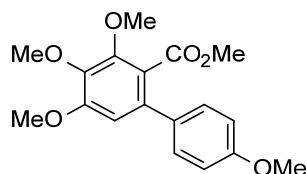
Methyl 3-(4-methoxyphenyl)-2-naphthoate (5.3.4-4ya) [CAS: 1415046-18-2]: Compound **5.3.4-4ya** was prepared following method A, starting from 2-naphthoic acid (176 mg, 1.00 mmol) and 4-methoxybenzenediazonium tetrafluoroborate (222 mg, 1.00 mmol). After purification, **5.3.4-4ya** was obtained as orange oil (193 mg, 0.66 mmol, 66%).

¹H-NMR (400 MHz, CDCl₃): δ = 8.37 (s, 1 H), 7.93 (d, J = 8.0 Hz, 1 H), 7.86 (d, J = 8.4 Hz, 1 H), 7.80 (s, 1 H), 7.60–7.51 (m, 2 H), 7.36–7.33 (m, 2 H), 6.99–6.96 (m, 2 H), 3.87 (s, 3 H), 3.74 (s, 3 H) ppm; **¹³C-NMR** (101 MHz, CDCl₃): δ = 169.2, 158.9, 138.3, 134.4, 133.8, 131.4, 130.8, 129.58, 129.55, 129.2, 128.5, 128.1, 127.7, 126.5, 113.5, 55.3, 52.1 ppm; **IR** (ATR): $\tilde{\nu}$ = 2948, 2835, 1722, 1515, 1277, 1240, 1214, 1176 cm⁻¹; **MS** (EI, 70 eV), m/z (%): 293 (19), 292 (100) [M⁺], 262 (14), 261 (62), 218 (14), 189 (10); **elemental analysis**: calcd. (%) for C₁₉H₁₆O₃: C 78.06, H 5.52; found: C 77.80, H 5.71.



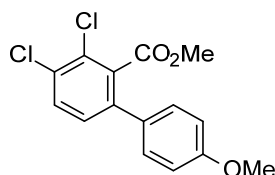
Methyl 3,4',5-trimethoxy-[1,1'-biphenyl]-2-carboxylate (5.3.4-4za) [CAS: 131035-41-1]: Compound **5.3.4-4za** was prepared following method A, starting from 2,4-dimethoxybenzoic acid (186 mg, 1.00 mmol) and 4-methoxybenzenediazonium tetrafluoroborate (222 mg, 1.00 mmol). After purification, **5.3.4-4za** was obtained as beige solid (236 mg, 0.78 mmol, 78%).

¹H-NMR (400 MHz, CDCl₃): δ = 7.33–7.30 (m, 2 H), 6.92–6.89 (m, 2 H), 6.46 (dd, J = 5.2 Hz, 2.0 Hz, 2 H), 3.82 (s, 3 H), 3.81 (s, 3 H), 3.80 (s, 3 H), 3.60 (s, 3 H) ppm; **¹³C-NMR** (101 MHz, CDCl₃): δ = 168.5, 161.1, 159.0, 157.9, 142.0, 132.6, 129.0, 115.7, 113.6, 105.9, 96.9, 55.8, 55.2, 55.0, 51.8 ppm; **IR** (ATR): $\tilde{\nu}$ = 2003, 2946, 2838, 1724, 1599, 1584, 1571, 1515, 1455, 1455, 1290, 1235, 1096, 830 cm⁻¹; **MS** (EI, 70 eV), m/z (%): 302 (51) [M⁺], 272 (18), 271 (100); **m.p.**: 57–58 °C.



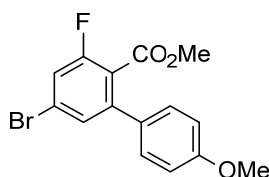
Methyl 3,4,4',5-tetramethoxy-[1,1'-biphenyl]-2-carboxylate (5.3.4-4aaa) [CAS: 1809272-47-6]: Compound **5.3.4-4aaa** was prepared following method A, starting from 2,3,4-trimethoxybenzoic acid (217 mg, 1.00 mmol) and 4-methoxybenzenediazonium tetrafluoroborate (222 mg, 1.00 mmol). After purification, **5.3.4-4aaa** was obtained as brown solid (226 mg, 0.68 mmol, 68%).

¹H-NMR (400 MHz, CDCl₃): δ = 7.31–7.27 (m, 2 H), 6.92–6.88 (m, 2 H), 6.64 (s, 1 H), 3.64 (s, 3 H), 3.89 (s, 3 H), 3.87 (s, 3 H), 3.81 (s, 3 H), 3.64 (s, 3 H) ppm; **¹³C-NMR** (101 MHz, CDCl₃): δ = 168.0, 159.0, 154.1, 150.9, 140.8, 135.5, 132.3, 129.1, 121.1, 113.7, 108.7, 61.7, 60.8, 56.0, 55.1, 51.9 ppm; **IR** (ATR): $\tilde{\nu}$ = 3004, 2941, 2842, 1723, 1248, 1212, 1107, 1019 cm⁻¹; **MS** (EI, 70 eV), m/z (%): 333 (18), 332 (100) [M⁺], 318 (11), 317 (65), 301 (20), 289 (11), 243 (14); **elemental analysis**: calcd. (%) for C₁₈H₂₀O₆: C 65.05, H 6.07; found: C 65.00, H 6.24; **m.p.**: 51–52 °C.



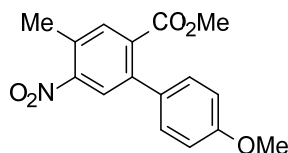
Methyl 3,4-dichloro-4'-methoxy-[1,1'-biphenyl]-2-carboxylate (**5.3.4-4aba**) [CAS: 1809272-48-7]: Compound **5.3.4-4aba** was prepared following method B, starting from 2,3-dichlorobenzoic acid (97.5 mg, 0.50 mmol) and 4-methoxybenzenediazonium tetrafluoroborate (111 mg, 0.50 mmol). After purification, **5.3.4-4aba** was obtained as brown solid (124 mg, 0.39 mmol, 79%).

¹H-NMR (400 MHz, CDCl₃): δ = 7.50 (d, *J* = 8.4 Hz, 1 H), 7.30–7.27 (m, 2 H), 7.21 (d, *J* = 8.4 Hz, 1 H), 6.95–6.91 (m, 2 H), 3.82 (s, 3 H), 3.72 (s, 3 H) ppm; **¹³C-NMR** (100 MHz, CDCl₃): δ = 167.0, 159.8, 142.6, 135.5, 132.0, 131.5, 130.4, 129.3, 128.2, 127.5, 114.0, 55.2, 52.5 ppm; **IR** (ATR): $\tilde{\nu}$ = 2951, 2837, 1734, 1250, 1178 cm⁻¹; **MS** (EI, 70 eV), *m/z* (%): 314 (14), 312 (79), 311 (17) [M⁺], 310 (100), 281 (35), 279 (46), 244 (19); **elemental analysis**: calcd. (%) for C₁₅H₁₂Cl₂O₃: C 57.90, H 3.89; found: C 58.09, H 3.96; **HRMS** (EI-TOF), *m/z*: [M⁺] calcd. for C₁₅H₁₂Cl₂O₃: 310.0163; found: 310.0161; **m.p.**: 87–88 °C.



Methyl 5-bromo-3-fluoro-4'-methoxy-[1,1'-biphenyl]-2-carboxylate (**5.3.4-4aca**) [CAS: 1809272-49-8]: Compound **5.3.4-4aca** was prepared following method B, starting from 4-bromo-2-fluorobenzoic acid (122 mg, 0.50 mmol) and 4-methoxybenzenediazonium tetrafluoroborate (111 mg, 0.50 mmol). After purification, **5.3.4-4aca** was obtained as brown oil (123 mg, 0.36 mmol, 73%).

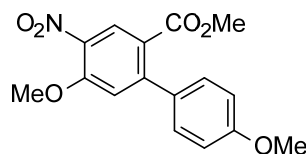
¹H-NMR (400 MHz, CDCl₃): δ = 7.24 (s, 1 H), 7.19–7.15 (m, 3 H), 6.85–6.81 (m, 2 H), 3.73 (s, 3 H), 3.60 (s, 3 H) ppm; **¹³C-NMR** (101 MHz, CDCl₃): δ = 165.5, 159.8, 159.5 (d, *J*_{C-F} = 256.1 Hz), 143.3 (d, *J*_{C-F} = 3.6 Hz), 130.2 (d, *J*_{C-F} = 1.8 Hz), 129.2, 128.5 (d, *J*_{C-F} = 3.6 Hz), 123.9 (d, *J*_{C-F} = 10.9 Hz), 120.3 (d, *J*_{C-F} = 16.4 Hz), 117.6, (d, *J*_{C-F} = 25.4 Hz), 114.0, 55.2, 52.5 ppm; **IR** (ATR): $\tilde{\nu}$ = 2952, 2838, 1732, 1515, 1247 cm⁻¹; **MS** (EI, 70 eV), *m/z* (%): 341 (17), 340 (100) [M⁺], 339 (18), 338 (72), 309 (39), 307 (35), 157 (13); **HRMS** (EI-TOF), *m/z*: [M⁺] calcd. for C₁₅H₁₂BrFO₃: 337.9954; found: 337.9952.



Methyl 4'-methoxy-4-methyl-5-nitro-[1,1'-biphenyl]-2-carboxylate (**5.3.4-4ada**)

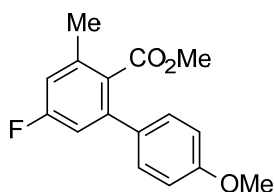
[CAS: 1809272-50-1]: Compound **5.3.4-4ada** was prepared following method B, starting from 3-methyl-4-nitrobenzoic acid (92.4 mg, 0.50 mmol) and 4-methoxybenzenediazonium tetrafluoroborate (111 mg, 0.50 mmol). After purification, **5.3.4-4ada** was obtained as brown solid (100 mg, 0.33 mmol, 66%).

¹H-NMR (400 MHz, CDCl₃): δ = 7.86 (s, 1 H), 7.62 (s, 1 H), 7.18–7.14 (m, 2 H), 6.87–6.85 (m, 2 H), 3.75 (s, 3 H), 3.61 (s, 3 H), 2.54 (s, 3 H) ppm; **¹³C-NMR** (101 MHz, CDCl₃): δ = 167.8, 159.5, 150.0, 140.6, 134.7, 133.8, 131.5, 130.8, 129.3, 126.2, 113.8, 55.2, 52.4, 19.7 ppm; **IR** (ATR): $\tilde{\nu}$ = 2969, 2940, 1725, 1510, 1293, 1236 cm⁻¹; **MS** (EI, 70 eV), *m/z* (%): 302 (17), 301 (100) [M⁺], 284 (19), 256 (26), 225 (7); **elemental analysis**: calcd. (%) for C₁₆H₁₅NO₅: C 63.78, H 5.02, N 4.65; found: C 63.52, H 5.00, N 4.44; **m.p.**: 83–84 °C.



Methyl 4',5-dimethoxy-4-nitro-[1,1'-biphenyl]-2-carboxylate (**5.3.4-4aea**) [CAS: 1809272-51-2]: Compound **5.3.4-4aea** was prepared following method A, starting from 4-methoxy-3-nitrobenzoic acid (201 mg, 1.00 mmol) and 4-methoxybenzenediazonium tetrafluoroborate (222 mg, 1.00 mmol). After purification, **5.3.4-4aea** was obtained as yellow solid (265 mg, 0.83 mmol, 83%).

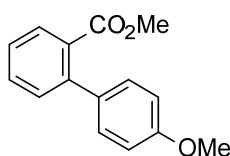
¹H-NMR (400 MHz, CDCl₃): δ = 8.40 (s, 1 H), 7.19–7.15 (m, 2 H), 6.93–6.87 (m, 3 H), 3.94 (s, 3 H), 3.79 (s, 3 H), 3.64 (s, 3 H) ppm; **¹³C-NMR** (101 MHz, CDCl₃): δ = 166.2, 159.8, 154.6, 149.6, 137.4, 131.8, 129.3, 128.7, 122.1, 115.8, 113.7, 56.8, 55.3, 52.2 ppm; **IR** (ATR): $\tilde{\nu}$ = 3016, 2970, 2951, 2926, 1728, 1350, 1229 cm⁻¹; **MS** (EI, 70 eV), *m/z* (%): 318 (18), 317 (100) [M⁺], 287 (10), 286 (44), 211 (17), 139 (7); **HRMS** (EI-TOF), *m/z*: [M⁺] calcd. for C₁₆H₁₅NO₆: 317.0899; found, 317.0906; **m.p.**: 136–137 °C.



Methyl 5-fluoro-4'-methoxy-3-methyl-[1,1'-biphenyl]-2-carboxylate (**5.3.4-4afa**)

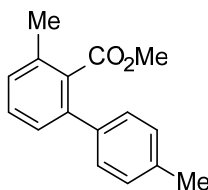
[CAS: 1809272-52-3]: Compound **5.3.4-4afa** was prepared following method A, starting from 4-fluoro-3-methylbenzoic acid (156 mg, 1.00 mmol) and 4-methoxybenzenediazonium tetrafluoroborate (222 mg, 1.00 mmol). After purification, **5.3.4-4afa** was obtained as yellow oil (202 mg, 0.74 mmol, 74%).

¹H-NMR (400 MHz, CDCl₃): δ = 7.15 (d, *J* = 8.4, 2 H), 6.80–6.74 (m, 4 H), 3.67 (s, 3 H), 3.47 (s, 3 H), 2.24 (s, 3 H) ppm; **¹³C-NMR** (101 MHz, CDCl₃): δ = 169.7, 162.4 (d, *J*_{C-F} = 248.0 Hz), 159.2, 142.2 (d, *J*_{C-F} = 9.1 Hz), 138.3 (d, *J*_{C-F} = 9.1 Hz), 132.1 (d, *J*_{C-F} = 1.8 Hz), 129.2 (d, *J*_{C-F} = 2.7 Hz), 129.0, 115.3 (d, *J*_{C-F} = 21.8 Hz), 113.9, 113.7, 55.0, 51.8, 19.6 ppm; **IR** (ATR): $\tilde{\nu}$ = 2950, 2837, 1723, 1597, 1515, 1246 cm⁻¹; **MS** (EI, 70 eV), *m/z* (%): 275 (16), 274 (96) [M⁺], 244 (15), 243 (100), 242 (67), 227 (17), 200 (16); **elemental analysis**: calcd. (%) for C₁₆H₁₅FO₃: C 70.06, H 5.51; found: C 70.08, H 5.54.



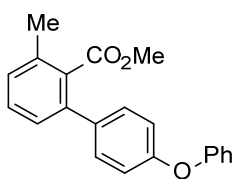
Methyl 4'-methoxy-[1,1'-biphenyl]-2-carboxylate (**5.3.4-4aga**) [CAS: 17103-25-2]: Compound **5.3.4-4aga** was prepared following method A, starting from benzoic acid (123 mg, 1.00 mmol) and 4-methoxybenzenediazonium tetrafluoroborate (222 mg, 1.00 mmol). After purification, **5.3.4-4aga** was obtained as colorless liquid (69 mg, 0.28 mmol, 28%) along with the diarylated product (92 mg, 0.26 mmol, 26%).

¹H-NMR (400 MHz, CDCl₃): δ = 7.82–7.78 (d, 1 H), 7.52 (td, *J* = 7.8 Hz, 1.3 Hz, 1 H), 7.41–7.36 (m, 2 H), 6.28–6.24 (m, 2 H), 6.97–6.93 (m, 2 H), 3.86 (s, 3 H), 3.68 (s, 3 H) ppm; **¹³C-NMR** (101 MHz, CDCl₃): δ = 169.4, 159.0, 142.0, 133.6, 131.2, 130.8, 130.7, 129.7, 129.4, 126.8, 113.5, 55.2, 52.0 ppm; **MS** (EI, 70 eV), *m/z* (%): 243 (19), 242 (100) [M⁺], 212 (10), 211 (74), 168 (17), 139 (14); the analytical data matched those reported in the literature.^[276]



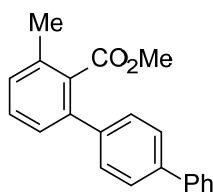
Methyl 3,4'-dimethyl-[1,1'-biphenyl]-2-carboxylate (**5.3.4-4ab**) [CAS: 1097018-21-7]: Compound **5.3.4-4ab** was prepared following method A1, starting from 2-methylbenzoic acid (138 mg, 1.00 mmol) and 4-methylbenzenediazonium tetrafluoroborate (247 mg, 1.20 mmol). After purification, **5.3.4-4ab** was obtained as yellow oil (180 mg, 0.75 mmol, 75%).

¹H-NMR (400 MHz, CDCl₃): δ = 7.26 (t, J = 7.8 Hz, 1 H), 7.20–7.17 (m, 2 H), 7.14–7.10 (m, 4 H), 3.54 (s, 3 H), 2.32 (s, 3 H), 2.30 (s, 3 H) ppm; **¹³C-NMR** (101 MHz, CDCl₃): δ = 170.4, 140.0, 137.9, 137.0, 135.3, 133.1, 129.4, 128.9, 128.9, 128.0, 127.2, 51.8, 21.2, 19.7 ppm; **IR** (ATR): $\tilde{\nu}$ = 3024, 2970, 2948, 1725, 1264 cm⁻¹; **MS** (EI, 70 eV), m/z (%): 241 (23), 240 (100) [M⁺], 210 (12), 209 (73), 208 (45), 166 (10), 165 (15); **elemental analysis**: calcd. (%) for C₁₆H₁₆O₂: C 79.97, H 6.71; found: C 79.85, H 6.75.



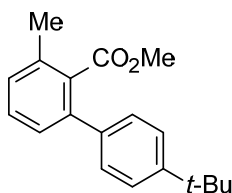
Methyl 3-methyl-4'-phenoxy-[1,1'-biphenyl]-2-carboxylate (**5.3.4-4ac**) [CAS: 1809272-55-6]: Compound **5.3.4-4ac** was prepared following method A1, starting from 2-methylbenzoic acid (138 mg, 1.00 mmol) and 4-phenoxybenzenediazonium tetrafluoroborate (341 mg, 1.20 mmol). After purification, **5.3.4-4ac** was obtained as brown oil (228 mg, 0.71 mmol, 71%).

¹H-NMR (400 MHz, CDCl₃): δ = 7.39–7.31 (m, 4 H), 7.33–7.31 (m, 1 H), 7.21 (d, J = 8.0 Hz, 2 H), 7.13 (t, J = 7.6 Hz, 1 H), 7.07–7.02 (m, 4 H), 3.64 (s, 3 H), 2.40 (s, 3 H) ppm; **¹³C-NMR** (101 MHz, CDCl₃): δ = 170.3, 156.9, 156.8, 139.4, 135.8, 135.4, 133.1, 129.8, 129.6, 129.4, 129.0, 127.2, 123.5, 119.1, 118.4, 51.9, 19.7 ppm; **IR** (ATR): $\tilde{\nu}$ = 3036, 2947, 1725, 1588, 1488, 1231 cm⁻¹; **MS** (EI, 70 eV), m/z (%): 319 (21), 318 (100) [M⁺], 287 (31), 286 (23), 194 (16), 193 (40), 165 (12); **elemental analysis**: calcd. (%) for C₂₁H₁₈O₃: C 79.23, H 5.70; found: C 79.28, H 5.94.



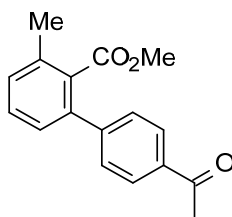
Methyl 3-methyl-[1,1':4',1''-terphenyl]-2-carboxylate (**5.3.4-4ad**) [CAS: 1809272-56-7]: Compound **5.3.4-4ad** was prepared following method A1, starting from 2-methylbenzoic acid (138 mg, 1.00 mmol) and 4-phenylbenzenediazonium tetrafluoroborate (322 mg, 1.20 mmol). After purification, **5.3.4-4ad** was obtained as colorless solid (222 mg, 0.73 mmol, 73%).

¹H-NMR (400 MHz, CDCl₃): δ = 7.74 (d, J = 8.0 Hz, 4 H), 7.58–7.50 (m, 4 H), 7.44 (t, J = 7.6 Hz, 2 H), 7.36 (d, J = 7.6 Hz, 1 H), 7.31 (d, J = 7.5 Hz, 1 H), 3.72 (s, 3 H), 2.53 (s, 3 H) ppm; **¹³C-NMR** (100 MHz, CDCl₃): δ = 170.2, 140.4, 139.9, 139.7, 139.5, 135.4, 133.0, 129.3, 129.0, 128.7, 128.5, 127.2, 127.1, 126.9, 126.8, 51.7, 19.6 ppm; **IR** (ATR): $\tilde{\nu}$ = 3024, 2952, 1728, 1258 cm⁻¹; **MS** (EI, 70 eV), m/z (%): 303 (21), 302 (100) [M⁺], 272 (15), 271 (73), 270 (26), 269 (25), 228 (8); **HRMS** (EI-TOF), m/z : [M⁺] calcd. for C₂₁H₁₈O₂: 302.1307; found: 302.1305; **m.p.**: 79–80 °C.



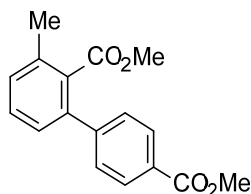
Methyl 4'-(tert-butyl)-3-methyl-[1,1'-biphenyl]-2-carboxylate (**5.3.4-4ae**) [CAS: 1809272-57-8]: Compound **5.3.4-4ae** was prepared following method A1, starting from 2-methylbenzoic acid (138 mg, 1.00 mmol) and 4-(*tert*-butyl)benzenediazonium tetrafluoroborate (298 mg, 1.20 mmol). After purification, **5.3.4-4ae** was obtained as yellow oil (172 mg, 0.61 mmol, 61%).

¹H-NMR (400 MHz, CDCl₃): δ = 7.43–7.40 (m, 2 H), 7.35 (t, J = 8.0 Hz, 1 H), 7.32–7.29 (m, 2 H), 7.24–7.19 (m, 2 H), 3.60 (s, 3 H), 2.40 (s, 3 H), 1.35 (s, 9 H) ppm; **¹³C-NMR** (101 MHz, CDCl₃): δ = 170.5, 150.2, 140.0, 137.8, 135.3, 133.1, 129.3, 128.8, 127.8, 127.2, 125.2, 51.8, 34.5, 31.3, 19.7 ppm; **IR** (ATR): $\tilde{\nu}$ = 2952, 1727, 1365, 1267, 1236 cm⁻¹; **MS** (EI, 70 eV), m/z (%): 282 (23) [M⁺], 268 (19), 267 (100); **elemental analysis**: calcd. (%) for C₁₉H₂₂O₂: C 80.82, H 7.85; found: C 80.82, H 8.00.



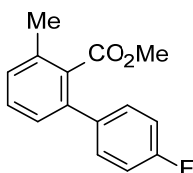
Dimethyl 3-methyl-[1,1'-biphenyl]-2,4'-dicarboxylate (**5.3.4-4af**) [CAS: 1809272-58-9]: Compound **5.3.4-4af** was prepared following method B, starting from 2-methylbenzoic acid (68.8 mg, 0.50 mmol) and 4-acetylbenzenediazonium tetrafluoroborate (117 mg, 0.50 mmol). After purification, **5.3.4-4af** was obtained as colorless solid (81 mg, 0.30 mmol, 60%).

¹H-NMR (400 MHz, CDCl₃): δ = 7.99–7.97 (m, 2 H), 7.45–7.43 (m, 2 H), 7.36 (t, J = 7.8 Hz, 1 H), 7.24 (d, J = 7.6 Hz, 1 H), 7.19 (d, J = 7.6 Hz, 1 H), 3.58 (s, 3 H), 2.61 (s, 3 H), 2.40 (s, 3 H) ppm; **¹³C-NMR** (101 MHz, CDCl₃): δ = 197.6, 169.8, 145.7, 138.9, 135.8, 135.7, 132.8, 129.8, 129.5, 128.34, 128.29, 126.9, 51.8, 26.5, 19.6 ppm; **IR** (ATR): $\tilde{\nu}$ = 3002, 2970, 2949, 1719, 1678, 1356, 1269 cm⁻¹; **MS** (EI, 70 eV), m/z (%): 314 (14), 312 (79), 311 (17) [M⁺], 310 (100), 281 (35), 279 (46), 244 (19); **elemental analysis**: calcd. (%) for C₁₇H₁₆O₃: C 76.10, H 6.01; found: C 76.19, H 6.24; **m.p.**: 114–115 °C.



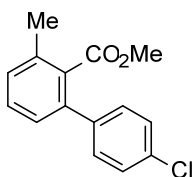
Dimethyl 3-methyl-[1,1'-biphenyl]-2,4'-dicarboxylate (**5.3.4-4ag**) [CAS: 1809272-59-0]: Compound **5.3.4-4ag** was prepared following method B, starting from 2-methylbenzoic acid (68.8 mg, 0.50 mmol) and 4-(methoxycarbonyl)benzenediazonium tetrafluoroborate (125 mg, 0.50 mmol). After purification, **5.3.4-4ag** was obtained as yellow solid (90 mg, 0.32 mmol, 63%).

¹H-NMR (400 MHz, CDCl₃): δ = 8.07–8.05 (m, 2 H), 7.42 (d, J = 8.4 Hz, 2 H), 7.35 (t, J = 7.6 Hz, 1 H), 7.24–7.19 (m, 2 H), 3.92 (s, 3 H), 3.56 (s, 3 H), 2.40 (s, 3 H) ppm; **¹³C-NMR** (101 MHz, CDCl₃): δ = 169.8, 166.8, 145.5, 139.0, 135.7, 132.9, 129.7, 129.5, 129.0, 128.1, 126.9, 52.0, 51.8, 19.6 ppm; **IR** (ATR): $\tilde{\nu}$ = 2947, 1709, 1264, 1115 cm⁻¹; **MS** (EI, 70 eV), m/z (%): 269 (8), 268 (36) [M⁺], 254 (17), 253 (100), 195 (7), 42 (8); **elemental analysis**: calcd. (%) for C₁₇H₁₆O₄: C, 71.82; H, 5.67; found: C, 71.69; H, 5.67; **m.p.**: 69–70 °C.



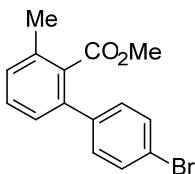
Methyl 4'-fluoro-3-methyl-[1,1'-biphenyl]-2-carboxylate (**5.3.4-4ah**) [CAS: 1809272-60-3]: Compound **5.3.4-4ah** was prepared following procedure B, starting from 2-methylbenzoic acid (68.8 mg, 0.50 mmol) and 4-fluorobenzenediazonium tetrafluoroborate (105 mg, 0.50 mmol). After purification, **5.3.4-4ah** was obtained as brown solid (71 mg, 0.29 mmol, 58%).

¹H-NMR (400 MHz, CDCl₃): δ = 7.37–7.31 (m, 3 H), 7.22 (d, J = 7.2 Hz, 1 H), 7.18 (d, J = 7.6 Hz, 1 H), 7.10–7.06 (m, 2 H), 3.61 (s, 3 H), 2.40 (s, 3H) ppm; **¹³C-NMR** (101 MHz, CDCl₃): δ = 170.2, 162.3 (d, J_{C-F} = 247.1 Hz), 139.0, 136.9 (d, J_{C-F} = 3.6 Hz), 135.5, 133.2, 129.8 (d, J_{C-F} = 8.5 Hz), 129.4, 129.2, 127.2, 115.2 (d, J_{C-F} = 21.8 Hz), 51.9, 19.7 ppm; **IR** (ATR): $\tilde{\nu}$ = 3004, 2970, 2948, 1737, 1366, 1218 cm⁻¹; **MS** (EI, 70 eV), m/z (%): 245 (29), 244 (100) [M⁺], 214 (13), 213 (88), 212 (26), 183 (11), 165 (11); **elemental analysis**: calcd. (%) for C₁₅H₁₃FO₂: C 73.76, H 5.36; found: C 73.47, H 5.52; **m.p.**: 62–63 °C.



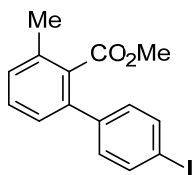
Methyl 4'-chloro-3-methyl-[1,1'-biphenyl]-2-carboxylate (**5.3.4-4ai**) [CAS: 1809272-61-4]: Compound **5.3.4-4ai** was prepared following method B, starting from 2-methylbenzoic acid (68.8 mg, 0.50 mmol) and 4-chlorobenzenediazonium tetrafluoroborate (113 mg, 0.50 mmol). After purification, **5.3.4-4ai** was obtained as brown oil (75 mg, 0.29 mmol, 58%).

¹H-NMR (400 MHz, CDCl₃): δ = 7.38–7.34 (m, 3 H), 7.31–7.28 (m, 2 H), 7.23 (d, J = 7.6 Hz, 1 H), 7.18 (d, J = 7.6 Hz, 1 H), 3.62 (s, 3 H), 2.40 (s, 3 H) ppm; **¹³C-NMR** (101 MHz, CDCl₃): δ = 170.1, 139.3, 138.8, 135.6, 133.5, 133.1, 129.53, 129.51, 129.4, 128.5, 127.1, 51.9, 19.7 ppm; **IR** (ATR): $\tilde{\nu}$ = 2970, 2948, 1725, 1459, 1366, 1265, 1235, 1121 cm⁻¹; **MS** (EI, 70 eV), m/z (%): 261 (21), 260 (67) [M⁺], 231 (37), 229 (100), 193 (28), 166 (20), 165 (27); **elemental analysis**: calcd. (%) for C₁₅H₁₃ClO₂: C 69.10, H 5.03; found: C 69.10, H 5.14.



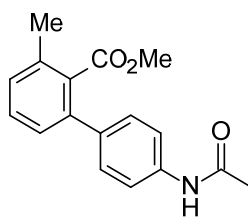
Methyl 4'-bromo-3-methyl-[1,1'-biphenyl]-2-carboxylate (**5.3.4-4aj**) [CAS: 1809272-62-5]: Compound **5.3.4-4aj** was prepared following method B, starting from 2-methylbenzoic acid (68.8 mg, 0.50 mmol) and 4-bromobenzenediazonium tetrafluoroborate (135 mg, 0.50 mmol). After purification, **5.3.4-4aj** was obtained as red solid (106 mg, 0.35 mmol, 70%).

¹H-NMR (400 MHz, CDCl₃): δ = 7.43–7.40 (m, 2 H), 7.25 (t, *J* = 7.6 Hz, 1 H), 7.15–7.12 (m, 3 H), 7.07 (d, *J* = 7.6 Hz, 1 H), 3.52 (s, 3 H), 2.30 (s, 3 H) ppm; **¹³C-NMR** (101 MHz, CDCl₃): δ = 170.0, 139.8, 138.8, 135.6, 132.9, 131.4, 129.8, 129.5, 129.4, 127.0, 121.7, 51.9, 19.6 ppm; **IR** (ATR): $\tilde{\nu}$ = 2948, 2925, 1728, 1457, 1266 cm⁻¹; **MS** (EI, 70 eV), *m/z* (%): 306 (70) [M⁺], 304 (66), 275 (71), 273 (70), 194 (100), 193 (38), 165 (29); **HRMS** (EI-TOF), *m/z*: [M⁺] calcd. for C₁₅H₁₃BrO₂: 304.0099; found: 304.0086; **m.p.**: 54–55 °C.



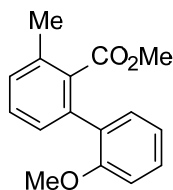
Methyl 4'-iodo-3-methyl-[1,1'-biphenyl]-2-carboxylate (**5.3.4-4ak**) [CAS: 1809272-63-6]: Compound **5.3.4-4ak** was prepared following method A (AgOAc (50.1 mg, 30 mol%) and Li₂CO₃ (22.2 mg, 30 mol%) were used), starting from 2-methylbenzoic acid (138 mg, 1.00 mmol) and 4-iodobenzenediazonium tetrafluoroborate (318 mg, 1.00 mmol). After purification, **5.3.4-4ak** was obtained as yellow solid (211 mg, 0.74 mmol, 74%).

¹H-NMR (400 MHz, CDCl₃): δ = 7.74–7.70 (m, 2 H), 7.35 (d, *J* = 7.6 Hz, 1 H), 7.23 (d, *J* = 7.6 Hz, 1 H), 7.17 (d, *J* = 7.6 Hz, 1 H), 7.12–7.09 (m, 2 H), 3.62 (s, 3 H), 2.40 (s, 3 H) ppm; **¹³C-NMR** (101 MHz, CDCl₃): δ = 167.0, 140.4, 138.9, 137.4, 135.6, 132.9, 130.1, 129.52, 129.46, 127.0, 93.3, 51.9, 19.7 ppm; **IR** (ATR): $\tilde{\nu}$ = 3001, 2970, 2947, 1737, 1366, 1217 cm⁻¹; **MS** (EI, 70 eV), *m/z* (%): 353 (16), 352 (100) [M⁺], 321 (23), 194 (27), 193 (12), 165 (11); **HRMS** (EI-TOF), *m/z*: [M⁺] calcd. for C₁₅H₁₃IO₂: 351.9960; found: 351.9945; **m.p.**: 73–74 °C.



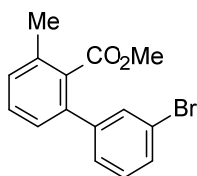
Methyl 4'-acetamido-3-methyl-[1,1'-biphenyl]-2-carboxylate (5.3.4-4al) [CAS: 1809272-64-7]: Compound **5.3.4-4al** was prepared following method A1, starting from 2-methylbenzoic acid (138 mg, 1.00 mmol) and 4-(acetylamino)benzenediazonium tetrafluoroborate (299 mg, 1.20 mmol). After purification, **5.3.4-4al** was obtained as beige solid (247 mg, 0.70 mmol, 70%).

¹H-NMR (400 MHz, DMSO-*d*₆): δ = 10.06 (s, 1 H), 7.65 (d, *J* = 8.4, Hz, 2 H), 7.41 (d, *J* = 7.6 Hz, 1 H), 7.28–7.22 (m, 4 H), 3.59 (s, 3 H), 2.30 (s, 3 H), 2.07 (s, 3 H) ppm; **¹³C-NMR** (101 MHz, DMSO-*d*₆): δ = 169.6, 168.4, 138.8, 138.7, 134.68, 134.67, 132.8, 129.6, 128.7, 128.2, 126.9, 118.9, 51.8, 24.0, 19.1 ppm; **IR** (ATR): $\tilde{\nu}$ = 3001, 2970, 2947, 1737, 1366, 1217 cm⁻¹; **HRMS** (EI-TOF), *m/z*: [*M*⁺] calcd. for C₁₇H₁₇NO₃: 283.1208; found: 283.1204; **m.p.**: 187–188 °C.



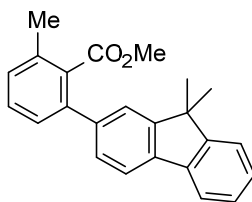
Methyl 2'-methoxy-3-methyl-[1,1'-biphenyl]-2-carboxylate (5.3.4-4am) [CAS: 1809272-65-8]: Compound **5.3.4-4am** was prepared following method A1, starting from 2-methylbenzoic acid (138 mg, 1.00 mmol) and 4-iodobenzenediazonium tetrafluoroborate (266 mg, 1.20 mmol). After purification, **5.3.4-4am** was obtained as orange oil (209 mg, 0.82 mmol, 82%).

¹H-NMR (400 MHz, CDCl₃): δ = 7.38–7.30 (m, 2 H), 7.22–7.19 (m, 3 H), 6.99 (td, *J* = 7.4 Hz, 0.9 Hz, 1 H), 6.93 (d, *J* = 8.0 Hz, 1 H), 3.75 (s, 3 H), 3.55 (s, 3 H), 2.44 (s, 3 H) ppm; **¹³C-NMR** (101 MHz, CDCl₃): δ = 169.6, 156.2, 137.3, 135.8, 133.3, 130.5, 130.0, 129.4, 129.3, 128.8, 128.4, 120.4, 110.4, 55.4, 51.4, 20.3 ppm; **IR** (ATR): $\tilde{\nu}$ = 2947, 2835, 1725, 1434, 1262, 1236 cm⁻¹; **MS** (EI, 70 eV), *m/z* (%): 256 (52) [*M*⁺], 225 (100), 224 (23), 210 (30), 209 (42), 181 (27), 163 (21); **elemental analysis**: calcd. (%) for C₁₆H₁₆O₃: C 74.98, H 6.29; found: C 75.01, H 6.29.



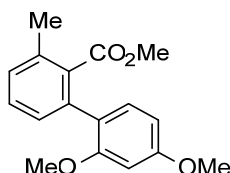
Methyl 3'-bromo-3-methyl-[1,1'-biphenyl]-2-carboxylate (5.3.4-4an) [CAS: 1809272-66-9]: Compound **5.3.4-4an** was prepared following method B, starting from 2-methylbenzoic acid (68.8 mg, 0.50 mmol) and 3-bromobenzenediazonium tetrafluoroborate (135 mg, 0.50 mmol). After purification, **5.3.4-4an** was obtained as brown oil (65 mg, 0.21 mmol, 43%).

¹H-NMR (400 MHz, CDCl₃): δ = 7.52 (t, J = 1.6 Hz, 1 H), 7.45 (dt, J = 7.6 Hz, 1.8 Hz, 1 H), 7.35 (t, J = 7.8 Hz, 1 H), 7.29–7.26 (m, 1 H), 7.25–7.22 (m, 2 H), 7.18 (d, J = 7.6 Hz, 1 H), 3.62 (s, 3 H), 2.39 (s, 3 H) ppm; **¹³C-NMR** (100 MHz, CDCl₃): δ = 169.9, 142.9, 138.5, 135.7, 133.1, 131.3, 130.4, 129.8, 129.7, 129.5, 127.1, 126.9, 122.3, 51.9, 19.7 ppm; **IR** (ATR): $\tilde{\nu}$ = 2970, 2947, 1726, 1457, 1267 cm⁻¹; **MS** (EI, 70 eV), m/z (%): 306 (95), 304 (95) [M⁺], 275 (100), 274 (89), 273 (90), 272 (63), 194 (93); **elemental analysis**: calcd. (%) for C₁₅H₁₃BrO₂: C 59.04, H 4.29; found: C 59.42, H 4.42.



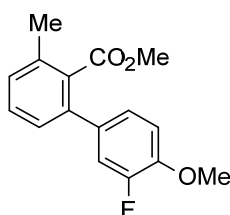
Methyl 2-(9,9-dimethyl-9H-fluoren-2-yl)-6-methylbenzoate (5.3.4-4ao) [CAS: 1809272-67-0]: Compound **5.3.4-4ao** was prepared following method B, starting from 2-methylbenzoic acid (68.8 mg, 0.50 mmol) and 9,9-dimethyl-9H-fluorene-2-diazonium tetrafluoroborate (154 mg, 0.50 mmol). After purification, **5.3.4-4ao** was obtained as colorless oil (140 mg, 0.41 mmol, 82%).

¹H-NMR (400 MHz, CDCl₃): δ = 7.77–7.75 (m, 2 H), 7.47–7.45 (m, 2 H), 7.41–7.31 (m, 5 H), 7.24 (d, J = 7.6 Hz, 1 H), 3.58 (s, 3 H), 2.44 (s, 3 H), 1.52 (s, 6 H) ppm; **¹³C-NMR** (101 MHz, CDCl₃): δ = 170.4, 153.74, 153.68, 140.5, 140.0, 138.8, 138.4, 135.5, 133.2, 129.4, 129.0, 127.3, 127.25, 127.17, 127.0, 122.6, 122.5, 120.1, 120.0, 51.8, 46.8, 27.2, 19.7 ppm; **IR** (ATR): $\tilde{\nu}$ = 2957, 2862, 1724, 1447, 1267 cm⁻¹; **MS** (EI, 70 eV), m/z (%): 343 (24), 342 (100) [M⁺], 327 (27), 311 (12), 296 (22), 295 (100), 252 (13); **elemental analysis**: calcd. (%) for C₂₄H₂₂O₂: C 84.18, H 6.48; found: C 83.81, H 6.51.



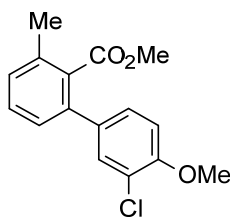
Methyl 2',4'-dimethoxy-3-methyl-[1,1'-biphenyl]-2-carboxylate (5.3.4-4ap) [CAS: 1809272-68-1]: Compound **5.3.4-4ap** was prepared following procedure A1, starting from 2-methylbenzoic acid (138 mg, 1.00 mmol) and 2,4-dimethoxybenzenediazonium tetrafluoroborate (302 mg, 1.20 mmol). After purification, **5.3.4-4ap** was obtained as colorless solid (226 mg, 0.79 mmol, 79%).

¹H-NMR (400 MHz, CDCl₃): δ = 7.33 (t, J = 7.6 Hz, 1 H), 7.20–7.16 (m, 2 H), 7.12 (d, J = 8.0 Hz, 1 H), 6.54–6.50 (m, 2 H), 3.84 (s, 3 H), 3.73 (s, 3 H), 3.59 (s, 3 H), 2.43 (s, 3 H) ppm; **¹³C-NMR** (100 MHz, CDCl₃): δ = 169.8, 160.4, 157.2, 137.0, 135.6, 133.5, 130.9, 129.2, 129.0, 128.6, 122.7, 104.0, 98.4, 55.34, 55.29, 51.4, 20.2 ppm; **IR** (ATR): $\tilde{\nu}$ = 3007, 2970, 1722, 1366, 1210 cm⁻¹; **MS** (EI, 70 eV), m/z (%): 287 (18), 286 (100) [M⁺], 255 (41), 254 (32), 240 (15), 239 (14), 197 (8); **elemental analysis**: calcd. (%) for C₁₇H₁₈O₄: C, 71.31; H, 6.34; found: C, 71.10; H, 6.39; **m.p.**: 73–74 °C.



Methyl 3'-fluoro-4'-methoxy-3-methyl-[1,1'-biphenyl]-2-carboxylate (5.3.4-4aq) [CAS: 1809272-69-2]: Compound **5.3.4-4aq** was prepared following method A, starting from 2-methylbenzoic acid (138 mg, 1.00 mmol) and 3-fluoro-4-methoxybenzenediazonium tetrafluoroborate (240 mg, 1.00 mmol). After purification, **5.3.4-4aq** was obtained as colorless solid (230 mg, 0.84 mmol, 84%).

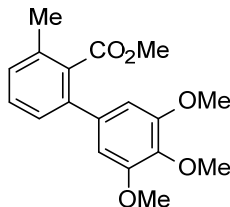
¹H-NMR (400 MHz, CDCl₃): δ = 7.32 (t, J = 7.6 Hz, 1 H), 7.19 (d, J = 7.6 Hz, 1 H), 7.17–7.11 (m, 2 H), 7.09–7.07 (m, 1 H), 6.97 (t, J = 8.6 Hz, 1 H), 3.89 (s, 3 H), 3.66 (s, 3 H), 2.38 (s, 3 H) ppm; **¹³C-NMR** (100 MHz, CDCl₃): δ = 170.0, 151.8 (d, J_{C-F} = 244.1 Hz), 146.9 (d, J_{C-F} = 10.7 Hz), 138.3 (d, J_{C-F} = 1.8 Hz), 135.3, 133.7 (d, J_{C-F} = 7.3 Hz), 133.0, 129.3, 129.0, 126.9, 123.9 (d, J_{C-F} = 3.6 Hz), 115.9 (d, J_{C-F} = 19.1 Hz), 112.9 (d, J_{C-F} = 1.8 Hz), 55.9, 51.7, 19.5 ppm; **IR** (ATR): $\tilde{\nu}$ = 3007, 2970, 1722, 1515, 1270 cm⁻¹; **MS** (EI, 70 eV), m/z (%): 275 (17), 274 (100) [M⁺], 244 (14), 243 (96), 242 (60), 227 (17), 200 (15); **elemental analysis**: calcd. (%) for C₁₆H₁₅FO₃: C, 70.06; H, 5.51; found: C, 69.98; H, 5.54; **m.p.**: 109–110 °C.



Methyl 3'-chloro-4'-methoxy-3-methyl-[1,1'-biphenyl]-2-carboxylate (**5.3.4-4ar**)

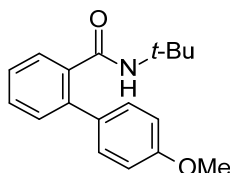
[CAS: 1809272-70-5]: Compound **5.3.4-4ar** was prepared following method B, starting from 2-methylbenzoic acid (68.8 mg, 0.50 mmol) and 3-chloro-4-methoxybenzenediazonium tetrafluoroborate (128 mg, 0.50 mmol). After purification, **5.3.4-4ar** was obtained as colorless solid (116 mg, 0.40 mmol, 80%).

¹H-NMR (400 MHz, CDCl₃): δ = 7.41 (d, J = 2.4 Hz, 1 H), 7.33 (t, J = 7.8 Hz, 1 H), 7.24–7.16 (m, 3 H), 6.94 (d, J = 8.4 Hz, 1 H), 3.92 (s, 3 H), 3.66 (s, 3 H), 2.38 (s, 3 H) ppm.; **¹³C-NMR** (101 MHz, CDCl₃): δ = 170.1, 154.3, 138.2, 135.4, 134.0, 133.1, 129.9, 129.4, 129.1, 127.5, 127.0, 122.2, 111.7, 56.0, 51.9, 19.6 ppm; **IR** (ATR): $\tilde{\nu}$ = 3005, 2970, 2948, 1724, 1439, 1366, 1229 cm⁻¹; **MS** (EI, 70 eV), m/z (%): 292 (32), 290 (100) [M⁺], 261 (18), 259 (54), 258 (19), 224 (60), 223 (64); **elemental analysis**: calcd. (%) for C₁₆H₁₅ClO₃: C 66.10, H 5.20; found: C 65.92, H 5.08; **m.p.**: 109–110 °C.



Methyl 3',4',5'-trimethoxy-3-methyl-[1,1'-biphenyl]-2-carboxylate (**5.3.4-4as**) [CAS: 1809272-71-6]: Compound **5.3.4-4as** was prepared following method A, starting from 2-methylbenzoic acid (138 mg, 1.00 mmol) and 3,4,5-trimethoxybenzenediazonium tetrafluoroborate (282 mg, 1.00 mmol). After purification, **5.3.4-4as** was obtained as yellow oil (263 mg, 0.83 mmol, 83%).

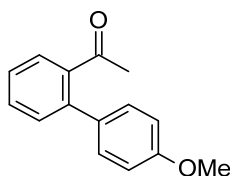
¹H-NMR (400 MHz, CDCl₃): δ = 7.29 (t, J = 7.6 Hz, 1 H), 7.19 (dd, J = 13.2 Hz, 7.2 Hz, 2 H), 6.57 (s, 2 H), 3.84 (s, 3 H), 3.81 (s, 6 H), 3.61 (s, 3 H), 2.35 (s, 3 H) ppm; **¹³C-NMR** (101 MHz, CDCl₃): δ = 170.2, 152.88, 139.6, 137.0, 136.2, 135.1, 132.9, 129.2, 128.9, 126.7, 105.2, 60.6, 55.8, 51.8, 19.3 ppm; **IR** (ATR): $\tilde{\nu}$ = 2942, 2836, 1724, 1577, 1240, 1120 cm⁻¹; **MS** (EI, 70 eV), m/z (%): 317 (17), 316 (87) [M⁺], 302 (18), 301 (100), 285 (7), 273 (14), 209 (9); **HRMS** (EI-TOF), m/z : [M⁺] calcd. for C₁₈H₂₀O₅: 316.1311; found, 316.1285.



N-(*tert*-butyl)-4'-methoxy-[1,1'-biphenyl]-2-carboxamide (**5.3.2-3aa** and **5.3.4-5aa**) [CAS: 1809272-53-4]: The screening reactions in 5.3.2 were performed following the procedure described in section 7.5.2.

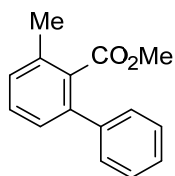
Compound **5.3.4-5aa** was prepared following method A without esterification, starting from *N*-*tert*-butylbenzamide (88.6 mg, 0.5 mmol) and 4-methoxybenzenediazonium tetrafluoroborate (111 mg, 0.5 mmol). After purification, **5.3.4-5aa** was obtained as colorless solid (83.5 mg, 0.295 mmol, 59%).

¹H-NMR (400 MHz, CDCl₃): δ = 7.69 (dd, J = 7.6 Hz, 1.2 Hz, 1 H), 7.42 (td, J = 7.6 Hz, 1.6 Hz, 1 H), 7.37 (dd, J = 7.6 Hz, 1.2 Hz, 1 H), 7.36–7.33 (m, 2 H), 7.30 (dd, J = 7.6 Hz, 1.2 Hz, 1 H), 6.98–6.94 (m, 2 H), 5.07 (s, 1 H), 3.85 (s, 3 H), 1.15 (s, 9 H) ppm; **¹³C-NMR** (101 MHz, CDCl₃): δ = 168.5, 159.3, 138.9, 136.7, 132.7, 130.1, 130.0, 129.7, 128.8, 127.2, 113.9, 55.4, 51.3, 28.2 ppm; **IR** (ATR): $\tilde{\nu}$ = 3295, 2976, 2935, 2837, 1630, 1518, 1476, 1441, 1241, 1176 cm⁻¹; **MS** (EI, 70 eV), m/z (%): 282 (24), 283 (100) [M⁺], 268 (10), 226 (40), 212 (12), 211 (68), 168 (10); **elemental analysis**: calcd. (%) for C₁₈H₂₁NO₂: C 76.30, H 7.47, N 4.94; found: C 76.24, H 7.46, N 4.77; **m.p.**: 134–135 °C.



1-(4'-Methoxy-[1,1'-biphenyl]-2-yl)ethanone (**5.3.4-5ba**) [CAS: 192863-43-7]: Compound **5.3.4-5ba** was prepared following method A without esterification, starting from acetophenone (60.7 mg, 0.5 mmol) and 4-methoxybenzenediazonium tetrafluoroborate (111 mg, 0.5 mmol). After purification, **5.3.4-5ba** was obtained as yellow oil (40.7 mg, 0.09 mmol, 18%).

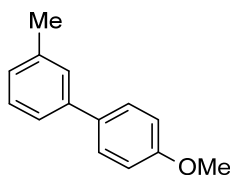
¹H-NMR (400 MHz, CDCl₃): δ = 7.45–7.39 (m, 2 H), 7.32–7.28 (m, 2 H), 7.20–7.17 (m, 2 H), 6.91–6.86 (m, 2 H), 3.77 (s, 3 H), 1.93 (s, 3 H) ppm; **¹³C-NMR** (101 MHz, CDCl₃): δ = 205.3, 159.5, 140.8, 140.1, 132.9, 130.6, 130.1, 129.9, 127.7, 127.0, 114.1, 55.3, 30.4 ppm; **IR** (ATR): $\tilde{\nu}$ = 3036, 2956, 2836, 1683, 1609, 1515, 1474, 1440, 1244 cm⁻¹; **MS** (EI, 70 eV), m/z (%): 227 (57), 226 (100) [M⁺], 225 (15), 212 (10), 211 (66), 168 (16), 139 (12); **elemental analysis**: calcd. (%) for C₁₅H₁₄O₂: C 79.62, H 6.24; found: C 79.58, H 6.50; **HRMS** (EI-TOF), m/z : [M⁺] calcd for C₁₅H₁₄O₂, 226.0994; found: 226.1000.



Methyl 3-methylbiphenyl-2-carboxylate (**5.3.4-6aa**) [CAS: 1261902-83-3]: Compound **5.3.4-6aa** was prepared following method A, starting from 2-methylbenzoic acid (68.8 mg, 0.5 mmol) and diphenyliodonium triflate (215 mg, 0.5 mmol). After purification, **5.3.4-6aa** was obtained as colorless oil (94.7 mg, 0.42 mmol, 84%).

¹H-NMR (400 MHz, CDCl₃): δ = 7.36–7.32 (m, 4 H), 7.30–7.27 (m, 2 H), 7.18–7.15 (m, 2 H), 3.53 (s, 3 H), 2.36 (s, 3 H) ppm; **¹³C-NMR** (101 MHz, CDCl₃): δ = 170.2, 140.8, 140.1, 135.3, 133.1, 129.3, 129.0, 128.2, 128.1, 127.3, 127.1, 51.7, 19.6 ppm; **IR** (ATR): $\tilde{\nu}$ = 2948, 1725, 1462, 1435, 1265 cm⁻¹; **MS** (EI, 70 eV), m/z (%): 227 (41), 226 (100) [M⁺], 196 (11), 195 (72), 194 (39), 167 (10), 165 (16); **HRMS** (EI-TOF), m/z : [M⁺] calcd. for C₁₅H₁₄O₂: 226.0994; found: 226.0993.

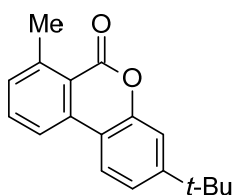
7.5.5 Procedure for the one-pot ortho-C–H arylation and protodecarboxylation



4'-Methoxy-3-methylbiphenyl (**5.3.4-7aa**) [CAS: 17171-17-4]: An oven-dried 20 mL vessel was charged with [IrCp*Cl₂]₂ (6.0 mg, 7.5 μ mol, 3 mol%), Ag₂CO₃ (10.3 mg, 37.5 μ mol, 15 mol%), Li₂CO₃ (9.2 mg, 125 μ mol, 50 mol%), 2-methylbenzoic acid (34.4 mg, 0.25 mmol) **5.3.4-1a** and 4-methoxybenzenediazonium tetrafluoroborate **5.3.4-2a** (66.6 mg, 0.3 mmol). After the vessel was flushed with 3 alternating vacuum and nitrogen purge cycles, degassed acetone (0.5 mL) was added *via* syringe. The resulting mixture was stirred at 60 °C for 24 h. After the reaction was complete, the acetone was removed under reduces pressure. Cu₂O (36.1 mg, 0.25 mmol), 1,10-phenanthroline (91.0 mg, 0.5 mmol) and NMP (1 mL) were added and the mixture was stirred at 190 °C for 12 h. The mixture was allowed to cool to RT, brine (20 mL) was added and the resulting mixture was extracted with ethyl acetate (3 \times 20 mL). The combined organic layers were dried over MgSO₄, filtered, and the volatiles were removed under reduced pressure. The residue was purified by column chromatography (SiO₂, ethyl acetate/hexane gradient) yielding the corresponding biaryl **5.3.4-7aa** as a colorless oil (41.2 mg, 0.21 mmol, 83%).

¹H-NMR (400 MHz, CDCl₃): δ = 7.56 (d, J = 8.0 Hz, 2 H), 7.40 (d, J = 9.6 Hz, 2 H), 7.34 (t, J = 7.2 Hz, 1 H), 7.16 (d, J = 7.2 Hz, 1 H), 7.02–7.00 (m, 2 H), 3.88 (s, 3 H), 2.45 (s, 3 H) ppm; **¹³C-NMR** (101 MHz, CDCl₃): δ = 159.0, 140.8, 138.2, 133.8, 128.6, 128.1, 127.5, 127.4, 123.8, 114.1, 55.3, 21.5 ppm; **IR** (ATR): $\tilde{\nu}$ = 3032, 2954, 2910, 2838, 1602, 1514, 1483, 1439, 1286, 1249 cm⁻¹; **MS** (EI, 70 eV), m/z (%): 199 (16), 198 (100) [M⁺], 184 (8), 183 (57), 155 (35), 153 (8); the analytical data matched those reported in the literature.^[277]

7.5.6 Procedure for the one-pot ortho-C–H arylation and cyclization



3-tert-Butyl-7-methyl-6H-benzo[c]chromen-6-one (5.3.4-7ab) [CAS: 1809272-72-7]: An oven-dried 20 mL vessel was charged with [IrCp*Cl₂]₂ (12.0 mg, 15 μ mol, 3 mol%), Ag₂CO₃ (41.4 mg, 0.15 mmol, 30 mol%), AgOTf (25.7 mg, 0.1 mmol, 20 mol%), Li₂CO₃ (11.1 mg, 0.15 mmol, 30 mol%), 2-methylbenzoic acid (68.8 mg, 0.5 mmol) **5.3.4-1a** and 4-(tert-butyl)benzenediazonium tetrafluoroborate **5.3.4-2e** (124 mg, 0.5 mmol). After the vessel was flushed with 3 alternating vacuum and nitrogen purge cycles, degassed acetone (1 mL) was added *via* syringe. The resulting mixture was stirred at 60 °C for 24 h. After the reaction was complete, the acetone was removed under reduces pressure. K₂S₂O₃ (410 mg, 1.5 mmol) and AgNO₃ (8.5 mg, 50 μ mol, 10 mol%) were added. A mixture of MeCN/H₂O (4 mL, 1:1) was added and the reaction was stirred at 50 °C for 18 h.^[278] The mixture was allowed to cool to RT, brine (20 mL) was added and the resulting mixture was extracted with ethyl acetate (3 \times 20 mL). The combined organic layers were dried over MgSO₄, filtered, and the volatiles were removed under reduced pressure. The residue was purified by column chromatography (SiO₂, ethyl acetate/hexane gradient) yielding **5.3.4-7ab** as a colorless oil (81 mg, 0.31 mmol, 61%).

¹H-NMR (400 MHz, CDCl₃): δ = 7.90–7.87 (m, 2 H), 7.58 (d, J = 7.6 Hz, 1 H), 7.32–7.28 (m, 3 H), 2.83 (s, 3 H), 1.36 (s, 9 H) ppm; **¹³C-NMR** (101 MHz, CDCl₃): δ = 160.7, 154.4, 151.2, 144.2, 136.2, 133.8, 131.7, 122.6, 121.6, 119.5, 119.4, 115.6, 114.0, 35.0, 31.1, 23.9 ppm; **IR** (ATR): $\tilde{\nu}$ = 2947, 2860, 1722, 1599, 1467, 1048 cm⁻¹; **MS** (EI, 70 eV), m/z (%): 267 (8), 266 (24) [M⁺], 252 (17), 251 (100), 223 (17); **HRMS** (EI-TOF), m/z : [M⁺] calcd. for C₁₈H₁₈O₂: 266.1306; found: 266.1302.

7.5.7 Control experiments

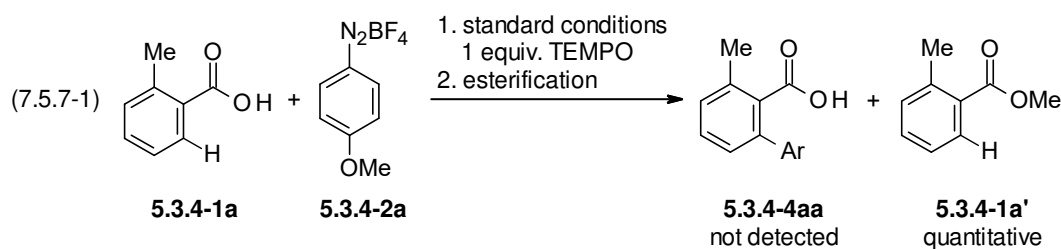
Control experiments showed that aryl halides, triflates, and tosylates are inactive as carbon electrophiles under the optimized conditions. However, diaryliodonium salts can alternatively be used as electrophiles (*Tabelle 38*).

Tabelle 38: Screening of aryl electrophiles for the Ir-catalyzed ortho-arylation.

5.3.4-1a	5.3.4-2	5.3.4-3
Entry	Aryl electrophile	5.3.4-4aa (%)
1	5.3.4-2 = ClPh, BrPh, or IPh	n.d.
2	5.3.4-2 = TfOPh or TsOPh	n.d.
3	5.3.4-2 = TfOIPh ₂	86

Reaction conditions: 5.3.4-1a (0.5 mmol), 5.3.4-2 (0.5 mmol), [IrCp*Cl₂]₂ (3 mol%), Ag₂CO₃ (3 mol%), Li₂CO₃ (50 mol%), acetone (1 mL), 60 °C, 24 h. Isolated yield after esterification with K₂CO₃ and MeI is given.

The presence of the radical scavenger TEMPO shuts down the reaction, which suggests that single-electron-transfer processes may be involved (Eq. 7.5.7-1).



7.6 *ortho*-C–H Arylation of Benzoic Acids with Aryl Bromides and Chlorides Catalyzed by Ruthenium

7.6.1 General remarks

The NMP used in the following reaction was not degassed prior to its use.

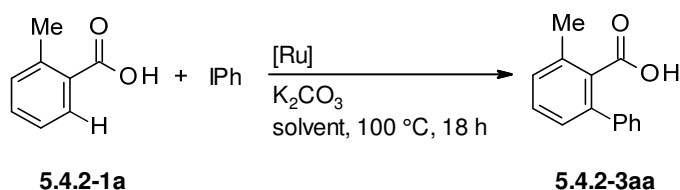
7.6.2 Optimization of the Ru-catalyzed *ortho*-arylation

General method:

An oven-dried 20 mL vessel was charged with the solid reagents. After the vessel was flushed with 3 alternating vacuum and nitrogen purge cycles, the solvent and the liquid reagents

were added *via* syringe and the resulting mixture was stirred at the given temperature for 16 h. The reaction mixture was allowed to cool to RT and *n*-tetradecane (50 μ L) was added *via* syringe. K₂CO₃ (138 mg, 2 equiv.), MeI (156 μ L, 5 equiv.) and NMP (2 mL) were added and the mixture was stirred at 60 °C for 2 h. The mixture was allowed to cool to RT and ethyl acetate (2 mL) was added. A sample of the reaction mixture (0.5 mL) was dissolved in ethyl acetate (2 mL), washed with water (2 mL), dried over MgSO₄, and analyzed by GC.

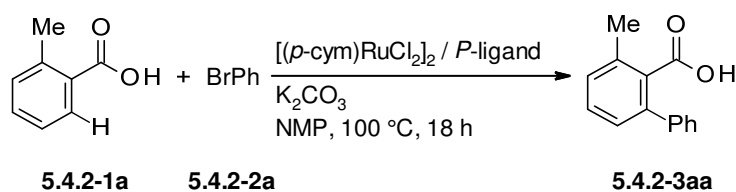
Tabelle 39: Ru-Catalyzed ortho-arylation with iodobenzene.



Entry	[Ru]	solvent	5.4.2-3aa (%)
1	[Ru(MeCN) ₆ (OTf) ₂]	Tol	n.d.
2	"	Dioxane	trace
3	"	<i>t</i> -AmylOH	5
4	"	NMP	12
5	[Ru(<i>p</i> -cym)Cl ₂] ₂	"	25
6	[Ru(<i>p</i> -cym)I ₂] ₂	"	15
7	[Ru(C ₆ H ₆)Cl ₂] ₂	"	16
8	[Ru(C ₆ Me ₆)Cl ₂] ₂	"	trace
9	(COD)RuCl ₂	"	8
10	(COD)RuCp*Cl	"	trace
11	RuCl ₃ × 3 H ₂ O	"	20
12	RuCl ₂ (PPh ₃) ₃	"	trace
13 ^[a]	[Ru(<i>p</i> -cym)Cl ₂] ₂	"	34

Reaction conditions: **5.4.2-1a** (0.5 mmol), IPh (0.5 mmol), [Ru] (8 mol%), K₂CO₃ (1 equiv.), solvent (3 mL), 100 °C, 18 h. Yields were determined by GC analysis after esterification with K₂CO₃ (2 equiv.) and MeI (5 equiv.) in NMP at 60 °C for 2 h with *n*-tetradecane as an internal standard. [a] IPh (2.0 mmol).

Tabelle 40: Supplementary ligand screening.



Entry	BrPh (equiv.)	P-ligand	5.4.2-3aa (%)
1	4	-	13
2	"	PPh ₃	35
3	"	P(o-Tol) ₃	trace
4	"	P(Mes) ₃	trace
5	"	XPhos	n.d.
6	"	P(Ad) ₃ Ph	n.d.
7	"	Pt-Bu ₃	trace
8	"	PCy ₃	76
9	2	"	73
10	1	"	20
11	"	PEt ₂ Ph	65
12	"	POct ₃	78
13	"	Pi-Pr ₃	43
14	"	PMe ₃	3
15	"	PMe ₃ × HBF ₄	73
16	"	PEt ₃ × HBF ₄	93

Reaction conditions: **5.4.2-1a** (0.5 mmol), **5.4.2-2a**, [Ru(*p*-cym)Cl₂]₂ (4 mol%), *P*-ligand (8 mol%), K₂CO₃ (1.1 equiv.), NMP (3 mL), 100 °C, 18 h. Yields were determined by GC analysis after esterification with K₂CO₃ (2 equiv.) and MeI (5 equiv.) in NMP at 60 °C for 2 h with *n*-tetradecane as an internal standard.

7.6.3 General procedure for the Ru-catalyzed ortho-arylation

Method A – coupling of aryl bromides:

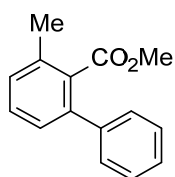
An oven-dried 20 mL vessel was charged with [Ru(*p*-cym)Cl₂]₂ (12.2 mg, 0.02 mmol, 4 mol%), triethylphosphonium tetrafluoroborate (8.3 mg, 0.04 mmol, 8 mol%), K₂CO₃ (76 mg, 0.55 mmol, 1.1 equiv.), and the benzoic acid **5.4.2-1** (0.50 mmol). After the vessel was flushed with 3 alternating vacuum and nitrogen purge cycles, NMP (3 mL) and the aryl bromide **5.4.2-2**

(0.50 mmol) were added *via* syringe. The resulting mixture was stirred at 100 °C for 18 h. After the reaction was complete, the mixture was allowed to cool to RT. NMP (2 mL), K₂CO₃ (207 mg, 3 equiv.) and MeI (156 µL, 5 equiv.) were added and the mixture was stirred at 60 °C for 2 h. The mixture was allowed to cool to RT, ethyl acetate (20 mL) was added and the resulting mixture was washed with water, aqueous LiCl solution (20%) and brine (20 mL each). The organic layer was dried over MgSO₄, filtered, and the volatiles were removed under reduced pressure. The residue was purified by column chromatography (SiO₂, ethyl acetate/cyclohexane gradient) yielding the corresponding biaryl.

Method B – coupling of aryl chlorides:

An oven-dried 20 mL vessel was charged with [Ru(*p*-cym)Cl₂]₂ (12.2 mg, 0.02 mmol, 4 mol%), DL-pipecolinic acid (5.17 mg, 0.04 mmol, 8 mol%), K₂CO₃ (76 mg, 0.55 mmol, 1.1 equiv.), and the corresponding carboxylic acid **5.4.2-1** (0.50 mmol, 1 equiv.). After the vessel was flushed with 3 alternating vacuum and nitrogen purge cycles, NMP (3 mL) and the corresponding aryl chloride **5.4.2-2'** (2.00 mmol, 4 equiv.) were added *via* syringe. The resulting mixture was stirred at 120 °C for 18 h. After the reaction was complete, the mixture was allowed to cool to RT. NMP (2 mL), K₂CO₃ (207 mg, 3 equiv.) and MeI (156 µL, 5 equiv.) were added and the mixture was stirred at 60 °C for 2 h. The mixture was allowed to cool to RT, ethyl acetate (20 mL) was added and the resulting mixture was washed with water, aqueous LiCl solution (20%) and brine (20 mL each). The organic layer was dried over MgSO₄, filtered, and the volatiles were removed under reduced pressure. The residue was purified by column chromatography (SiO₂, ethyl acetate/cyclohexane gradient) yielding the corresponding biaryl.

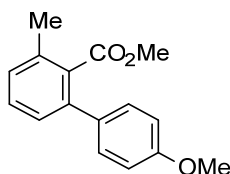
7.6.4 Synthesis and characterization of the corresponding products



Methyl 3-methylbiphenyl-2-carboxylate (**5.4.2-3aa**) [CAS: 941320-77-0]: Compound **5.4.2-3aa** was prepared following the general method A from 2-methylbenzoic acid (**5.4.2-1a**) (68.8 mg, 0.50 mmol) and bromobenzene (**5.4.2-2a**) (79.3 mg, 53.2 µL, 0.50 mmol). **5.4.2-3aa** was isolated as colorless oil (105 mg, 93%).

Compound **5.4.2-3aa** was prepared following the general method B from 2-methylbenzoic acid (**5.4.2-1a**) (68.8 mg, 0.50 mmol) and chlorobenzene (**5.4.2-2a'**) (227 mg, 205 µL, 2.00 mmol). **5.4.2-3aa** was isolated as colorless oil (85 mg, 75%).

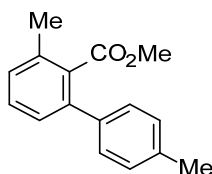
¹H-NMR (400 MHz, CDCl₃): δ = 7.30–7.45 (m, 6 H), 7.24 (d, J = 7.5 Hz, 2 H), 3.60 (s, 3 H), 2.42 (s, 3 H) ppm; **¹³C-NMR** (101 MHz, CDCl₃): δ = 170.3, 140.9, 140.2, 135.5, 133.2, 129.5, 129.1, 128.3, 128.2, 127.4, 127.3, 51.9, 19.7 ppm; **IR** (ATR): $\tilde{\nu}$ = 3062, 2950, 1726, 1463, 1436, 1267, 1122, 1066 cm⁻¹; **MS** (EI, 70 eV), m/z (%): 226 (100) [M⁺], 195 (90), 165 (22); the analytical data matched those reported earlier in this document.



Methyl 4'-methoxy-3-methylbiphenyl-2-carboxylate (**5.4.2-3ab**) [CAS: 1097018-19-3]: Compound **5.4.2-3ab** was prepared following the general method A from 2-methylbenzoic acid (**5.4.2-1a**) (68.8 mg, 0.50 mmol) and 4-bromoanisole (**5.4.2-2b**) (93.5 mg, 62.8 μ L, 0.50 mmol). **5.4.2-3ab** was isolated as colorless solid (105 mg, 82%).

Compound **5.4.2-3ab** was prepared following the general method B from 2-methylbenzoic acid (**5.4.2-1a**) (68.8 mg, 0.50 mmol) and 4-chloroanisole (**5.4.2-2b'**) (291 mg, 251 μ L, 2.00 mmol). **5.4.2-3ab** was isolated as colorless solid (92 mg, 72%).

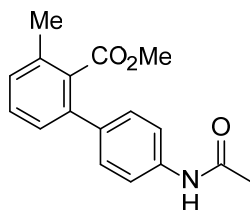
¹H-NMR (400 MHz, CDCl₃): δ = 7.28–7.37 (m, 3 H), 7.17–7.23 (m, 2 H), 6.91–6.97 (m, 2 H), 3.85 (s, 3 H), 3.64 (s, 3 H), 2.40 (s, 3 H) ppm; **¹³C-NMR** (101 MHz, CDCl₃): δ = 170.5, 159.0, 139.6, 135.3, 133.3, 133.1, 129.3, 129.3, 128.7, 127.2, 113.7, 55.2, 51.9, 19.7 ppm; **IR** (ATR): $\tilde{\nu}$ = 2946, 2839, 1726, 1609, 1512, 1440, 1247, 1183 cm⁻¹; **MS** (EI, 70 eV), m/z (%): 256 (100) [M⁺], 225 (62), 209 (15), 181 (9), 153 (8); **HRMS** (EI-TOF), m/z : [M⁺] calcd. for C₁₆H₁₆O₃: 256.1099; found: 256.1091; **m.p.**: 69–70 °C; the analytical data matched those reported earlier in this document.



Methyl 3,4'-dimethylbiphenyl-2-carboxylate (**5.4.2-3ac**) [CAS: 1097018-21-7]: Compound **5.4.2-3ac** was prepared following the general method B from 2-methylbenzoic acid (**5.4.2-1a**) (68.8 mg, 0.50 mmol) and 4-chlorotoluene (**5.4.2-2c'**) (258 mg, 241 μ L, 2.00 mmol). **5.4.2-3ac** was isolated as colorless oil (66 mg, 55%).

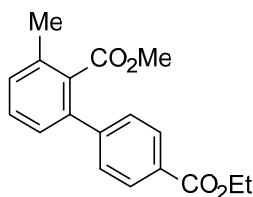
¹H-NMR (400 MHz, CDCl₃): δ = 7.32–7.38 (m, 1 H), 7.25–7.29 (m, 2 H), 7.18–7.24 (m, 4 H), 3.63 (s, 3 H), 2.40 (s, 3 H), 2.39 (s, 3 H) ppm; **¹³C-NMR** (101 MHz, CDCl₃): δ = 170.5, 140.0, 137.9, 137.0, 135.3, 133.1, 129.4, 129.0, 128.9, 128.0, 127.2, 51.8, 21.2, 19.7 ppm; **IR** (ATR):

$\tilde{\nu}$ = 2949, 1725, 1265, 1122, 1088, 1067, 783 cm^{-1} ; **MS** (EI, 70 eV), m/z (%): 240 (100) [M^+], 209 (55), 165 (17); the analytical data matched those reported earlier in this document.



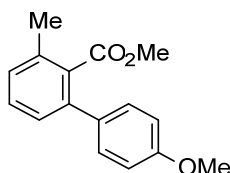
Methyl 4'-(acetamino)-3-methylbiphenyl-2-carboxylate (**5.4.2-3ad**) [CAS: 1809272-64-7]: Compound **5.4.2-3ad** was prepared following the general method A from 2-methylbenzoic acid (**5.4.2-1a**) (68.8 mg, 0.50 mmol) and *N*-(4-bromophenyl)acetamide (**5.4.2-2d**) (109 mg, 0.50 mmol). **5.4.2-3ad** was isolated as colorless solid (131 mg, 93%).

$^1\text{H-NMR}$ (400 MHz, CDCl_3): δ = 7.52 (d, J = 8.5 Hz, 2 H), 7.29–7.40 (m, 4 H), 7.18–7.24 (m, 2 H), 3.64 (s, 3 H), 2.40 (s, 3 H), 2.17 (s, 3 H) ppm; **$^{13}\text{C-NMR}$** (101 MHz, CDCl_3): δ = 170.5, 168.3, 139.4, 137.3, 136.7, 135.4, 133.1, 129.5, 129.0, 128.8, 127.2, 119.4, 51.9, 24.6, 19.7 ppm; **IR** (ATR): $\tilde{\nu}$ = 3322, 3275, 1679, 1532, 1456, 1320, 1288, 1257 cm^{-1} ; **MS** (EI, 70 eV), m/z (%): 283 (100) [M^+], 252 (11), 241 (43), 235 (12), 209 (50); **m.p.**: 189–190 $^{\circ}\text{C}$; the analytical data matched those reported earlier in this document.



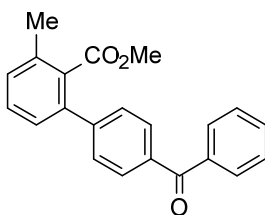
4'-Ethyl 2-methyl 3-methylbiphenyl-2,4'-dicarboxylate (**5.4.2-3ae**): Compound **5.4.2-3ae** was prepared following the general method A from 2-methylbenzoic acid (**5.4.2-1a**) (68.8 mg, 0.50 mmol) and ethyl 4-bromobenzoate (**5.4.2-2e**) (116 mg, 82.6 μL , 0.50 mmol). **5.4.2-3ae** was isolated as colorless oil (124 mg, 83%).

$^1\text{H-NMR}$ (400 MHz, CDCl_3): δ = 8.08 (s, 2 H), 7.42–7.46 (m, 2 H), 7.36–7.41 (m, 1 H), 7.21–7.29 (m, 2 H), 4.41 (q, J = 7.0 Hz, 2 H), 3.59 (s, 3 H), 2.42 (s, 3 H), 1.42 (t, J = 7.2 Hz, 3 H) ppm; **$^{13}\text{C-NMR}$** (101 MHz, CDCl_3): δ = 169.9, 166.4, 145.5, 139.2, 135.8, 133.0, 129.8, 129.6 (s, 2 C) 129.4, 128.2, 127.1, 61.0, 51.9, 19.7, 14.3 ppm; **IR** (ATR): $\tilde{\nu}$ = 2982, 2951, 1714, 1461, 1438, 1269, 1180, 1103 cm^{-1} ; **MS** (EI, 70 eV), m/z (%): 298 (100) [M^+], 266 (14), 253 (41), 239 (11), 195 (29), 165 (11); **HRMS** (EI-TOF), m/z : [M^+] calcd. for $\text{C}_{18}\text{H}_{18}\text{O}_4$: 298.1205; found: 298.1203.



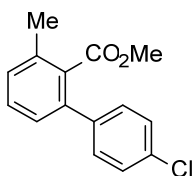
Methyl 4'-methoxy-3-methylbiphenyl-2-carboxylate (**5.4.2-3af**) [CAS: 1097018-19-3]: Compound **5.4.2-3af** was prepared following the general method A from 2-methylbenzoic acid (**5.4.2-1a**) (68.8 mg, 0.50 mmol) and 4-bromophenol (**5.4.2-2f**) (87.4 mg, 0.5 mmol). **5.4.2-3af** was isolated as yellow oil (67 mg, 52%).

¹H-NMR (400 MHz, CDCl₃): δ = 7.28–7.37 (m, 3 H), 7.17–7.23 (m, 2 H), 6.92–6.96 (m, 2 H), 3.85 (s, 3 H), 3.64 (s, 3 H), 2.40 (s, 3 H) ppm; **¹³C-NMR** (101 MHz, CDCl₃): δ = 170.5, 159.0, 139.6, 135.3, 133.3, 133.1, 129.3, 129.3, 128.7, 127.2, 113.7, 55.2, 51.8, 19.6 ppm; **IR** (ATR): $\tilde{\nu}$ = 2946, 2839, 1726, 1609, 1512, 1440, 1247, 1183 cm⁻¹; **MS** (EI, 70 eV), m/z (%): 256 (100) [M⁺], 225 (62), 209 (15), 181 (9), 153 (8); **m.p.**: 69–70 °C; the analytical data matched those reported earlier in this document.



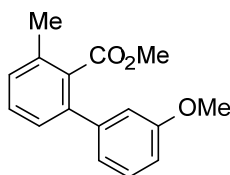
Methyl 4'-benzoyl-3-methylbiphenyl-2-carboxylate (**5.4.2-3ag**): Compound **5.4.2-3ag** was prepared following the general method A from 2-methylbenzoic acid (**5.4.2-1a**) (68.8 mg, 0.50 mmol) and (4-bromophenyl)(phenyl)methanone (**5.4.2-2g**) (135 mg, 0.50 mmol). **5.4.2-3ag** was isolated as colorless solid (134 mg, 81%).

¹H-NMR (400 MHz, CDCl₃): δ = 7.80–7.90 (m, 4 H), 7.58–7.65 (m, 1 H), 7.47–7.55 (m, 4 H), 7.41 (t, J = 7.7 Hz, 1 H), 7.24–7.31 (m, 2 H), 3.63 (s, 3 H), 2.43 (s, 3 H) ppm; **¹³C-NMR** (101 MHz, CDCl₃): δ = 196.4, 170.0, 145.2, 139.1, 137.6, 136.4, 135.9, 133.0, 132.5, 130.3, 130.0, 129.9, 129.7, 128.4, 128.2, 127.2, 52.0, 19.8 ppm; **IR** (ATR): $\tilde{\nu}$ = 3066, 2949, 1721, 1655, 1599, 1400, 1315, 1124 cm⁻¹; **MS** (EI, 70 eV), m/z (%): 330 (100) [M⁺], 315 (54), 299 (22), 253 (66), 195 (8), 165 (13), 105 (60); **HRMS** (EI-TOF), m/z : [M⁺] calcd. for C₂₂H₁₈O₃: 330.1256; found: 330.1259; **m.p.**: 83–84 °C.



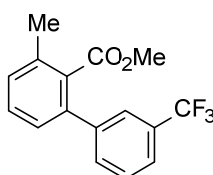
Methyl 4'-chloro-3-methylbiphenyl-2-carboxylate (**5.4.2-3ah**) [CAS: 1809272-61-4]: Compound **5.4.2-3ah** was prepared following the general method A from 2-methylbenzoic acid (**5.4.2-1a**) (68.8 mg, 0.50 mmol) and 4-chlorobromobenzene (**5.4.2-2h**) (95.7 mg, 58 μ L, 0.50 mmol). **5.4.2-3ah** was isolated as colorless oil (80 mg, 61%).

¹H-NMR (400 MHz, CDCl₃): δ = 7.34–7.40 (m, 3 H), 7.28–7.33 (m, 2 H), 7.22–7.26 (m, 1 H), 7.16–7.21 (m, 1 H), 3.63 (s, 3 H), 2.41 (s, 3 H) ppm; **¹³C-NMR** (101 MHz, CDCl₃): δ = 170.0, 139.3, 138.8, 135.6, 133.5, 133.1, 129.5, 129.5, 129.4, 128.5, 127.1, 51.9, 19.7 ppm; **IR** (ATR): $\tilde{\nu}$ = 2948, 1725, 1494, 1459, 1395, 1265, 1121, 835 cm⁻¹; **MS** (EI, 70 eV), m/z (%): 260 (88) [M⁺], 229 (100), 193 (22), 165 (20); the analytical data matched those reported earlier in this document.



Methyl 3'-methoxy-3-methylbiphenyl-2-carboxylate (**5.4.2-3ai**): Compound **5.4.2-3ai** was prepared following the general method A from 2-methylbenzoic acid (**5.4.2-1a**) (68.8 mg, 0.50 mmol) and 3-bromoanisole (**5.4.2-2i**) (95.4 mg, 64.5 μ L, 0.50 mmol). **5.4.2-3ai** was isolated as colorless solid (111 mg, 87%).

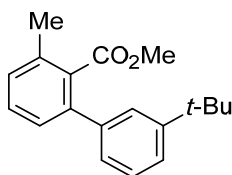
¹H-NMR (400 MHz, CDCl₃): δ = 7.36 (t, J = 7.8 Hz, 1 H), 7.28–7.33 (m, 1 H), 7.21–7.26 (m, 2 H), 6.87–6.99 (m, 3 H), 3.83 (s, 3 H), 3.63 (s, 3 H), 2.41 (s, 3 H) ppm; **¹³C-NMR** (101 MHz, CDCl₃): δ = 170.3, 159.4, 142.2, 139.9, 135.4, 133.1, 129.4, 129.3, 129.2, 127.1, 120.6, 113.5, 113.3, 55.2, 51.9, 19.7 ppm; **IR** (ATR): $\tilde{\nu}$ = 2948, 2835, 1725, 1576, 1466, 1433, 1267, 1228 cm⁻¹; **MS** (EI, 70 eV), m/z (%): 256 (94) [M⁺], 224 (100), 182 (12), 153 (9); **HRMS** (EI-TOF), m/z : [M⁺] calcd. for C₁₆H₁₆O₃: 256.1099; found: 256.1082.



Methyl 3-methyl-3'-(trifluoromethyl)biphenyl-2-carboxylate (**5.4.2-3aj**): Compound **5.4.2-3aj** was prepared following the general method A from 2-methylbenzoic acid (**5.4.2-1a**) (68.8 mg,

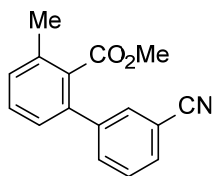
0.50 mmol) and 1-bromo-3-(trifluoromethyl)benzene (**5.4.2-2j**) (114 mg, 70.6 μ L, 0.50 mmol). **5.4.2-3aj** was isolated as colorless oil (105 mg, 71%).

¹H-NMR (400 MHz, CDCl₃): δ = 7.59–7.67 (m, 2 H), 7.49–7.58 (m, 2 H), 7.40 (t, J = 7.7 Hz, 1 H), 7.26–7.30 (m, 1 H), 7.21–7.25 (m, 1 H), 3.62 (s, 3 H), 2.42 (s, 3 H) ppm; **¹³C-NMR** (101 MHz, CDCl₃): δ = 169.9, 141.6, 138.6, 135.8, 133.2, 131.6 (d, J_{C-F} = 1.8 Hz), 130.7 (q, J_{C-F} = 32.7 Hz), 129.8, 129.6, 128.8, 127.1, 125.1 (q, J_{C-F} = 3.0 Hz), 124.1 (q, J_{C-F} = 3.0 Hz), 123.8 (q, J_{C-F} = 272.5 Hz), 51.9, 19.8 ppm; **¹⁹F-NMR** (377 MHz, CDCl₃): δ = -62.59 ppm; **IR** (ATR): $\tilde{\nu}$ = 2953, 1728, 1433, 1335, 1263, 1164, 1120, 1067 cm⁻¹; **MS** (EI, 70 eV), m/z (%): 294 (68) [M⁺], 263 (100), 215 (8), 165 (13); **HRMS** (EI-TOF), m/z : [M⁺] calcd. for C₁₆H₁₃F₃O₂: 294.0868; found: 294.0870.



Methyl 3'-tert-butyl-3-methylbiphenyl-2-carboxylate (**5.4.2-3ak**): Compound **5.4.2-3ak** was prepared following the general method A from 2-methylbenzoic acid (**5.4.2-1a**) (68.8 mg, 0.50 mmol) and 1-bromo-3-*tert*-butylbenzene (**5.4.2-2k**) (107 mg, 85.2 μ L, 0.50 mmol). **5.4.2-3ak** was isolated as colorless oil (111 mg, 79%).

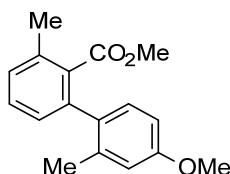
¹H-NMR (400 MHz, CDCl₃): δ = 7.30–7.46 (m, 4 H), 7.17–7.28 (m, 3 H), 3.60 (s, 3 H), 2.42 (s, 3 H), 1.35 (s, 9 H) ppm; **¹³C-NMR** (101 MHz, CDCl₃): δ = 170.4, 151.1, 140.6, 140.5, 135.4, 133.2, 129.4, 128.9, 128.1, 127.2, 125.4, 125.3, 124.2, 51.8, 34.7, 31.4, 19.7 ppm; **IR** (ATR): $\tilde{\nu}$ = 2952, 2867, 1727, 1589, 1463, 1436, 1365, 1117 cm⁻¹; **MS** (EI, 70 eV), m/z (%): 282 (67) [M⁺], 235 (100), 207 (16), 193 (42); **HRMS** (EI-TOF), m/z : [M⁺] calcd. for: C₁₉H₂₂O₂: 282.1620; found: 282.1624.



Methyl 3'-cyano-3-methylbiphenyl-2-carboxylate (**5.4.2-3al**): Compound **5.4.2-3al** was prepared following the general method A from 2-methylbenzoic acid (**5.4.2-1a**) (68.8 mg, 0.50 mmol) and 3-cyanobromobenzene (**5.4.2-2l**) (91.0 mg, 0.50 mmol). **5.4.2-3al** was isolated as colorless oil (65 mg, 52%).

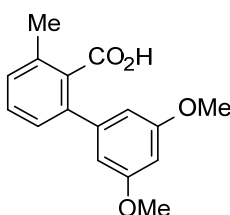
¹H-NMR (400 MHz, CDCl₃): δ = 7.62–7.68 (m, 2 H), 7.57–7.62 (m, 1 H), 7.48–7.54 (m, 1 H), 7.37–7.43 (m, 1 H), 7.29 (d, J = 7.5 Hz, 1 H), 7.18 (d, J = 7.5 Hz, 1 H), 3.63 (s, 3 H), 2.42 (s,

3 H) ppm; $^{13}\text{C-NMR}$ (101 MHz, CDCl_3): δ = 169.6, 142.2, 137.8, 136.0, 133.0, 132.7, 131.7, 131.0, 130.2, 129.7, 129.1, 127.0, 118.6, 112.5, 52.0, 19.7 ppm; **IR** (ATR): $\tilde{\nu}$ = 2949, 2231, 1726, 1591, 1460, 1436, 1120, 1068 cm^{-1} ; **MS** (EI, 70 eV), m/z (%): 251 (64) [M^+], 220 (100), 190 (9), 165 (9); **HRMS** (EI-TOF), m/z : [M^+] calcd. for $\text{C}_{16}\text{H}_{13}\text{NO}_2$: 251.0946; found: 251.0950.



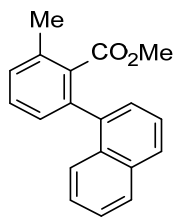
Methyl 4'-methoxy-2',3-dimethylbiphenyl-2-carboxylate (**5.4.2-3am**): Compound **5.4.2-3am** was prepared following the general method A from 2-methylbenzoic acid (**5.4.2-1a**) (68.8 mg, 0.50 mmol) and 1-bromo-4-methoxy-2-methylbenzene (**5.4.2-2m**) (104 mg, 114 μL , 0.50 mmol). **5.4.2-3am** was isolated as yellow oil (54.0 mg, 40%).

$^1\text{H-NMR}$ (400 MHz, CDCl_3): δ = 7.31 (t, J = 8.0 Hz, 1 H), 7.20 (d, J = 7.3 Hz, 1 H), 7.01–7.08 (m, 2 H), 6.79 (d, J = 2.5 Hz, 1 H), 6.72 (dd, J = 8.3, 2.8 Hz, 1 H), 3.83 (s, 3 H), 3.52 (s, 3 H), 2.40 (s, 3 H), 2.12 (s, 3 H) ppm; $^{13}\text{C-NMR}$ (101 MHz, CDCl_3): δ = 169.9, 158.8, 139.6, 137.5, 135.0, 134.2, 132.6, 130.2, 128.9, 128.7, 127.6, 115.2, 110.3, 55.1, 51.6, 20.4, 19.7 ppm; **IR** (ATR): $\tilde{\nu}$ = 2948, 2835, 1728, 1608, 1573, 1461, 1266, 1237 cm^{-1} ; **MS** (EI, 70 eV), m/z (%): 270 (100) [M^+], 238 (55), 223 (10), 195 (25), 152 (6); **HRMS** (EI-TOF), m/z : [M^+] calcd. for $\text{C}_{17}\text{H}_{18}\text{O}_3$: 270.1256; found: 270.1257.



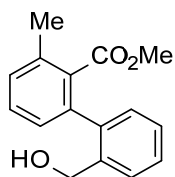
3',5'-Dimethoxy-3-methylbiphenyl-2-carboxylic acid (**5.4.2-3an**) [CAS: 1261980-73-7]: Compound **5.4.2-3an** was prepared following the general method B from 2-methylbenzoic acid (**5.4.2-1a**) (68.8 mg, 0.50 mmol) and 5-chloro-1,3-dimethoxybenzene (**5.4.2-2n'**) (356 mg, 2.00 mmol). **5.4.2-3an** was isolated as colorless oil (97 mg, 68%).

$^1\text{H-NMR}$ (400 MHz, CDCl_3): δ = 7.38 (t, J = 7.8 Hz, 1 H), 7.25 (d, J = 7.8 Hz, 2 H), 6.60 (d, J = 2.3 Hz, 2 H), 6.48 (t, J = 2.3 Hz, 1 H), 3.78 (s, 6 H), 2.46 (s, 3 H) ppm; $^{13}\text{C-NMR}$ (CDCl_3 , 101 MHz): δ = 174.9, 160.6, 142.5, 139.9, 135.3, 132.1, 129.7, 129.3, 127.2, 106.4, 100.1, 55.3, 19.7 ppm; **IR** (ATR): $\tilde{\nu}$ = 2962, 2937, 2838, 1695, 1584, 1456, 1421, 1204, 1153, 1063, 907, 727, 695 cm^{-1} ; the analytical data matched those reported in the literature.^[131]



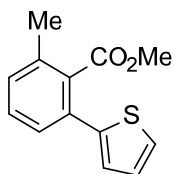
Methyl 3-phenylnaphthalene-2-carboxylate (5.4.2-3ao): Compound **5.4.2-3ao** was prepared following the general method A from 2-methylbenzoic acid (**5.4.2-1a**) (68.8 mg, 0.50 mmol) and 1-bromonaphthalene (**5.4.2-2o**) (158 mg, 106 μ L, 0.75 mmol). **5.4.2-3ao** was isolated as colorless oil (117 mg, 85%).

$^1\text{H-NMR}$ (400 MHz, CDCl_3): δ = 7.82–7.92 (m, 2 H), 7.63–7.69 (m, 1 H), 7.46–7.52 (m, 2 H), 7.39–7.45 (m, 2 H), 7.29–7.37 (m, 2 H), 7.23–7.27 (m, 1 H), 3.27 (s, 3 H), 2.47 (s, 3 H) ppm; **$^{13}\text{C-NMR}$** (101 MHz, CDCl_3): δ = 169.6, 138.7, 138.4, 135.7, 134.4, 133.4, 131.9, 129.4, 129.0, 128.4, 128.0, 127.8, 126.6, 126.2, 125.9, 125.7, 124.9, 51.5, 19.9 ppm; **IR** (ATR): $\tilde{\nu}$ = 3053, 2948, 1726, 1587, 1508, 1435, 1394, 1111 cm^{-1} ; **MS** (EI, 70 eV), m/z (%): 276 (100) [M^+], 245 (50), 202 (12), 107 (6); **HRMS** (EI-TOF), m/z : [M^+] calcd. for: $\text{C}_{19}\text{H}_{16}\text{O}_2$: 276.1150; found: 276.1138.



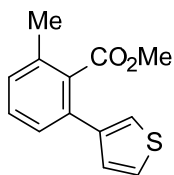
Methyl 2'-(hydroxymethyl)-3-methylbiphenyl-2-carboxylate (5.4.2-3ap): Compound **5.4.2-3ap** was prepared following the general method A from 2-methylbenzoic acid (**5.4.2-1a**) (68.8 mg, 0.50 mmol) and 3-bromobenzyl alcohol (**5.4.2-2p**) (95.4 mg, 0.50 mmol). **5.4.2-3ap** was isolated as colorless oil (66 mg, 52%).

$^1\text{H-NMR}$ (400 MHz, CDCl_3): δ = 7.53 (dd, J = 7.7, 1.1 Hz, 1 H), 7.32–7.42 (m, 2 H), 7.23–7.32 (m, 2 H), 7.10 (ddd, J = 12.4, 7.6, 0.9 Hz, 2 H), 4.46–4.54 (m, 1 H), 4.33–4.40 (m, 1 H), 3.53 (s, 3 H), 2.40 (s, 3 H) ppm; **$^{13}\text{C-NMR}$** (101 MHz, CDCl_3): δ = 170.4, 139.2, 138.8, 138.6, 135.1, 133.7, 129.4, 129.2, 129.1, 129.1, 128.3, 127.2, 127.2, 63.1, 52.0, 19.7 ppm; **IR** (ATR): $\tilde{\nu}$ = 3420, 2949, 1727, 1589, 1438, 1110, 1066, 1012 cm^{-1} ; **MS** (EI, 70 eV), m/z (%): 239 (29) [$\text{M}^+ - \text{OH}$], 224 (100), 206 (60), 195 (59), 181 (38), 165 (25); **HRMS** (EI-TOF), m/z : [M^+] calcd. for $\text{C}_{16}\text{H}_{14}\text{O}_2$: 238.0994; found: 238.0998 [$\text{M}^+ - (\text{H}_2\text{O})$].



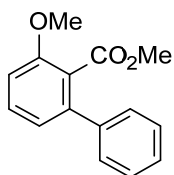
Methyl 2-methyl-6-(thiophen-2-yl)benzoate (5.4.2-3aq): Compound **5.4.2-3aq** was prepared following the general method A from 2-methylbenzoic acid (**5.4.2-1a**) (68.8 mg, 0.50 mmol) and 2-bromothiophene (**5.4.2-2q**) (83.2 mg, 49.5 μ L, 0.50 mmol). **5.4.2-3aq** was isolated as orange oil (100 mg, 86%).

¹H-NMR (400 MHz, CDCl₃): δ = 7.30–7.36 (m, 3 H), 7.18–7.24 (m, 1 H), 7.08–7.11 (m, 1 H), 7.03–7.07 (m, 1 H), 3.76 (s, 3 H), 2.38 (s, 3 H) ppm; **¹³C-NMR** (101 MHz, CDCl₃): δ = 170.2, 141.9, 135.3, 133.3, 132.0, 129.5, 129.3, 127.5, 127.4, 125.9, 52.1, 19.5 ppm; **IR** (ATR): $\tilde{\nu}$ = 2948, 2920, 1727, 1589, 1432, 1266, 1119, 1072 cm⁻¹; **MS** (EI, 70 eV), m/z (%): 232 (100) [M⁺], 200 (70), 171 (12), 129 (6); **HRMS** (EI-TOF), m/z : [M⁺] calcd. for: C₁₃H₁₂O₂S: 231.0480; found: 231.0490 [M⁺-H].



Methyl 2-methyl-6-(thiophen-3-yl)benzoate (5.4.2-3ar): Compound **5.4.2-3ar** was prepared following the general method A from 2-methylbenzoic acid (**5.4.2-1a**) (68.8 mg, 0.50 mmol) and 3-bromothiophene (**5.4.2-2r**) (84 mg, 48.3 μ L, 0.50 mmol). **5.4.2-3ar** was isolated as orange oil (79.0 mg, 68%).

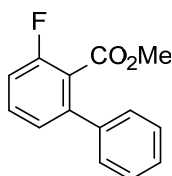
¹H-NMR (400 MHz, CDCl₃): δ = 7.28–7.32 (m, 2 H), 7.2–7.25 (m, 2 H), 7.13–7.17 (m, 1 H), 7.10–7.13 (m, 1 H), 3.66 (s, 3 H), 2.33 (s, 3 H) ppm; **¹³C-NMR** (101 MHz, CDCl₃): δ = 170.5, 140.9, 135.2, 134.3, 133.0, 129.4, 129.0, 127.9, 126.8, 125.6, 122.3, 52.0, 19.5 ppm; **IR** (ATR): $\tilde{\nu}$ = 2948, 1723, 1591, 1461, 1437, 1265, 1119, 1090 cm⁻¹; **MS** (EI, 70 eV), m/z (%): 232 (100) [M⁺], 200 (85), 171 (13), 129 (7); **HRMS** (EI-TOF), m/z : [M⁺] calcd. for C₁₃H₁₂O₂S: 232.0558; found: 232.0564.



Methyl 3-methoxybiphenyl-2-carboxylate (5.4.2-3ba) [CAS: 773134-32-0]: Compound **5.4.2-3ba** was prepared following the general method A from 2-methoxybenzoic acid

(**5.4.2-3b**) (76.8 mg, 0.50 mmol) and bromobenzene (**5.4.2-2a**) (119.0 mg, 79.8 μ L, 0.75 mmol). **5.4.2-3ba** was isolated as colorless solid (117 mg, 97%).

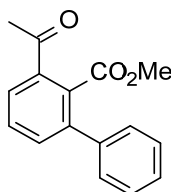
¹H-NMR (400 MHz, CDCl₃): δ = 7.32–7.45 (m, 6 H), 7.01 (dd, J = 7.7, 0.9 Hz, 1 H), 6.95 (dd, J = 8.3, 0.8 Hz, 1 H), 3.90 (s, 3 H), 3.64 (s, 3 H) ppm; **¹³C-NMR** (101 MHz, CDCl₃): δ = 168.5, 156.4, 141.2, 140.0, 130.5, 128.3, 128.2, 127.6, 123.0, 122.0, 109.8, 56.0, 52.1 ppm; **IR** (ATR): $\tilde{\nu}$ = 2947, 2839, 1730, 1570, 1462, 1257, 1128, 1108 cm⁻¹; **MS** (EI, 70 eV), m/z (%): 242 (63) [M⁺], 211 (100), 168 (12), 139 (8); **m.p.**: 84–85 °C; the analytical data matched those reported in the literature.^[131]



Methyl 3-fluorobiphenyl-2-carboxylate (**5.4.2-3ca**) [CAS: 1528793-42-1]: Compound **5.4.2-3ca** was prepared following the general method A from 2-fluorobenzoic acid (**5.4.2-1c**) (119 mg, 0.50 mmol) and bromobenzene (**5.4.2-2a**) (119.0 mg, 79.8 μ L, 0.75 mmol). **5.4.2-3ca** was isolated as colorless oil (102 mg, 88%).

Compound **5.4.2-3ca** was prepared following the general method B from 2-fluorobenzoic acid (**5.4.2-1c**) (119 mg, 0.50 mmol) and chlorobenzene (**5.4.2-2a'**) (227.0 mg, 205 μ L, 2 mmol). **5.4.2-3ca** was isolated as colorless oil (108 mg, 94%).

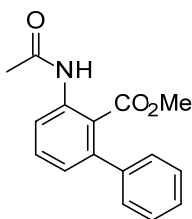
¹H-NMR (400 MHz, CDCl₃): δ = 7.35–7.50 (m, 6 H), 7.21 (dd, J = 7.9, 0.9 Hz, 1 H), 7.14 (ddd, J = 9.3, 8.3, 1.0 Hz, 1 H), 3.69 (s, 3 H) ppm; **¹³C-NMR** (101 MHz, CDCl₃): δ = 166.2, 159.7 (d, J_{C-F} = 251.6 Hz), 142.5 (d, J_{C-F} = 2.7 Hz), 139.3 (d, J_{C-F} = 2.7 Hz), 131.2 (d, J_{C-F} = 8.2 Hz), 128.5, 128.1, 127.9, 125.5 (d, J_{C-F} = 2.7 Hz), 121.4 (d, J_{C-F} = 16.3 Hz), 114.7, 114.5, 52.4, ppm; **¹⁹F-NMR** (377 MHz, CDCl₃): δ = -115.3 ppm; **IR** (ATR): $\tilde{\nu}$ = 2952, 1732, 1612, 1568, 1462, 1261, 1239, 1115 cm⁻¹; **MS** (EI, 70 eV), m/z (%): 230 (79) [M⁺], 199 (100), 170 (16); the analytical data matched those reported in the literature.^[278]



Methyl 3-acetylbiphenyl-2-carboxylate (**5.4.2-3da**) [CAS: 1097018-12-6]: Compound **5.4.2-3da** was prepared following the general method A from 2-acetylbenzoic acid (**5.4.2-1d**)

(82.9 mg, 0.50 mmol) and bromobenzene (**5.4.2-2a**) (119 mg, 80.0 μ L, 0.75 mmol). **5.4.2-3da** was isolated as yellow solid (79 mg, 62%).

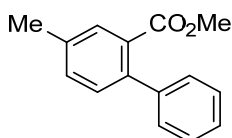
¹H-NMR (400 MHz, CDCl₃): δ = 7.81–7.86 (m, 1 H), 7.53–7.59 (m, 2 H), 7.34–7.44 (m, 5 H), 3.67 (s, 3 H), 2.65 (s, 3 H) ppm; **¹³C-NMR** (101 MHz, CDCl₃): δ = 198.3, 169.7, 141.1, 135.9, 134.2, 132.9, 129.2, 128.5, 128.3, 127.9, 127.9, 52.3, 27.6 ppm; **IR** (ATR): $\tilde{\nu}$ = 2952, 1727, 1677, 1578, 1454, 1428, 1193, 1125 cm⁻¹; **MS** (EI, 70 eV), m/z (%): 254 (10) [M⁺], 239 (100), 207 (7), 179 (6), 152 (9); **HRMS** (EI-TOF), m/z : [M⁺] calcd. for C₁₆H₁₄O₃: 254.0943; found: 254.0945; **m.p.**: 92–93 °C; the analytical data matched those reported in the literature.^[131]



Methyl 3-acetamidobiphenyl-2-carboxylate (**5.4.2-3ea**): Compound **5.4.2-3ea** was prepared following the general method A from *N*-acetylanthranilic acid (**5.4.2-1a**) (90.5 mg, 0.50 mmol) and bromobenzene (**5.4.2-2a**) (91.0 mg, 0.50 mmol). **5.4.2-3ea** was isolated as colorless solid (95 mg, 71%).

Compound **5.4.2-3ea** was prepared following the general method b from *N*-acetylanthranilic acid (**5.4.2-1a**) (90.5 mg, 0.50 mmol) and chlorobenzene (**5.4.2-2a'**) (227 mg, 205 μ L, 2.00 mmol). **5.4.2-3ea** was isolated as colorless solid (78 mg, 58%).

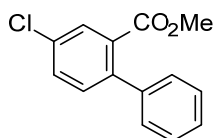
¹H-NMR (400 MHz, CDCl₃): δ = 9.32 (brs, 1 H), 8.39 (d, J = 8.3 Hz, 1 H), 7.51 (t, J = 7.9 Hz, 1 H), 7.31–7.43 (m, 3 H), 7.24–7.30 (m, 3 H), 7.10–7.17 (m, 1 H), 3.44 (s, 3 H), 2.22 (s, 3 H) ppm; **¹³C-NMR** (101 MHz, CDCl₃): δ = 169.9, 168.6, 143.0, 141.9, 137.8, 131.6, 128.2, 127.9, 127.2, 125.6, 120.5, 119.6, 51.9, 25.1 ppm; **IR** (ATR): $\tilde{\nu}$ = 3236, 3037, 2949, 1722, 1548, 1466, 1369, 1266 cm⁻¹; **MS** (EI, 70 eV), m/z (%): 269 (62) [M⁺], 227 (68), 195 (100), 168 (22), 139 (9); **HRMS** (EI-TOF), m/z : [M⁺] calcd. for C₁₆H₁₅NO₃: 269.1052; found: 269.1063; **m.p.**: 162–163 °C.



Methyl 4-methylbiphenyl-2-carboxylate (**5.4.2-3fa**) [CAS: 152620-33-2]: Compound **5.4.2-3ga** was prepared following the general method A from 3-methylbenzoic acid (**5.4.2-1f**) (68.8 mg, 0.50 mmol) and bromobenzene (**5.4.2-2a**) (119.0 mg, 79.8 μ L, 0.75 mmol). **5.4.2-3fa** was isolated as colorless oil (96 mg, 85%).

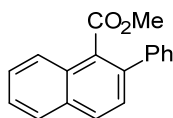
Compound **5.4.2-3fa** was prepared following the general method B from 3-methylbenzoic acid (**5.4.2-1f**) (68.8 mg, 0.50 mmol) and chlorobenzene (**5.4.2-2a'**) (227 mg, 205 μ L, 0.75 mmol). **5.4.2-3fa** was isolated as colorless oil (67 mg, 59%).

¹H-NMR (400 MHz, CDCl₃): δ = 7.65 (d, J = 0.5 Hz, 1 H), 7.27–7.44 (m, 7 H), 3.64 (s, 3 H), 2.44 (s, 3 H) ppm; **¹³C-NMR** (101 MHz, CDCl₃): δ = 169.4, 141.3, 139.6, 137.1, 130.7, 130.6, 130.3, 128.4, 128.0, 127.1, 51.9, 21.0 ppm; **IR** (ATR): $\tilde{\nu}$ = 3027, 2949, 1717, 1482, 1434, 1296, 1243, 1089 cm⁻¹; **MS** (EI, 70 eV), m/z (%): 226 (100) [M⁺], 195 (67), 165 (13); the analytical data matched those reported in the literature.^[278]



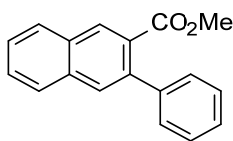
Methyl 4-chlorobiphenyl-2-carboxylate (**5.4.2-3ga**) [CAS: 1092775-67-1]: Compound **5.4.2-3ga** was prepared following the general method A from 3-chlorobenzoic acid (**5.4.2-1g**) (79.1 mg, 0.50 mmol) and bromobenzene (**5.4.2-2a**) (79.3 mg, 53.2 μ L, 0.50 mmol). **5.4.2-3ga** was isolated as colorless oil (93.3 mg, 76%).

¹H-NMR (400 MHz, CDCl₃): δ = 7.80–7.85 (m, 1 H), 7.51 (dd, J = 8.2, 2.4 Hz, 1 H), 7.35–7.45 (m, 3 H), 7.33 (d, J = 8.3 Hz, 1 H), 7.27–7.31 (m, 2 H), 3.66 (s, 3 H) ppm; **¹³C-NMR** (101 MHz, CDCl₃): δ = 167.8, 140.9, 140.1, 133.2, 132.1, 132.0, 131.2, 129.7, 128.2, 128.1, 127.5, 52.2 ppm; **IR** (ATR): $\tilde{\nu}$ = 3064, 2950, 1721, 1472, 1396, 1142, 1107, 1009 cm⁻¹; **MS** (EI, 70 eV), m/z (%): 246 (94) [M⁺], 215 (100), 152 (40), 76 (11); the analytical data matched those reported in the literature.^[279]



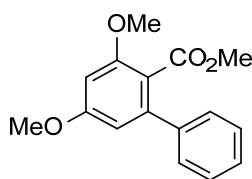
Methyl 2-phenylnaphthalene-1-carboxylate (**5.4.2-3ha**) [CAS: 109251-89-0]: Compound **5.4.2-3ha** was prepared following the general method B from naphthalene-1-carboxylic acid (**5.4.2-1h**) (87.8 mg, 0.50 mmol) and chlorobenzene (**5.4.2-2a'**) (227 mg, 205 μ L, 2.00 mmol). **5.4.2-3ha** was isolated as colorless solid (120 mg, 92%).

¹H-NMR (400 MHz, CDCl₃): δ = 7.98 (d, J = 8.3 Hz, 2 H), 7.89–7.94 (m, 1 H), 7.37–7.63 (m, 8 H), 3.71 (s, 3 H) ppm; **¹³C-NMR** (CDCl₃, 101 MHz): δ = 170.0, 140.9, 138.0, 132.3, 130.0, 129.9, 128.5, 128.4, 128.1, 127.6, 127.5, 127.4, 126.3, 125.0, 52.2 ppm; **IR** (ATR): $\tilde{\nu}$ = 3051, 2997, 2946, 1716, 1427, 1371, 1341, 1036 cm⁻¹; **MS** (EI, 70 eV), m/z (%): 262 (100) [M⁺], 231 (85), 202 (15); **m.p.**: 75–76 °C; the analytical data matched those reported in the literature.^[131]



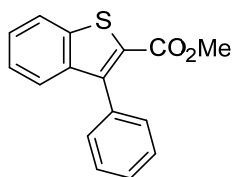
Methyl 3-phenylnaphthalene-2-carboxylate (**5.4.2-3ia**) [CAS: 68376-11-4]: Compound **5.4.2-3ia** was prepared following the general method A from naphthalene-2-carboxylic acid (**5.4.2-1i**) (70.8 mg, 0.50 mmol) and bromobenzene (**5.4.2-2a**) (119 mg, 79.8 μ L, 0.75 mmol). **5.4.2-3ia** was isolated as colorless oil (115 mg, 88%).

¹H-NMR (400 MHz, CDCl₃): δ = 8.39–8.44 (m, 1 H), 7.93–7.99 (m, 1 H), 7.86–7.92 (m, 1 H), 7.84 (s, 1 H), 7.52–7.65 (m, 2 H), 7.34–7.49 (m, 5 H), 3.67–3.76 (m, 3 H) ppm; **¹³C-NMR** (101 MHz, CDCl₃): δ = 169.0, 141.4, 138.8, 134.4, 131.5, 131.0, 129.7, 129.1, 128.6, 128.5, 128.2, 128.0, 127.8, 127.1, 126.7, 52.1 ppm; **IR** (ATR): $\tilde{\nu}$ = 3055, 3020, 2948, 1717, 1491, 1441, 1276, 1214 cm⁻¹; **MS** (EI, 70 eV), m/z (%): 262 (100) [M⁺], 231 (49), 202 (14); the analytical data matched those reported in the literature.^[280]



Methyl 3,5-dimethoxybiphenyl-2-carboxylate (**5.4.2-3ja**) [CAS: 131035-40-0]: Compound **5.4.2-3ja** was prepared following the general method A from 2,4-dimethoxybenzoic acid (**5.4.2-1j**) (92.9 mg, 0.50 mmol) and bromobenzene (**5.4.2-2a**) (79.3 mg, 53.2 μ L, 0.50 mmol). **5.4.2-3ja** was isolated as purple oil (114 mg, 84%).

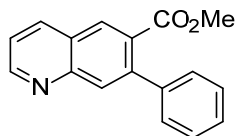
¹H-NMR (400 MHz, CDCl₃): δ = 7.30–7.43 (m, 5 H), 6.50 (s, 2 H), 3.87 (s, 3 H), 3.85 (s, 3 H), 3.58 (s, 3 H) ppm; **¹³C-NMR** (101 MHz, CDCl₃): δ = 168.4, 161.3, 158.1, 142.7, 140.5, 128.3, 128.0, 127.6, 116.0, 106.1, 97.5, 56.0, 55.5, 51.9 ppm; **IR** (ATR): $\tilde{\nu}$ = 2942, 2841, 1726, 1598, 1456, 1415, 1339, 12612 cm⁻¹; **MS** (EI, 70 eV), m/z (%): 272 (71) [M⁺], 241.2 (100); the analytical data matched those reported in the literature.^[281]



Methyl 3-phenyl-1-benzothiophene-2-carboxylate (**5.4.2-3ka**) [CAS: 58878-44-7]: Compound **5.4.2-3ka** was prepared following the general method A from 1-benzothiophene-2-carboxylic

acid (**5.4.2-1k**) (89.1 mg, 0.50 mmol) and bromobenzene (**5.4.2-2a**) (119 mg, 79.8 μ L, 0.75 mmol). **5.4.2-3ka** was isolated as colorless solid (73 mg, 54%).

¹H-NMR (400 MHz, CDCl₃): δ = 7.88–7.92 (m, 1 H), 7.34–7.57 (m, 8 H), 3.80 (s, 3 H) ppm; **¹³C-NMR** (101 MHz, CDCl₃): δ = 162.9, 144.2, 140.4, 134.5, 129.6, 128.1, 128.0, 127.8, 127.2, 125.3, 124.8, 122.5, 120.0, 52.2 ppm; **IR** (ATR): $\tilde{\nu}$ = 2943, 2845, 1700, 1516, 1440, 1291, 1177, 1155 cm⁻¹; **MS** (EI, 70 eV), m/z (%): 268 (100) [M⁺], 237 (72), 208 (7), 165 (15); **m.p.**: 65–66 °C; the analytical data matched those reported in the literature.^[282]

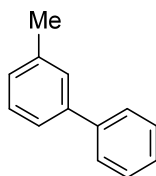


Methyl 7-phenylquinoline-6-carboxylate (**5.4.2-3la**): Compound **5.4.2-3la** was prepared following the general method A from 6-quinolinecarboxylic acid (**5.4.2-1l**) (89.3 mg, 0.50 mmol) and bromobenzene (**5.4.2-2a**) (79.3 mg, 53.2 μ L, 0.50 mmol). **5.4.2-3la** was isolated as orange oil (53 mg, 40%).

¹H-NMR (400 MHz, CDCl₃): δ = 9.03 (dd, J = 4.3, 1.8 Hz, 1 H), 8.36 (s, 1 H), 8.25–8.29 (m, 1 H), 8.13 (s, 1 H), 7.39–7.50 (m, 6 H), 3.71 (s, 3 H) ppm; **¹³C-NMR** (101 MHz, CDCl₃): δ = 168.6, 152.6, 148.8, 142.5, 140.6, 136.6, 131.1, 130.7, 130.1, 128.4, 128.2, 127.5, 126.5, 121.8, 52.2 ppm; **IR** (ATR): $\tilde{\nu}$ = 2948, 1720, 1623, 1456, 1430, 1342, 1268, 1200 cm⁻¹; **MS** (EI, 70 eV), m/z (%): 263 (100) [M⁺], 232 (86), 204 (14), 176 (9); **HRMS** (EI-TOF), m/z : [M⁺] calcd. for C₁₇H₁₃NO₂: 263.0936; found: 263.0941.

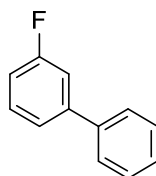
7.6.5 Procedure for the one-pot *ortho*-C–H arylation and protodecarboxylation

An oven-dried 20 mL vessel was charged with [Ru(*p*-cym)Cl₂]₂ (12.2 mg, 0.02 mmol, 4 mol%), PEt₃ × HBF₄ (8.32 mg, 0.04 mmol, 8 mol%), K₂CO₃ (76 mg, 0.55 mmol, 1.1 equiv.), Cu₂O (7.23 mg, 0.05 mmol, 10 mol%) and the *ortho*-substituted benzoic acid (**5.4.2-1**) (0.50 mmol). After the vessel was flushed with 3 alternating vacuum and nitrogen purge cycles, NMP (3 mL) and bromobenzene (**5.4.2-2a**) (79.3 mg, 53.2 μ L, 0.50 mmol) were added *via* syringe. The resulting mixture was stirred at 180 °C for 18 h. After the reaction was complete, the mixture was allowed to cool to RT, then ethyl acetate (20 mL) was added and the resulting mixture was washed with water, aqueous LiCl solution (20%) and brine (20 mL each). The organic layer was dried over MgSO₄, filtered, and the volatiles were removed under reduced pressure. The residue was purified by column chromatography (SiO₂, ethyl acetate/cyclohexane gradient) yielding the corresponding biaryl.



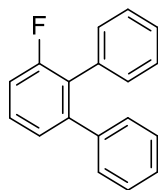
3-Methyl-1,1'-biphenyl (**5.4.2-4aa**) [CAS: 643-93-6]: Compound **5.4.2-4aa** was prepared following the general method for the one-pot *ortho*-C–H arylation and protodecarboxylation starting from 2-methylbenzoic acid (**5.4.2-1a**) (68.8 mg, 0.50 mmol). **5.4.2-4aa** was isolated as colorless oil (45 mg, 54%).

¹H-NMR (400 MHz, CDCl₃): δ = 7.58–7.65 (m, 2 H), 7.39–7.49 (m, 4 H), 7.33–7.39 (m, 2 H), 7.19 (d, J = 7.3 Hz, 1 H), 2.45 (s, 3 H) ppm; **¹³C-NMR** (CDCl₃, 101 MHz): δ = 141.3, 141.2, 138.3, 128.7, 128.6, 128.0, 127.2, 127.1, 124.2, 21.5 ppm; **IR** (ATR): $\tilde{\nu}$ = 3057, 3031, 2916, 1601, 1481, 791, 752, 698 cm⁻¹; **MS** (EI, 70 eV), m/z (%): 168 (100) [M⁺], 165 (19), 153 (15), 152 (18); the analytical data matched those reported in the literature.^[283]



3-Fluoro-1,1'-biphenyl (**5.4.2-4ca**) [CAS: 2367-22-8]: Compound **5.4.2-4ca** was prepared following the general method for the one-pot *ortho*-C–H arylation and protodecarboxylation, starting from 2-fluorobenzoic acid (**5.4.2-1c**) (70.8 mg, 0.50 mmol). **5.4.2-4ca** was isolated as colorless oil (61 mg, 71%).

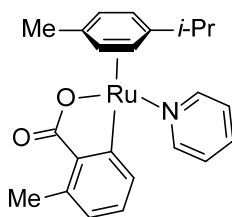
¹H-NMR (400 MHz, CDCl₃): δ = 7.58–7.65 (m, 2 H), 7.40–7.49 (m, 5 H), 7.32–7.39 (m, 2 H), 7.19 (d, J = 7.3 Hz, 1 H), 2.45 (s, 3 H) ppm; **¹³C-NMR** (CDCl₃, 101 MHz): δ = 164.4 (d, J_{C-F} = 246.1 Hz), 143.5 (d, J_{C-F} = 7.3 Hz), 139.9 (d, J_{C-F} = 2.7 Hz), 130.2 (d, J_{C-F} = 8.2 Hz), 128.9, 127.8, 127.1, 122.8 (d, J_{C-F} = 2.7 Hz), 114.1, 113.9 (d, J_{C-F} = 1.82 Hz) ppm; **¹⁹F-NMR** (375 MHz, CDCl₃): δ = -113.16 ppm; **IR** (ATR): $\tilde{\nu}$ = 3065, 3035, 1576, 1474, 1422, 1260, 1186, 1158, 1076, 877, 788, 755, 695 cm⁻¹; **MS** (EI, 70 eV), m/z (%): 172 (100) [M⁺], 154 (4), 98 (6), 85 (12), 74 (11); the analytical data matched those reported in the literature.^[284]

7.6.6 Procedure for the one-pot ortho-C–H arylation and decarboxylative cross coupling

3'-Fluoro-1,1':2',1''-terphenyl (5.4.2-5ca): An oven-dried 20 mL vessel was charged with [Ru(*p*-cym)Cl₂]₂ (12.2 mg, 0.02 mmol, 4 mol%), PEt₃ × HBF₄ (8.32 mg, 0.04 mmol, 8 mol%), K₂CO₃ (76 mg, 0.55 mmol, 1.1 equiv.), and 2-fluorobenzoic acid (**5.4.2-1c**) (70.8 mg, 0.50 mmol). After the vessel was flushed with 3 alternating vacuum and nitrogen purge cycles, NMP (3 mL) and bromobenzene (**5.4.2-2a**) (79.3 mg, 53.2 μL, 0.50 mmol) were added *via* syringe. The resulting mixture was stirred at 100 °C for 18 h. After the reaction time, the mixture was allowed to cool to RT, then a stock solution of Pd(acac)₂ (7.62 mg, 25.0 μmol, 5 mol%) and XPhos (12.0 mg, 25.0 μmol, 5 mol%) in NMP (1 mL), a slurry of Cu₂O (7.16 mg, 0.05 mmol, 10 mol%) in NMP (0.5 mL) and bromobenzene (64.0 μL, 0.6 mmol, 1.20 equiv.) were added *via* syringe. The vessel was heated at 180 °C for 6 h, then allowed to cool to RT. Ethyl acetate (20 mL) was added and the resulting mixture was washed with water, aqueous LiCl solution (20%) and brine (20 mL each). The organic layer was dried over MgSO₄, filtered, and the volatiles were removed under reduced pressure. The residue was purified by column chromatography (SiO₂, cyclohexane isocratic) yielding **5.4.2-5ca** as colorless oil (68 mg, 55%).

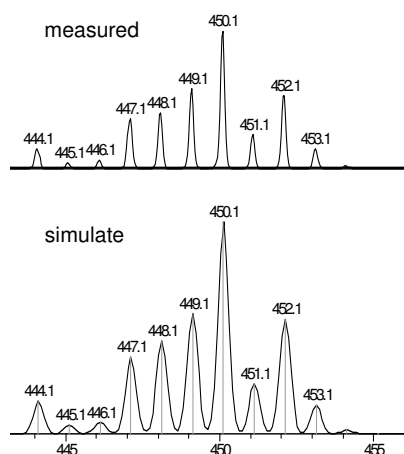
¹H-NMR (400 MHz, CDCl₃): δ = 6.97–7.35 (m, 13 H) ppm; **¹³C-NMR** (CDCl₃, 101 MHz): δ = 160.0 (d, *J*_{C-F} = 246.1 Hz), 143.3 (d, *J*_{C-F} = 2.7 Hz), 140.2 (d, *J*_{C-F} = 2.7 Hz), 134.2, 130.9 (d, *J*_{C-F} = 1.9 Hz), 129.8, 128.6 (d, *J*_{C-F} = 9.1 Hz), 128.2 (d, *J*_{C-F} = 15.4 Hz), 127.8, 127.8, 127.1, 126.7, 126.0 (d, *J*_{C-F} = 3.5 Hz), 114.6 (d, *J*_{C-F} = 23.6 Hz) ppm; **¹⁹F-NMR** (375 MHz, CDCl₃): δ = -115 ppm; **IR** (ATR): $\tilde{\nu}$ = 3053, 3021, 2916, 1601, 1487, 792, 752, 698 cm⁻¹; **MS** (EI, 70 eV), *m/z* (%): 248 (100) [M⁺], 228 (5); **HRMS** (EI-TOF), *m/z*: [M⁺] calcd. for C₁₈H₁₃F: 248.1001; found: 248.0994.

7.6.7 Synthesis of $[Ru(2\text{-Me-benzoato}^{2-}\text{-C}^6\text{,O}^1)(p\text{-cymene})(pyridine)]$



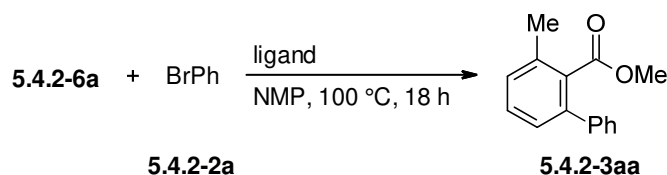
Compound **5.4.2-6a** was synthesized following the literature procedure,^[285] starting from potassium 2-methyl benzoate (**5.4.2-1a**) (261 mg, 1.5 mmol), $[Ru(p\text{-cym})Cl_2]_2$ (312 mg, 0.5 mmol), pyridine (79 mg, 8.1 μ L, 1 mmol) and trimethylamine (715 mg, 983 μ L, 7 mmol). **5.4.2-6a** was isolated as a red wax (82 mg, 37%).

¹H-NMR (400 MHz, $CDCl_3$): δ = 8.54–8.60 (m, 2 H), 7.86–7.91 (m, 1 H), 7.46 (tt, J = 7.7, 1.5 Hz, 1 H), 7.10 (t, J = 7.3 Hz, 1 H), 6.99–7.04 (m, 2 H), 6.73 (dd, J = 6.9, 0.6 Hz, 1 H), 5.52 (dd, J = 5.8, 1.0 Hz, 1 H), 5.45 (dd, J = 6.0, 0.8 Hz, 1 H), 5.22 (dd, J = 5.9, 1.1 Hz, 1 H), 4.79 (dd, J = 5.8, 1.0 Hz, 1 H), 2.46 (s, 3 H), 2.36 (quin, J = 6.9 Hz, 2 H), 1.70 (s, 1 H), 0.99 (dd, J = 6.8, 1.5 Hz, 6 H) ppm; **¹³C-NMR** ($CDCl_3$, 101 MHz): δ = 181.3, 177.5, 153.6, 140.0, 136.6, 135.5, 134.5, 129.6, 126.6, 124.3, 101.8, 97.9, 87.9, 87.2, 84.3, 80.2, 30.7, 22.6, 22.2, 19.9, 17.9 ppm; **IR** (ATR): $\tilde{\nu}$ = 3050, 2965, 2926, 2872, 1600, 1468, 1443, 1213, 1091, 1008, 907, 759, 692 cm^{-1} ; **ESI-MS**, m/z :



7.6.8 Mechanistic studies

The stoichiometric reaction of **5.4.2-6a** and $PEt_3 \times HBF_4$ with **5.4.2-2a** yielded **5.4.2-3aa** in 57%. This result supports the intermediacy of an *ortho*-metalated species in the catalytic cycle. Without the phosphine, no product formation was observed (*Tabelle 41*).

Tabelle 41: Stoichiometric reaction of ruthenacycle **5.4.2-6a** with bromobenzene **5.4.2-2a**.

Entry	ligand (mol%)	5.4.2-3aa (%)
1	PEt ₃ × HBF ₄ (100)	57
2	-	0

Reaction conditions: **5.4.2-6a** (0.1 mmol), **5.4.2-2a** (0.1 mmol), NMP (3 mL), 100 °C, 18 h. Yields were determined by GC analysis after esterification with K₂CO₃ (3 equiv.) and MeI (5 equiv.) in NMP at 60 °C for 2 h with *n*-tetradecane as an internal standard.

7.7 Branched Arylalkenes from Cinnamates: Selectivity Inversion in Heck Reactions by Carboxylates as Deciduous Directing Groups

7.7.1 General remarks

The β-deuterium-labeled potassium cinnamate **5.5.2-D-1d** was prepared according to the literature procedure.^[286] The carboxylates were prepared from the corresponding carboxylic acids following the procedure below and were directly used.

7.7.2 General procedure for the protodecarboxylation experiments

An oven-dried vessel was charged with the cinammic acid (0.30 mmol), copper(I) oxide (2.2 mg, 15 μmol, 5mol%), and 1,10 phenanthroline (5.4 mg, 30 μmol, 10 mol%). After the vessel was flushed with 3 alternating vacuum and nitrogen purge cycles, degassed NMP (1 mL) was added *via* syringe. The resulting mixture was stirred at the given temperature for 16 h. The reaction mixture was allowed to cool to RT, *n*-tetradecane (30 μL) was added *via* syringe and the mixture was diluted with ethyl acetate (4 mL). A sample of the reaction mixture (0.25 mL) was dissolved in ethyl acetate (2 mL), washed with brine (2 mL), dried over MgSO₄, and analyzed by GC.

7.7.3 Preparation of starting materials

General procedure for the preparation of potassium carboxylates:

A 250 mL, two-necked, round-bottomed flask was charged with the carboxylic acid (20.0 mmol) and ethanol (20.0 mL). To this, a solution of potassium *tert*-butoxide (2.24 g, 20.0 mmol) in ethanol (20.0 mL) was added dropwise over 1 h. After complete addition, the

reaction mixture was stirred for another 1 h at RT. A gradual formation of a white precipitate was observed. The resulting solid was collected by filtration washed sequentially with ethanol (2×10.0 mL) and cold ($0\text{ }^{\circ}\text{C}$) diethyl ether (10.0 mL), and dried in vacuum to provide the corresponding potassium salts of the carboxylic acids.

7.7.4 Optimization of the decarboxylative Mizoroki-Heck coupling

General method:

An oven-dried 20 mL vessel was charged with the solid reagents. After the vessel was flushed with 3 alternating vacuum and nitrogen purge cycles, the solvent and the liquid reagents were added *via* syringe and the resulting mixture was stirred at the given temperature for 16 h. The reaction mixture was allowed to cool to RT and *n*-tetradecane (50 μL) was added *via* syringe. K_2CO_3 (207 mg, 3 equiv.), MeI (156 μL , 5 equiv.) and MeCN (3 mL) were added and the mixture was stirred at $60\text{ }^{\circ}\text{C}$ for 2 h. After the mixture was cooled to RT, a sample of the reaction mixture (0.25 mL) was dissolved in ethyl acetate (2 mL), washed with brine (2 mL), dried over MgSO_4 , and analyzed by GC.

Tabelle 42: Optimization of the reaction conditions.

$ \begin{array}{c} \text{Ph}-\text{CH}=\text{CH}-\text{C}(=\text{O})\text{OK} + \text{Br}(p\text{-Tol}) \xrightarrow[\text{- CO}_2]{\begin{array}{c} [\text{Pd}] / P\text{-ligand} \\ [\text{M}] / 1,10\text{-Phen} \\ \text{solvent, } \Delta, 16 \text{ h} \end{array}} \text{Ph}-\text{CH}=\text{CH}-\text{C}(=\text{O})\text{OMe} + \text{Ph}-\text{CH}=\text{CH}-\text{C}(=\text{O})\text{OMe} + \text{Ph}-\text{CH}=\text{CH}-\text{C}(=\text{O})\text{OMe} \\ \text{5.5.2-1a} \quad \text{5.5.2-2a} \quad \quad \quad \text{5.5.2-3aa} \quad \text{5.5.2-4aa} \quad \text{5.5.2-5aa} \end{array} $							
Entry	[M]	[Pd]	P-ligand	T ($^{\circ}\text{C}$)	Yield (%)		
					5.5.2-3aa	5.5.2-4aa	5.5.2-5aa
1	-	$\text{Pd}(\text{acac})_2$	PPh_3	130	4	12	10
2	CuBr	"	"	"	2	23	4
3	$\text{Sc}(\text{OTf})_3$	"	"	"	6	40	12
4	$\text{Pb}(\text{NO}_3)_2$	"	"	"	6	30	11
5	FeCl_2	"	"	"	5	25	15
6 ^[a]	-	"	"	"	5	<1	<1
7	Ag_2CO_3	"	"	"	6	<1	12
8	CuBr	"	"	150	28	9	7
9	"	"	"	170	73	n.d.	12
10	"	"	$\text{P}(p\text{-Tol})_3$	"	76	"	14

11	"	"	P(<i>o</i> -Tol) ₃	"	92	"	8
12	"	"	P(<i>p</i> -F-C ₆ H ₄) ₃	"	73	"	12
13	"	"	PCy ₃	"	76	"	12
14	"	"	Pt-Bu ₃ ·HBF ₄	"	87	"	12
15	"	"	BINAP	"	87	"	12
16	"	"	dppf	"	70	"	11
17	"	"	JohnPhos	"	77	"	11
18	"	"	DavePhos	"	81	"	13
19	"	"	XPhos	"	80	"	12
20	"	Pd(F ₆ -acac) ₂	P(<i>o</i> -Tol) ₃	"	85	"	13
21	"	PdCl ₂	"	"	83	"	13
22	"	PdBr ₂	"	"	82	"	12
23	"	Pd(OAc) ₂	"	"	86	"	14
24	"	Pd(TFA) ₂	"	"	86	"	14
25	"	(MeCN) ₂ PdCl ₂	"	"	83	"	13
26	"	Pd(dba) ₂	"	"	88	"	12
27	CuCl	Pd(acac) ₂	"	"	90	"	10
28	CuI	"	"	"	58	"	8
29	Cu ₂ O	"	"	"	75	"	10
30 ^[b]	CuBr	"	"	"	88	"	12
31 ^[c]	"	"	"	"	43	"	15
32 ^[d]	"	"	"	"	n.d.	"	n.d.
33 ^[e]	"	"	"	"	25	"	11
34 ^[f]	"	"	"	"	42	"	7
35	"	-	-	"	trace	"	trace
36	-	Pd(acac) ₂	P(<i>o</i> -Tol) ₃	"	6	"	16

Reaction conditions: **5.5.2-1a** (0.6 mmol), **5.5.2-2a** (0.5 mmol), [M] (10 mol%), 1,10-Phen (10 mol%), [Pd] (2 mol%), *P*-ligand (5 mol%), NMP/quinoline (1:1, 3mL), 16 h. Yields were determined by GC analysis after esterification with K₂CO₃ (3 equiv.) and MeI (5 equiv.) in MeCN at 60 °C for 2 h with *n*-tetradecane as an internal standard. [a] copper cinnamate was used instead of **5.5.2-1a**. [b] *in situ* generation of **5.5.2-1a** from cinammic acid and KOAc. [c] *in situ* generation of **5.5.2-1a** from cinammic acid and K₂CO₃. [d] starting from cinammic acid. [e] in NMP (3 mL). [f] in NMP/Mes (1:1, 3 mL).

7.7.5 General procedure for the decarboxylative Mizoroki-Heck coupling

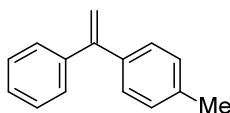
Method A – coupling of aryl bromides:

An oven-dried, nitrogen-flushed 20 mL crimp cap vessel was charged with Pd(acac)₂ (6.1 mg, 0.02 mmol, 2.0 mol%), P(*o*-Tol)₃ (15.7 mg, 0.05 mmol, 5.0 mol%), CuBr (14.6 mg, 0.10 mmol, 10.0 mol%), 1,10-phenanthroline (18.2 mg, 0.10 mmol, 10.0 mol%), and the potassium carboxylate **5.5.2-1** (1.2 mmol, 1.2 equiv.). A degassed mixture of NMP and quinoline (1:1, 3.0 mL) and the aryl bromide **5.5.2-2** (1.0 mmol, 1 equiv.) were added *via* syringe. The resulting solution was then stirred at 170 °C for 16 h. After the reaction was complete, the mixture was cooled to RT, diluted with 1 N HCl (20 mL) and extracted with ethyl acetate (3 × 50 mL). The combined organic layers were washed with water and brine, dried over MgSO₄, filtered, and concentrated in vacuo. The residue was purified by column chromatography (SiO₂, ethyl acetate/cyclohexane gradient) yielding the corresponding product.

Method B – coupling of aryl chlorides:

An oven-dried, nitrogen-flushed 20 mL crimp cap vessel was charged with Pd(acac)₂ (3.1 mg, 0.01 mmol, 2.0 mol%), XPhos (12.3 mg, 0.025 mmol, 5.0 mol%), CuBr (7.3 mg, 0.05 mmol, 10.0 mol%), 1,10-phenanthroline (9.1 mg, 0.05 mmol, 10.0 mol%), and the potassium carboxylate **5.5.2-1** (0.6 mmol, 1.2 equiv.). A degassed mixture of NMP and quinoline (1:1, 3.0 mL) and the aryl chloride **5.5.2-2'** (0.5 mmol, 1 equiv.) were added *via* syringe. The resulting solution was then stirred at 170 °C for 16 h. After the reaction was complete, the mixture was cooled to RT, diluted with 1 N HCl (20 mL) and extracted with ethyl acetate (3 × 50 mL). The combined organic layers were washed with water and brine, dried over MgSO₄, filtered, and concentrated in vacuo. The residue was purified by column chromatography (SiO₂, ethyl acetate/cyclohexane gradient) yielding the corresponding product.

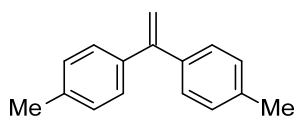
7.7.6 Synthesis and characterization of the corresponding products



1-Methyl-4-(1-phenylvinyl)benzene (**5.5.2-3aa**) [CAS: 948-55-0]: Compound **5.5.2-3aa** was prepared following the general method A from potassium cinnamate (**5.5.2-1a**) (223 mg, 1.2 mmol) and 4-bromotoluene (**5.5.2-2a**) (175 mg, 126 μ L, 1.0 mmol). **5.5.2-3aa** was isolated as a colorless liquid (178 mg, 92%).

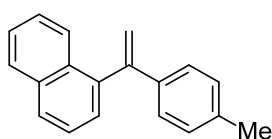
Compound **5.5.2-3aa** was prepared following the general method B from potassium cinnamate (**5.5.2-1a**) (112 mg, 0.6 mmol) and 4-chlorotoluene (**5.5.2-2a'**) (65 mg, 60 μ L, 0.5 mmol). **5.5.2-3aa** was isolated as a colorless liquid (89 mg, 90%).

¹H-NMR (400 MHz, CDCl₃): δ = 7.37–7.33 (m, 5 H), 7.26 (d, J = 8.0 Hz, 2 H), 7.16 (d, J = 9.0 Hz, 2 H), 5.45 (d, J = 1.0 Hz, 1 H), 5.43 (d, J = 1.3 Hz, 1 H), 2.39 (s, 3 H) ppm; **¹³C-NMR** (101 MHz, CDCl₃): δ = 149.9, 141.7, 138.6, 137.5, 128.8, 128.3, 128.1, 128.1, 127.6, 113.6, 21.2 ppm; **IR** (ATR): $\tilde{\nu}$ = 3086, 3053, 2924, 1659, 1606, 1509, 1492, 1327, 1028, 894, 825 cm⁻¹; **MS** (EI, 70 eV), m/z (%): 194 (72) [M⁺], 179 (100), 165 (8), 115 (9), 89 (5); **HRMS** (EI-TOF), m/z : [M⁺] calcd. for C₁₅H₁₄: 194.1096; found: 194.1093.



4,4'-(Ethene-1,1-diyl)bis(methylbenzene) (5.5.2-3ba) [CAS: 2919-20-2]: Compound **5.5.2-3ba** was prepared following the general method A from potassium (*E*)-3-*p*-tolylacrylate (**5.5.2-1b**) (240 mg, 1.2 mmol) and 4-bromotoluene (**5.5.2-2a**) (175 mg, 126 μ L, 1.0 mmol). **5.5.2-3ba** was isolated as a colorless liquid (188 mg, 90%).

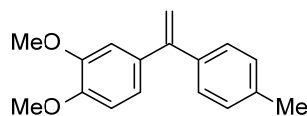
¹H-NMR (400 MHz, CDCl₃): δ = 7.26 (d, J = 8.0 Hz, 4 H), 7.16 (d, J = 8.0 Hz, 4 H), 5.40 (s, 2 H), 2.39 (s, 6 H) ppm; **¹³C-NMR** (101 MHz, CDCl₃): δ = 149.7, 138.8, 137.4, 128.8, 128.2, 113.0, 21.2 ppm; **IR** (ATR): $\tilde{\nu}$ = 3028, 2922, 1725, 1654, 1607, 1511, 1312, 1277, 1177, 925 cm⁻¹; **MS** (EI, 70 eV), m/z (%): 208 (99) [M⁺], 193 (100), 178 (38), 115 (14), 89 (17); **HRMS** (EI-TOF), m/z : [M⁺] calcd. for C₁₆H₁₆: 208.1252; found: 208.1250.



1-[1-(4-Methylphenyl)ethenyl]naphthalene (5.5.2-3ca) [CAS: 127236-58-2]: Compound **5.5.2-3ca** was prepared following the general method A from potassium (*E*)-3-(1-naphthalenyl)acrylate (**5.5.2-1c**) (284 mg, 1.2 mmol) and 4-bromotoluene (**5.5.2-2a**) (175 mg, 126 μ L, 1.0 mmol). **5.5.2-3ca** was isolated as a colorless oil (142 mg, 58%).

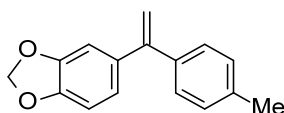
¹H-NMR (400 MHz, CDCl₃): δ = 7.87 (dd, J = 8.0, 5.2 Hz, 2 H), 7.79 (d, J = 8.5 Hz, 1 H), 7.51 (dd, J = 8.0, 7.0 Hz, 1 H), 7.48–7.42 (m, 2 H), 7.34 (ddd, J = 8.3, 6.9, 1.5 Hz, 1 H), 7.25–7.20 (m, 2 H), 7.08 (d, J = 8.0 Hz, 2 H), 5.96 (d, J = 1.5 Hz, 1 H), 5.35 (d, J = 1.5 Hz, 1 H), 2.33 (s, 3 H) ppm; **¹³C-NMR** (101 MHz, CDCl₃): δ = 148.0, 140.0, 138.2, 137.5, 133.6, 131.9, 129.1, 128.1, 127.8, 127.1, 126.5, 126.4, 125.8, 125.6, 125.4, 115.3, 21.1 ppm; **IR** (ATR): $\tilde{\nu}$ = 3043,

2917, 1608, 1509, 1399, 896, 776 cm^{-1} ; **MS** (EI, 70 eV), m/z (%): 244 (100) [M^+], 243 (39), 229 (64), 228 (20), 152 (25), 91 (18); **HRMS** (EI-TOF), m/z : [M^+] calcd. for $\text{C}_{19}\text{H}_{16}$: 244.1252; found: 244.1260.



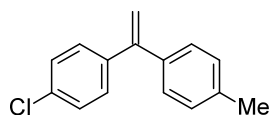
1,2-Dimethoxy-4-(1-p-tolylvinyl)benzene (**5.5.2-3da**) [CAS: 94752-74-6]: Compound **5.5.2-3da** was prepared following the general method A from potassium (*E*)-3-(3,4-dimethoxyphenyl)acrylate (**5.5.2-1d**) (275 mg, 1.2 mmol) and 4-bromotoluene (**5.5.2-2a**) (175 mg, 126 μL , 1.0 mmol). **5.5.2-3da** was isolated as a yellow solid (212 mg, 83%).

$^1\text{H-NMR}$ (400 MHz, CDCl_3): δ = 7.26 (d, J = 8.0 Hz, 2 H), 7.16 (d, J = 8.0 Hz, 2 H), 6.92–6.89 (m, 2 H), 6.84 (d, J = 8.0 Hz, 1 H), 5.37 (s, 2 H), 3.91 (s, 3 H), 3.85 (s, 3 H), 2.38 (s, 3 H) ppm; **$^{13}\text{C-NMR}$** (101 MHz, CDCl_3): δ = 149.5, 148.7, 148.5, 138.7, 137.5, 134.5, 128.8, 128.2, 120.8, 112.5, 111.4, 110.6, 55.9, 55.8, 21.2 ppm; **IR** (ATR): $\tilde{\nu}$ = 3086, 2998, 2961, 2913, 2837, 1738, 1509, 1464, 1413, 1247, 1132, 1026, 899 cm^{-1} ; **MS** (EI, 70 eV), m/z (%): 254 (100) [M^+], 239 (29), 223 (12), 207 (8), 117 (11); **HRMS** (EI-TOF), m/z : [M^+] calcd. for $\text{C}_{17}\text{H}_{18}\text{O}_2$: 254.1207; found: 254.1306.



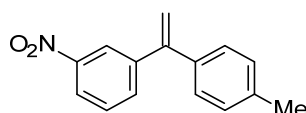
5-(1-p-Tolylvinyl)benzo[d][1,3]dioxole (**5.5.2-3ea**): Compound **5.5.2-3ea** was prepared following the general method A from potassium (*E*)-3-(benzo[d][1,3]dioxol-5-yl)acrylate (**5.5.2-1e**) (230 mg, 1.2 mmol) and 4-bromotoluene (**5.5.2-2a**) (175 mg, 126 μL , 1.0 mmol). **5.5.2-3ea** was isolated as a colorless liquid (95 mg, 40%).

$^1\text{H-NMR}$ (400 MHz, CDCl_3): δ = 7.27–7.25 (m, 2 H), 7.16 (d, J = 8.0 Hz, 2 H), 6.88–6.83 (m, 2 H), 6.79 (d, J = 8.0 Hz, 1 H), 5.98 (s, 2 H), 5.35 (d, J = 0.8 Hz, 2 H), 2.39 (s, 3 H) ppm; **$^{13}\text{C-NMR}$** (101 MHz, CDCl_3): δ = 149.4, 147.4, 147.2, 138.7, 137.5, 135.9, 128.8, 128.2, 122.0, 112.7, 108.7, 107.9, 101.0, 21.2 ppm; **IR** (ATR): $\tilde{\nu}$ = 2894, 2776, 1725, 1652, 1603, 1501, 1485, 1436, 1230, 1034, 934 cm^{-1} ; **MS** (EI, 70 eV), m/z (%): 238 (100) [M^+], 223 (40), 193 (20), 180 (23), 165 (22), 63 (13); **HRMS** (EI-TOF), m/z : [M^+] calcd. for $\text{C}_{16}\text{H}_{14}\text{O}_2$: 238.0994; found: 238.0985.



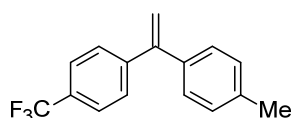
1-Chloro-4-(1-p-tolylvinyl)benzene (**5.5.2-3fa**) [CAS: 69416-93-9]: Compound **5.5.2-3fa** was prepared following the general method A from potassium (*E*)-3-(4-chlorophenyl)acrylate (**5.5.2-1f**) (265 mg, 1.2 mmol) and 4-bromotoluene (**5.5.2-2a**) (175 mg, 126 μ L, 1.0 mmol). **5.5.2-3fa** was isolated as a yellow liquid (152 mg, 67%).

¹H-NMR (400 MHz, CDCl₃): δ = 7.33–7.27 (m, 4 H), 7.23–7.21 (m, 2 H), 7.16 (d, J = 8.0 Hz, 2 H), 5.45 (d, J = 1.3 Hz, 1 H), 5.40 (d, J = 1.3 Hz, 1 H), 2.39 (s, 3 H) ppm; **¹³C-NMR** (101 MHz, CDCl₃): δ = 148.8, 140.1, 138.1, 137.8, 133.5, 129.6, 128.9, 128.3, 128.1, 114.0, 21.2 ppm; **IR** (ATR): $\tilde{\nu}$ = 3093, 3030, 2923, 2856, 1916, 1743, 1605, 1510, 1485, 1089, 1011, 897 cm⁻¹; **MS** (EI, 70 eV), m/z (%): 230 (29) [M^+], 228 (100), 213 (23), 193 (63), 178 (57), 50 (13); **HRMS** (EI-TOF), m/z : [M^+] calcd. for C₁₅H₁₃³⁵Cl: 228.0706; found: 228.0697; C₁₅H₁₃³⁷Cl: 230.0676; found: 230.0699.



1-Nitro-3-(1-p-tolylvinyl)benzene (**5.5.2-3ga**) [CAS: 34564-93-7]: Compound **5.5.2-3ga** was prepared following the general method A from potassium (*E*)-3-(3-nitrophenyl)acrylate (**5.5.2-1g**) (277 mg, 1.2 mmol) and 4-bromotoluene (**5.5.2-2a**) (175 mg, 126 μ L, 1.0 mmol). **5.5.2-3ga** was isolated as a yellow liquid (177 mg, 74%).

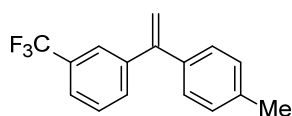
¹H-NMR (400 MHz, CDCl₃): δ = 8.23 (t, J = 1.9 Hz, 1 H), 8.18 (ddd, J = 8.0, 2.3, 1.0 Hz, 1 H), 7.67 (dt, J = 7.7, 1.3 Hz, 1 H), 7.51 (t, J = 8.0 Hz, 1 H), 7.22–7.17 (m, 4 H), 5.58 (d, J = 0.8 Hz, 1 H), 5.52 (d, J = 0.8 Hz, 1 H), 2.40 (s, 3 H) ppm; **¹³C-NMR** (101 MHz, CDCl₃): δ = 148.3, 148.0, 143.5, 138.3, 137.2, 134.2, 129.2, 129.1, 127.9, 123.0, 122.5, 115.8, 21.2 ppm; **IR** (ATR): $\tilde{\nu}$ = 3084, 3047, 3027, 2920, 2863, 1744, 1510, 1346, 1084, 908 cm⁻¹; **MS** (EI, 70 eV), m/z (%): 239 (100) [M^+], 221 (16), 207 (14), 192 (20), 178 (27), 44 (43); **HRMS** (EI-TOF), m/z : [M^+] calcd. for C₁₅H₁₃NO₂: 239.0946; found: 239.0944.



1-Methyl-4-(1-(4-(trifluoromethyl)phenyl)vinyl)benzene (**5.5.2-3ha**) [CAS: 1257310-40-9]: Compound **5.5.2-3ha** was prepared following the general method A from potassium (*E*)-3-(4-

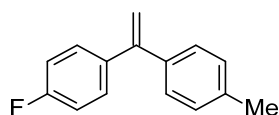
(trifluoromethyl)phenyl)acrylate (**5.5.2-1h**) (305 mg, 1.2 mmol) and 4-bromotoluene (**5.5.2-2a**) (175 mg, 126 μ L, 1.0 mmol). **5.5.2-3ha** was isolated as a colorless liquid (215 mg, 82%).

¹H-NMR (400 MHz, CDCl₃): δ = 7.61 (d, J = 8.3 Hz, 2 H), 7.47 (d, J = 8.0 Hz, 2 H), 7.24–7.17 (m, 4 H), 5.55 (d, J = 0.8 Hz, 1 H), 5.48 (d, J = 0.8 Hz, 1 H), 2.40 (s, 3 H) ppm; **¹³C-NMR** (101 MHz, CDCl₃): δ = 148.8, 145.3, 137.96, 137.7, 129.6 (d, J_{C-F} = 33.7 Hz), 129.0, 128.6, 128.0, 125.1 (q, J_{C-F} = 3.7 Hz), 124.2 (d, J_{C-F} = 270.0 Hz), 115.2, 21.2 ppm; **¹⁹F-NMR** (377 MHz, CDCl₃): δ = -62.4 ppm; **IR** (ATR): $\tilde{\nu}$ = 3028, 2970, 2925, 2875, 1741, 1614, 1509, 1320, 1164, 1110, 1060, 907, 855 cm⁻¹; **MS** (EI, 70 eV), m/z (%): 262 (100) [M⁺], 247 (48), 226 (13), 193 (29), 178 (29), 69 (10); **HRMS** (EI-TOF), m/z : [M⁺] calcd. for C₁₆H₁₃F₃: 262.0969; found: 262.0979.



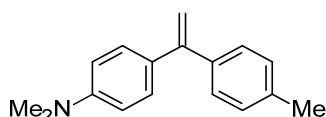
1-(1-p-Tolylvinyl)-3-(trifluoromethyl)benzene (**5.5.2-3ia**): Compound **5.5.2-3ia** was prepared following the general method A from potassium (*E*)-3-(3-(trifluoromethyl)phenyl)acrylate (**5.5.2-1i**) (254 mg, 1.2 mmol) and 4-bromotoluene (**5.5.2-2a**) (175 mg, 126 μ L, 1.0 mmol). **5.5.2-3ia** was isolated as a colorless solid (246 mg, 94%).

¹H-NMR (400 MHz, CDCl₃): δ = 7.63 (s, 1 H), 7.59 (d, J = 8.0 Hz, 1 H), 7.52 (d, J = 8.0 Hz, 1 H), 7.46 (t, J = 8.0 Hz, 1 H), 7.24–7.21 (m, 2 H), 7.18 (d, J = 8.0 Hz, 2 H), 5.54 (d, J = 1.0 Hz, 1 H), 5.46 (d, J = 1.0 Hz, 1 H), 2.40 (s, 3 H) ppm; **¹³C-NMR** (101 MHz, CDCl₃): δ = 148.8, 142.5, 138.0, 137.7, 131.6, 130.6 (d, J_{C-F} = 31.0 Hz), 129.1, 128.6, 128.0, 125.0 (q, J_{C-F} = 3.7 Hz), 124.4 (q, J_{C-F} = 3.7 Hz), 122.8, 115.0, 21.2 ppm; **¹⁹F-NMR** (377 MHz, CDCl₃): δ = -62.5 ppm; **IR** (ATR): $\tilde{\nu}$ = 3012, 2925, 1735, 1511, 1439, 1312, 1338, 1296, 1165, 1149, 1119, 1069, 902 cm⁻¹; **MS** (EI, 70 eV), m/z (%): 262 (100) [M⁺], 247 (64), 193 (25), 178 (28), 69 (13); **HRMS** (EI-TOF), m/z : [M⁺] calcd. for C₁₆H₁₃F₃: 262.0969; found: 262.0967; **m.p.**: 66–67 °C.



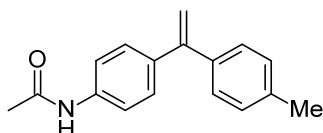
1-Fluoro-4-(1-p-tolylvinyl)benzene (**5.5.2-3ja**) [CAS: 365-23-1]: Compound **5.5.2-3ja** was prepared following the general method A from potassium (*E*)-3-(4-fluorophenyl)acrylate (**5.5.2-1j**) (245 mg, 1.2 mmol) and 4-bromotoluene (**5.5.2-2a**) (175 mg, 126 μ L, 1.0 mmol). **5.5.2-3ja** was isolated as a colorless liquid (156 mg, 74%).

¹H-NMR (400 MHz, CDCl₃): δ = 7.35–7.30 (m, 2 H), 7.25–7.23 (m, 2 H), 7.17 (d, J = 8.0 Hz, 2 H), 7.06–7.00 (m, 2 H), 5.43 (d, J = 1.3 Hz, 1 H), 5.38 (d, J = 1.3 Hz, 1 H), 2.39 (s, 3 H) ppm; **¹³C-NMR** (101 MHz, CDCl₃): δ = 162.5 (d, $J_{\text{C-F}}$ = 247.1 Hz), 148.9, 138.4, 137.72 (d, $J_{\text{C-F}}$ = 3.6 Hz), 137.68, 129.9 (d, $J_{\text{C-F}}$ = 8.2 Hz), 128.9, 128.1, 115.0 (d, $J_{\text{C-F}}$ = 20.9 Hz), 113.5 (d, $J_{\text{C-F}}$ = 1.8 Hz), 21.2 ppm; **¹⁹F-NMR** (377 MHz, CDCl₃): δ = -114.9 ppm; **IR** (ATR): $\tilde{\nu}$ = 3047, 3027, 2924, 1659, 1601, 1506, 1222, 1157, 825 cm⁻¹; **MS** (EI, 70 eV), m/z (%): 212 (100) [M⁺], 211 (11), 197 (64), 196 (34), 177 (26), 50 (11); **HRMS** (EI-TOF), m/z : [M⁺] calcd. for C₁₅H₁₃F: 212.1001; found: 212.0995.



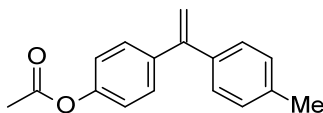
N,N-Dimethyl-4-(1-*p*-tolylvinyl)aniline (**5.5.2-3ka**) [CAS: 116330-41-7]: Compound **5.5.2-3ka** was prepared following the general method A from potassium (*E*)-3-(4-(dimethylamino)phenyl)acrylate (**5.5.2-1k**) (275 mg, 1.2 mmol) and 4-bromotoluene (**5.5.2-2a**) (175 mg, 126 μ L, 1.0 mmol). **5.5.2-3ka** was isolated as a colorless solid (196 mg, 82%).

¹H-NMR (400 MHz, CDCl₃): δ = 7.30–7.25 (m, 4 H), 7.17 (d, J = 8.0 Hz, 2 H), 6.72 (d, J = 8.0 Hz, 2 H), 5.36 (d, J = 1.5 Hz, 1 H), 5.26 (d, J = 1.5 Hz, 1 H), 2.99 (s, 6 H), 2.40 (s, 3 H) ppm; **¹³C-NMR** (101 MHz, CDCl₃): δ = 150.1, 149.6, 139.3, 137.2, 129.0, 128.7, 128.3, 127.1, 111.9, 110.9, 40.5, 21.2 ppm; **IR** (ATR): $\tilde{\nu}$ = 3082, 2891, 2807, 1742, 1611, 1520, 1443, 1362, 1230, 1199, 870 cm⁻¹; **MS** (EI, 70 eV), m/z (%): 237 (100) [M⁺], 222 (11), 178 (14), 44 (19); **HRMS** (EI-TOF), m/z : [M⁺] calcd. for C₁₇H₁₉N: 237.1517; found: 237.1531; **m.p.**: 90–91 °C.



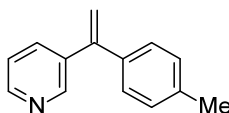
N-(4-(1-Tolylvinyl)phenyl)acetamide (**5.5.2-3la**): Compound **5.5.2-3la** was prepared following the general method A from potassium (*E*)-3-(4-(acetamido)phenyl)acrylate (**5.5.2-1l**) (292 mg, 1.2 mmol) and 4-bromotoluene (**5.5.2-2a**) (175 mg, 126 μ L, 1.0 mmol). **5.5.2-3la** was isolated as a colorless solid (204 mg, 81%).

¹H-NMR (400 MHz): δ = 7.58 (brs, 1 H), 7.48 (d, J = 8.5 Hz, 2 H), 7.30 (d, J = 8.5 Hz, 2 H), 7.23 (d, J = 8.3 Hz, 2 H), 7.15 (d, J = 7.8 Hz, 2 H), 5.39 (s, 2 H), 2.38 (s, 3 H), 2.19 (s, 3 H) ppm; **¹³C-NMR** (101 MHz, CDCl₃): δ = 168.3, 149.2, 138.5, 137.6, 137.5, 137.3, 128.9, 128.8, 128.1, 119.5, 113.2, 24.6, 21.1 ppm; **IR** (ATR): $\tilde{\nu}$ = 3291, 3029, 3922, 1736, 1658, 1591, 1528, 1369, 1314 cm⁻¹; **HRMS** (EI-TOF), m/z : [M⁺] calcd. for C₁₇H₁₇NO: 251.1310; found: 251.1323; **m.p.**: 125–126 °C.



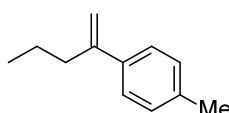
1-Acetyloxy-4-(1-p-tolylvinyl)benzene (**5.5.2-3ma**): Compound **5.5.2-3ma** was prepared following the general method A from potassium (*E*)-3-(4-acetyloxy)acrylate (**5.5.2-1m**) (293 mg, 1.2 mmol) and 4-bromotoluene (**5.5.2-2a**) (175 mg, 126 μ L, 1.0 mmol). **5.5.2-3ma** was isolated as a colorless oil (57 mg, 23%).

¹H-NMR (400 MHz, CDCl₃): δ = 7.39–7.35 (m, 2 H), 7.26 (d, *J* = 8.0 Hz, 2 H), 7.17 (d, *J* = 8.0 Hz, 2 H), 7.08–7.05 (m, 2 H), 5.44 (d, *J* = 1.0 Hz, 1 H), 5.41 (d, *J* = 1.0 Hz, 1 H), 2.39 (s, 3 H), 2.33 (s, 3 H) ppm; **¹³C-NMR** (101 MHz, CDCl₃): δ = 169.5, 150.2, 150.0, 139.3, 138.3, 137.6, 129.3, 128.9, 128.1, 121.2, 113.8, 21.1 (2 C) ppm; **IR** (ATR): $\tilde{\nu}$ = 3025, 2923, 1763, 1506, 1368, 1191, 1163, 1014, 909, 825 cm⁻¹; **MS** (EI, 70 eV), *m/z* (%): 252 (34) [M⁺], 210 (100), 207 (26), 195 (59), 44 (50), 43 (30), 40 (53); **HRMS** (EI-TOF), *m/z*: [M⁺] calcd. for C₁₇H₁₆O₂: 252.1150; found: 252.1144.



3-(1-p-Tolylvinyl)pyridine (**5.5.2-3na**) [CAS: 857436-03-4]: Compound **5.5.2-3na** was prepared following the general method A from potassium (*E*)-3-(pyridin-3-yl)acrylate (**5.5.2-1n**) (225 mg, 1.2 mmol) and 4-bromotoluene (**5.5.2-2a**) (175 mg, 126 μ L, 1.0 mmol). **5.5.2-3na** was isolated as a colorless liquid (140 mg, 72%).

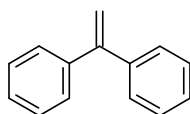
¹H-NMR (400 MHz, CDCl₃): δ = 8.65 (s, 1 H), 8.58 (d, *J* = 4.0 Hz, 1 H), 7.63 (dt, *J* = 8.0, 1.9 Hz, 1 H), 7.29–7.26 (m, 1 H), 7.24–7.22 (m, 2 H), 7.19–7.17 (m, 2 H), 5.56 (d, *J* = 0.8 Hz, 1 H), 5.46 (d, *J* = 0.8 Hz, 1 H), 2.39 (s, 3 H) ppm; **¹³C-NMR** (101 MHz, CDCl₃): δ = 149.2, 148.8, 146.7, 138.0, 137.4, 137.3, 135.6, 129.1, 127.8, 123.0, 115.1, 21.1 ppm; **IR** (ATR): $\tilde{\nu}$ = 3085, 3026, 2921, 1609, 1565, 1510, 1473, 1412, 1021, 899, 824 cm⁻¹; **MS** (EI, 70 eV), *m/z* (%): 195 (100) [M⁺], 180 (70), 115 (14), 51 (20); **HRMS** (EI-TOF), *m/z*: [M⁺] calcd. for C₁₄H₁₃N: 195.1049; found: 195.1047.



1-Methyl-4-(pent-1-en-2-yl)benzene (**5.5.2-3oa**) [CAS: 91176-31-7]: Compound **5.5.2-3oa** was prepared following the general method A from potassium (*E*)-hex-2-enoate (**5.5.2-1o**) (183 mg,

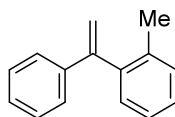
1.2 mmol) and 4-bromotoluene (**5.5.2-2a**) (175 mg, 126 μL , 1.0 mmol). **5.5.2-3oa** was isolated as a colorless liquid (130 mg, 81%).

$^1\text{H-NMR}$ (400 MHz, CDCl_3): δ = 7.32 (d, J = 8.0 Hz, 2 H), 7.15 (d, J = 8.0 Hz, 2 H), 5.25 (s, 1 H), 5.02 (s, 1 H), 2.48 (t, J = 7.5 Hz, 2 H), 2.36 (s, 3 H), 1.53–1.44 (m, 2 H), 0.93 (td, J = 7.4, 0.8 Hz, 3 H) ppm; **$^{13}\text{C-NMR}$** (101 MHz, CDCl_3): δ = 148.2, 138.5, 136.9, 128.9, 126.0, 111.4, 37.4, 21.3, 21.1, 13.8 ppm; **IR** (ATR): $\tilde{\nu}$ = 3085, 2959, 2930, 2872, 1739, 1626, 1513, 1455, 1377, 893 cm^{-1} ; **MS** (EI, 70 eV), m/z (%): 160 (18) [M^+], 145 (47), 132 (100), 117 (48), 115 (30), 91 (26); **HRMS** (EI-TOF), m/z : [M^+] calcd. for $\text{C}_{12}\text{H}_{16}$: 160.1252; found: 160.1259.



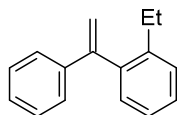
1,1'-Ethenylidenebisbenzene (**5.5.2-3ab**) [CAS: 530-48-3]: Compound **5.5.2-3ab** was prepared following the general method A from potassium cinnamate (**5.5.2-1a**) (223 mg, 1.2 mmol) and bromobenzene (**5.5.2-2b**) (159 mg, 106 μL , 1.0 mmol). **5.5.2-3ab** was isolated as a colorless liquid (132 mg, 73%).

$^1\text{H-NMR}$ (400 MHz, CDCl_3): δ = 7.40–7.30 (m, 10 H), 5.51–45.47 (m, 2 H) ppm; **$^{13}\text{C-NMR}$** (101 MHz, CDCl_3): δ = 150.0, 141.5, 128.2, 128.1, 127.7, 114.3 ppm; **IR** (ATR): $\tilde{\nu}$ = 3080, 3056, 3029, 1610, 1574, 1492, 1444, 1328, 1027, 896 cm^{-1} ; **MS** (EI, 70 eV), m/z (%): 180 (100) [M^+], 179 (80), 178 (53), 165 (49), 73 (37), 50 (30), 44 (33); **HRMS** (EI-TOF), m/z : [M^+] calcd. for $\text{C}_{14}\text{H}_{12}$: 180.0939; found: 180.0942.



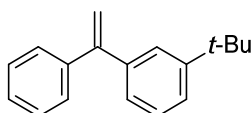
1-Methyl-2-(1-phenylvinyl)benzene (**5.5.2-3ac**) [CAS: 947-77-3]: Compound **5.5.2-3ac** was prepared following the general method A from potassium cinnamate (**5.5.2-1a**) (223 mg, 1.2 mmol) and 2-bromotoluene (**5.5.2-2c**) (171 mg, 120 μL , 1.0 mmol). **5.5.2-3ac** was isolated as a colorless liquid (86 mg, 44%).

$^1\text{H-NMR}$ (400 MHz, CDCl_3): δ = 9.30–9.17 (m, 9 H), 5.77 (d, J = 1.3 Hz, 1 H), 5.20 (d, J = 1.3 Hz, 1 H), 2.07 (s, 3 H) ppm; **$^{13}\text{C-NMR}$** (101 MHz, CDCl_3): δ = 149.4, 141.6, 140.6, 136.1, 130.04, 129.99, 128.3, 127.53, 127.5, 126.4, 125.7, 114.9, 20.1 ppm; **IR** (ATR): $\tilde{\nu}$ = 3058, 3022, 2923, 1614, 1494, 1445, 1028, 901 cm^{-1} ; **MS** (EI, 70 eV), m/z (%): 194 (17) [M^+], 179 (100), 178 (56), 115 (15), 89 (14), 51 (15), 50 (18); **HRMS** (EI-TOF), m/z : [M^+] calcd. for $\text{C}_{15}\text{H}_{14}$: 194.1096; found: 194.1088.



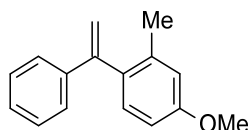
1-Ethyl-2-(1-phenylvinyl)benzene (**5.5.2-3ad**) [CAS: 859315-62-1]: Compound **5.5.2-3ad** was prepared following the general method A from potassium cinnamate (**5.5.2-1a**) (223 mg, 1.2 mmol) and 1-bromo-2-ethylbenzene (**5.5.2-2d**) (227 mg, 170 μ L, 1.0 mmol). **5.5.2-3ad** was isolated as a colorless liquid (120 mg, 57%).

¹H-NMR (400 MHz, CDCl₃): δ = 7.35–7.21 (m, 9 H), 5.80 (d, J = 1.3 Hz, 1 H), 5.23 (d, J = 1.3 Hz, 1 H), 2.44 (q, J = 7.5 Hz, 2 H), 1.06 (t, J = 7.5 Hz, 3 H) ppm; **¹³C-NMR** (101 MHz, CDCl₃): δ = 149.1, 142.1, 141.1, 140.8, 130.2, 128.4, 128.2, 127.7, 127.6, 126.5, 125.6, 114.9, 26.3, 15.2 ppm; **IR** (ATR): $\tilde{\nu}$ = 3024, 2970, 2927, 2873, 1738, 1615, 1322, 1166, 1112, 1062, 905, 854 cm⁻¹; **MS** (EI, 70 eV), m/z (%): 208 (100) [M⁺], 193 (79), 178 (28), 130 (24), 115 (48), 44 (32); **HRMS** (EI-TOF), m/z : [M⁺] calcd. for C₁₆H₁₆: 208.1252; found: 208.1245.



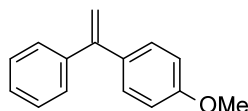
1-tert-Butyl-3-(1-phenylvinyl)benzene (**5.5.2-3ae**) [CAS: 1459147-48-8]: Compound **5.5.2-3ae** was prepared following the general method A from potassium cinnamate (**5.5.2-1a**) (223 mg, 1.2 mmol) and 1-bromo-3-*tert*-butylbenzene (**5.5.2-2e**) (213 mg, 170 μ L, 1.0 mmol). **5.5.2-3ae** was isolated as a yellow liquid (212 mg, 90%).

¹H-NMR (400 MHz, CDCl₃): δ = 7.41–7.33 (m, 7 H), 7.29 (t, J = 8.0 Hz, 1 H), 7.15 (dd, J = 7.5, 1.0 Hz, 1 H), 5.49 (s, 1 H), 5.47 (s, 1 H), 1.33 (s, 9 H) ppm; **¹³C-NMR** (101 MHz, CDCl₃): δ = 151.0, 150.4, 141.5, 141.08, 128.2, 128.1, 127.8, 127.6, 125.6, 125.3, 124.7, 114.0, 34.7, 31.3 ppm; **IR** (ATR): $\tilde{\nu}$ = 3052, 3025, 2962, 1598, 1493, 1364, 1259, 890, 800, 776 cm⁻¹; **MS** (EI, 70 eV), m/z (%): 236 (34) [M⁺], 221 (100), 103 (26), 77 (7), **HRMS** (EI-TOF), m/z : [M⁺] calcd. for C₁₈H₂₀: 236.1565; found: 236.1567.



4-Methoxy-2-methyl-1-(1-phenylvinyl)benzene (**5.5.2-3af**) [CAS: 24890-56-0]: Compound **5.5.2-3af** was prepared following the general method A from potassium cinnamate (**5.5.2-1a**) (223 mg, 1.2 mmol) and 2-bromo-5-methoxytoluene (**5.5.2-2f**) (207 mg, 228 μ L, 1.0 mmol). **5.5.2-3af** was isolated as yellow liquid (213 mg, 95%).

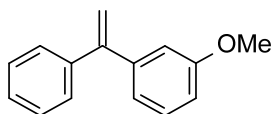
¹H-NMR (400 MHz, CDCl₃): δ = 7.31–7.25 (m, 5 H), 7.17 (d, J = 7.8 Hz, 1 H), 6.80–6.77 (m, 2 H), 5.75 (d, J = 1.5 Hz, 1 H), 5.20 (d, J = 1.3 Hz, 1 H), 3.85 (s, 3 H), 2.05 (s, 3 H) ppm; **¹³C-NMR** (101 MHz, CDCl₃): δ = 158.9, 149.1, 141.0, 137.6, 134.2, 131.1, 128.3, 127.5, 126.5, 115.6, 114.9, 110.7, 55.2, 20.5 ppm; **IR** (ATR): $\tilde{\nu}$ = 3083, 3025, 2953, 2834, 1605, 1572, 1498, 1444, 1293, 1238, 1163, 1040, 899, 807, 777 cm⁻¹; **MS** (EI, 70 eV), m/z (%): 224 (100) [M⁺], 209 (95), 192 (13); **HRMS** (EI-TOF), m/z : [M⁺] calcd. for C₁₆H₁₆O: 224.1201; found: 224.1211.



1-Methoxy-4-(1-phenylvinyl)benzene (**5.5.2-3ag**) [CAS: 4333-75-9]: Compound **5.5.2-3ag** was prepared following the general method A from potassium cinnamate (**5.5.2-1a**) (223 mg, 1.2 mmol) and 4-bromoanisole (**5.5.2-2g**) (189 mg, 127 μ L, 1.0 mmol). **5.5.2-3ag** was isolated as a colorless solid (184 mg, 87%).

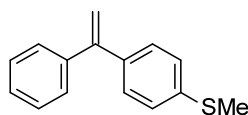
Compound **5.5.2-3ag** was prepared following the general method B from potassium cinnamate (**5.5.2-1a**) (112 mg, 0.6 mmol) and 4-chloroanisole (**5.5.2-2g'**) (73 mg, 63 μ L, 0.5 mmol). **5.5.2-3ag** was isolated as a colorless solid (80 mg, 76%).

¹H-NMR (400 MHz, CDCl₃): δ = 7.38–7.32 (m, 5 H), 7.31–7.28 (m, 2 H), 6.90–6.87 (m, 2 H), 5.42 (d, J = 1.3 Hz, 1 H), 5.37 (d, J = 1.3 Hz, 1 H), 3.84 (s, 3 H) ppm; **¹³C-NMR** (101 MHz, CDCl₃): δ = 159.3, 149.5, 141.8, 136.0, 129.4, 128.3, 128.1, 127.6, 113.5, 112.9, 55.3 ppm; **IR** (ATR): $\tilde{\nu}$ = 3095, 3031, 3005, 2952, 2835, 1737, 1598, 1505, 1242, 1177, 1026, 900, 840 cm⁻¹; **HRMS** (EI-TOF), m/z : [M⁺] calcd. for C₁₅H₁₄O: 210.1045; found: 210.1039; **m.p.**: 74–75 °C.



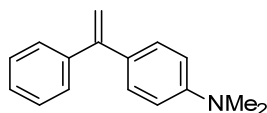
1-Methoxy-3-(1-phenylvinyl)benzene (**5.5.2-3ah**) [CAS: 34564-79-9]: Compound **5.5.2-3ag** was prepared following the general method A from potassium cinnamate (**5.5.2-1a**) (223 mg, 1.2 mmol) and 3-bromoanisole (**5.5.2-2h**) (191 mg, 129 μ L, 1.0 mmol). **5.5.2-3ah** was isolated as a yellow liquid (170 mg, 81%).

¹H-NMR (400 MHz, CDCl₃): δ = 7.37–7.32 (m, 5 H), 7.27 (t, J = 8.0 Hz, 1 H), 6.94 (d, J = 7.5 Hz, 1 H), 6.91–6.87 (m, 2 H), 5.48 (s, 2 H), 3.81 (s, 3 H) ppm; **¹³C-NMR** (101 MHz, CDCl₃): δ = 159.4, 149.9, 143.0, 141.3, 129.1, 128.2, 128.1, 127.7, 120.9, 114.4, 113.9, 113.2, 55.2 ppm; **IR** (ATR): $\tilde{\nu}$ = 3055, 3002, 2937, 2834, 1738, 1596, 1574, 1485, 1283, 1226, 1040, 893, 774 cm⁻¹; **HRMS** (EI-TOF), m/z : [M⁺] calcd. for C₁₅H₁₄O: 210.1045; found: 210.1040.



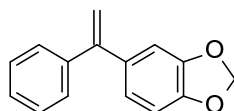
Methyl(4-(1-phenylvinyl)phenyl)sulfane (**5.5.2-3ai**) [CAS: 138534-58-4]: Compound **5.5.2-3ai** was prepared following the general method A from potassium cinnamate (**5.5.2-1a**) (223 mg, 1.2 mmol) and 4-bromothioanisole (**5.5.2-2i**) (207 mg, 1.0 mmol). **5.5.2-3ai** was isolated as a yellow liquid (146 mg, 64%).

¹H-NMR (400 MHz, CDCl₃): δ = 7.35–7.33 (m, 5 H), 7.29–7.26 (m, 2 H), 7.23–7.20 (m, 2 H), 5.45 (d, *J* = 1.0 Hz, 1 H), 5.42 (d, *J* = 1.0 Hz, 1 H), 2.51 (s, 3 H) ppm; **¹³C-NMR** (101 MHz, CDCl₃): δ = 149.4, 141.4, 138.2, 138.0, 128.6, 128.3, 128.2, 127.7, 126.1, 113.87, 15.7 ppm; **IR** (ATR): $\tilde{\nu}$ = 3091, 3017, 2921, 1741, 1590, 1489, 1392, 1078, 901, 830 cm⁻¹; **MS** (EI, 70 eV), *m/z* (%): 226 (100) [M⁺], 211 (10), 179 (31); **HRMS** (EI-TOF), *m/z*: [M⁺] calcd. for C₁₅H₁₄S: 226.0816; found: 226.0757.



N,N-Dimethyl-4-(1-phenylethenyl)benzenamine (**5.5.2-3aj**) [CAS: 22057-80-3]: Compound **5.5.2-3aj** was prepared following the general method A from potassium cinnamate (**5.5.2-1a**) (223 mg, 1.2 mmol) and 1-bromo-*N,N*-dimethylaniline (**5.5.2-2j**) (204 mg, 1.0 mmol). **5.5.2-3aj** was isolated as a yellow liquid (184 mg, 82%).

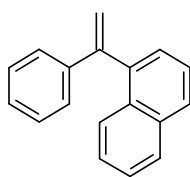
¹H-NMR (400 MHz, CDCl₃): δ = 7.41–7.31 (m, 5 H), 7.28–7.24 (m, 2 H), 6.71 (d, *J* = 8.0 Hz, 2 H), 5.40 (d, *J* = 1.3 Hz, 1 H), 5.27 (d, *J* = 1.3 Hz, 1 H), 2.99 (s, 6 H) ppm; **¹³C-NMR** (101 MHz, CDCl₃): δ = 150.2, 149.8, 142.2, 129.4, 129.0, 128.4, 128.0, 127.4, 111.9, 111.4, 40.5 ppm; **IR** (ATR): $\tilde{\nu}$ = 3084, 3023, 2884, 2851, 2801, 1742, 1604, 1519, 1443, 1350, 1198, 946 cm⁻¹; **MS** (EI, 70 eV), *m/z* (%): 223 (100) [M⁺], 208 (25), 179 (8), 102 (7); **HRMS** (EI-TOF), *m/z*: [M⁺] calcd. for C₁₆H₁₇N: 223.1361; found: 223.1364.



5-(1-Phenylethenyl)benzo[d][1,3]dioxole (**5.5.2-3ak**) [CAS: 51003-88-4]: Compound **5.5.2-3ak** was prepared following the general method A from potassium cinnamate (**5.5.2-1a**) (223 mg, 1.2 mmol) and 1-bromo-3,4-(methylenedioxy)benzene (**5.5.2-2k**) (207 mg, 1.0 mmol). **5.5.2-3ak** was isolated as a colorless liquid (192 mg, 86%).

Compound **5.5.2-3ak** was prepared following the general method B from potassium cinnamate (**5.5.2-1a**) (112 mg, 0.6 mmol) and 1-chloro-3,4-(methylenedioxy)benzene (**5.5.2-2k'**) (80 mg, 60 μ L, 0.5 mmol). **5.5.2-3ak** was isolated as a colorless liquid (100 mg, 88%).

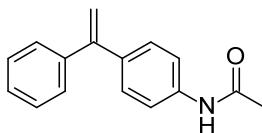
¹H-NMR (400 MHz, CDCl₃): δ = 7.36–7.31 (m, 5 H), 6.85–6.82 (m, 2 H), 6.79 (d, J = 8.0 Hz, 1 H), 5.98 (s, 2 H), 5.40 (d, J = 1.0 Hz, 1 H), 5.37 (d, J = 1.0 Hz, 1 H) ppm; **¹³C-NMR** (101 MHz, CDCl₃): δ = 149.6, 147.5, 147.2, 141.6, 135.7, 128.3, 128.1, 127.7, 122.0, 113.4, 108.6, 107.9, 101.1 ppm; **IR** (ATR): $\tilde{\nu}$ = 3024, 2887, 2778, 1485, 1439, 1231, 1097, 937, 917 cm⁻¹; **MS** (EI, 70 eV), m/z (%): 224 (100) [M⁺], 223 (18), 209 (17), 193 (14), 166 (22), 1645 (33); **HRMS** (EI-TOF), m/z : [M⁺] calcd. for C₁₅H₁₂O₂: 224.0837; found: 224.0855.



1-(1-Phenylvinyl)naphthalene (**5.5.2-3al**) [CAS: 28358-65-8]: Compound **5.5.2-3al** was prepared following the general method A from potassium cinnamate (**5.5.2-1a**) (223 mg, 1.2 mmol) and 1-bromonaphthalene (**5.5.2-2l**) (211 mg, 142 μ L, 1.0 mmol). **5.5.2-3al** was isolated as a yellow liquid (152 mg, 66%).

Compound **5.5.2-3al** was prepared following the general method B from potassium cinnamate (**5.5.2-1a**) (112 mg, 0.6 mmol) and 1-chloronaphthalene (**5.5.2-2l'**) (90 mg, 76 μ L, 0.5 mmol). **5.5.2-3al** was isolated as a yellow liquid (47 mg, 40%).

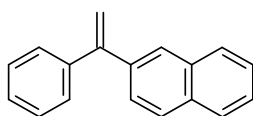
¹H-NMR (400 MHz, CDCl₃): δ = 7.87 (dd, J = 8.0, 4.0 Hz, 2 H), 7.77 (d, J = 8.5 Hz, 1 H), 7.52 (t, J = 8.0 Hz, 1 H), 7.47–7.42 (m, 2 H), 7.36–7.31 (m, 3 H), 7.29–7.25 (m, 3 H), 6.00 (d, J = 1.3 Hz, 1 H), 5.41 (d, J = 1.3 Hz, 1 H) ppm; **¹³C-NMR** (101 MHz, CDCl₃): δ = 148.23, 141.02, 139.76, 133.65, 131.82, 128.35, 128.15, 127.92, 127.67, 127.21, 126.60, 126.40, 125.84, 125.65, 125.41, 116.23 ppm; **IR** (ATR): $\tilde{\nu}$ = 3077, 3050, 3030, 2923, 2855, 1610, 1491, 1339, 1023, 906, 805 cm⁻¹; **MS** (EI, 70 eV), m/z (%): 230 (100) [M⁺], 228 (26), 207 (33), 152 (36), 44 (78); **HRMS** (EI-TOF), m/z : [M⁺] calcd. for C₁₈H₁₄: 230.1096; found: 230.1082.



N-(4-(1-Phenylvinyl)phenyl)acetamide (**5.5.2-3am**) [CAS: 22101-32-2]: Compound **5.5.2-3am** was prepared following the general method A from potassium cinnamate (**5.5.2-1a**) (223 mg,

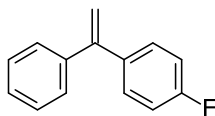
1.2 mmol) and 4-bromoacetanilide (**5.5.2-2m**) (218 mg, 1.0 mmol). **5.5.2-3am** was isolated as a colorless solid (218 mg, 92%).

¹H-NMR (400 MHz, CDCl₃): δ = 7.82 (brs, 1 H), 7.49 (d, J = 8.0 Hz, 2 H), 7.33–7.29 (m, 7 H), 5.42 (d, J = 8.0 Hz, 2 H), 2.19 (s, 3 H) ppm; **¹³C-NMR** (101 MHz, CDCl₃): δ = 168.6, 149.3, 141.4, 137.4, 137.4, 128.7, 128.2, 128.1, 127.7, 119.6, 113.8, 24.5 ppm; **IR** (ATR): $\tilde{\nu}$ = 3299, 3179, 3106, 3032, 2971, 1739, 1666, 1594, 1537, 1506, 1491, 1399, 1373, 1314, 1258, 1009, 897 cm⁻¹; **MS** (EI, 70 eV), m/z (%): 237 (85) [M⁺], 195 (100), 180 (65), 178 (15), 165 (17), 152 (11); **HRMS** (EI-TOF), m/z : [M⁺] calcd. for C₁₆H₁₅NO: 237.1154; found: 237.1155; **m.p.**: 119–120 °C.



2-[1-(Phenylethenyl)]naphthalene (5.5.2-3an) [CAS: 28358-66-9]: Compound **5.5.2-3an** was prepared following the general method A from potassium cinnamate (**5.5.2-1a**) (223 mg, 1.2 mmol) and 2-bromonaphthalene (**5.5.2-2n**) (209 mg, 1.0 mmol). **5.5.2-3an** was isolated as a colorless oil (165 mg, 83%).

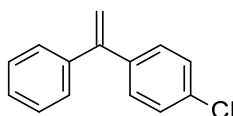
¹H-NMR (400 MHz, CDCl₃): δ = 7.88–7.82 (m, 4 H), 7.52–7.48 (m, 3 H), 7.43–7.37 (m, 5 H), 5.62 (s, 1 H), 5.58 (s, 1 H) ppm; **¹³C-NMR** (101 MHz, CDCl₃): δ = 150.0, 141.5, 138.9, 133.3, 132.9, 128.4, 128.2, 128.2, 127.8, 127.7, 127.6, 127.3, 126.4, 126.1, 126.0, 114.8 ppm; **IR** (ATR): $\tilde{\nu}$ = 3051, 3022, 1505, 1490, 901, 825 cm⁻¹; **MS** (EI, 70 eV), m/z (%): 230 (100) [M⁺], 229 (41), 228 (24), 215 (46), 51 (18), 44 (18); **HRMS** (EI-TOF), m/z : [M⁺] calcd. for C₁₈H₁₄: 230.1096; found: 230.1077.



1-Fluoro-4-(1-phenylvinyl)benzene (5.5.2-3ao) [CAS: 395-21-1]: Compound **5.5.2-3ao** was prepared following the general method A from potassium cinnamate (**5.5.2-1a**) (223 mg, 1.2 mmol) and 4-bromofluorobenzene (**5.5.2-2o**) (177 mg, 111 μ L, 1.0 mmol). **5.5.2-3ao** was isolated as a colorless liquid (182 mg, 92%).

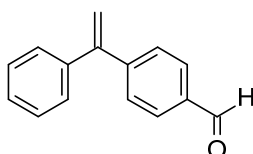
Compound **5.5.2-3ao** was prepared following the general method B from potassium cinnamate (**5.5.2-1a**) (112 mg, 0.6 mmol) and 4-chlorofluorobenzene (**5.5.2-2o'**) (67 mg, 54 μ L, 0.5 mmol). **5.5.2-3ao** was isolated as a colorless liquid (79 mg, 80%).

¹H-NMR (400 MHz, CDCl₃): δ = 7.39–7.30 (m, 7 H), 7.04 (tt, J = 8.0, 4.0 Hz, 2 H), 5.46 (d, J = 1.0 Hz, 1 H), 5.43 (d, J = 1.0 Hz, 1 H) ppm; **¹³C-NMR** (101 MHz, CDCl₃): δ = 162.6 (d, $J_{\text{C-F}}$ = 246.5 Hz), 149.0, 141.3, 137.5 (d, $J_{\text{C-F}}$ = 3.7 Hz), 129.8 (d, $J_{\text{C-F}}$ = 8.1 Hz), 128.23, 128.18, 127.9, 115.0 (d, $J_{\text{C-F}}$ = 22.1 Hz), 114.2 (d, $J_{\text{C-F}}$ = 1.5 Hz) ppm; **¹⁹F-NMR** (377 MHz, CDCl₃): δ = -114.7 ppm; **IR** (ATR): $\tilde{\nu}$ = 3047, 2926, 2854, 1737, 1601, 1504, 1222, 1158, 897, 840 cm⁻¹; **MS** (EI, 70 eV), m/z (%): 198 (100) [M⁺], 182 (63), 177 (25), 51 (15); **HRMS** (EI-TOF), m/z : [M⁺] calcd. for C₁₄H₁₁F: 198.0845; found: 198.0843.



1-Chloro-4-(1-phenylethenyl)benzene (**5.5.2-3ap**) [CAS: 18218-20-7]: Compound **5.5.2-3ap** was prepared following the general method A from potassium cinnamate (**5.5.2-1a**) (223 mg, 1.2 mmol) and 1-bromo-4-chlorobenzene (**5.5.2-2p**) (191 mg, 116 μ L, 1.0 mmol). **5.5.2-3ap** was isolated as a colorless liquid (150 mg, 70%).

¹H-NMR (400 MHz, CDCl₃): δ = 7.40–7.25 (m, 9 H), 5.47 (s, 1 H), 5.46 (s, 1 H) ppm; **¹³C-NMR** (101 MHz, CDCl₃): δ = 149.0, 141.0, 139.9, 133.6, 129.5, 128.33, 128.26, 128.17, 127.9, 144.7 ppm; **IR** (ATR): $\tilde{\nu}$ = 3056, 3028, 2971, 1739, 1661, 1598, 1487, 1445, 1366, 1229, 1217, 1090, 1012 cm⁻¹; **MS** (EI, 70 eV), m/z (%): 216 (23) [M⁺], 214 (78), 199 (11), 179 (100), 152 (10); **HRMS** (EI-TOF), m/z : [M⁺] calcd. for C₁₄H₁₁³⁵Cl: 214.0549; found: 214.0543; C₁₄H₁₁³⁷Cl: 216.0520; found: 216.0524.

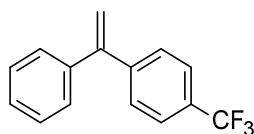


4-(1-Phenylvinyl)benzaldehyde (**5.5.2-3aq**) [CAS: 389582-37-0]: Compound **5.5.2-3aq** was prepared following the general method A from potassium cinnamate (**5.5.2-1a**) (223 mg, 1.2 mmol) and 4-bromobenzaldehyde (**5.5.2-2q**) (187 mg, 1.0 mmol). **5.5.2-3aq** was isolated as a colorless solid (126 mg, 60%).

Compound **5.5.2-3aq** was prepared following the general method B from potassium cinnamate (**5.5.2-1a**) (112 mg, 0.6 mmol) and 4-chlorobenzaldehyde (**5.5.2-2q'**) (70 mg, 59 μ L, 0.5 mmol). **5.5.2-3aq** was isolated as a colorless solid (60 mg, 58%).

¹H-NMR (400 MHz, CDCl₃): δ = 10.0 (s, 1 H), 7.87 (dt, J = 8.0, 4.0 Hz, 2 H), 7.52 (dd, J = 8.0, 4.0 Hz, 2 H), 7.40–7.30 (m, 5 H), 5.60 (dd, J = 4.8, 0.8 Hz, 2 H) ppm; **¹³C-NMR** (101 MHz, CDCl₃): δ = 191.9, 149.1, 147.6, 140.5, 135.6, 129.7, 128.6, 128.4, 128.2, 128.1, 116.5 ppm;

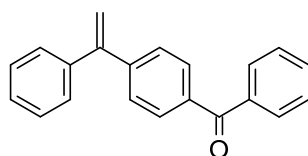
IR (ATR): $\tilde{\nu}$ = 3050, 2833, 2740, 1696, 1602, 1562, 1488, 1208, 913 cm^{-1} ; **MS** (EI, 70 eV), m/z (%): 237 (85) [M^+], 195 (100), 180 (65), 178 (15), 165 (17), 152 (11); **HRMS** (EI-TOF), m/z : [M^+] calcd. for $\text{C}_{15}\text{H}_{12}\text{O}$: 208.0888; found: 208.0883; **m.p.**: 54–55 $^{\circ}\text{C}$.



1-(1-Phenylethenyl)-4-(trifluoromethyl)benzene (**5.5.2-3ar**) [CAS: 345-88-0]: Compound **5.5.2-3ar** was prepared following the general method A from potassium cinnamate (**5.5.2-1a**) (223 mg, 1.2 mmol) and 1-bromo-4-(trifluoromethyl)benzene (**5.5.2-2r**) (227 mg, 142 μL , 1.0 mmol). **5.5.2-3ar** was isolated as a colorless oil (155 mg, 62%).

Compound **5.5.2-3ar** was prepared following the general method B from potassium cinnamate (**5.5.2-1a**) (112 mg, 0.6 mmol) and 1-chloro-4-(trifluoromethyl)benzene (**5.5.2-2r'**) (92 mg, 68 μL , 0.5 mmol). **5.5.2-3ar** was isolated as a colorless oil (80 mg, 65%).

$^1\text{H-NMR}$ (400 MHz, CDCl_3): δ = 7.61 (d, J = 8.3 Hz, 2 H), 7.47 (d, J = 8.3 Hz, 2 H), 7.40–7.31 (m, 5 H), 5.58 (s, 1 H), 5.53 (s, 1 H) ppm; **$^{13}\text{C-NMR}$** (101 MHz, CDCl_3): δ = 149.0, 145.1 (q, $J_{\text{C-F}}$ = 1.5 Hz), 140.6, 129.7 (q, $J_{\text{C-F}}$ = 33.0 Hz), 128.5, 128.4, 128.14, 128.08, 125.2 (q, $J_{\text{C-F}}$ = 3.7 Hz), 124.2 (q, $J_{\text{C-F}}$ = 272.2 Hz), 115.9 ppm; **$^{19}\text{F-NMR}$** (377 MHz, CDCl_3): δ = -62.5 ppm; **IR** (ATR): $\tilde{\nu}$ = 3057, 2926, 2856, 1740, 1616, 1319, 1164, 1121, 1063, 1016, 905, 850 cm^{-1} ; **MS** (EI, 70 eV), m/z (%): 248 (100) [M^+], 233 (32), 227 (15), 179 (76), 151 (7); **HRMS** (EI-TOF), m/z : [M^+] calcd. for $\text{C}_{15}\text{H}_{11}\text{F}_3$: 248.0813; found: 248.0791.

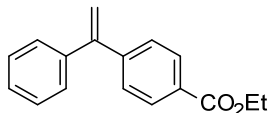


Phenyl(4-(1-phenylvinyl)phenyl)methanone (**5.5.2-3as**) [CAS: 682748-25-0]: Compound **5.5.2-3as** was prepared following the general method A from potassium cinnamate (**5.5.2-1a**) (223 mg, 1.2 mmol) and 4-bromobenzophenone (**5.5.2-2s**) (269 mg, 1.0 mmol). **5.5.2-3as** was isolated as a yellow solid (188 mg, 66%).

Compound **5.5.2-3as** was prepared following the general method B from potassium cinnamate (**5.5.2-1a**) (112 mg, 0.6 mmol) and 4-chlorobenzophenone (**5.5.2-2s'**) (109 mg, 0.5 mmol). **5.5.2-3as** was isolated as a yellow solid (89 mg, 63%).

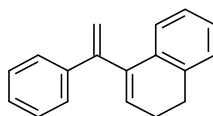
$^1\text{H-NMR}$ (400 MHz, CDCl_3): δ = 7.86–7.83 (m, 2 H), 7.81 (dt, J = 8.0, 4.0 Hz, 2 H), 7.63–7.59 (m, 1 H), 7.53–7.46 (m, 4 H), 7.41–7.34 (m, 5 H), 5.59 (s, 2 H) ppm; **$^{13}\text{C-NMR}$** (101 MHz,

CDCl₃): δ = 196.3, 149.3, 145.6, 140.7, 137.6, 136.7, 132.4, 130.1, 123.0, 128.3, 128.3, 128.2, 128.1, 128.0, 115.9 ppm; **IR** (ATR): $\tilde{\nu}$ = 3096, 3050, 3029, 1648, 1595, 1442, 1311, 1274, 905, 859 cm⁻¹; **MS** (EI, 70 eV), m/z (%): 284 (100) [M⁺], 207 (69), 178 (17), 105 (24), 77 (25); **HRMS** (EI-TOF), m/z : [M⁺] calcd. for C₂₁H₁₆O: 284.1201; found: 284.1199; **m.p.**: 73–74 °C.



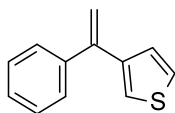
Ethyl 4-(1-phenylvinyl)benzoate (**5.5.2-3at**) [CAS: 679390-82-0]: Compound **5.5.2-3at** was prepared following the general method A from potassium cinnamate (**5.5.2-1a**) (223 mg, 1.2 mmol) and ethyl 4-bromobenzoate (**5.5.2-2t**) (232 mg, 162 μ L, 1.0 mmol). **5.5.2-3at** was isolated as a yellow liquid (126 mg, 50%).

¹H-NMR (400 MHz, CDCl₃): δ = 8.02 (dt, J = 8.0, 4.0 Hz, 2 H), 7.42 (dt, J = 8.0, 4.0 Hz, 2 H), 7.38–7.31 (m, 5 H), 5.55 (dd, J = 5.5, 0.8 Hz, 2 H), 4.40 (q, J = 7.0 Hz, 2 H), 1.41 (t, J = 7.2 Hz, 3 H) ppm; **¹³C-NMR** (101 MHz, CDCl₃): δ = 166.4, 149.3, 145.9, 140.8, 129.7, 129.5, 128.3, 128.2, 128.0, 115.8, 60.9, 14.3 ppm; **IR** (ATR): $\tilde{\nu}$ = 3091, 3029, 2990, 2934, 1703, 1605, 1367, 1271, 1178, 1104, 1017, 907, 866 cm⁻¹; **MS** (EI, 70 eV), m/z (%): 252 (65) [M⁺], 240 (41), 224 (21), 207 (100), 180 (30), 163 (40), 105 (49); **HRMS** (EI-TOF), m/z : [M⁺] calcd. for C₁₇H₁₆O₂: 252.1150; found: 252.1159.



4-(1-Phenylvinyl)-1,2-dihydronaphthalene (**5.5.2-3au**): Compound **5.5.2-3au** was prepared following the general method A from potassium cinnamate (**5.5.2-1a**) (223 mg, 1.2 mmol) and 4-bromo-1,2-dihydronaphthalene (**5.5.2-2u**) (209 mg, 1.0 mmol). **5.5.2-3au** was isolated as a colorless oil (93 mg, 40%) along with the approximate 5% of the s-cis isomer.

¹H-NMR (400 MHz, CDCl₃): δ = 7.46–7.43 (m, 2 H), 7.30–7.22 (m, 3 H), 7.16 (d, J = 4.0 Hz, 2 H), 7.08 (td, J = 7.3 Hz, 1 H), 7.01 (td, J = 7.5 Hz, 1 H), 6.93 (d, J = 8.0 Hz, 1 H), 6.16 (t, J = 4.6 Hz, 1 H), 5.66 (d, J = 1.8 Hz, 1 H), 5.36 (d, J = 1.8 Hz, 1 H), 2.89 (t, J = 8.0 Hz, 1 H), 2.45–2.40 (m, 2 H) ppm; **¹³C-NMR** (101 MHz, CDCl₃): δ = 148.5, 140.0, 139.5, 136.1, 134.3, 128.7, 128.3, 127.6, 127.4, 126.7, 126.6, 126.3, 125.6, 114.8, 28.2, 23.4 ppm; **IR** (ATR): $\tilde{\nu}$ = 3057, 3024, 2932, 2882, 2829, 1493, 1484, 1446, 1022, 899 cm⁻¹; **MS** (EI, 70 eV), m/z (%): 232.0 (100) [M⁺], 231.1 (24), 217.1 (32), 128.0 (22), 77.0 (15), 51.0 (13); **HRMS** (EI-TOF), m/z : [M⁺] calcd. for C₁₈H₁₆: 232.1252; found: 232.1259.



3-(1-Phenylethenyl)-thiophen (**5.5.2-3av**) [CAS: 75488-46-9]: Compound **5.5.2-3av** was prepared following the general method A from potassium cinnamate (**5.5.2-1a**) (223 mg, 1.2 mmol) and 3-bromothiophene (**5.5.2-2v**) (168 mg, 97 μ L, 1.0 mmol). **5.5.2-3av** was isolated as a colorless oil (55 mg, 29%).

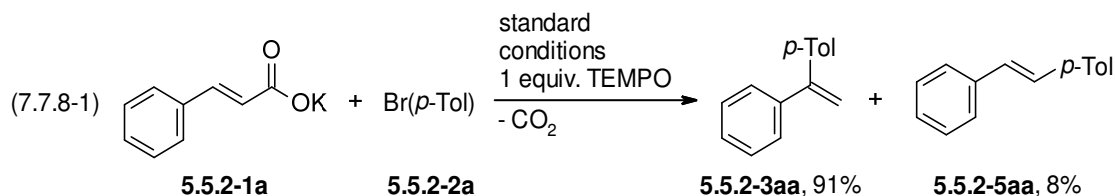
¹H-NMR (400 MHz, CDCl₃): δ = 7.43–7.34 (m, 5 H), 7.33–7.30 (m, 1 H), 7.21–7.18 (m, 1 H), 7.15–7.13 (m, 1 H), 5.55 (d, J = 1.3 Hz, 1 H), 5.35 (d, J = 1.3 Hz, 1 H) ppm; **¹³C-NMR** (101 MHz, CDCl₃): δ = 144.5, 142.5, 141.5, 128.2, 128.1, 127.8, 127.2, 125.4, 123.3, 113.4 ppm; **IR** (ATR): $\tilde{\nu}$ = 3104, 3058, 3023, 1607, 1492, 1444, 1302, 1081, 1027, 891 cm⁻¹; **MS** (EI, 70 eV), m/z (%): 186.0 (100) [M⁺], 185.1 (63), 184.2 (27), 171.1 (34), 50.0 (21), 44.9 (18); **HRMS** (EI-TOF), m/z : [M⁺] calcd. for C₁₂H₁₀S: 186.0503; found: 186.0501.

7.7.7 Procedure for the one-pot three-step process

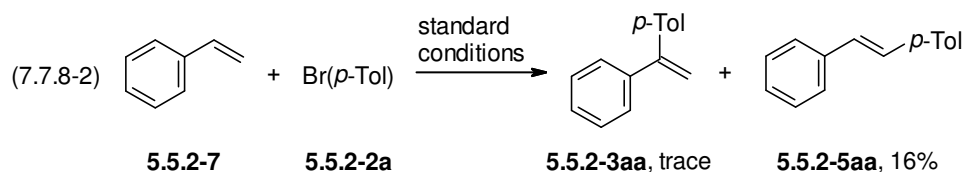
An oven-dried, nitrogen-flushed 20 mL crimp cap vessel was charged with Pd(acac)₂ (3.1 mg, 0.01 mmol, 2.0 mol%), P(*o*-Tol)₃ (7.8 mg, 0.025 mmol, 5.0 mol%) and potassium acetate (32.7 mg, 0.6 mmol). A degassed mixture of NMP and quinoline (1:1, 2.0 mL), bromobenzene (**5.5.2-2b**) (79.3 mg, 53 μ L, 0.5 mmol) and methyl acrylate (**5.5.2-6**) (43.5 mg, 46 μ L, 0.5 mmol) were added *via* syringe. The resulting mixture was then stirred at 150 °C for 16 h. After the reaction was complete, the mixture was cooled to RT. The vessel was opened inside a glove box and potassium *tert*-butoxide (137 mg, 1.1 mmol) was added. Outside the glove box water (10 mg, 10 μ L, 0.55 mmol) was added *via* syringe. The resulting mixture was then stirred at 100 °C for 2 h. After the reaction was complete, the mixture was cooled to RT. A degassed solution of Pd(acac)₂ (3.1 mg, 0.01 mmol, 2.0 mol%), P(*o*-Tol)₃ (7.8 mg, 0.025 mmol, 5.0 mol%), CuBr (7.3 mg, 0.05 mmol, 10.0 mol%), 1,10-phenanthroline (9.1 mg, 0.05 mmol, 10.0 mol%) in a mixture of NMP and quinoline (1:1, 1.0 mL) and 4-bromotoluene (**5.5.2-2a**) (85.5 mg, 62 μ L, 0.5 mmol) were added *via* syringe. The resulting mixture was then stirred at 170 °C for 16 h. After the reaction was complete, the mixture was cooled to RT, diluted with 1 N HCl (20 mL) and extracted with ethyl acetate (3 \times 50 mL). The combined organic layers were washed with water and brine, dried over MgSO₄, filtered, and concentrated in vacuo. The residue was purified by column chromatography (SiO₂, ethyl acetate/cyclohexane gradient) yielding **5.5.2-3aa** as a colorless liquid (60 mg, 62%).

7.7.8 Control experiments

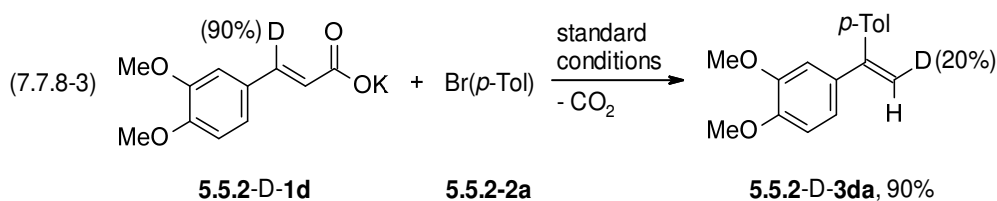
The standard reaction was conducted in the presence of the radical scavenger TEMPO (Eq. 7.7.8-1). This did not quench the reaction, which suggests that it does not proceed *via* a radical process.



The reaction of styrene **5.5.2-7** with 4-bromotoluene **5.5.2-2a** under standard conditions yields the linear product **5.5.2-5** in high selectivity, which rules out a reaction pathway *via* a protodecarboxylation followed by a Heck reaction (Eq. 7.7.8-2).



When the reaction was performed with the deuterium-labelled starting material **5.5.2-D-1d**, only 20% of the deuterium was incorporated in the previous position of the carboxylate group. This indicates that the Heck coupling and the decarboxylation are not concerted but separate steps (Eq. 7.7.8-3).



8 Literaturverzeichnis

- [1] G. S. Zweifel, M. H. Nantz, P. Somfai, *Modern Organic Synthesis: An Introduction*, John Wiley & Sons, Hoboken, **2017**.
- [2] L. J. Goossen, C. Linder, N. Rodríguez, P. P. Lange, *Chem. – Eur. J.* **2009**, *15*, 9336–9349.
- [3] A. de Meijere, F. Diederich, *Metal-Catalyzed Cross-Coupling Reactions*, Wiley-VCH, Weinheim, **2004**.
- [4] P. T. Anastas, J. C. Warner, *Green Chemistry: Theory and Practice*, Oxford Univ. Press, Oxford, **2000**.
- [5] P. T. Anastas, R. H. Crabtree, Eds., *Handbook of Green Chemistry*, Wiley-VCH, Weinheim, **2009**.
- [6] P. Anastas, N. Eghbali, *Chem. Soc. Rev.* **2009**, *39*, 301–312.
- [7] R. A. Sheldon, *Pure Appl. Chem.* **2000**, *72*, 1233–1246.
- [8] D. J. C. Constable, P. J. Dunn, J. D. Hayler, G. R. Humphrey, J. Johnnie L. Leazer, R. J. Linderman, K. Lorenz, J. Manley, B. A. Pearlman, A. Wells, et al., *Green Chem.* **2007**, *9*, 411–420.
- [9] G. W. V. Cave, C. L. Raston, J. L. Scott, *Chem. Commun.* **2001**, 2159–2169.
- [10] L. J. Gooßen, N. Rodríguez, K. Gooßen, *Angew. Chem. Int. Ed.* **2008**, *47*, 3100–3120.
- [11] T. Patra, D. Maiti, *Chem. – Eur. J.* **2017**, *23*, 7383–7401.
- [12] N. Rodríguez, L. J. Goossen, *Chem. Soc. Rev.* **2011**, *40*, 5030–5048.
- [13] K. P. C. Vollhardt, N. E. Schore, H. Butenschön, K.-M. Roy, *Organische Chemie*, Wiley-VCH, Weinheim, **2011**.
- [14] M. Smith, J. March, *March's Advanced Organic Chemistry: Reactions, Mechanisms, and Structure*, Wiley-Interscience, Hoboken, **2007**.
- [15] E. Breitmaier, G. Jung, *Organische Chemie*, Thieme, Stuttgart, **2009**.
- [16] H. Kolbe, *J. Für Prakt. Chem.* **1874**, *10*, 89–112.
- [17] E. Knoevenagel, *Berichte Dtsch. Chem. Ges.* **1898**, *31*, 2596–2619.
- [18] W. H. Perkin, *J. Chem. Soc.* **1877**, *31*, 388–427.
- [19] G. P. Chiusoli, P. M. Maitlis, Royal Society of Chemistry (Great Britain), Eds., *Metal-Catalysis in Industrial Organic Processes*, RSC Pub, Cambridge, **2006**.
- [20] K. Weissmehl, H.-J. Arpe, *Industrielle Organische Chemie: Bedeutende Vor- und Zwischenprodukte*, Wiley-VCH, Weinheim, New York, **1998**.
- [21] R. A. F. Tomás, J. C. M. Bordado, J. F. P. Gomes, *Chem. Rev.* **2013**, *113*, 7421–7469.

- [22] O. Hromatka, H. Ebner, *Ind. Eng. Chem.* **1959**, *51*, 1279–1280.
- [23] G. J. Sunley, D. J. Watson, *Catal. Today* **2000**, *58*, 293–307.
- [24] P. N. R. Vennestrøm, C. M. Osmundsen, C. H. Christensen, E. Taarning, *Angew. Chem. Int. Ed.* **2011**, *50*, 10502–10509.
- [25] U. Biermann, U. Bornscheuer, M. A. R. Meier, J. O. Metzger, H. J. Schäfer, *Angew. Chem. Int. Ed.* **2011**, *50*, 3854–3871.
- [26] A. Behr, J. P. Gomes, *Eur. J. Lipid Sci. Technol.* **2010**, *112*, 31–50.
- [27] W. I. Dzik, P. P. Lange, L. J. Gooßen, *Chem. Sci.* **2012**, *3*, 2671–2678.
- [28] H. A. Chiong, Q.-N. Pham, O. Daugulis, *J. Am. Chem. Soc.* **2007**, *129*, 9879–9884.
- [29] M. Miura, T. Tsuda, T. Satoh, S. Pivsa-Art, M. Nomura, *J. Org. Chem.* **1998**, *63*, 5211–5215.
- [30] R. Giri, N. Mangel, J.-J. Li, D.-H. Wang, S. P. Breazzano, L. B. Saunders, J.-Q. Yu, *J. Am. Chem. Soc.* **2007**, *129*, 3510–3511.
- [31] K. Ueura, T. Satoh, M. Miura, *Org. Lett.* **2007**, *9*, 1407–1409.
- [32] G. Shi, Y. Zhang, *Adv. Synth. Catal.* **2014**, *356*, 1419–1442.
- [33] M. Pichette-Drapeau, L. J. Gooßen, *Chem. – Eur. J.* **2016**, *22*, 18654–18677.
- [34] M. O. Konev, E. R. Jarvo, *Angew. Chem. Int. Ed.* **2016**, *55*, 11340–11342.
- [35] J. Xuan, Z.-G. Zhang, W.-J. Xiao, *Angew. Chem.* **2015**, *127*, 15854–15864.
- [36] K. Okada, K. Okamoto, N. Morita, K. Okubo, M. Oda, *J. Am. Chem. Soc.* **1991**, *113*, 9401–9402.
- [37] Y. Wei, P. Hu, M. Zhang, W. Su, *Chem. Rev.* **2017**, *117*, 8864–8907.
- [38] G. J. P. Perry, I. Larrosa, *Eur. J. Org. Chem.* **2017**, 3517–3527.
- [39] M. Font, J. M. Quibell, G. J. P. Perry, I. Larrosa, *Chem. Commun.* **2017**, *53*, 5584–5597.
- [40] G. Chen, Z. Zhuang, G.-C. Li, T. G. Saint-Denis, Y. Hsiao, C. L. Joe, J.-Q. Yu, *Angew. Chem. Int. Ed.* **2017**, *56*, 1506–1509.
- [41] Y. Zhu, X. Chen, C. Yuan, G. Li, J. Zhang, Y. Zhao, *Nat. Commun.* **2017**, *8*, 14904.
- [42] M. H. Shaw, J. Twilton, D. W. C. MacMillan, *J. Org. Chem.* **2016**, *81*, 6898–6926.
- [43] Z. Zuo, D. T. Ahneman, L. Chu, J. A. Terrett, A. G. Doyle, D. W. C. MacMillan, *Science* **2014**, *345*, 437–440.
- [44] Z. Zuo, D. W. C. MacMillan, *J. Am. Chem. Soc.* **2014**, *136*, 5257–5260.
- [45] S. Ventre, F. R. Petronijevic, D. W. C. MacMillan, *J. Am. Chem. Soc.* **2015**, *137*, 5654–5657.
- [46] T. Qin, J. Cornella, C. Li, L. R. Malins, J. T. Edwards, S. Kawamura, B. D. Maxwell, M. D. Eastgate, P. S. Baran, *Science* **2016**, *352*, 801–805.

- [47] K. M. M. Huihui, J. A. Caputo, Z. Melchor, A. M. Olivares, A. M. Spiewak, K. A. Johnson, T. A. DiBenedetto, S. Kim, L. K. G. Ackerman, D. J. Weix, *J. Am. Chem. Soc.* **2016**, *138*, 5016–5019.
- [48] M. J. Schnermann, L. E. Overman, *Angew. Chem. Int. Ed.* **2012**, *51*, 9576–9580.
- [49] G. Pratsch, G. L. Lackner, L. E. Overman, *J. Org. Chem.* **2015**, *80*, 6025–6036.
- [50] J.-A. García-López, M. F. Greaney, *Chem. Soc. Rev.* **2016**, *45*, 6766–6798.
- [51] L. Pu, *Chem. Rev.* **1998**, *98*, 2405–2494.
- [52] D. A. Horton, G. T. Bourne, M. L. Smythe, *Chem. Rev.* **2003**, *103*, 893–930.
- [53] P. J. Hajduk, M. Bures, J. Praestgaard, S. W. Fesik, *J. Med. Chem.* **2000**, *43*, 3443–3447.
- [54] A. V. R. Rao, M. K. Gurjar, K. L. Reddy, A. S. Rao, *Chem. Rev.* **1995**, *95*, 2135–2167.
- [55] X. Mei, C. Wolf, *Chem. Commun.* **2004**, 2078–2079.
- [56] A. Zahn, C. Brotschi, C. J. Leumann, *Chem. – Eur. J.* **2005**, *11*, 2125–2129.
- [57] J. R. Nitschke, T. D. Tilley, *J. Am. Chem. Soc.* **2001**, *123*, 10183–10190.
- [58] F. Babudri, G. M. Farinola, F. Naso, R. Ragni, *Chem. Commun.* **2007**, 1003–1022.
- [59] M. Nilsson, E. Kulonen, S. Sunner, V. Frank, J. Brunvoll, E. Bunnenberg, C. Djerassi, R. Records, *Acta Chem. Scand.* **1966**, *20*, 423–426.
- [60] M. Nilsson, C. Ullenius, U.-Å. Blom, N. A. Zaidi, *Acta Chem. Scand.* **1968**, *22*, 1998–2002.
- [61] P. E. Fanta, *Synthesis* **1974**, *1974*, 9–21.
- [62] A. F. Shepard, N. R. Winslow, J. R. Johnson, *J. Am. Chem. Soc.* **1930**, *52*, 2083–2090.
- [63] L. J. Gooßen, G. Deng, L. M. Levy, *Science* **2006**, *313*, 662–664.
- [64] L. J. Goossen, N. Rodríguez, B. Melzer, C. Linder, G. Deng, L. M. Levy, *J. Am. Chem. Soc.* **2007**, *129*, 4824–4833.
- [65] Z.-C. Cao, Q.-Y. Luo, Z.-J. Shi, *Org. Lett.* **2016**, *18*, 5978–5981.
- [66] G. A. Grasa, S. P. Nolan, *Org. Lett.* **2001**, *3*, 119–122.
- [67] L. J. Gooßen, B. Zimmermann, T. Knauber, *Angew. Chem. Int. Ed.* **2008**, *47*, 7103–7106.
- [68] L. J. Goossen, N. Rodríguez, C. Linder, *J. Am. Chem. Soc.* **2008**, *130*, 15248–15249.
- [69] L. J. Gooßen, N. Rodríguez, P. P. Lange, C. Linder, *Angew. Chem. Int. Ed.* **2010**, *49*, 1111–1114.
- [70] B. Song, T. Knauber, L. J. Gooßen, *Angew. Chem. Int. Ed.* **2013**, *52*, 2954–2958.
- [71] L. J. Goossen, B. Melzer, *J. Org. Chem.* **2007**, *72*, 7473–7476.
- [72] L. J. Goossen, T. Knauber, *J. Org. Chem.* **2008**, *73*, 8631–8634.

- [73] L. J. Gooßen, N. Rodríguez, C. Linder, B. Zimmermann, T. Knauber, *Org. Synth.* **2008**, 85, 196.
- [74] L. J. Gooßen, F. Rudolphi, C. Oppel, N. Rodríguez, *Angew. Chem. Int. Ed.* **2008**, 47, 3043–3045.
- [75] F. Rudolphi, B. Song, L. J. Gooßen, *Adv. Synth. Catal.* **2011**, 353, 337–342.
- [76] J. Tang, L. J. Gooßen, *Org. Lett.* **2014**, 16, 2664–2667.
- [77] S. Bhowmik, G. Pandey, S. Batra, *Chem. – Eur. J.* **2013**, 19, 10487–10491.
- [78] P. P. Lange, L. J. Gooßen, P. Podmore, T. Underwood, N. Sciammetta, *Chem. Commun.* **2011**, 47, 3628–3630.
- [79] L. J. Gooßen, B. Zimmermann, C. Linder, N. Rodríguez, P. P. Lange, J. Hartung, *Adv. Synth. Catal.* **2009**, 351, 2667–2674.
- [80] J.-M. Becht, C. Catala, C. Le Drian, A. Wagner, *Org. Lett.* **2007**, 9, 1781–1783.
- [81] J.-M. Becht, C. L. Drian, *Org. Lett.* **2008**, 10, 3161–3164.
- [82] Z. Wang, Q. Ding, X. He, J. Wu, *Tetrahedron* **2009**, 65, 4635–4638.
- [83] Z. Wang, Q. Ding, X. He, J. Wu, *Org. Biomol. Chem.* **2009**, 7, 863–865.
- [84] L. J. Gooßen, P. P. Lange, N. Rodríguez, C. Linder, *Chem. – Eur. J.* **2010**, 16, 3906–3909.
- [85] L. J. Gooßen, C. Linder, N. Rodríguez, P. P. Lange, A. Fromm, *Chem. Commun.* **2009**, 7173–7175.
- [86] L. J. Gooßen, N. Rodríguez, C. Linder, P. P. Lange, A. Fromm, *ChemCatChem* **2010**, 2, 430–442.
- [87] R. Shang, Y. Fu, Y. Wang, Q. Xu, H.-Z. Yu, L. Liu, *Angew. Chem. Int. Ed.* **2009**, 48, 9350–9354.
- [88] R. Shang, Q. Xu, Y.-Y. Jiang, Y. Wang, L. Liu, *Org. Lett.* **2010**, 12, 1000–1003.
- [89] L. W. Sardzinski, W. C. Wertjes, A. M. Schnaith, D. Kalyani, *Org. Lett.* **2015**, 17, 1256–1259.
- [90] M. Yamashita, K. Hirano, T. Satoh, M. Miura, *Org. Lett.* **2010**, 12, 592–595.
- [91] R. Shang, Y. Fu, J.-B. Li, S.-L. Zhang, Q.-X. Guo, L. Liu, *J. Am. Chem. Soc.* **2009**, 131, 5738–5739.
- [92] K. Park, G. Bae, J. Moon, J. Choe, K. H. Song, S. Lee, *J. Org. Chem.* **2010**, 75, 6244–6251.
- [93] D. Zhao, C. Gao, X. Su, Y. He, J. You, Y. Xue, *Chem. Commun.* **2010**, 46, 9049–9051.
- [94] P. Forgione, M.-C. Brochu, M. St-Onge, K. H. Thesen, M. D. Bailey, F. Bilodeau, *J. Am. Chem. Soc.* **2006**, 128, 11350–11351.

- [95] F. Bilodeau, M.-C. Brochu, N. Guimond, K. H. Thesen, P. Forgione, *J. Org. Chem.* **2010**, *75*, 1550–1560.
- [96] C. Peschko, C. Winklhofer, W. Steglich, *Chem. – Eur. J.* **2000**, *6*, 1147–1152.
- [97] M. Nakano, H. Tsurugi, T. Satoh, M. Miura, *Org. Lett.* **2008**, *10*, 1851–1854.
- [98] M. Miyasaka, A. Fukushima, T. Satoh, K. Hirano, M. Miura, *Chem. – Eur. J.* **2009**, *15*, 3674–3677.
- [99] M. Miyasaka, K. Hirano, T. Satoh, M. Miura, *Adv. Synth. Catal.* **2009**, *351*, 2683–2688.
- [100] F. Zhang, M. F. Greaney, *Org. Lett.* **2010**, *12*, 4745–4747.
- [101] R.-T. He, J.-F. Wang, H.-F. Wang, Z.-G. Ren, J.-P. Lang, *Dalton Trans.* **2014**, *43*, 9786.
- [102] X. Li, D. Zou, F. Leng, C. Sun, J. Li, Y. Wu, Y. Wu, *Chem Commun* **2013**, *49*, 312–314.
- [103] C. K. Haley, C. D. Gilmore, B. M. Stoltz, *Tetrahedron* **2013**, *69*, 5732–5736.
- [104] L.-C. Campeau, K. Fagnou, *Chem Soc Rev* **2007**, *36*, 1058–1068.
- [105] J.-B. Rouchet, C. Schneider, C. Spitz, J. Lefèvre, G. Dupas, C. Fruit, C. Hoarau, *Chem. – Eur. J.* **2014**, *20*, 3610–3615.
- [106] O. Daugulis, H.-Q. Do, D. Shabashov, *Acc. Chem. Res.* **2009**, *42*, 1074–1086.
- [107] D. A. Colby, R. G. Bergman, J. A. Ellman, *Chem. Rev.* **2010**, *110*, 624–655.
- [108] P. B. Arockiam, C. Bruneau, P. H. Dixneuf, *Chem. Rev.* **2012**, *112*, 5879–5918.
- [109] T. W. Lyons, M. S. Sanford, *Chem. Rev.* **2010**, *110*, 1147–1169.
- [110] B. Liu, B.-F. Shi, *Tetrahedron Lett.* **2015**, *56*, 15–22.
- [111] Y. Zhou, J. Yuan, Q. Yang, Q. Xiao, Y. Peng, *ChemCatChem* **2016**, *8*, 2178–2192.
- [112] T. Gensch, M. N. Hopkinson, F. Glorius, J. Wencel-Delord, *Chem. Soc. Rev.* **2016**, *45*, 2900–2936.
- [113] R. J. Phipps, M. J. Gaunt, *Science* **2009**, *323*, 1593–1597.
- [114] J. Li, S. Warratz, D. Zell, S. De Sarkar, E. E. Ishikawa, L. Ackermann, *J. Am. Chem. Soc.* **2015**, *137*, 13894–13901.
- [115] S. Li, L. Cai, H. Ji, L. Yang, G. Li, *Nat. Commun.* **2016**, *7*, 10443.
- [116] T. Patra, S. Bag, R. Kancharla, A. Mondal, A. Dey, S. Pimparkar, S. Agasti, A. Modak, D. Maiti, *Angew. Chem. Int. Ed.* **2016**, *55*, 7751–7755.
- [117] F. Zhang, D. R. Spring, *Chem. Soc. Rev.* **2014**, *43*, 6906–6919.
- [118] D. Katayev, K. F. Pfister, T. Wendling, L. J. Gooßen, *Chem. – Eur. J.* **2014**, *20*, 9902–9905.
- [119] T. Truong, K. Klimovica, O. Daugulis, *J. Am. Chem. Soc.* **2013**, *135*, 9342–9345.
- [120] K. M. Engle, T.-S. Mei, M. Wasa, J.-Q. Yu, *Acc. Chem. Res.* **2012**, *45*, 788–802.

- [121] T. Satoh, M. Miura, *Synthesis* **2010**, 2010, 3395–3409.
- [122] J. Cornella, M. Righi, I. Larrosa, *Angew. Chem. Int. Ed.* **2011**, 50, 9429–9432.
- [123] C. Arroniz, A. Ironmonger, G. Rassias, I. Larrosa, *Org. Lett.* **2013**, 15, 910–913.
- [124] J. Luo, S. Preciado, I. Larrosa, *Chem. Commun.* **2015**, 51, 3127–3130.
- [125] J. Luo, S. Preciado, S. O. Araromi, I. Larrosa, *Chem. – Asian J.* **2016**, 11, 347–350.
- [126] J. Luo, S. Preciado, I. Larrosa, *J. Am. Chem. Soc.* **2014**, 136, 4109–4112.
- [127] C. Zhu, Y. Zhang, J. Kan, H. Zhao, W. Su, *Org. Lett.* **2015**, 17, 3418–3421.
- [128] C. Arroniz, J. G. Denis, A. Ironmonger, G. Rassias, I. Larrosa, *Chem. Sci.* **2014**, 5, 3509–3514.
- [129] Z. Wu, S. Chen, C. Hu, Z. Li, H. Xiang, X. Zhou, *ChemCatChem* **2013**, 5, 2839–2842.
- [130] A. J. S. Johnston, K. B. Ling, D. Sale, N. Lebrasseur, I. Larrosa, *Org. Lett.* **2016**, 18, 6094–6097.
- [131] D.-H. Wang, T.-S. Mei, J.-Q. Yu, *J. Am. Chem. Soc.* **2008**, 130, 17676–17677.
- [132] Y. Zhang, H. Zhao, M. Zhang, W. Su, *Angew. Chem.* **2015**, 127, 3888–3892.
- [133] X. Qin, D. Sun, Q. You, Y. Cheng, J. Lan, J. You, *Org. Lett.* **2015**, 17, 1762–1765.
- [134] X. Qin, X. Li, Q. Huang, H. Liu, D. Wu, Q. Guo, J. Lan, R. Wang, J. You, *Angew. Chem.* **2015**, 127, 7273–7276.
- [135] H. Gong, H. Zeng, F. Zhou, C.-J. Li, *Angew. Chem.* **2015**, 127, 5810–5813.
- [136] A. Biafora, L. Gooßen, *Synlett* **2017**, 28, DOI: 10.1055/s-0036-1588450.
- [137] S. Bhadra, W. I. Dzik, L. J. Gooßen, *Angew. Chem. Int. Ed.* **2013**, 52, 2959–2962.
- [138] L. Huang, A. Biafora, G. Zhang, V. Bragoni, L. J. Gooßen, *Angew. Chem. Int. Ed.* **2016**, 55, 6933–6937.
- [139] N. Y. P. Kumar, A. Bechtoldt, K. Raghuvanshi, L. Ackermann, *Angew. Chem. Int. Ed.* **2016**, 55, 6929–6932.
- [140] J. Zhang, R. Shrestha, J. F. Hartwig, P. Zhao, *Nat. Chem.* **2016**, 8, 1144–1151.
- [141] M. Simonetti, I. Larrosa, *Nat. Chem.* **2016**, 8, 1086–1088.
- [142] A. Biafora, B. A. Khan, J. Bahri, J. M. Hewer, L. J. Goossen, *Org. Lett.* **2017**, 19, 1232–1235.
- [143] L. J. Gooßen, W. R. Thiel, N. Rodríguez, C. Linder, B. Melzer, *Adv. Synth. Catal.* **2007**, 349, 2241–2246.
- [144] L. J. Goossen, C. Linder, *Unveröffentlichte Ergebnisse*, Technische Universität Kaiserslautern, **2009**.
- [145] C. Amatore, A. Jutand, *J. Organomet. Chem.* **1999**, 576, 254–278.
- [146] S. Kozuch, S. Shaik, *Acc. Chem. Res.* **2011**, 44, 101–110.

- [147] J. Tang, A. Biafora, L. J. Goossen, *Angew. Chem. Int. Ed.* **2015**, *54*, 13130–13133.
- [148] G. Cahiez, A. Moyeux, O. Gager, M. Poizat, *Adv. Synth. Catal.* **2013**, *355*, 790–796.
- [149] D. Hackenberger, *Diplomarbeit*, Technische Universität Kaiserslautern, **2013**.
- [150] J. Menges, *Diplomarbeit*, Technische Universität Kaiserslautern, **2014**.
- [151] A. Reis, D. Dehe, S. Farsadpour, I. Munstein, Y. Sun, W. R. Thiel, *New J. Chem.* **2011**, *35*, 2488–2495.
- [152] S. Farsadpour, L. T. Ghoochany, Y. Sun, W. R. Thiel, *Eur. J. Inorg. Chem.* **2011**, *2011*, 4603–4609.
- [153] B. Song, *Dissertation*, Technische Universität Kaiserslautern, **2013**.
- [154] N. Tsukada, N. Ohnishi, S. Aono, F. Takahashi, *Organometallics* **2012**, *31*, 7336–7338.
- [155] J. P. Michael, *Nat. Prod. Rep.* **2005**, *22*, 627–646.
- [156] S. Zheng, Q. Zhong, M. Mottamal, Q. Zhang, C. Zhang, E. LeMelle, H. McFerrin, G. Wang, *J. Med. Chem.* **2014**, *57*, 3369–3381.
- [157] T. J. Donohoe, C. R. Jones, L. C. A. Barbosa, *J. Am. Chem. Soc.* **2011**, *133*, 16418–16421.
- [158] J. R. Roppe, B. Wang, D. Huang, L. Tehrani, T. Kamenecka, E. J. Schweiger, J. J. Anderson, J. Brodtkin, X. Jiang, M. Cramer, et al., *Bioorg. Med. Chem. Lett.* **2004**, *14*, 3993–3996.
- [159] A. G. Fang, J. V. Mello, N. S. Finney, *Org. Lett.* **2003**, *5*, 967–970.
- [160] S. W. Thomas, K. Venkatesan, P. Müller, T. M. Swager, *J. Am. Chem. Soc.* **2006**, *128*, 16641–16648.
- [161] K. L. Billingsley, S. L. Buchwald, *Angew. Chem. Int. Ed.* **2008**, *47*, 4695–4698.
- [162] G. R. Dick, E. M. Woerly, M. D. Burke, *Angew. Chem. Int. Ed.* **2012**, *51*, 2667–2672.
- [163] D. M. Knapp, E. P. Gillis, M. D. Burke, *J. Am. Chem. Soc.* **2009**, *131*, 6961–6963.
- [164] L.-C. Campeau, S. Rousseaux, K. Fagnou, *J. Am. Chem. Soc.* **2005**, *127*, 18020–18021.
- [165] L.-C. Campeau, D. R. Stuart, J.-P. Leclerc, M. Bertrand-Laperle, E. Villemure, H.-Y. Sun, S. Lasserre, N. Guimond, M. Lecavallier, K. Fagnou, *J. Am. Chem. Soc.* **2009**, *131*, 3291–3306.
- [166] D. J. Schipper, M. El-Salfiti, C. J. Whipp, K. Fagnou, *Tetrahedron* **2009**, *65*, 4977–4983.
- [167] H.-Y. Sun, S. I. Gorelsky, D. R. Stuart, L.-C. Campeau, K. Fagnou, *J. Org. Chem.* **2010**, *75*, 8180–8189.
- [168] L. Ackermann, S. Fenner, *Chem Commun* **2011**, *47*, 430–432.
- [169] P. Dyson, D. L. Hammick, *J. Chem. Soc. Resumed* **1937**, 1724–1725.

- [170] M. R. F. Ashworth, R. P. Daffern, D. L. Hammick, *J. Chem. Soc. Resumed* **1939**, 809–812.
- [171] E. V. Brown, M. B. Shambhu, *J. Org. Chem.* **1971**, 36, 2002–2004.
- [172] P. Lu, C. Sanchez, J. Cornella, I. Larrosa, *Org. Lett.* **2009**, 11, 5710–5713.
- [173] H. G. O. Becker, R. Beckert, Eds., *Organikum: organisch-chemisches Grundpraktikum*, Wiley VCH, Weinheim, **2009**.
- [174] F. Mo, G. Dong, Y. Zhang, J. Wang, *Org. Biomol. Chem.* **2013**, 11, 1582–1593.
- [175] D. P. Hari, B. König, *Angew. Chem.* **2013**, 125, 4832–4842.
- [176] L. He, G. Qiu, Y. Gao, J. Wu, *Org. Biomol. Chem.* **2014**, 12, 6965–6971.
- [177] T. Sandmeyer, *Berichte Dtsch. Chem. Ges.* **1884**, 17, 1633–1635.
- [178] H. H. Hodgson, *Chem. Rev.* **1947**, 40, 251–277.
- [179] G. Balz, G. Schiemann, *Berichte Dtsch. Chem. Ges. B Ser.* **1927**, 60, 1186–1190.
- [180] M. Gomberg, W. E. Bachmann, *J. Am. Chem. Soc.* **1924**, 46, 2339–2343.
- [181] R. Pschorr, *Berichte Dtsch. Chem. Ges.* **1896**, 29, 496–501.
- [182] H. Meerwein, E. Büchner, K. van Emster, *J. Für Prakt. Chem.* **1939**, 152, 237–266.
- [183] D. P. Hari, P. Schroll, B. König, *J. Am. Chem. Soc.* **2012**, 134, 2958–2961.
- [184] S. Crespi, S. Jäger, B. König, M. Fagnoni, *Eur. J. Org. Chem.* **2017**, 2147–2153.
- [185] A. Wetzels, V. Ehrhardt, M. R. Heinrich, *Angew. Chem. Int. Ed.* **2008**, 47, 9130–9133.
- [186] A. Wetzels, G. Pratsch, R. Kolb, M. R. Heinrich, *Chem. – Eur. J.* **2010**, 16, 2547–2556.
- [187] F. P. Crisóstomo, T. Martín, R. Carrillo, *Angew. Chem. Int. Ed.* **2014**, 53, 2181–2185.
- [188] A. Honraedt, M.-A. Raux, E. L. Grogne, D. Jacquemin, F.-X. Felpin, *Chem. Commun.* **2014**, 50, 5236–5238.
- [189] A. Roglans, A. Pla-Quintana, M. Moreno-Mañas, *Chem. Rev.* **2006**, 106, 4622–4643.
- [190] C. Galli, *Chem. Rev.* **1988**, 88, 765–792.
- [191] D. Kalyani, K. B. McMurtrey, S. R. Neufeldt, M. S. Sanford, *J. Am. Chem. Soc.* **2011**, 133, 18566–18569.
- [192] S. R. Neufeldt, M. S. Sanford, *Adv. Synth. Catal.* **2012**, 354, 3517–3522.
- [193] D. Lee, Y. Kim, S. Chang, *J. Org. Chem.* **2013**, 78, 11102–11109.
- [194] J. Ryu, J. Kwak, K. Shin, D. Lee, S. Chang, *J. Am. Chem. Soc.* **2013**, 135, 12861–12868.
- [195] J. Kim, S. Chang, *Angew. Chem. Int. Ed.* **2014**, 53, 2203–2207.
- [196] D. Shabashov, O. Daugulis, *Org. Lett.* **2006**, 8, 4947–4949.
- [197] D.-D. Li, T.-T. Yuan, G.-W. Wang, *J. Org. Chem.* **2012**, 77, 3341–3347.
- [198] Q. Gui, X. Chen, L. Hu, D. Wang, J. Liu, Z. Tan, *Adv. Synth. Catal.* **2016**, 358, 509–514.

- [199] C. S. Yeung, X. Zhao, N. Borduas, V. M. Dong, *Chem. Sci.* **2010**, *1*, 331–336.
- [200] L. Hu, Q. Gui, X. Chen, Z. Tan, G. Zhu, *Org. Biomol. Chem.* **2016**, *14*, 11070–11075.
- [201] P. Nareddy, F. Jordan, S. E. Brenner-Moyer, M. Szostak, *ACS Catal.* **2016**, *6*, 4755–4759.
- [202] R. K. Chinnagolla, M. Jeganmohan, *Org. Lett.* **2012**, *14*, 5246–5249.
- [203] L. Ilies, E. Konno, Q. Chen, E. Nakamura, *Asian J. Org. Chem.* **2012**, *1*, 142–145.
- [204] D. Prat, A. Wells, J. Hayler, H. Sneddon, C. R. McElroy, S. Abou-Shehada, P. J. Dunn, *Green Chem.* **2015**, *18*, 288–296.
- [205] F. P. Byrne, S. Jin, G. Paggiola, T. H. M. Petchey, J. H. Clark, T. J. Farmer, A. J. Hunt, C. R. McElroy, J. Sherwood, *Sustain. Chem. Process.* **2016**, *4*, 7.
- [206] K. Shin, S.-W. Park, S. Chang, *J. Am. Chem. Soc.* **2015**, *137*, 8584–8592.
- [207] Für eine Übersicht der durchschnittlichen Preise für Palladium, Iridium, Rhodium und Ruthenium zwischen Januar 2016 und Mai 2017 siehe: <http://www.platinum.matthey.com/prices/price-charts>, letzter Aufruf: 28. Mai 2017.
- [208] S. De Sarkar, W. Liu, S. I. Kozhushkov, L. Ackermann, *Adv. Synth. Catal.* **2014**, *356*, 1461–1479.
- [209] A. Bechtoldt, C. Tirlir, K. Raghuvanshi, S. Warratz, C. Kornhaaß, L. Ackermann, *Angew. Chem. Int. Ed.* **2016**, *55*, 264–267.
- [210] P. S. Thuy-Boun, G. Villa, D. Dang, P. Richardson, S. Su, J.-Q. Yu, *J. Am. Chem. Soc.* **2013**, *135*, 17508–17513.
- [211] B.-F. Shi, Y.-H. Zhang, J. K. Lam, D.-H. Wang, J.-Q. Yu, *J. Am. Chem. Soc.* **2010**, *132*, 460–461.
- [212] K. M. Engle, D.-H. Wang, J.-Q. Yu, *J. Am. Chem. Soc.* **2010**, *132*, 14137–14151.
- [213] D.-H. Wang, K. M. Engle, B.-F. Shi, J.-Q. Yu, *Science* **2010**, *327*, 315–319.
- [214] K. M. Engle, P. S. Thuy-Boun, M. Dang, J.-Q. Yu, *J. Am. Chem. Soc.* **2011**, *133*, 18183–18193.
- [215] G. Cheng, T.-J. Li, J.-Q. Yu, *J. Am. Chem. Soc.* **2015**, *137*, 10950–10953.
- [216] L. Huang, D. J. Weix, *Org. Lett.* **2016**, *18*, 5432–5435.
- [217] R. Mei, C. Zhu, L. Ackermann, *Chem. Commun.* **2016**, *52*, 13171–13174.
- [218] M. Simonetti, D. M. Cannas, A. Panigrahi, S. Kujawa, M. Kryjewski, P. Xie, I. Larrosa, *Chem. – Eur. J.* **2017**, *23*, 549–553.
- [219] J. Kobayashi, M. Ishibashi, *Chem. Rev.* **1993**, *93*, 1753–1769.
- [220] P. Moosophon, S. Kanokmedhakul, K. Kanokmedhakul, K. Soyong, *J. Nat. Prod.* **2009**, *72*, 1442–1446.

- [221] C. Singh, M. Hassam, V. P. Verma, A. S. Singh, N. K. Naikade, S. K. Puri, P. R. Maulik, R. Kant, *J. Med. Chem.* **2012**, *55*, 10662–10673.
- [222] S. Messaoudi, B. Tréguier, A. Hamze, O. Provot, J.-F. Peyrat, J. R. De Losada, J.-M. Liu, J. Bignon, J. Wdzieczak-Bakala, S. Thoret, et al., *J. Med. Chem.* **2009**, *52*, 4538–4542.
- [223] L. Qu, X. Tang, *Cancer Chemother. Pharmacol.* **2010**, *65*, 201–205.
- [224] M. C. Heck, C. E. Wagner, P. H. Shahani, M. MacNeill, A. Grozic, T. Darwaiz, M. Shimabuku, D. G. Deans, N. M. Robinson, S. H. Salama, et al., *J. Med. Chem.* **2016**, *59*, 8924–8940.
- [225] R. F. Heck, J. P. Nolley, *J. Org. Chem.* **1972**, *37*, 2320–2322.
- [226] T. Mizoroki, K. Mori, A. Ozaki, *Bull. Chem. Soc. Jpn.* **1971**, *44*, 581–581.
- [227] M. Oestreich, *The Mizoroki-Heck Reaction*, Wiley, Hoboken, **2009**.
- [228] I. P. Beletskaya, A. V. Cheprakov, *Chem. Rev.* **2000**, *100*, 3009–3066.
- [229] J. Ruan, J. Xiao, *Acc. Chem. Res.* **2011**, *44*, 614–626.
- [230] J. Ruan, J. A. Iggo, N. G. Berry, J. Xiao, *J. Am. Chem. Soc.* **2010**, *132*, 16689–16699.
- [231] J. Mo, L. Xu, J. Xiao, *J. Am. Chem. Soc.* **2005**, *127*, 751–760.
- [232] T. M. Gøgsig, A. T. Lindhardt, M. Dekhane, J. Grouleff, T. Skrydstrup, *Chem. – Eur. J.* **2009**, *15*, 5950–5955.
- [233] J. Mo, J. Xiao, *Angew. Chem. Int. Ed.* **2006**, *45*, 4152–4157.
- [234] A. L. Hansen, T. Skrydstrup, *J. Org. Chem.* **2005**, *70*, 5997–6003.
- [235] P. Harrison, G. Meek, *Tetrahedron Lett.* **2004**, *45*, 9277–9280.
- [236] M. M. S. Andappan, P. Nilsson, H. von Schenck, M. Larhed, *J. Org. Chem.* **2004**, *69*, 5212–5218.
- [237] L. Qin, X. Ren, Y. Lu, Y. Li, J. (Steve) Zhou, *Angew. Chem.* **2012**, *124*, 6017–6021.
- [238] L. Qin, H. Hirao, J. (Steve) Zhou, *Chem. Commun.* **2013**, *49*, 10236–10238.
- [239] C. Zheng, S. S. Stahl, *Chem. Commun.* **2015**, *51*, 12771–12774.
- [240] C. Zheng, D. Wang, S. S. Stahl, *J. Am. Chem. Soc.* **2012**, *134*, 16496–16499.
- [241] A. Deb, D. Maiti, *Eur. J. Org. Chem.* **2017**, *2017*, 1239–1252.
- [242] R. Matsubara, A. C. Gutierrez, T. F. Jamison, *J. Am. Chem. Soc.* **2011**, *133*, 19020–19023.
- [243] E. A. Standley, T. F. Jamison, *J. Am. Chem. Soc.* **2013**, *135*, 1585–1592.
- [244] S. Z. Tasker, A. C. Gutierrez, T. F. Jamison, *Angew. Chem. Int. Ed.* **2014**, *53*, 1858–1861.
- [245] A. F. Littke, G. C. Fu, *J. Am. Chem. Soc.* **2001**, *123*, 6989–7000.

- [246] R. F. Heck, *Acc. Chem. Res.* **1979**, *12*, 146–151.
- [247] M.-P. Denieul, T. Skrydstrup, *Tetrahedron Lett.* **1999**, *40*, 4901–4904.
- [248] L. F. Tietze, S. G. Stewart, M. E. Polomska, A. Modi, A. Zeeck, *Chem. – Eur. J.* **2004**, *10*, 5233–5242.
- [249] Y. Zou, L. Qin, X. Ren, Y. Lu, Y. Li, J. (Steve) Zhou, *Chem. – Eur. J.* **2013**, *19*, 3504–3511.
- [250] L. Botella, C. Nájera, *J. Org. Chem.* **2005**, *70*, 4360–4369.
- [251] R. Martin, S. L. Buchwald, *Acc. Chem. Res.* **2008**, *41*, 1461–1473.
- [252] S. Agasti, A. Dey, D. Maiti, *Chem. Commun.* **2016**, *52*, 12191–12194.
- [253] T. Kitamura, Y. Fujiwara, in *From C–H to C–C Bonds*, **2014**, 33–54.
- [254] C. Jia, W. Lu, T. Kitamura, Y. Fujiwara, *Org. Lett.* **1999**, *1*, 2097–2100.
- [255] W. L. F. Armarego, C. L. L. Chai, *Purification of Laboratory Chemicals*, Elsevier/Butterworth-Heinemann, Amsterdam; Boston, **2009**.
- [256] F. Rudolphi, L. J. Goossen, *J. Chem. Inf. Model.* **2012**, *52*, 293–301.
- [257] G. R. Fulmer, A. J. M. Miller, N. H. Sherden, H. E. Gottlieb, A. Nudelman, B. M. Stoltz, J. E. Bercaw, K. I. Goldberg, *Organometallics* **2010**, *29*, 2176–2179.
- [258] A. L. S. Thompson, G. W. Kabalka, M. R. Akula, J. W. Huffman, *Synthesis* **2005**, *2005*, 547–550.
- [259] K. Pal, *Synthesis* **1995**, *1995*, 1485–1487.
- [260] A. Herrera, R. Martínez-Alvarez, M. Chioua, R. Chatt, R. Chioua, A. Sánchez, J. Almy, *Tetrahedron* **2006**, *62*, 2799–2811.
- [261] Y. Sun, A. Hienzsch, J. Grasser, E. Herdtweck, W. R. Thiel, *J. Organomet. Chem.* **2006**, *691*, 291–298.
- [262] C. Sarcher, S. Farsadpour, L. Taghizadeh Ghoochany, Y. Sun, W. R. Thiel, P. W. Roesky, *Dalton Trans.* **2014**, *43*, 2397–2405.
- [263] E. Ioachim, E. A. Medlycott, M. I. J. Polson, G. S. Hanan, *Eur. J. Org. Chem.* **2005**, *2005*, 3775–3780.
- [264] S. Dalai, V. N. Belov, S. Nizamov, K. Rauch, D. Finsinger, A. de Meijere, *Eur. J. Org. Chem.* **2006**, *2006*, 2753–2765.
- [265] D. Gelman, L. Jiang, S. L. Buchwald, *Org. Lett.* **2003**, *5*, 2315–2318.
- [266] D. Zhao, T. M. Neubauer, B. L. Feringa, *Nat. Commun.* **2015**, *6*, 6652.
- [267] Y. Engel, A. Dahan, E. Rozenshine-Kemelmakher, M. Gozin, *J. Org. Chem.* **2007**, *72*, 2318–2328.
- [268] M. Moreno-Mañas, R. Pleixats, A. Serra-Muns, *Synlett* **2006**, *2006*, 3001–3004.

- [269] A. Núñez, A. Sánchez, C. Burgos, J. Alvarez-Builla, *Tetrahedron* **2004**, *60*, 6217–6224.
- [270] L. Ackermann, A. Althammer, *Org. Lett.* **2006**, *8*, 3457–3460.
- [271] B. Song, X. Zheng, J. Mo, B. Xu, *Adv. Synth. Catal.* **2010**, *352*, 329–335.
- [272] A. S. Henderson, S. Medina, J. F. Bower, M. C. Galan, *Org. Lett.* **2015**, *17*, 4846–4849.
- [273] A. Lemire, M. Grenon, M. Pourashraf, A. B. Charette, *Org. Lett.* **2004**, *6*, 3517–3520.
- [274] Y.-J. Cherng, *Tetrahedron* **2002**, *58*, 4931–4935.
- [275] G. H. Posner, S. B. Lu, E. Asirvatham, E. F. Silversmith, E. M. Shulman, *J. Am. Chem. Soc.* **1986**, *108*, 511–512.
- [276] F. M. Pillar, P. Appukkuttan, A. Gavryushin, M. Helm, P. Knochel, *Angew. Chem. Int. Ed.* **2008**, *47*, 6802–6806.
- [277] L. Ackermann, C. J. Gschrei, A. Althammer, M. Riederer, *Chem. Commun.* **2006**, 1419–1421.
- [278] Y. Wang, A. V. Gulevich, V. Gevorgyan, *Chem. – Eur. J.* **2013**, *19*, 15836–15840.
- [279] Y. Li, Y.-J. Ding, J.-Y. Wang, Y.-M. Su, X.-S. Wang, *Org. Lett.* **2013**, *15*, 2574–2577.
- [280] K. H. Kim, H. S. Lee, S. H. Kim, S. H. Kim, J. N. Kim, *Chem. – Eur. J.* **2010**, *16*, 2375–2380.
- [281] C. C. Kanakam, N. S. Mani, G. S. R. S. Rao, *J. Chem. Soc. [Perkin 1]* **1990**, 2233–2237.
- [282] M. Raduán, J. Padrosa, A. Pla-Quintana, T. Parella, A. Roglans, *Adv. Synth. Catal.* **2011**, *353*, 2003–2012.
- [283] M. Lafrance, K. Fagnou, *J. Am. Chem. Soc.* **2006**, *128*, 16496–16497.
- [284] T. Zhu, X. Li, H. Chang, W. Gao, W. Wei, *Synlett* **2016**, *27*, 880–887.
- [285] S. Warratz, C. Kornhaaß, A. Cajaraville, B. Niepötter, D. Stalke, L. Ackermann, *Angew. Chem. Int. Ed.* **2015**, *54*, 5513–5517.
- [286] J. Krüger, B. Manmontri, G. Fels, *Eur. J. Org. Chem.* **2005**, *2005*, 1402–1408.

9 Curriculum Vitae

Persönliche Daten

Name: Dagmar Isabell Hackenberger

Ausbildung

01/2014 – 08/2017	Promotion im Arbeitskreis von Prof. Dr. L. J. Gooßen, Technische Universität Kaiserslautern und Ruhr-Universität Bochum (seit 07/2016)
10/2008 – 09/2013	Studium der Chemie, Technische Universität Kaiserslautern Vertiefungsrichtung: Organische Chemie Diplomarbeit bei Prof. Dr. L. J. Gooßen: „Bimetallisch-katalysierte decarboxylierende Kreuzkupplung mit bidentaten Liganden“
08/2005 – 03/2008	Abitur, Gymnasium Saarburg
08/1999 – 06/2005	Mittlere Reife, Realschule Saarburg

Berufserfahrung

01/2014 – 08/2017	Wissenschaftliche Mitarbeiterin im Arbeitskreis von Prof. Dr. L. J. Gooßen, Technische Universität Kaiserslautern und Ruhr-Universität Bochum (seit 07/2016)
10/2013 bis 12/2013	Praktikum, Evonik Industries AG, Inorganic Materials, Abteilung Catalysts – homogene Katalyse, Hanau

Stipendien

10/2014 – 09/2016	Promotionsstipendium der Stipendienstiftung Rheinland-Pfalz – Graduiertenförderung
-------------------	--

Universitäres Engagement

07/2014 – 06/2016	Sprecherin des Jungchemikerforums Kaiserslautern
01/2014 – 06/2016	Aktives Mitglied des Jungchemikerforums Kaiserslautern